A POTENTIAL EFFECT OF CORDYCEPIN ON THE FEEDBACK BETWEEN POLYADENYLATION AND PI3K/AKT/MTOR SIGNALLING

STEVEN JAMES LAWRENCE, M.Sc

Thesis submitted to the University of Nottingham for the degree of Doctor of Philosophy

MAY 2023

Declaration

Except where acknowledged in the text, I declare that this dissertation is my own work and is based on research that was undertaken by myself in the School of Pharmacy, Faculty of Science, University of Nottingham, UK.

Acknowledgements

Firstly, I would like to thank my supervisor, Dr. Cornelia H. de Moor. It has been a privilege to work with someone who has so much knowledge, patience, and upbeat attitude which has kept me on the right path throughout my PhD. Lia has always known exactly what to say and when to say it to keep me motivated and has gone way above and beyond to help make sure this PhD is as great as it can be. Even though Lia has faced some unimaginable challenges towards the end of my PhD, she has always had the time to help me, which just exemplifies how incredible she is as a leader, mentor, and friend. I honestly couldn't describe Lia well enough to justify how amazing she has been throughout my PhD. I honestly think I will never have a supervisor as selfless, and eager to see me grow as a scientist and a person in my lifetime.

This PhD would not have been possible without the funding from the BBSRC and the University of Nottingham. I also would like to acknowledge Professor Grahame Hardie and Dr. Simon Hawley (University of Dundee) for their kindness with supplying us with CRISPR-Cas9 knockout HEK293 cells which was used in this PhD.

My PhD would not have been the same without members of the Gene Regulation and RNA Biology (GRRB) lab. These included:

- Athena Martin, who was my 'RAW macrophage and tissue culture buddy' in the lab and helped keep our macrophages going. Athena was also always a ray of sunshine and helped normalise the day with friendly chats.
- Ruby Chrisp, Ryan Morris, and Hannah Tomlin who always had an incredible sense of humour and helped keep me sane.
- Dr. Kathryn Williams & Dr. Alexander Kondrashov who gave me excellent advice in the lab.
- Ammar Khamis, Asraa Thiyab, Hong Kai, and Elizabeth Rider for allowing me to supervise them in the lab and were always great to work with.
- Joe Tomlinson for helping interpret the proteomics data.

- Barbara Rampersad and Stephen Hall for providing amazing technical support.
- Dr. Hilary Collins for training me on confocal microscopy and for technical advice.
- Dr. Keith Spriggs, my second supervisor, for being amazing at critiquing my PhD Thesis and for helping with bioinformatics.

Finally, but certainly not least, I would like to acknowledge my amazing husband, Daniel Lawrence-Eyre, for purpose, constant praise, and for managing my life around me whilst I have been on this PhD. Dan has been my rock and put me above anything else to ensure I had the time to write the PhD around maintaining a full-time job. It has been incredibly difficult to write the PhD thesis after working 9-5 shifts in my day job, and Dan has sacrificed a lot of his evenings and weekends to keep me going. I wouldn't be where I am today without him, so this PhD is as much his as it is mine. I would also like to acknowledge my fantastic family, including my Mum and Dad, who have never put any pressure on me, but celebrate every little success I have made. I wouldn't be the person I am today if it wasn't for them, and I hope I have made them proud.

Abstract

Polyadenylation is a key step in mRNA maturation and leads to the sequential addition of adenosines forming a poly(A) tail, which is important in mRNA stability, nuclear export, transcription termination, and translational control. This process requires RNA-binding proteins, such as polyadenylation machinery, in pre-mRNA 3'processing multiprotein complexes. Cordycepin (3'-deoxyadenosine) is a natural compound known to metabolise to cordycepin triphosphate (CoTP), which once incorporated into the poly(A) tail, causes chain termination and is thought to restrict the dissociation of polyadenylation machinery such as WDR33. There are known effects of cordycepin on inflammation, cancer progression, and signal transduction pathways, such as PI3K/Akt/mTOR signalling, however the clear mechanism of action of cordycepin is still elusive.

This study analysed multiple microarray and RNA-Seq datasets with cordycepin treatment and found that cordycepin had a similar effect on gene expression to the known PI3K inhibitor, LY294002. Consistently, differentially expressed genes with cordycepin treatment were also linked with repression of PI3K/Akt signalling. Furthermore, through western blotting, cordycepin and PI3K inhibition was found to repress phosphorylation of kinases downstream to AKT and mTORC1, in RAW264.7 macrophages and MCF-7 cells, and phosphorylated AMPK (Thr172) in RAW264.7 macrophages only. These effects demonstrate that cordycepin can repress AKT and mTORC1 probably by inhibiting PI3K.

Through Ingenuity Pathway Analysis, cordycepin treatment was found to have opposite effects to gene expression to the stimulation and activation of upstream regulators such as LPS, TNF, multiple interleukins, EGF, TGF-β, PDGF, and their respective receptors. In RAW264.7 macrophages, differentially expressed genes with cordycepin treatment showed repression of NF-κB signalling, and immunofluorescence confirmed that cordycepin represses LPS-induced NF-κB (p65) nuclear translocation. Also, cordycepin treatment repressed relative mRNA expression of both inflammatory mRNA markers in RAW264.7 macrophages, and growth factor-dependent mRNA markers and transcriptions factors, such as MYC and JUN in MCF-7 cells. Cordycepin treatment prior to EGF stimulation in HEK293 cells also repressed relative

mRNA expression of immediate early genes (IEG's), c-MYC and c-JUN through qPCR. This altogether showed that cordycepin represses gene expression downstream from inflammatory and growth factor responses via inhibiting activity of signalling pathways and transcription factors.

AMPK has previously been suggested to be the key mechanistic target of cordycepin. However, this study has shown that cordycepin can still repress mRNA expression of IEG's and biological pathways such as chromatin remodelling and transcription in CRISPR-Cas9 AMPK knockout HEK293 cells with EGF stimulation. Cordycepin also repressed genes linked to multiple inositol phosphate metabolic pathways in the presence of growth factors in MCF-7, MDA-MB-231 cells, NIH3T3 fibroblasts, and in CRISPR-Cas9 AMPK Knockout HEK293 cells. This included key kinases important for generating inositol phosphates upstream to PI3K signalling, indicating that cordycepin can still affect PI3K activity in the absence of AMPK.

Label-free quantitative proteomics of Orthogonal Organic Phase Separation (OOPS) fractions showed that both cordycepin and LY294002 treatments can shift RBP's, including polyadenylation factors, towards the RNA-bound Interphase. PI3K inhibition had a more substantial effect than cordycepin treatment and shifted WDR33 towards the Interphase suggesting that PI3K inhibition traps WDR33 on RNA, similarly to CoTP. Knockdown of WDR33 in RAW264.7 macrophages was found to repress PI3K/Akt/mTOR signalling through phosphorylating AMPK (Thr172), and repressing GSK3β (Ser9), 4E-BP1 (Thr37/46) phosphorylation. Coupled together, this study suggests that there is a feedback effect between PI3K and WDR33.

The findings in this study therefore both complement known effects of cordycepin on inflammatory, and growth factor stimulation, shows that cordycepin probably acts through PI3K inhibition, and suggesting that cordycepin may act through affecting the feedback between PI3K and the polyadenylation machinery.

List of figures

List of tables

List of abbreviations

3'DI	3'deoxyadenosine
3'UTR	3'untranslated region
4E-BP	4E-binding protein
ADA	Adenosine deaminase
ADK	Adenosine kinase
AGPC	Acidic Guanidinium Thiocyanate-Phenol-Chloroform
AMP	Adenosine monophosphate
AMPK	AMP kinase
APA	Alternative polyadenylation
ARE	AU-rich element
ATP	Adenosine triphosphate
cAMP	Cyclic AMP
cDNA	Complementary deoxyribonucleic acid
CF	Cleavage factor
CoDP	Cordycepin diphosphate
CoMP	Cordycepin monophosphate
CoTP	Cordycepin triphosphate
CPA	Cleavage and polyadenylation
CPE	Cytoplasmic polyadenylation element
CPEB	CPE-binding
CPSF	Cleavage and polyadenylation specificity factor
CREB	cAMP response element-binding protein
CstF	Cleavage stimulation factor
CTD	Carboxy-terminal domain
DMEM	Dulbecco's Modified Eagle Medium
DMSO	Dimethyl sulfoxide
DSE	Downstream GU or U rich element
ECL	Enhanced chemiluminescence
EDTA	Ethylenediaminetetraacetic acid
EGF	Epidermal growth factor
EGFR	EGF receptor
EGR	Early growth receptor
EIF	Eukaryotic translation initiation factor

ER	Estrogen receptor
ERK	Extracellular signal-regulated kinase
FBS	Foetal bovine serum
FDR	False discovery rate
FGF	Fibroblast growth factor
FOS	Fos proto-oncogene, AP-1 transcription factor
FOSB	FosB proto-oncogene, AP-1 transcription factor
GPER	G protein-coupled estrogen receptor
GSK	Glycogen synthase kinase
HCL	Hydrochloric acid
HER2	Human epithelial growth factor receptor 2
IGF	Insulin-like growth factor
IL1β	Interleukin 1-beta
InsP	Inositol phosphate
IPA	Ingenuity pathway analysis
IPK	Inositol polyphosphate kinase
JNK	c-JUN N-terminal kinase
KO	Knockout
LIMMA	Linear models for microarray data
Log_2FC	Logarithmic to base 2 of Fold Change
LPS	Lipopolysaccharide
LXR/RXR	Liver X receptor/Retinoid X receptor
MAPK	Mitogen-activated protein kinase
MD2	Myeloid differentiation protein 2
MEK	MAPK kinase
mRNA	Messenger RNA
MS	Mass spectrometry
mtDNA	Mitochondrial DNA
mTOR	Mechanistic target of rapamycin
mTORC1	Mechanistic target of rapamycin 1
mTORC2	Mechanistic target of rapamycin 2
MYC	MYC proto-oncogene, bHLH transcription factor
MyD88	Myeloid differentiation primary response 88
NF-κB	Nuclear factor kappa-light-chain-enhancer of activated B cells

OOPS	Orthogonal Organic Phase Separation
PABP	Poly(A) binding protein
PABPC	Cytoplasmic poly(A) binding protein
PABPN1	Nuclear poly(A) binding protein
PAMP	Pathogen-associated molecular patterns
PAP	Poly(A) polymerase
PARP1	poly(ADP-ribose) polymerase 1
PAS	Poly(A) signal
PBS	Phosphate buffered saline
PCR	Polymerase chain reaction
PDGF	Platelet-derived growth factor
PH domain	Pleckstrin homology domain
PI	Phosphoinositide
PI3K	Phosphoinositide 3-kinase
PMSF	Phenylmethylsulfonyl fluoride
Poly(A)	Polyadenosine
PPAR	Peroxisome proliferator-activated receptor
PR	Progesterone receptor
PRR	Pattern-recognition receptor
PSF	Polyadenylation specificity factor
PtdIns	Phosphatidylinositols
PVDF	Polyvinylidene fluoride
qPCR	Quantitative real-time PCR
RBD	RNA-binding domain
RBP	RNA-binding protein
RNA	Ribonucleic acid
RNA-Seq	RNA-sequencing
RNAP II	RNA polymerase II
RNP	Ribonucleoprotein
RTK	Receptor tyrosine kinase
RRM	RNA-recognition motif
rRNA	Ribosomal RNA
RBP	RNA-binding protein
RPKM	Reads per kilobase of exon model per million

SDS	Sodium dodecyl sulfate
Ser	Serine
siRNA	Small interfering RNA
TBST	Tris-buffered saline and Tween 20
TEMED	N,N,N',N'-tetramethylethane-1,2-diamine
TENT	Terminal nucleotidyltransferase
TGF-β	Transforming growth factor-beta
Thr	Threonine
TLR	Toll-like receptor
TME	Tumour microenvironment
TNBC	Triple-negative breast cancer
TNF	Tumour necrosis factor
TNFR	TNF receptor
TREX	TRanscription EXport
TUTase	Terminal uridyl transferases
UQ	Upper quartile
USE	U(G/A)UA upstream element
VEGF	Vascular endothelial growth factor
WDR33	WD repeat domain 33

1 Introduction

Signal transduction initiating from growth factor receptors, Toll like receptors and cytokine receptors usually involve several pathways, including the PI3K/Akt/mTOR, RAF/MEK/ERK, and AMPK signalling pathways. These pathways have been heavily investigated previously as drug targets for a variety of conditions, such as cancer, inflammatory diseases, and metabolic syndromes. However, targeting these pathways with current therapies can have undesirable side-effects and become ineffective over time, and therefore have been disappointing.

The bioactive compound, cordycepin (3'deoxyadenosine), is isolated from the caterpillar fungus, *Cordyceps militaris* and has been incorporated into traditional herbal medicine in East Asia to alleviate afflictions of many illnesses[1, 2]. Cordycepin has been well publicised to effect signal transduction, with recent reviews from Radhi *et al*. 2021[3] and Khan *et al*. 2022[4] finding consistent effects of cordycepin to PI3K/Akt/mTOR, AMPK, p38 MAPK, JNK, and MEK/ERK signalling. Although these effects on signalling are known, the precise mechanism of action of cordycepin is still elusive.

Cordycepin is an adenosine analogue with a similar structure to adenosine but has an absence of oxygen at the 3'position of its ribose backbone (figure 1.1)[5]. Early tissue culture studies identified that cordycepin is metabolised intracellularly into cordycepin mono-, di-, and triphosphate (CoMP, CoDP, CoTP) through phosphorylation by adenosine kinase (ADK) (figure 1.1)[5]. CoTP is known to be the active metabolite associated with cordycepins anti-inflammatory[6, 7], anti-cancerous[8, 9], immunomodulatory[10], and anti-microbial biological activities[11, 12]. Due to the structural similarity to adenosine (figure 1.1), cordycepin is known to be a chain terminator for cleavage and polyadenylation, a process involved in the addition of multiple adenosines to the end of mRNA which will be described in more detail in Chapter 1.5.

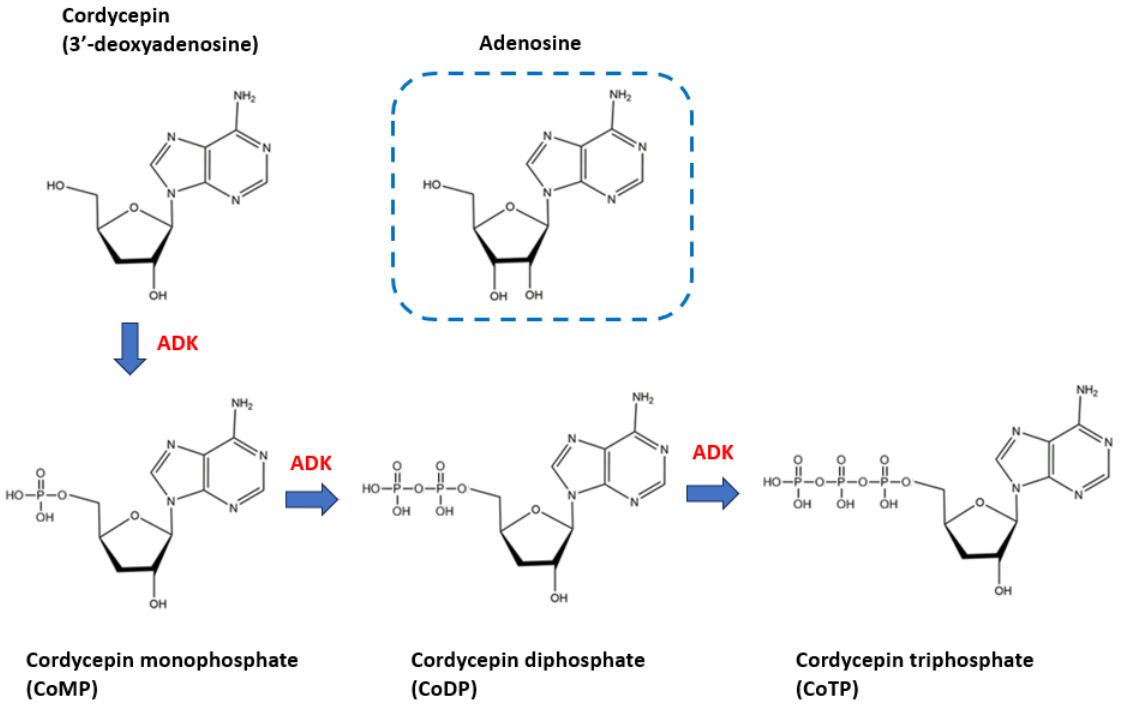

Figure 1.1: Structure and metabolism of cordycepin. As highlighted, cordycepin has a similar structure to adenosine (circled), however it differs through the absence of 3'hydroxyl moiety. Cordycepin is metabolised to CoMP, CoDP, and CoTP through phosphorylation by adenosine kinase (ADK).

It is known that adenosine deaminase (ADA) can deaminate cordycepin into 3'-deoxyinosine, leading to a short plasma half-life of cordycepin[13, 14]. Recently, a new approach was used to evade ADA deamination by encapsulating CoMP fused to a protective cap made of a phosphoramidate motif known as a ProTide (NUC-7738). It was found that CoMP metabolised to CoDP and CoTP intracellularly using this method[15], and current Phase I/II clinical trials have shown significant promise with NUC-7738 (trial ID: NCT03829254). Considering this therapeutic potential of cordycepin, and its effects on signal transduction and polyadenylation, I will introduce in more detail the PI3K/Akt/mTOR, RAF/MEK/ERK, and AMPK signalling pathways, and the process of cleavage and polyadenylation in this Introduction chapter. I will then discuss current literature on the effects of cordycepin on signalling and polyadenylation machinery and show gaps in current research to highlight the importance of understanding the clear mechanism of action of cordycepin. Finally, I will set out the aims of this PhD study and describe how my research can expand current knowledge on the effects of cordycepin on signalling and polyadenylation.

1.1 Signal Transduction Pathways

1.1.1 Plasma membrane Inositol Phosphates

Membrane phospholipids are important precursors of signal transduction. Inositols are polyols which constitute as the head group component of the membrane phospholipids known as lipid phosphatidylinositols (PtdIns). The most common inositol is *myo*-inositol, which plays a role in mediating osmoregulation[16]. Inositols as part of the PtdIns can be selectively phosphorylated by cytoplasmic lipid kinases and phosphatases at positions 3, 4, and 5 generating seven unique species of phospholipids[17-19]. This includes the three monophosphates, PtdIns 3, 4, or 5 phosphate (PI3P, PI4P, or PI5P), the three diphosphates, PtdIns 4,5 biphosphate ($PI(4,5)P_2$), PtdIns 3,4 biphosphate ($PI(3,4)P_2$), and PtdIns 3,5 biphosphate ($PI(3,5)P_2$), and a single triphosphate, PtdIns 3, 4, 5 biphosphate ($PI(3,4,5)P_3$)[17, 18]. These phospholipids are primarily enriched at organelle membranes, aren't freely diffusible in the aqueous cytoplasm, and are spatially restricted to the membrane that they are produced on[20]. They act as second messengers in signal transduction pathways mediating the phosphorylation of downstream proteins, play a role in chromatin remodelling and gene expression, and facilitate nuclear export of mRNA[21-25].

The Phosphoinositide 3-kinase (PI3K) phosphorylates the 3-hydroxyl group of the Inositol ring of the initial PtdIns (PIP) to produce PI3P, and PI4P to produce the $PI(3,4)P_2$ biphosphate. PI3K also phosphorylates $PtdIns(4,5)P_2$ (PIP_2) to synthesise PtdIns-3,4,5-p3 (PIP_3), which is important in downstream signalling pathways and controls cell division[26, 27]. The PI3P monophosphate is predominantly localised on late endosomes and autophagosomal membranes and has roles in endosomal trafficking and autophagy[28, 29]. The PI4P monophosphate is generated by the Phosphatidylinositol 4-kinase (PI4K) family, localises to the Golgi complex and plasma membrane, and plays a role in vesicle trafficking, and lipid homeostasis[30, 31]. The mechanism of the synthesis of PI5P has been speculated to be through phosphorylation by PtdIns 5-kinase (PIKFyve) to PIP and plays a role in insulin stimulated glucose uptake from the extracellular environment[32, 33]. Alternatively, PIKFyve can also catalyse the phosphorylation of PI3P to form $PI(3,5)P_2$, important for lysosomal localisation of downstream signalling pathways[34].

Besides lipid-bound phosphoinositides (PIPs), there are also many derivatives of soluble inositol phosphates (InsPs) due to variable attachment of phosphate moieties to inositol. InsPs are second messengers mediating many downstream cellular processes, including proliferation, differentiation,

apoptosis, migration, and the release of intracellular calcium (through Ins(1,4,5)P3, IP_3)[35, 36]. Based on cellular conditions and stimulus, InsP's can be dynamically turned over to mediate signalling cascades. These InsP's are synthesised by four distinct kinase classes in eukaryotes. These are the inositol polyphosphate kinase (IPK), inositol pentakisphosphate 2-kinase (IPPK), the inositol 1,3,4-trisphosphate 5/6-kinase (ITPK1), and the diphosphoinositol pentakisphosphate kinase (PPIP5K) families[35]. The most characterised group is IPK, which further subdivides into Ins(1,4,5)P_3-3 kinase (IP_3-3K), the inositol polyphosphate multikinase (IPMK, IPK2), and inositol hexakisphosphate kinase (IP6K)[35].

Initial synthesis of the precursor, IP_3, can be through PIP_2 cleavage by phosphatidylinositol-specific phospholipase C (PI-PLC), or through isomerisation of glucose-6-phosphate (G6P) by myo-inositol 1-phosphate synthase (MIPS)[35]. IPMK is known to generate multiple inositol phosphates, through the conversion of IP_3 to Ins(1,3,4,5)P4 (InsP4, IP_4), and IP_4 to Ins(1,3,4,5,6)P5 (InsP5, IP_5)[37]. IPPK is important in the phosphorylation IP_5 to Ins(1,2,3,4,5,6)P6 (InsP6, IP_6). In the presence of growth factors or insulin, PPIP5K2 and IP_6 Kinases (IP6Ks, such as IP6K1) can convert IP_6 to the inositol pyrophosphate, 5PP-InsP5 (InsP7, IP_7). IP_7 is known to interact with the PH-domain of proteins at subcellular membranes and compete with PIP_2 and PIP_3 in protein binding[35, 38]. PPIP5K2 can then phosphorylate IP_7 to 1,5PPInsP4 (InsP8, IP_8)[35, 38]. This altogether shows the dynamic roles InsPs play in signalling pathways and modulating protein interactions with PIPs.

1.1.2 Phosphoinositide 3-kinase (PI3K) signalling

The PI3K/protein kinase B (PKB/Akt) pathway is a crucial pathway in a variety of cellular functions such as quiescence, proliferation, motility, survival, and intracellular trafficking[39]. PI3Ks are lipid kinases divided into three classes (I-III) which all share a core region with a C2 domain, helical domain, and a bilobal kinase domain[19, 40, 41]. The kinase domain is the enzymatic core which contains N- and C-lobe regions forming a cleft, which mediates phosphorylation of lipid substrates via the activation, catalytic, and P-loops[19, 42].

Class I PI3Ks are heterodimeric molecules composed of a p85 regulatory subunit and a p110 catalytic subunit[40, 41]. Mammals express four p110 Class I isoforms (p110α, p110β, p110δ and p110γ encoded by

PIK3CA, *PIK3CB*, *PIK3CD* and *PIK3CG* respectively) important for catalysing the phosphorylation of the phosphatidylinositol 4,5-biphosphate (PtdIns(4,5)P2, or PIP_2) to Phosphatidylinositol-3,4,5-biphosphate (PtdIns-3,4,5-p3, PIP_3)[27, 41, 43-47]. There are also five variants of the p85 subunit, p85α, p55α, p50α (splice variants encoded by *PIK3R1*), p85β and p55γ (expressed by *PIK3R2* and *PIK3R3* respectively), with p85α showing the highest expression[40, 48-52]. Class I PI3Ks are subdivided into Class IA and IB, with Class IA comprising of catalytic subunits p110α, β, and δ which associate with the coiled-coil C and N-terminal Src homology 2 domains (C-SH2 and N-SH2 respectively) and inter-SH2 (iSH2) domain in all five p85 regulatory subunits[39, 53-55]. This SH2 coiled-coil complex preferentially binds to a phosphotyrosyl residue motif YXXM located on growth factor receptors and adaptor protein complexes, such as the insulin receptor substrate 1 (IRS1)[56]. Class IB comprises of the catalytic isoform p110γ which binds to the βγ subunit of heterotrimeric G proteins after activation by GPCRs in a Ras/p101-dependent manner[57], or through inflammatory downstream receptor tyrosine kinases (RTKs) and Toll-like/IL-1 receptor (TLR/IL1R) Ras/p87-dependent manner[58].

There are three Mammalian Class II PI3K isoforms comprising of catalytic subunits, C2α, C2β, and C2γ (encoded by *PI3KC2α*, *PI3KC2β*, and *PI3KC2γ* respectively). These isoforms lack regulatory subunits and can therefore be activated by monomers[59, 60]. The C2α and C2β isoforms are ubiquitously expressed, however the C2γ isoform is predominantly expressed in metabolic tissues including the liver and pancreas[61]. Structurally, Class II PI3K's have a C-terminal phox-homology (PX) domain and C2 domain, as well as a unique extended N-terminal regions with additional protein-binding domains known to aid in intracellular localisation[62]. Similarly to Class I PI3Ks, Class II PI3Ks contain a Ras-binding domain (RBD) on the N-terminal side of the core region. As opposed to Class I PI3Ks, Class II PI3Ks do not produce PIP_3 *in vitro*; but instead use PIP as a substrate to generate PIP_2[63, 64]. Class II PI3K isoforms play different roles due to slight structural changes, with PI3KC2α involved in vesicular trafficking and mitosis by scaffolding to mitotic spindle[65, 66].

There is currently only one Class III PI3K, which is a complex containing a regulatory subunit, Vps15 (p150), and a catalytic lipid kinase, Vps34, and plays a central role in autophagy[67]. The Vps15 subunit is a putative Ser/Thr kinase required for Vps34 stability and activity. The Vps34 kinase facilitates synthesis of Phosphatidylinositol 3-phosphate (PtdIns3P; PI3P; PIP), which is a docking signal for proteins containing

the PIP binding domains (FYVE or PX domains)[68, 69]. The Atg14-related protein (Atg14) can stimulate Vps34 at the phagophore membrane which is required for autophagy initiation in conditions of nutrient withdrawal[70, 71]. Altogether, the PI3K classes are diverse and regulate downstream signalling through lipid metabolism, which can activate substrates downstream on the plasma membranes.

1.1.3 PI3K/Akt Signalling

AKT is a central PIP_3-effector Ser/Thr kinase, which is activated through recruitment and binding of AKT's Pleckstrin Homology (PH) domain to the inositol head group of PIP_3 at the plasma membrane. AKT can be divided into three highly homologous isoforms, AKT1 (PKB), AKT2 (PKBβ), and AKT3 (PKBγ)[72]. The AKT1 isoform is known to be ubiquitously expressed, whereas AKT2 is more highly expressed in insulin-sensitive tissues such as liver and skeletal muscle, and AKT3 is highly expressed in the brain and testes[73-76]. Structurally, the AKT isoforms share architectural homology by containing a catalytic domain flanked by an amino-terminal PH domain, and regulatory carboxyl-terminal domain[77-79]. The PH domain of AKT is also known to bind directly with PIP_2, however this induces a significantly less activation of AKT compared to PIP_3 *in vitro*[80-82].

Full activation of AKT occurs through phosphorylation of the key phosphorylation site, Threonine 308 (Thr308), by Phosphoinositide-dependent kinase-1 (PDK1)[78]. PDK1 is also translocated to the plasma membrane by PIP_3 through interaction with AKT's catalytic domain. This is followed by phosphorylation at Serine 473 (Ser473) in the PH domain by the mechanistic target of rapamycin (mTOR) complex 2 (mTORC2)[83]. Phosphorylation at Ser473 stabilises Thr308 phosphorylation of AKT, however AKT is still active without phosphorylation of Ser473, but has significantly less activity[84, 85]. The protein phosphatases, PP2A, and PH domain leucine-rich repeat protein phosphatase 1 and 2 (PHLPP1 and PHLPP2) can dephosphorylate AKT at Thr308 and Ser473 respectively, thereby inactivating AKT activity[86, 87].

Once fully activated, AKT modulates many downstream proteins and lipid kinases, transcription factors, small G proteins, E3 ubiquitin ligases, metabolic enzymes, and cell cycle regulators through

phosphorylation[88]. These include notable target proteins such as glycogen synthase kinase 3 (GSK3)[89], tuberous sclerosis 2 (TSC2)[90], and PRAS40 (AKT1S1; component of mTORC1)[91]. AKT is also known to phosphorylate and activate the Forkhead transcription factor family, such as FoxO[92, 93]. These factors function by phosphorylating and acetylating posttranscriptional modifications at serine, threonine, and lysine residues of mRNA associated with cellular proliferation, survival, glucose metabolism, and oxidative stress resistance[93]. Two GSK3 subtypes exist with high sequence homology; GSK3α and GSK3β, which function as Serine/Threonine kinases[94]. GSK3β is known to phosphorylate numerous proteins and transcription factors associated with the Wnt/β-catenin signalling pathway linked to cellular growth, tumourigenesis, and glycogen metabolism[95]. GSK3 is constitutively active in the absence of exogeneous signal, and AKT is known to phosphorylate and inhibit GSK3α via Ser21, and GSK3β via Ser9 in their conserved amino-terminal motif[88]. This altogether shows that AKT is a master kinase which regulates many downstream substrates associated with cellular metabolism and survival.

1.1.4 mTOR signalling

1.1.4.1 mTORC1 signalling

mTOR is another Ser/Thr protein kinase incorporated into two distinct complexes, mTORC1 and mTORC2, which differ in composition, activation, and sensitivity to the natural compound, rapamycin[96]. The mTORC1 complex comprises of mTOR, and the core subunits, mLST8 (GβL), Raptor (regulatory protein associated with mTOR), PRAS40 (proline-rich AKT substrate of 40 kDa), and DEPTOR (DEP domain containing mTOR interacting protein)[97]. The Raptor subunit aids in facilitating recruitment of substrates to the TOR signalling (TOS) motif of mTORC1, and subcellular localisation which is detailed further in this chapter[98]. The PRAS40 subunit inhibits mTORC1 through binding to the β-strand of the FKBP12-rapamycin-binding (FRB) domain of mTOR and binds directly to the WD40 domain of mLST8[99]. The DEPTOR subunit interplays and forms a feedback loop with mTOR in the mTORC1 complex[100].

mTORC1 plays a key role in regulating anabolic processes, including cell division, by interrogating intra- and extracellular information, including energy status and stress, growth factors and nutrient

availability[96]. mTORC1 acts on multiple upstream sensor proteins, such as the conserved leucine sensor, SAR1B, which regulates mTORC1 signalling in the presence of intracellular leucine[101]. Another leucine sensor, Sestrin2 (in a dual complex with Sestrin1), is known to interact with and inhibit the GTPase activating protein, GATOR2, which is disrupted by leucine[102, 103]. The amino acid arginine is also known to disrupt the formation of CASTOR1-GATOR2 homodimer and CASTOR1/2-GATOR2 heterodimer complexes which would otherwise inhibit GATOR2 activity[104]. GATOR2 is a pentameric protein complex composing of Mios, WDR24, WDR59, SEH1L, and SEC13[105, 106], which acts upstream to GATOR1, a trimeric protein complex composing of DEPDC5, NPRL2 and NPRL3 known to inhibit Rag (Ras-related guanosine triphosphate (GTP)-binding) GTPase[105] (figure 1.2). In the presence of leucine, Sestrin2 dissociates from the ring domain of WDR24, leading to GATOR2-mediated GATOR1 inactivation, and activation of Rag GTPases[107], which leads to mTORC1 activation as described below.

In the presence of amino acids, Rag GTPase form an active module heterodimer configuration incorporating GTP-bound RagA/B and GDP-bound RagC/D[108]. This configuration anchors lysosomal recruitment of mTORC1 via its subunit, Raptor, which is sustained by the microspherule protein 1 (MCRS1) on the lysosome. At the lysosome, Raptor binds and couples with GTP-bound Rheb (Ras homolog enriched in brain), activating mTORC1[109, 110]. Lysosomal translocation of Rag GTPases and mTORC1 is facilitated by a pentameric complex known as the Ragulator complex[111] (figure 1.2). This complex directly binds to the C-terminal roadblock domains (CRDs) of Rag GTPases and tethers Rag heterodimers on the lysosomal membrane[112]. The putative lysosomal arginine sensor, SLC38A9, forms part of the Ragulator complex through binding to the Rag-Ragulator complex via it's N-terminus. Once regulated by arginine, SLC38A9 transmits amino acids such as leucine from the lysosome to the cytosolic environment, thereby activating mTORC1 via Sestrin1/2[113, 114]. The proton pump, v-ATPase, increases the affinity of Rags and mTORC1 through stimulating the GEF activity of the Ragulator complex, catalysing the conversion of GDP-bound RagA/B, to GTP-bound[115]. The KICSTOR quadruplex also interacts with the Ragulator complex, and contains SZT2, KPTN, ITFG2, and C12orf66, which coordinates sensing of amino acid depletion with GATOR1/2 and inactivates mTORC1 through recruiting GATOR1 to the lysosome in catabolic conditions[116, 117].

During amino acid deprivation, RagA/B is GDP-bound, and Rag C/D is GTP-bound, causing cytoplasmic accumulation and repression of mTORC1, through the recruitment of the TSC1/2 complex which stimulates $Rheb^{GTP}$ to $Rheb^{GDP}$ conversion[118]. TSC1 aids in stabilising TSC2 in the complex, and TSC2 acts as a GTPase-activating protein for the small GTPase, Rheb[119-121]. Under conditions of leucine deficiency, SAR1B can inhibit mTORC1 through physically targeting and inhibiting GATOR2[101] (figure 1.2).

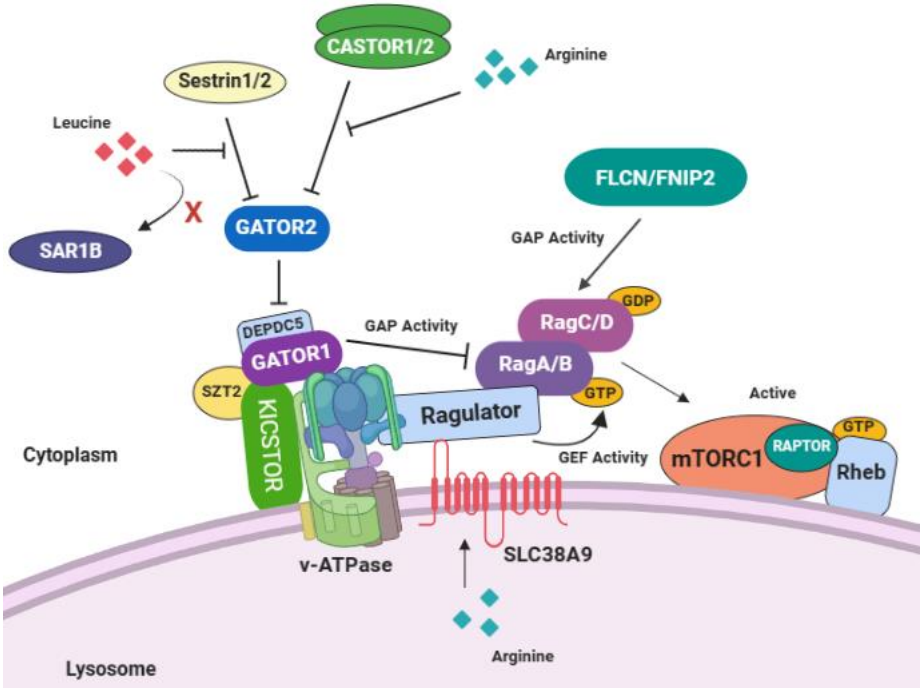

Figure 1.2: Diagram of the Ragulator complex and mTORC1 lysosomal localisation. The lysosomal localisation of mTORC1 and Rag GTPases are facilitated by the Ragulator complex located on the lysosome. This diagram was created using BioRender.com.

Once activated, mTORC1 regulates downstream cellular functions, including cap-dependent translation initiation through the Eukaryotic translation initiation factor 4E (eIF4E)-binding proteins (4E-BP1 and 2), and cellular proliferation via direct phosphorylation of ribosomal protein S6 kinase (S6K)[122, 123]. Phosphorylation of 4E-BP1/2 releases the cap-binding translation initiation factor, eIF4E, increasing 5'-

cap-dependent translation[124, 125]. mTORC1 phosphorylates 4E-BP2 at the Threonine 37/46 (Thr37/46) residues which induces structural remodelling of 4E-BP2, leading to a 100-fold decrease in the affinity between 4E-BP1/2 and eIF4E[126]. Additional phosphorylation at Serine 65, 85, and Thr70 of 4E-BP1 leads to a further decrease in affinity and complete dissociation to eIF4E[127]. mTORC1 induces activation of S6K1 through direct phosphorylation at Thr389, enabling subsequent phosphorylation by PDK1. Once activated, S6K1 phosphorylates and activates multiple substrates which promote mRNA translation initiation, including eIF4B, which is a positive regulator of the 5'cap binding translation initiation complex[128].

1.1.4.2 mTORC2 signalling

Just like mTORC1, the mTORC2 complex contains the core mLST8 subunit. Specifically, the mTORC2 complex contains the scaffolding rapamycin-insensitive companion of mTOR (RICTOR) subunit, and the mammalian stress-activated Map kinase-interacting 1 (mSIN1) important for subcellular localisation[129, 130]. The C-terminal domain of RICTOR interacts and forms multiple contacts with mTOR and masks the FKBP-rapamycin binding domain of mTOR, which makes mTORC2 insensitive to rapamycin[131, 132]. The mLST8 subunit plays a crucial scaffolding role in the mTORC2 complex, with polyubiquitination and ablation of mLST8 from the complex weakens mTOR's interaction with RICTOR and mSIN1, disrupting substrate recruitment of mTORC2[129, 132, 133]. The regulation of mTORC2 is not fully elucidated, with recent research linking activation to conditions of intracellular alkaline pH and amino acid starvation, which further activates AKT to restrict apoptosis[134]. Recent findings have also shown that non-functioning TSC1/2 impairs mTORC2 activity independently of mTORC1, and that TSC1/2 can bind directly to RICTOR in the mTORC2 complex[135].

More is known about downstream substrates of mTORC2, including the regulation of AKT, AGC protein kinases (PKA, PKG, and PKC), and SGK1, all of which are important in cellular proliferation, survival, cytoskeletal remodelling, and cell migration[97]. The best characterised kinase activity of mTORC2 is through the phosphorylation of AKT at Ser473. Knockout of mSIN1 has been shown to restrict AKT

phosphorylation of the transcription factor, FoxO1/3a, but not other downstream substrates such as GSK3α/β and TSC2[136]. In comparison, knockout of RICTOR disrupts liver-specific AKT signalling of Fox01 and GSKα/β, but not with adipose-specific RICTOR knockout[137, 138]. mTORC2 is known to have regulatory effects in insulin signalling, as Sestrin 3 (SESN3) has been found to regulate hepatic insulin sensitivity and glucose metabolism through mTORC2-mediated activation of AKT[139]. The mTORC2 complex also associates with the ribosome where it can phosphorylate nascent AKT at site Thr450 on its turn motif during translation, preventing premature ubiquitination and increasing AKT stability[140]. This altogether shows that although the precise mechanism of mTORC2 activation still not fully understood, mTORC2 can facilitate cellular processes via substrates like AKT.

1.1.5 AMPK Signalling

Conditions of nutrient deprivation and high intracellular adenosine monophosphate/adenosine triphosphate (AMP/ATP) ratios stimulates the AMPK pathway, regulating growth and reprogramming of cellular metabolism via suppression of the mTORC1 pathway[141]. For this reason, AMPK is a sensor of cellular energy. AMPK is a heterotrimeric complex, comprising a catalytic α subunit, and regulatory β and γ subunits[142]. The α subunit contains an amino-terminal region with a serine/threonine kinase domain and an activation T-loop which is vital for AMPKs regulation[143]. Significant activation of AMPK is through phosphorylation at Thr172 in the T-loop by LKB1 (liver kinase B1), which is activated under increased cyclic adenosine monophosphate (cAMP) levels by cAMP-dependent protein kinase (PKA)[144]. LKB1 is further regulated through tethering with AXIN, and associating with Ste20-related adaptor protein-α/β (STRADα/β) and mouse protein 25-α (MO25α, or β for Human)[145]. Alternatively, phosphorylation at Thr172 can also be induced by calcium flux via CAMKK2 (CAMKKβ; calcium/calmodulin dependent protein kinase kinase)[146].

The ligand to AMPK, AMP, binds to the γ subunit of AMPK, which activates it through three complementary mechanisms; allosteric activation[147], promoting upstream kinases to phosphorylate at Thr172[148, 149], and inhibition of protein phosphatases which can dephosphorylate at Thr172[150]. Allosteric

activation of AMPK is dependent on AMP; however, promotion of upstream kinases and inhibition of protein phosphatases can also be mimicked by adenosine diphosphate (ADP)[151, 152]. These activating effects of AMP and ADP are antagonised by ATP, thus AMPK when activated restores energy homeostasis by switching on catabolic pathways and restricting anabolic processes[142, 152]. Once activated, AMPK inhibits mTORC1 through phosphorylation of TSC2 at Ser1387, and Raptor at two conserved serine motifs, Ser722 and Ser792, leading to cell-cycle arrest[153, 154].

1.1.6 Diseases linked to PI3K/Akt/mTOR and AMPK signalling

Among the four Class I isoforms, PIK3CA encoding the p110α catalytic subunit, is the most frequently associated isoform with mutations linking to cancer pathogenesis[155-157]. Mutations of the *PIK3CA* gene is known to be an early activation event in breast and colon cancer, highlighting the importance of PIK3CA in breast cancer development[156]. Expression of the Class II PI3K C2α isoform is associated with genomic stability, with downregulation linked to spindle alterations and delayed anaphase onset. Reduced abundance of PI3K-C2α is also linked to breast cancer clones with mitotic checkpoint defects[158].

The PTEN protein phosphatase is known to inhibit AKT signalling pathway through dephosphorylating PIP_3 to PIP_2, and therefore plays a role regulating cell metabolism, survival, proliferation, apoptosis, growth and migration, and thus is known also as a tumour suppressor[159, 160]. Somatic mutations and epigenetic silencing leading to the loss of PTEN has been linked to the progression of many cancers, including glioblastoma, prostate, and breast cancer, which is thought to lead to accumulation of PIP_3 and activation of AKT[161, 162]. Mutations in PTEN and loss of function is also linked to neurological disorders, including autism and extreme macrocephaly through diminished synaptic plasticity, dendritic and axonal growth, and accelerated spine maturation[163]. Conversely, a reduction in the PI3K/Akt signalling pathway is linked to Alzheimer's Disease, characterised by the formation of senile plaque with amyloid protein (Aβ), and abnormally high phosphorylation of Tau protein in brain nerves[164]. Activated GSK3β can increase Aβ production and hyperphosphorylate Tau protein, and as AKT inactivates GSK3β through phosphorylation

at Ser9, the PI3K/Akt pathway can restrict the formation of neurofibrillary tangles and development of disease[165].

The intramolecular interaction of the PH and kinase domains of AKT1 was found to be important in maintaining AKT activity, with disruption or mutations of these domains linked to inefficient binding to phosphoinositols and a lack of plasma membrane localisation and activation[166]. Disruption and/or mutations of the PH domain has thereby been associated in diseases, such as cancer. An example of this is a G > A point mutation, resulting in a lysine substitution for glutamic acid at amino acid 17 (E17K), in breast, colorectal, and ovarian cancers[167], which leads to constitutive activation of AKT[168]. The E17K mutation is also known to affect the sensitivity of allosteric inhibitors, but not ATP-competitive inhibitors to AKT[167].

Currently, the role of AMPK signalling in the progression of cancer is ambiguous. Research has found that genetic ablation of the α1 catalytic subunit can promote Myc-induced lymphomagenesis, suggesting that AMPK represses tumour development and progression to metastasis[169]. However, AMPK was found to have an oncogenic effect in T-cell acute lymphoblastic leukaemia, as AMPK deficiency led to cell death, whereas AMPK activation promoted survival through upregulating mitochondrial metabolism[170]. Under conditions of intracellular alkaline pH and amino acid deprivation, AMPK is known to be upregulated, which in turn is linked to mTORC2/AKT activation, which aids in tumourigenesis and evasion of apoptosis[134]. Furthermore, other research groups have shown that AMPK signalling has beneficial effects in improving diabetes, mitochondrial disease, and the ability to extend life span[171-173].

1.2 Inflammation and Disease

Inflammation is a broad and complex biological mechanism crucial in orchestrating long-term adaptive immunity of the innate immune system in response to recognition of foreign structures, such as the evolutionarily conserved pathogen-associated molecular patterns (PAMPs), and tissue damage. These PAMPs are recognised by pattern-recognition receptor (PRR's), which are highly expressed by myeloid cells such as monocytes, macrophages, lymphocytes, neutrophils, fibroblasts, and dendritic cells. These can activate gene expression programmes that lead to the secretion of chemokines that attract other immune cells to initiate tissue remodelling[174-178]. PRRs can be membrane-bound, such as Interleukin receptors (ILRs) and TNF receptors (TNFRs), or cytosolic such as RIG-1-like receptors (RLRs) which detect markers of RNA viruses[179-181]. There are also Nucleotide-binding and oligomerization domain (NOD)-like receptors (NLRs), such as NOD, NLRC, and NLPR proteins, important for sensing intracellular pathogens and the secretion of IL-1β and IL-18 cytokines downstream from caspase-1 cleavage[182, 183].

1.2.1 LPS:TLR4:MD2 inflammation in Macrophages

Toll-like receptors (TLRs) are examples of a membrane-bound PRR, and are type I transmembrane proteins encompassing leucine-rich repeat ectodomains which help mediate recognition of PAMPs, transmembrane domains, and intracellular Toll-interleukin 1 (IL-1) receptor (TIR) domains which mediate downstream signal transduction[176, 177]. Structural studies using x-ray crystallography of TLR ectodomains have highlighted that there are several PAMPs which can act as ligand to TLRs, including lipids, lipoproteins, proteins, and nucleic acids derived from multiple microbial pathogens[184-186]. A well-publicised PAMP is lipopolysaccharide (LPS), found on gram-negative bacteria outer membranes, in stimulating TLR4 in macrophages[187, 188]. LPS is shuttled by the LPS binding protein (LBP) to the glycosylphosphatidylinositol-anchored protein, CD14, which facilitates transfer and modulates recognition of LPS to the TLR4:MD2 receptor complex[189, 190]. LPS binds directly and independently to MD2, which non-covalently associates with TRL4[191, 192]. TLR4 then undergoes oligomerisation to allow for the recruitment of adaptor proteins to TIR domains, such as MyD88, TIR domain-containing adaptor

protein (TIRAP), TIR domain-containing adaptor inducing IFN-β (TRIF or TICAM1), and TRIF-related adaptor molecule (TRAM)[193]. Two key pathways activated downstream to LPS stimulation is MyD88-dependent and MyD88-independent signalling pathways.

1.2.2 MyD88-dependent and MyD88-independent pathways in Macrophages

During the MyD88-dependent pathway; MyD88 is recruited to the TIR domain and activates IL-1 receptor-associated kinase-4 (IRAK-4), which further recruits IRAK2 or IRAK1 forming a Myddosome complex. This results in phosphorylation and activation of the IRAK2 and IRAK1[194, 195]. Once activated, IRAK1 undergoes autophosphorylation at multiple sites and leads to dissociation of IRAK1/4 from MyD88[196, 197]. IRAK1/4 phosphorylates the E3 ligase Pellino isoforms 1-3 (PELI1/2/3) and promotes Lys^{63}-linked polyubiquitination of IRAK1 *in vivo*[198]. This leads to the binding and interaction of the E3 ubiquitin ligase, TRAF6, Ubc13 and Uev1a[199, 200]. Once TRAF6 is covalently attached to the K63-pUb (Lys^{63}-linked polyubiquitin) chain of IRAK1 (K63-pUb-IRAK1), it further recruits the transforming growth factor β (TGFβ)-activated kinase1 (TAK1), and TAK1 binding proteins 2 and 3 (TAB2/3) complex, leading to dimerization and autophosphorylation of TAK1[201]. The K63-pUb-IRAK1 chain also associates with the NF-κB essential modifier (NEMO), a regulatory subunit of the IκBα kinase (IKK) complex, the catalytic subunits IKKαβ, and A20-binding inhibitor of NF-κB2 (ABIN2), a regulatory subunit of Tumour progression locus 2 (Tpl2) kinase[202]. Once anchored, the NEMO:IKKα:IKKβ complex interacts with the IRAK1:TAK1:TRAF6 complex leading to phosphorylation of IκB kinase, which would otherwise inhibit the NF-κB transcription regulator complex[203, 204]. This leads to tagging IκB proteins for degradation by the 26S proteasome, allowing NF-κB translocation to the nucleus and transcription of primary response cytokine, chemokines such as TNF, IL-1β, and Cxcl2[205], as highlighted by figure 1.3.

NF-κB is known to be composed of homo- and hetero-dimeric complexes of the Rel family polypeptides, characterised through containing an N-terminal Rel Homology Domain (RHD) which mediates DNA binding, nuclear localisation, and subunit dimerization[206]. Mammals express five core NF-κB proteins: RelA (p65), RelB, c-Rel, NF-κB1 (p50), and NF-κB2 (p52). NF-κB1 (p50) and NF-κB2 (p52) are partially

proteolyzed by the proteasome which removes part of their C-terminus, including the C-terminal transcriptional activation domain (TAD). Due to this, NF-κB dimers composed solely of NF-κB1 (p50) and/or NF-κB2 (p52) fail to activate transcription *in vitro* or *in vivo*, and require RelA and/or c-Rel which enhances NF-κB transcription through their RHDs[207, 208]. Genes encoding the NF-κB polypeptides are upregulated by NF-κB, which generates a positive feedback loop, with the exception of RelA expression, which is controlled through a housekeeping promoter[209].

During the MyD88-independent pathway; the TRIF adaptor protein is the key mediator of the activation of IFN regulatory factor 3 (IRF3) transcription factors. TRIF mediates the recruitment of TRAF3, which forms a complex with TRAF family member-associated NF-κB activator (TANK), TANK binding kinase 1 (TBK1) and the inhibitor of NF-κB subunit epsilon (IKBKE; IKKε)[210, 211]. TBK1 and IKKε phosphorylate IRF3 leading to dimerization and interaction with coactivators CREB-binding protein (CBP) and p300 modulating translocation to the nucleus, and transcriptional promotion at IRF3-binding sites of interferons including IFN-β[212-214]. Besides LPS stimulation, the MyD88-independent pathway is most notably associated with stimulation of viral double-stranded RNA (dsRNA), which has been proven in studies involving synthetic polyrI:rC-RNA[215, 216].

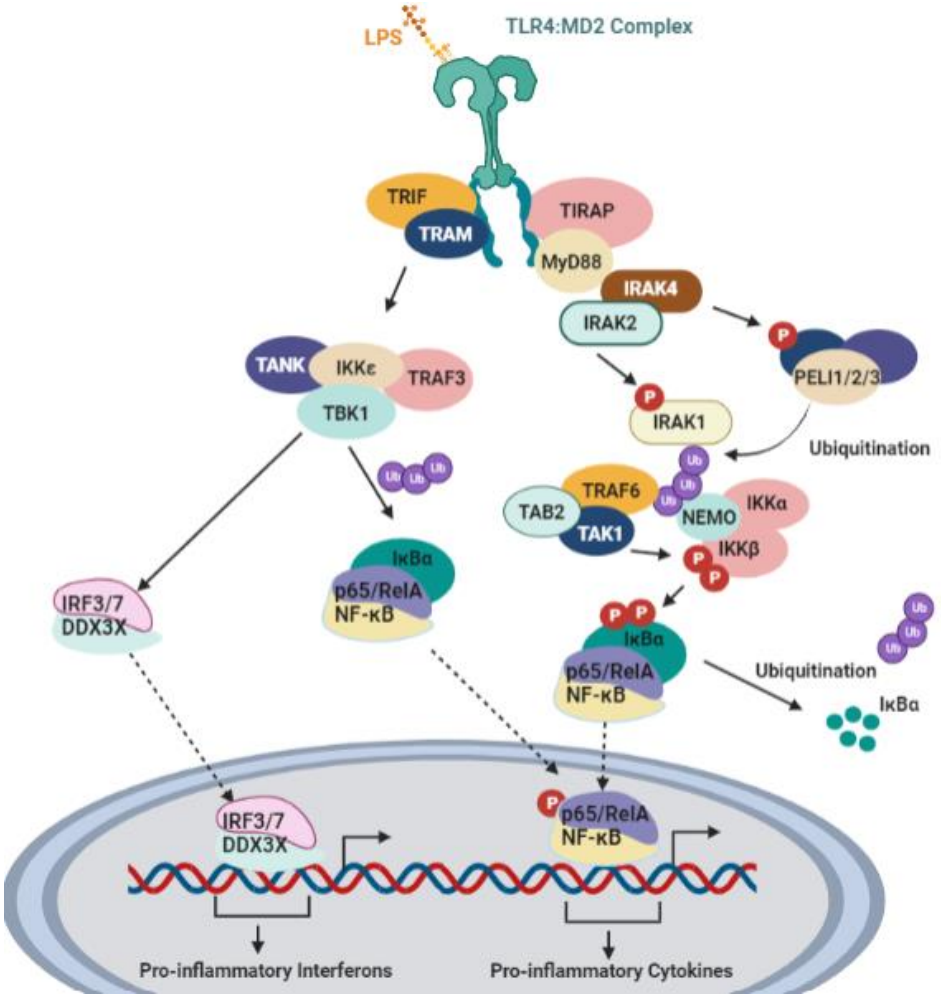

Figure 1.3: Schematic of the LPS:TLR4:MD2 signalling pathway. LPS stimulation of the TLR4:MD4 complex in macrophages induces MyD88-dependent and MyD88-independent pathways upstream to IRF3 and NF-κB nuclear translocation and production of anti-inflammatory interferons and cytokines.

1.2.3 PI3K/Akt signalling in inflammation (PI3K/Akt/NF-κB signalling)

PI3K/Akt/mTOR signalling has a key role downstream to LPS:TLR4 stimulation in immune cells with myeloid origin, such as macrophages, monocytes, and dendritic cells. Upon bacterial Lipopolysaccharide (LPS) inflammatory stimulation, TLR4 associates with the extracellular Myloid differentiation protein 2 (MD2), forming a LPS:TLR4:MD2 complex[185]. This complex recruits the B-cell adaptor for PI3K (BCAP), which is a multifunctional signal transducer interacting with Myeloid differentiation primary response 88

(MyD88) and activating PI3K/Akt signalling[217, 218]. Once activated, AKT phosphorylates IκB kinase-α (IKKα), a Ser/Thr kinase which forms a holocomplex with IKKβ and NF-κB essential modifier (NEMO, or IKKγ), at the T23 site[219, 220]. The activated NEMO:IKKα:IKKβ complex then phosphorylates the negative regulator IκBα at two key serine sites, leading to polyubiquitination and degradation by a E3 ligase complex[221]. This allows nuclear translocation of the NF-κB:p65:RelA heterodimer and regulated transcription of pro-inflammatory cytokines such as the interleukins, IL1β, IL18, and tumour necrosis factor-α (TNFα)[222, 223], highlighted by figure 1.4. AKT is not the only kinase that can mediate IKK activation, as MAP3K7 (TAK1)[224], NF-κB-inducing kinase (NIK)[225], and the TNF receptor (TNFR)-associated factors (TRAFs)[226] all induce NF-κB signalling[227, 228].

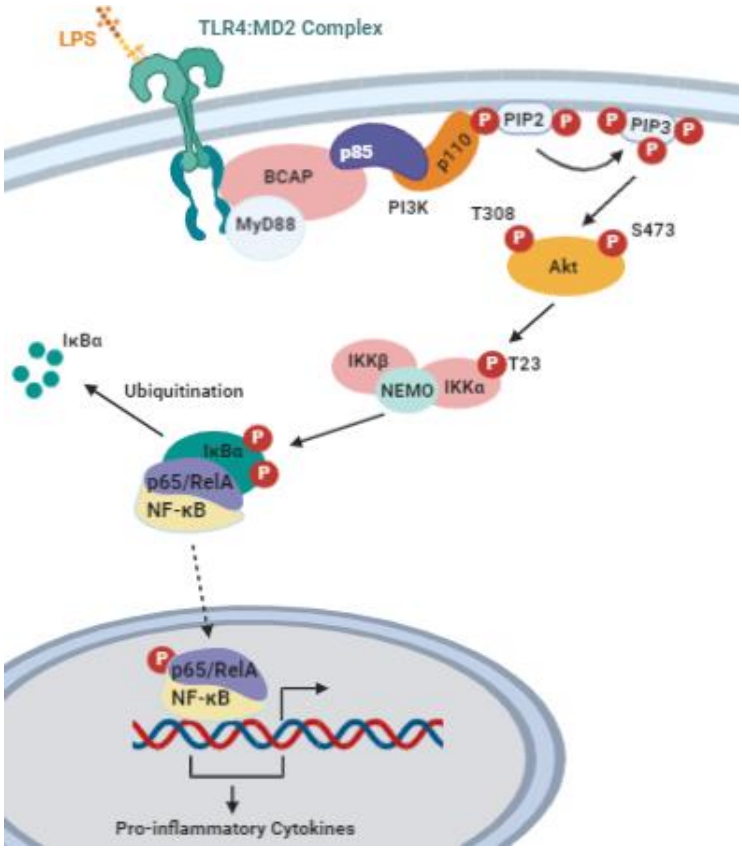

Figure 1.4: Diagram of the LPS:TLR4:MD2 activation of PI3K/Akt/NF-κB signalling cascade in macrophages. This diagram is based on current literature for AKT kinase induction[185, 218, 219, 221]. This diagram was created using BioRender.com.

1.2.4 MAPK signalling in inflammation

Mitogen-activated protein kinases (MAPKs) are highly conserved serine/threonine kinases implicated in the regulation of gene expression, cell survival, apoptosis, proliferation, and differentiation during stress and inflammatory responses[229, 230]. There are three classes of MAPKs, including extracellular signal-regulated kinases (ERKs), and stress-activated protein kinases (SAPKs) families, c-jun N-terminal kinase (JNK) and p38 (p38MAPKs)[231]. Inflammatory cytokines such as TNF are known to stimulate MAPK signalling cascades, and once bound to its receptor, TNF stimulates recruitment of TNF receptor-associated factors TRAF2, TRAF3, and TRAF6, as well as IKK's to the TNFR complex[232]. Once at the TNFR, TRAF6 oligomerises and activates, catalysing the synthesis of unanchored Lys-63 (K63)-linked polyubiquitin chains which binds to the zinc finger (ZNF) domains of TAB2 and TAB3. This stimulates autophosphorylation of TGF-β activated kinase (TAK1) at Thr184 and Thr187, which phosphorylates IKKs and MAPKs[229, 233-238]. TAK1 is also activated through polyubiquitination and proteasomal degradation of TRAF3, which otherwise inhibits the activation of TAK1[239-241]. Activated TAK1 and other MAPK's such as MEKK1, ASK1, and MLK2/3 activate other MAPK kinases such as MKK4/7 and MKK3/6, upstream from JNK and p38 signalling respectively[242-245]. Activation of MAPK kinases lead to nuclear translocation and activation of transcription factors such as the ternary complex factor Elk-1, AP-1, CREB, and Activating transcription factors (ATFs), leading to transcription of proinflammatory cytokines[246, 247]. Alternatively, phosphorylation of IκB after LPS activation of TLR4 also leads to release of the serine/threonine kinase, Tpl2, from a stoichiometric complex, which further phosphorylates and activates MAPKs such as ERK1/2, MEK1 and JNK[248-250]. Once activated through LPS stimulation, Tpl2 phosphorylates MEK1/2, which then phosphorylates and activates ERK1/2.

1.2.5 Inflammatory diseases and current treatments

When immune response and inflammation is not moderated, uncontrolled and chronic inflammation can occur, leading to severe tissue damage and pathogenicity[251]. In occurrences of severe infection or injury, cytokines and chemokines can be released in vast quantities, known as cytokine/chemokine storms or

hypercyto or hyperchemokinemia. This can also lead changes of acute phase proteins in blood plasma, and uncontrolled secretion of cytokines affecting distant tissues, known as the Acute Phase Response (APR)[252, 253]. Chronic inflammation is a feature of many diseases such as cancer, arthritis, Alzheimer's disease, and diseases of the immune, cardiovascular, and pulmonary systems[251, 254]. A common analgesic medicine used to treat pain associated with chronic inflammation are nonsteroidal anti-inflammatory drugs (NSAIDs). However, these are responsible for worsening symptoms such as excessive bleeding, strokes, heart attacks and renal damage in patients over the age of 65 with pre-existing illnesses, contributing to 30% of hospital admissions of adverse drug reactions in the UK[255, 256].

Besides NSAIDs, steroidal-based treatments are also administered for inflammatory diseases such as Crohn's disease and ulcerative colitis, which are inflammatory bowel diseases afflicting 1 in 250 people in the UK[257]. Corticosteroids such as prednisone or prednisolone are administered orally for people with inflammatory bowel diseases which can manage flare ups of inflammation and lead to remission[258]. Corticosteroids function through binding to glucocorticoid receptors, translocating into the nucleus, and binding to response elements which blocks transcription of pro-inflammatory mRNA mediators such as AP-1, CREB, and NF-κB[258, 259]. However, corticosteroids have some severe side-effects through prolonged usage such as hypertension, hyperglycemia, osteoporosis, and steroid addiction/dependency, impotence, and mental health issues[258]. Altogether, current treatments for inflammatory diseases have beneficial anti-inflammatory effects, however side effects can be severe, and prolonged usage is not advisable. Moreover, these treatments are not always effective. Therefore, alternative treatment methods with different modes of action and milder side-effects have the potential to help many people.

1.3 Breast Cancer

1.3.1 Molecular Features of Breast Cancer

Currently, 1 in 7 women in the UK will be diagnosed with Breast Cancer in their lifetime. Between 2016-2018, close to 56,000 breast cancer cases were diagnosed, of which 81% underwent surgery to remove primary tumour, 63% received radiotherapy, and 34% had chemotherapy, with over 11,000 recorded deaths[260]. Worldwide, breast cancer is the most prevalent cancer in women, with almost 50% of breast cancer cases transitioning into metastatic disease, able to evade clinical intervention[261].

Breast cancer is known to be phenotypically diverse with a large degree of genetic and epigenetic heterogeneity characterised by hormone and growth factor receptor status[262-264]. Through gene expression profiling, breast cancer has been classified into four intrinsic molecular subtypes; luminal A, luminal B, v-erb-b2 (ERBB2)/Human epithelial growth factor receptor 2 (HER2) gene-overexpressing, and basal-like triple-negative breast cancer (TNBC)[265-267]. Luminal A breast cancers are known to have estrogen receptors (ERs) and/or progesterone receptors (PRs), but little to none HER2, whereas luminal B breast cancers can include cell surface HER2 and has worse prognosis. HER2-positive breast cancers have little to no cell surface ERs or PRs, and TNBCs are triple-negative for ERs, PRs, and HER2, but can express EGFR[268].

HER2-positive breast cancers account for 15-20% of breast cancer occurrences, with 50% also positive for hormone receptors, and are considered to have poor prognosis[269-271]. TNBC is highly invasive and prevalent in premenopausal women under the age of 40, and accounts for ~15-20% of breast cancer occurrences. In women with TNBC, 46% are diagnosed with distant metastasis, and mortality rates reaching 40% within 5 years[272, 273]. Many breast carcinomas (~70%) are ER and PR-positive and are subclassed in the luminal A and B groups, with ~20-30% of ER-positive breast cancer patients experiencing recurrence with distant metastasis post treatment[265, 274].

The initiation of metastasis in breast cancer is coordinated by complex biological processes regulated by events in the tumour microenvironment (TME; stromal)[275]. The TME is known to promote the epithelial-to-mesenchymal transition (EMT), which involves epithelial cell reprograming to acquire traits common in mesenchymal cells, such as detachment, enhanced motility and invasiveness[276]. The EMT promotes

the formation of cancer stem cell (CSC's), tumour growth and migration[277]. Prominent regulatory factors of EMT are insulin-like growth factors (IGF's), hepatocyte growth factors (HGFs), epidermal growth factors (EGFs), platelet-derived growth factors (PDGFs), transforming growth factor β (TGF-β), and cytokines[276].

1.3.2 Growth factor-dependent stimulation and Signalling in Breast Cancer

Growth factors play important roles in the activation of associated receptor tyrosine kinases (RTKs), such as EGF binding to EGFR, to mediate downstream PI3K/Akt, Ras/Raf/MEK/ERK, MAPK, and JAK/STAT signalling. These pathways are crucial in cancer pathogenesis through promoting proliferation, angiogenesis, and metastasis[278-280]. For this reason, amplification of the growth factor receptors is common in many cancers, making them targets in anti-cancerous therapeutics[281-284]. These receptors can also be constitutively active through mutations, such as the known mutations of the ligand-binding domain of the ER-alpha (ERα) receptor, which leads to poor patient outcome[285]. This is evident for immortalised Breast Adenocarcinomas, MCF-7 cells, which have functional estrogen and EGF receptors, whereas MDA-MB-231 cells are triple-negative (hormone-independent) and more aggressive[286, 287].

The EGFR family are commonly associated with cancer and consists of four homologous members: EGFR1 (ERBB1/HER1), EGFR2 (ERBB2/HER2), EGFR3 (ERBB3/HER3), and EGFR4 (ERBB4/HER4)[288, 289]. They are known to function as tyrosine kinases, which phosphorylate tyrosine via transfer of a γ phosphate of ATP to tyrosine residues on protein substrates[290]. Typically, EGFRs contain an extracellular domain, transmembrane segment, and an intracellular region[288, 289]. The extracellular domain is important for ligand binding, and disulfide bond formation through two cysteine-rich regions[291, 292]. The intracellular region contains the functional tyrosine kinase domain which must be partnered with another EGFR to be activated[293]. This kinase domain region contains a conserved catalytic ATP binding pocket, essential for ATP binding and kinase activity[294]. EGFRs also contain a C-terminal tail which contains multiple phosphorylation sites required for downstream signal transduction[292].

Activation of EGFRs can be through binding of several types of ligands, including EGF, epigen (EPG), TGFα, and heparin-binding EGF-like growth factor (HBEGF)[295]. Once bound, EGFR receptors undergo

conformational changes exposing their extracellular regions enabling homo- and heterodimerisation with other EGFRs[296]. These dimers mediate transphosphorylation of tyrosine residues between each other, and recruitment of downstream signalling proteins[297, 298]. Adaptor proteins known to bind to activated EGFR are Grb2 and Src homology 2 (Shc2), which can further recruit and activate the guanine nucleotide exchange factor (GEF), son of sevenless (SOS). This GEF protein regulates Ras and Rho family GTPases, which increases GTP loading of Ras, and the recruitment Raf kinases, leading to sequential activation of MEK1/2 and ERK1/2, which stimulates cell proliferation[299, 300]. Activated ERK then phosphorylates downstream MAPK kinases and ribosomal S6 kinases (RSK's), such as RSK1/2, which translocates to the nucleus with ERK1/2 triggering phosphorylation and activation of transcription factors, Sp1, E2F, Elk-1, and AP-1. This induces transcription of immediate early genes (IEG's) such as JUN and FOS[301].

Certain heterodimer compositions enhance activity of specific signalling pathways, such as EGFR2-EGFR3 (HER2-HER3) heterodimers, which exhibit potent mitogenic activity of PI3K/Akt signalling in breast cancer progression[302]. EGFR3 is also known to have multiple binding sites with the p85 subunit of PI3K, which stimulates plasma membrane localisation of PI3K[303]. Also, EGF-bound EGFR3 recruits the docking protein, Gab1, which also binds to the p85 subunit[304, 305]. The EGFR1-EGFR4 heterodimer also has docking binding sites for Grb2 which interacts with the PI3KC2β isoform, thereby localising and activating PI3K to the plasma membrane[303, 306]. This altogether highlights that multiple EGFR's can stimulate PI3K localisation and activation of PI3K/Akt signalling.

EGFR2 also activates JNK signalling, which is known to regulate cytokine expression, influencing breast cancer metastasis and poor prognosis through nuclear translocation of RAS, NF-κB, and JUN transcription factors[307-310]. EGFR2 can also activate and form complexes with other receptors, such as insulin-like growth factor 1 receptor (IGF-1R)[311], which has tyrosine kinase activity and autophosphorylates itself and downstream proteins upon ligand binding and activation[312]. Activation of IGF-1R through binding to IGF-1 has been shown to induce bone metastasis of MDA-MB-231 cells, and activation AKT and NF-κB signalling downstream[313-315]. IGF-1 has also been shown to regulate the G protein-coupled estrogen receptor (GPER/GPR30) expression and function in ER-positive breast cancer cells through HIF-1α, leading to stimulation of vascular endothelial growth factor (VEGF) signalling in the breast tumour microenvironment[316]. GPER's are transmembrane proteins with seven domains expressed in ~50-60% of

breast cancer tissues and is an alternative estrogen receptor which is structurally distinct to the canonical ERα and Erβ receptors[317-319]. GPERs can directly interact with EGFR, IGF-1Rs, HIF-1α, and Notch signalling components to trigger release of growth factors such as VEGF, FGF (fibroblast growth factors), and proinflammatory cytokine IL1β[320, 321], which mediate activation ERK1/2, PI3K/Akt signalling cascades and second messengers such as cAMP[322].

GPER expression has been shown to correlate with VEGF activation and production[316]. There are three VEGF receptors (VEGFR1, VEGFR2, and VEGFR3), which contain seven extracellular immunoglobulin (Ig)-like domains, and two intracellular tyrosine kinase domains[323]. These VEGFRs bind to disulfide bonds of the VEGF growth factor isoforms (VEGFA-D) forming homo- and heterodimers, which triggers tyrosine autophosphorylation, providing binding sites for adaptor proteins[323, 324]. VEGFRs have selective binding affinity for the VEGF isoforms, with the VEGFA-VEGFR1[325, 326], and VEGFA-VEGFR2[327, 328] heterodimers known to modulate MAPK/ERK and PI3K/Akt signalling in invasive breast cancer.

GPERs also link to FGF receptors (FGFRs) isoforms, FGFR1-4, which contain intracellular tyrosine kinase domain[329, 330]. There are 22 known conserved FGF ligands, which upon binding, lead to dimerization of FGFRs and activation via autophoshorylation. Phosphorylation of FGFR changes the receptors conformation exposing molecular docking sites for adaptor proteins. These proteins then orchestrate downstream PKC, phospholipase Cγ, PI3K/Akt, and MAPK signalling pathways for cell proliferation, growth, differentiation, vascular repair, and cell survival[329, 330]. FGFRs can also induce activation of platelet-derived growth factor receptors (PDGFRs) and promote acquirement of resistance to inhibitors to these receptors[331, 332]. There are five known PDGF isoforms, consisting of PDGFAA, PDGFBB, PDGFAB, PDGFCC, and PDGFDD, which bind to the RTK receptors, PDGFRα and PDGFRβ[333]. Breast cancer are known to have highly expressed PDGFRα, which can induce EGFR2 activation and trigger downstream ERK1/2 and PI3K/Akt signalling, promoting cell proliferation, survival, and lymph node metastasis[334].

Another growth factor receptor associated with cancer progression is the TGF-β receptor (TGF-βR) family, which comprises of three homologs; TGF-βR1, TGF-βR2, and TGF-βR3[335, 336]. Once TGF binds to TGF-βR2, it recruits and transphosphorylates TGF-βR1, further activating transcription factors for TGF-β responsive genes linked to cellular proliferation, survival, migration, and differentiation[281]. Activated TGF-βR1 can

form a tetrameric receptor complex with TGF-βR2 which mediates recruitment and formation of the ShcA-Grb2-Sos complex which activates Ras at the plasma membrane, and further triggers MEK1/2 and ERK1/2 signalling[337]. TGF-β stimulation of TGF-βR1 can also lead to the activation of MAPK kinases, MKK4, and MKK3/6 inducing the activation of JNK and p38 MAPK signalling[338, 339]. Activated TGF-βR2 can interact with the p85 subunit of PI3K[340], demonstrating that TGF-βR's play important roles in activating signalling pathways.

1.3.3 Therapeutic advances in Breast Cancer

As growth factor receptors are implicated in the development of breast cancers, there have been many clinical trials and research studies reviewing the clinical benefit of the modulation of growth factor receptors and downstream signalling pathways. Current standard treatments for breast cancer is surgery, such as total excision of the breast (mastectomy) or breast-conserving (lumpectomy), post-surgery radiotherapy, chemotherapy using alkylating agents, antimetabolites, and tubulin inhibitors, and personalised treatments[341]. Radiotherapy after a mastectomy in the chest walls and associated lymph nodes has already been attributed to reduced recurrence and mortality[342]. However, irradiation can cause major side effects such as cardiotoxicity, thus exposure is minimised to reduce damaging surrounding healthy tissue[343]. Chemotherapeutic agents for breast cancer also have side-effects, including neurocognitive dysfunction, fatigue, cytopenia, cardiomyopathy, early menopause, and psychosocial impacts[344]. Due to the phenotypically diverse nature of breast cancer, subtype-specific treatments have been proposed to be more effective in restricting tumour growth and metastasis.

HER2-positive breast cancer tumours are known to be sensitive to standard chemotherapy and the monoclonal antibody antagonist, trastuzumab (Herceptin), can extend survival[345, 346]. However, breast cancers can become resistant to first-line anti-HER2 therapies[270, 347]. An example of resistance to Herceptin is through PTEN loss, expression of the highly metastatic p95HER2 truncated isoform, and IGF-1R-HER2 heterodimerisation[311, 348, 349]. Alternatively, PI3K overexpression is also an important resistance mechanism to anti-HER2 therapies with initial clinical studies showing promise in combating HER2-

positive metastatic breast cancer. A Phase I clinical study has shown the benefits and accepted tolerance of combining PI3K inhibitors, such as alpelisib, with the antibody-drug conjugate target of HER2, trastuzumab emtansine (T-DM1), however side effects were common in the patients[350].

The selective allosteric pan-AKT inhibitor, MK-2206, is known to inhibit autophosphorylation of AKT at Thr308 and Ser473, and has been used in trials, such as a phase II clinical trial for advanced breast cancer with PI3K/Akt mutations and PTEN loss, which showed a lack of clinical benefit[351]. However, in combination with neoadjuvant chemotherapy, this inhibitor showed complete response in a hormone receptor- and HER2-positive breast cancer cohort in the I-SPY 2 clinical trial[352]. Furthermore, MK-2206 also induced apoptosis in ER+, and HER2 negative metastatic breast cancer cell lines, but required additional endocrine treatments to maintain the apoptotic effect in long-term estrogen-deprived cells[353]. This altogether suggests that this AKT inhibitor needs additional treatment for clinical use.

There are currently no targeted treatments for triple-negative breast cancers (TNBC's), with standardised treatment being chemotherapy and surgery, which can become refractory and require alternative therapies such as immunotherapy and subtype-specific therapies[354]. The basal-like 1 (BL1) TNBC subtype has high amplification of MYC, PIK3CA, KRAS, IGF1R, and CDK6, as well as deletion of DNA damage repair genes, BRCA2, PTEN, MDM2, RB1, and TP53, highlighting sensitivity to PARP inhibitors[355]. PARP inhibitors, such as olaparib, promotes apoptosis through restricting the DNA repair function of PARP enzymes, and have been shown to have antitumoural effects in BRCA1/2-deficient breast cancer patients, which make up ~19.5% of TNBC patients[356]. The treatment of olaparib on its own however does not show a significant response rate in TNBC patients with and without BRCA1/2 mutations[357], but in combination with PI3K inhibitors, such as alpelisib, there was increased sensitivity of metastatic TNBC to olaparib[358].

For the mesenchymal (M) TNBC subtype, which are characterised by overexpressed Wnt/β-catenin and TGF-β signalling pathways, it has been suggested that patients can benefit from mTOR inhibitors which target EMT[359]. A phase I clinical trial has already shown a response rate of 21% in breast cancer patients with a combination of mTOR inhibitors, temsirolimus and/or everolimus, and VEGF inhibitors[360]. It is also known that ~47% of the M subtype of TNBC harbour mutations in PIK3CA[360]. A recent phase II/III clinical trial, the BELLE-4 study, showed that one patient had improved survival with a combination of paclitaxel

chemotherapy and the pan-PI3K inhibitor, buparlisib. However, this patient experienced grade 3 hyperglycaemia[361]. Altogether, this shows that current inhibitors of PI3K/Akt/mTOR signalling machinery have been disappointing with a lack of efficacy and with bad side-effects. This PhD will expand on the ProTide (NUC-7738) study[15] on the use of nucleotide analogues as a potential way of modulating polyadenylation and PI3K/Akt/mTOR signalling. This will show that cordycepin has potential as a therapeutic agent for signalling pathways, with currently known effects expanded in the next section.

1.4 Effects of Cordycepin on Signalling Pathways

The effects of cordycepin on signalling pathways in current literature have been recently reviewed by Radhi *et al*. 2021[3] and Khan *et al*. 2022[4]. These reviews have shown consistent repression of PI3K/Akt/mTOR signalling, activation of AMPK signalling, and modulation of p38 MAPK, JNK, and MEK/ERK signalling pathways which are linked to the anti-inflammatory and anti-proliferative effects of cordycepin[3] (figure 1.5). These signalling pathways are explained in more detail in Chapter 1.1.

Holbein *et al*. (2009)[362] has previously showed that a mutant yeast strain, vps15, of a regulatory subunit of PI3K affects poly(A) tail metabolism leading to aberrant poly(A) tail length distribution. This strain was sensitive to cordycepin, highlighting a repressive effect to PI3K. Furthermore, cordycepin also leads to reduction of the phosphorylation of AKT (pAKT; Ser473) and total AKT levels in multiple cell lines[3], with an exacerbated effect of cordycepin through pre-treatment of Wortmannin (PI3K inhibitor)[363]. This effect of cordycepin on pAKT has also been shown in RAW264.7 macrophages and SKOV-3 Human Ovarian cancer cell lines via suppression of the pAKT-IκB-NF-κB signalling cascade[364, 365], and cordycepin was proposed to also inhibit cell migration and invasiveness of LNCaP prostate cells and reduced AKT phosphorylation[366]. Cordycepin can also repress NF-κB-mediated transcription during inflammation via repression of PI3K/Akt signalling, which is upstream from the IKKα:IKKβ:NEMO complex involved in nuclear translocation of Nuclear Factor Kappa-B (NF-κB) and transcription of proinflammatory cytokines[217-219].

The mammalian target of rapamycin complex 2 (mTORC2) phosphorylates AKT at Ser473[83], and consistent with the repression of phosphorylation of AKT (Ser473), cordycepin also is known to repress phosphorylation and activation of mTOR. This was shown in repressed phosphorylation of mTOR (Ser2448) and AKT (Ser473) in MA-10 Leydig tumour cells[367], and induction of autophagy via reduced mTOR phosphorylation in HepG2 cells[368] with cordycepin treatment. Moreover, cordycepin also prevents phosphorylation of 4E-BP1 (Thr37/46) in NIH3T3 Fibroblasts, downstream to mTOR signalling, which was abrogated through 4E-BP1 knockdown and AMP kinase (AMPK) inhibition (Compound C)[369]. Compound C however has very poor selectivity for AMPK, suggesting that this effect of cordycepin may not be entirely through AMPK[370] (figure 1.5). Wong, *et al*. (2010)[369] also found that compound C treatment substantially increases AKT phosphorylation in otherwise untreated cells. This suggests that overactivation of mTOR may be responsible for the reduced effect of cordycepin.

Alternatively, activated AMPK is known to negatively regulate mTORC1[153, 154], and cordycepin is known to consistently activate AMPK signalling in literature[3]. This includes the phosphorylation and activation of AMPK (Thr172) in LPS-induced RAW264.7 macrophages which inhibited NF-κB and transcription of TNFα[371], the augmentation of chemosensitivity in glioma cells[372], and repression of drug resistant genes such as HIF-1α in gallbladder cells through cordycepin-induced AMPK activation[373]. Research from Hawley *et al*. (2020)[13] suggests that cordycepin monophosphate (CoMP) could act as a mimic of adenosine monophosphate (AMP) and activate AMPK with lower potency to AMP. This was suggested to be the causal effect of cordycepin; however, CoMP was not conclusively found intracellularly[13]. Also, this paper does not show any preference of CoMP over AMP as a ligand for AMPK, and that knockout of AMPK appears to convey sensitivity, rather than resistance to cordycepin, suggesting that this may be an adaptive response.

Besides PI3K/Akt/mTOR and AMPK signalling pathways, the MAP kinase (MAPK) signalling pathways such as p38 MAPK, ERK, and JNK, have also been shown to be affected by cordycepin treatment[3, 4]. The effects of cordycepin on p38 MAPK and JNK signalling are however ambiguous[3]. For p38 MAPK, research shows both repression at Thr180/Tyr182 in LPS-induced RAW264.7 macrophages[364], TNFα-induced vascular muscle cells[374], and activation at Thr180/Tyr182, which was abrogated by the p38 MAPK inhibitor (SB203580)[367, 375]. Similarly, cordycepin both repressed JNK phosphorylation at Thr183/Tyr185 during

TNFα stimulation[374], and during ER stress to restrict apoptosis[376], and induced phosphorylation of JNK during G2/M-phase cell cycle arrest[375], and apoptosis in MA-10 Leydig tumour cells[367]. Unlike p38 MAPK and JNK, phosphorylation and activation of ERK signalling at Thr202/Tyr204 was found to be more consistently repressed by cordycepin in systematic reviews[3, 4]. This repression of ERK phosphorylation (Thr202/Tyr204) through cordycepin was shown to induce cell cycle arrest and apoptosis of leukaemia cells[377], and was found to be downstream to EGF stimulation of EGFR in mouse oral cancer cells[378] and lung cancer cells[379]. This shows that there can be variable effects of cordycepin on MAPK signalling, however literature suggests that cordycepin usually inhibits ERK signalling (figure 1.5).

An outstanding issue restricting cordycepin from being a lead compound is the lack of a clear binding target molecule or mechanism of action that connects cordycepin with its therapeutic effects. Proposed binding targets of cordycepin, besides the signalling components, AKT and AMPK, include adenosine receptors[7, 369, 380-384], CDK2[367, 377, 385], PARP1[386, 387], and FGFR2[388]. CDK2 is a cyclin-dependent serine/threonine kinase important in G1/S transition, initiation of DNA synthesis, and exit of the S phase during the cell cycle[377]. Cordycepin is thought to dock to the binding pocket of CDK2[385], and inhibit expression of CDK2 leading to S-phase accumulation and apoptosis through activation of the Chk2-Cdc25A pathway[377]. AKT is known to regulate CDK2[389], therefore it is likely that the cordycepin effects CDK2 through repressing phosphorylation and activation of AKT (figure 1.5). Furthermore, Li *et al*. (2020)[388] confirmed reduced activation of CDK2 and found that cordycepin can bind to the fibroblast growth factor receptor 2 (FGFR2), leading to cell cycle arrest through blocking a FGFR/Ras/ERK signalling cascade. This altogether could suggest that cordycepin affects signalling pathways via upstream receptors, which needs further clarity.

Cordycepin is also thought to target the poly(ADP-ribose) polymerase, PARP1, which like CDK2, also links cordycepin to DNA damage responses. PARP1 is known to mediate nuclear translocation of phosphorylated ERK, inducing transcription of immediate early genes (IEGs), and help modulate multiple pathways linked to DNA strand break repair[390]. Cordycepin has been previously found to repress NF-κB signalling through inhibiting PARP1 activity[387], suggesting that cordycepin can repress signalling cascades through PARP1 (figure 1.5). Alternatively, the effect of cordycepin on inhibiting PARP has been proposed to be through adenosine receptors[386]. However, research is ambiguous for the effect of cordycepin

through adenosine receptors, with the consensus suggesting that intracellular import and phosphorylation of cordycepin is required for function, as opposed to binding directly to the receptors[7, 369, 384]. The necessity of intracellular phosphorylation of cordycepin to the active CoTP was confirmed by Schwenzer *et al*. (2021)[15], who found that mutation of adenosine kinase (ADK), which metabolises and phosphorylates adenosine intracellularly, confers resistance to cordycepin in an insertional mutagenesis screen. This altogether shows the effect of cordycepin on PARP1 is not through binding to adenosine receptors, and alternative mechanisms of action of cordycepin still needs further investigation. This effect of cordycepin on signalling pathways could be through its effect on cleavage and polyadenylation. This process and the biological importance of the poly(A) tail will be expanded in the next section.

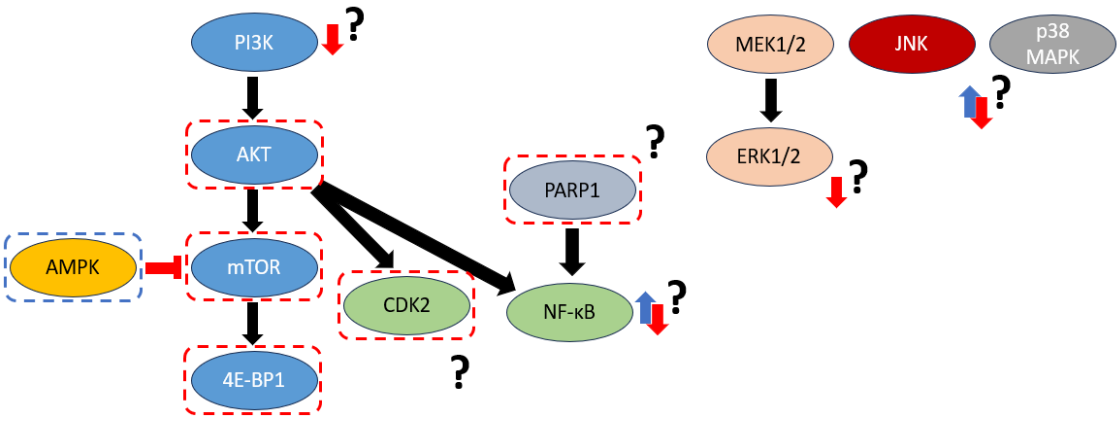

Figure 1.5: Current potential signalling targets of cordycepin. Schematic diagram of the currently known targets of cordycepin based on literature. Proteins highlighted in red are known to be repressed, whereas blue indicates upregulation with cordycepin treatment. The effect of cordycepin on some targets are ambiguous based on current literature and highlighted with a question mark.

1.5 Formation and Biological Functions of the Poly(A) tail

The poly(A) tail and 3'end processing machinery contributes to transcription termination, translational control, and the stability of mRNA, thereby regulating gene expression. mRNA poly(A) shortening (deadenylation) can trigger repression of translation and subsequent mRNA degradation. This highlights the importance of the poly(A) tail and a dynamic transcriptome and translatome, which is described in depth in this chapter[391, 392].

1.5.1 Cleavage and Nuclear Polyadenylation

Nuclear poly(A) tail synthesis involves the assembly of a cleavage and polyadenylation specificity factor (CPSF) pre-mRNA 3'processing multiprotein complex (detailed in figure 1.6). The CPSF multicomplex has seven core subunits organised into two stable multi-protein complexes: polyadenylation specificity factor (PSF) and cleavage factor (CF) complexes[393, 394]. Additionally, the cleavage factor I(m) (CFIm), CFIIm, and cleavage stimulation factor (CSTF) complexes aids in pre-mRNA cleavage. Altogether, the CPSF, CFIm, CFIIm, and CSTF complexes form a heterooligomeric multi-complex which interacts with scaffolding proteins. Many of these scaffolding proteins interact with the carboxyl-terminal domain (CTD) of RNA Polymerase II (RNAP II), linking the cleavage and polyadenylation complexes to transcription[395-399].

These subcomplexes recognise four cis-acting RNA sequence elements flanking a cleavage and polyadenylation (CPA) site on the 3' untranslated regions (3'UTR). These include the highly conserved A(A/U)UAAA poly(A) signal (PAS) hexamer motif, the U(G/A)UA upstream element (USE), the downstream GU or U rich element (DSE), and G rich auxiliary element[400-403]. The AAUAAA PAS hexamer is the most common canonical variant found in human protein-coding genes[404], and there are also other hexamers with reduced functionality, such as the AUUAAA hexamer[405-408].

The core PSF subcomplex comprises of CPSF1 (CPSF160), CPSF4 (CPSF30), WDR33, and FIP1L1 (Fip1/hFip1). The complex co-transcriptionally recognise the PAS motif through direct interaction with CPSF4 and WDR33[403, 409-411]. Analysis of these interactions through Cryo-EM showed that CPSF1 orientates CPSF4 and WDR33 to directly bind to the PAS site[402, 403]. The ZF2 and ZF3 CCCH zinc finger motifs of CPSF4 interact with the A1, A2, A4, and A5 bases on the PAS site, and the Hoogstein base pairing

of the U3 and A6 bases of the PAS site interact with the WD40 domain of WDR33[402, 403]. The CPSF1 subunit is known to form a rigid scaffold which interacts with CPSF4 and the cleavage factor, CPSF2 (CPSF100)[393, 402, 403, 412]. CPSF4 is recruited by the transcription factor TFIID, important for initiating RNAP II transcription, to the preinitiation complex at DNA promoter regions. This links transcription initiation and 3'end mRNA processing. Upon the start of transcription, CPSF4 dissociates from TFIID and becomes associated with the PAS site[413].

The core CF subcomplexes required for efficient pre-mRNA 3'end cleavage are CPSF2, CPSF3 (CPSF73), and scaffold protein Symplekin (SYMPK)[393]. The CF core complex is tethered to the core PSF subcomplex through a conserved interaction between CPSF1 and CPSF2 through a polyadenylation specificity factor interaction motif (PIM)[393]. The CPA site is usually close to the PAS site (~10-30 nucleotides downstream)[414, 415], allowing CPSF3 mediated endonucleolytic cleavage. After cleavage, Fip1 and CPSF1 recruits a Poly(A) Polymerase (PAP) which sequentially adds adenosines to form the poly(A) tail[409, 416, 417]. The PSF subunit, Fip1, preferentially binds to the U-rich region of the USE site through an C-terminal arginine-rich RNA-binding motif, and interacts with PAP and CPSF1 via it's N-terminus region, and CPSF4 on its conserved central domain[409, 412, 418]. CPSF3 is zinc-dependent hydrolase with an endoribonuclease active site crucial for cleavage activity situated in the interface between a N-terminal canonical metallo-β-lactamase domain and a novel β-CASP domain. Recently it has been found that the Ubiquitin-ligase, RBBP6, a constitutive subunit of the CF complex, interacts with CPSF3 and WDR33 and plays a crucial role in activating cleavage in the presence of CSTF and CFIIm subcomplexes[394, 419]. Symplekin is also known to interact with CPSF2, which contains a canonical metallo-β-lactamase domain and a novel β-CASP domain, and CPSF3 through interaction with Symplekin's CTD[420, 421].

The CSTF heterotrimeric protein complex consists of CSTF1 (CstF-50), CSTF2 (CstF-64), and CSTF3 (CstF-77), binds to the DSE site and enables efficient cleavage of the CPA site. The subunit CSTF2 mediates recognition and binding to the GU- and U-rich DSE region via it's N-terminal RNA-recognition motif (RRM)[422, 423]. The CSTF3 subunit is known to enhance nuclear recruitment of CSTF2 and increase stability of RNA-binding of CSTF2 via the RRM via interaction with the last 30 amino acids of CSTF3[424]. Symplekin also interacts with CSTF2, coupling the RNA-bound CPSF and CSTF subcomplexes and is important for catalysing CPSF3-mediated cleavage of the CPA site and recruitment of CFIm subcomplex and PAP

factors[420, 421]. The CSTF1 subunit is a WD-repeat containing protein which interacts directly to the C-terminal heptad domain (CTD) of RNAP II via it's amino terminus *in vivo*[425-427]. CSTF3 was also found to bind specifically to the CTD of RNAP II, but at less efficiency than CSTF1, and to the N-terminus of Fip1 which associates with PAP at the USE site[409, 428]. Due to these interactions, it is now known that CSTF3 can compete with PAP for Fip1 binding, thereby attenuating polyadenylation efficiency[429].

The final, less well-characterised complexes are the CFIm and CFIIm subcomplexes. The CFIm subcomplex composes of three subunits: CFIm 25 (CPSF5, encoded by NUDT21), CFIm 68 (CPSF6), and CFIm 59 (CPSF7). These interact with the USE element (~40 nucleotides upstream to the CPA site) and facilitate 3'end processing complex assembly. The CFIIm subcomplex consists of two fractions: CFIIAm and CFIIBm. The CFIIBm fraction contains stimulating factors for CFIIAm which are not fully understood[398]. CFIIAm is a heterodimer of the cleavage and polyadenylation factor I subunit 1 (CLP1) and the cleavage and polyadenylation factor subunit (PCF11)[430]. This heterodimer has the potential to bind to downstream RNA G-rich sequences, recognise and bridge the CFIm-CPSF complexes during cleavage, and enhance RNAP II-mediated transcription termination[430-434]. Altogether the CPSF, CSTF, and CFIm subcomplexes, a canonical PAPα or PAPγ (PAPOLA or PAPOLG), and the nuclear poly(A) binding protein (PABPN1) act as a transient multi-protein cleavage and polyadenylation complex[402, 435-438], shown in figure 1.6.

Sequential addition of adenylate residues by PAP occurs after cleavage at the CPA site of the 5'end product. PABPN1 speeds up PAP polyadenylation by tethering PAP to mRNA via it's C-terminal domain on polyadenylated RNAs with ~10 adenylate residues, increasing PAP-RNA affinity ~80-fold which would otherwise have a low affinity to RNA due to a lack of sequence specificity[436, 439, 440]. PAP is transiently stabilised on the RNA upon formation of a processive polyadenylation complex containing CPSF-PABPN1-PAP, which aids in the synthesis of mRNA transcripts with poly(A) tail of ~250 adenylate residues[438, 441], shown in figure 1.6.

Besides the nuclear canonical PAPs, PAPα/PAPγ, and testis-specific PAPβ, other non-canonical PAP's such as the speckle targeted PIPKIα regulated poly(a) polymerase (TUT1, also known as Star-PAP, RBM21, or TENT1). TUT1 is part of another group of enzymes important for mammalian 3'non-templated polyadenylation of mRNA and non-coding RNA known as terminal nucleotidyltransferases (TENTs)[442].

These TENTS separate into non-canonical PAPs and terminal uridyl transferases (TUTases) and share a catalytic helix-turn motif with highly conserved aspartate residues[443, 444]. TUT1 is also highly selective to the spliceosome component, U6 snRNA, and functions as a U6-TUTase[445]. TUT1 also promotes 3'end CPSF3 cleavage by recruiting CPSF3 and CPSF1 to the CPA site, and forms a complex incorporating CSTF2, RNAP II and Symplekin to promote 3'end CPSF3 cleavage[446, 447]. This altogether demonstrates that PAPs have a diverse role in regulating cleavage and nuclear polyadenylation based on proteins they interact with and protein complexes they bind to.

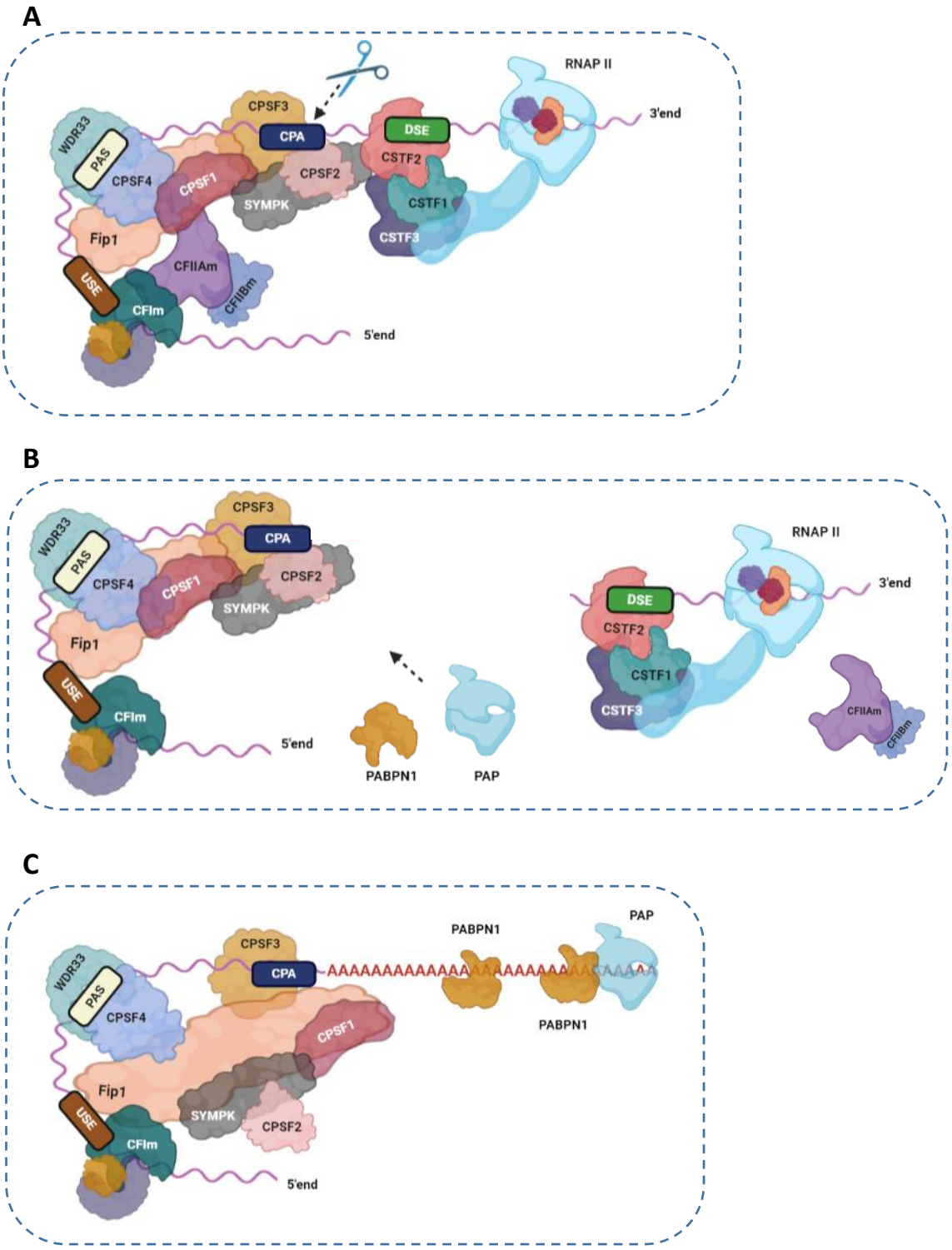

Figure 1.6: Overview of cleavage and nuclear polyadenylation. A) Schematic diagram of the key protein complexes attached to the cis-acting RNA sequence elements in the mRNA 3'UTR. **B)** Cleavage at the CPA site dissociates RNAP II and DSE elements and stimulates recruitment of PAP and PABPN1. **C)** PAP is tethered to mRNA via it's C-terminal domain, stabilised by CPSF-PABPN1 and sequential addition of adenosine residues added to form the poly(A) tail.

1.5.2 Poly(A) Machinery and Transcription Termination

During 3'end processing of eukaryotic protein-coding pre-mRNA transcripts, the cleavage at the CPA site defines the 3'end of the mature mRNA, essential for mRNA maturation and transcription termination[448]. The termination of transcription occurs when the nascent RNA and polymerase release from the DNA template, and is thought to be required for recycling RNAP II for subsequent rounds of transcription, controlling pervasive transcription, and regulates gene expression[449].

There are two main mechanisms of termination downstream of mRNA cleavage, the allosteric mechanism and the 'torpedo model'[449-451]. In the allosteric mechanism, termination is mediated by changes to RNAP II processivity due to conformational changes induced by transcription of the end of the mRNA. This is thought to be facilitated by a loss of elongation factors and acquisition of termination factors[449-451]. Elongation factors include SCAF4/8 which bind to hyperphosphorylated RNAP II CTD and are involved in selection of PAS site and regulate transition of transcription elongation to termination[452]. Depletion of SCAF4/8 can lead to premature cleavage and polyadenylation, which has also been seen with reduced levels of CDK12, PABPN1, and U1-snRNP[452-455]. This process does not necessarily require cleavage and the PAS site before termination, as conformational changes of RNAP II from PAS transcription can promote termination without cleavage[456, 457].

In the 'torpedo model', CPSF3 cleaves at the PAS, allowing XRN2-mediated 5'-3' exonuclease digestion of nascent RNA, and release of RNAP II from the DNA template through contact with the exonuclease[449-451]. When XRN2 is inhibited, PAS-dependent termination is also inhibited, which is potentially due to a delay in the time taken for XRN2 to reach and dissociate RNAP II from the DNA template[450, 458]. This was further proven by Fong *et al*. (2015)[459] who found that PAS-dependent termination is dependent on elongation rate of RNAP II. XRN2 termination shifted upstream by slowing RNAP II elongation (R749H substitution), and speeding transcription up (E1126G substitution) extended termination downstream[459]. The CFIIm subunit, PCF11, is also known to be important for efficient degradation of the 3'end product after cleavage and enhances transcription termination in the presence of an intact poly(A) signal[433, 434], highlighting an association of the PAS site and transcription termination. This altogether shows that CPSF3-mediated cleavage, an intact PAS site, and the activity of RNAP II are important for the 'torpedo model' of transcription termination.

1.5.3 Alternative Polyadenylation (APA)

It is now well established that the majority of Human genes have multiple poly(A) signals (PAS; A(A/U)UAAA motif's), causing alternative polyadenylation (APA), found in internal coding regions (IE-APA, or CR-APA), and intronic/untranslated regions (IT-APA or UTR-APA), giving rise to transcript isoforms of various 3'UTRs, affecting gene regulation and the transcriptome[404, 460]. This categorisation of APA has broadened, with tandem occurrences of APA (TR-APA), and Upstream APA (UR-APA), a PAS upstream from the last exon with a prevalence of ~40% in the mouse genome. Proximal PAS sites which are upstream can also lead to exon skipping (Splicing APA; SP-APA)[461-463].

Alternative polyadenylation can generate multiple RNA isoforms with variable 3'UTR lengths. These isoforms can therefore contain variable amounts of *cis*-elements, such the protein binding motifs; AU-rich elements (AREs), GU-rich elements (GREs), and PUF protein-binding elements, and microRNA binding sites important for mRNA stability and translation[464-466]. In cellular proliferation, the pro-proliferation mRNA transcripts with shortened 3'UTRs through APA are more stable, as they have less target sites for microRNA-mediate repression[464]. However, it has also been proposed that longer 3'UTRs can also evade microRNA-mediated repression by forming occlusive structures blocking the accessibility of regulatory elements, such as microRNA sites[467]. The subcellular localisation and roles of proteins also vary depending on the positioning of the APA site, and length of 3'UTR. This is apparent for immunoglobulin M (IgM) heavy chain isoforms isolated from B lymphocytes, as the longer transcript is membrane-bound, whereas the shorter isoform is not[468]. Alternative 3'UTR lengths can also alter mRNA localisation and mediate local synthesis of proteins[469, 470]. Berkovits and Mayr (2015)[471] also demonstrated that shorter CD47 proteins from shorter 3'UTR transcripts localised in the endoplasmic reticulum (ER), whereas proteins from longer 3'UTR transcripts localised on the cell surface and functioned as a scaffolding protein. Through transcriptomics of cumulative human cell lines, APA isoforms with a longer 3'UTR and inverted Alu repeats tend to be more abundant in the nucleus compared to the cytoplasm[472, 473]. This nuclear retention is thought to be a quality control mechanism to prevent inappropriate translation of promiscuously edited RNA with inverted repeats[474, 475]. This highlights that 3'UTR length and *cis* elements can play a role in protein subcellular localisation and function, however mRNA stability does not always correlate with 3'UTR length.

It has been found that changes in the levels of polyadenylation factors can affect the choice of PAS site as CFIm and CFIIm subunits are known to regulate APA. The CFIm complex is known to preferentially interact with distal PAS sites in terminal exons to help facilitate CstF-CPSF-PAP-RNA stabilisation. Additionally, loss-of-function of the CFIm subunits, NUDT21 and CPSF6, leads to transcriptome wide proximal PAS selection in HEK293 cells[476-478]. Short mRNA isoforms through APA of these subunits are associated with spermatogenesis as they are enriched in mouse male germ cells, and CFIm binding sites accumulate near the 3'ends of germ cell mRNA[479]. Similarly, Fip1 has been found to preferentially select proximal PAS sites, generating APA transcript isoforms crucial for embryonic stem cell self-renewal and somatic cell reprogramming[480]. Conversely, PABPN1 and PABPC1 were found to promote usage of distal PAS sites, with PABPN1 found to inhibit expression of APA transcripts with PAS sites near the TSS[481]. PABPC1 also interacts with hnRNPLL and regulates immunoglobulin secretion in B cells by promoting proximal APA, shifting expression of the membrane isoform to secreted isoform promoting differentiation[482]. This altogether highlights that cleavage and polyadenylation factors contribute to PAS site selection in APA, which have biological roles in differentiation and development.

1.5.4 Cytoplasmic Polyadenylation

The extension of the poly(A) tail during cytoplasmic polyadenylation can mediate the switch of otherwise dormant mRNAs during oogenesis and early development to translationally active mRNA[483-487]. Poly(A) polymerases, cytoplasmic poly(A) binding proteins (such as PABPC1), and the cytoplasmic polyadenylation element (CPE) binding proteins, CPEBs 1-4, are often required for efficient cytoplasmic polyadenylation and mRNA translation[488-490]**.** PABPC1 requires ~12 adenosine residues to bind to the poly(A) tail, and help PAPs extend the poly(A) tail by ~20-30 adenosine resides. The most abundant PABPC in the cytoplasm is PABPC1, found predominantly in somatic tissue[491]. There are other PABPC's which are testis-specific (known as tPABP, or PABPC3), embryonic (ePAB), X-linked (PABPC5), and an inducible protein in stimulated T-cells (known as PABPC4, or iPABP)[492-496].

The CPEB proteins (CPEB1-4) are important in posttranscriptional gene regulation, as dependent on phosphorylation state, they can both repress and enhance translation[497]. CPEBs have conserved C-terminal RNA-binding domains incorporating two RNA-recognition motifs (RRMs) which precede zinc-binding domains, which help bind to CPE sites on mRNA[498]. In immature oocytes, mRNA containing CPE sites are translationally dormant and have been proposed to reside in a complex containing unphosphorylated CPEB1, eIF4E, a cap-binding Eukaryotic translation initiation factor, and Maskin, a CPEB-associated factor[499, 500]. However, Maskin was not found to be co-fractionated with CPEB1, but CPSF2, DDX6, eIF4ENIF (4ET), and eIF4E1b was, suggesting that Maskin is not associated to CPEB1-mediated translation repression[501], but repression is likely to be mediated by blocking eIF4G recruitment through 4ET or eIF4E1b. In the absence of CPEB1 at the CPE site, eIF4G would normally bridge eIF4E on the 5'cap of mRNA to PABP, circularising the mRNA towards the poly(A) tail, forming a closed-loop structure, and facilitating translation[502-505]. During maturation in vertebrates, CPEB1 is phosphorylated at serine reside 174 by Eg2 (also known as Aurora A), a serine/threonine protein, increasing the affinity of CPEB1 in recruiting CPSF through breaking the closed-loop inhibitory structure between the 5' and 3'UTR[506-508]. Altogether, CPEB1 plays an important role in translational efficiency in development, and the recruitment of canonical cytoplasmic PAPs such as GLD2 (PAPD4) and PAPβ (PAPOLB, also known as TPAP) to the 3'UTR, or non-canonical cytoplasmic PAPs, TENT4A (PAPD5), TENT4B (PAPD7), or TENT5 (FAM46), to elongate the poly(A) tail[509-511].

1.5.5 Mitochondrial Polyadenylation

In Metazoans, the very compact, circular mitochondrial genome (mtDNA) is well conserved, encoding a core set of ~13 mRNAs and 2 rRNAs punctuated by ~22 tRNAs[512, 513]. These mRNAs are core components of the mitochondrial respiratory chain complex important for the synthesis of ATP[514]. In the mitochondrial genome, mt-tRNAs intersperse mRNAs and rRNAs, known as the tRNA punctuation model, and form the structural basis for RNaseP and RNaseZ complexes at tRNA-mRNA junctions. These complexes help release mtRNAs through efficient 5' and 3' cleavage at tRNA-mRNA junctions[515-518].

It is still under investigation as to the key roles of mitochondrial polyadenylation in RNA stability, turnover and translation. It is however understood that 3'-end polyadenylation is crucial for mt-mRNAs which lack a complete stop codon, and thus an open reading frame, as mt-mRNAs carry over a 3'-end proximal sequence ending in U or UA after endoribonucleolytic processing[515, 519]. Mitochondrial polyadenylation is orchestrated by the non-canonical PAP, MTPAP (also known as TENT6, or PAPD1), which adds sequential adenosine residues to incomplete U or UA stop codons, completing the UAA stop codon of mitochondrial mRNA[520-522]. MTPAP does not appear to have a specificity towards nucleotides, and uses all nucleotides as a substrate with its strongest activity linked with using ATP and UTP forming diverse 3'end tails[523].

MTPAP is found predominantly localised in mitochondrial RNA granules (MRGs) with other RNA processing and translation machinery[520-522]. These MRG's are membraneless compartments of RNA-protein complexes, found close to mitoribosomes, and are important in mitochondrial gene expression[524, 525]. The Helicase SUV3 and polynucleotide phosphorylase (PNPase) form a SUV3/PNPase degradosome complex cooperates with the G-rich RNA sequence binding factor 1 (GRSF1) and co-localise to MRGs with MTPAP[526, 527]. The SUV3/PNPase complex is important for mt-RNA surveillance and degradation of antisense G-quadraplexes (G4s)-containing mt-RNAs, which are transcribed in abundance as the mitochondria genome has skewed G-rich strand regions[527, 528]. MTPAP is known to polyadenylate abnormal mt-tRNAs, which are degraded by the SUV2/PNPase complex, suggesting a potential role of mitochondrial polyadenylation on mt-tRNA surveillance[529]. This altogether shows mitochondrial polyadenylation may be pivotal in degradation of abnormally polyadenylated RNAs, and mitochondrial translation but the relative importance of these processes remains to be elucidated.

Table 1.1: Summary of known PAPs. Additional functions of each PAP based on literature are described which are not related to the sequential addition of adenosine residues during cleavage and polyadenylation.

Official name	Localisation	Additional Functions
PAPOLA/PAPOLG (PAPα/PAPγ)	Nuclear	Contributes to APA[530, 531]. Associated in the PABPN1 and PAPα/γ-mediated decay (PPD) pathway of deficiently spliced and nuclear-retained transcripts[532, 533].
TUT1 (RBM21/TENT1/ Star-PAP/PAPD2)	Nuclear	Known as a terminal nucleotidyltransferase (TENT)[442]. Acts as a U6-TUTase with U6 snRNA[445]. Promotes 3'end cleavage through CPSF3 & CPSF1 recruitment[446, 447]. Implicated in disease pathogenesis[534, 535].
TENT2 (GLD2/PAPD4/TUT2)	Cytoplasmic	Associates with Symplekin through CPEB & CPSF interaction[536-538].
TENT4A (PAPD7/POLK/LAK1)	Cytoplasmic	Restricts rapid deadenylation by impeding the CCR4-NOT complex[510, 539].
TENT4B (GLD4/PAPD5/TUT3)	Cytoplasmic	Associated with synaptic plasticity[540], carbohydrate metabolism and glucose homeostasis[541]. Restricts rapid deadenylation with TENT4A[510, 539].
PAPβ (PAPOLB/TPAP)	Cytoplasmic	Mostly associated with polyadenylation of sperm-related mRNAs[485, 509].
TENT5A (FAM46A)	Cytoplasmic	Implicated in disease pathogenesis[542-546]. TENT5 (FAM46) group associated in promotion of cell death through polyadenylation of ER-targeted mRNAs[511, 547], and regulating immune response[548].
TENT5B (FAM46B)	Cytoplasmic	Thought to be specific to pluripotent stem cell-specific mRNA and important in early embryonic development[549].
TENT5C (FAM46C)	Cytoplasmic	Acts as a potential onco-suppressor, with loss-of-function linked to cancer development[547, 550-556].
MTPAP (TENT6/PAPD1)	Mitochondria	Completes the UAA stop codon of mitochondrial mRNA[520-522]. Associated with the SUV3/PNPase/GRSF1 degradsome complex in mt-tRNA surveillance[526, 527]. Associated with lethal autosomal recessive perinatal encephalopathy[557].

1.5.6 Roles of Polyadenylation in Health and Disease

Due to the role of cleavage and polyadenylation in mRNA maturation, stability, export, and function of mature transcripts, it is not surprising that perturbance of this process is linked to health and disease. Cleavage and polyadenylation factors are known to be associated with cancer progression. The CSTF1 subunit and the CTD of RNAP II is known to interact with the BRCA1-associated RING domain protein (BARD1), and BRCA1. This CSTF1-BARD1-BRCA1 interaction has been found to inhibit mRNA 3'end formation and the degradation of RNAP II through ubiquitination under genotoxic stress[558, 559]. BARD1 has also been implicated to colocalise with the DNA replication and repair protein, RAD51, which is known to interact with BRCA1, and the largest subunit of RNAP II (RPB1)[560-563]. During DNA damage, CSTF1 forms a complex with PARN, the poly(A)-specific 3'exoribonuclease and enhances BARD1 activation of PARN leading to deadenylation of nuclear mRNA[564]. Altogether, this links transcription-coupled RNA processing and DNA repair through interactions with CSTF1, and potential anti-cancerous effects of CSTF1 and BARD1.

Alternative polyadenylation is implicated in many diseases, with relatively high prevalence of transcript isoforms with shortened 3'UTRs in cancer[565, 566]. Alternative polyadenylation of PABPN1 and PCF11, crucial for bridging the CFIm-CPSF complexes, stimulating cleavage, and enhancing PAP activity is linked to cancer pathogenesis. Across 17 different cancer types, APA of PABPN1 was found to be a modulator of 3'UTR shortening by suppressing proximal PAS site selection and cleavage[530]. Knockdown of PABPN1 also resulted in 3'UTR shortening of cell cycle related genes, inhibition of proliferation, and S phase arrest in triple-negative breast cancer[567]. Truncated mRNA isoforms derived from Intronic APA are also associated with cancers, such as Isoform 3 (Iso3), formed by Intronic APA of the retinoblastoma-binding protein 6 (RBBP6). Iso3 is downregulated in several human cancers, and outcompetes RBBP6 from binding to CSTF2, and inhibiting CPSF3-mediated 3'end cleavage[568, 569]. RBBP6 is known to interfere in DNA binding of tumour suppressor, p53, and facilitates ubiquitination and degradation through interacting with the negative regulator of p53, Mdm2. Due to lower expression of competitive Iso3 in cancer, RBBP6-mediated degradation of p53 isn't impeded, allowing for cancer growth[570]. This altogether suggests that APA of cleavage and polyadenylation factors may play a role in cancer progression.

Poly(A) polymerases have also been implicated in cancer and various diseases. For example, protein-coding mutations of TENT5 PAPs are prevalent in multiple myeloma, a B-cell malignancy, occurring in ~3-13% of primary malignancies, with ~20% of patients also showing deletion of the 1p12 locus of TENT5C[550-553]. TENT5C also acts as a onco-suppressor, as knockout enhances B lymphocyte proliferation, and introduction of wild type TENT5C significantly reduces multiple myeloma growth, which is thought to be partly due to specific polyadenylation of ER mRNAs of TENT5 PAPs linked to cell death[547]. Alternatively to cancer, impairment of the ubiquitin specific peptidase 15 (USP15), which is known to aid TUT1 stabilisation of the U6 snRNA in the nucleoplasm is linked to chronic ER stress and unconventional cerebellar formation, linking abrogated TUT1 to neurogenerative phenotypes[571]. Knockout of TENT5A in mice was found to cause skeletal abnormalities, with high expression of TENT5A found in mineralised tissues in wild type mice[543]. Also, biallelic mutations of MTPAP leads to short poly(A) tailed mt-RNA transcripts, and development of lethal autosomal recessive perinatal encephalopathy[557]. Altogether, PAPs are associated with variety of diseases highlighting the diverse roles PAPs have in biological functions.

1.5.7 Role of the Poly(A) tail in Nuclear Export

In eukaryotes the nuclear envelope is important for separating transcription from translation and allows modification of mRNA. During maturation, mRNA is capped (m^7G 5'end), spliced, and poly-adenylated to form packaged messenger ribonucleoprotein complexes (mRNPs) prior to nuclear export[572, 573]. The m^7G 5'end cap identifies the molecule as self and interacts with nuclear export factors[574, 575]. The mechanism of nuclear export in most mRNAs is conserved in eukaryotes incorporating three pathways; NXF1:NXT1 (TAP:P15), CRM1 (exportin) and Exportin-5. The CRM1 and Exportin-5 pathways preferentially export microRNAs, rRNAs, and snRNAs out of the nucleus[576]. The homologous NXF1:NXT1 (TAP:P15) complex mediates the export of mature mRNAs through nuclear pores to the cytoplasm[577].

NXF1:NXT1 binds to RNA non-specifically, and requires additional factors associated with the TREX (TRanscription EXport) complex to stimulate RNA-binding and promote mRNA export. The TREX complex

contains a THO subcomplex comprising of THOC1-3 and THOC5-7, the DEAD-box helicases UAP56 (DDX39B) and DDX39A, RNA export adaptors such as Aly/REF, CHTOP, Ulf, and export factors such as POLDIP3 and ZC3H11A[578-582]. Aly/REF is an important adaptor which contains N- and C-terminal helices acting as the UAP56-binding motif (UBM)[583]. Aly/REF has a weak RNA recognition motif (RRM), flanked by arginine-rich regions allowing binding to NXF1:NXT1 and transfer of RNA from Aly/REF to NXF1:NXT1[584, 585]. The THO subcomplex is recruited early in mRNA synthesis and mediates packaging of nascent mRNA into a mRNP complex with components of the TREX complex, such as UAP56 which aids in binding to mRNA[586].

1.5.8 The Poly(A) tail and Translation

The cytoplasmic poly(A) binding protein, PABPC1, is influential in translation initiation. PABPC's contain four N-terminal RNA recognition motif (RRM) domains with a nanomolar affinity to bind to the poly(A) RNA[587-589]. PABPC's also contain a proline-rich C-terminal mademoiselle (MLLE) domain which recognises the peptide motif, poly(A)-interacting motif 2 (PAM2), which regulates poly(A) tail dynamics by interacting with PABP-binding proteins[590]. PABPC1 requires ~12 adenosine residues for RRM1 and RRM2 high-affinity binding to the 3'-end of mRNA and extends the poly(A) tail by ~20-30 adenosine resides, physically covering ~30 nucleotides[590, 591]. PABPC1 is known to bind across the poly(A) tail, binding in a 'head-to-tail' formation, linking RRM1 to RRM4[592]. This supports the interaction and stability of translation machinery including the Eukaryotic translation initiation factor eIF4G and translation termination factor, eRF3[505, 589, 593-596].

The m^7G 5'end cap of mRNAs binds directly to translation factors promoting translation initiation[597, 598]. This aids in the formation of the closed loop between the 5'end eukaryotic translation initiation factor, eIF4E, the scaffolding protein eIF4G, and PABPC on the 3'end poly(A) tail[597, 599]. Altogether, the 5'-m^7G cap-eIF4E-eIF4G-PABPC-poly(A)-3' complex aids in the stimulation of translation through the recruitment of the small (40S) ribosomal subunit[600, 601]. Interestingly, depletion of eIF4E at 80-90% does not affect global protein synthesis rate, demonstrating that eIF4E is not a rate-limiting factor in translation[602, 603].

The poly(A) tail also enhances translation in m^7G-uncapped mRNA's, even though translational activity is weaker when compared to in the presence of the m^7G 5'end cap[601, 604, 605]. Altogether, this shows that the poly(A) tail and PABPC are important factors for the activation of translation, even in the absence of the 5'end cap. However, the length of the poly(A) tail itself has minimal correlation to translation efficiency[606].

1.5.9 Regulation of Poly(A) tail length & mRNA Stability

The length of the poly(A) tail has been an area of ongoing research. Measurements using radiolabelling techniques in HeLa cells suggested that the range of 150-250 adenosine residues was added to RNA[607, 608]. Restriction to a ~250 poly(A) tail length appeared to be in part through stimulation of PAP through the nuclear poly(A) binding protein (PABPN1) and Cleavage and Polyadenylation Specificity Factors (CPSF)[438, 440, 532]. Advances in sequencing has now enabled the analysis of poly(A) length and sequences on a global scale. These studies identified huge variations in poly(A) tail length, with a median measurement of ~60 nucleotides in total RNA, and low abundant mRNA with longer than ~250 nucleotide poly(A) tails in the Human transcriptome[609-615]. Altogether these studies mostly investigated the link between stability and poly(A) tail length through genome-wide stability studies in steady-state, which shows no positive correlation with poly(A) tail length and stability.

Prior to degradation, deadenylation and the release of PABPC is required before mRNA decay[616]. Due to this, one alternative hypothesis of a link of poly(A) tail length and mRNA stability is that PABPC on the poly(A) tail contributes to mRNA stability. Formation of the 5'-m^7G cap-eIF4E-eIF4G-PABPC-poly(A)-3' closed loop structure is thought to be important for restricting access to exonucleases to mRNA[599, 617], and as PABPC requires ~12 adenosine residues for binding[590, 591], this links tail length and stability. PABPC was also found to sequester from the poly(A) tail through addition of excess poly(A) RNA in a reporter mRNA decay system, destabilising and exposing the poly(A) tail complex leading to degradation[618]. PABPC is also known to play a role in the removal of adenosine during deadenylation through forming a PAM3-PABPC-poly(A) RNP complex with the cytoplasmic deadenylation complex, PAN2-PAN3[590, 619, 620].

Besides PAN2-PAN3, the other canonical deadenylation complex is the CCR4-NOT (CNOT) complex, which incorporates exonucleases (CNOT6/7/8), decapping (CNOT2/3) and scaffolding subunits (CNOT1/9), and a E3 ubiquitin ligase (CNOT4)[621-628]. These two core deadenylase complexes have been hypothesised to act in a biphasic (or sequential) manner, as initial removal of distal adenosines is through PAN2-PAN3, presumably through interaction with PABPC's, and proximal deadenylation to the 3'UTR is through CCR4-NOT[629]. This altogether shows that the stability of mRNA can be linked to the interaction of the poly(A) tail, translation machinery of the 5'cap, and mRNA deadenylation. As it is clear that cleavage and polyadenylation machinery regulates the poly(A) tail and mRNA stability, the next section will expand on the roles of cleavage and polyadenylation machinery in signalling pathways.

1.5.10 The roles of Cleavage and Polyadenylation factors in Signalling Pathways

As detailed previously, cleavage and polyadenylation factors have diverse roles in health and disease, and research has started to suggest that inhibition of polyadenylation may affect signal transduction and inflammation. It has been shown by Ashraf *et al*. (2019)[384] who showed that knockdown of CPSF4 and WDR33 can repress NF-κB nuclear translocation and inflammatory mRNA marker expression in RAW264.7 macrophages. CPSF4 was also found to be elevated in inflamed synovial tissues associated with osteoarthritis[384]. Furthermore, depletion of CPSF4 also reduces mRNA transcription of cyclooxygenase 2 (COX-2, PTGS2) through decreased phosphorylation of IKKα/β and IκBα and nuclear translocation of NF-κB to promotor regions. Conversely, upregulation of CPSF4 leads to increased expression of COX-2 and lung cancer tumorigenesis[630]. CPSF4 was also found to be overexpressed in human colon cancer, facilitating tumorigenesis through upregulating NF-κB transcription of the telomerase reverse transcriptase, hTERT[631]. The influenza A virus has been found to express the NS1A protein which blocks the ZF2 and ZF3 motifs and CPSF4 interaction to the AAUAAA PAS site. This abrogated global 3'-end processing, and reduced inflammatory mRNA marker expression to reduce host response[632]. This altogether shows that CPSF4 can repress inflammatory response and mRNA marker expression through NF-κB signalling.

Interestingly, the influenza virus protein, NS1, also interacts with the SH2 domain of the p85β subunit of PI3K and shows linked interactions with both CPSF4 and PI3K[632, 633]. The link between CPSF4 and PI3K/Akt/mTOR signalling has previously been substantiated through the repression of AKT (Ser473) and mTOR (Ser2448) through knockdown of CPSF4 in CAL27 squamous cell carcinomas[634]. Knockdown of CPSF4 was also shown to reduce phosphorylation and activation of PI3K p85 (Tyr458)/p55 (Tyr199), AKT (Ser473), ERK1/2 (Thr202/Tyr204), and JNK (Thr183/Tyr185) in H1299 non-small cell lung carcinomas[635]. Combinational treatment of the selective pan-PI3K inhibitor, NVP-BKM120 (Buparlisib), with the mutant p53 gain-of-function compound, Prima-1^{Met}, was found to synergistically abrogate CPSF4-binding of hTERT. This suppressed hTERT mRNA expression, and reduced metastasis and growth of thyroid cancer cells and tumour xenografts, highlighting the link between PI3K/Akt/mTOR signalling and CPSF4/hTERT[636]. The microRNA, miR-4458, can directly target the 3'UTR of CPSF4 and suppress mRNA expression of CPSF4. In MDA-MB-231 cells, overexpression of miR-4458 can also repress the phosphorylation and activation of PI3K p85 (Tyr458)/p55 (Tyr199), AKT (Ser473), and ERK1/2 (Thr202/Tyr204)[637]. Altogether, these findings suggest that targeting CPSF4 can affect PI3K/Akt/mTOR, ERK, and JNK signalling.

Besides CPSF4, other components of cleavage and polyadenylation are also linked to PI3K/Akt/mTOR signalling. This includes CPSF3 which mediates endonucleolytic cleavage on the 3'UTR prior to the addition of the poly(A) tail, as knockdown of CPSF3 in hepatocellular carcinoma cells results in reduced phosphorylation of AKT (Ser473). This also led to increased GSK3β downstream from AKT, inducing cell cycle arrest[638]. The cleavage factor I(m) (CFIm) subcomplex plays a role in cleavage and polyadenylation, and high-throughput analysis of the silencing of CFIm subcomplex subunit, CPSF6, in A549 lung adenocarcinoma cells illustrated affects to mTOR, PTEN, and NF-κB signalling pathways. CPSF6 silencing also induced increased GSK3β protein expression, but reduced JUN and IRS1, which altogether suggests that CPSF6 plays a role in the expression of key transcription factors downstream from PI3K/Akt/mTOR and NF-κB signalling in growth factor stimulation[639]. Knockdown of another CFIm factor, CFIm 59 (CPSF7), also represses PI3K/Akt/mTOR signalling in lung adenocarcinoma cells, which inhibits colony formation, migration and invasion[640]. This all show that multiple cleavage and polyadenylation factors play a role in PI3K/Akt/mTOR signalling.

Cleavage and polyadenylation factors also play a role in alternative polyadenylation (APA) and selection of poly(A) site (PAS), which has been linked to signalling pathways. This includes the pre-mRNA cleavage complex 2 protein, PCF11, which when depleted in mouse C2C12 cells led to global 3'UTR lengthening through the promotion of distal PAS site selection. This led to reduced neuroblastoma tumorigenesis by upregulating the long 3'UTR GNB1 transcript, which is less stable than the canonical isoform, and modulates Wnt signalling[641]. Similarly to loss of CPSF6, downregulation of CFIm 25 (CPSF5, encoded by NUDT21), leads to global proximity PAS site selection and 3'UTR shortening[477]. CFIm 25 also modulates Wnt/β-catenin and NF-κB signalling pathways through regulating the 3'UTR APA of ANXA2 and LIMK2 mRNA, leading to poor prognosis in bladder cancer[642]. Interestingly, knockdown of all three-cleavage factor I(m) factors, CFIm 25, 59, and 68, increased PTEN protein abundance in NIH3T3 fibroblasts, with CFIm 25 and 68 shifting APA towards proximal PAS site selection of PTEN 3'UTR, aiding in increased stability of PTEN[643]. As PTEN is a negative regulator of PI3K/Akt signalling, altogether the data suggests that effects on APA through cleavage and polyadenylation factors also play a role in modulating signalling pathways. As cleavage and polyadenylation plays a role in signal transduction pathways, and cordycepin is known to affect signalling pathways, the next section will highlight what is known about the effects of cordycepin on cleavage and polyadenylation machinery.

1.6 Effects of Cordycepin on Cleavage and Polyadenylation

It is now clear that cordycepin is a chain terminator of polyadenylation. Once inside the cell, cordycepin is phosphorylated to cordycepin triphosphate (CoTP), which inhibits cleavage and polyadenylation in both nuclear extracts and tissue culture[644, 645]. When CoTP is incorporated into the poly(A) tail, it traps a protein complex on the incomplete mRNA transcript, including CPSF4 and WDR33, restricting dissociation from the 3'UTR, leading to chain termination and reduction in selective mRNA poly(A) tail length[5, 369, 646]. Through genetic screens in yeast by Holbein *et al.* (2009)[362], it was shown that cordycepin does indeed act through inhibiting polyadenylation, as mutation of the yeast Poly(A) Polymerase (PAP) reverses the

effects of cordycepin. This research also illustrated that many genes involved in polyadenylation can affect the sensitivity of yeast to cordycepin[362].

It is known that genes can contain multiple PAS sites across the transcript, with alternative selection of PAS sites, known as alternative polyadenylation (APA), causing transcript isoforms of various 3'UTRs and functions[404, 460]. In *S. cerevisiae*, cordycepin treatment was found to increase abundance of longer APA isoforms in favour of more distal PAS site selection in ACT1 and ASC1 mRNA. This led to longer, unstable heterogeneous 3'end mRNA transcripts susceptible to miRNA-mediated degradation[362]. Yeast strains with mutant alleles for cleavage and polyadenylation factors also demonstrated that inactivation of 3'end processing machinery promotes distal cleavage site selection. This led to higher expression of longer 3'UTR isoforms, and suggested deficiency of RNAP II CTD and 3'end processing machinery interaction for transcription[647]. Cordycepin treatment was also compared to 3'end factor mutants and was found to significantly correlate in the switch of cleavage site selection for select genes, highlighting again that cordycepin affects polyadenylation machinery. However, cordycepin-induced APA was suggested to not act through direct interaction and RNA chain termination (via CoTP), but instead by altering the RNAP II elongation rate of transcription and affecting nucleotide metabolism[647]. This altogether demonstrates that cordycepin acts through 3'end processing machinery and alter transcription rate, inducing APA of select mRNAs.

Current limitations of cordycepin as a viable lead therapeutic compound is poor uptake into cells and short plasma half-life due to enzymatic deamination by adenosine deaminase (ADA). For this reason, an alternative method of delivering cordycepin is required[13, 14]. A recent approach encapsulating cordycepin monophosphate (CoMP) fused to a protective cap made of a phosphoramidate motif known as a ProTide (NUC-7738) was found to evade deamination by ADA. The monophosphate was also successfully converted into 3'-dADP (3'-deoxyadenosine 5'-diphosphate; CoDP) and 3'-dATP (3'-deoxyadenosine 5'-triphosphate; CoTP) by the intracellular phosphoramidase, HINT1[15]. It was also found through haploid genetic screening that mutating WDR33 led to resistance to NUC-7738, implicating polyadenylation in its mechanism of action in cancer cell apoptosis[15]. This result couples with previous findings that CoTP restricts dissociation of WDR33 from the 3'UTR[5, 369, 646]. NUC-7738 has already shown promise in Phase I clinical trials (NuTide:701), and patients are currently being recruited with advanced solid tumours and

lymphoma for a Phase I/II trial in combination with the PD-1 inhibitor, pembrolizumab (trial ID: NCT03829254). Altogether, cordycepin can act through cleavage and polyadenylation machinery such as CPSF4 and WDR33, and targeted therapeutics such as NUC-7738 show promise in using cordycepin to alleviate disease such as cancer. This PhD will try and build on previous literature described in this thesis and identify clear binding target molecules or mechanisms of action that connects cordycepin with its therapeutic effects.

1.7 Aims of the Study

Despite the fact that there are clear effects of cordycepin on inflammation, cancer progression, and PI3K/Akt/mTOR signalling[3], and that cordycepin analogues are entering the clinic[15], the mechanism of action of cordycepin is still elusive[3, 4]. This PhD study aims to contribute to the elucidation of the mechanism of action of cordycepin.

The effect of cordycepin on gene and protein expression will be compared against known modulators of PI3K/Akt/mTOR, AMPK, and MEK signalling pathways to assess consistency of effects to literature and show whether specific components of these pathways are affected by cordycepin. This will be through treating RAW264.7 macrophages and MCF-7 Human Breast Adenocarcinomas.

The effect of WDR33 knockdown on inflammatory stimulation in RAW264.7 macrophages will be assessed through analysis of RNA-Seq data and confirmed through qPCR of inflammatory gene markers compared to siRNA control (siCtrl). The RNA-Seq data will be compared to RNA-Seq data with cordycepin treatment to review whether the effect on inflammation by cordycepin is through knockdown of WDR33. Furthermore, the effect of WDR33 knockdown on PI3K/Akt and AMPK signalling will be reviewed through western blotting of phosphorylated substrates of the pathways to link cleavage and polyadenylation machinery and signalling machinery.

Multiple high-throughput datasets of cell lines which have been treated with cordycepin to assess response to inflammatory or growth-factor stimuli will be assessed in this study to exclude cell and

experiment specific effects of cordycepin. Furthermore, comparative analysis tools will be used with the output of these datasets to highlight predicted biological pathways and master regulators which have similar effects on expression to cordycepin treatment, thereby highlighting potential targets of cordycepin.

As AMPK has been proposed to be the main effector of CoMP[13], and AMPK signalling is consistently upregulated in literature with cordycepin treatment[3], the effect of cordycepin treatment will be assessed in a cell line with abrogated AMPK, thereby elucidating whether AMPK is a core target of cordycepin.

Lastly, quantitative proteomics will be used to assess the changes in abundance of RBPs with cordycepin treatment and PI3K inhibition to investigate whether the effects we see with cordycepin is through shifting RBP's from being bound in RNA-RNP complexes, as would be expected for regulation by RNA polyadenylation. A comparison will be made with PI3K inhibition. Output from these aims to identify currently unknown RBPs which change between being bound in an RNA-RNP complex and unbound with cordycepin treatment, which could highlight unknown targets linking to known downstream effects of cordycepin.

The results found in this PhD study will progress our understanding of the effect of cordycepin, and thereby polyadenylation machinery, on signal transduction, and show whether cordycepin changes RBP abundance to RNA in comparison to PI3K inhibition. Altogether, the outcomes from this study will aim to identify mechanisms of action and regulatory targets of cordycepin.

2 Materials and Methods

2.1 Cell culture and Treatments

2.1.1 Cell culture

RAW264.7 macrophages were cultured in Dulbecco's Modified Eagle Medium (DMEM; Sigma; 6429) supplemented with 10% Fetal Bovine Serum (FBS; Gibco; 11550356). Cells were passaged when confluency reached ~70-80% in culture flasks at ratios of 1:12. For passaging; RAW264.7 macrophages were suspended in culture media through scraping with sterile cell scrapers (FisherScientific; 11597692). RAW264.7 macrophages were used at passages ranging from 10-30 throughout this study. Prior to treatments, RAW264.7 macrophages were incubated for 24 hours in DMEM media supplemented with 0.5% FBS.

MCF-7 Human Breast Adenocarcinoma cells were cultured in DMEM supplemented with 10% FBS, 1% L-glutamine (Sigma; G7513), and 1% Penicillin/Streptomycin (Sigma; P4333). Cells were passaged when confluency reached ~70-80% in culture flasks at ratios of 1:3. For passaging; MCF-7 cells were washed with sterile PBS prior to suspension from the flask through 5 minutes incubation at 37°C at 5% CO_2 in 1x Trypsin-EDTA in PBS (FisherScientific; 10779413). Fresh culture media was used to collect the cells from the flask for passaging. MCF-7 cells were used at passages ranging from 4-25 throughout this study. MCF-7 cells were treated after a maximum of 24 hours, and no longer, of seeding into plates and dishes to restrict the depletion of growth factors in serum.

Wild type and CRISPR-Cas9 AMPK knockout HEK293 Human Embryonic Kidney cells were a gift from Professor Grahame Hardie's lab at the University of Dundee. HEK293 cells were cultured in DMEM supplemented with 10% FBS and 1% Penicillin/Streptomycin as used in Professor Grahame Hardie's lab[13, 648, 649]. Cells were passaged when confluency reached ~70-80% in culture flasks at ratios of 1:12. HEK293 cells were used at passages ranging from 5-15 throughout this study. Prior to treatments, HEK293 cells were incubated for 24 hours in DMEM media containing only 0.1% FBS and 1% Penicillin/Streptomycin.

For passaging, all cell lines were pelleted through centrifugation at 1,500 rpm for 5 minutes, and the old media removed from the pellets. The pellets were then re-suspended in fresh culturing media to the

desired ratio prior to addition into a fresh culture flask up to a volume of 12 ml new media. All cell cultures were maintained in 37°C and 5% CO_2 in tissue culture incubators.

For long-term cryostorage, cells were cultured in 150 mm culture dishes, pelleted through centrifugation at 1,500 rpm for 5 minutes, the supernatant was removed, and the pellets were re-suspended in ice-cold FBS containing 10% DMSO. Suspended cells (~1 ml) were aliquoted into cryovials on ice, quickly transferred to a -80°C freezer, and transferred to liquid nitrogen 24 hours later for long-term storage. Cells were revived through thawing, addition of the cell suspension to 9 ml culture media, pelleted through centrifugation at 1,500 rpm for 5 minutes, supernatant was removed, and the cell pellet was re-suspended to 12 ml culture media before addition to a fresh T75 culture flask.

2.1.2 Treatment Conditions

A variety of bioactive compounds and kinase modulators were used throughout this study, and at various concentrations dependent on the cell line. Throughout the study, RAW264.7 macrophages and HEK293 cells were seeded at specific cell densities through cell counting using a haemocytometer, after 24 hours, the original culture media highlighted in section 2.1.1 was removed, PBS-washed, and cells were cultured for 24-hours in fresh media with less FBS (0.5% for RAW264.7 macrophages and 0.1% for HEK293 cells) prior to treatment. Bacterial lipopolysaccharide (LPS; Sigma; L4774) was used to induce inflammatory response in RAW264.7 macrophages as described in figure legends. Human recombinant Epidermal Growth Factor (EGF; Gibco; PHG0314) was used to stimulate growth factor response in HEK293 cells as they express endogenous EGFR[650, 651]. MCF-7 cells were seeded at specific cell densities through cell counting using a haemocytometer 24 hours before treatment, and not starved from growth factors, to ensure that serum responses are still active prior to treatment to assess effects on serum-dependent signalling.

All treatment concentrations are highlighted in table 2.1 and in figure legends in the Results section. These concentrations were validated through validation experiments by myself (Section 9.2, Appendix) or from

previous Researchers in my lab. Specific seeding densities are highlighted below dependent on the experiment.

Table 2.1: The bioactive compounds and kinase modulator concentrations used throughout this study.

Official name	Molecule Type	Product Code	Final concentrations		
			RAW264.7	MCF-7	HEK293
Cordycepin	Bioactive compound	C3394 (Sigma)	20 µM	50 µM	25 µM
Adenosine	Nucleoside	A4036 (Sigma)	20 µM	X	X
3'deoxyinosine	Bioactive compound	13146-72-0 (Santa Cruz)	200 µM	X	X
LY294002	PI3K/mTOR/CSK2 inhibitor (ATP-competitive)[652]	HY-10108 (Insight Bio.)	100 µM	50 µM	X
Pictilisib	Pan-PI3K inhibitor (ATP-competitive)[653]	HY-50094 (Insight Bio.)	500 nM	500 nM	X
BYL-719 (Alpelisib)	PI3Kα inhibitor (ATP-competitive)[654, 655]	HY-15244 (Insight Bio.)	25 µM	5 µM	X
Torin1	mTOR inhibitor (ATP-competitive)[656]	4247 (Tocris)	500 nM	250 nM	X
MK-2206	AKT inhibitor (Allosteric)[351]	ABE4221 (Source Bio.)	10 µM	5 µM	X
A-769662	AMPK activator (Allosteric & AMP mimic)[171, 657, 658]	3336 (Tocris)	20 µM	10 µM	X
PD98059	MEK inhibitor (Allosteric)[659]	9900 (Cell Signalling)	10 µM	15 µM	X

2.1.3 siRNA Knockdown

RAW264.7 macrophages were seeded into 6-well tissue culture plates at a density of $15x10^4$ cells per well to restrict over-confluency as this procedure requires an extra 24-hour incubation compared to other procedures.

After 24 hours, all culture media was taken off the RAW264.7 macrophages and replaced by 1.7 ml fresh DMEM + 10% FBS media to each well. For transfections, two separate Gibco Opti-MEM reduced serum media (FisherScientific; Cat. Number: 15392402) mixes were made and incubated at room temperature for 10-15 seconds, one containing ON-TARGETplus siRNA for WDR33 (Dharmacon; Cat. Number: L-051645-01-0005 5) or siRNA for unspecific scrambled control (Dharmacon; Cat. Number: D-001810-10), and the other containing Lipofectamine™ RNAiMAX Transfection Reagent (FisherScientific; Cat. Number: 13778075) highlighted in table 2.2.

Table 2.2: siRNA and Lipofectamine RNAiMAX mixes.

siRNA Transfection mixes		
Reagent	**siRNA mix**	**Lipofectamine mix**
Opti-MEM	147.5 µl	142.5 µl
siRNA (4µM)	2.5 µl	X
Lipofectamine RNAiMAX	X	7.5 µl

As highlighted by table 2.2; for the mix containing siRNA, 2.5 µl of siRNA (4 µM stock) was added to 147.5 µl Opti-MEM. For the mix containing Lipofectamine RNAiMAX, 7.5 µl Lipofectamine was added to 142.5 µl Opti-MEM. These two mixes were combined, making up a 300 µl mix, and incubated at room temperature for a maximum of 10 minutes to form siRNA and Lipofectamine complexes. All 300 µl of this mix was added drop-by-drop into each well and incubated for a further 24 hours. The final concentration of siRNA used is 5 nM in 2 ml media in each well.

After 24 hours, this transfection procedure was repeated but with media containing less FBS (DMEM + 0.5% FBS) prior to treatment. The following day, the cells were treated as highlighted in the results figure legends, and then harvested for either total RNA, followed by cDNA synthesis, or protein for western blotting using the procedures highlighted in Methods section 2.3.

2.2 RNA isolation, cDNA Synthesis, and Quantitative Real-time Polymerase Chain Reaction (qPCR)

For all cell lines, $0.3x10^6$ cells were seeded into 6-well tissue culture plates in a maximum of 3 ml cell culture media. Total RNA was extracted from the cells using the ReliaPrep™ RNA Cell Miniprep System (Cat. Number: Z6012) following the protocol of the manufacturer (Promega), except with a 1-hour DNase treatment rather than 15 minutes. RNA was eluted in 15-20 µl nuclease-free water into non-stick RNase-free tubes provided in the ReliaPrep™ kit. RNA concentrations were determined using the NanoDrop 1000 (ThermoFisher), with 260/280 ratios of 2.00-2.20 considered as good quality RNA, and adequate for cDNA synthesis. Samples were not eliminated for cDNA synthesis based on the 260/230 ratio but was recorded to explain for any anomalies in the data downstream. RNA was stored short-term in -20°C, and long-term in -80°C to restrict degradation of RNA.

cDNA synthesis was performed using SuperScript III Reverse Transcriptase (Invitrogen, Cat. Number: 10368252) according to manufacturer protocol to synthesise cDNA from 500 ng/µl of RNA. For a 500 ng/µl reaction, RNA was initially incubated for 5 minutes at 65-70°C with 2 µl random primers (30 ng/µl, Fisher Scientific Limited, Cat. Number: 10646313), 1 µl dNTP's (10 mM, Fisher Scientific Limited, Cat. Number: 11863933), and nuclease-free water to make a final volume of 14.5 µl. Samples were then incubated on ice for 5 minutes, followed by addition of 4 µl of 5x First Strand Buffer, 1 µl DTT (100 mM), and 0.5 µl SuperScript III to make up a volume of 20 µl. For the reaction, samples were incubated at 50°C for 1 hour, followed by incubation at 70°C for 15 minutes to stop the reaction. cDNA samples were diluted 1:10 with nuclease-free water for qPCR.

Relative mRNA levels were measured through qPCR with a Qiagen Rotor-Gene Q qPCR cycler using the GoTaq qPCR system (Promega, Cat. Number: A6002). A GoTaq qPCR master mix was made containing 5 µl GoTaq qPCR Mastermix (2x), 2 µl nuclease-free water, and 0.5 µl gene-specific primer pairs (Forward and Reverse primers (20 µM)). Primer sequences are detailed in table 2.3. A 10 µl mix was made containing 2 µl 1:10 diluted cDNA and 8 µl GoTaq qPCR master mix in triplicate per target mRNA.

The thermal profile setup of qPCR in a Qiagen Rotor-Gene Q cycler started with an initialisation step at 95°C for 5 minutes, followed by 40 cycles incorporating a 10 second denaturation step at 95°C, 20 second Annealing step at 60°C, and 20 second Elongation step at 72°C. Relative mRNA levels were recorded in

triplicate and normalised to GAPDH reference gene, gaining a calculated relative mean value per gene. All qPCR data were analysed using the Fold Change (2^-ΔΔCT) method[660].

2.2.1 qPCR primer design for mature RNA (mRNA)

For primers designed for mRNA, NCBI Primer-Blast was used to choose primers based on the mRNA sequence obtained from NCBI. To detect spliced mRNA, at least one of the primer pairs must span an exon-exon junction. Chosen primers were then counter-checked in NCBI Primer-Blast for target mRNA specificity. Product size produced by the primer pairs were between 150 to 250 nucleotides and aimed for no more than a 2°C difference in melting temperatures (Tm). The Guanine-Cytosine (GC) content was between 40-60%. Self-complementarity and self-3'-complementarity of the primers was as low as possible to restrict primer hairpins from forming. All primer sequences used in this study is highlighted in table 2.3.

Table 2.3: qPCR primer sequences.

Mouse (*Mus musculus*) Primers			
Target RNA (mature)	**Strand Orientation**	**Primer Sequence (5'-3')**	**Tm (°C)**
Acod1 (Irg1)	Forward	ACTCCTGAGCCAGTTACCCT	61.70
	Reverse	CTGTGACAGACTTGAGCATCAT	62.00
Ccl4	Forward	CATGAAGCTCTGCGTGTCTG	59.28
	Reverse	TCTTTTGGTCAGGAATACCACAG	58.35
Clec4e	Forward	ATGTGTCGTAACATATCGCAGC	59.21
	Reverse	TGCTCTTCCTGTGTGTCGAT	59.03
Cxcl2	Forward	CCAGACAGAAGTCATAGCCAC	61.30
	Reverse	TCAGGTACGATCCAGGCTTC	62.00
Dusp4	Forward	AAACCACTCTATCCCCAGCC	64.10
	Reverse	TTGGTCACTTTTGCAGCTGG	64.30
Errfi1	Forward	CTAACAACTGTTGGATGTGCTG	57.85
	Reverse	GAAGTGCAGACCCCATTCAC	58.83
Gapdh	Forward	AAGAAGGTGGTGAAGCAGGC	65.60
	Reverse	ATCGAAGGTGGAAGAGTGGG	65.30
Il1ϐ	Forward	AGATGAAGGGCTGCTTCCAAA	67.00
	Reverse	GGAAGGTCCACGGGAAAGAC	66.90
Ptgs2	Forward	CAGCCAGGCAGCAAATCCTT	68.60
	Reverse	AGTCCGGGTACAGTCACACT	68.10

Rpl28	Forward	TACAGCACGGAGCCAAATAA	63.10
	Reverse	ACGGTCTTGCGGTGAATTAG	63.90
Tnf	Forward	CTATGGCCCAGACCCTCACA	67.30
	Reverse	CCACTTGGTGGTTTGCTACGA	67.00
Wdr33	Forward	ATCAGAGAGATATGCGGGCAA	59.03
	Reverse	GGTCCACCTCACAACAAATACTG	59.50

Human (*Homo sapiens*) Primers

Target RNA (mature)	Strand Orientation	Primer Sequence (5'-3')	Tm (°C)
ACTB	Forward	AACCGCGAGAAGATG	55.20
	Reverse	CCAGAGGCGTACAGGGATAG	57.10
ATF3	Forward	CACAAAAGCCGAGGTAGC	62.00
	Reverse	AGCCTTCAGTTCAGCATTCAC	63.30
BCAR3	Forward	GGCACCAGTACACCCAAACT	63.80
	Reverse	CACATGTCGGTTCCTTCAAA	63.60
DUSP1	Forward	GAGCTGTGCAGCAAACAGT	61.90
	Reverse	CAGGTACAGAAAGGGCAGGA	63.10
c-JUN	Forward	CGTGAAGTGACGGACTGTTC	63.50
	Reverse	GTGAGGAGGTCCGAGTTCTT	62.30
c-FOS	Forward	CTGTCAACGCGCAGGACTT	60.96
	Reverse	GTCATGGTCTTCACAACGCC	59.48
FOSL1	Forward	CAGGCGGAGACTGACAAAC	63.60
	Reverse	CCTGGGGAAAGGGAGATACA	65.00
GAPDH	Forward	CATCGCTCAGACACCATGGG	69.10
	Reverse	CGTTCTCAGCCTTGACGGTG	68.20
JUNB	Forward	AAGGGACACGCCTTCTGAA	64.80
	Reverse	AAACGTCGAGGTGGAAGGA	64.70
MYC	Forward	TCCTCGGATTCTCTGCTCTC	63.60
	Reverse	CTCTGACCTTTTGCCAGGAG	63.90
PLK2	Forward	AAAGGTGTTGACAGAGCCAGA	63.80
	Reverse	AGACCGAAGTCCCCAACTTT	63.70
RPL10A	Forward	TCTCTCGCGACACCCTGT	65.00
	Reverse	TTAGCCTCGTCACAGTGCTG	64.30
SGK1	Forward	ATGAAGCAGAGGAGGATGGG	65.40
	Reverse	GGCCAAGGTTGATTTGCTGA	67.20

2.3 Protein extraction and western blotting

2.3.1 Extracting whole-cell protein

For all cell lines, $3x10^6$ cells were seeded into 15 cm dishes made up to 20 ml culture medium. Cells were treated as described by the results figure legends. MCF-7 cells were treated 24 hours after seeding,

whereas RAW264.7 macrophages and HEK293 cells were treated 48 hours after seeding. This was so they were starved from growth factors (FBS) for 24-hours prior to treatment a day after seeding. For western blotting of whole cell protein, the cells were washed with sterile ice-cold PBS after treatment to remove media, scraped using sterile cell scrapers, and pelleted in 1 ml sterile ice-cold PBS through centrifugation at 10,000xg for 1 minute in sterile 1.5 ml centrifuge tubes. Supernatant was discarded, and the pellet was lysed on ice with 125 µl RIPA lysis buffer (recipe detailed below). Protein supernatant was collected through 20,000xg centrifugation for 10 minutes at 4°C and stored at -20°C short-term and -80°C long-term.

RIPA lysis buffer recipe: 50 mM Tris-HCL (pH 7.5), 1% NP-40, 0.5% Sodium deoxycholate, 0.1% Sodium dodecyl sulfate (SDS), 1 mM EDTA, 150 mM NaCl, 1mM PMSF, 1mM Sodium orthovanadate, and 1 mM β-Glycerophosphate diluted in deionised MilliQ water. 1 tablet of cOmplete, Mini, EDTA-free Protease Inhibitor Cocktail tablet (Roche; 11836170001) was added per 10 ml RIPA lysis buffer prior to use.

2.3.2 Bradford Assay

Protein was quantified against BSA standards using Pierce Coomassie (Bradford) protein assay kit (ThermoFisher Scientific, Cat. 23200). BSA standards were made at 10, 5, 2.5, 2.0, 1.5, 1.0, 0.75, and 0.0 mg/ml. These BSA standards was diluted using the same RIPA lysis buffer as the protein samples for quantification. All BSA standards and protein samples were diluted further by 1:10 with nuclease-free water. Nuclease-free water was the 0.0 mg/ml negative control standard. 5 µl of each protein sample and BSA standard was added in triplicate into individual wells of a 96-well plate. To each well, 200 µl of Pierce Coomassie stain was added and mixed through repetitive pipetting.

Protein was quantified at an absorbance of 595 nm in a plate reader. The quantification reading obtained with the 0.0 mg/ml nuclease-free water sample was subtracted to all protein samples and BSA standards. A graph was created from the BSA standard readings with the y-axis indicating BSA standard

concentration (mg/ml) over Bradford quantification output. A line of best fit was created for the BSA standards, and the protein from the samples were quantified through the line of best fit equation: $\boldsymbol{y = mx + c}$ (where $\boldsymbol{m}$ is the gradient, $\boldsymbol{c}$ is the y-intercept, and $\boldsymbol{x}$ is the absorbance obtained in Bradford assay for each protein sample).

2.3.3 Western blotting

2.3.3.1 Gel casting and electrophoresis

After quantification, 50 µg of protein was diluted with 3x SDS-PAGE loading buffer (recipe detailed below), heated to 90-95°C for a maximum of 5 minutes to break down protein complexes, and loaded into individual Stacking gel 1.5 mm thick wells solidified above SDS-PAGE acrylamide gel (recipes detailed below). Protein molecular weight markers (NEB; P7719S, or ThermoFisher Scientific; 26625) was also loaded into an individual well. The percentage of the SDS-PAGE acrylamide gel ranged between 6-20% based on the protein weight (kDa) of interest(s). SDS-PAGE acrylamide gels were casted in 1.5 mm thick mini-gels, levelled by addition of ~1 mL deionised MilliQ water, and poured off once set prior to addition of the Stacking gel. Protein migrated through gel electrophoresis at 20 mA constant current per SDS-PAGE acrylamide gel in a BIO-RAD Mini-PROTEAN System in 1% Running buffer (recipe detailed below).

Semi-dry transfer of the SDS-PAGE acrylamide gel to a Polyvinylidene fluoride (PVDF) membrane followed completion of gel electrophoresis. Three square sheets of Whatman gel blotting paper were soaked in western blot transfer buffer (recipe detailed below) and placed underneath the PVDF membrane, which was soaked in methanol and western blot transfer buffer. The SDS-PAGE acrylamide gel was stacked between the PVDF membrane and three more-square sheets of Whatman gel blotting paper soaked in western blot transfer buffer. Blotting occurred at 0.8 mA constant current per square cm of blotting stack for a maximum of 2 hours.

3x SDS-PAGE loading buffer recipe: 1M Tris/HCL (pH 6.8), 9% SDS (w/v), 30% Glycerol (v/v), 15% Beta-mercaptoethanol (w/v), and 0.01% Bromophenol Blue (w/v) diluted in deionised MilliQ water.

SDS-PAGE acrylamide gel recipe (10.5 ml): **** mL 30% Acrylamide/Bis-acrylamide 37.5:1 solution (Merck; A3699), 3.45 ml 1.5M Tris/HCL (pH 8.8), 105 µl 10% SDS, 105 µl 10% ammonium persulfate, and 13.5 µl TEMED (N,N,N',N'-tetramethylethane-1,2-diamine; ThermoFisher Scientific; 17919), diluted up to 10.5 ml total volume of deionised MilliQ water.

****quantity of 30% Acrylamide/Bis-acrylamide 37.5:1 solution differs based on percentage of the gel.

Stacking gel (3 ml) recipe: 495 µl 30% Acrylamide/Bis-acrylamide 37.5:1 solution, 375 µl 1M Tris/HCL (pH 6.8), 37.5 µl 10% SDS, 37.5 µl 10% ammonium persulfate, 6 µl TEMED, diluted up to 3 ml total volume of deionised MilliQ water.

10x Running buffer (1 Litre stock) recipe: 144g Glycine, 30g Tris base, and 1% SDS diluted up to 1 Litre total volume of deionised MilliQ water. 50 ml of 10% Running buffer was further diluted in 450 ml deionised MilliQ water to make up 1% Running buffer.

Western blot transfer buffer recipe (250 ml): 1.45g Tris base, 0.725g Glycine, 9.25 ml 10% SDS, 50 ml Methanol, and 200 ml deionised MilliQ water.

2.3.3.2 Incubation of Primary and Secondary antibodies

After the semi-dry transfer, the PVDF membranes were washed three times for 5 minutes in TBST (recipe detailed below). Membranes were blocked in 5% skimmed milk in TBST for 1 hour at room temperature. Membranes were washed another three times for 5 minutes in TBST and incubated with primary antibodies in either 3% BSA in TBST for phosphorylated-proteins or 5% milk in TBST for total proteins overnight at 4°C based on dilutions highlighted in table 2.4. The membranes were washed a further three times for 5 minutes in TBST and incubated at room temperature for 1-hour in secondary antibody (HRP-coupled) diluted in 5% milk in TBST (table 2.4). For every whole membrane, a protein loading control (GAPDH or Vinculin) was used to highlight any discrepancies in protein loading quantity.

TBST solution (1 Litre): 10 ml 1M Tris/HCL (pH 8.0), 30 ml 5M NaCl, and 0.5 ml Tween 20 made up to 1 Litre with deionised MilliQ water.

Table 2.4: Primary and Secondary antibodies used for western blotting and immunofluorescence.

Antibody	Type	Product Code	Manufacturer	Dilution
Phospho-4E-BP1 (Thr37/46)	Primary	4060S (D9E)	Cell Signalling	1:1000
Total 4E-BP1	Primary	9452S	Cell Signalling	1:1000
Phospho-p70 S6 Kinase (Thr389)	Primary	9234S (108D2)	Cell Signalling	1:1000
Total p70 S6 Kinase	Primary	2708S (49D7)	Cell Signalling	1:1000
Anti-pan-AKT (Total AKT)	Primary	ab8805	Abcam	1:500
Phospho-AKT (Ser473)	Primary	4058S (193H12)	Cell Signalling	1:1000
Phospho-AKT (Ser473)	Primary	4060S (D9E)	Cell Signalling	1:1000
Phospho-AKT (Ser473)	Primary	587F11	Cell Signalling	1:1000
Phospho-AKT (Ser473)	Primary	9271S	Cell Signalling	1:1000
Phospho-AKT (Thr308)	Primary	4056S (244F9)	Cell Signalling	1:1000
Total AKT	Primary	9272S	Cell Signalling	1:1000
Phospho-AKT (Ser473)	Primary	AF3263	NKT Scientific	1:1000
Phospho-AKT (Thr308)	Primary	AF3262	NKT Scientific	1:1000
Phospho-AKT 1/2/3 (Ser473)	Primary	BS-0876R	ThermoFisher	1:300
Phospho-AMPKα (Thr172)	Primary	2535S (40H9)	Cell Signalling	1:750
Total AMPKα	Primary	5831S (D5A2)	Cell Signalling	1:1000
CELF1	Primary	ab31262-100 (3B1)	Abcam	1:500
DRAQ5*	Nuclei	ab108410	Abcam	1:5000*
GAPDH	Primary	60004-1-lg	ProteinTech	1:50000
Phospho-GSK3β (Ser9)	Primary	9336S	Cell Signalling	1:1000
Total GSK3β	Primary	9315S (27C10)	Cell Signalling	1:1000
NF-κB p65*	Primary	4764S (C22B4)	Cell Signalling	1:200*
Vinculin	Primary	sc-5573 (H-300)	Santa Cruz	1:1000
WDR33	Primary	sc-374466 (D-1)	Santa Cruz	1:1000
Anti-Mouse IgG (HRP)	Secondary	P0447	Dako	1:5000
Anti-Rabbit IgG (HRP)	Secondary	P0217	Dako	1:5000
AlexaFluor 488*	Secondary	A11034	Invitrogen	1:400*
AlexaFluor 546*	Secondary	A11003	Invitrogen	1:400*

***Antibodies and dilutions used for immunofluorescence.**

2.3.3.3 Protein band image analysis

After incubation of secondary antibody, the membranes were washed a further three times in TBST at room temperature. Peroxidase activity was detected through chemiluminescence with ECL buffer solutions (GE Healthcare; RPN2236). Just before use, ECL solutions A and B were mixed at equal volume

before adding onto the western blot membrane. Blots were imaged using the ImageQuant LAS 4000 biomolecular imager using chemiluminescence. Exposure times varied according to protein signal and quality of the antibodies. The high-resolution setting was used where possible for exposure times ranging from seconds to ~10 minutes. Separate images were obtained per blot for the protein molecular weight markers.

Images from the ImageQuant LAS 4000 biomolecular imager were saved as .tif files and opened within the BIO-RAD Image Lab software (version 6.0.1). Blot images of proteins of interest were merged and overlayed with the same blots protein molecular weight markers to highlight protein signal molecular weight.

2.3.3.4 Stripping and re-use of membranes

Where necessary, membranes were stripped from a previous primary antibody, such as a less abundant phosphorylated-protein, and re-probed with a new primary antibody for total protein. The membranes were stripped in Stripping buffer (recipe detailed below) in sealed 50 mL falcon tubes, with the protein side facing inwards to ensure equal stripping across the membrane. The membranes in Stripping buffer were incubated in a benchtop incubator shaker for 30 minutes at 50°C to ensure regular rotation of the falcon tubes and membranes. Stripping buffer was discarded and washed for 5 minutes at least six times in TBST until the β-mercaptoethanol was no longer detectable. Before use, the membranes were re-blocked in 5% milk in TBST and incubated with new primary antibody as described previously (section 2.3.3.2).

Stripping buffer recipe: 62.5 mM Tris/HCL (pH 6.8), 2% SDS, 0.8% β-mercaptoethanol.

2.4 Immunofluorescence (IFF)

2.4.1 Seeding into Ibidi Chambers and treatments

RAW264.7 macrophages were seeded at a density of $1x10^4$/chamber into 8-well Ibidi Chambers (Ibidi, Cat. Number: 80826). After 24 hours, the media was replaced with media containing less FBS (0.5%) and incubated for another 24 hours. The cells were treated with various conditions, initially by 10 minutes of LPS (1 µg/ml) stimulation, then treated for a further 50 minutes with either DMSO (vehicle control) or cordycepin (20 µM). DMSO only control chambers were incubated with the same volume as cordycepin for the full 1 hour without LPS.

After treatment, the cells were washed three times with ice-cold sterile PBS and fixed with 4% paraformaldehyde (PFA) in PBS for 12 minutes. The chambers were washed three times with ice-cold sterile PBS and permeabilised using 0.1% Saponin in PBS for 10 minutes. The chambers were blocked with 3% bovine serum albumin (BSA) with 0.1% Saponin in PBS for 1 hour at room temperature before probing with primary antibodies (table 2.4) overnight in 4°C. Chambers were then washed three times with ice-cold sterile PBS and incubated with Alexa Fluorophore-conjugated secondary antibodies (table 2.4) for 1 hour at room temperature covered in aluminium foil. Both the primary and secondary antibodies were diluted in 3% BSA with 0.1% Saponin in PBS according to manufacturer protocol. For contrast, the cells were washed three times with ice-cold sterile PBS and the cell nuclei were stained with DRAQ5 (table 2.4) in PBS and 0.1% Saponin for 5 minutes at room temperature in aluminium foil. Cells were washed three times with ice-cold sterile PBS and stored with ~100 µL of PBS in aluminium foil at 4°C in a fridge until imaging.

For every secondary antibody used, one well was dedicated to incubation with only the secondary antibody to show that the fluorescence of the primary antibodies is through specific binding and not background noise of the secondary antibody. Saponin was used for permeabilization as it is not as harsh as the Triton X-100 detergent, however it is not a permanent permeabilizer, so it is added in each step to keep pores from closing.

2.4.2 Confocal microscopy

The chambers were imaged using the Zeiss LSM510 confocal microscope with 488 nm argon, 543 nm Helium-Neon and 633 nm Helium-Neon lasers under conditions of minimal ambient lighting under the guidance of Dr. Hilary Collins. A drop of immersion oil was used to coat the 40x objective lens, and the slides were placed on the platform above. To find cells and focus the microscope, one fluorescence colour (emitted colour) was chosen, and the cells were visualised through the microscope eyepiece using the microscope light rather than the lasers. Images in each channel were adjusted based on gain and offset to ensure the images were neither over- or underexposed and to reduce any background signal outside of the cell. The wells with secondary antibody staining only were used to check for background staining, and if necessary, was used to adjust settings and subtract background before imaging primary antibody wells. Images were taken where possible in two fields of view per well to gain accurate images for the localisation of the proteins corresponding to the primary antibodies (table 2.4).

2.4.3 Image analysis (Nuclear/Cytoplasmic quantification)

All confocal images were analysed based on the intensity of nuclear:cytoplasmic staining of primary antibody using Image J (Fiji). Within ImageJ, the merged fluorescent channels of the confocal images were split to reveal the DRAQ5 nuclei staining and primary antibody staining separately by going through 'Image', 'Colour', then 'Split Channels'. ImageJ detects objects through particle analysis by making binary (black and white) images, making the background black and the nuclei staining white. This is achieved by going through 'Process', 'Binary', 'Make Binary' within ImageJ (figure 2.1A). The white nuclei staining area of the DRAQ5 split channel was subtracted from the primary antibody split channel. This step creates a split channel of the primary antibody with nuclear fluorescence removed, leaving only cytoplasmic primary antibody staining around the nuclei (figure 2.1B). The cytoplasmic fluorescence intensity of the primary antibody is then quantified for at least three cells in the same channel by going through 'Analyse', and then 'Measure' in ImageJ, to obtain a mean quantification for cytoplasmic primary antibody intensity. This cytoplasmic value was used to subtract from the whole cell to obtain a value for nuclear primary

antibody fluorescence intensity. The mean quantification of the primary antibody nuclear and cytoplasmic staining was then used to calculate a ratio of nuclear/cytoplasm. Graphs of nuclear:cytoplasmic intensity was created within GraphPad PRISM.

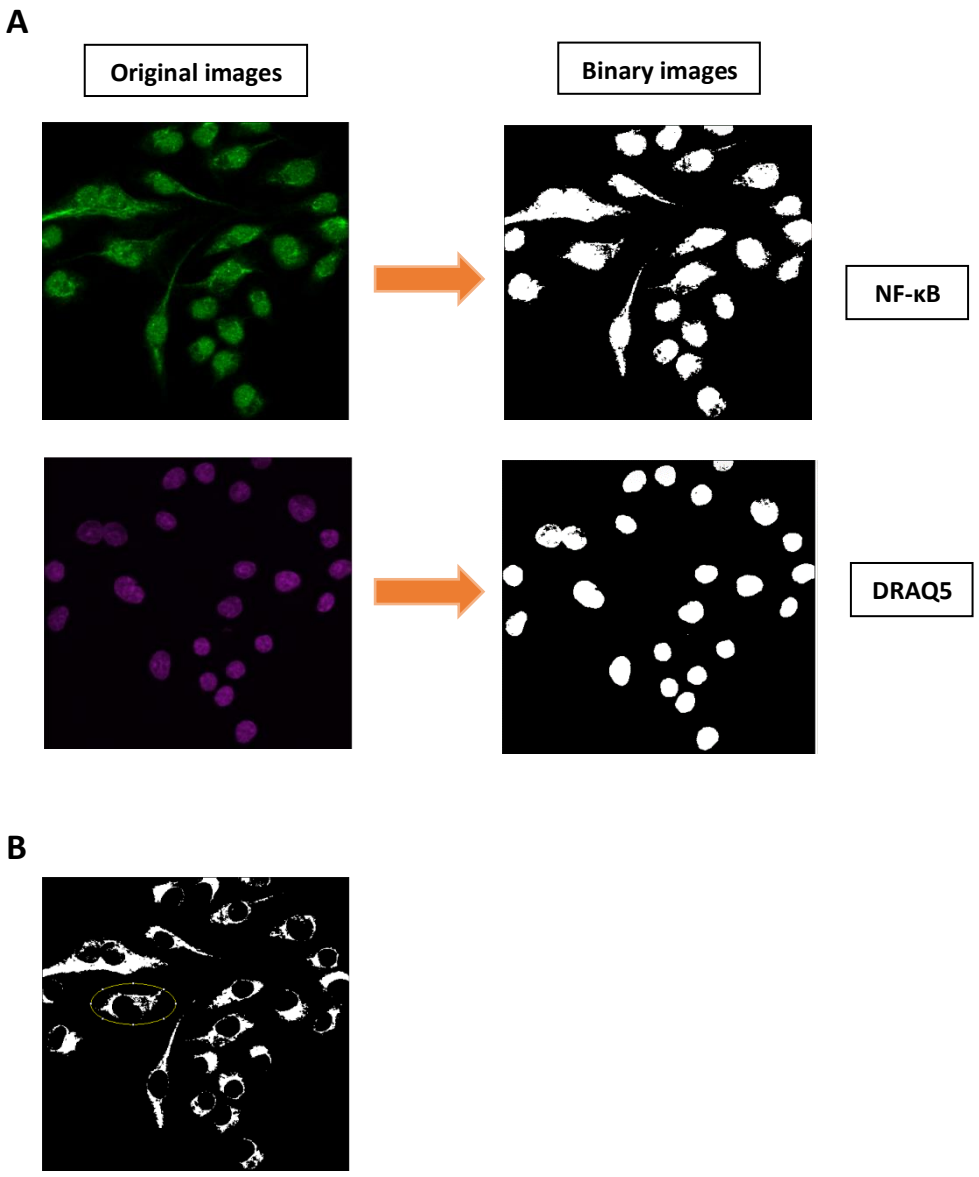

Figure 2.1: ImageJ (Fiji) confocal microscopy images of nuclear:cytoplasmic quantification. **A)** Original and binary images of NF-κB staining of RAW264.7 macrophages as 546 nm, and DRAQ5 nuclei staining at 633 nm. **B)** Subtraction of the DRAQ5 nuclei stain from the original NF-κB binary image, leaving only cytoplasmic NF-κB staining for quantification prior to NF-κB nuclear quantification to calculate the nuclear:cytoplasmic ratio.

2.5 Orthogonal Organic Phase Separation (OOPS)

2.5.1 Original protocol

The original OOPS procedure published in *Nature Biotechnology* by Queiroz, R.M.L., *et al*. (2019)[661] is a technique to isolate RNA-binding proteins (RBP's) in the aqueous-organic interface (Interphase) through acidified guanidinium thiocyanate-phenol-chloroform (AGPC) phase partitioning. Initially the method involves crosslinking through UV-irradiation at 254 nm to generate RNA-protein adducts directly to PBS-washed cell culture in tissue culture dishes before cell lysis in Acidic Guanidinium Thiocyanate-Phenol (TriZol). Homogenised lysate is then transferred to a centrifuge tube and incubated at room temperature for 5 minutes to dissociate un-stabilised RNA-protein interactions, followed by biphasic extraction by addition of 200 µl chloroform. Phases were separated through an initial vortex and centrifugation at 12,000 xg at 4°C for 15 minutes. The upper aqueous phase containing non-crosslinked RNA is transferred to a separate tube and followed by RNA precipitation, and the lower organic phase containing non-crosslinked protein is separated from the Interphase and precipitated through addition of 9 volumes of methanol. The Interphase containing RNA-protein adducts is subjected to three more repeated AGPC separations to enrich the Interphase and remove non-crosslinked proteins, precipitated through addition of 9 volumes of methanol, and centrifuged at 14,000 xg at room temperature for 10 minutes.

2.5.2 Adaptation of original protocol

The original OOPS procedure[661] has been adapted to incorporate formaldehyde crosslinking as opposed to UV crosslinking (detailed in figure 2.2). Formaldehyde crosslinking was used as it sustains stronger protein-RBP associations and is reversible in comparison to UV crosslinking, and the priority was to retrieve and identify proteins associated with RNA either directly or indirectly. This adaptation to the OOPS method is also based on the Ribonucleoprotein (RNP) immunoprecipitation method used in Christine Mayr's lab[471], and previously described in chromatin immunoprecipitations[662, 663].

RAW264.7 macrophages were seeded at $3x10^6$ in 150 mm tissue culture plates per treatment condition, with the inclusion of a formaldehyde crosslinking control sample which does not undergo formaldehyde crosslinking. Culture media was aspirated after 24 hours and replaced with media containing less FBS

(0.5%) for further 24 hours. The cells were then treated as detailed in the Results section figure legends. After treatment, original media was removed, and the cells were washed twice with ice-cold PBS. Except for the formaldehyde crosslinking control sample; methanol-free formaldehyde (Thermo Scientific; 28906) was added to the cells at a final concentration of 0.5% in PBS on ice for 2 minutes based on treatment validations which will be highlighted in Chapter 8. The crosslinking was quenched through addition of Glycine (pH 7) to a final concentration of 0.25M and incubation at room temperature for 5 minutes (figure 2.2). Cells were harvested and pelleted through centrifugation at 3,000 rpm for 4 minutes at 4°C.

Immediately after centrifugation, the pellets were broken down in 1 ml TRIzol lysis reagent (FisherScientific; Cat. 12044977) and incubated for 5 minutes at room temperature followed by addition of 200 µl chloroform (FisherScientific; 15204228), vortexing for 5-10 seconds, and incubated for 5 minutes at room temperature. Phases were separated through centrifugation at 12,000xg for 15 minutes at 4°C. Using gel loading tips, the upper aqueous phase, and lower organic phase were carefully transferred to separate 1.5 centrifuge tubes, leaving the Interphase section (containing RBP's) in the original tubes. The original OOPS procedure[661] incorporates additional AGPC phase separations, however this adaptation only involves the one AGPC separation based on treatment validations detailed in Chapter 8. The Interphase and Organic phases were precipitated with 9 volumes of methanol as also included in the original OOPS procedure[661], and then solubilised with 100 µl 3x SDS-PAGE Loading Buffer and stored at -20°C ready for western blotting (figure 2.2).

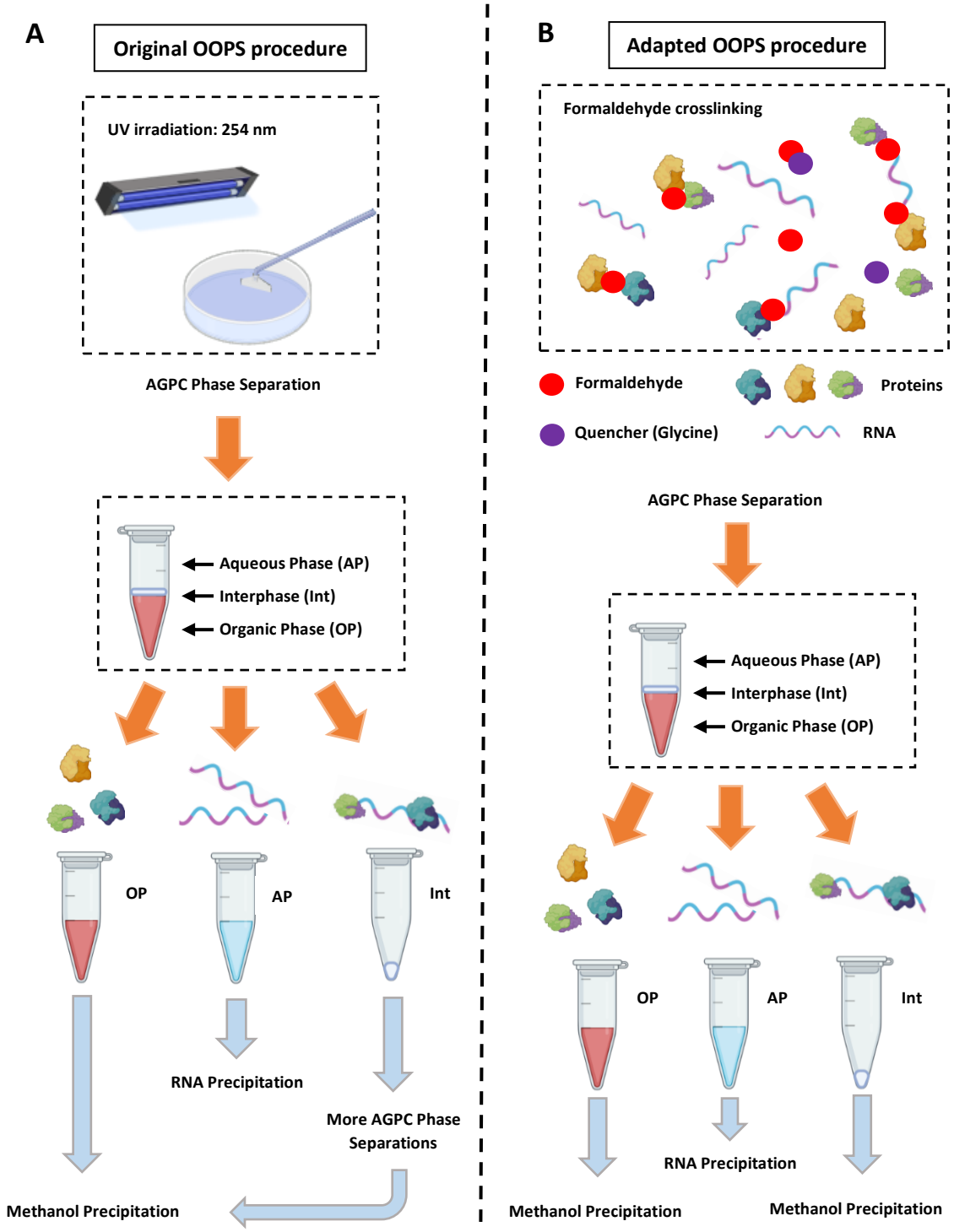

Figure 2.2: Schematic of the original and adapted OOPS methods. The original method[661] (left) involves UV crosslinking of RNA-proteins adducts, and multiple sequential AGPC separations of the Interphase containing RNA-protein complexes. The adapted method (right) involves formaldehyde crosslinking, and only one AGPC phase separation of the Interphase based on treatment validations. Diagram abbreviations; Aqueous Phase (AP), Interphase (Int), Organic Phase (OP).

2.6 Microarray, RNA-Seq, and Bioinformatics

2.6.1 Microarray platforms

In this thesis, two microarray datasets are analysed directly from the original fluorescent signal data in .txt file format. One dataset regards an MCF-7 microarray dataset, performed in quadruplicate by Dr. Asma Khurshid in collaboration with Professor Anne Willis (MRC Toxicology Unit, University of Cambridge), using the Agilent microarray platform; Human GE 8x60K (v2). This dataset was initially analysed by Asma in her Thesis[664] but has been re-analysed in this Thesis. The other microarray dataset was for murine RAW264.7 macrophages, which was performed Dr. Sadaf Ashraf using the Agilent-028005 SurePrint G3 Mouse GE 8x60K Microarray platform (GPL13912) and initially analysed and described in Ashraf, *et al.* (2019)[384]. This dataset has been deposited in NCBI's Gene Expression Omnibus repository (GSE126157) by Dr. Graeme Thorn (Queen Mary, University of London).

2.6.1.1 Differential gene expression of Microarray data: LIMMA pipeline

The Linear Models for Microarray (LIMMA) method[665] is a popular pipeline used predominantly for the analysing microarray data[666, 667], high-throughput PCR's[668], protein arrays[669], and can be incorporated into pipelines analysing RNA sequencing (RNA-Seq) data[670]. The LIMMA method allows for analysing comparison between many RNA targets simultaneously and can stably analyse small numbers of arrays through borrowing information across genes in both single-channel and dual-channel microarrays[665].

The pipeline below details the methods used within R[671] for analysing microarray data throughout the study using the LIMMA method[665]. LIMMA identifies the raw fluorescent microarray data as a raw expression list and creates a matrix of this data within R (EListRaw matrix). The raw microarray fluorescent data (in .txt file format) is uploaded into R and read based on the platform used (i.e. Agilent), and whether the array was single-channel or dual-channel. LIMMA allows the inclusion of extra information from the raw .txt microarray files, including whether the fluorescence of each probe is above background fluorescence. The following command allows for this:

```
>Microarray_data <- read.maimages(Microarray_file_location, source = "agilent", green.only = TRUE,
other.columns = "gIsWellAboveBG")
```

Based on how the files are uploaded within R, the files must be identified based on experimental treatment condition. An example command is below for treatment (cordycepin; C60) or control (DMSO; D60):

```
>Microarray_data$targets$treatments <- c("C60", "D60", "D60", "C60", "C60", "D60", "D60", "C60")
```

For single-channel arrays, the LIMMA method suggests normalising expression values between the arrays to achieve consistency between the arrays as normalisation within the arrays is not relevant to single-channel arrays[665]. The microarray data was corrected for background noise by using negative control probes in the array. This method compared to other correction methods was found to produce the lowest false-discovery rate by Silver, Ritchie, and Smyth (2009)[672] and is commonly used in the LIMMA method[665]. The quartile method of normalisation was used to force the empirical distribution of each column (microarray probe) to be identical[673], and allowed for more direct comparison to RNA-Seq quartile normalised data, which is described later on. After normalisation, the control probes were filtered out of the dataset and all probes which fall below background fluorescence in all arrays. The following commands performs these steps:

```
>Microarray_data <- backgroundCorrect(Microarray_data, method = "normexp")
>Microarray_data <- normalizeBetweenArrays(Microarray_data, method = "quantile")
>Negative_Control <- Microarray_data$genes$ControlType==-1L
>Positive_Control <- Microarray_data$genes$ControlType==1L
>IsExpr <- rowSums(Microarray_data$other$gIsWellAboveBG > 0) >= 4
>Micrarray_data <- Microarray_data[!Negative_Control & !Positive_Control & IsExpr, ]
```

After normalisation, design matrices were created and used in the estimation process of model parameters, such as numerical normalised fluorescence, through the 'model.matrix' function of LIMMA[665]. The modelled design matrices of normalised fluorescence values are grouped based on experimental condition (i.e treatment and control), following the commands below:

```
>Microarray_Design <- model.matrix(~0+Microarray_data$targets$treatments)
>Colnames(Microarray_Design) <- Microarray_data$targets$Treatment
>Microarray_Groups <- c(rep("C60", 4), rep("D60", 4))
>Microarray_Groups <- factor(Microarray_Groups)
```

The 'makeContrasts' function in LIMMA[665] was then used to make contracts between the grouped design matrices of treatment and control. A linear model based on the design matrices was then fitted using the Log expression values for each probe after the normalisation step using the 'lmfit' function. The linear models were compared between treatment and control with 'contrasts.fit'. The empirical bayes statistics for differential expression (eBayes)[674] was used to compute moderated t-statistics, F-statistics, and log-odds of differential expression based on the contrast of the linear models. By default, eBayes assumes that the proportion of genes which are differentially expressed is 0.01 (1%)[674]. The p-value statistics from eBayes are adjusted for multiple testing, which by default is through the Benjamini & Hochberg ("BH") method[675] which controls the expected false discovery rate (FDR). The following commands performs these steps:

```
>C60_vs_D60 <- makeContrasts(C60-D60, levels = Microarray_Design)
>Treatment_vs_Control_fit <- lmFit(Microarray_data, Microarray_Design)
>Treatment_vs_Control_fit <- contrasts.fit(Treatment_vs_Control_fit, C60_vs_D60)
>Treatment_vs_Control_fit <- eBayes(Treatment_vs_Control_fit, 0.01)
>tT_Treatment_vs_Control <- topTable(Treatment_vs_Control_fit, adjust.method = "BH", n=Inf)
```

2.6.2 RNA-Sequencing (RNA-Seq)

2.6.2.1 RNA extraction and preparation for RNA-Seq

Total RNA extracted using the ReliaPrep™ RNA Cell Miniprep System was sent to GENEWIZ (Azenta) for next-generation sequencing (standard RNA-Seq). The total RNA was assessed for quantity and quality using the NanoDrop 1000 (ThermoFisher). GENEWIZ required DNA-free total RNA diluted at concentration 50 ng/µl in nuclease-free water per sample, with a A260/A280 quality between 1.8-2.2 for

standard RNA-Seq. RNA was depleted from ribosomal RNA through rRNA depletion performed by GENEWIZ as these can be highly abundant and interfere with measurements of lowly-expressed RNAs[676, 677]. RNA extracted by Dr. Masar Radhi for WDR33 knockdown, and diluted by Dr. Asta Tranholm, was sequenced using the Illumina HiSeq platform, whereas the RNA extracted for cordycepin and PI3K inhibitor was sequenced using Illumina NovaSeq platform due to advances in high-throughput machinery. Data output from the RNA-Seq was compressed into Fastq.gz files.

2.6.2.2 Qualitative analysis of RNA-Seq Fastq.gz files

Before analysing the RNA-Seq output, quality control of the data was necessary to ensure that the data quality of replicates would not hinder the downstream output. The FastQC[678] program (version 0.11.9) from Babraham Bioinformatics was used to perform quality control checks on the raw RNA-Seq sequence data in the Fastq.gz files. For every Fastq.gz file; the per base sequence quality, average quality per read, nucleotide content, GC content, number of 'N' base calls, and overrepresented sequences were reviewed. These measurements indicate the quality of sequence base calling, quality of sequence runs, whether certain nucleotide(s) and sequences are overrepresented, and whether there are sequence contamination(s) through high-throughput methods. RNA-Seq Fastq.gz files were taken forward to downstream analysis based on these quality checks. Any file with per base sequence quality consistently at ≥ 28, which is considered good by FastQC was included for the next steps.

2.6.2.3 Obtaining read counts & expression data for RNA-Seq

The general RNA-Seq pipeline for differential gene expression from Fastq.gz files are separated into four core steps: mapping to a genome, gene level expression estimation, normalisation, and comparison of the normalised expression data[679, 680].

Primary genome assembly files were obtained from Ensembl (Human genome; GRCh38.p13, Mouse genome, GRCm38.p6). Within the R environment, the buildindex function from the Rsubread[681, 682] package was used to generate a genome index from the genome sequence file obtained from Ensembl using commands below:

```
>RAW_fastq <- dir(path = "**folder path for RNA-Seq files**", pattern = ".fastq.gz", full.names = TRUE).
>Rsubread::buildindex(basename = "mm10_Index", reference = GRCm38_p6_DNA_Primary_Assembly).
```

The Rsubread[681, 682] package was also used for mapping and alignment of RNA-Seq short sequence reads from the Fastq.gz files to a reference genome index using the 'align' function. This function uses the 'seed-and-vote' algorithm when aligning to the reference genome. A 'seed', or short segment of the RNA-seq sequence reads, is aligned simultaneously in multiple parts of the genome sequence, and followed by an in-fill step to complete the alignment. It uses a relatively large number of short equi-spaced seeds from each read, which are called 'subreads'. This strategy of alignment is both sensitive, and specific because the final location must be supported by several different subreads, optimal for gene-level counting. Alignment of the paired-end RNA-Seq Fastq.gz files to the reference genome index creates binary alignment map (BAM) files, through the example commands below:

```
>ForwardFiles <- dir(path = ""**folder path for RNA-Seq files**"", pattern = "R1_001.fastq.gz",
full.names = TRUE).
>ReverseFiles <- dir(path = ""**folder path for RNA-Seq files**"", pattern = "R2_001.fastq.gz",
full.names = TRUE).
>Rsubread_Aligned_Files <- c("CoR_LPS_1.bam", "CoR_LPS_2.bam", "CoR_LPS_3.bam",
"DMSO_1.bam", "DMSO_2.bam", "DMSO_3.bam", "DMSO_LPS_1.bam", "DMSO_LPS_2.bam",
"DMSO_LPS_3.bam", "LY294002_LPS_1.bam", "LY294002_LPS_2.bam", "LY294002_LPS_3.bam")
>Rsubread::align(index = "mm10_Index", readfile1 = ForwardFiles, readfile2 = ReverseFiles, type =
"rna", input_format = "gzFASTQ", output_format = "BAM", output_file= Rsubread_Aligned_Files)
```

After mapping to the reference genome file, a gene transfer format (GTF) file, detailing genome sequences linked to genomic features obtained from Ensembl, was used to assign the mapped sequencing reads to specific reference genome features (such as exon location). This is performed using the featureCounts[683] function in Rsubread[682]. This function also quantifies reads mapped to the genomic

features and takes into account that the RNA-Seq data is paired-end by restricting the duplication of the mapping counts of the pairs to each feature[683]. The following commands is used below:

```
>GRCm38_100_GTF <- list.files(path ="**folder path for RNA-Seq BAM files**", pattern = ".gtf.gz", full.names = TRUE)

>FeatureCount_Results <- Rsubread::featureCounts(RAW_BAM_Files, annot.ext = GRCm38_100_GTF, isGTFAnnotationFile = TRUE, GTF.featureType = "exon", GTF.attrType = "gene_id", useMetaFeatures = TRUE, allowMultiOverlap = FALSE, countMultiMappingReads = FALSE, isPairedEnd = TRUE)
```

The numerical matrix containing the mapped read counts data to genomic features from the previous step was then manipulated into a digital gene expression list to obtain modelled expression data. The empirical analysis of digital gene expression in R (edgeR)[684] package was then used for the analysis of replicated count-based expression data. This package is analogous to how LIMMA[665] uses eBayes modelling to moderate probe-wise variances, however edgeR models count data using an overdispersed Poisson model and eBayes to moderate the degree of overdispersion across genes in RNA-Seq[684]. The commands below detail the grouping of the biological replicates based on treatment condition and creation of digital expression lists from mapped counts:

```
>Groups <- c(rep("CoR_LPS", 3), rep("DMSO", 3), rep("DMSO_LPS", 3), rep("LY294002_LPS", 3))

>Groups <- factor(Groups)

>install.packages("edgeR")

>library(edgeR)

>RNA_Seq_DGEList <- edgeR::DGEList(FeatureCount_Results$counts, group = Groups)
```

2.6.2.4 Differential gene expression analysis of RNA-Seq: Upper Quartile Normalisation and Log_2FC method

Raw read counts are not sufficient on their own to compare expression level changes among samples due to limitations from factors such as transcript length, total number of reads, and biases during sequencing[685]. Reads per kilobase of exon model per million reads (RPKM) is a value generated by within-

normalisation methods which removes the feature-lengths and library size effects which bias raw counts[685]. RPKM values can be calculated with the following equation:

$$RPKM = number\ of\ mapped\ reads\ \div \left(\frac{Gene\ length}{1{,}000} \times \frac{total\ of\ mapped\ reads\ per\ sample}{1{,}000{,}000}\right)$$

The Upper Quartile (UQ) normalisation method was used to normalise the RPKM values as it considers and ignores highly variable/expressed features as well as different library sizes[686, 687]. UQ normalisation also does not contain assumptions within its statistical framework, and only considers RNAs with reads in at least one sample. For UQ normalisation, the RPKM values were divided by the 75th percentile value calculated from all the RPKM values of the RNA-Seq sample, and then subsequently multiplied by the mean value of the upper quartile values across all RNA-Seq samples[688, 689]. Normalisation of technical artifacts was not performed additionally to UQ normalisation due to potential risks of removing real biological effects in differential expression[688].

After UQ normalisation of the RPKM values, differential gene expression was calculated through Log_2 Fold Change (Log_2FC) between treatment and control treatment conditions. This was formulated through dividing the treatment RPKM value to control RPKM value, creating a Fold Change (FC) value, and then using the =LOG(FC,2) formula in Excel to gain the Log_2FC. The two-sample t-test was used to calculate the p-value statistical significance in the change in RPKM/expression providing variance is equal between the two independent groups, and corrected by using the Benjamini & Hochberg ("BH") method[675] to obtain adjusted false-discovery rates.

2.6.3 Gene Ontology Analysis of enriched biological pathways

High-throughput gene expression data can be interpreted through consideration of biological, molecular, and cellular functions to highlight the biological significance (or gene ontology). The Database for Annotation, Visualisation and Integrated Discovery (DAVID)[690] tool was used to assess enrichment

through providing a comprehensive set of functional annotations based on many data sources and annotation sources in the DAVID Knowledgebase.

For inclusion in DAVID gene ontology analysis, differentially expressed genes needed to meet the following cut-offs of: ≥ 1 Log_2FC & 0.05 p-value for upregulated genes, or ≤ -1 Log_2FC & 0.05 p-value for downregulated genes. Biological pathways associated with these gene lists are detailed in the Results sections to show biological effects of the differential expression of treatment against control.

2.6.4 Qiagen's Ingenuity Pathway Analysis (IPA)

The Ingenuity Pathway Analysis (IPA)[691] from Qiagen is an advanced tool which allows in-depth comparative analysis of input gene lists to biological pathways from publicly available databases and extensive libraries of high-throughput datasets. IPA also contains analytical tools which allows exploration of predicted upstream regulators, causal networks, mechanistic networks, pathway activation analysis, and downstream effects analysis. The analytical tools in IPA for these produces z-scores which indicate predicted activation or inhibition based on the gene expression patterns of the input genes for a canonical pathway, upstream regulator, or downstream functions. For inclusion into IPA, output of RNA-Seq or microarray data met the following cut-offs for differential expression of: ≥ 1 Log_2FC & 0.05 p-value for upregulated genes, or ≤ -1 Log_2FC & 0.05 p-value for downregulated genes. Comparative analysis in IPA of different treatment conditions and datasets has been used to show comparisons between gene expression patterns between the datasets on effects to biological pathways and upstream regulators.

2.6.5 Quantitative Proteomics methods

2.6.5.1 Identification of RNA-binding proteins after OOPS

To identify changes in proteins between various treatment conditions in OOPS separations, samples were sent for label-free quantitative proteomics to the Advanced Mass Spectrometry Facility of the University

of Birmingham. Organic (unbound proteins) and Interphase (RNA-protein bound complexes) separations for RAW264.7 macrophages were achieved following the OOPS method detailed in section 2.5. Organic and Interphase separations were sent for treatments of DMSO (0.02% v/v), DMSO (0.02% v/v) & LPS (1 μg/ml), Cordycepin (20 μM) & LPS (1 μg/ml), and LY294002 (100 μM) & LPS (1 μg/ml) with formaldehyde crosslinking. A DMSO (0.02% v/v) & LPS (1 μg/ml) sample without formaldehyde crosslinking was also sent as a crosslinking control.

All samples were trypsin digested and peptides were separated through liquid chromatography. There were five biological replicates sent to the University of Birmingham, with two biological replicates undergoing 1-hour liquid chromatography, and three biological replicates undergoing a 2-hour liquid chromatography step. Label-free MS-based proteomics was performed on the samples using the Q-Executive HF mass spectrometer. The facility used the Proteome Discoverer platform from ThermoFisher Scientific to obtain output from precursor ion intensities which was sent back to me. The facility sent output only for identified proteins which had at least two unique peptides present, which is a golden rule in protein identification.

Proteins were identified as being an RNA-binding protein through using EMBL's RBPbase (v0.2.1), which is a comprehensive database which integrates high-throughput RBP detection studies of Eukaryotic RBPs. Relative abundances for proteins were normalised through UQ normalisation (detailed in section 2.6.2.4), and changes of abundance between samples and OOPS phases were quantified through calculating the ratio of change through dividing the normalised abundances.

3 Polyadenylation inhibition represses inflammatory stimulation in RAW264.7 Macrophages

3.1 Introduction

Modification of mRNA through polyadenylation and the addition of the poly(A) tail is important for the formation of a dynamic transcriptome and translatome[391, 392], and thereby regulates gene expression. The poly(A) tail machinery is known to play crucial roles in the termination of transcription[449-451], the nuclear export of mRNP complexes[692-695], and translation[600, 601, 604, 605]. Polyadenylation at the PAS site through a canonical or non-canonical PAP occurs after CPSF3-mediated cleavage ~10-30 nucleotides upstream at the CPA site on the 3'UTR[409, 414-417]. The CPSF subunits, CPSF4 and WDR33, recognise and bind directly to the PAS site, which are correctly orientated to the site by CPSF1. These subunits need to dissociate from the PAS site to mediate full and repeated cleavage and polyadenylation[402, 403, 408, 410]. An active metabolite of cordycepin, cordycepin triphosphate (CoTP), has been found to incorporate into the poly(A) tail, restricting dissociation of CPSF4 and WDR33 from the 3'UTR of mRNA causing chain termination and reduction in selective mRNA poly(A) tail length[644, 645, 696, 697]. Previous studies have shown that cordycepin has anti-inflammatory[6, 7], immunomodulatory[10], and anti-microbial effects[11, 12], however a clear mechanism of how cordycepin exerts these effects is still not conclusive.

Inflammation is known to induce rapid mRNA transcription in response to stimulus such as through recognition of PAMPs, such as lipopolysaccharides (LPS) by pattern recognition receptors (PRRs)[176-178]. Toll-like receptors (TLRs) are PRRs known to initiate signalling cascades through adaptors such as MyD88, leading to transcription of proinflammatory cytokines and chemokines via nuclear translocation of transcription factors such as NF-κB, AP-1, and interferon (IFN)-regulatory factors (IRFS)[176-178]. When immune response and inflammation is not moderated, chronic and uncontrolled inflammation and tissue damage can occur[251]. This can lead to cytokine/chemokine storms or hypercyto or hyperchemokinemia, non-specific distant inflammatory Acute Phase Response (APR)[252, 253], and a plethora of diseases such as cancer, arthritis, Alzheimer's disease, and diseases of the autoimmune, cardiovascular, and pulmonary systems[251, 254].

The role cleavage and polyadenylation plays in inflammation is still not fully understood, however CPSF4 has been found to be elevated in inflamed synovial tissues of patients with osteoarthritis[384]. It is also

known that sensitivity of the CXCL2 chemokine by cordycepin is dependent on the presence of 3'UTR sequence[7]. Knockdown of CPSF4 has been shown to repress expression of phosphorylated IKKα/β and IκBα and reduced nuclear translocation of NF-κB at COX-2 promoter regions[630]. It has also been shown that knockdown of both CPSF4 and WDR33 can repress NF-κB nuclear translocation and some inflammatory mRNA markers in RAW264.7 macrophages[384]. The effect of cordycepin on NF-κB-mediated transcription has been reviewed as part of a systematic review of the biological effects of cordycepin by Radhi, *et al.* (2021)[3]. This review found variable effects of cordycepin on NF-κB transcription in current literature, as some studies highlight repression of nuclear translocation[364, 365, 698-700] and phosphorylation of NF-κB subunits[371, 700-702], whereas others show no effect on NF-κB with cordycepin[7, 703, 704]. This altogether shows that there could be a role of polyadenylation in inflammatory NF-κB-mediated transcription which needs further investigation.

This chapter attempts to confirm and broaden our understanding of inflammatory targets of cordycepin and the association of poly(A) machinery, WDR33, on key inflammatory markers, regulators, and biological pathways. High-throughput data analysis and confirmational qPCR gene expression experiments will be used to investigate whether polyadenylation has a role in inflammation through cordycepin treatment and knockdown of WDR33 in RAW264.7 macrophages.

3.2 Cordycepin represses inflammatory master regulators and biological pathways

To distinguish whether cordycepin represses genome-wide expression of proinflammatory markers and to identify downregulated inflammatory pathways, a microarray dataset of cordycepin treatment of RAW264.7 macrophages was re-analysed using the LIMMA method[665] detailed in the Methods section (2.6.3). RAW264.7 macrophages were seeded and cultured in DMEM & 10% FBS media for 24-hours. After 24-hours, the media was taken off and the cells were incubated for 24-hours in media with less FBS (0.5%). RAW264.7 cells were then treated in this media for either cordycepin (20 μM) or DMSO (0.02% v/v) for 1-hour prior to a further 1-hour LPS (1 μg/mL) inflammatory stimulation. This dataset was initially analysed using an alternative method, and described in the publication, Ashraf, *et al.* (2019)[384]. This dataset has been deposited in NCBI's Gene Expression Omnibus repository (GSE126157).

A volcano plot illustrating the spread of expression of cordycepin treatment compared against DMSO with LPS (1 μg/mL) inflammatory stimulation demonstrates a higher number of upregulated genes (899; ≥ 1 Log_2FC & ≤ 0.05 p-value), compared to downregulated genes (342; ≤ -1 Log_2FC & ≤ 0.05 p-value) (figure 3.1). Most of the genes (20,740) did not meet a statistical significance of ≤ 0.05 p-value and were within the Log_2FC range of +1 to -1. These genes were excluded from further analysis as they were not statistically significant and did not reach a threshold of ≥ 1 or ≤ -1 Log_2FC change in expression with cordycepin treatment.

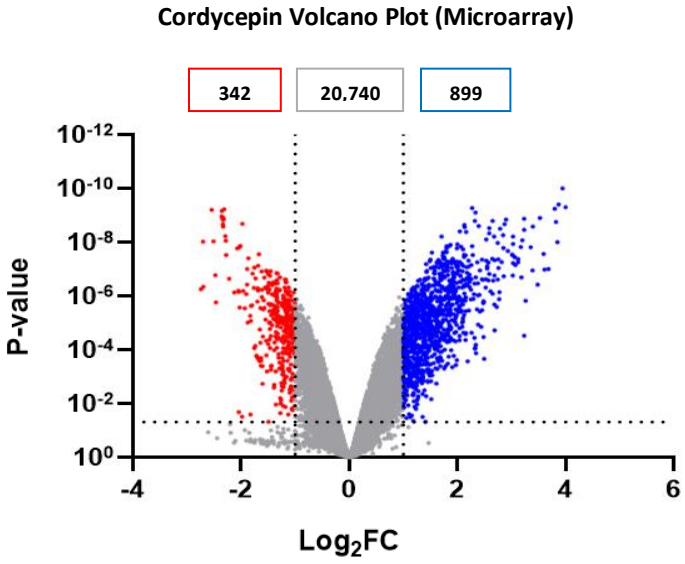

Figure 3.1: Volcano plot indicating the spread of differentially expressed genes with cordycepin treatment in RAW264.7 macrophages (microarray). Each dot represents a differentially expressed gene for cordycepin (20 µM) treatment compared to DMSO (0.02% v/v) with LPS (1 µg/mL) inflammatory stimulation. Microarray output was analysed using the LIMMA method[665]. Red denotes downregulated genes with ≤ -1 Log_2FC & ≤ 0.05 p-value, blue denotes upregulated genes with ≥ 1 Log_2FC & ≤ 0.05 p-value, grey denotes genes which do not meet these requirements.

The Functional Annotation Tool in the DAVID Bioinformatics Resource (LHRI, version 6.8)[690] was used to obtain Gene Ontology (GO) analysis output of enriched biological pathways associated with the upregulated genes and downregulated genes illustrated in the volcano plot (figure 3.1). Downregulated genes with cordycepin treatment with LPS inflammatory stimulation show an enrichment of many proinflammatory biological pathways, such as the cellular response to LPS, TNF and IL-1 stimulation, and general inflammatory and immune responses (figure 3.2A). The biological pathway which had the most associated downregulated genes with cordycepin treatment was transcription (DNA-templated) biological pathway (~35 genes; figure 3.2A). The transcription (DNA-templated) biological pathway however had the lowest enrichment value (≤ ~2-fold enrichment) in the downregulated genes with cordycepin treatment (figure 3.2A). Cellular responses and biological pathways associated with inflammation and immunity are predominantly downregulated with cordycepin treatment (figure 3.2A). Statistically significant downregulated genes with cordycepin treatment with LPS inflammatory stimulation enriched with these biological pathways show repression of regulators of inflammation, immunity, and transcription.

Upregulated genes with cordycepin treatment with LPS (1 μg/ml) inflammatory stimulation are more heterogeneous, with input of upregulated genes into DAVID GO analysis suggesting that cordycepin can upregulate membrane protein ectodomain proteolysis, cholesterol efflux, organism development, and response to hypoxia (figures 3.2B). This altogether shows that cordycepin exerts a clear repression of immune and inflammatory mRNA and may upregulate cholesterol efflux with inflammatory stimulation.

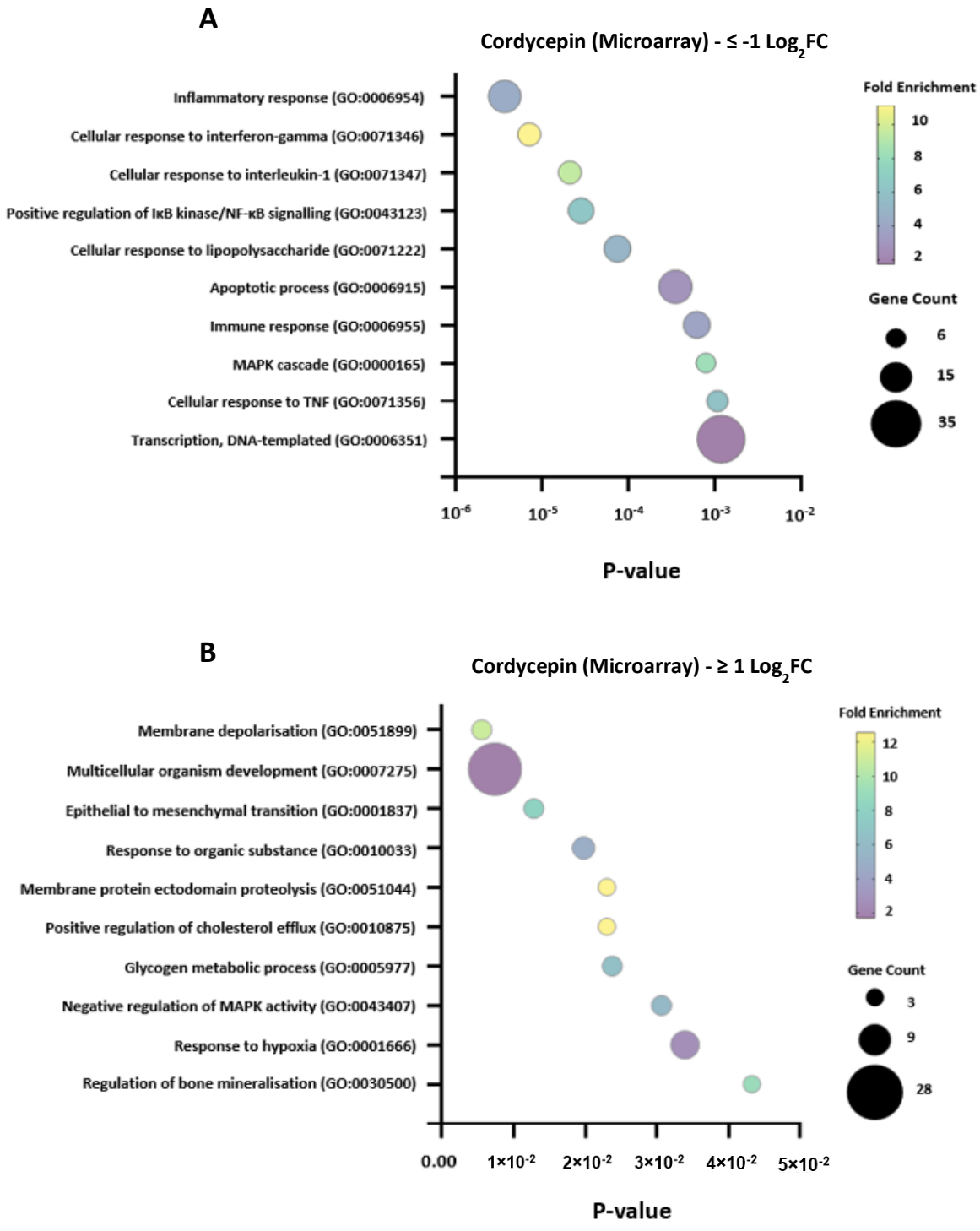

Figure 3.2: Differential expression analysis of cordycepin treatment indicates repression of key proinflammatory biological pathways (microarray). Differentially expressed genes obtained from microarray output analysed in LIMMA[665] of cordycepin (20 µM) treatment compared to DMSO (0.02% v/v) treatment with LPS inflammatory stimulation were inputted into DAVID Gene Ontology[690]. Bubble plots indicate enriched biological pathways associated with **A)** significantly repressed genes (≤ 0.05 p-value and Log_2FC of ≤ -1), and **B)** significantly upregulated genes (≤ 0.05 p-value and Log_2FC of ≥ 1) with cordycepin treatment.

All differentially expressed genes with statistical significance (≤ 0.05 p-value) with cordycepin treatment were analysed through the Expression Analysis tool in QIAGEN's Ingenuity Pathway Analysis (IPA) platform[691]. Activation z-scores, a predictive score used to infer activation states of biological pathways based on the direction of gene regulation, were obtained through IPA. Pathways including cell-membrane receptors, TLR3 and 4, Interferon-α/β receptor (IFNAR), RIG-1, and TNF-receptors 1 and 2 (TNFR1 and 2), were found to have negative activation z-scores and enrichment in repressed genes (figure 3.3). This implies that cordycepin can affect the activation of inflammation by a variety of receptors upstream to proinflammatory transcription. Biological effects of known PAMP's are also predicted to be repressed with cordycepin treatment such as LPS, TNF, IFN-γ, CSF2, CD40LG, and TNFSF11 (figure 3.3). Through IPA and GO analysis, the MyD88-dependent and independent pathways are both predicted to be repressed with cordycepin treatment. Downstream regulators and pathways of MyD88/LPS stimulation are repressed including the MyD88 adaptor protein, multiple pathogen response pathways, DNA-templated transcription, NF-κB complex and signalling, and the MAPK cascade (figures 3.2A & 3.3).

Differential expression analysis was performed for the comparison of RAW264.7 macrophages treated with 1-hour DMSO (0.02% v/v) treatment, followed by a further 1-hour LPS (1 μg/ml) inflammatory stimulation, compared to DMSO (0.02% v/v) treatment alone. This was to show that the RAW264.7 macrophages were inducible with LPS (1 μg/ml) inflammatory stimulation, and that the effect seen with cordycepin treatment is not through DMSO (figure A.2.1). All statistically significant upregulated genes (≥ 1 Log_2FC & ≤ 0.05 p-value) were used in DAVID Gene Ontology analysis[690], which showed that upregulated genes were associated with pro-immune and inflammatory biological pathways, providing evidence that the RAW264.7 macrophages were inducible with LPS (1 μg/ml) inflammatory stimulation (figure A.2.1B).

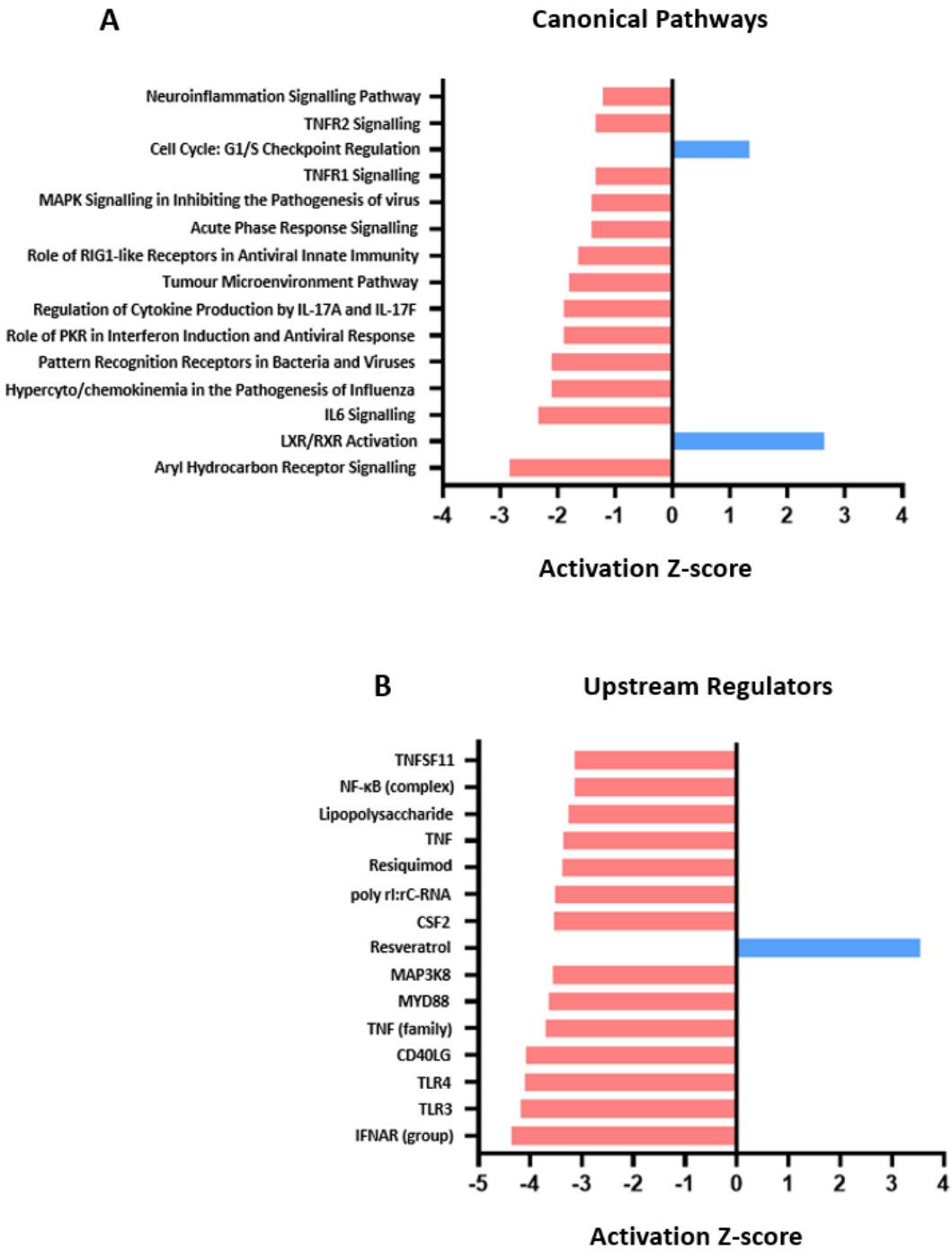

Figure 3.3: Cordycepin represses pro-inflammatory canonical biological pathways and upstream regulators. All statistically significant differentially expressed genes (≤ 0.05 p-value) obtained from microarray output analysed in LIMMA[665] of cordycepin (20 µM) treatment compared to DMSO (0.02% v/v) treatment with LPS inflammatory stimulation were inputted into IPA[691]. **A)** Indicates the top 15 biological canonical pathways which are repressed (red bars) or upregulated (blue bars) with cordycepin treatment. **B)** Indicates the top 15 upstream regulators which act in an opposite way (red bars) or act similarly (blue bars) to cordycepin treatment based on differential gene expression.

As the MyD88 pathway was suggested to be repressed with cordycepin treatment based on the DAVID GO and IPA tools (figures 3.2A, and 3.3B), immunofluorescence was performed to visualise the effect of cordycepin on localisation of NF-κB (p65). RAW264.7 macrophages were treated with cordycepin (20 μM) or DMSO (0.02% v/v) for 10 minutes prior to 50 minutes LPS inflammatory stimulation (figure 3.4). RAW264.7 macrophages were treated with DMSO without LPS as an inflammatory control to compare against DMSO and LPS treated RAW264.7 macrophages. With LPS stimulation, there is higher fluorescence of NF-κB (p65) and a ~1.75-fold increase in nuclear:cytoplasmic fluorescent ratio, confirming that LPS is inducing an inflammatory response through NF-κB transcription (figure 3.4). There is a statistically significant repression of nuclear translocation of NF-κB (p65) necessary for transcription in comparison to DMSO treatment with LPS, from a 2-fold to 0.7-fold nuclear:cytoplasmic fluorescent ratio with cordycepin & LPS treatment (p-value = ≤ 0.001). This effect of cordycepin repression nuclear translocation of NF-κB correlates with previous studies[364, 365, 698-700]. The morphology of RAW264.7 macrophages treated with cordycepin resembles DMSO treatment without LPS stimulation, again suggesting that cordycepin is inhibiting inflammatory stimulation of LPS u pstream of NF-κB transcription.

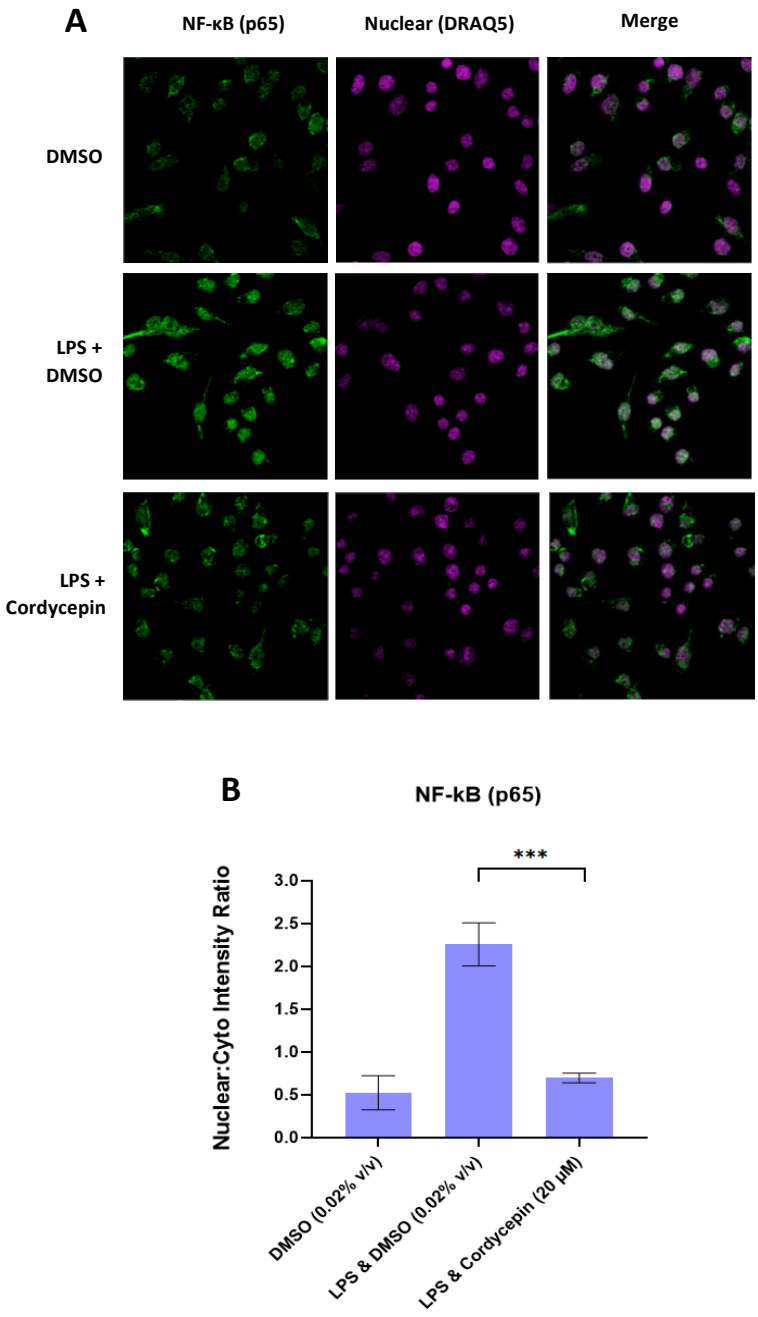

Figure 3.4: Cordycepin represses NF-κB (p65) nuclear translocation. RAW264.7 macrophages were treated with LPS (1 µg/mL) for an initial 10 minutes, followed by 50 minutes treatments with either cordycepin (20 µM) or DMSO (0.02% v/v). DMSO only treatment (0.02% v/v) was used without LPS to demonstrate NF-κB (p65) localisation without inflammatory stimulation. **A)** Confocal images of cells with various treatment conditions stained with anti-NF-κB (p65), DRAQ5 nuclear staining, and merged overlay. **B)** Nuclear:cytoplasmic intensity ratio of NF-κB (p65) fluorescence was calculated using ImageJ (Fiji). (mean ± SD; N = 2 independent experiments; Student t-test was used to obtain statistical significance against LPS & DMSO (0.02% v/v) and representative of; *P<0.05, **P<0.01, ***P<0.001, ****P<0.0001).

Key inflammatory markers which were consistently found in repressed biological pathways of cordycepin treatment through DAVID GO and IPA analysis (figures 3.2A & 3.3A) were confirmed further through qPCR to assess mRNA abundance changes (figure 3.5; method detailed in 2.2). Cordycepin (20 μM) treatment for 1 hour prior to a further 1-hour LPS (1 μg/ml) stimulation resulted in significant repression of relative mRNA abundance of proinflammatory cytokines; Il1β (p-value = ≤ 0.0001) and Tnf (p-value = ≤ 0.05) compared to DMSO and LPS treatment. The chemokine, Ccl4, also has a significant repression in mRNA expression (p-value = ≤ 0.0001), however another chemokine, Cxcl2, did not have a statistically significant repression in mRNA expression. Clec4e which is a calcium-dependent lectin PRR of innate immunity[705], and Acod1 (Irg1), an important regulator in immunometabolism of inflammation[706], were both significantly repressed with cordycepin treatment (p-value = ≤ 0.05). Cordycepin treatment also significantly repressed Ptgs2 (Cox2) mRNA expression (p-value = ≤ 0.001), which is a rate-limiting enzyme important in prostaglandin production during inflammation[707], suggesting that cordycepin represses prostaglandin production.

In contrast to the repression of proinflammatory mRNA markers, cordycepin also appears to have a statistically significant repression (p-value = ≤ 0.01) of Dusp4, which is a negative regulator of MAPK signalling, known to increase cytokine levels in knockout macrophages[708]. This result is the opposite of what is seen in figures 3.2 and 3.3, as DAVID GO and IPA analysis output suggests that cordycepin is repressing MAPK signalling. Cordycepin also significantly represses mRNA abundance of Errfi1 (p-value = ≤ 0.05), which has anti-proliferative and anti-inflammatory effects with LPS stimulation[709]. Rpl28 is an abundant mRNA used in this experiment as a housekeeping gene and shows that there is not a statistically significant difference in expression of Rpl28 mRNA between cordycepin and DMSO treatment (figure 3.5).

These results confirm and are as predicted compared to the microarray analysis output that these genes are repressed by cordycepin treatment. Cordycepin appears to affect genes that are induced by LPS including proinflammatory markers. Anti-inflammatory genes such as Dusp4 and Errfi1 are induced by LPS inflammatory stimulus and might be targets of NF-κB involved in the resolution of acute inflammation (figure 3.5).

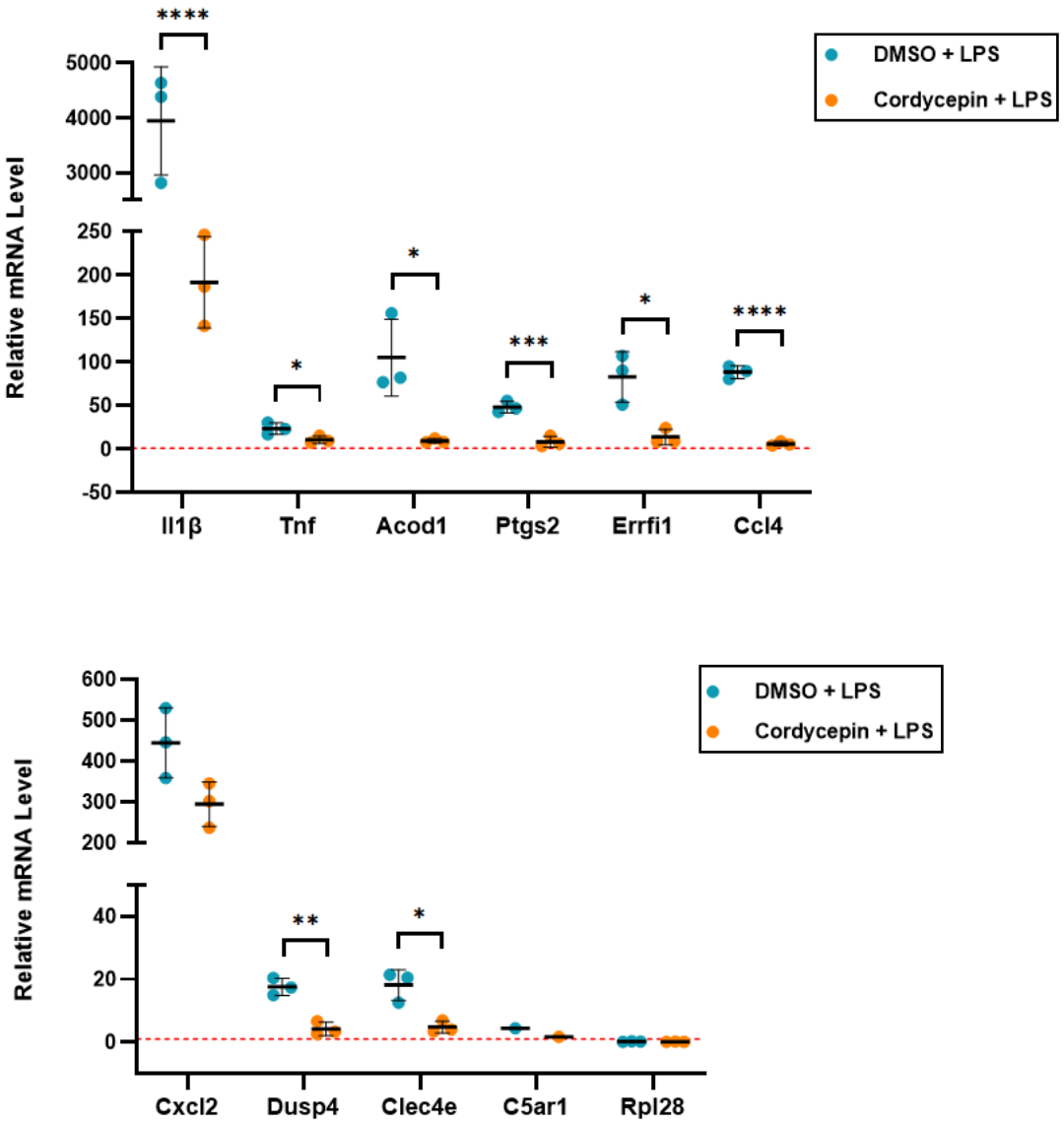

Figure 3.5: Cordycepin represses relative mRNA expression of inflammatory markers. RAW264.7 macrophages were treated for 1 hour with cordycepin (20 µM) or DMSO (0.02% v/v) prior to a further 1-hour LPS (1 µg/mL) inflammatory stimulation. Total RNA was extracted followed by cDNA synthesis, and qPCR. Copy threshold (Ct) values of qPCR for key inflammatory genes were analysed using the 2-ΔΔCt method[660] and normalised to the Ct values of Gapdh (housekeeping gene). Relative mRNA expression of tested genes is presented as the Log_2 Fold Change relative to untreated control. (mean ± SD; n=3 independent experiments; Student t-test was used to obtain statistical significance against LPS & DMSO (0.02% v/v) and representative of; *P<0.05, **P<0.01, ***P<0.001, ****P<0.0001).

3.3 Cordycepin represses more inflammatory genes than adenosine and 3'-deoxyinosine

Due to the structural similarity, it has been proposed that cordycepin could act in a similar manner to adenosine (figure 3.6), such as modulating adenosine receptors (A_1, A_{2A}, A_{2B}, or A_3). Research currently has contrasting results on this theory, as agonists and antagonists of adenosine receptors have been found to both repress[380, 386], and to have no effect to the mechanisms of cordycepin[382].

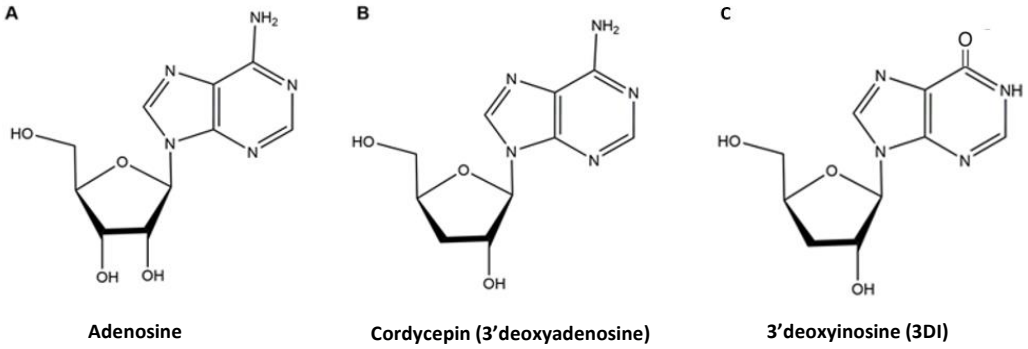

Figure 3.6: Structural comparison between adenosine, cordycepin and 3'deoxyinosine (3DI). As highlighted, cordycepin (B) and 3'deoxyinosine (C) differs from adenosine (A) through the absence of 3'hydroxyl moiety. 3'deoxyinosine (3DI) differs from adenosine and cordycepin through the presence of a hypoxanthine purine derivative.

To exclude the possibility that cordycepin affects inflammation predominantly through association with adenosine receptors, RAW264.7 macrophages were treated for 1 hour with either DMSO (vehicle control; 0.02% v/v), cordycepin (20 µM), adenosine (20 µM; same concentration at cordycepin), or 3'deoxyinosine (3DI; 200 µM) prior to a further 1-hour LPS (1 µg/ml) inflammatory stimulation. 3DI is a potent inhibitor of growth of the promastigote form of *Leishmania tropica*, which is reaminated to form 3'-deoxyinosine-5'-monophopshate and CoMP, CoDP and CoTP[710]. 3DI has been found to convert to CoTP at a 10-fold lower ratio compared to cordycepin in RAW264.7 macrophages[711], so for this reason, 10x the concentration of 3DI was used in this experiment (200 µM). Total RNA was extracted post-treatments, followed by cDNA synthesis and qPCR looking at the same consistent inflammatory mRNA markers in the

DAVID GO and IPA output as before, which have already seen effects from cordycepin treatment (figure 3.5).

In comparison to LPS and DMSO treatment, cordycepin consistently produces the same statistically significant repression of inflammatory mRNA markers, apart from the chemokine, Cxcl2, as seen previously (figures 3.5 and 3.7), however the same effect is not seen for adenosine and 3DI (figure 3.7). Adenosine treatment in RAW264.7 macrophages had no repression on inflammatory mRNA markers compared to LPS and DMSO. For proinflammatory markers Il1β, Acod1, Clec4e, and Ccl4, adenosine had no change in expression compared to DMSO, and only slight upregulation of mRNA markers; Tnf, Ptgs2, Errfi1, Cxcl2, and Dusp4, which were not statistically significant (figure 3.7). 3DI treatment led to statistically significant repression of proinflammatory mRNA markers, Il1β, Acod1, Ptgs2, and Ccl4 ($p = \leq 0.05$). Little to no effect was seen by 3DI on relative mRNA expression of Tnf and Dusp4, and repression of Clec4e which was not statistically significant. In comparison to DMSO, 3DI upregulated the mRNA expression of Errfi1 and Cxcl2, but this was not statistically significant (figure 3.7).

Altogether, cordycepin treatment consistently represses the mRNA expression of inflammatory markers induced by LPS, whereas 3DI has a similar, but weaker, effect to cordycepin, even at x10 higher concentration. Adenosine does not have the same anti-inflammatory effect to cordycepin or 3DI for all the mRNA markers, suggesting that the effect of cordycepin in RAW264.7 macrophages is not through modulating adenosine receptors (figure 3.7), and thus other mechanisms need to be explored further.

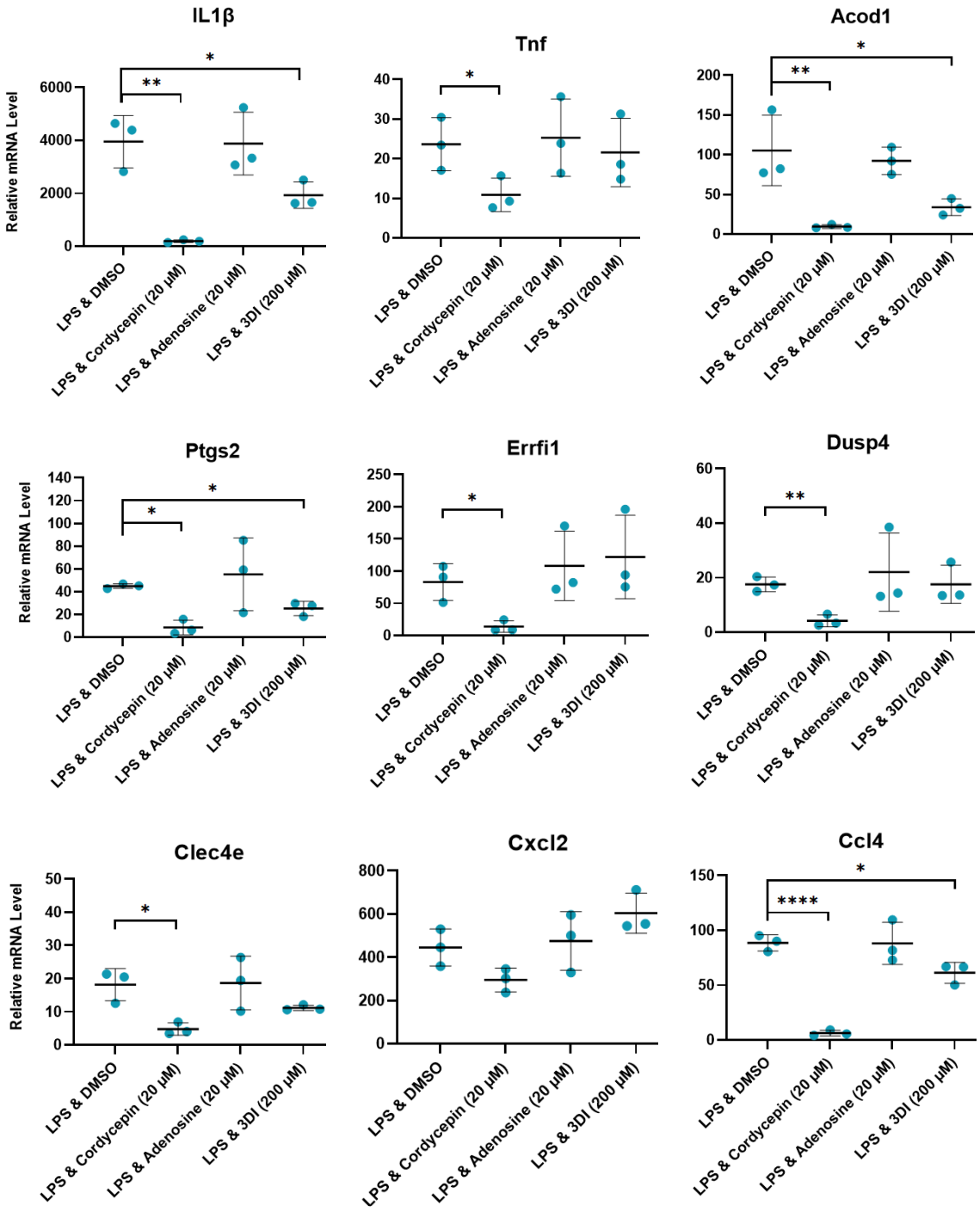

Figure 3.7: More inflammatory genes are repressed by cordycepin compared to adenosine and 3'deoxyinosine. RAW264.7 macrophages were treated for 1 hour with either cordycepin (20 μM), adenosine (20 μM), 3Di (200 μM) or DMSO (0.02% v/v) prior to LPS (1 μg/mL) inflammatory stimulation. qPCR output was analysed using the 2-ΔΔCt method[660] and normalised to Gapdh (housekeeping gene). Relative mRNA expression level of tested genes are presented relative to untreated control. (mean ± SD; n=3 independent experiments; One-way Anova was used to obtain statistical significance against LPS & DMSO (0.02% v/v) and representative of; *P<0.05, **P<0.01, ***P<0.001, ****P<0.0001).

3.4 WDR33 knockdown represses inflammatory master regulators and biological pathways

It is clear that CoTP incorporated into RNA can lead to poly(A) chain termination[646] and the qPCR results from figures 3.5 and 3.7 suggest that CoTP is indeed the active metabolite. It can be hypothesised that cordycepin represses inflammation through affecting mRNA 3'processing. Indeed, CoTP has also been shown to restrict dissociation of CPSF4 and WDR33 from the AAUAAA PAS site on the 3'UTR of cleaved pre-mRNA[644, 645, 696, 697]. Previous publications in our lab has already highlighted that depleting polyadenylation machinery can restrict NF-κB nuclear translocation, and repress inflammatory gene expression[384]. More research has been done on the repression of inflammation through CPSF4 knockdown compared to WDR33 knockdown[634-636], so further work is required to see whether depleting WDR33 does repress inflammatory stimulation.

To add clarity on this, Dr. Masar Radhi extracted RNA from RAW264.7 macrophages after 48-hours of siRNA knockdown of either WDR33 or scramble control (siCtrl). After 48-hours of knockdown, RAW264.7 macrophages were stimulated for 1-hour with LPS to induce inflammation prior to RNA extraction to compare to cells which were not treated with LPS. RNA was sent to GENEWIZ (Azenta Life Sciences) for RNA-Seq, and output was analysed for the first time in this project through Log_2 fold change of treatment versus control of RPKM values after Upper Quartile normalisation (UQ)[688, 689, 712]. Details of the method of the WDR33 knockdown by Dr. Masar Radhi and coding used for analysis is explained in the Methods sections (2.1.3 and 2.6.2). This is the first time this RNA-Seq dataset has been analysed and interpreted.

A volcano plot illustrating the spread of expression of WDR33 knockdown compared against scrambled control siRNA demonstrates a higher number of upregulated genes (799; ≥ 1 Log_2FC & ≤ 0.05 p-value), compared to downregulated genes (245; ≤ -1 Log_2FC & ≤ 0.05 p-value) (figure 3.8). Most of the genes (16,507) did not meet a statistical significance of ≤ 0.05 p-value and were within the Log_2FC range of +1 to -1. These genes were excluded from further analysis as they were not statistically significant and did not reach a substantial change in expression with WDR33 knockdown.

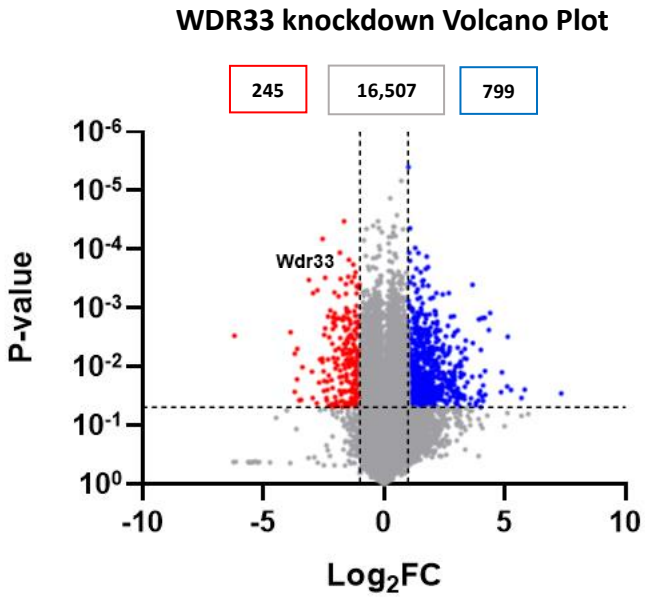

Figure 3.8: Volcano plot indicating the spread of differentially expressed genes with WDR33 knockdown in RAW264.7 macrophages. Each dot represents a differentially expressed gene for WDR33 knockdown compared to scramble control (Ctrl) with LPS (1 µg/mL) inflammatory stimulation. RNA-Seq was analysed through Log_2 fold change of treatment versus control of RPKM values after Upper Quartile normalisation (UQ)[688, 689, 712]. Red denotes downregulated genes with ≤ -1 Log_2FC & ≤ 0.05 p-value, blue denotes upregulated genes with ≥ 1 Log_2FC & ≤ 0.05 p-value, grey denotes genes which do not meet these requirements.

The Functional Annotation Tool in the DAVID Bioinformatics Resource (LHRI, version 6.8)[690] was used to obtain Gene Ontology (GO) analysis output of enriched biological pathways associated with the upregulated genes and downregulated genes illustrated in the volcano plot (figure 3.8). Downregulated genes with WDR33 knockdown (245, figure 3.8) show an enrichment of many proinflammatory biological pathways, which highlight repression of LPS, cytokine, and IL-1 inflammatory and immune responses (figure 3.9A). Key regulators of inflammatory response such as *TNF*, *ACOD1*, *IL1β*, *PTGS2*, and multiple cytokines were also shown to be downregulated with WDR33 knockdown and LPS inflammatory stimulation (figure A.2.4A). Apoptosis appears also to be repressed with WDR33 knockdown, as this pathway shows enrichment of downregulated genes (figure 3.9A). The highest enrichment of downregulated genes associated with WDR33 knockdown (~25-fold enrichment) is associated with the

p38 MAPK cascade, which is known to mediate inflammation[713] (figure 3.9A). Downregulated genes (~25) with WDR33 knockdown are associated with the regulation of transcription by RNAP II promoter, however ~84 genes are upregulated in transcription (DNA-templated) biological pathway, altogether demonstrating a link of knocking down WDR33 and affecting transcription of mRNA (figure 3.9). Key regulators downregulated in the transcription by RNAP II promoter pathway were transcription factors and mRNA linked to early growth response, *EGR1*, *EGR2*, *JUN*, *FOSL1*, and multiple interleukin mRNA's (figure A.2.4A).

Based on just upregulated genes (799, figure 3.8), knockdown of WDR33 show enrichment of genes associated with protein processing, cell-adhesion, actin nucleation, formation of actinomyosin structures, and signal transduction, including adenylate cyclase-activating G Protein-Coupled Receptor (GPCR) signalling (figure 3.8B). Upregulated genes were also enriched in the regulation of transcription, DNA-templated biological pathway, however these genes were predominantly zinc-finger proteins, which are abundantly associated with a wide-range of molecular functions (figure A.2.4A). Genes associated with negative regulation of cytokine production are also upregulated with WDR33 knockdown, which suggests again that WDR33 knockdown represses inflammatory response (figure 3.8 B).

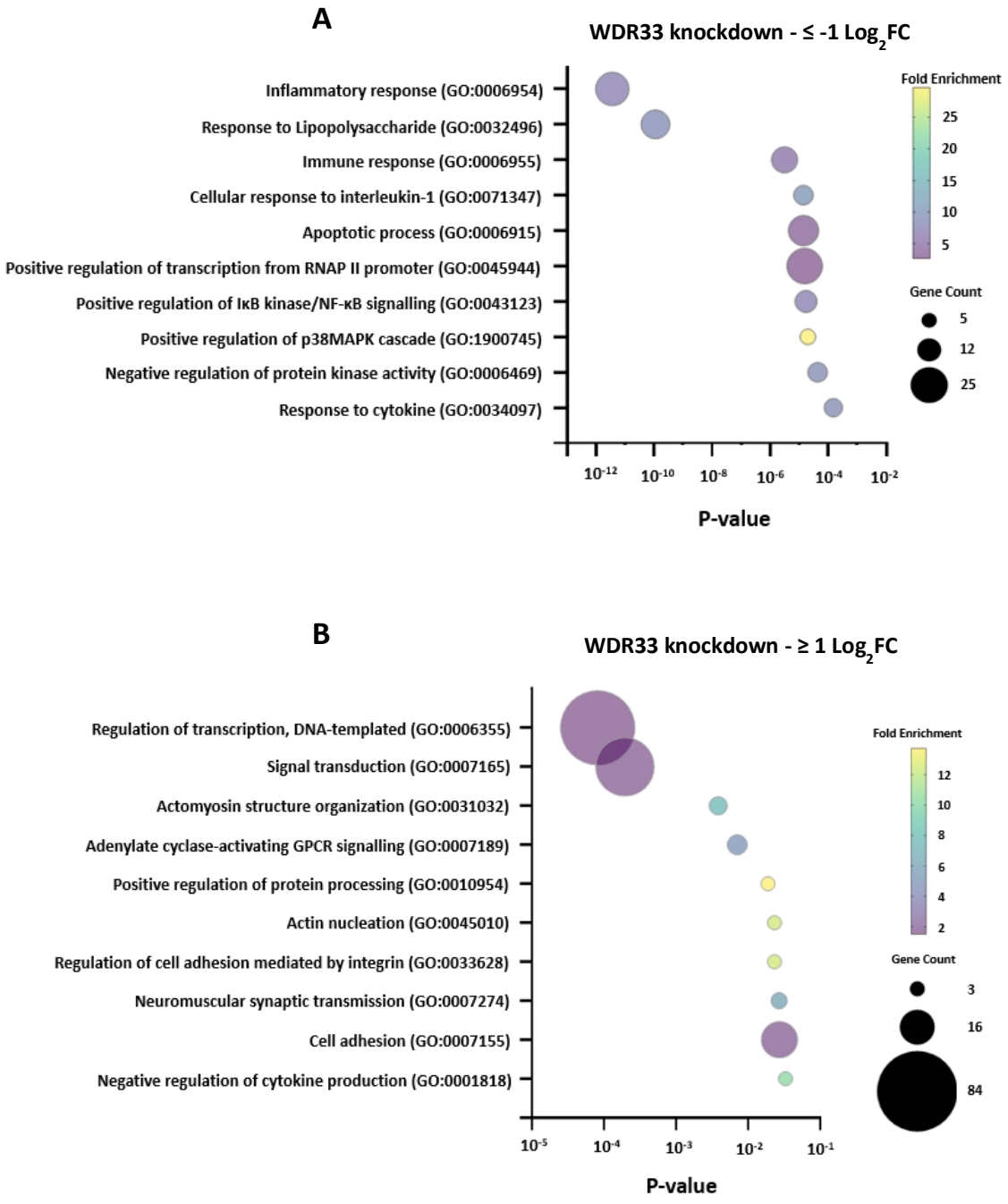

Figure 3.9: Differential expression analysis of WDR33 knockdown indicates repression of key proinflammatory biological pathways. Differentially expressed genes were obtained from RNA-Seq output through Log_2 fold change of treatment versus control of RPKM values after Upper Quartile normalisation (UQ)[688, 689, 712]. RPKM values for WDR33 knockdown was compared to RPKM values of scramble control (Ctrl) with LPS (1 µg/mL) inflammatory stimulation. Differentially expressed genes were inputted into DAVID Gene Ontology[690]. Bubble plots indicate enriched biological pathways associated with **A)** significantly repressed genes (≤ 0.05 p-value and Log_2FC of ≤ -1), and **B)** significantly upregulated genes (≤ 0.05 p-value and Log_2FC of ≥ 1) with WDR33 knockdown.

All differentially expressed genes with statistical significance (≤ 0.05 p-value) with WDR33 knockdown were analysed through the Expression Analysis tool in QIAGEN's Ingenuity Pathway Analysis (IPA) platform[691]. Consistently with the DAVID GO output, WDR33 knockdown negatively regulates inflammatory canonical biological pathways, including TNF receptor signalling, Toll-like receptor signalling, PRR response to pathogens, Acute Phase Response, and Interleukin signalling pathways (figure 3.10A). Upstream regulators which mediate inflammation also have negative activation z-scores, including the effect of TNF members, IFN-γ, Interleukin 1-α (IL1A), IL1β, LPS and NF-κB, indicating that WDR33 knockdown acts in an opposite way and mitigate the stimulation of these regulators (figure 3.10B). Even though WDR33 knockdown represses PRR response to pathogens, phagosome formation appears to be upregulated, suggesting that phagocytosis still occurs with WDR33 knockdown (figure 3.10).

Similarly to upregulated genes in the adenylate cyclase-activated GPCR signalling pathway, cAMP-mediated signalling also has a positive activation z-score, suggesting a feedback effect with WDR33 knockdown on reduced polyadenylation (figures 3.9B and 3.10B). Interestingly, the MEK 1/2 inhibitor (U0126) has a positive activation z-score, and the upstream regulator, ERK, has a negative activation z-score with WDR33 knockdown. This suggests that knocking down WDR33 has a similar effect to MEK 1/2 inhibition, and the repression of ERK signalling (figure 3.10B), linking the poly(A) machinery WDR33 to MEK/ERK signalling.

To confirm that siRNA scramble control (siCtrl) is not causing this effect, and that the RAW264.7 macrophages were inducible for LPS (1 μg/ml) inflammatory stimulation, RNA-Seq datasets for 48-hour siCtrl knockdown and LPS inflammatory stimulation was compared to siCtrl without LPS stimulation. Statistically significant upregulated genes (≥ 1 Log_2FC, and ≤ 0.05 p-value) with siCtrl and LPS treatment were found to be enriched in pro-immune and inflammatory biological pathways (figure A.2.3B). Regulators of pro-inflammatory response and transcription, CXCL2, TNF, IL1β, and FOSB, were also found to be upregulated (figure A.2.3A). This altogether confirms that siRNA knockdown of WDR33 is causing this anti-inflammatory and transcriptional effect in RAW264.7 macrophages induced with LPS inflammatory stimulation.

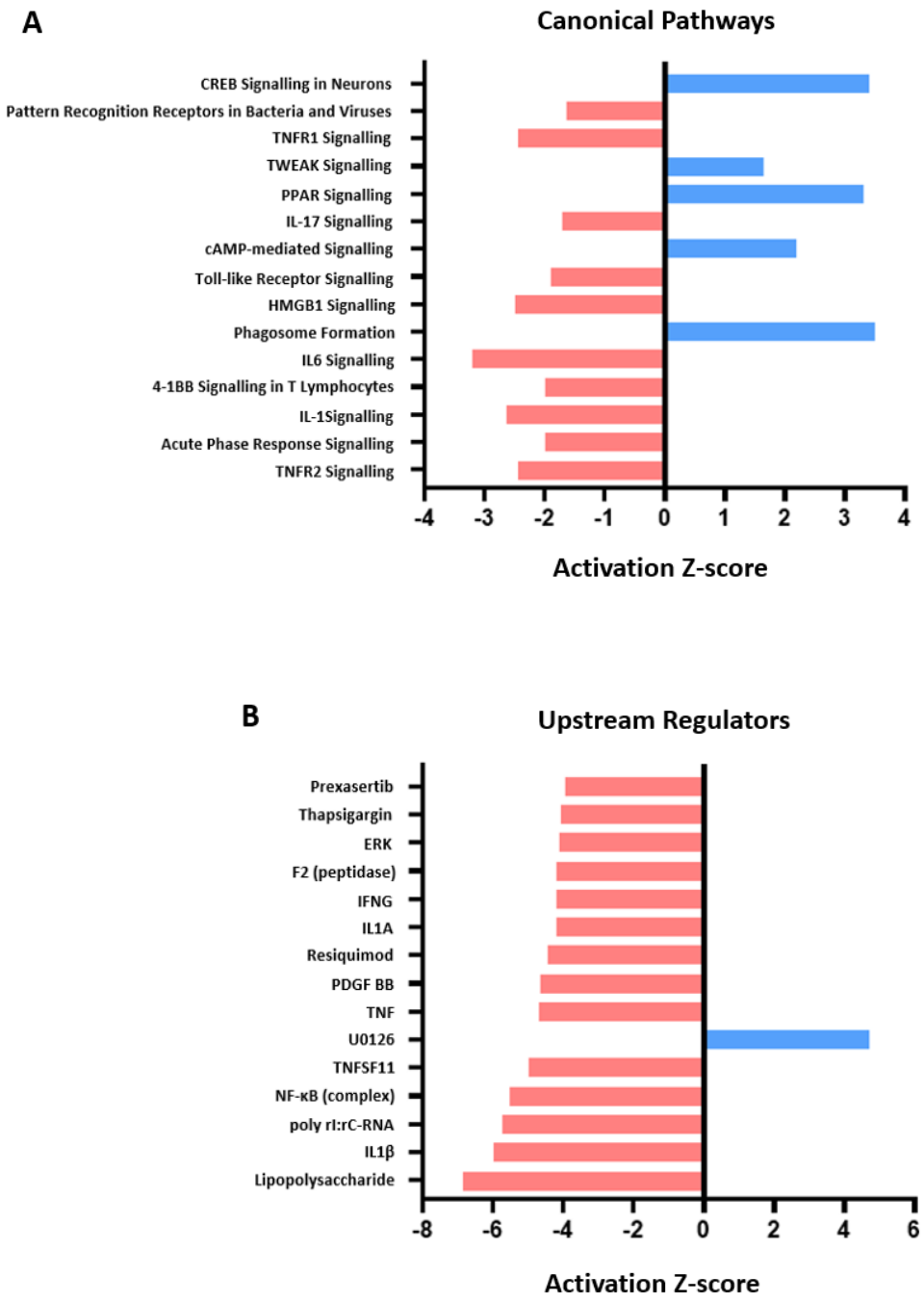

Figure 3.10: WDR33 knockdown represses pro-inflammatory canonical biological pathways and upstream regulators. All statistically significant differentially expressed genes (≤ 0.05 p-value) obtained from RNA-Seq output analysed using RPKM values after Upper Quartile normalisation (UQ)[688, 689, 712] for WDR33 knockdown compared to scramble control (Ctrl) with LPS (1 µg/mL) inflammatory stimulation were inputted into IPA[691]. **A)** Indicates the top 15 biological canonical pathways which are repressed (red bars) or upregulated (blue bars) with WDR33 knockdown. **B)** Indicates the top 15 upstream regulators which have a different (red bars) or similar (blue bars) differential gene expression profile to WDR33 knockdown.

To confirm the effect of WDR33 knockdown on inflammation, qPCR of key inflammatory mRNA markers identified in the multiple biological pathways in the DAVID GO and IPA analysis of WDR33 knockdown (figures 3.9A and 3.10A) was used to assess changes in relative mRNA abundance. These mRNA markers were also consistently repressed with cordycepin treatment (figure 3.5 and 3.7). Knockdown of WDR33 in RAW264.7 macrophages, RNA extraction, cDNA synthesis and qPCR methods are detailed in the Methods section (2.1.3 and 2.2). Knockdown of WDR33 was initially confirmed through measuring the relative mRNA abundance of WDR33 mRNA expression with knockdown in comparison to siRNA knockdown of scramble control (Ctrl) with and without LPS inflammatory stimulation. Consistently, the relative mRNA expression of WDR33 was ~0.45 (figure 3.11B) with WDR33 knockdown, confirming a ~55% knockdown efficiency.

Knockdown of WDR33 prior to 1-hour LPS (1 μg/ml) inflammatory stimulation resulted in statistically significant repression of proinflammatory cytokine mRNA markers, Il1β and Tnf ($p = \leq 0.05$ and $p = \leq 0.01$ respectively) (figure 3.11A). These results are consistent with repression of Il1β and Tnf stimulation in figure 3.10. In contrast, WDR33 knockdown also appears to have a statistically significant repression (p-value = ≤ 0.05) of Dusp4, an inhibitor of MAPK[708], which was not expected based on repression of p38 MAPK signalling (figure 3.9A). This effect is also seen with cordycepin treatment (figures 3.2, 3.3, 3.5). WDR33 knockdown did lead to repression of the inflammatory markers, Ptgs2, Errfi1, Cxcl2, Clec4e, Ccl4 and C5ar1, but this effect was not statistically significant. Acod1 mRNA expression appears to be upregulated in WDR33 knockdown compared to siRNA Ctrl, which is not statistically significant (Figure 3.11A). Rpl28 was used in this experiment as a housekeeping gene and shows that there is not a statistically significant difference in expression of Rpl28 mRNA between WDR33 knockdown and siRNA control (figure 3.11A). Altogether, WDR33 knockdown does repress inflammatory mRNA marker expression, excluding Acod1, which is consistent with the repression of inflammatory biological pathways in DAVID GO and IPA output (3.9A and 3.10), but the majority are not statistically significant, including none of the chemokine mRNAs. More statistically significant changes with WDR33 knockdown on mRNA expression could be achieved with more biological replicates to reduce high standard deviation (figure 3.11A), or with a bigger knockdown of WDR33 relative mRNA level (figure 3.11B).

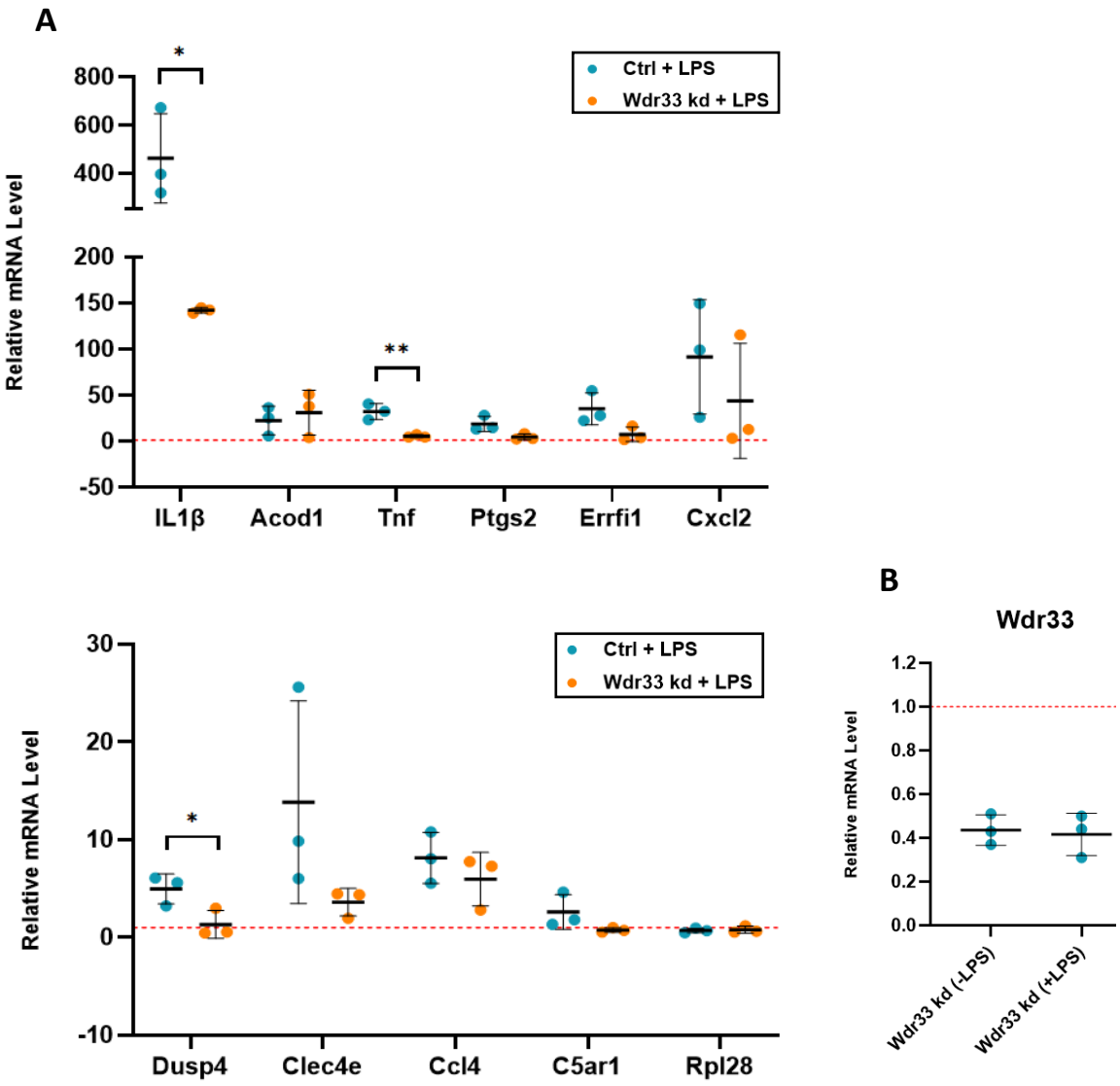

Figure 3.11: Wdr33 knockdown represses relative mRNA expression of inflammatory markers. RAW264.7 macrophages were subjected to siRNA knockdown of either Wdr33 or scramble control (Ctrl) for a total of 48 hours prior to 1-hour LPS (1 µg/mL) inflammatory stimulation. Total RNA was extracted followed by cDNA synthesis, and qPCR. Copy threshold (Ct) values of qPCR for **A)** key inflammatory genes and **B)** Wdr33 were analysed using the 2-ΔΔCt method[660] and normalised to the Ct values of Gapdh (housekeeping gene). Relative mRNA expression of tested genes is presented as the Log_2 Fold Change relative to siRNA Ctrl without LPS. (mean ± SD; n=3 independent experiments; Student t-test was used to obtain statistical significance against siRNA Ctrl + LPS and representative of; *P<0.05, **P<0.01, ***P<0.001, ****P<0.0001).

3.5 Downregulated overlapping genes linked to repression of inflammatory stimulation

As CoTP restricts dissociation of WDR33 on the 3'UTR[644, 645, 696, 697], and the fact both cordycepin treatment (figures 3.2-3.5) and WDR33 knockdown (figures 3.9-3.11), both repress multiple inflammatory pathways, a comparison of these datasets was needed to demonstrate if cordycepin acts through WDR33 on inflammation. As of yet, this comparison has not been done before with these datasets, however Ashraf *et al*. (2019)[384], has previously also shown that both cordycepin and WDR33 knockdown can repress inflammatory mRNA expression. Based on figures 3.2, 3.3, 3.9, and 3.10, it can be hypothesised that overlapping genes for cordycepin and WDR33 knockdown treatments are associated with repression of inflammatory biological pathways and upstream regulators. However, there are clear differences in statistical significance of the repression of inflammatory mRNA marker expression (figures 3.5 and 3.11), showing that there may be a big variation in expression profile between the two treatments. To confirm this, all statistically significant genes (p-value = ≤ 0.05) were overlapped based on gene nomenclature, highlighted by the Venn diagram in figure 3.12A. This comparison highlights that 1,510 differentially expressed genes overlap between the two treatment conditions; however, most of the genes did not overlap, showing treatment-specific differential expression changes (figure 3.12A). To highlight this variability in expression profile, all statistically significant genes which overlapped (1,510), were visualised through a scatter plot based on Log_2 fold change, showing that there was a positive correlation between these genes (R^2 = 0.135, goodness of fit) (figures 3.12A and B). This outcome could be due to the very different time frames of the two treatment conditions, as cordycepin treatment (20 μM) occurred for one hour, whereas WDR33 knockdown occurred twice over a 48-hour period (detailed in Methods section 2.1.3).

To show that overlapped genes between the two treatment conditions are related to repression of inflammatory stimulation, all downregulated genes (lower-left quadrant of the scatter plot (3.12B)) were used in DAVID GO analysis. Biological pathways enriched with downregulated overlapped genes are association with cellular response to LPS, interleukin-1, TNF, and general inflammatory and immune responses (figure 3.12C). Positive regulation of NF-κB signalling, RNAP II promoter transcription, and interleukin-8 production are enriched with downregulated genes, as well as apoptotic process and

neutrophil chemotaxis. Repression of the pathways is consistent with the previous results in figures 3.2A and 3.9A.

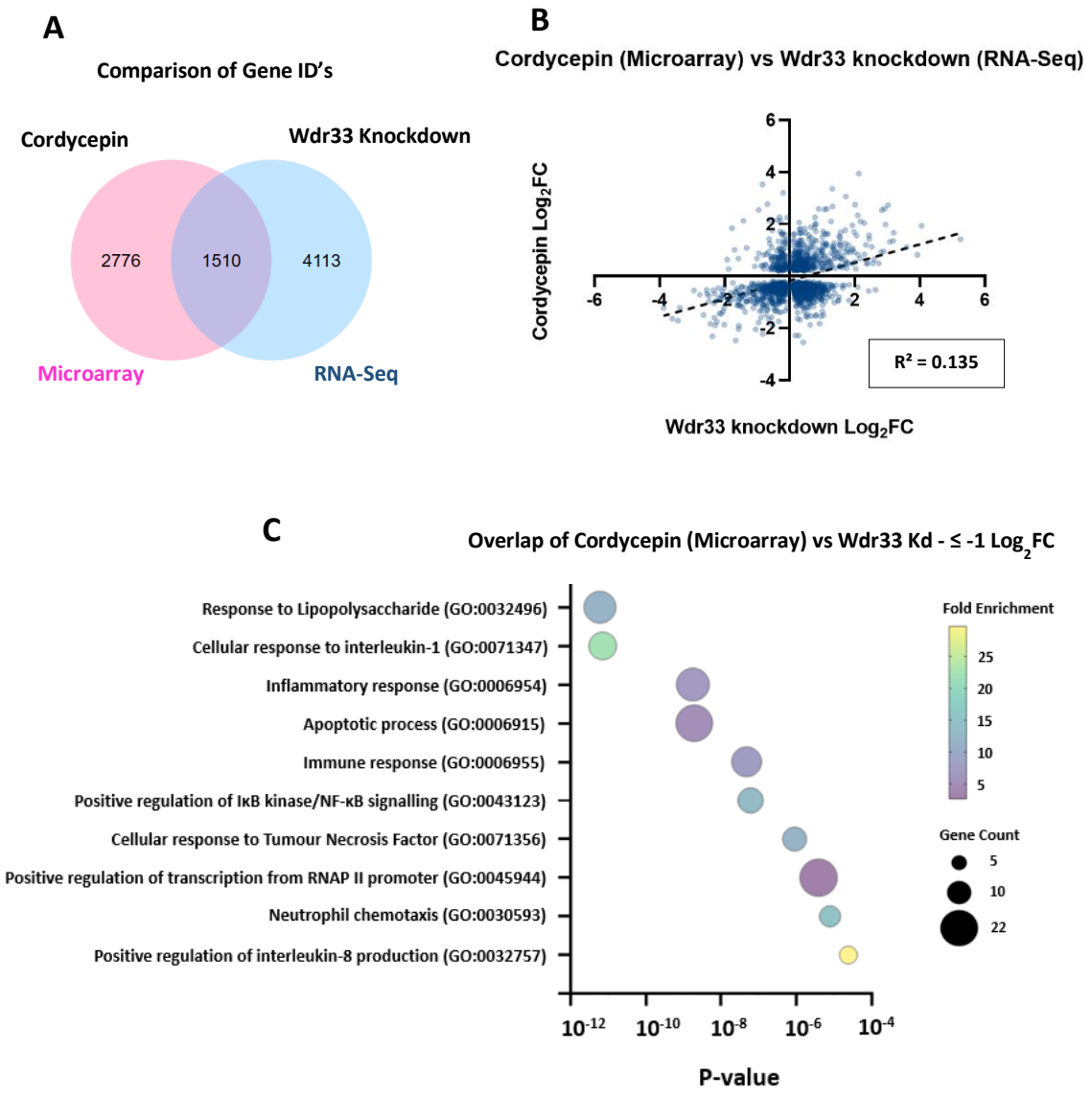

Figure 3.12: Overlap of differentially expressed genes between cordycepin treatment and Wdr33 knockdown. Differentially expressed genes for cordycepin treatment (20 µM; microarray data) was compared to Wdr33 knockdown (double knockdown of 5 nM; RNA-Seq) with 1-hour LPS inflammatory stimulation (1 µg/mL) in RAW264.7 macrophages. **A)** Venn diagram of all genes with statistical significance (≤0.05 p-value) for each treatment condition. **B)** Scatter plot of Log_2FC comparison with 'Goodness of fit' R^2 value. **C)** Top 10 enriched GO biological pathway terms obtained through DAVID[690] for all repressed genes which overlapped between cordycepin and Wdr33 knockdown.

To build on the output of DAVID GO analysis, the Comparison Analysis tool within QIAGEN's Ingenuity Pathway Analysis (IPA) platform[691] was used to compare both affected canonical biological pathways and upstream regulators for cordycepin treatment (microarray) and WDR33 knockdown (RNA-Seq). All differentially expressed genes with statistical significance (≤ 0.05 p-value) were used for the Comparison Analysis, with activation z-scores indicating predictive activation states based on the direction of gene regulation. Consistent with figure 3.12C, many proinflammatory canonical biological pathways are repressed with both treatment conditions, including TNF receptors 1/2 signalling, interleukin-6 (IL-6) signalling, interleukin-17 (IL-17) signalling in regulating cytokine production, APR signalling, and responses to pathogenesis and immunity (figure 3.13A). Both treatments have opposite effects in inflammatory stimulation to many cytokines, including TNF, IL1β, IL33, IFN-γ (IFNG), CSF2, and TNFSF11, providing more evidence that inflammatory stimulation is repressed (figure 3.13B). The MyD88-dependent and -independent pathways, and NF-κB transcription is repressed in both treatments, as MyD88, IRAK4, NOD2, TICAM1 (TRIF), and the NF-κB complex has negative activation z-scores as upstream regulators (figure 3.13B).

Biological pathways which are upregulated in statistically significant genes with both treatment conditions includes PPAR signalling and LXR/RXR activation, which are both known to heterodimerise and is linked to repression of cytokine production and NF-κB signalling[714-717]. WDR33 knockdown has already shown an upregulation of phagosome formation, cAMP and CREB signalling (figure 3.10A), which is also seen with overlapping genes with cordycepin treatment (figure 3.13A).

Consistent with previous results on repression of MAPK signalling (figures 3.2A and 3.9A), and MEK inhibition (figure 3.10B), cordycepin and WDR33 knockdown appears to affect signal transduction pathways and upstream regulators of signal transduction (figure 3.13). The PI3K/Akt biological pathway has a negative activation z-score with both treatments (figure 3.13A), and upstream inhibitors, SB203580 (p39 MAPK inhibitor), PD98059 (MEK1 inhibitor), U0126 (MEK 1/2 inhibitor), and LY294002 (PI3K inhibitor), have positive activation z-scores, indicating a similar effect of cordycepin and WDR33 knockdown on gene expression to these inhibitors (figure 3.13). This altogether suggests that affecting polyadenylation can inhibit signalling pathways in inflammatory stimulation.

A

Canonical Pathways

	siWdr33 kd (+LPS)	Cordycepin (+LPS)
PPAR Signaling	3.317	2.646
IL-6 Signalling	-3.207	-2.333
Phagosome Formation	3.507	1.606
Hypercyto/chemokinemia in the Pathogenesis of Influenza	-3.000	-2.111
LXR/RXR Activation	2.449	2.646
Coronavirus Pathogenesis Pathway	-2.309	-2.324
CREB Signalling in Neurons	3.413	1.213
Cholecystokinin/Gastrin-mediated Signalling	-2.530	-2.000
cAMP-mediated Signalling	2.183	2.333
PI3K/AKT Signalling	-2.828	-1.633
Osteoarthritis Pathway	-2.530	-1.667
Aryl Hydrocarbon Receptor Signalling	-1.342	-2.828
Regulation of Cytokine Production by IL-17A and IL-17F	-2.000	-1.890
TNFR2 Signalling	-2.449	-1.342
TNFR1 Signalling	-2.449	-1.342
Acute Phase Response Signalling	-2.000	-1.414
TREM1 Signalling	-2.121	-1.134
Role of PKR in Interferon Induction and Antiviral Response	-1.265	-1.897
MIF Regulation of Innate Immunity	-1.633	-1.000
IL-17 Signalling	-1.698	-0.775

Activation Z-score

B

Upstream Regulators

Upstream Regulator	Molecule Type	siWdr33 kd (+LPS)	Cordycepin (+LPS)
Lipopolysaccharide	Chemical drug	-6.856	-4.096
TNF	Cytokine	-4.692	-4.088
IL1B	Cytokine	-5.983	-2.784
IL33	Cytokine	-3.250	-2.319
IRAK4	Kinase	-2.350	-2.056
PDGF BB	Complex	-4.668	-2.736
IFNG	Cytokine	-4.180	-2.994
CSF2	Cytokine	-2.022	-3.564
TNFSF11	Cytokine	-4.992	-4.369
NF-κB (complex)	Complex	-5.530	-4.176
SB203580	Kinase inhibitor	2.282	2.223
MYD88	Adaptor	-4.449	-3.526
PD98059	Kinase inhibitor	3.948	1.946
Prexasertib	Chemical drug	-3.951	-1.474
ERK	Group	-4.110	-2.069
NOD2	NF-κB subunit	-4.313	-3.115
LY294002	Kinase inhibitor	3.143	2.397
U0126	Kinase inhibitor	4.724	2.373
poly rI:rC-RNA	Biologic drug	-5.749	-3.635
TICAM1	Adaptor	-3.517	-2.574

Activation Z-score

Figure 3.13: Comparison of biological canonical pathways and upstream regulators consistently affected between cordycepin treatment (microarray) and Wdr33 knockdown. Differentially expressed genes for cordycepin treatment (20 µM; Microarray data) was compared to Wdr33 knockdown (double knockdown of 5 nM; RNA-Seq) with 1-hour LPS inflammatory stimulation (1 µg/mL) in RAW264.7 macrophages. All significantly differentially expressed genes (≤ -1 log_2FC and ≥ 1 log_2FC; ≤ 0.05 p-value) for both treatments were compared in IPA[691]. **A)** biological canonical pathways and **B)** upstream regulators.

As shown previously, both cordycepin and WDR33 knockdown can repress inflammatory stimulation (figures 3.12C, and 3.13), however a majority of statistically significant differentially expressed genes were treatment-specific and had a low positive correlation in Log_2 fold change (R^2 = 0.135, figures 3.12A and 3.12B). This could be through differences in treatment time frames and because of variability in high-throughput profiling methodologies between microarray, profiling predefined transcripts through hybridisation, and RNA-Seq, full sequencing of the genome/transcriptome. Previous publications have already shown that there are differences in differential expression output in comparison between microarray and RNA-Seq platforms[718-720]. To try and improve comparison between cordycepin treatment and WDR33 knockdown and eliminate biases between comparing microarray and RNA-Seq data, an RNA-Seq has been performed for RAW264.7 macrophages with 1-hour cordycepin treatment (20 µM), followed by a further hour inflammatory stimulation with LPS (1 µg/ml). Differential expression of this RNA-Seq dataset was achieved through comparison to DMSO and LPS treatment and analysed through comparison of RPKM values after Upper Quartile normalisation (UQ)[688, 689, 712] (Methods section 2.6.2). Initially, LPS & DMSO was compared to DMSO (0.02% v/v) treatments to confirm inflammatory stimulation. As shown in figure A.2.2, RAW264.7 macrophages were stimulated with LPS as multiple inflammatory biological pathways were enriched with upregulated genes with LPS & DMSO treatment.

A volcano plot illustrating the spread of expression of cordycepin treatment compared to DMSO with LPS inflammatory stimulation demonstrates a higher number of upregulated genes (3,095; ≥ 1 Log_2FC & ≤ 0.05 p-value), compared to downregulated genes (1,000; ≤ -1 Log_2FC & ≤ 0.05 p-value) (figure 3.14). Most of the genes (14,947) did not meet a statistical significance of ≤ 0.05 p-value and were within the Log_2FC range of +1 to -1. This differential expression profile of cordycepin treatment was also seen with the microarray dataset (figure 3.1).

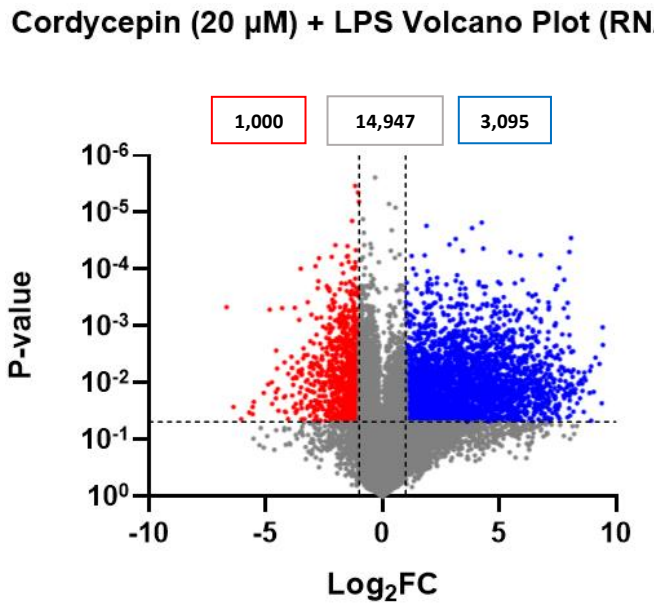

Figure 3.14: Volcano plot indicating the spread of differentially expressed genes with cordycepin treatment in RAW264.7 macrophages (RNA-Seq). Each dot represents a differentially expressed gene for cordycepin (20 µM) treatment compared to DMSO (0.02% v/v) with LPS (1 µg/mL) inflammatory stimulation. RNA-Seq was analysed through Log_2 fold change of RPKM values after Upper Quartile normalisation (UQ)[688, 689, 712]. Red denotes downregulated genes with ≤ -1 Log_2FC & ≤ 0.05 p-value, blue denotes upregulated genes with ≥ 1 Log_2FC & ≤ 0.05 p-value, grey denotes genes which do not meet these requirements.

Consistently with the microarray dataset of cordycepin treatment, the downregulated genes (≤ -1 Log_2FC & ≤ 0.05 p-value) were enriched in multiple inflammatory biological pathways. This included IFN-α -β -γ, regulation of TNF, IL-6 and cytokine production, response to LPS, and general inflammatory and Type-2 immune response with the highest fold enrichment (~50-fold, figure 3.15A). Transcription from RNAP II promoter was also enriched with the highest number of downregulated genes (~80), with transcription also repressed in the microarray dataset (figure 3.2A). DAVID GO analysis of upregulated genes (≥ 1 Log_2FC & ≤ 0.05 p-value) enriched ion and transmembrane transport, cilium movement, cell adhesion and differentiation, extracellular matrix organisation, phosphorylation, and signal transduction (figure 3.15B). Like with WDR33 knockdown (figure 3.9B), RNA-Seq output of cordycepin treatment also upregulates genes enriched in adenylated cyclase-activating GPCR signalling (figure 3.15B).

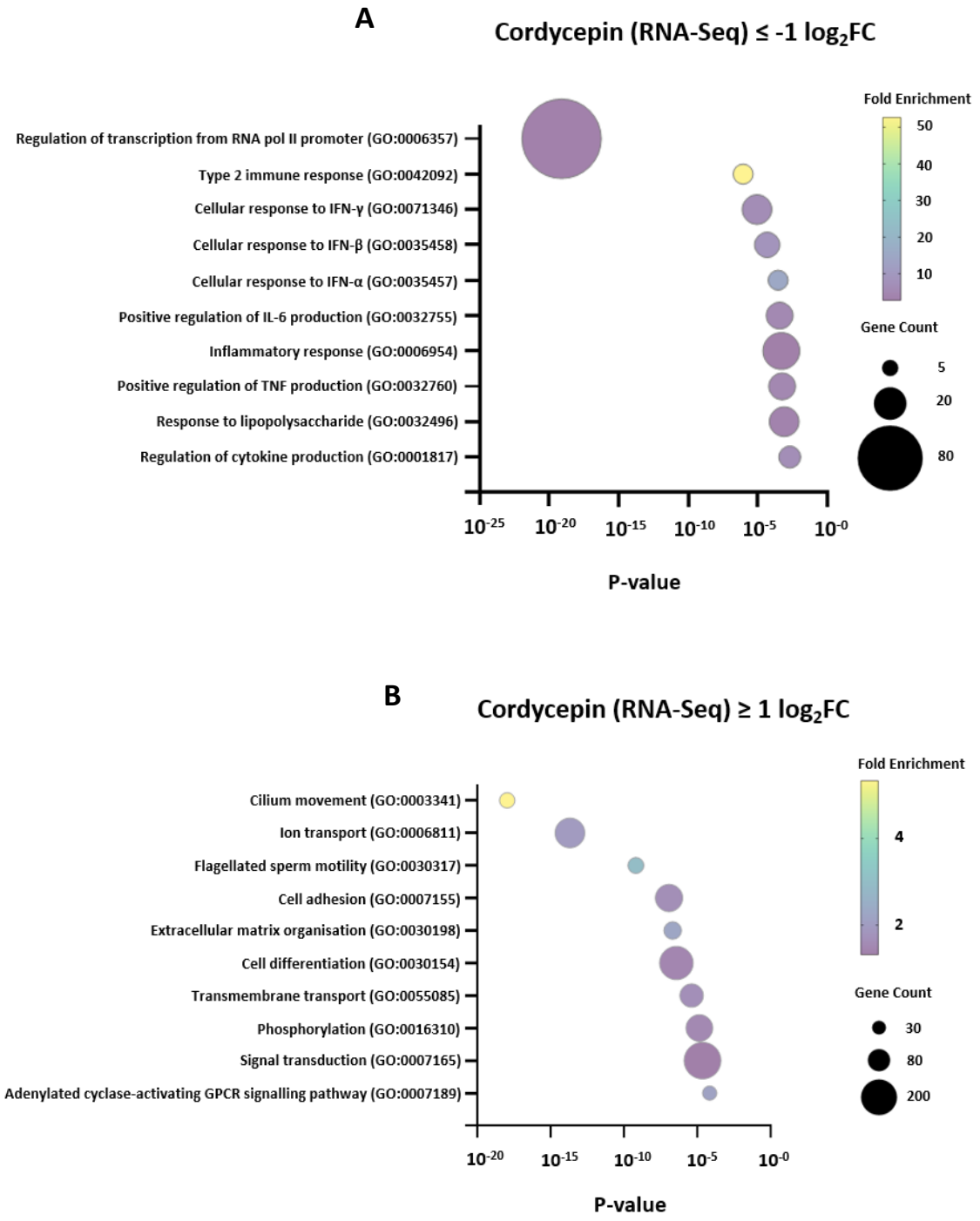

Figure 3.15: Differential expression analysis of cordycepin treatment indicates repression of key proinflammatory biological pathways (RNA-Seq). Differentially expressed genes were obtained from RPKM values from RNA-Seq was analysed through computing the Log_2 fold change of cordycepin (20 µM) treatment compared to DMSO (0.02% v/v) with LPS inflammatory stimulations (1 µg/ml) after Upper Quartile normalisation (UQ)[688, 689, 712]. Statistically significant genes (≤ 0.05 p-value) were inputted into DAVID Gene Ontology[690]. Bubble plots indicate enriched biological pathways associated with **A)** significantly repressed genes (≤ 0.05 p-value and Log_2FC of ≤ -1), and **B)** significantly upregulated genes (≤ 0.05 p-value and Log_2FC of ≥ 1) with cordycepin treatment.

Inclusion of all statistically significant genes for cordycepin treatment (RNA-Seq) into the Expression Analysis tool in IPA[691] shows repression of inflammatory biological pathways associated with APR signalling, TNFR2 and toll-like receptor signalling, PRR of pathogens, and IL6 signalling (figure 3.16A). Key upstream regulators of inflammation, LPS, TNF, TNFSF11, and IL1β, all have negative activation z-scores with cordycepin treatment, as well as MyD88, TICAM1 and the NF-κB complex (figure 3.16B). The transcription factor, KLF6, was also found to have a negative activation z-score and is also thought to mediate inflammation in macrophages[721]. The JAK/STAT signalling pathway has a negative activation z-score and is associated with interferon response[722, 723], which contributes with the output from DAVID GO analysis that cordycepin has an opposite effect to response to interferon stimulation (figures 3.15A and 3.16A).

The effect of cordycepin treatment also has a repressive effect on PI3K/Akt signalling, as shown with a negative activation z-score, and has been shown to have a similar effect on gene expression to the PI3K inhibitor, LY294002, which has a positive activation z-score (figure 3.16). The Superpathway of Inositol Phosphate Compounds pathway contributes to the production of PIP2, which is phosphorylated by PI3K to form PIP_3[27, 43-47], and this pathway is upregulated in cordycepin treatment, which could be a feedback loop from repressed PI3K/Akt signalling (figure 3.16). Similarly to WDR33 knockdown (figure 3.10B), cordycepin treatment also has a similar effect to the MEK1/2 inhibitor, U0126, which demonstrates further that affecting polyadenylation represses signalling pathways. Both cordycepin treatment and WDR33 knockdown upregulate cAMP, CREB, and GPCR signalling pathways, and phagosome formation (figures 3.9B, 3.10, 3.15B, and 3.16).

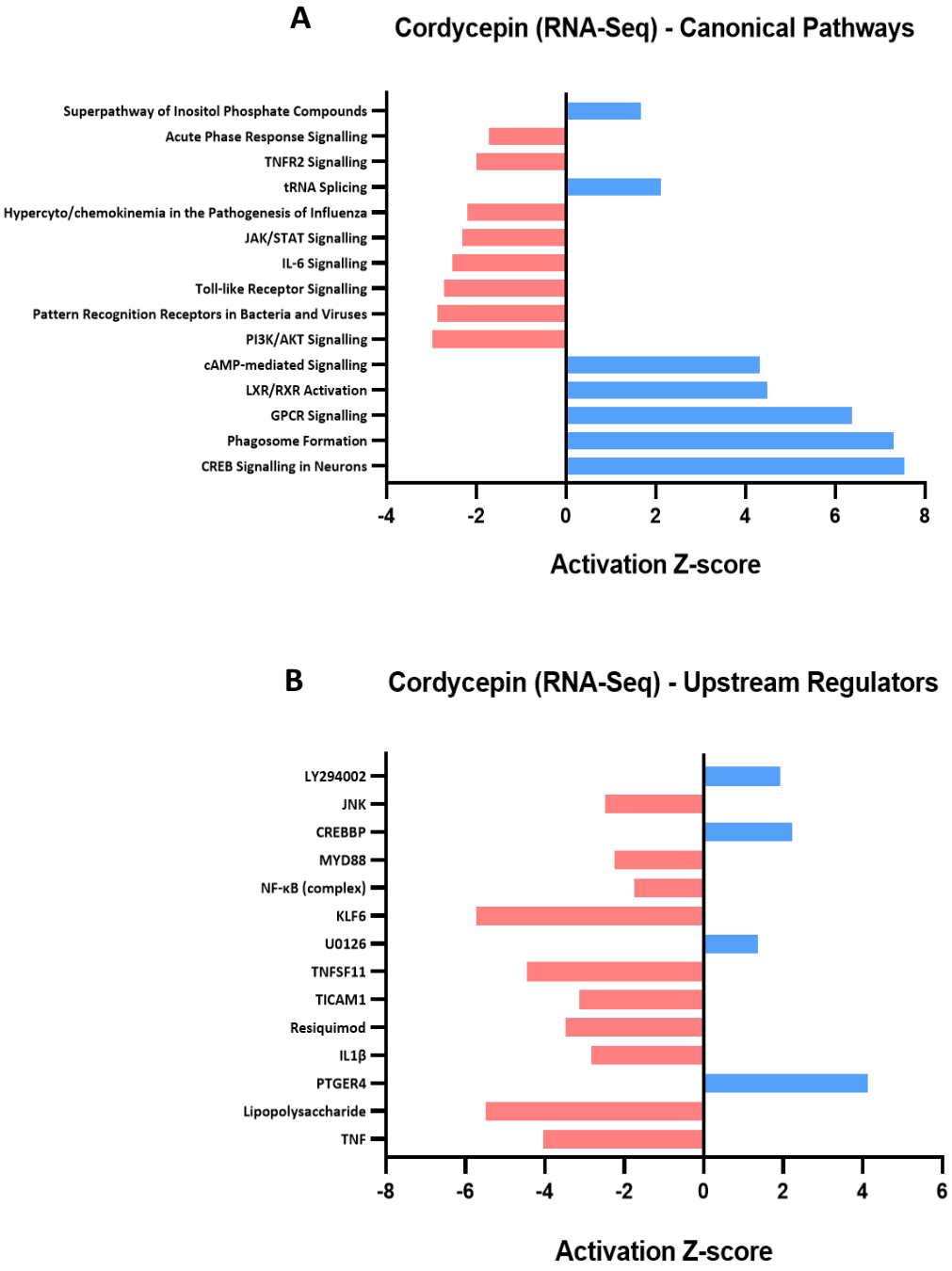

Figure 3.16: Cordycepin represses pro-inflammatory canonical biological pathways and upstream regulators. RPKM values from RNA-Seq was analysed through computing the Log_2 fold change of cordycepin (20 µM) treatment compared to DMSO (0.02% v/v) with LPS inflammatory stimulations (1 µg/ml) after Upper Quartile normalisation (UQ)[688, 689, 712]. All statistically significant differentially expressed genes (≤ 0.05 p-value) were inputted into IPA[691]. **A)** Indicates the top biological canonical pathways which are repressed (red bars) or upregulated (blue bars) with cordycepin treatment. **B)** Indicates the top upstream regulators which act in an opposite way (red bars) or act similarly (blue bars) to cordycepin treatment based on differential gene expression.

To show that cordycepin clearly represses inflammatory stimulation, and to see whether there is variation between microarray and RNA-Seq analysis, the two datasets were compared against each based on differential gene expression (figure 3.17). All statistically significant genes (≤0.05 p-value) for both datasets were compared to each other based on gene nomenclature, with 1,885 genes overlapping between the two datasets (figure 3.17A). By separating these overlapping genes and comparing Log_2 fold changes between the microarray and RNA-Seq cordycepin datasets, there is a positive correlation in differential expression (R^2 = 0.539) for both datasets (figure 3.17B). This shows that these two datasets are far from identical at the individual gene level, despite the identical treatment of the cells.

DAVID GO analysis of the overlapped downregulated genes for both the microarray and RNA-Seq datasets show enrichment of transcription by RNAP II promoter, LPS-mediated signalling, immune response, MAPK cascade, and NF-κB signalling (figure 3.17C), consistent with previous results (figures 3.2A and 3.15A). Unlike the individual GO analyses shown previously, overlapped downregulated genes of microarray and RNA-Seq datasets of cordycepin treatment were enriched in protein ubiquitination, protein transport, chromatin organisation and cell cycle biological pathways (figure 3.17C).

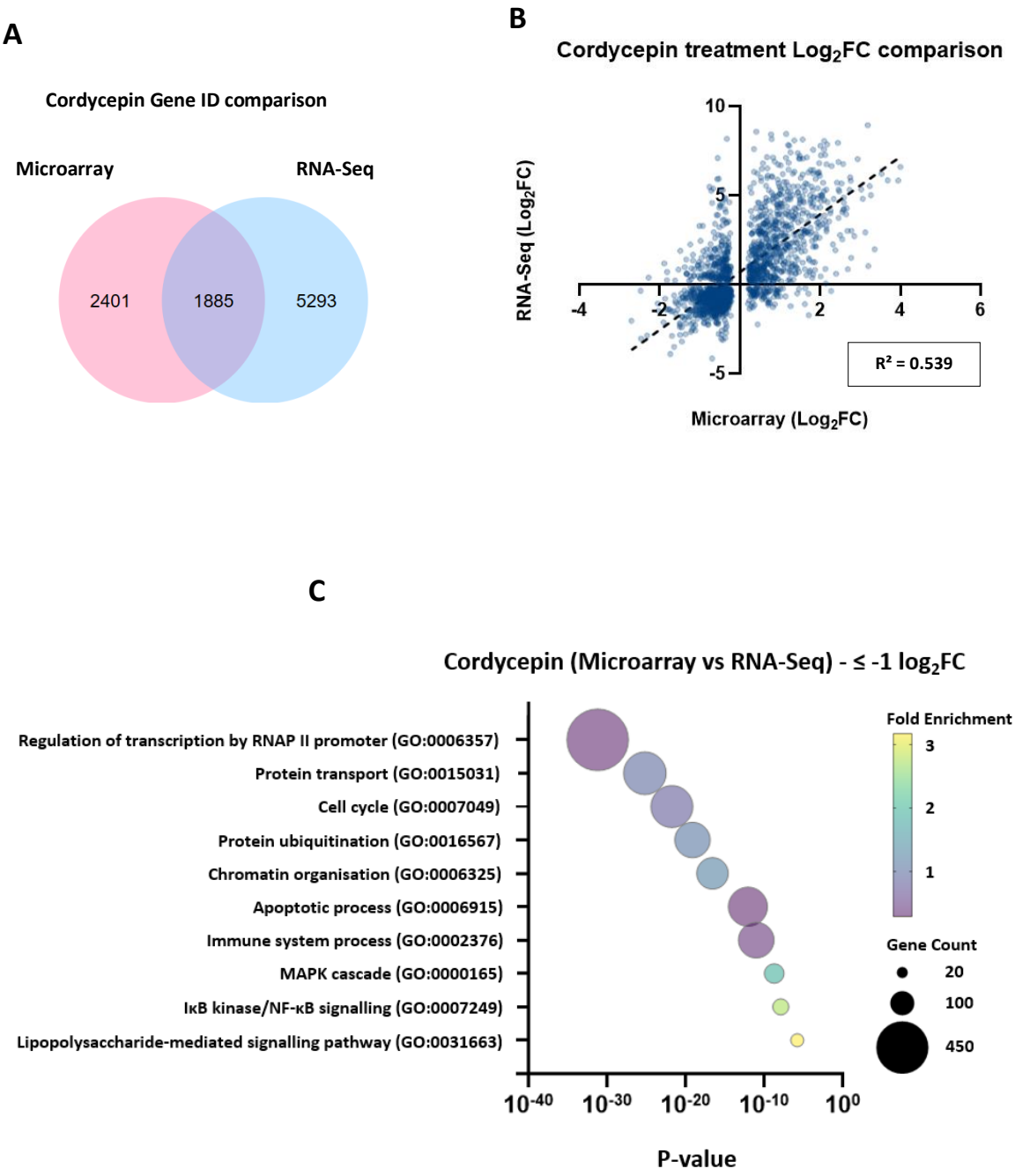

Figure 3.17: Overlap of differentially expressed genes between the microarray and RNA-Seq datasets with cordycepin treatment. Differentially expressed genes for cordycepin treatment (20 µM) was compared to DMSO (0.02% v/v) treatment with LPS inflammatory stimulation in RAW264.7 macrophages. **A)** Venn diagram of all genes with statistical significance (≤ 0.05 p-value) for both datasets including overlapping genes. **B)** Scatter plot of Log_2FC of the overlapping genes (1,885). **C)** Top 10 enriched GO biological pathway terms obtained through DAVID[690] for all repressed genes (≤ -1 Log_2FC) which overlapped between the microarray and RNA-Seq datasets for cordycepin treatment.

The RNA-Seq dataset of cordycepin treatment was compared to the WDR33 knockdown dataset as previously there was a relatively low positive correlation (R^2 = 0.135) and overlap between the microarray dataset of cordycepin treatment and RNA-Seq dataset of WDR33 knockdown (figure 3.12A and B). As before, all statistically significant genes were compared based on gene nomenclature, showing an overlap of 2,163 genes between cordycepin treatment and WDR33 knockdown (figure 3.18A), which is smaller than genes which are only differentially expressed with cordycepin treatment (5,015). There was a positive correlation between the cordycepin treatment and WDR33 knockdown based on Log_2 fold change (R^2 = 0.207), somewhat higher than the positive correlation with the microarray dataset of cordycepin treatment with WDR33 knockdown (R^2 = 0.135; figure 3.12B). Many inflammatory biological pathways were repressed based on downregulated overlapped genes between cordycepin treatment and WDR33 knockdown (figure 3.18C). These pathways include cellular response to TNF, LPS, and interleukin-1, general inflammatory response and NF-κB signalling, regulation of interleukin-2 production, apoptotic process, and angiogenesis (figure 3.18C). MAPK and ERK1/2 signalling cascades are upregulated as negative regulation of these cascades are enriched by downregulated overlapping genes. This effect could be through feedback mechanisms, which need further investigation.

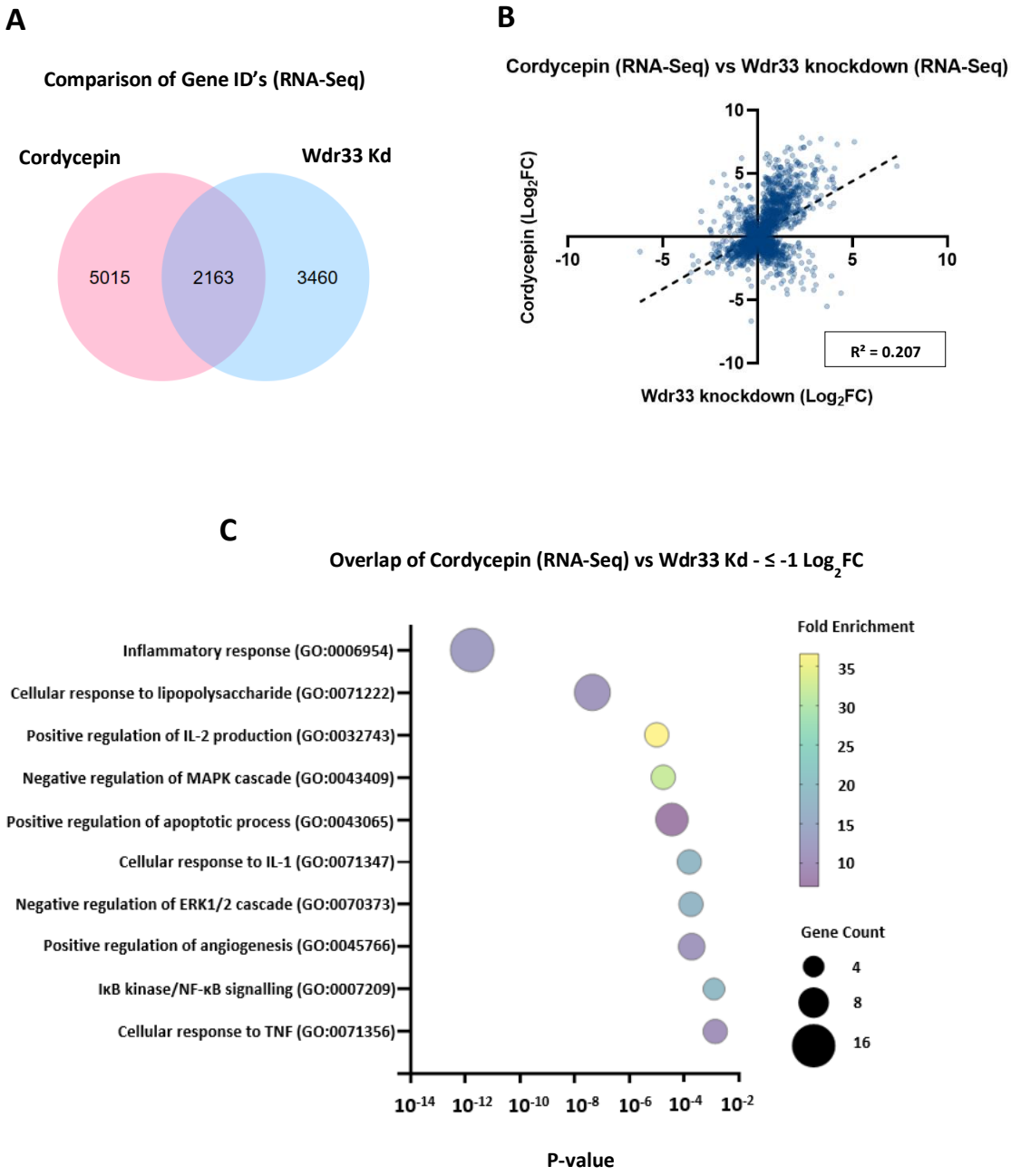

Figure 3.18: Overlap of differentially expressed genes between cordycepin treatment (RNA-Seq) and Wdr33 knockdown. Differentially expressed genes for cordycepin treatment (20 µM; RNA-Seq) was compared to Wdr33 knockdown (double knockdown of 5 nM; RNA-Seq) with 1-hour LPS inflammatory stimulation (1 µg/mL) in RAW264.7 macrophages. **A)** Venn diagram of all genes with statistical significance (≤0.05 p-value) for each treatment condition including overlapping genes. **B)** Scatter plot of Log_2FC of the overlapping genes (2,163). **C)** Top 10 enriched GO biological pathway terms obtained through DAVID[690] for all repressed genes which overlapped between cordycepin and Wdr33 knockdown.

Comparison of all significantly differentially expressed genes (≤ -1 log_2FC and ≥ 1 log_2FC; ≤ 0.05 p-value) for cordycepin treatment (RNA-Seq) and WDR33 knockdown are linked to repression of PI3K/Akt signalling, toll-like receptor signalling, interleukin-6 signalling, and multiple response pathways to pathogens through Comparison analysis in IPA (figure 3.19A). Consistent with repression of PI3K/Akt signalling, the PI3K inhibitor, LY294002, has a positive activation z-score, highlighting similar effects to gene expression to cordycepin treatment and WDR33 knockdown (figure 3.19B). As seen before (figures 3.10B & 3.13B), MEK1/2 signalling also appears to be repressed as the inhibitor, U0126, also has a positive activation z-score, however negative regulation of ERK1/2 signalling is enriched with downregulated genes, suggesting upregulation as feedback from MEK1/2 inhibition (figure 3.18C). Upstream regulators which show negative activation z-scores and opposite effects for both cordycepin treatment and WDR33 knockdown were linked to inflammation, including toll-like receptors (TLR3/4/9), TNF, TNFSF11, IL1β, LPS, and interferon-γ (IFNG). The NF-κB complex, including subunits RELA and NOD2, the adaptor TICAM1, and the RIPK2 kinase, known to modulate NOD1/2 and NF-κB signalling[724, 725], also have opposite effects to cordycepin treatment and WDR33 knockdown, suggesting reduced NF-κB transcription of proinflammatory cytokine mRNA (figure 3.19B). Upregulated canonical biological pathways include PPAR and LXR/RXR activation, known to repress cytokine production and NF-κB signalling[714-717], as well as repression of the upstream transcription factor, BHLHE40 (also known as DEC1), which is a co-repressor of RXR and LXR/RXR heterodimers[726] (figure 3.19). As shown previously (figures 3.9B, 3.10A, 3.13A, 3.15B, & 3.16A), Adenylate cyclase-activating GPCR, CREB, cAMP signalling, and phagosome formation have positive activation z-scores. This is potentially why signalling of protein kinase A (PKA), which is a cAMP-dependent kinase[727], G Beta Gamma (Gβγ) and Gαs signalling, subunits of GPCRs which activates adenylate cyclase[728-731], and Calcium signalling, which can be regulated by GPCRs[732], are upregulated in figure 3.19A. Altogether, inflammatory biological pathways and regulators are repressed by both cordycepin treatment and WDR33 knockdown, whereas GPCR-mediated regulation of cAMP and CREB transcription are upregulated (figures 3.13A & 3.19).

A

Canonical Pathways

	Cordycepin + LPS	Wdr33 knockdown (+LPS)
PI3K/AKT Signalling	-2.982	-2.828
Role of PRR's in Recognition of Bacteria and Viruses	-2.858	-1.633
Toll-like Receptor Signalling	-2.714	-1.890
IL-6 Signalling	-2.524	-3.207
Hypercyto/chemokinemia in the Pathogenesis of Influenza	-2.200	-3.000
Type II Diabetes Mellitus Signalling	-2.111	-1.890
Role of PKR in Interferon Induction and Antiviral Response	-2.065	-1.265
PPARα/RXRα Activation	2.132	1.134
PPAR Signalling	2.500	3.317
Gαs Signalling	2.558	2.236
Protein Kinase A Signalling	2.626	2.357
Ephrin Receptor Signalling	3.402	1.890
G Beta Gamma Signalling	3.545	1.000
cAMP-mediated signalling	4.323	2.183
LXR/RXR Activation	4.491	2.449
Calcium Signalling	4.768	1.342
Breast Cancer Regulation by Stathmin1	5.277	3.536
Synaptogenesis Signalling Pathway	6.677	2.530
Phagosome Formation	7.309	3.507
CREB Signalling in Neurons	7.544	3.413

Activation Z-score

B

Upstream Regulators

Upstream Regulator	Molecule Type	Cordycepin (+LPS)	Wdr33 knockdown (+LPS)
TICAM1	Adaptor	-3.140	-3.517
Lipopolysaccharide	Chemical drug	-5.492	-6.856
poly rI:rC-RNA	Chemical drug	-4.399	-5.749
Resiquimod	Chemical drug	-3.475	-4.461
PDGF BB	Complex	-3.681	-4.668
IL1β	Cytokine	-2.826	-5.983
TNFSF11	Cytokine	-4.445	-4.992
TNF	Cytokine	-4.038	-4.692
IFNG	Cytokine	-2.957	-4.180
RIPK2	Kinase	-3.002	-3.423
MAPK8	Kinase	-2.555	-3.234
U0126	Kinase inhibitor (MEK1/2)	1.355	4.724
LY294002	Kinase inhibitor (PI3K; mTOR; CSK2)	1.908	3.143
RELA	NF-κB subunit	-2.966	-4.677
NOD2	NF-κB subunit	-2.690	-4.313
TLR4	Toll-like receptor	-3.250	-4.322
TLR9	Toll-like receptor	-2.592	-3.678
TLR3	Toll-like receptor	-2.919	-3.027
NF-κB (complex)	Transcription factor	-1.745	-5.530
BHLHE40	Transcription factor	-4.850	-2.714

Activation Z-score

Figure 3.19: Comparison of biological canonical pathways and upstream regulators consistently affected between cordycepin treatment and Wdr33 knockdown (RNA-Seq). Differentially expressed genes for cordycepin treatment (20 µM; RNA-Seq) was compared to Wdr33 knockdown (double knockdown of 5 nM; RNA-Seq) with 1-hour LPS inflammatory stimulation (1 µg/mL) in RAW 264.7 macrophages. All significantly differentially expressed genes (≤ -1 log_2FC and ≥ 1 log_2FC; ≤ 0.05 p-value) for both treatments were compared in IPA[691]. **A)** biological canonical pathways and **B)** upstream regulators.

3.6 Discussion

The data in this chapter on RAW264.7 macrophage inflammatory stimulation demonstrates the broad genome-wide anti-inflammatory effects of cordycepin treatment and knockdown of WDR33, to further link polyadenylation to inflammatory stimulation. Consistently, there is repression to LPS and cytokine stimulations, immune response, and inflammatory biological pathways through enrichment of downregulated genes (figures 3.2A, 3.3, 3.5, 3.7, 3.9A, 3.10-12, 3.13B, 3.15A, 3.16B, & 3.19). This anti-inflammatory effect associated with polyadenylation machinery has been seen with knockdown of CPSF4, linked to decreased COX-2 transcription through repressed NF-κB nuclear translocation in lung cancer progression, and with both CPSF4 and WDR33 knockdown in Osteoarthritis[384, 630]. The overlap of the statistically significant differentially expressed genes between cordycepin treatment and WDR33 knockdown is not very large (positive correlation R^2 range = 0.135 (microarray) to 0.207 (RNA-Seq); figures 3.12B & 3.18B), which is further confirmed through qPCR of inflammatory mRNA markers (figures 3.5 & 3.11). However, this positive correlation is quite remarkable considering WDR33 knockdown is a 48-hour protocol, and cordycepin treatment is for only 1-hour prior to 1-hour LPS inflammatory stimulation. However, considering the microarray and RNA-Seq datasets for cordycepin treatment had a higher, but relatively poor correlation (R^2 range = 0.539; figure 3.17B), potentially through differences in the two platforms or technical variability, the RNA-Seq correlation between WDR33 knockdown and cordycepin is relatively close (figure 3.18B). The differences seen in expression profile and qPCR results of WDR33 knockdown could be through RAW264.7 macrophages adapting to the reduced polyadenylation machinery over the 48-hour period, or potentially through suboptimal knockdown of WDR33 mRNA (~55% knockdown; figure 3.11B). Future work should include prolonged cordycepin treatment at a lower concentration over a 48-hour period in RAW264.7 macrophages, to directly compare against the 48-hour WDR33 knockdown to substantiate whether cordycepin exerts its anti-inflammatory effects through WDR33.

Repression of the LPS stimulation of MyD88-dependent and independent pathways and NF-κB transcription in RAW264.7 macrophages is also notably affected by cordycepin treatment and WDR33 knockdown. Crucial key mediators including multiple toll-like receptors (TLR3/4/9), LPS, MyD88, TICAM1 (TRIF), RIPK2 kinase, RELA, NOD2, and the NF-κB complex all have negative activation z-scores for

cordycepin treatment and WDR33 knockdown (figures 3.3B, 3.10B, 3.13B, 3.16B, & 3.19B). This altogether suggests that cordycepin affects LPS:TLR4:MD2 signalling upstream to NF-κB transcription, demonstrated in figure 3.20. Furthermore, nuclear translocation and activation of NF-κB (p65) is also significantly repressed by cordycepin treatment (figure 3.4). Coupled with reduced NF-κB nuclear localisation with WDR33 knockdown in RAW264.7 macrophages by Ashraf *et al.* (2019)[384], it is clear that NF-κB-mediated transcription of proinflammatory cytokine and interferon mRNA is repressed. This result contrasts with previous published work by Kondrashov *et al*. (2012)[7], which demonstrated that IκBα degraded normally and NF-κB (p65) translocated to the nucleus with cordycepin treatment in Human airway smooth muscle cells. It could be that this is a cell-specific effect, as highlighted in the review by Radhi *et al*. (2021)[3], and that cordycepin represses NF-κB activation predominantly in RAW264.7 macrophages, as previous research supports the findings demonstrated in this chapter[364, 384, 699].

Due to this repression of NF-κB, there may be an increase in the transcription factor HIF-1α, important in response to hypoxia, which is known to cross-talk with NF-κB[733]. HIF-1α is known to counteract NF-κB repression through the indirect hyperphosphorylation of IκB and phosphorylation of the p65 subunit of NF-κB[734]. This is potentially why response to hypoxia is an upregulated biological pathway for cordycepin treatment, counteracting the repression of NF-κB (figure 3.2B). Polyubiquitination, induced by interleukin-1, plays a crucial role in the formation of polyubquitin chains interacting with IRAK1, TRAF6, and NF-κB regulatory elements upstream to NF-κB activation[198, 201, 202]. This process is clearly affected by both cordycepin treatment and WDR33 knockdown, as cellular response to interleukin-1 is enriched with downregulated genes (figures 3.2A, 3.9A, & 3.18C), and protein ubiquitination is enriched with overlapped downregulated genes of cordycepin treatment (figure 3.17C). IRAK4, important for promoting polyubiquitination of IRAK1 *in vivo*[198], also has opposing effects to cordycepin and WDR33 knockdown (figure 3.13B), further substantiating that cordycepin and WDR33 knockdown represses NF-κB signalling.

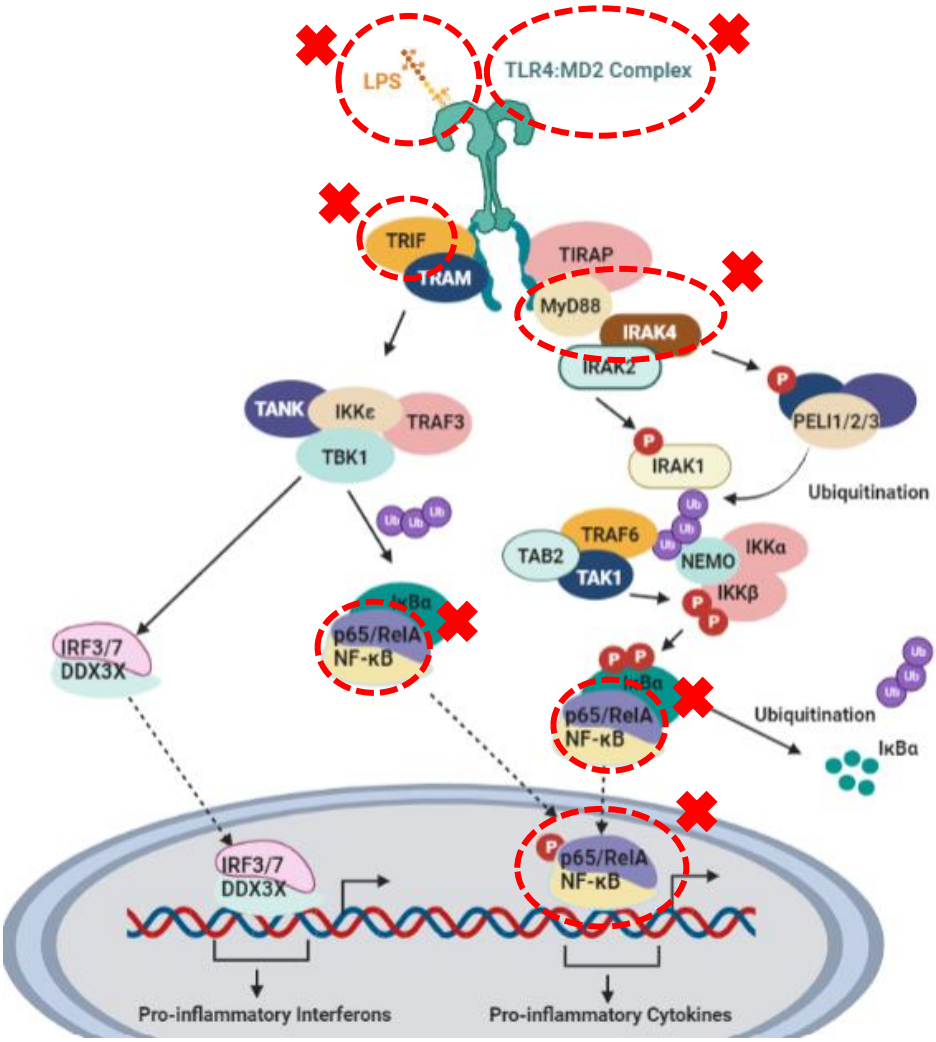

Figure 3.20: Cordycepin affects multiple components of the LPS:TLR4:MD2 signalling pathway. Based on differential expression output of cordycepin treatment from Chapter 3, cordycepin has been found to repress multiple components of LPS:TLR4:MD4 signalling (circled in red), leading to reduced nuclear translocation of NF-κB.

Through IPA analysis, Resveratrol, had a positive activation z-score, indicating a similar effect on gene expression to cordycepin (figure 3.3B). This link could be due to the repression of PTGS2 and NF-κB by Resveratrol[735, 736]. Alternatively, cordycepin treatment and WDR33 knockdown was found to act in an opposite manner to Resiquimod (figure 3.3B, 3.10B, & 3.16B), which is an agonist of TLR7/8 and has a role in immune stimulation[737]. Both cordycepin treatment (microarray dataset) and knockdown of WDR33

were found to have an opposite effect to Prexasertib activity (figure 3.13B). Prexasertib is a selective ATP-competitive small-molecule inhibitor of checkpoint kinase 1 (CHK1) known to upregulate transcription of proinflammatory cytokines, chemokines, and activate Macrophages and T-cells[738, 739]. This effect to CHK1 potentially links to the effect seen by cordycepin treatment on cell cycle G1/S checkpoint regulation (figure 3.3A).

Both cordycepin treatment and WDR33 knockdown upregulate biological pathways for adenylate cyclase-activating GPCR, CREB, cAMP signalling, and phagosome formation (figures 3.9B, 3.10A, 3.13A, 3.15B, & 3.16A), which as described previously, is most likely why PKA[727], Gβγ and Gαs[728-731], and Calcium signalling[732] are also upregulated (figure 3.19A). Consistent with data in this chapter, cordycepin upregulating cAMP and CREB signalling could be linked to inhibition of NF-κB transcription[740]. Activation of GPCRs, coupled to the Gαs subunit proteins, activate adenylate cyclase and elevates levels of cAMP, which thereby activates PKA[727, 730, 741, 742]. PKA has been found to inhibit mTORC1, through phosphorylating Raptor at Ser791, potentially through interaction with PKA anchoring protein, AKAP8L[743, 744]. Data presented in this chapter also shows that cordycepin treatment and WDR33 knockdown can repress PI3K/Akt signalling (figures 3.13A & 3.19A) and has similar effects to gene expression as the PI3K inhibitor, LY294002. Coupled with similar effects to MEK1/2 inhibitor, U0126, this indicates that polyadenylation can influence PI3K/Akt/mTOR and MEK1/2 signal transduction pathways, which needs further investigation.

Cordycepin treatment and WDR33 knockdown appears to be associated with positive regulation of cholesterol efflux (figure 3.2 B), which is linked to LXR/RXR activation, a pathway which is also associated with WDR33 knockdown (figures 3.3A, 3.10A, 3.13A, 3.16A, & 3.19A). The LXR pathway represses AP-1 through forming a complex with small ubiquitin-like modifier (SUMO) and the nuclear corepressor (NCoR) leading to SUMOylation[745, 746], which in turn represses the ATP-binding cassette transporter, ABCA1, leading to cholesterol efflux[747]. The LXR pathway is also essential for lipid metabolism and plays an important role in macrophage apoptotic cell clearance and repression of pro-inflammatory cytokine production[748, 749]. Alternatively, LXR activation also leads to repression of TLR4 and LPS stimulation of Il1β and Ptgs2 expression in macrophages[750]. The RXR pathway heterodimerises to PPARs[715], in which PPARγ is a known inhibitor of the transcription factors NF-κB, AP-1, and STAT in macrophages and

monocyte production of cytokines[716, 717]. PPARγ also simultaneously induces induction of LXRα and the ATP-binding cassette transporter, ABCA1, leading to cholesterol efflux and atherogenesis in macrophages[751]. This accumulatively highlights a potential mechanism of cordycepin, as activation of PPARs and LXR/RXR signalling links to the repression of NF-κB and proinflammatory biological pathways, which needs further research.

Altogether, these results suggest that both cordycepin treatment and WDR33 knockdown can exert repression of LPS:TLR4:NF-κB pro-inflammatory cytokine production. This effect could potentially be through upregulation of the LXR/RXR or RXR/PPAR pathways, which would be an interesting future direction of this research. The difference between cordycepin treatment and WDR33 knockdown may be because arresting WDR33, potentially through cordycepin treatment, is not the same as removing the protein entirely, during inflammatory stimulation. It is also probable that the cells have somewhat adapted to the reduced polyadenylation machinery in the WDR33 knockdown over the treatment time course. Given there is a big difference in treatment timescales between the treatment conditions, the overlap is quite remarkable (figures 3.12B & 3.18B). Altogether, cordycepin and WDR33 knockdown do have significant anti-inflammatory effects in RAW264.7 macrophages, which correlates with previous research in the lab[7, 384], with a prominent link to repression as upstream to LPS:TLR4 to NF-κB transcription. Furthermore, biological pathways associated with chronic inflammation are also repressed by cordycepin treatment, such as hypercyto -chemokinemia, and APR for both treatment conditions (figures 3.3A, 3.10A, 3.13A, 3.16A, & 3.19A). This provides a rationale for further research on potential therapeutic benefits of cordycepin and poly(A) machinery modulation to chronic inflammatory pathogenesis, and whether the effect of cordycepin is through polyadenylation.

As PI3K/Akt and MEK1/2 signalling are repressed by cordycepin and WDR33 knockdown (figures 3.13A & 3.19A), more work is needed to see whether repression of these pathways is the mechanism in which cordycepin affects inflammation. Going forward, further work is needed to research consistent effects with cordycepin treatment in other cell types and conditions, such as serum-dependent stimulation, to gain a provide a clearer idea of mechanisms of action of polyadenylation through cordycepin treatment, which will be addressed in the next chapter.

4 Cordycepin represses growth-factor responses and serum-dependent signalling

4.1 Introduction

Breast cancer is the most prevalent cancer worldwide for women and is a phenotypically diverse cancer with a large degree of genetic and epigenetic heterogeneity characterised by hormone receptor status[261-264, 752, 753]. This is evident for immortalised Breast Adenocarcinomas, MCF-7 cells, which have functional estrogen and EGF receptors, whereas MDA-MB-231 cells are triple-negative for ERs, PRs and HER2 (hormone-independent for estrogen and progesterone) and more aggressive[268, 286, 287]. Metastasis initiation in breast cancer relies on the complex coordination of biological processes regulated by events in the tumour microenvironment (TME; stromal)[275]. This promotes epithelial-to-mesenchymal transition (EMT), the formation of cancer stem cell (CSC's), tumour growth and migration of tumour into the bloodstream through angiogenesis[277]. Prominent regulatory hormone factors of EMT are insulin-like growth factors (IGF's), hepatocyte growth factors (HGFs), epidermal growth factors (EGFs), platelet-derived growth factors (PDGFs), transforming growth factor β (TGF-β), and cytokines[276]. These factors bind and activate associated receptor tyrosine kinases (RTKs), such as EGF binding to EGFR, and mediate downstream PI3K/Akt, MAPK/ERK, and JAK/STAT signalling. These pathways are crucial in cancer pathogenesis through promoting proliferation, angiogenesis, and metastasis[278, 279]. Amplification of the growth factor receptors are common in many cancers, making them targets in anti-cancerous therapeutics[281-284]. Clearly therefore, growth factors, their receptors and their influence on gene expression are very important in cancer, including breast cancer.

In the previous chapter, cordycepin and knockdown of poly(A) machinery were found to repress inflammatory stimulation, highlighting a potential role of polyadenylation in inflammation. It is already well established that alternative polyadenylation is implicated in many cancers, producing mRNA transcript isoforms with shortened 3'UTRs able to evade miRNA-mediated degradation[469, 470, 565, 566, 754]. Components of polyadenylation are also associated with cancer progression, such as the roles of CPSF1 and PABPN1[567], and reduced function of NUDT21 or loss-of-function of CPSF6[477, 642, 755, 756]. Upregulation of CPSF3 is known to promote triple-negative breast cancer stemness and metastasis, with inactivation of CPSF3 linked to reduced tumorigenesis[757]. It is also known that CPSF4 plays a key role in upregulating

human telomerase reverse transcriptase (hTERT) leading to lung tumorigenesis and poor prognosis[758]. It has also been recently found that CPSF4 binds to MDM4 promoter and significantly enhances metastasis through mediating EMT of triple-negative breast cancer cells, such as MDA-MB-231[759]. It has been publicised and described in a systematic review that cordycepin can repress metalloproteinases, which are important for the activation of TGF-β cytokines and degradation of the EMT to mediate metastasis[3, 703, 760-762]. Altogether this demonstrates the importance of further research into the roles of polyadenylation in cancer progression and the potential therapeutic effect of modulating polyadenylation in cancer. This will be explored in this chapter through the comparison of multiple high-throughput datasets with cordycepin treatment in cell lines with serum stimulation, as FBS used to supplement media contains many growth factors, such as EGF, FGF, IGF, PDGF, and TGF[763].

4.2 Cordycepin affects multiple serum-dependent signalling pathways stimulated by growth factor response

In order to get an overview of the effect of cordycepin on serum-dependent signalling, microarray data which was analysed previously by Dr. Asma Khurshid[664] was re-analysed in this study using the LIMMA method[665] to allow comparison to other datasets. Differentially expressed genes for cordycepin treatment compared to DMSO control was obtained following the method detailed in Methods section 2.6.1.1. Expanding on Methods section 2.6.1; Asma seeded MCF-7 cells 24-hours prior to 2-hour treatment of either cordycepin (50 μM) or DMSO (0.05% v/v). This was performed in quadruplicate, with RNA extracted before cDNA synthesis and use in an Agilent microarray platform.

A volcano plot of the spread of expression highlights that there are an almost equal number of upregulated genes (300; ≥ 1 Log_2FC & ≤ 0.05 p-value) and downregulated genes (525; ≤ -1 Log_2FC & ≤ 0.05) (figure 4.1A). Most genes (33,268) did not meet a statistical significance of ≤ 0.05 p-value and were within the Log_2FC range of +1 to -1. These genes were excluded from further analysis as they were not statistically significant and did not reach a threshold of ≥ 1 or ≤ -1 Log_2FC change in expression with cordycepin treatment (figure 4.1A).

The Functional Annotation Tool in the DAVID Bioinformatics Resource (LHRI, version 6.8)[690] was used to obtain Gene Ontology (GO) analysis output of enriched biological pathways associated with the downregulated genes illustrated in the volcano plot (figure 4.1A). Downregulated genes with cordycepin treatment show repression of transcription from RNAP II promoter, protein ubiquitination, cellular response to glucose starvation, cell cycle pathways, vasculogenesis and angiogenesis (figure 4.1B). Predominantly, zinc-finger protein mRNAs are repressed by cordycepin treatment in the regulation of transcription from Pol II, however some early response genes are also repressed, such as *JUNB*, *EGR1*, *ATF3*, and *MYC* (figure A.2.5A). Negative regulation of Notch signalling and apoptotic process were also enriched with downregulated genes with cordycepin treatment (figure 4.1B). Upregulated genes with cordycepin treatment of MCF-7 cells are associated with translation reinitiation and ribosome disassembly, however this is only based on two mRNAs; *MCTS1* and *DENR* (figure A.2.5B).

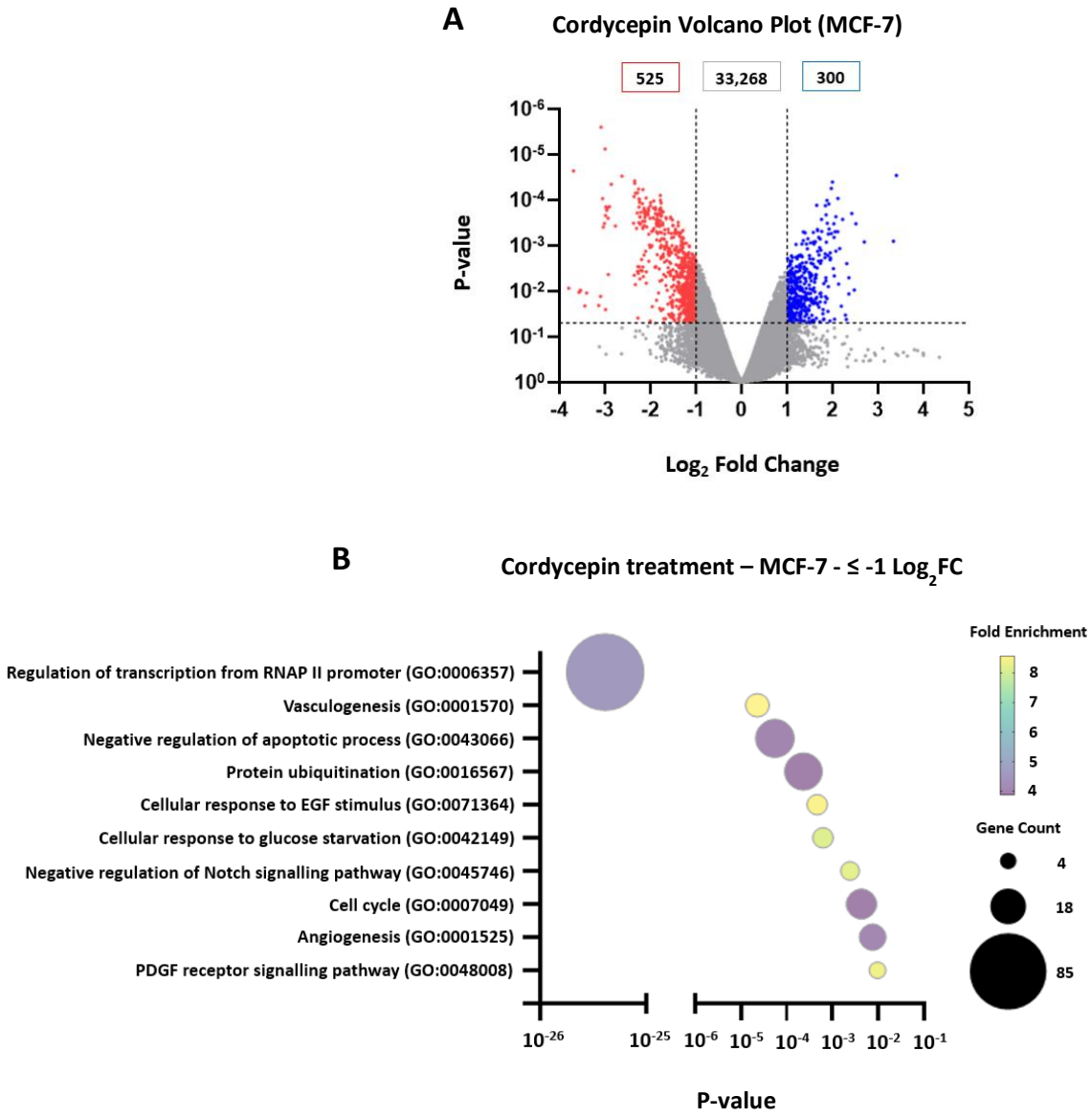

Figure 4.1: Differential expression analysis of cordycepin treatment in MCF-7 indicates repression of serum-dependent signalling. Differentially expressed genes obtained from microarray output was analysed using the LIMMA method[665] of 2-hour cordycepin (50 µM) compared to DMSO (0.05% v/v). **A)** Volcano plot showing the spread of expression with cordycepin treatment. Red denotes downregulated genes with ≤ -1 Log_2FC & ≤ 0.05 p-value, blue denotes upregulated genes with ≥ 1 Log_2FC & ≤ 0.05 p-value, grey denotes genes which do not meet these requirements. **B)** Bubble plot indicate enriched biological pathways associated with repressed genes (red dots from **A)**) through DAVID Gene Ontology[690].

Inclusion of all statistically significant genes (≤ 0.05 p-value) with cordycepin treatment of MCF-7 cells into the Expression Analysis tool of IPA[764] also highlighted biological pathways and upstream regulators associated with the stimulation of growth factors. Signalling pathways such as TGF-β signalling, Estrogen-mediated S-phase entry, mTOR, and ERK5 signalling were also repressed with cordycepin treatment (figure 4.2A). This was shown with negative activation z-scores, a predictive score used to infer activation states of biological pathways based on the direction of gene regulation. Multiple inflammatory pathways were also repressed with cordycepin treatment including CXCR4 signalling, RIG1-like receptors, HMGB1 signalling, toll-like receptors, TNFR1 signalling, and interleukin-1, 6, and 17 signalling (figure 4.2A). The only biological pathway which is upregulated with cordycepin treatment is PPAR signalling (figure 4.2A).

Upstream regulators which had a positive activation z-score and similar effect to cordycepin treatment in MCF-7 cells was inhibitors of kinase modulators, such as LY294002 (PI3K inhibitor), U0126 (MEK1/2 inhibitor), SU6656 (Src and PDGF receptor inhibitor), and SP600125 (JNK inhibitor) (figure 4.2B). Regulators which have a negative activation z-score and an opposite effect on downstream expression to cordycepin treatment in MCF-7 cells was associated with TNF, EGF, HGF and PDGF BB stimulation, PI3K, p38 MAPK and ERK1/2 signalling (figure 4.2B). The transcription regulator, NUPR1, cAMP responsive elements CREM and CREB1, and G protein-coupled estrogen receptor, GPER1, were also found to have an opposite effect on expression to cordycepin treatment (figure 4.2B). Altogether, cordycepin can repress biological pathways and upstream regulators associated with growth factor response in MCF-7 Breast Adenocarcinomas (figures 4.1 and 4.2).

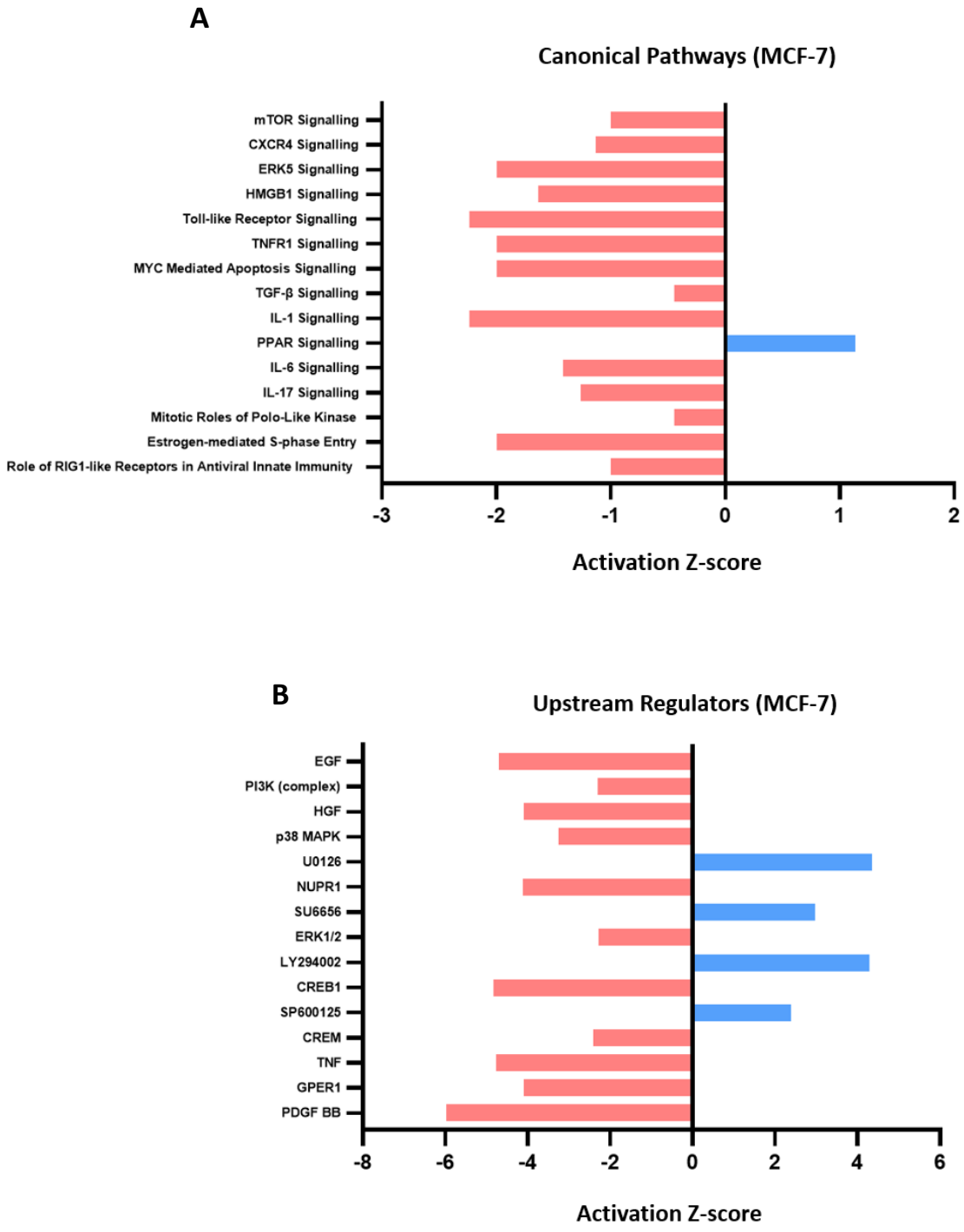

Figure 4.2: Cordycepin represses growth factor-dependent canonical biological pathways and upstream regulators in MCF-7 cells. Differentially expressed genes with statistical significance (≤ 0.05 p-value from moderated t-statistic) of 2-hour cordycepin (50 µM) treatment compared to DMSO (0.05% v/v) in MCF-7 cells obtained using the LIMMA method[665] were used for entry into IPA[691]. **A)** Indicates the top biological canonical pathways which are repressed (red bars) or upregulated (blue bars) with cordycepin treatment. **B)** Indicates the top upstream regulators which act in an opposite way (red bars) or act similarly (blue bars) to cordycepin treatment based on activation z-score.

4.3 Cordycepin represses serum-dependent mRNA expression in MCF-7 Breast Adenocarcinomas

To provide further evidence that cordycepin represses growth factor response in MCF-7 cells to previous results in the chapter (figures 4.1 & 4.2), the abundance of serum-dependent mRNA markers was assessed through qPCR. These markers used in figure 4.3 were chosen based on association with breast cancer development and are known to be stimulated in the presence of growth factors (figure 4.1). MCF-7 cells were seeded 24-hours prior to 2-hour treatment of cordycepin (50 µM) or DMSO (0.05% v/v) added directly into media detailed in Methods section 2.1.1, before RNA extraction and cDNA synthesis in triplicate.

In comparison to DMSO, cordycepin (50 µM) resulted in statistically significant repression of mRNA levels of key proto-oncogene transcription factors MYC (p-value = ≤ 0.0001) and JUNB (p-value = ≤ 0.001), and the stress-induced transcription factor ATF3 (p-value = ≤ 0.01) (figure 4.3). The serine/threonine protein kinases SGK1 (p-value = ≤ 0.01), and PLK2 (p-value = ≤ 0.0001), were also repressed with cordycepin (50 µM) treatment, suggesting reduced phosphorylation of SGK1 and PLK2 targets (figure 4.3). The protein tyrosine/threonine phosphatase oncogene, DUSP1, was also significantly repressed (p-value = ≤ 0.01) with cordycepin (50 µM) treatment, suggesting oncogenesis is repressed with cordycepin treatment (figure 4.3). Expression of BCAR3, a marker of anti-estrogen resistance in breast cancer[765], is also repressed with cordycepin (50 µM) treatment, highlighting that cordycepin could affect breast cancer progression (p-value = ≤ 0.01; figure 4.3).

ACTB is an abundant mRNA used in this experiment as a housekeeping gene and shows that there is not a statistically significant difference in expression between cordycepin (50 µM) and DMSO treatments (figure 4.3).

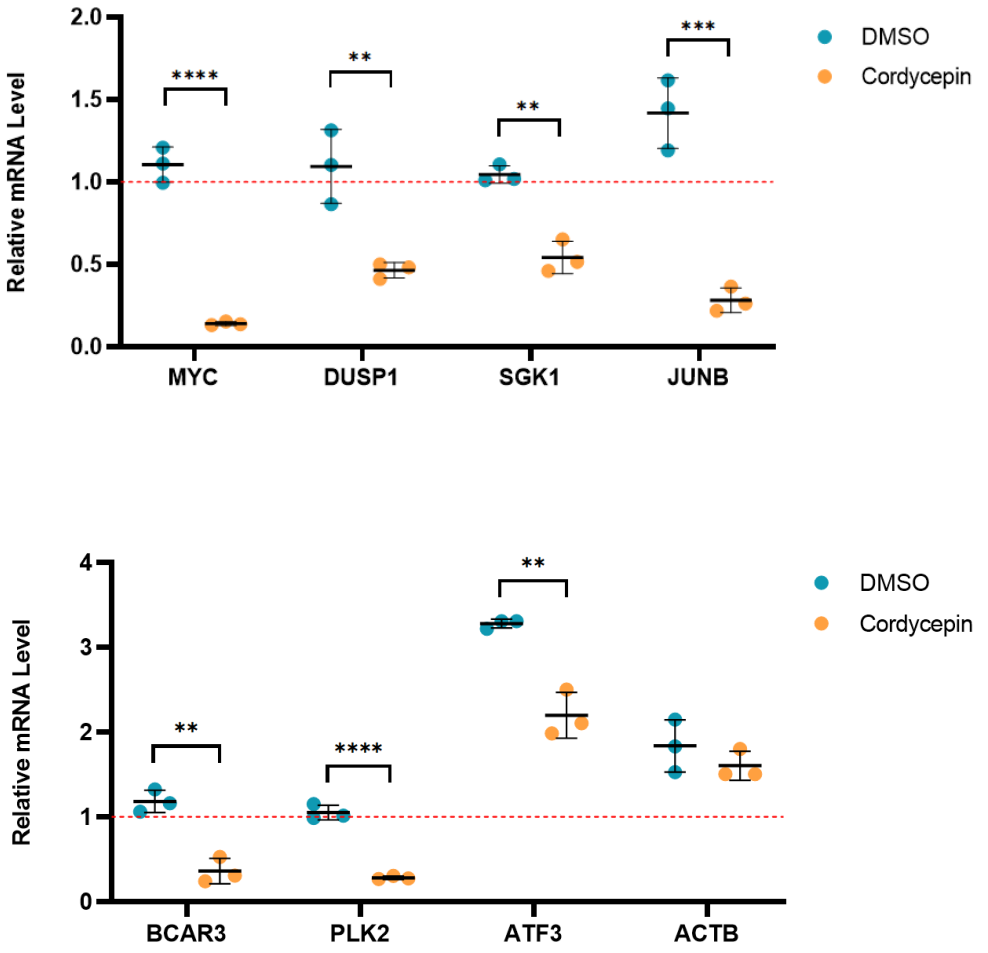

Figure 4.3: Cordycepin represses relative mRNA expression of serum-dependent markers. MCF-7 Breast adenocarcinomas were seeded for 24-hours prior to treatment for 2 hours with cordycepin (50 µM) or DMSO (0.05% v/v) before total RNA extraction, cDNA synthesis, and qPCR. Copy threshold (Ct) values for serum-dependent genes were analysed using the 2-ΔΔCt method[660] and normalised to the Ct values of GAPDH (housekeeping gene). Relative mRNA expression of tested genes is presented as the Log_2 Fold Change relative to untreated MCF-7 cells. (mean ± SD; n=3 independent experiments; Student's t-test was used to determine statistical significance against DMSO (0.05% v/v) and representative of; *P<0.05, **P<0.01, ***P<0.001, ****P<0.0001).

This chapter has shown the effects of cordycepin treatment on MCF-7 cells, which have functional estrogen and EGF receptors (figures 4.1-4.3). For comparison to this cell line, RNA-Seq analysis of cordycepin treatment of triple-negative hormone insensitive MDA-MB-231 cells was used to determine consistent effects to growth factor response with cordycepin treatment[286, 287]. This dataset was obtained

from Dr. Jialiang Lin[766]. This RNA-Seq dataset was reanalysed using the Upper Quartile normalisation (UQ) method[688, 689, 712] instead of the Rsubread method[764] as this reduced variability in the spread of differential expression (figure A.3).

A volcano plot illustrating the spread of expression of cordycepin treatment compared against DMSO demonstrates a higher number of downregulated genes (2,070; ≤ -1 Log_2FC & ≤ 0.05 p-value) compared to upregulated genes (1,125; ≥ 1 Log_2FC & ≤ 0.05 p-value) (figure 4.4A). Most of the genes (27,815) did not meet a statistical significance of ≤ 0.05 p-value and were within the Log_2FC range of +1 to -1. This high amount of non-statistically significant genes is most likely due to the presence of technical artifacts. Normalisation and removal of these artifacts was not carried out to reduce the risk of removing real biological effects as suggested previously[688]. These genes were excluded from further analysis as they were not statistically significant and did not reach a threshold of ≥ 1 or ≤ -1 Log_2FC change in expression with cordycepin treatment.

The Functional Annotation Tool in the DAVID Bioinformatics Resource (LHRI, version 6.8)[690] was used to obtain Gene Ontology (GO) analysis output of enriched biological pathways associated with the downregulated genes illustrated in the volcano plot (figure 4.4A). Downregulated genes with cordycepin treatment are enriched in transcription from RNAP II promoter, EGF stimulation, chromatin organisation and remodelling, apoptosis, and stem cell population maintenance (figure 4.4B). Multiple lysine demethylase (KDM) mRNAs and chromodomain helicase DNA binding protein mRNAs are downregulated by cordycepin treatment and enriched in chromatin organisations and remodelling (figure A.2.6A). As found previously in MCF-7 cells (figure A.2.5A), many downregulated genes enriched in the regulation of transcription with cordycepin treatment are zinc-finger mRNAs (figure A.2.6A). Besides zinc-finger mRNAs, repressed transcription factors and early growth response mRNAs were also enriched in transcription such as MYC, JUNB, MEF2C, FOS, FOXO1/3, and ELF mRNAs (figure A.2.6A).

Signalling pathways are also affected by cordycepin due to enrichment of downregulated genes associated with PI3K activity, and negative regulation of MAPK activity (figure 4.4B). The gene encoding the catalytic subunit p85β of PI3K, *PIK3R2*, is enriched in both signalling pathways and downregulated by cordycepin treatment, whereas multiple DUSP mRNAs are specifically enriched in the MAPK signalling

pathway, and multiple suppressor of cytokine signalling (SOCS) mRNAs are specifically enriched in the PI3K signalling pathway, and downregulated by cordycepin (figure A.2.6A). Repression of protein ubiquitination also appears to be associated with cordycepin treatment in MDA-MB-231 Breast Adenocarcinomas (figure 4.4B), which includes enrichment of multiple mRNAs encoding ring finger proteins (RNFs), F-box proteins (FBX), and tripartite motif proteins (TRIM) (figure A.2.6A). The mRNA's encoding NXF1, important in the nuclear export of mRNAs through association with the poly(A) tail[576], and the mRNA encoding the E3 ubiquitin ligase subunit of the CCR4-NOT deadenylation complex (*CNOT4*), are both downregulated by cordycepin and enriched in protein ubiquitination (figure A.2.6A).

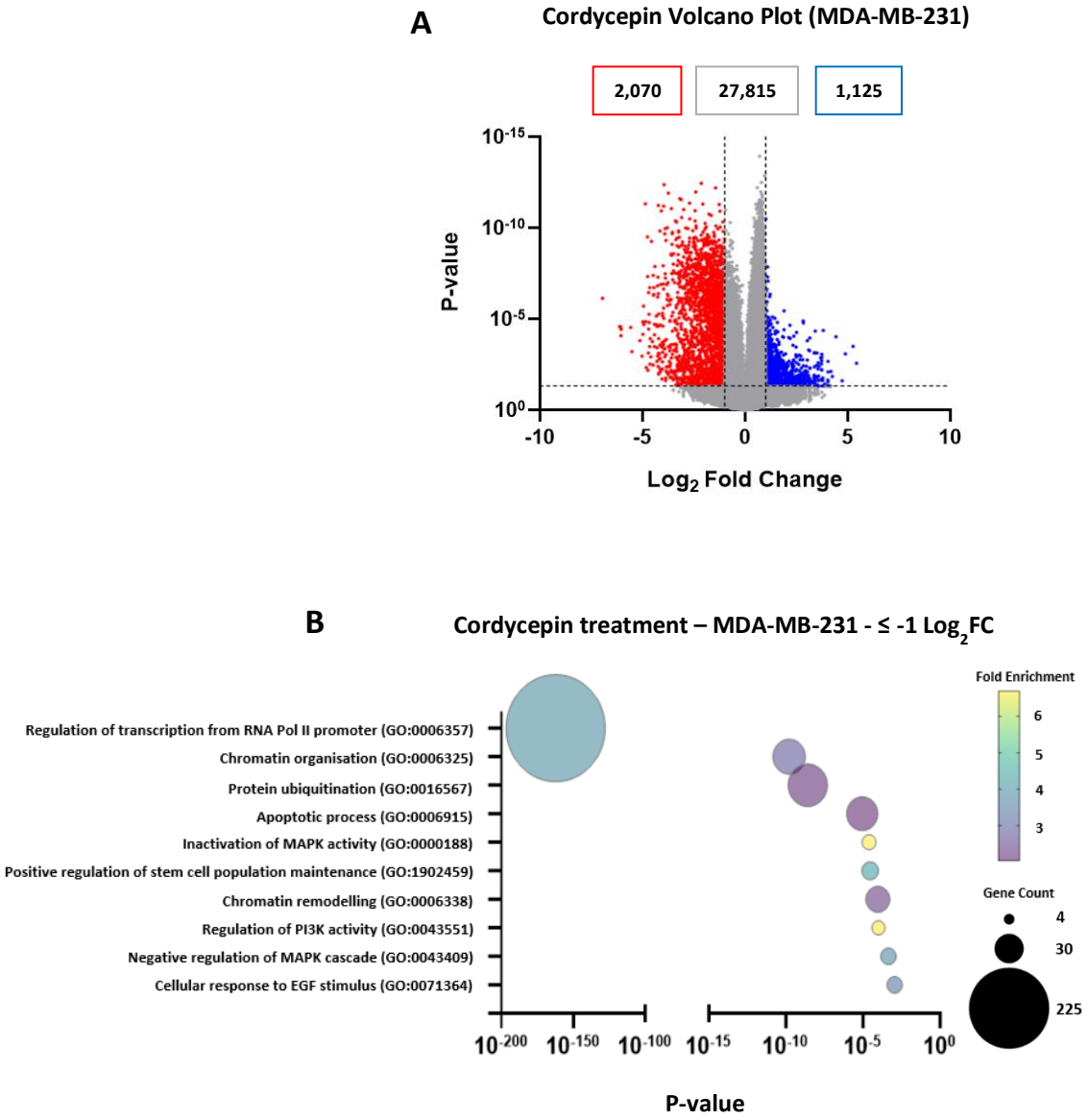

Figure 4.4: Differential expression analysis of cordycepin treatment in MDA-MB-231 indicates repression of serum-dependent signalling. Differentially expressed genes obtained from RNA-Seq RPKM values for the comparison of 2-hour cordycepin (50 µM) treatment against DMSO (0.05% v/v) treatment was analysed for Log_2FC after Upper Quartile normalisation[688, 689, 712]. **A)** Volcano plot showing the spread of expression with cordycepin treatment. Red denotes downregulated genes with ≤ -1 Log_2FC & ≤ 0.05 p-value, blue denotes upregulated genes with ≥ 1 Log_2FC & ≤ 0.05 p-value, grey denotes genes which did not meet these requirements. **B)** Bubble plot indicate enriched biological pathways associated with repressed genes (red dots from **A)**) through DAVID Gene Ontology[690].

Inclusion of all statistically significant genes (≤ 0.05 p-value) of the MDA-MB-231 RNA-Seq dataset with cordycepin treatment into the Expression Analysis tool of IPA[764] also highlighted repression of serum-dependent signalling and cancer progression (figure 4.5). Multiple growth factor signalling pathways have negative activation z-scores, including HGF, IGF-1, and TGF-β signalling (figure 4.5A). Growth factors were also shown to have opposite effects to expression compared to cordycepin treatment as the upstream regulators EGF, HGF, and PDGF BB also had negative z-scores (figure 4.5B). Inflammatory pathways associated with cancer progression, IL-6 signalling, NF-κB, and TNFR1/2 signalling, were also shown to be repressed by cordycepin treatment (figure 4.5A). Signalling pathways associated with cancer progression were also repressed with cordycepin, such as HER2 signalling in Breast Cancer, Estrogen-mediated S-phase Entry, Unfolded protein response, iNOS signalling, Prolactin signalling, and MYC-mediated apoptosis (figure 4.5A). The only biological pathway which was found to be upregulated with cordycepin treatment in MDA-MB-231 cells was PPAR signalling (figure 4.5A).

Upstream regulators which had a positive activation z-score and similar effect to cordycepin treatment in MDA-MB-231 cells was the zinc-finger protein GLI1, the kinase CDK19, PI3K inhibitor LY294002, MEK1/2 inhibitor U0126, and CDK7 inhibitor THZ2 (figure 4.5B). Regulators which have an opposite effect to downstream expression to cordycepin treatment in MDA-MB-231 cells is the effect of ERK and PI3K activity, the Eukaryotic initiation factor EIF2AK3, the GPER1 receptor, and transcription regulator, NUPR1. Inhibitors of topoisomerase, Camptothecin, and CHK1/2 inhibitor, Prexasertib, also had similar effects to cordycepin treatment (figure 4.5B). This together shows that cordycepin can repress serum-dependent signalling pathways and pathways associated with cancer progression in MDA-MB-231.

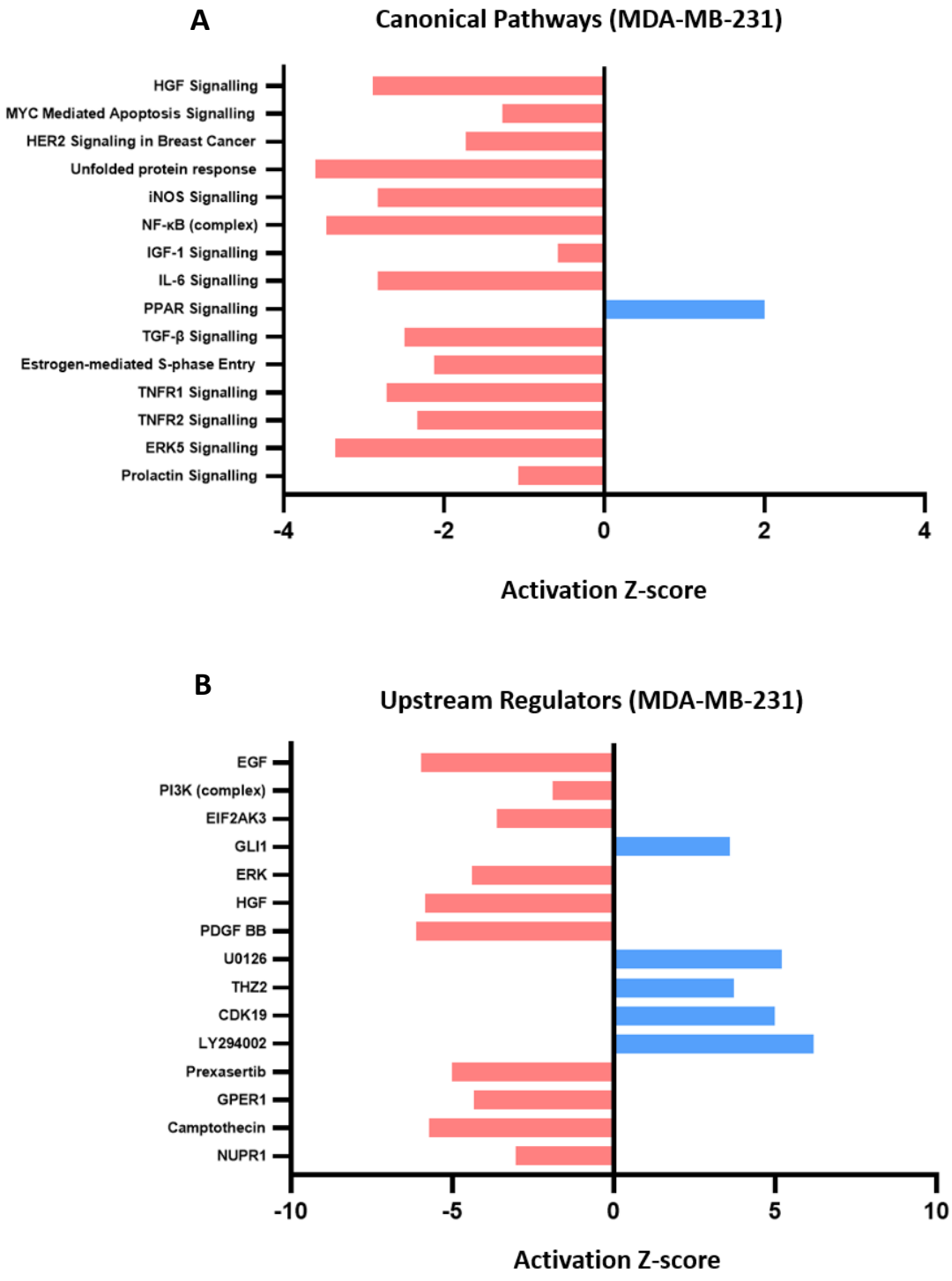

Figure 4.5: Cordycepin represses serum-dependent canonical biological pathways and upstream regulators in MDA-MB-231 Breast Adenocarcinoma. All statistically significant differentially expressed genes (≤ 0.05 p-value) obtained from RNA-Seq RPKM output analysed through Log_2FC after Upper Quartile normalisation[688, 689, 712] of 2-hour cordycepin (50 µM) treatment compared to DMSO (0.05% v/v) were used for entry into IPA[691]. **A)** Indicates the top biological canonical pathways which are repressed (red bars) or upregulated (blue bars) with cordycepin treatment. **B)** Indicates the top upstream regulators which act in an opposite way (red bars) or act similarly (blue bars) to cordycepin treatment based on activation z-score.

As shown in this chapter, cordycepin has been found to repress biological pathways and upstream regulators associated with serum-dependent signalling in Breast Adenocarcinomas (figures 4.1-4.5). To test directly that cordycepin affects growth factor signalling, the effect of FBS serum response which contain multiple growth factors[763] will be investigated in NIH3T3 fibroblasts. These fibroblasts are well characterised in growth factor response, as transcriptionally induced mRNA transcripts of immediate early genes (IEGs) are known to be polyadenylated with a ~150-200 nucleotide poly(A) tails within 15-20 minutes of serum-stimulation[767-769]. For comparison to Breast Adenocarcinomas, NIH3T3 cells will be pre-treated with cordycepin prior to addition of FBS serum with growth factors to examine if cordycepin can repress the initial growth factor response of NIH3T3 when compared to serum stimulation alone. Differential gene expression analysis of a microarray dataset of NIH3T3 fibroblasts using the LIMMA[665] method was used to identify biological pathways affected by cordycepin treatment on serum induced NIH3T3 fibroblasts. NIH3T3 cells were serum-starved for 24 hours prior to 90-minute cordycepin (20 µM) treatment, followed by 30-minute 10% NBCS serum stimulation to see if cordycepin represses serum response. This experiment was performed, and the dataset was initially analysed by Dr. Richa Singhania and Dr. Cornelia H. de Moor (unpublished data) and reanalysed in this thesis.

Differential expression of cordycepin treatment in NIH3T3 fibroblasts is illustrated in a volcano plot (figure 4.6A). The spread of expression of cordycepin treatment prior to serum stimulation highlights higher upregulated genes (1,600; ≥ 1 Log_2FC & ≤ 0.05 p-value) compared to downregulated genes (901; ≤ -1 Log_2FC & ≤ 0.05 p-value) (figure 4.6A). Consistently with other datasets (figures 4.1A and 4.4A), most of the genes (30,664) did not meet a statistical significance of ≤ 0.05 p-value and were within the Log_2FC range of +1 to -1. These genes were excluded from further analysis as they were not statistically significant and did not reach a threshold of ≥ 1 or ≤ -1 Log_2FC change in expression with cordycepin treatment.

The statistically significant downregulated genes from figure 4.6A were used in the Functional Annotation Tool in the DAVID Bioinformatics Resource (LHRI, version 6.8)[690] to obtain Gene Ontology (GO) analysis output of enriched biological pathways. Consistently with figures 4.1B and 4.4B, downregulated genes with cordycepin treatment in NIH3T3 fibroblasts show repression of transcription from RNAP II promoter, angiogenesis, inactivation of MAPK kinase, and apoptotic process (figure 4.6B). As found previously, many of the downregulated genes associated with transcription from RNAP II are mRNAs encoding zinc-finger

proteins, however transcription factors and early growth response genes are also downregulated, including *EGR1*, *EGR3*, *EGR4*, *MYC*, *JUNB*, and Kruppel-like factors (KLFs) (figure A.2.7A). Growth factor pathways, FGF and TGF-β receptor signalling, as well as cellular response to TNF are also enriched with downregulated genes (figure 4.6B). Cellular differentiation and circadian rhythm biological processes are also repressed by cordycepin treatment in NIH3T3 fibroblasts (figure 4.6B), which is an effect not seen in Breast Adenocarcinoma cells in figures 4.1B and 4.4B.

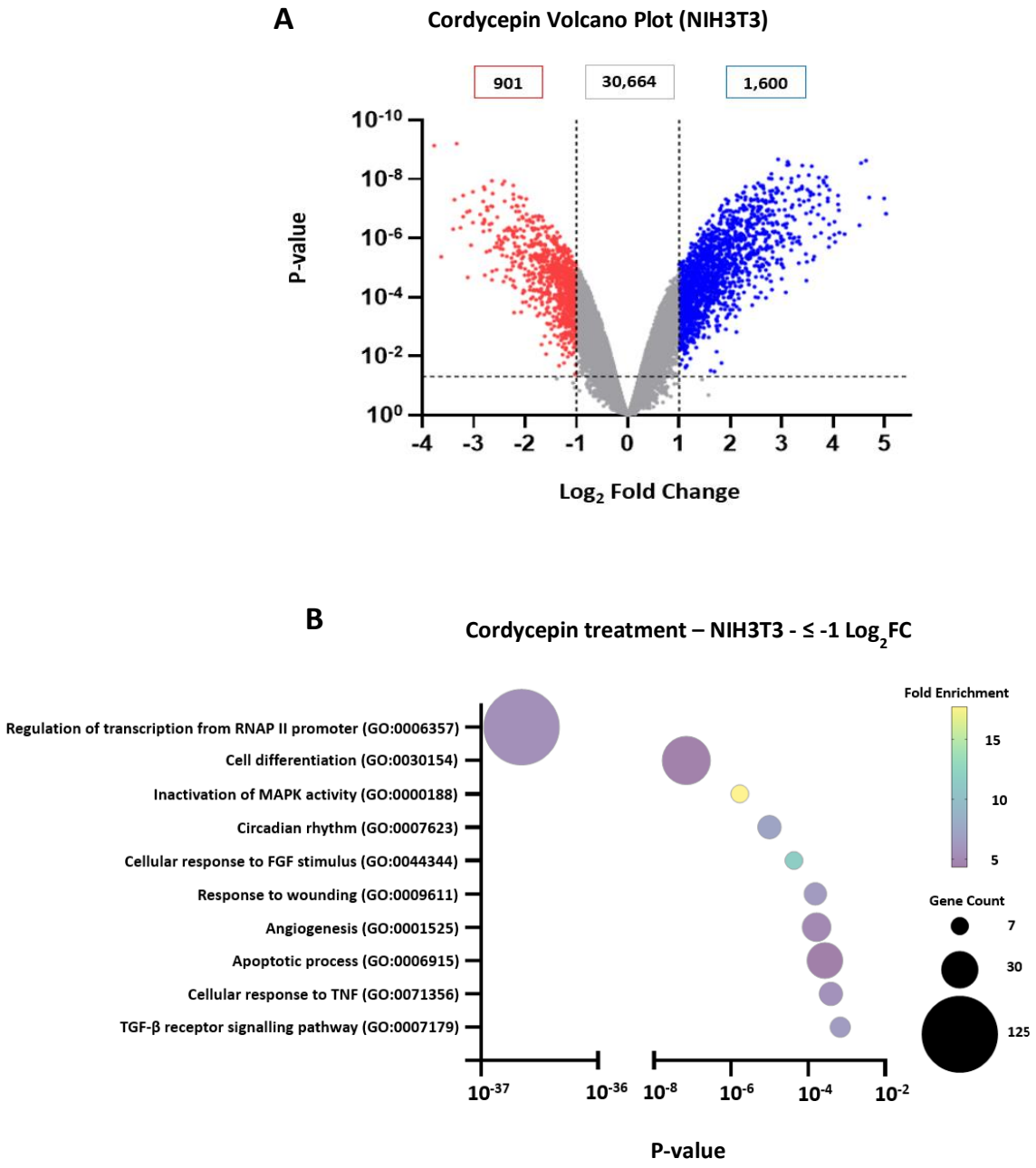

Figure 4.6: Differential expression analysis of cordycepin treatment in NIH3T3 indicates repression of growth response and serum-dependent signalling. Differentially expressed genes obtained from Microarray output was analysed using the LIMMA method[665]. NIH3T3 cells were treated after 24-hour serum-starvation for 90-minute cordycepin (20 µM) prior to 30-minute 10% NBCS serum stimulation compared to serum stimulation alone. **A)** Volcano plot showing the spread of expression with cordycepin treatment. Red denotes genes with ≤ -1 Log_2FC & ≤ 0.05 p-value, blue denotes genes with ≥ 1 Log_2FC & ≤ 0.05 p-value, grey denotes genes with -1 to 1 Log_2FC & > 0.05 p-value. **B)** Bubble plot indicate enriched biological pathways associated with repressed genes (red dots from **A)**) through DAVID Gene Ontology[690].

Inclusion of all statistically significant genes (≤ 0.05 p-value) of the NIH3T3 microarray dataset with cordycepin treatment into the Expression Analysis tool of IPA[764] also highlighted repression of serum-dependent signalling (figure 4.7). As seen previously in Breast Adenocarcinomas; EGF stimulus, TNFR1/2 signalling, CXCR4, ERK5, IL-6, and TGF-β signalling biological pathways are repressed with cordycepin treatment with negative activation z-scores (figures 4.2, 4.5 and 4.7). The tumour microenvironment pathway, CSDE1 signalling, WNT/β-catenin signalling, 3-phosphoinositide biosynthesis and superpathway of inositol phosphate compounds pathways are also repressed in NIH3T3 fibroblasts with cordycepin treatment (figure 4.7A). Upregulated biological pathways included LXR/RXR signalling, already seen in RAW264.7 macrophages (figures 3.3A, 3.10A, 3.13A, 3.16A, & 3.19A), and cAMP-mediated signalling (figures 3.9B, 3.10, 3.15B, and 3.16), suggesting a consistent effect of cordycepin treatment on mouse cell lines (figure 4.7A).

Upstream regulators which had a positive activation z-score and similar effect to cordycepin treatment in NIH3T3 fibroblasts were kinase inhibitors, LY294002 (PI3K inhibitor), SU6656 (Src and PDGF receptor inhibitor), U0126 (MEK1/2 inhibitor), and Prexasertib (CHK1/2 inhibitor). Regulators which have an opposite effect to downstream expression to cordycepin treatment in NIH3T3 fibroblasts is the effect of growth factors, TGFB1, EGF, PDGF BB, and IGF1 (figure 4.7B). Inflammatory upstream regulators, NF-κB, TNF, LPS and IL1β also have negative activation z-scores and opposite effects to cordycepin treatment on gene expression (figure 4.7B). Stimulation of receptors, EGR1 and GPER1 also have opposing effects to cordycepin treatment in NIH3T3 fibroblasts (figure 4.7B). Cordycepin treatment was also found to upregulate multiple mRNAs encoding interferon alpha (IFNA) paralogs enriched in multiple biological pathways linked with anti-viral immune responses (figure A.2.7B).

There are conflicting effects of cordycepin treatment on p38 MAPK in NIH3T3 fibroblasts as it shows both activation of signalling (figure 4.7A) but has an opposite effect to p38 MAPK as an upstream regulator (figure 4.7B). This suggests a potential feedback effect on p38 MAPK signalling with cordycepin in NIH3T3 fibroblasts. However consistently, cordycepin downregulates mRNAs encoding dual-specificity phosphatases (DUSPs), which are enriched in the inactivation of MAPK activity biological pathway (figure A.2.7A).

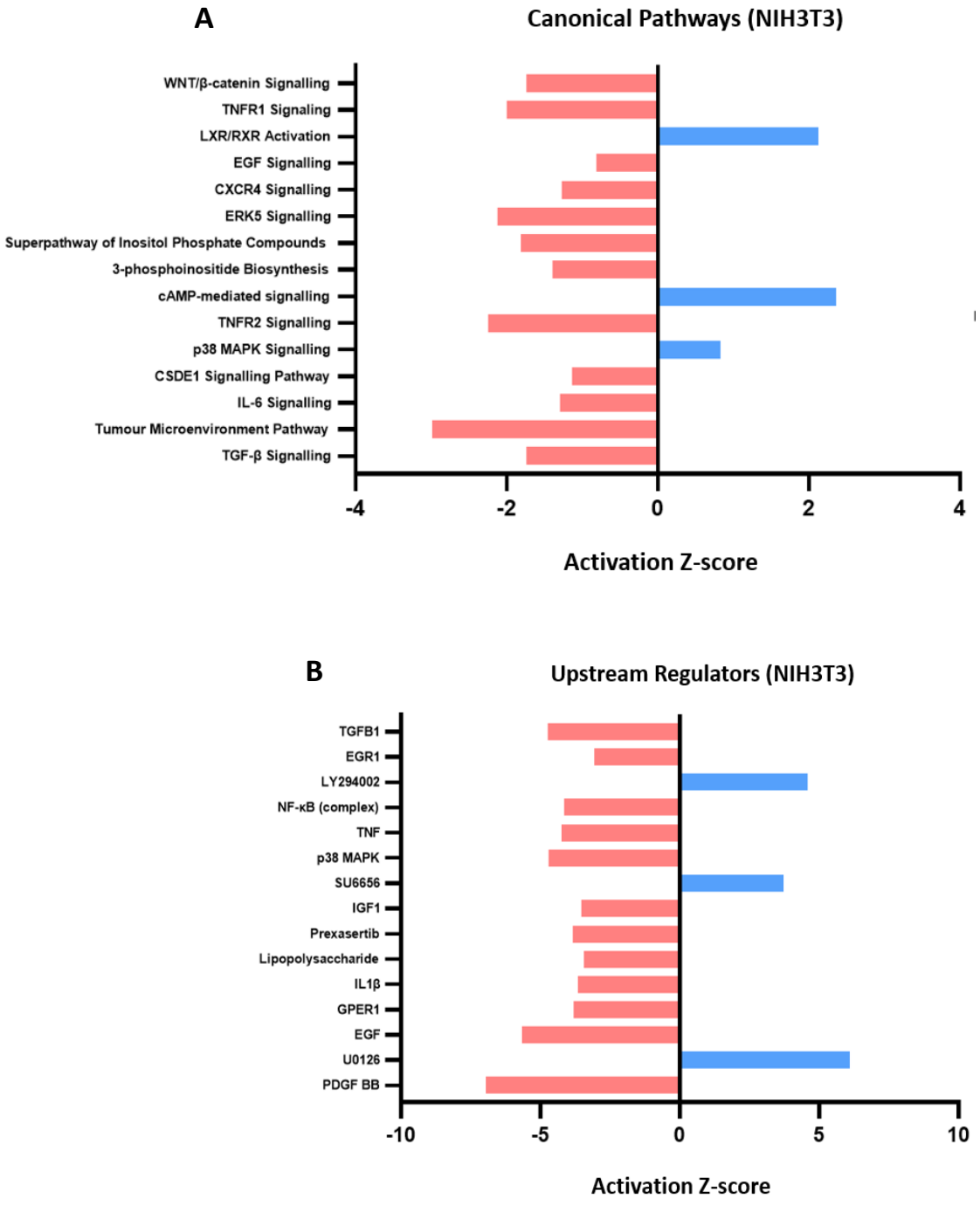

Figure 4.7: Cordycepin represses serum-dependent and Inflammatory canonical biological pathways and upstream regulators in NIH3T3 Fibroblasts. All statistically significant differentially expressed genes (≤ 0.05 p-value from moderated t-statistic) obtained through Microarray output was analysed using the LIMMA method[665] and entered into IPA[691]. NIH3T3 cells were treated after 24-hour serum-starvation for 90-minute cordycepin (20 µM) prior to 30-minute 10% NBCS serum stimulation compared to serum stimulation alone. **A)** Indicates the top biological canonical pathways which are repressed (red bars) or upregulated (blue bars) with cordycepin treatment. **B)** Indicates the top upstream regulators which act in an opposite way (red bars) or act similarly (blue bars) to cordycepin treatment based on activation z-score.

To build on the individual analysis of cordycepin treatment on serum-dependent signalling in this chapter, the Comparison Analysis tool within QIAGEN's Ingenuity Pathway Analysis (IPA) platform[691] was used to compare affected canonical biological pathways and upstream regulators (figure 4.8). During serum stimulation, cordycepin represses the TGF-β growth factor signalling pathway, as well as inflammatory pathways IL-6 and IL-8, ILK, TNFR1, CD40, and CXCR4 signalling (figure 4.8A). Cancer progression the tumour microenvironment, thyroid and colorectal cancer signalling pathways also have negative activation z-scores based on differential expression of cordycepin treatment in all three cell lines (figure 4.8A). Multiple inositol metabolism pathways and 3-phosphoinositide pathways are repressed with cordycepin treatment, suggesting a consistent repression of inositol signal transduction in serum stimulated cell lines with cordycepin treatment (figure 4.8A). Upregulation of PPARα/RXRα activation and PPAR signalling (figure 4.8A), is consistent to the effects of cordycepin treatment in RAW264.7 macrophages with inflammatory stimulation (figures 3.13A, and 3.19A).

Upstream regulators which had consistent positive activation z-score and similar effect to cordycepin treatment were activation of the CDK19 kinase, and the modulators LY294002 (PI3K inhibitor), U0126 and PD98059 (MEK1/2 inhibitors), and SB203580 (p38 MAPK inhibitor) (figure 4.8B). Regulators which have a consistent opposite effect to downstream expression to cordycepin treatment is the effect of growth factors, PDGF BB, EGF, VEGF, TGFB1, and HGF (figure 4.8B). Inflammatory upstream regulators, NF-κB, TNF, TNFSF11, LPS and IL-6 also have negative activation z-scores and opposite effects to cordycepin treatment on gene expression (figure 4.8B). Stimulation of kinases, ERK and p38 MAPK, G protein-coupled receptor, GPER1, and the CHK1/2 inhibitor, Prexasertib, were also found to have negative z-scores as upstream regulators and opposing effects to expression to cordycepin treatment (figure 4.8B). Altogether, these results show that kinases and biological pathways associated with serum-dependent signalling and growth factor responses are consistently repressed with cordycepin treatment in three separate serum-stimulated datasets.

A

Canonical Pathways (overlapping)

	MCF-7	NIH3T3	MDA-MB-231
PPARα/RXRα Activation	2.000	1.508	1.213
PPAR Signalling	1.134	1.414	2.000
Superpathway of Inositol Phosphate Compounds	-2.000	-1.807	-4.690
3-phosphoinositide Biosynthesis	-2.000	-1.387	-3.873
IL-8 Signalling	-1.414	-1.265	-3.742
ILK Signalling	-1.414	-1.291	-3.742
3-phosphoinositide Degradation	-2.000	-1.508	-3.742
D-myo-inositol-5-phosphate Metabolism	-2.000	-1.732	-3.742
D-myo-inositol (1,4,5,6)-Tetrakisphosphate Biosynthesis	-2.000	-1.508	-3.606
D-myo-inositol (3,4,5,6)-tetrakisphosphate Biosynthesis	-2.000	-1.508	-3.606
P2Y Purigenic Receptor Signalling Pathway	-1.000	-1.508	-3.464
ERK5 Signalling	-2.000	-2.121	-3.357
Thyroid Cancer Signalling	-1.342	-1.414	-3.207
CXCR4 Signalling	-1.134	-1.265	-3.162
Colorectal Cancer Metastasis Signalling	-1.890	-1.807	-3.000
IL-6 Signalling	-1.414	-1.291	-2.828
TNFR1 Signalling	-2.000	-2.000	-2.714
TGF-β Signalling	-0.447	-1.732	-2.496
Tumour Microenvironment Pathway	-1.342	-2.982	-2.138
CD40 Signalling	-1.000	-1.134	-1.265

Activation Z-score

B

Upstream Regulators (overlapping)

Upstream Regulator	Molecule Type	MCF-7	NIH3T3	MDA-MB-231
PDGF BB	Complex	-5.978	-6.942	-6.124
Lipopolysaccharide	Chemical drug	-4.793	-3.437	-8.169
EGF	Growth factor	-4.709	-5.648	-5.965
Vegf	Group	-4.398	-4.938	-6.873
U0126	Kinase inhibitor (MEK1/2)	4.347	6.102	5.194
TNF	Cytokine	-4.757	-4.255	-6.496
LY294002	Kinase inhibitor (PI3K; mTOR; CSK2)	4.285	4.580	6.186
NF-κB (complex)	Complex	-4.456	-4.138	-6.420
TGFB1	Growth factor	-3.876	-4.714	-6.147
PD98059	Kinase inhibitor (MEK1/2)	4.231	4.640	5.424
HGF	Growth factor	-4.102	-4.095	-5.833
CREB1	Transcription regulator	-4.823	-3.916	-4.974
SB203580	Kinase inhibitor (p38 MAPK)	3.632	3.673	5.512
ERK	Group	-4.003	-4.104	-4.410
Prexasertib	Chemical drug	-3.606	-3.838	-5.000
TNFSF11	Cytokine	-2.080	-4.739	-5.427
GPER1	G-protein coupled receptor	-4.088	-3.822	-4.314
p38 MAPK	Group	-3.246	-4.696	-4.271
IL6	Cytokine	-4.069	-2.653	-5.441
CDK19	Kinase	3.873	1.929	5.005

Activation Z-score

Figure 4.8: Comparison of biological canonical pathways and upstream regulators consistently affected between with cordycepin treatment with serum stimulation: Differentially expressed genes for cordycepin treatments was compared between MDA-MB-231, MCF-7 and NIH3T3 cells. All significantly differentially expressed genes (≤ -1 log_2FC and ≥ 1 log_2FC; ≤ 0.05 p-value) were compared in IPA[691]. **A)** biological canonical pathways and **B)** upstream regulators.

4.4 Cordycepin represses the EGF stimulation of HEK293 cells

This chapter has showed that cordycepin treatment can regulate serum-dependent and growth factor-dependent signalling pathways. As seen in figure 4.8, the growth factors such as EGF, has a negative activation z-score for all three serum stimulated cell lines, suggesting that stimulation of EGF has an opposite effect on expression to cordycepin treatment. It is also established that activation of EGFRs stimulate downstream PI3K/Akt, RAS/RAF/MEK, ERK/MAPK and JNK signalling cascades[155, 770-776], which were found to be repressed by cordycepin treatment during serum response (figures 4.2B, 4.5B, 4.7B, and 4.8). This altogether suggests that cordycepin can affect kinases and signalling pathways associated with serum response through repressing the stimulation of growth factors such as EGF, which needs further clarification.

HEK293 Human embryonic kidney cells are known to express endogenous EGF receptors and are well-characterised to respond to EGF stimulation[650, 651, 777-780]. HEK293 wild type cells were gifted to us from Professor Grahame Hardie's lab at the University of Dundee. These cells were cultured in DMEM & 10% FBS for 24-hours before the media was taken off, and fresh DMEM media with reduced FBS (0.1%) was added to the HEK293 cells for 24 hours. HEK293 cells were then treated with cordycepin (25 µM) for 20 minutes before 30 minutes of EGF (15 nM) stimulation and compared to DMSO (0.025 v/v) treatment with EGF stimulation. These concentrations were chosen based on validations performed by Elizabeth Rider (figure A.6). EGF-related mRNA markers were chosen based on genes which were consistently found to be associated with EGF as an upstream regulator from IPA analysis output (figure 4.8). Total RNA was extracted prior to cDNA synthesis and qPCR to validate changes in EGF-induced mRNA markers with cordycepin treatment.

In comparison to DMSO, cordycepin (25 µM) treatment before EGF stimulation (15 nM) resulted in statistically significant repression of immediate early response genes c-FOS (p-value = ≤ 0.01), and c-JUN (p-value = ≤ 0.001) (figure 4.9). The stress-induced transcription factor, ATF3, also has statistically significant repression of mRNA abundance with cordycepin treatment (p-value = ≤ 0.01), and the TG-interacting factor, TGIF1 (p-value = ≤ 0.05) (figure 4.9). The receptor tyrosine kinase signalling antagonist, SPRY2, Phosphatase, DUSP1, and housekeeping gene, ACTB, were slightly repressed with cordycepin treatment, but was not statistically significant. The mRNA markers of the serine/threonine protein kinase,

PLK2, and ERBB receptor feedback inhibitor, ERRFI1, did not significantly change in expression with EGF stimulation or cordycepin treatment prior to EGF stimulation (figure 4.9). Altogether, cordycepin treatment has a clear repression of EGF-stimulated early response and transcriptional mRNA markers, even after only 20 minutes of treatment prior to EGF stimulation.

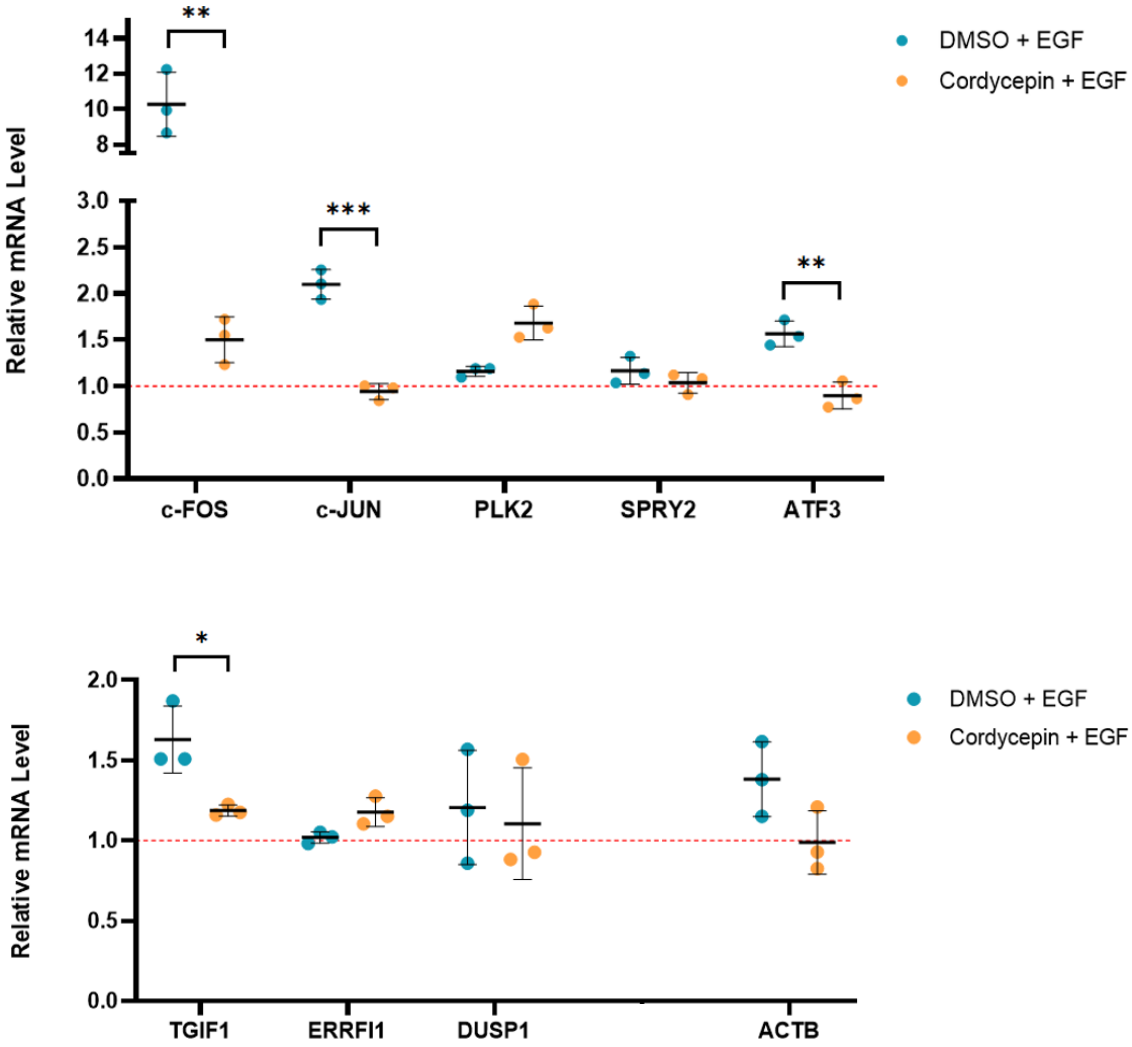

Figure 4.9: Cordycepin represses EGF-stimulated relative mRNA marker expression. HEK293 (wild type) cells were incubated in media containing less FBS (0.1%) for 24-hours prior to 20 minutes cordycepin (25 µM) treatment before a further 30-minute EGF (15 nM) stimulation compared to EGF-stimulation alone. Total RNA was extracted, followed by cDNA synthesis, and qPCR. Copy threshold (Ct) values of qPCR for EGF-stimulated genes were analysed using the 2-ΔΔCt method[660] and normalised to the Ct values of GAPDH (housekeeping gene). Relative mRNA expression of tested genes is presented as the Log_2 Fold Change relative to untreated control. (mean ± SD; n=3 independent experiments; Student t-test was used to obtain statistical significance against DMSO (0.05% v/v) and representative of; *P<0.05, **P<0.01, ***P<0.001, ****P<0.0001).

4.5 Discussion

This chapter has shown that cordycepin represses mRNA marker abundances for growth factor-dependent signalling in MCF-7 cells, which have functional estrogen and EGF receptors, and HEK293 cells prior to EGF stimulation (figures 4.2 & 4.9). Immediate early response genes, c-FOS and c-JUN were repressed with pre-treatment of cordycepin before EGF stimulation (figures 4.9). Both c-JUN and c-FOS are important transcription factors in cancer, known to be upregulated in invasive breast cancer and malignant glioma through regulating proliferation, apoptosis, and migration[781-784]. In Human osteoblast cell lines, knockdown of c-FOS was found to inhibit expression of Wnt2 and Fzd9 mRNA[785]. Wnt2 is known to activate Fzd9 which mediates Wnt/β-catenin signalling[786, 787], a pathway which has a negative activation z-score with cordycepin treatment of NIH3T3 Fibroblasts (figure 4.7A). This pathway is also upregulated in breast cancer cells with TGIF1[788], which has repressed mRNA abundance with cordycepin treatment in MCF-7 cells (figure 4.2).

The mRNA abundance of transcription factors MYC and JUNB, were found to be repressed with cordycepin treatment (figure 4.2). MYC is known to dimerize with Max, a helix-loop-helix zipper protein, and bind to Enhancer box (E-box) CANNTG DNA sequences[789, 790]. The MYC/Max dimer recruits the transformation/transcription domain-associated protein (TRRAP), histone acetyltransferase complexes TIPS60 and GCN5, and TIP48, a p300/CBP-associated factor and ATP-binding protein, to E-box sites. This complex acetylates histone H3 and H4, opening chromatin structure and allowing RNAP II machinery to access the E-box promoter and induce transcription[791, 792]. MYC is also known to interact with cofactors to stabilise to chromatin, such as WDR5 and the bromodomain protein, BRD4, in HEK293 cells, and PAF1 (RNAP II-associated factor) in *Drosophila*[793, 794]. Downregulated genes with cordycepin treatment were found to be enriched in the chromatin organisation biological pathway in MDA-MB-231 triple-negative cells (figure 4.4B). Transcription from RNAP II promoter was also consistently enriched in downregulates genes (figure 4.1B, 4.4B, 4.6B, A.2.5A, A.2.6A, & A.2.7A). The effect to these biological pathways is likely due to downregulation of transcription factors such as MYC and JUNB and could suggest that cordycepin affect chromatin through acetylation of H3 and H4 histones.

The CTD site of RNAP II interacts with the BRCA1-BARD1-CSTF1, leading to inhibition of mRNA 3' end formation *in vitro* and degradation of RNAP II under genotoxic stress through ubiquitination[558, 559].

Protein ubiquitination is enriched with downregulated genes with cordycepin treatment of MCF-7 and MDA-MB-231 breast cancer cells (figures 4.1B, 4.4B, A.2.5A, & A.2.6A), but not NIH3T3 Fibroblasts (figure 4.6B). This suggests that cordycepin treatment is most likely not causing downregulated regulation of transcription from RNAP II promoter through ubiquitination and degradation of RNAP II in breast cancer cells. The effect on transcription by cordycepin could however be through affecting upstream transcription regulators such as NUPR1. This regulator had an opposite effect to downstream expression compared to cordycepin treatment due to negative activation z-scores (figures 4.2B & 4.5B). TGF-β is known to regulate NUPR1 transcription[795], so repression of TGFB1 and TGF-β signalling (figures 4.2, 4.5, 4.6, 4.7, & 4.8) could be why NUPR1 also has a negative activation z-score.

Hedgehog (Hh) signalling is normally involved in animal development and tissue homeostasis, and plays a role in cancer malignant transformation, proliferation, drug-resistance, and metastasis[796, 797]. The Hh signalling component, GLI1, has a similar effect on downstream expression to cordycepin treatment in MDA-MB-231 cells (figure 4.5B). This zinc-finger protein is known to be upregulated in mammospheres, spheroid clumps of cancer stem cells (CSCs) involved in tumour resistance to chemotherapy[798, 799]. The adaptive response gene, ATF3, regulated by TGF-β, TNF-α, and IL1β, is repressed by cordycepin treatment in MCF-7 and HEK293 cells (figures 4.2 & 4.9). This gene is known to promote morphological and molecular changes reminiscent to EMT activation and stimulates formation of mammospheres and tumorigenesis[800]. This could suggest that cordycepin regulates Hh signalling and mammosphere production, which corroborates a previous publication in breast cancer cells[801].

As mentioned previously, regulatory factors such as EGF, IGF, HGF, PDGF and TGF-β are known to facilitate EMT[276]. Cordycepin has been publicised previously to revert EMT through upregulating E-cadherin, which is a tumour suppressor important for maintaining the epithelial phenotype[760, 802, 803]. Cordycepin has also been shown to repress metalloproteinases, which are important for the activation of TGF-β cytokines and degradation of the EMT to mediate metastasis[3, 703, 760-762]. EMT is also promoted through secretion of cytokines and chemokines from cancer-associated fibroblasts (CAFs) in the TME, known to remodel the extracellular matrix (ECM) and impact adaptive resistance to chemotherapy[804-806]. IGF-1 released by CAFs was found to trigger metastasis in MDA-MB-231 breast cancer cells, which aids in guiding metastatic cells towards IGF1-receptor rich locations in the presence of CXCR4, such as bone[313,

[314]. Bone-orientated IGF-1 is also known to bridge crosstalk between bone and metastatic cancer cells through the tyrosine autophosphorylation of IGF-1-receptors, which activates AKT and NF-κB signalling[315]. CXCR4 signalling (figures 4.2A, 4.7A, & 4.8A), IGF-1 (figures 4.5A & 4.7B), and NF-κB activity (figures 4.5A, 4.7B, & 4.8) were all found to be repressed with cordycepin treatment. This altogether could suggest that cordycepin can reduce bone-directed metastasis and IGF-1 mediated activation of NF-κB.

Consistently, the LXR/RXR and PPAR signalling pathways which were upregulated with cordycepin and treatment prior to inflammatory stimulation (figures 3.3A, and 3.16A), are also upregulated with all three datasets for cordycepin treatment prior to growth factor stimulation (figures 4.2A, 4.5A, 4.7A, & 4.8A). Diminished expression of RXRα is known to be associated with the development of malignant cancers[807-810]. As previously stated, RXRs can heterodimerise and activate PPARs[715], with PPARγ known to inhibit transcription factors such as NF-κB[716, 717]. PPARα has also been shown to upregulate expression of inhibitors of angiogenesis such as endostatin, and thrombospondin 1, and modulates NADPH oxidase-1-mediated angiogenesis[811, 812]. Altogether, as cordycepin treatment prior to growth factor stimulation upregulates PPARα/RXRα signalling, it is likely that cordycepin has an anti-malignant effect which is repressing NF-κB-mediated transcription of proinflammatory mRNAs, and tumour metastasis through angiogenesis.

The G protein-coupled estrogen receptor, GPER1, was consistently found to have an opposite effect to expression compared to cordycepin treatment (figures 4.2B, 4.5B, 4.7B, & 4.8B). It has been found that GPER and phosphorylated EGFR are recruited by estrogens to promoter regions of CAF target genes such as c-FOS and induce production of secretory factors which promote tumorigenesis[813, 814]. GPER is also known to functional interact with EGFR, IGF-1-receptors, HIF-1α, and Notch signalling components to trigger release of growth factors such as VEGF, FGF, and proinflammatory cytokine IL1β[320, 321]. These effects of GPER on growth factor receptors mediate activation of ERK1/2, PI3K/Akt signalling cascades and second messengers such as cAMP[322]. Cordycepin treatment in this chapter has consistently shown repression of MEK1/2, ERK, and PI3K/Akt signalling, and modulate MAPK signalling either directly or through having similar effects to known inhibitors of these pathways (figures 4.2, 4.4, 4.5, 4.7, & 4.8). This suggests that cordycepin can repress GPER-mediated activation of growth factor receptors, and ERK1/2 and PI3K/Akt/mTOR signalling. The cAMP signalling however is upregulated in NIH3T3 Fibroblasts with

cordycepin treatment (figure 4.7), and CREB1 has an opposite effect on expression to cordycepin treatment (figures 4.2 & 4.8). This suggests that cordycepin does not repress the effect of growth factors on downstream cAMP signalling.

Altogether this chapter highlights consistently that cordycepin represses growth factor response and serum-dependent signalling in multiple cell lines. Multiple growth factors, growth factor receptors, and inflammatory pathways important in cancer tumorigenesis are repressed throughout this chapter with cordycepin treatment. As growth factor response is repressed, MEK1/2, MAPK/ERK, and PI3K/Akt signalling is also downregulated, which is shown to be a similar effect to known inhibitors of these pathways (figures 4.2, 4.4, 4.5, 4.7, & 4.8). The effect of cordycepin and poly(A) machinery knockdown on signalling is also supported by results of the previous chapter in RAW264.7 macrophages (figures 3.13A & 3.19A). Interestingly, multiple phosphoinositide metabolic pathways are repressed by cordycepin treatment in serum-response (figure 4.8). Altogether this suggests that cordycepin, and polyadenylation, could act through PI3K/Akt signalling, which will be explored further in the next chapter.

5 Cordycepin represses PI3K/Akt/mTOR signal transduction and growth factor-dependent gene expression

5.1 Introduction

The PI3K/Akt/mTOR signalling pathway is important in regulating the cell cycle, and mediates many cellular functions including anabolic reactions, nutrient uptake, mRNA transcription and translation, and cellular growth and survival[39, 815, 816]. Activation of this pathway through PI3K is related to many factors, including growth factors and oncogenes associating with small Ras-related GTPases, receptor-coupled tyrosine kinases (RTKs), and heterotrimeric GPCR's[39]. Growth factors, such as EGF, bind to their respective receptors leading to activation of RTK domains and phosphorylation of multiple tyrosine residues leading to the activation of downstream signalling cascades[278, 279, 817]. This could for example be through direct binding, such as with EGFR3 and the p85 subunit of PI3K, or through recruiting docking proteins such as Gab1, which also binds to p85, which stimulates localisation of PI3K, and AKT afterwards, at the plasma membrane[303-305]. Once activated, AKT is known to phosphorylate downstream targets such as GSK3[89], TSC2[90], and PRAS40 (AKT1S1; component of mTORC1)[91], which in turn activates mTORC1. This mediates processes such as cell growth by S6K, protein synthesis by 4E-BP1/2, and autophagy through ULK1[123]. mTORC1 activation can be moderated by AMPK, which regulates growth and reprogramming of cellular metabolism via suppression of the mTORC1 pathway[141].

The PI3K/Akt/mTOR signalling pathway is known to cross-talk with other pathways such as MAPK/ERK, and JAK/STAT signalling, all of which are implicated in disease through over-stimulation or amplification of growth factor receptors, which are common in cancer[281-284]. Aberrations of these pathways also can lead to uncontrolled proliferation, angiogenesis, and metastasis[278, 279], with mutations in the p110α catalytic subunit of PI3K found frequently in cancer[155-157], such as breast cancer[156]. Due to the importance of PI3K/Akt/mTOR signalling in disease, many modulators have been synthesised to modulate aberrant activation of the pathway and restrict the progression of disease[39, 815]. In the previous chapter, cordycepin was found to repress growth factor response, downregulate MEK1/2, MAPK/ERK, and PI3K/Akt signalling, and was shown to have a similar effect on downstream expression to known inhibitors of these pathways (figures 4.2, 4.4, 4.5, 4.7, & 4.8). This builds on the systematic review of Radhi *et al*. (2021)[3] which found clear repression of AKT (Ser473), and ERK phosphorylation (Thr202/Tyr204) in

current literature for cordycepin treatment. To try and clarify if the effect of cordycepin on repressing growth factor stimulation from the previous chapter is through modulating signalling pathways such as the PI3K/Akt/mTOR pathway, cordycepin will be compared against known modulators of signalling pathways to test for similarity in downstream effects.

5.2 Cordycepin affects PI3K/Akt/mTOR Signalling kinases similarly to LY294002 in MCF-7 Breast Adenocarcinomas

As shown in the previous chapter, cordycepin can repress PI3K activity and has a consistently similar effect to gene expression to the PI3K inhibitor, LY294002 (figures 4.2B, 4.4B, 4.5B, 4.7B, and 4.8B). To provide experimental evidence that cordycepin has a similar effect to PI3K inhibition, serum-stimulated MCF-7 Breast Adenocarcinomas were treated for 2-hours with cordycepin treatment (50 µM), DMSO (0.05% v/v) or PI3K inhibitors (figure 5.1). DMSO treatment of MCF-7 cells had no effect to the phosphorylation of AMPK (Thr172) and S6K1 (Thr389), downstream to mTOR signalling, and slightly increased the phosphorylation of GSK3β (Ser9) and 4E-BP1 (Thr37/46) compared to no treatment (figure 5.1). When compared to DMSO treatment, both cordycepin and PI3K inhibition through LY294002 showed a decrease in phosphorylation of S6K1 (Thr389), GSK3β (Ser9) and 4E-BP1 (Thr37/46) but had no effect to the phosphorylation of AMPK (Thr172) (figure 5.1). The PI3K inhibitors, Pictilisib and Alpelisib, had similar effects to cordycepin treatment with repression of S6K1 (Thr389), GSK3β (Ser9) and 4E-BP1 (Thr37/46), however these inhibitors increased phosphorylation of AMPK (Thr172) (figure 5.1). GAPDH was used as a loading control and highlights that the same amount of protein was loaded per treatment condition into the western blot (figure 5.1).

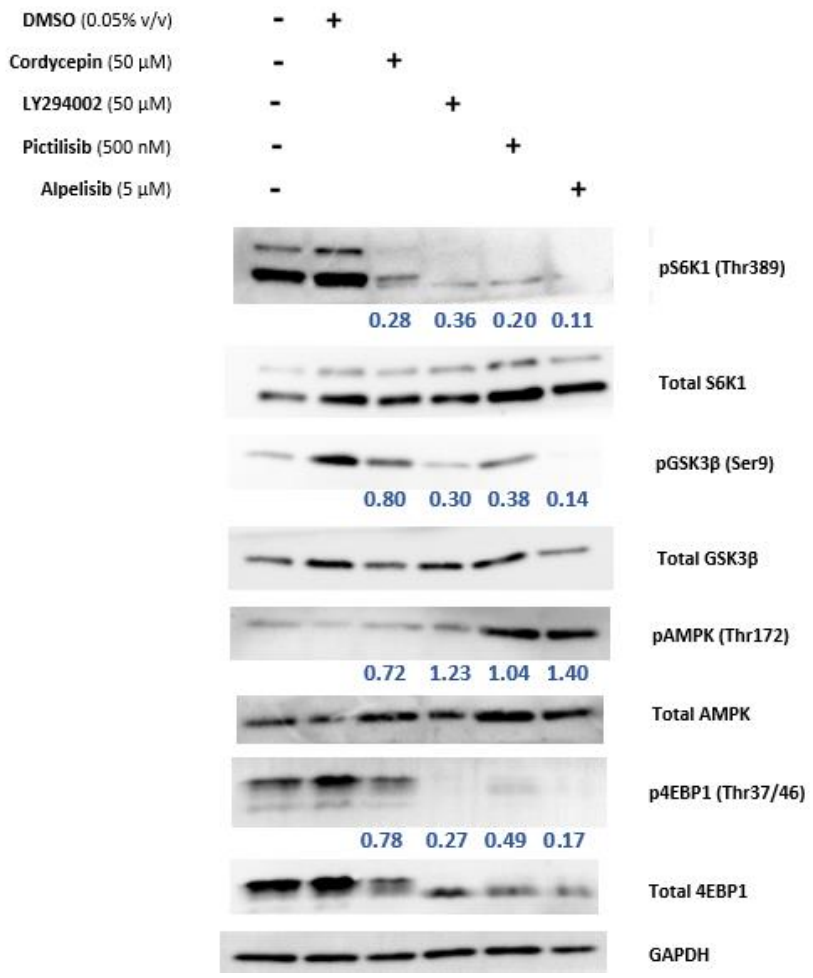

Figure 5.1: Cordycepin represses serum dependent PI3K/Akt/mTOR signalling and modulates kinase activation similarly to PI3K inhibitors. MCF-7 cells were treated for 2-hours with either cordycepin (50 µM), DMSO (0.05% v/v) or PI3K inhibitors; LY294002 (50 µM), Pictilisib (500 nM), or Alpelisib (5 µM). Total protein was extracted following Methods section 2.3.1. Western blotting and primary antibody incubation followed Methods section 2.3.3. Antibodies used are described in Table 2.4. Phosphorylated protein quantified using band intensity values obtained from Image Lab 6.0.1. All band intensities were normalised to GAPDH, then phosphorylated bands were normalised to Total protein band intensities per treatment condition. Finally, cordycepin and PI3K inhibitor band intensities were divided by the DMSO band intensity for each phosphorylated protein target (values displayed underneath are representative to the average of all three biological replicates). (Figure is representative to N = 3 biological replicates, with the other replicates shown in figure A.7).

5.3 Cordycepin represses serum-dependent mRNA expression more consistently than signalling modulators

As highlighted in the previous chapter, cordycepin was found to repress serum-dependent mRNA expression when compared to DMSO (figure 4.2). To try and identify target(s) of cordycepin in serum-dependent PI3K/Akt/mTOR signalling; MCF-7 Breast Adenocarcinoma's were treated with either cordycepin (50 µM), DMSO (0.05% v/v), or PI3K inhibitors for 2-hours. Cells were seeded in fresh DMEM & 10% FBS media and cultured for 24-hours prior to treatment with direct addition of cordycepin (50 µM) or DMSO (0.05% v/v) in the media for 2 hours before RNA extraction and cDNA synthesis following Methods section 2.2. Serum-dependent mRNA markers were chosen based on association to Breast cancer development and known to be stimulated in the presence of growth factors, which were investigated previously (figure 4.2).

Consistent with previous results (figure 4.2), in comparison to DMSO, cordycepin (50 µM) resulted in statistically significant repression of key proto-oncogene transcription factors MYC (p-value = ≤ 0.01) and JUNB (p-value = ≤ 0.001) (figure 5.2). The serine/threonine protein kinase PLK2 (p-value = ≤ 0.001), and the protein tyrosine/threonine phosphatase oncogene, DUSP1, were both significantly repressed (p-value = ≤ 0.01) with cordycepin treatment (figure 5.2). Expression of BCAR3 (p-value = ≤ 0.05), a marker of anti-estrogen resistance in breast cancer[765], and FOSL1 (p-value = ≤ 0.05), known to promote drug resistance to doxorubicin in breast cancer[818], were also repressed with cordycepin treatment (figure 5.2).

In comparison to DMSO, PI3K inhibitors repressed mRNA expression of MYC, DUSP1, and FOSL1 which was not statistically significant, except for Alpelisib treatment with FOSL1 (p-value = ≤ 0.05). The PI3K inhibitor, LY294002, had upregulated BCAR3 expression, whereas pictilisib and alpelisib had hardly any change in expression of BCAR3 (figure 5.2). All three PI3K inhibitors had a statistically significant repression of PLK2 (p-value = ≤ 0.05), and JUNB (p-value = ≤ 0.01-0.001) (figure 5.2). ACTB is an abundant housekeeping gene which shows no statistically significant difference in expression between cordycepin treatment and PI3K inhibition compared to DMSO (figure 5.2). Altogether, these results suggest that cordycepin gives a more consistent repression of these genes than PI3K inhibition, despite it's somewhat weaker effect on signal transduction.

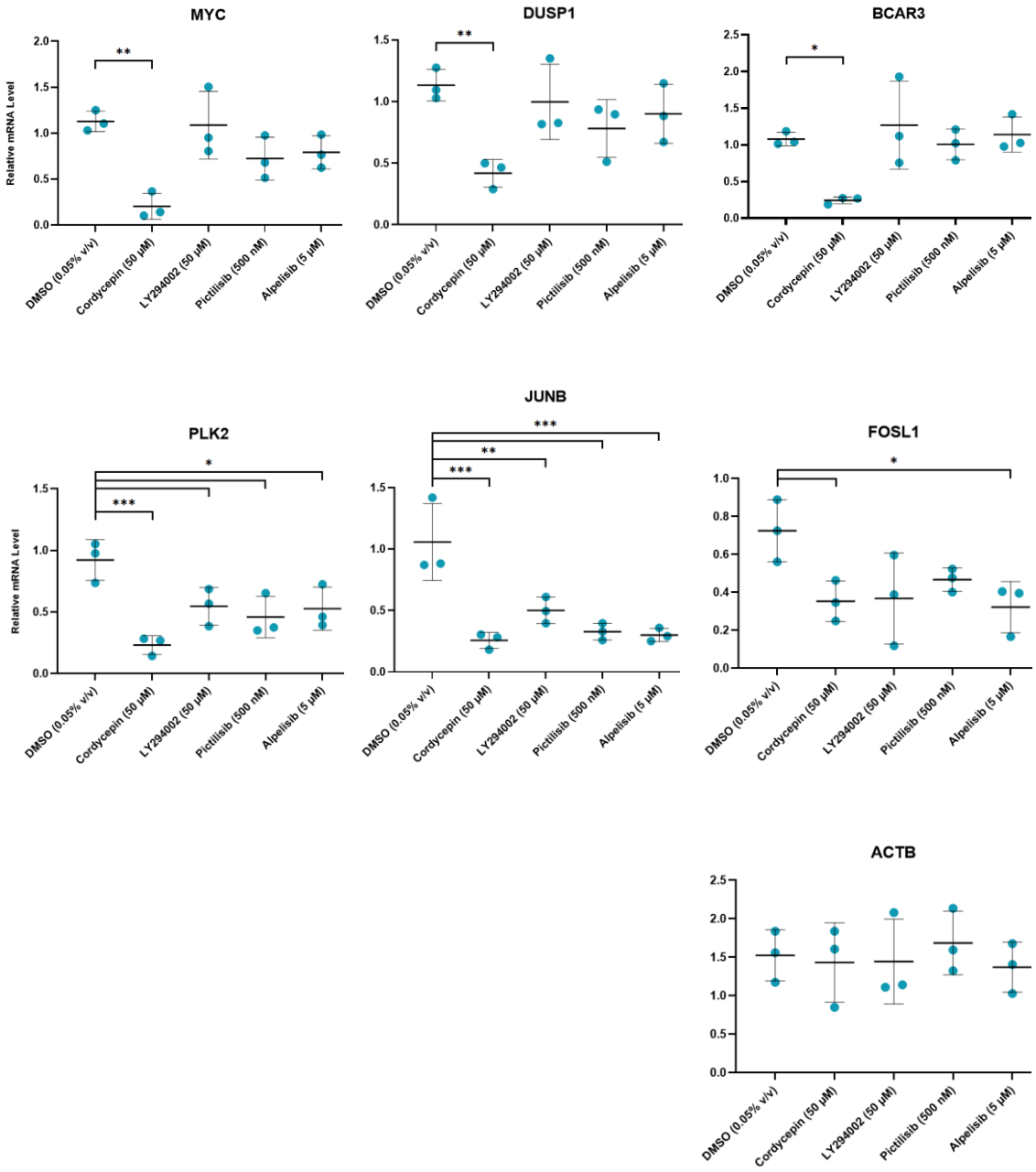

Figure 5.2: More serum-dependent markers are repressed by cordycepin treatment compared to PI3K inhibitors. MCF-7 breast adenocarcinomas were treated for 2 hours with either cordycepin (50 µM), DMSO (0.05% v/v), or PI3K inhibitors LY294002 (50 µM), Pictilisib (500 nM), or Alpelisib (5 µM) prior to total RNA extraction, cDNA synthesis and qPCR. Output was analysed using the 2-ΔΔCt method[660] and normalised to GAPDH (housekeeping gene). Relative mRNA expression level of tested genes were obtained through comparison to RNA from untreated MCF-7 cells. (mean ± SD; n=3 independent experiments; One-way Anova was used to obtain statistical significance against DMSO (0.05% v/v) and representative of; *P<0.05, **P<0.01, ***P<0.001, ****P<0.0001). Inhibitors: LY294002 (PI3K/mTOR/CSK2), Pictilisib (PI3K), Alpelisib (PI3Kα).

To investigate further whether cordycepin represses serum-dependent signalling through modulating signalling kinases, MCF-7 cells were treated with either DMSO (0.05% v/v), cordycepin (50 µM), an AMPK activator, mTOR, AKT, or MEK inhibitor for 2-hours prior to total RNA extraction and qPCR. In comparison to DMSO, cordycepin was again found to repress MYC, DUSP1, BCAR3, JUNB (p-value = ≤ 0.05), and PLK2 (p-value = ≤ 0.01) (figure 5.3). AMPK activation and MEK inhibition were also able to repress PLK2 mRNA expression (p-value = ≤ 0.05), whereas mTOR and AKT inhibition did not lead to statistically significant repression (figure 5.3).

Inhibition of mTOR through Torin1 was found to have a non-statistically significant upregulation in MYC, DUSP1, and BCAR3, and repression of PLK2 and JUNB mRNA expression compared to DMSO treatment (figure 5.3). Treatment with an AKT inhibitor, MK-2206, upregulated MYC, DUSP1, BCAR3, and JUNB mRNA expression, as well as a repression of PLK2, which were not statistically significant. Cordycepin, mTOR and AKT inhibition also led to non-statistically significant repression of FOSL1 (figure 5.3).

Activation of AMPK had no change in differential expression of MYC, BCAR3, and FOSL1, and a non-statistically significant repression of DUSP1 and JUNB compared to DMSO (figure 5.3). Inhibition of MEK through PD98059, had no change in differential expression of MYC and DUSP1, as well as a non-statistically significant upregulation of BCAR3, JUNB, and FOSL1 (figure 5.3). There were no statistically significant changes in expression for all treatment conditions for the housekeeping gene, ACTB. Altogether, as with the effect of PI3K inhibition (figure 5.2), cordycepin has a more consistent repression of serum-dependent signalling mRNA markers compared to kinase modulators (figure 5.3).

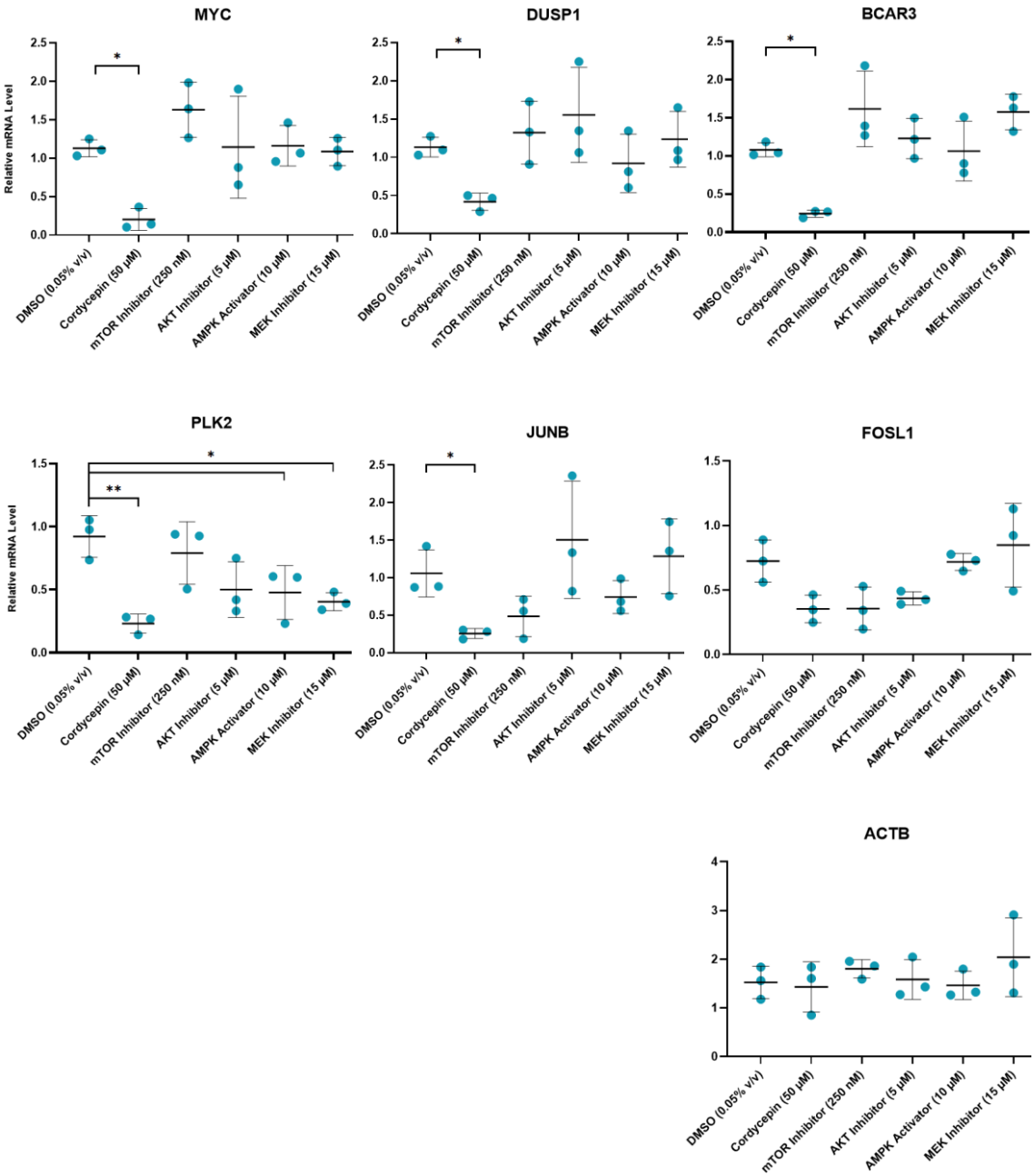

Figure 5.3: More serum-dependent markers are repressed by cordycepin treatment compared to kinase modulators. MCF-7 breast adenocarcinomas were treated for 2 hours with either cordycepin (50 µM), DMSO (0.05% v/v), or kinase modulators Torin1 (500 nM; mTOR inhibitor), MK-2206 (5 µM; AKT inhibitor), A-769662 (10 µM; AMPK activator), or PD98059 (15 µM; MEK inhibitor). Total RNA was extracted prior to cDNA synthesis and qPCR. Output was analysed using the 2-ΔΔCt method[660] and normalised to GAPDH (housekeeping gene). Relative mRNA expression level of tested genes are presented relative to untreated control. (mean ± SD; n=3 independent experiments; One-way Anova was used to obtain statistical significance against DMSO (0.05% v/v) and representative of; *P<0.05, **P<0.01, ***P<0.001, ****P<0.0001).

5.4 Discussion

This chapter has built on previous results on the repression of mRNA marker expression of serum-dependent response with cordycepin treatment (figures 4.2 & 4.9). Cordycepin treatment in this chapter has shown more statistically significant repression of mRNA marker expression compared to PI3K, mTOR, AKT, and MEK inhibitors, and an AMPK activator (figures 5.2 & 5.3). Both cordycepin treatment and PI3K inhibition repressed PLK2, JUNB, and FOSL1 mRNA expression (figure 5.2), which relates to previous results on the similarity of downstream expression (figures 4.2B, 4.5B, 4.7B, & 4.8B) and repression of PI3K/Akt signalling (figure 4.4B). The only other modulator with consistent repression of JUNB and FOSL1 was the mTOR inhibitor, Torin1 (figure 5.3). JUNB and FOS are immediate early genes (IEG's) which can be transcribed downstream from EGFR via ERK1/2 and JNK-mediated activation of transcription factors, Sp1, E2F, Elk-1, and AP-1[301, 307-310]. The MAPK/ERK signalling pathway is also known to be triggered through activation of GPERs[322], PDGFR[334], VEGFR's[325-328], and stimulation through TGF-β[819]. The TGF-β growth factor also induces expression of BCAR3, which is associated with anti-estrogen resistance and metastasis in breast cancer[765]. Expression of BCAR3 was found to be repressed by cordycepin, but no other kinase modulator (figure 5.2 & 5.3). There is a crosstalk between MAPK/ERK signalling pathway and PI3K/Akt signalling[281-284], which could be why cordycepin and PI3K inhibition are influencing JUNB expression, as the MEK inhibitor did not have the same effect as cordycepin or PI3K inhibition (figures 5.2 & 5.3).

Repression of FOSL1 with cordycepin treatment, PI3K, and mTOR inhibition (figures 5.2 & 5.3) could lead to sensitivity to therapies such as the anthracycline, doxorubicin, as FOSL1 is known to lead to resistance to doxorubicin[818]. Doxorubicin is also a VEGF inhibitor, which once combined with an mTOR inhibitors, can produce a 21% response rate in advanced metaplastic breast cancer[360]. This reiterates the repression of FOSL1 with mTOR inhibitor, Torin1 (figure 5.3). The transcription factor, MYC, plays a role in basal-like breast cancer progression[355], and is known to be upregulated through mTORC2-mediated FoxO acetylation in glycolysis[820], and downregulation of AMPK signalling through ablation of the α1 catalytic subunit[169]. This was however not supported in the results of this chapter, as inhibition of mTOR through Torin1 led to an increase in MYC expression, and activation of AMPK had no effect on expression to MYC (figure 5.3). Altogether, the effects on JUNB and FOSL1 expression by cordycepin could be through PI3K

or mTOR inhibition, however there is a lack of correlation with the repression of other mRNA markers, MYC and BCAR3, suggesting that cordycepin acts through an alternative mechanism in MCF-7 cells (figure 5.2 & 5.3).

Cordycepin treatment of MCF-7 cells was found to repress the phosphorylation and activation of downstream AKT target, GSK3β (Ser9)[89], and downstream mTORC1 targets, 4E-BP1 (Thr37/46) and S6K1 (Thr389), associated with protein synthesis[123], which was consistent with PI3K inhibition (figure 5.1). Activated S6K1 promotes translation initiation through phosphorylating eIF4B, a positive regulator of the eIF4F complex[128]. Phosphorylated 4E-BP1 is inactive and would otherwise block translation by outcompeting translation initiation factor, eIF4G, from binding to eIF4E[124, 125]. For this reason, results from figure 5.1 suggests that cordycepin could act through PI3K inhibition in repressing translation downstream. Previous results in this thesis have suggested that cordycepin treatment has a similar effect on gene expression as the PI3K inhibitor, LY294002 (figures 4.2B, 4.5B, 4.7B, & 4.8B) in serum stimulation, and just like LY294002 treatment, cordycepin had no effect on activating AMPK in MCF-7 cells (figure 5.1). This result on AMPK activation with cordycepin does not correlate with previous findings in MCF-7 cells by Dr. Jialiang Lin[766], as well as other research groups detailed in the systematic review of the biological effects of cordycepin by Radhi, *et al.* (2021)[3]. Besides LY294002, the other PI3K inhibitors, Pictilisib and Alpelisib, did lead to phosphorylation of AMPK (Thr172)(figure 5.1), which could be due to the fact LY294002 acts predominantly as an ATP-competitive inhibitor and is less specific to PI3K[652], than the allosteric inhibitors, Pictilisib and Alpelisib[653-655]. Alternatively, Alpelisib is PI3Kα-specific[654, 655], and this could also suggest AMPK activation is dependent on inhibition of the PI3Kα isoform in MCF-7 cells.

Altogether, this chapter suggests that cordycepin could repress phosphorylation of downstream AKT and mTORC1 targets through PI3K inhibition. However, as cordycepin has a more significant repression of mRNA markers in serum response, there could be alternative effects which are not through modulating specific signalling kinases. These results could be specific to MCF-7 cells and will be further assessed in inflammatory stimulation of RAW264.7 macrophages in the next chapter.

6 Cordycepin & PI3K Inhibition affect inflammatory mRNA markers and upstream regulators

6.1 Introduction

Inflammation is an important mechanism which orchestrates a response to pathogen-associated molecular patterns (PAMPs), such as bacterial lipopolysaccharides (LPS), leading to transcription of pro-inflammatory cytokines and chemokines[174-178]. These PAMPs are recognised by pattern-recognition receptors (PRRs), such as the toll-like receptor, TLR4[176, 177]. Upon binding of LPS, TLR4 recruits the extracellular Myloid differentiation protein 2 (MD2), forming a LPS:TLR4:MD2 complex[185]. This further recruits the signal transducer, BCAP, and MyD88, which leads to the activation of downstream signalling pathways, such as PI3K/Akt/mTOR signalling[217, 218] (figure 1.5). Alternatively, LPS stimulation of TLR4 can also release and activate the kinase, Tpl2, which further phosphorylates and activates MAPK signalling pathways such as ERK1/2, MEK1/2 and JNK signalling[248-250]. Activation of these MAPK signalling pathways leads to nuclear translocation of transcription factors such as Elk-1, AP-1, CREB, and Activating transcription factors (ATFs). This promotes the transcription of proinflammatory cytokines IL-10, IL-6, and TNF-α[246, 247]. Once activated, AKT phosphorylates kinases which leads to the nuclear translocation of transcription factors, such as the NF-κB:p65:RelA heterodimer, and regulates transcription of pro-inflammatory cytokines[222, 223]. AKT can also phosphorylate another kinase, TAK1, which can activate MKK4/7 and MKK3/6 kinases, upstream from JNK and p38 signalling respectively[242-245], and the IKK kinase upstream from NF-κB[224].

Cordycepin treatment has already been shown to broadly repress inflammatory stimulation in LPS-induced RAW264.7 macrophages (figures 3.2A, 3.3A, & 3.15A), as well as MyD88 activation (figures 3.3B & 3.16B). This suggests that cordycepin can restrict the activation of signalling pathways, upstream from transcription of pro-inflammatory mRNAs. This was shown to occur with the repression of NF-κB (p65) nuclear translocation (figure 3.4), and repression of inflammatory mRNA marker expression with cordycepin treatment (figures 3.5 & 3.7). This effect of cordycepin has also been seen previously through the repression of TNFα production and NF-κB activation in LPS-induced RAW264.7 macrophages through triggering AMPK activation[371]. Also, cordycepin treatment has been shown to repress PI3K/Akt, JAK, and

MAPK signalling pathways (figures 3.16 & 3.17C), suggesting cordycepin effect on inflammation is through signalling pathways.

Cleavage and polyadenylation factors have also been found to play a role in inflammatory stimulation. This includes NUDT21, which is known to modulate Wnt/β-catenin and NF-κB signalling pathways through regulating alternative polyadenylation[642]. Likewise, CPSF4 knockdown has been linked to reduction in the phosphorylation of IKKα/β and IκBα and nuclear translocation of NF-κB, leading to reduced PTGS2 mRNA expression[630]. Knockdown of WDR33 can also repress NF-κB nuclear translocation and inflammatory mRNA markers in RAW264.7 macrophages, and CPSF4 was also elevated in inflamed synovial tissues associated with osteoarthritis[384]. This was further proven through previous results showing that knockdown of WDR33 can broadly repress inflammatory pathways (figures 3.9A & 3.10A), and NF-κB signalling (figure 3.10B), which altogether demonstrates a link between cleavage and polyadenylation machinery and inflammation.

Cordycepin can deplete polyadenylation factors, such as WDR33, through trapping them on the 3'UTR[644, 645, 696, 697]. Both cordycepin and WDR33 knockdown was seen to repress PI3K/Akt signalling (figures 3.13 & 3.19). WDR33 was also found to affect MEK and ERK signalling (figure 3.10B & 3.11), and both treatments were found to have a similar effect on downstream expression to PI3K, MEK, and p38 MAPK inhibitors (figures 3.13, 3.18C, & 3.19). Altogether, there is a clear effect on inflammatory stimulation through cordycepin, and clear associations with both cordycepin treatment and WDR33 knockdown to known modulators of signalling pathways. To substantiate whether cordycepin acts through signalling kinases on inflammation, this chapter will compare cordycepin treatment to known kinase modulators on their effects on inflammatory stimulation. High-throughput comparison between cordycepin treatment and PI3K inhibition through LY294002, shown to have similarities previously (figures 3.16 & 3.17C), will aim to elucidate whether cordycepin affects inflammation through PI3K inhibition. Lastly, western blots of WDR33 knockdown will show whether phosphorylation machinery is linked to signalling kinases.

6.2 Cordycepin affects inflammatory activation of key kinases of PI3K/Akt/mTOR signalling

As highlighted previously, the effect of cordycepin treatment prior to LPS inflammatory stimulation has a repressive effect to PI3K/Akt signalling and has a similar effect on downstream expression to a known PI3K inhibitor, LY294002 (figures 3.13, 3.16, & 3.19). To further validate whether cordycepin represses inflammatory stimulation through modulating PI3K/Akt signalling, RAW264.7 macrophages were treated for 1 hour with either DMSO (0.02% v/v), cordycepin (20 μM), PI3K inhibitors, mTOR and AKT inhibitors, and an AMPK activator prior to a further 1-hour LPS (1 μg/ml) inflammatory stimulation. Total protein was then extracted and western blotting of downstream phosphorylation sites of PI3K/Akt/mTOR and AMPK signalling was used to indicate effects of cordycepin treatment (figure 6.1). As indicated in Appendix results (figure A.4) the antibodies for the phosphorylation of AKT are too non-specific to use to investigate the effects of cordycepin treatment on AKT activity directly (figure A.4). For this reason, the downstream AKT phosphorylation site of GSK3β (Ser9) was used to indicate activity of AKT.

The downstream phosphorylation sites, Threonine 37 and 46 (Thr37/46) of 4E-BP1 was used as an indicator of mTOR activity[821]. In RAW264.7 macrophages, both LPS and LPS & DMSO treatments increased the phosphorylation of 4E-BP1 (Thr37/46) (figure 6.1). When compared to LPS & DMSO, the PI3K inhibitor LY294002, and mTOR inhibitor (Torin1), were found to substantially repress phosphorylation of 4E-BP1 (Thr37/46) (figure 6.1). All the other modulators and cordycepin were also shown to reduce phosphorylation of 4E-BP1 (Thr37/46), but to a lesser extent (figure 6.1). This repression of phosphorylation through cordycepin is consistent with previous papers, including Wong *et al*. (2010)[369].

The nutrient-sensing AMPK signalling pathway, which upon activation represses mTOR signalling, was also assessed through the phosphorylation of AMPK at threonine 172 (Thr172) within the α-catalytic subunit[146, 822]. Upon stimulation with LPS or LPS & DMSO (0.02% v/v), the phosphorylation of AMPK (Thr172) is substantially reduced compared to RAW264.7 macrophages with no treatment, which is expected with unimpeded inflammatory stimulation (figure 6.1). When compared to LPS & DMSO, LPS & cordycepin treatment, and the PI3K inhibitors LY294002 and Alpelisib substantially increases phosphorylation of AMPK (Thr172), with more subtle increases in phosphorylation seen with Pictilisib,

and the mTOR and AKT inhibitors (figure 6.1). Interestingly, the AMPK activator did not increase phosphorylation of AMPK (Thr172) as much as cordycepin treatment (figure 6.1). The loading control, Vinculin, demonstrated that equal protein per treatment condition was loaded into the western blot (figure 6.1).

Altogether, cordycepin treatment prior to LPS inflammatory stimulation in RAW264.7 macrophages leads to increased AMPK (Thr172) phosphorylation, and reduced phosphorylation of GSK3β (Ser9), and 4E-BP1 (Thr37/46). This effect is not seen consistently with the PI3K inhibitors, AKT and mTOR inhibitors, or with the AMPK activator (figure 6.1). In MCF-7 cells, cordycepin was found to have a similar effect to LY294002 and did not increase phosphorylation of AMPK (Thr172). Further comparison of cordycepin and kinase modulators on inflammatory mRNA markers will be performed next to consolidate these inconsistent effects.

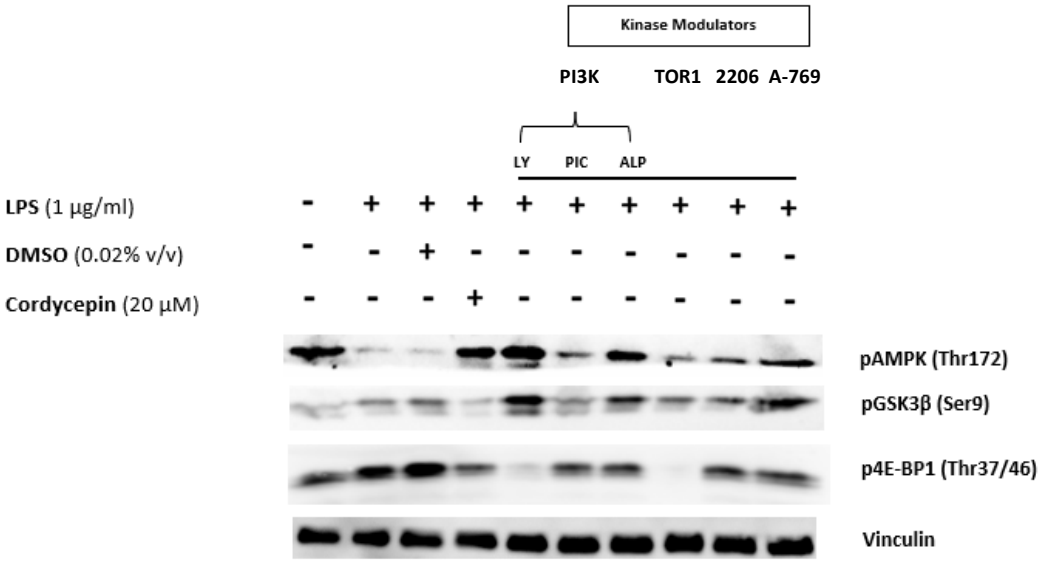

Figure 6.1: Cordycepin represses PI3K/Akt/mTOR signalling and modulates kinase activation similarly to PI3K inhibitors. RAW264.7 macrophages were treated with 1-hour cordycepin (20 µM), DMSO (0.02% v/v), PI3K inhibitors, LY294002 (100 µM), Pictilisib (500 nM), or Alpelisib (25 µM), mTOR inhibitor (Torin1 (TOR1); 500 nM), AKT inhibitor (MK-2206 (2206); 10 µM), or AMPK activator (A-769662 (A-769); 20 µM) treatments (described in Table 2.1) prior to 1-hour LPS (1 µg/ml) inflammatory stimulation. Protein was extracted following Methods section 2.3.1. Western blotting and primary antibody incubation followed Methods section 2.3.3. Antibodies used is described in Table 2.4. (Figure is representative to N = 2 biological replicates).

6.3 Cordycepin represses mRNA expression of inflammatory markers more consistently than PI3K/Akt/mTOR modulators

It has been shown previously that treatment of cordycepin (20 μM) for 1-hour prior to a further 1-hour LPS (1 μg/ml) inflammatory stimulation in RAW264.7 macrophages regulates MAPK signalling (figures 3.2, 3.3A, 3.17C, & 3.18C), and PI3K/Akt signalling (figures 3.13A, 3.16A, & 3.19A). Cordycepin also had similar effects on downstream gene expression to the known PI3K inhibitor, LY294002, and MEK1/2 inhibitor, U0126 (figures 3.13B, 3.16B, & 3.19B). To investigate whether the repression on inflammatory mRNA expression by cordycepin treatment (figure 3.5) is consistent with inhibition of PI3K signalling, RAW264.7 macrophages were treated with DMSO (0.02% v/v), cordycepin (20 μM), or PI3K inhibitors for 1-hour prior to a further 1-hour LPS (1 μg/ml) inflammatory stimulation. Concentrations used for these inhibitors are detailed in Table 2.1 and were initially validated and used by Dr. Masar Radhi in RAW264.7 macrophages which provided evidence that the inhibitors modulated kinases as expected, apart from Alpelisib. Concentrations were checked to ensure they had minimal effects on cell viability detailed in the Appendix (figure A.1). qPCR was used to measure mRNA abundance of inflammatory markers shown to be repressed by cordycepin previously (figure 3.5).

In comparison to LPS & DMSO (0.02% v/v), cordycepin treatment (20 μM) resulted in statistically significant repression of proinflammatory cytokines; Il1β (p-value = ≤ 0.0001) and Tnf (p-value = ≤ 0.05) (figure 6.2). Consistently to previous results (figure 3.5), cordycepin repressed the chemokine, Ccl4 (p-value = ≤ 0.0001), but did not statistically significantly repress another chemokine, Cxcl2 (figure 6.2). Other regulators of inflammatory response were also repressed with cordycepin treatment, such as Acod1 (p-value = ≤ 0.01), Ptgs2 (p-value = ≤ 0.05), Errfi1 (p-value = ≤ 0.05), Dusp4 (p-value = ≤ 0.01), and Clec4e (p-value = ≤ 0.05) (figure 6.2).

Inhibition of PI3K through LY294002 (100 μM) compared to DMSO showed repression of Il1β (p-value = ≤ 0.01), Acod1 (p-value = ≤ 0.01), & Clec4e (p-value = ≤ 0.05) (figure 6.2). Errfi1 is known to have anti-proliferative and anti-inflammatory effects with LPS stimulation[709], and was found to be statistically significantly upregulated (p-value = ≤ 0.05) with LY294002 treatment (figure 6.2). There was a non-statistically significant repression of Tnf, and upregulation of Ptgs2, Cxcl2, & Ccl4 with LY294002

treatment. Dusp4 had no change in mRNA abundance compared to DMSO with PI3K inhibition by LY294002 (figure 6.2).

Treatment with the potent PI3K inhibitor, Pictilisib (500 nM), led to statistically significant repression of Il1β (p-value = ≤ 0.001), and Ptgs2 (p-value = ≤ 0.05) compared to DMSO (figure 6.2). Pictilisib had a non-statistically significant repression of Errifi1, Cxcl2 and Ccl4, and non-statistically significant upregulation of Tnf and Dusp4 (figure 6.2). There was no change in mRNA abundance for Acod1 and Clec4e compared to DMSO with Pictilisib treatment (figure 6.2).

The PI3K α-catalytic subunit-specific inhibitor, Alpelisib (25 μM), had statistically significant repression of Tnf (p-value = ≤ 0.05), Acod1 (p-value = ≤ 0.05), Dusp4 (p-value = ≤ 0.05), Clec4e (p-value = ≤ 0.05), and Ccl4 (p-value = ≤ 0.01) compared to DMSO (figure 6.2). Alpelisib also led to repression of Il1β, Ptgs2, and Cxcl2, which was not statistically significant. Similarly to LY294002 treatment, there was a statistically significant upregulation of Errfi1 (p-value = ≤ 0.05) with Alpelisib treatment compared to DMSO (figure 6.2).

Altogether, cordycepin repressed all inflammatory mRNA markers, whereas the PI3K inhibitors led in some cases to upregulation and were less consistent in repression of inflammatory mRNA markers. The PI3K inhibitor LY294002 was consistently seen to have a similar effect to cordycepin treatment in IPA analysis (figures 3.13B, 3.16B, & 3.19B). The effects of PI3K inhibitors for inflammatory mRNA markers (figure 6.2) shows that there were varying effects between all three PI3K inhibitors, and that LY294002 treatment is not identical to the effects of cordycepin treatment, and as such, further comparison of other modulators will be reviewed next.

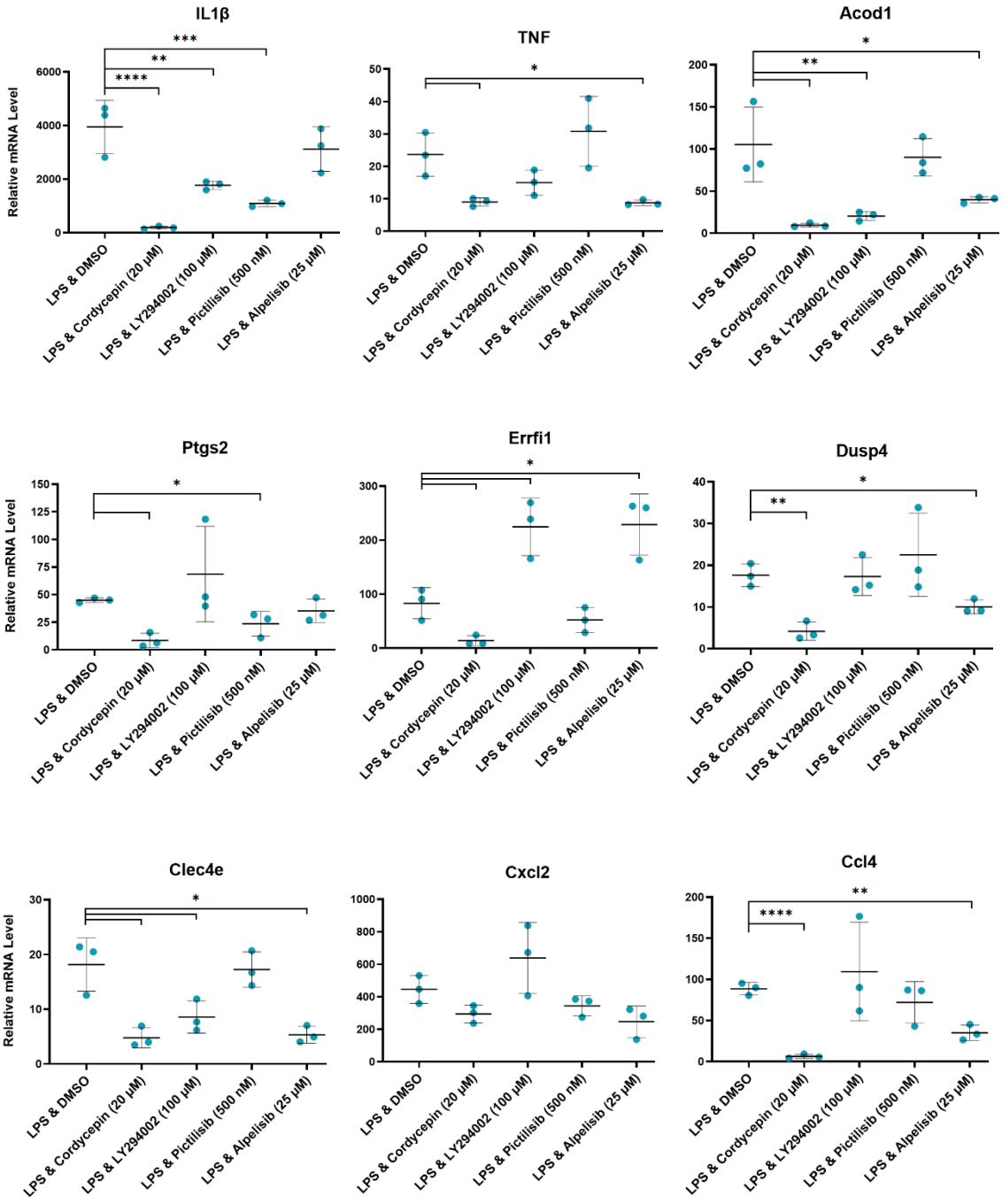

Figure 6.2: More inflammatory genes are repressed by cordycepin treatment compared to PI3K inhibitors. RAW264.7 macrophages were treated for 1 hour with either cordycepin (20 µM), DMSO (0.02% v/v), or PI3K inhibitors LY294002 (100 µM), Pictilisib (500 nM), or Alpelisib (25 µM) prior to LPS (1 µg/mL) inflammatory stimulation. qPCR output was analysed using the 2-ΔΔCt method[660] and normalised to Gapdh (housekeeping gene). Relative mRNA expression level of tested genes was obtained through comparing to RAW264.7 macrophages without any treatment (0 relative mRNA level). (mean ± SD; n=3 independent experiments; One-way Anova was used to obtain statistical significance against LPS & DMSO (0.02% v/v) and representative of; *P<0.05, **P<0.01, ***P<0.001, ****P<0.0001). Inhibitors: LY294002 (PI3K/mTOR/CSK2), Pictilisib (PI3K), Alpelisib (PI3Kα).

Due to differences between cordycepin treatment and PI3K inhibitors (figure 6.2), further comparison to other modulators of PI3K/Akt/mTOR and AMPK signalling was needed. Inhibition of mTOR through Torin1 (500 nM) for 1-hour prior to a further 1-hour LPS (1 μg/ml) inflammatory stimulation showed statistically significant repression of Il1β only (p-value = ≤ 0.001) (figure 6.3). There was statistically significant upregulation of Dusp4 (p-value = ≤ 0.05), Cxcl2 (p-value = ≤ 0.01), and Ccl4 (p-value = ≤ 0.05), and non-statistically significant upregulation of Tnf, Acod1, Ptgs2, and Clec4e, and downregulation of Errfi1 (figure 6.3) compared to LPS & DMSO treatment.

Similarly to mTOR inhibition, the only inflammatory mRNA marker with statistically significant repression was Il1β (p-value = ≤ 0.001) with inhibition of AKT (MK-2206; 10 μM) (figure 6.3). The only mRNA marker with statistically significant upregulation with AKT inhibition was Dusp4 (p-value = ≤ 0.05), the negative regulator of MAPK signalling[708] (figure 6.3). Inhibition of AKT led to a non-statistically significant upregulation of Tnf, Errfi1, Clec4e, and Cxcl2, and a non-statistically significant downregulation of Acod1, and Ptgs2 compared to LPS & DMSO (figure 6.3).

Activation of AMPK, known to regulate mTORC1 activity, showed a statistically significant upregulation of Il1β (p-value = ≤ 0.01) and Dusp4 (p-value = ≤ 0.05) compared to LPS & DMSO, similarly to both mTOR and AKT inhibition (figure 6.3). Other mRNA markers, Erffi1 (p-value = ≤ 0.05) and Cxcl2 (p-value = ≤ 0.01), were also upregulated with AMPK activation (figure 6.3). There was non-statistically significant upregulation of Tnf, Acod1, Ptgs2, Ccl4, and Clec4e with AMPK activation compared to LPS & DMSO (figure 6.3).

Apart from Cxcl2, treatment with cordycepin consistently repressed inflammatory mRNA markers as seen previously (figure 3.5 and 6.2), including Tnf, Acod1, Ptgs2, Errfi1, Clec4e (p-value = ≤ 0.05), Il1β and Ccl4 (p-value = ≤ 0.0001), and Dusp4 (p-value = ≤ 0.01) (figure 6.3). Altogether, mTOR inhibition and AMPK activation consistently upregulated inflammatory mRNA markers apart from Il1β, compared to LPS & DMSO (figure 6.3). In comparison to cordycepin, AKT inhibition also upregulated mRNA markers of inflammation, highlighting that the effect of cordycepin treatment on inflammatory expression is not the same as inhibition of AKT and mTOR, or activation of AMPK (figure 6.3). High-throughput comparison of cordycepin treatment and LY294002 will be further investigated to elaborate on figures 6.1 & 6.2.

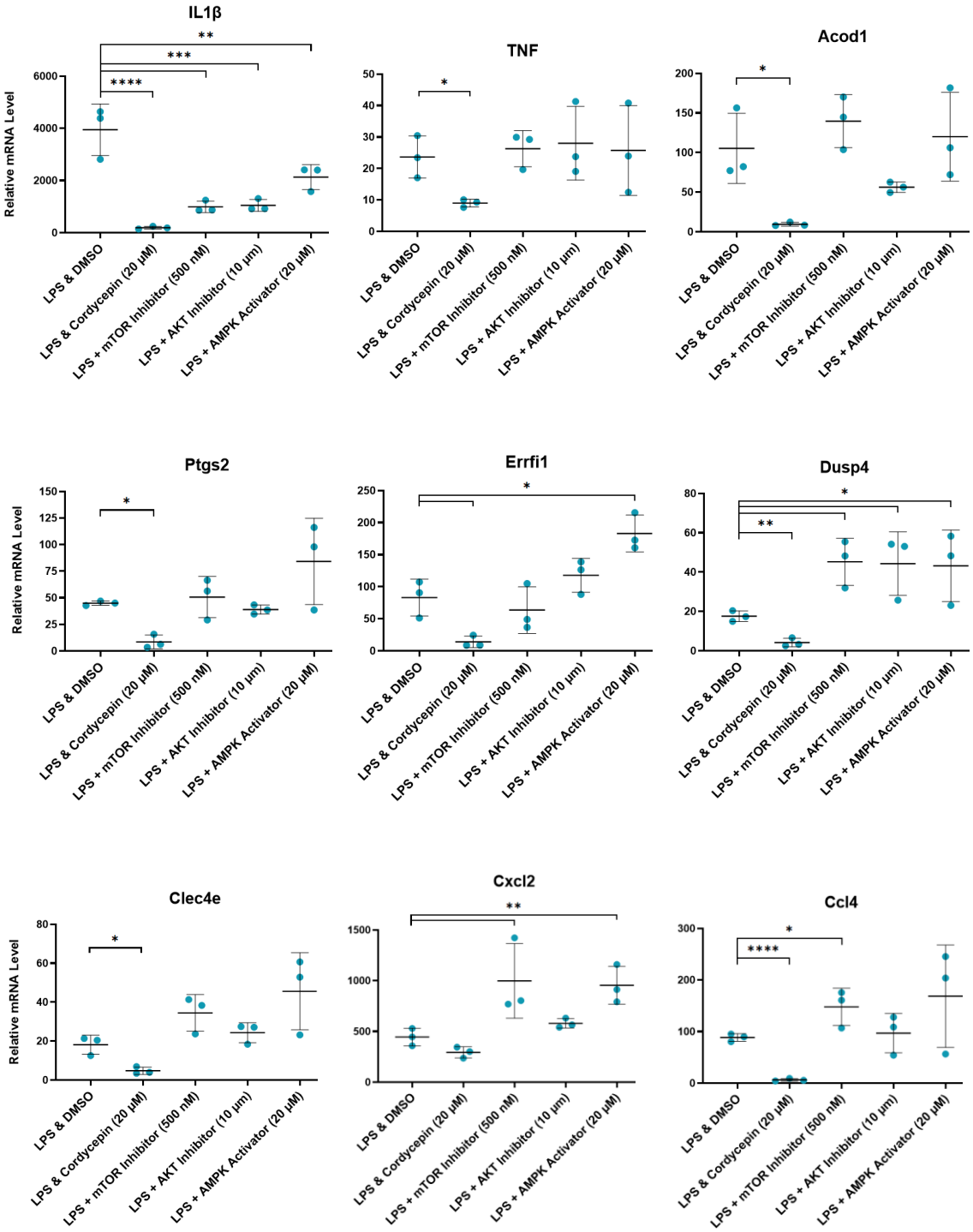

Figure 6.3: More inflammatory genes are repressed by cordycepin treatment compared to kinase modulators. RAW264.7 macrophages were treated for 1 hour with either cordycepin (20 μM), DMSO (0.02% v/v), or kinase modulators Torin1 (500 nM; mTOR inhibitor), MK-2206 (10 μM; AKT inhibitor), or A-769662 (20 μM; AMPK activator) prior to LPS (1 μg/mL) inflammatory stimulation. qPCR output was analysed using the 2-ΔΔCt method[660] and normalised to Gapdh (housekeeping gene). Relative mRNA expression level of tested genes was obtained through comparing to RAW264.7 macrophages without any treatment (0 relative mRNA level). (mean ± SD; n=3 independent experiments; One-way Anova was used to obtain statistical significance against LPS & DMSO and representative of; *P<0.05, **P<0.01, ***P<0.001, ****P<0.0001).

6.4 The effects of cordycepin and LY294002 on gene expression have a large overlap

As shown previously in this chapter, both cordycepin treatment and PI3K inhibition in RAW264.7 macrophages can significantly affect expression of inflammatory mRNA markers, with cordycepin consistently repressing mRNA abundance (figure 6.2). Cordycepin treatment was found to modulate many inflammatory biological pathways and regulators (figures 3.2, 3.3, 3.15-3.17) through analysis of RNA-Seq data. As the effect of cordycepin and PI3K inhibition leads to differences in the change of expression of inflammatory mRNA markers (figure 6.2), further work was needed to investigate whether PI3K inhibition has similar overall effects on inflammation. The PI3K inhibitor, LY294002, was chosen to be tested further through RNA-Seq of RAW264.7 macrophages as it has been shown to have a similar effect to cordycepin treatment on downstream expression (figures 3.16B, 4.2B, 4.5B, 4.7B, & 4.8B). RAW264.7 cells were treated for 1 hour with either DMSO (0.02% v/v), cordycepin (20 µM), or LY294002 (100 µM) before a further 1-hour LPS (1 µg/ml) inflammatory stimulation. For comparison to LPS & DMSO, cells were also treated solely with DMSO (0.02% v/v), to compare against treatment with LPS and confirm inflammatory stimulation.

Differential expressed genes were obtained from LPS & LY294002 treatment through comparison to LPS & DMSO and analysed through Log_2 fold change of RPKM values after Upper Quartile normalisation (UQ)[688, 689, 712] for RNA-Seq data (Methods section 2.6.2). A volcano plot illustrating the spread of expression of LPS & LY294002 treatment demonstrates a higher number of upregulated genes (891; ≥ 1 Log_2FC & ≤ 0.05 p-value), compared to downregulated genes (254; ≤ -1 Log_2FC & ≤ 0.05 p-value) (figure 6.4). Most of the genes (17,845) did not meet a statistical significance of ≤ 0.05 p-value and were within the Log_2FC range of +1 to -1 (figure 6.4).

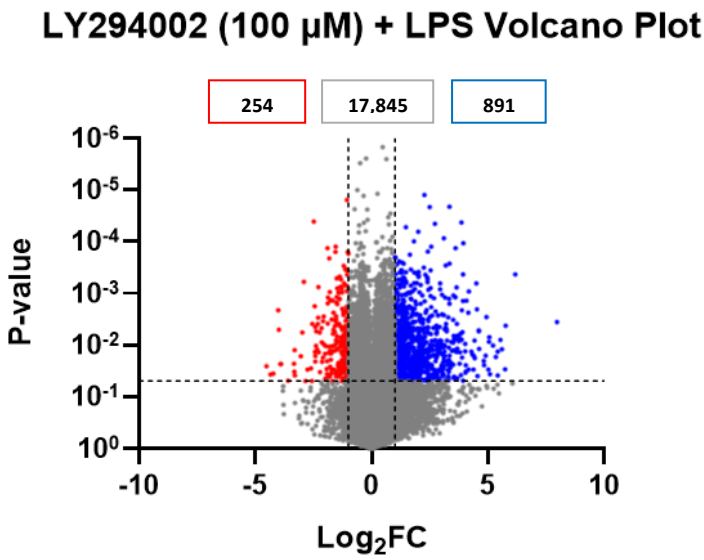

Figure 6.4: Volcano plot indicating the spread of differentially expressed genes with PI3K inhibition in RAW264.7 macrophages. Each dot represents a differentially expressed gene for LY294002 (100 µM; PI3K inhibitor) treatment compared to DMSO (0.02% v/v) with LPS (1 µg/mL) inflammatory stimulation. RNA-Seq was analysed through Log_2 fold change of treatment versus control of RPKM values after Upper Quartile normalisation (UQ)[688, 689, 712]. Red denotes downregulated genes with ≤ -1 Log_2FC & ≤ 0.05 p-value, blue denotes upregulated genes with ≥ 1 Log_2FC & ≤ 0.05 p-value, grey denotes genes which do not meet these requirements.

Consistently with the RNA-Seq dataset of cordycepin treatment (figure 3.15), the downregulated genes (≤ -1 Log_2FC & ≤ 0.05 p-value) for LY294002 treatment were enriched in multiple inflammatory biological pathways (figure 6.5A). This included inflammatory response, the immune system process, NF-κB signalling, and cellular responses to IFN-γ, IL-1, TNF and LPS (figure 6.5A). Inflammatory based upstream regulators also had negative z-scores and were predicted to be repressed, including TLR9, MYD88, and DUSP5, which is known to increase inflammatory gene expression in response to TNFα and dephosphorylate ERK1/2[823] (figure 6.6B). It is possible that the positive activation z-score of ERK is a feedback loop through DUSP5. The transcription factor, FOXO3, has a positive activation z-score (figure 6.6B), and is known to have pro- and anti-inflammatory effects, with inactivation leading to sustained interferon response to TNFα[824]. The negative regulation of transcription by RNAP II promoter, signal

transduction, and adenylate cyclase-inhibiting GPCR signalling pathways were also enriched by downregulated genes with LY294002 treatment (figure 6.5A). DAVID GO analysis of upregulated genes (≥ 1 Log_2FC & ≤ 0.05 p-value) were enriched in cilium and microtubule-based movement, extracellular matrix organisation, leukocyte migration, cellular differentiation, and adhesion, as well as SMAD, Wnt, and general signal transduction (figure 6.5B).

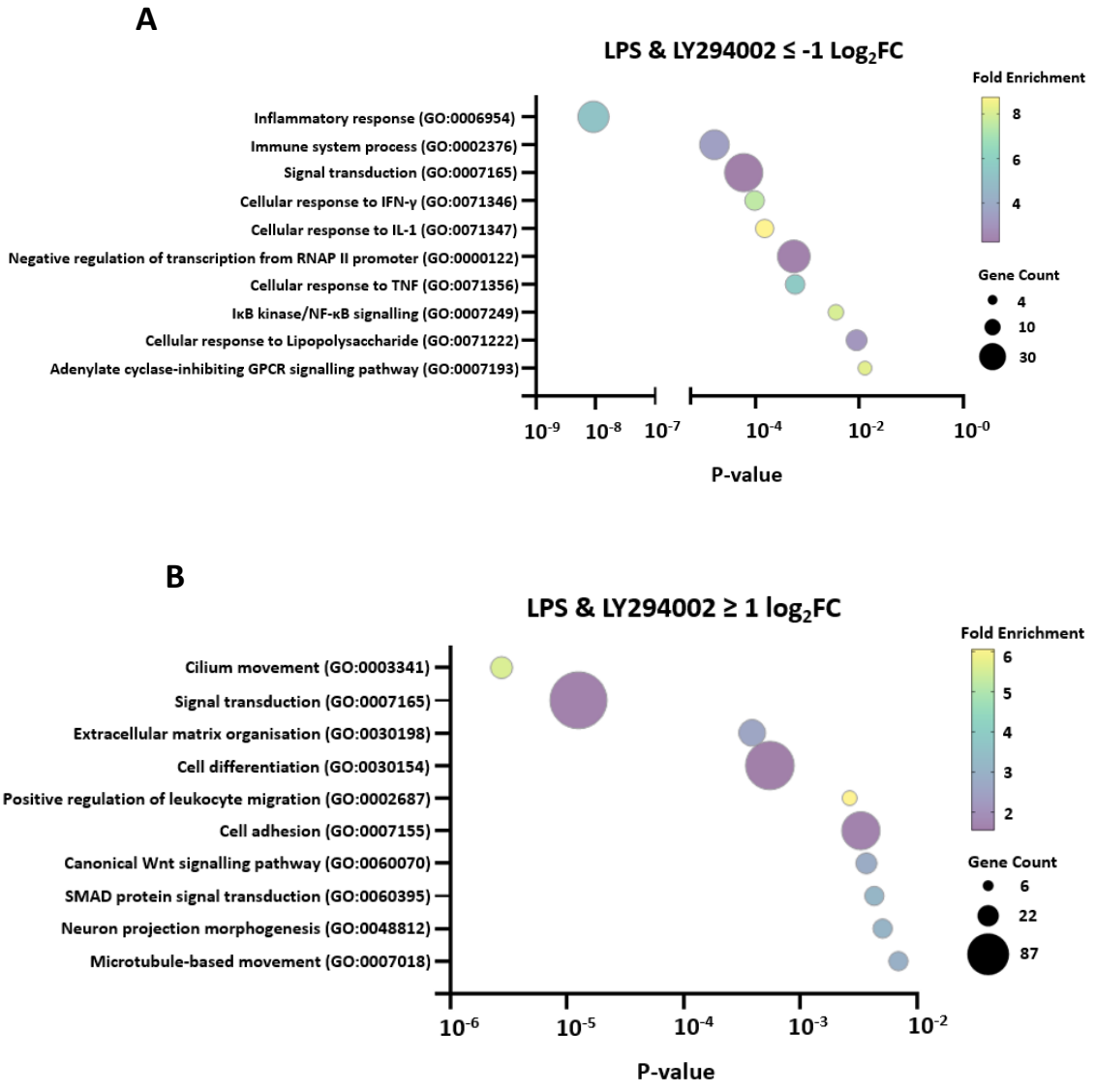

Figure 6.5: Differential expression analysis of PI3K inhibition indicates repression of key proinflammatory biological pathways. Differentially expressed genes obtained from RNA-Seq output of LY294002 (100 µM; PI3K inhibitor) treatment compared to DMSO (0.02% v/v) treatment with LPS inflammatory stimulation were inputted into DAVID Gene Ontology[690]. Bubble plots indicate enriched biological pathways associated with **A)** significantly repressed genes (≤ 0.05 p-value and Log_2FC of ≤ -1), and **B)** significantly upregulated genes (≤ 0.05 p-value and Log_2FC of ≥ 1) with cordycepin treatment.

Inclusion of all statistically significant genes for LY294002 treatment into the Expression Analysis tool in IPA[691] shows predicted repression of inflammatory biological pathways with negative activation z-scores. This included interferon and antiviral response, toll-like receptor signalling, IL-7 and IL-13 signalling, PI3K/Akt, p38 MAPK, and PTEN signalling (figure 6.6A). Multiple signalling pathways were upregulated with LY294002 treatment, including GPCR, Wnt, EGF, AMPK, and ERK/MAPK signalling which had positive activation z-scores. Transcription factors and growth factors such as EGF, JUN, ERK, p38 MAPK, STAT3, PDGF BB, TBGB1, and HGF were predicted to have similar effects to downstream expression to LY294002 treatment with positive activation z-scores (figure 6.6B). Alternatively, phagosome formation, and the superpathway of inositol phosphate compounds were also upregulated with LY294002 treatment (figure 6.6A). Unlike with cordycepin treatment, the MEK1/2 inhibitors, U0126 and PD098059 had negative activation z-scores with LY294002 treatment, highlighting opposite effects to downstream expression to these inhibitors (figure 6.6B). Due to these differences to cordycepin treatment on signalling modulators, the RNA-Seq datasets of cordycepin treatment and LY294002 will be compared to find consistent effects on downstream expression.

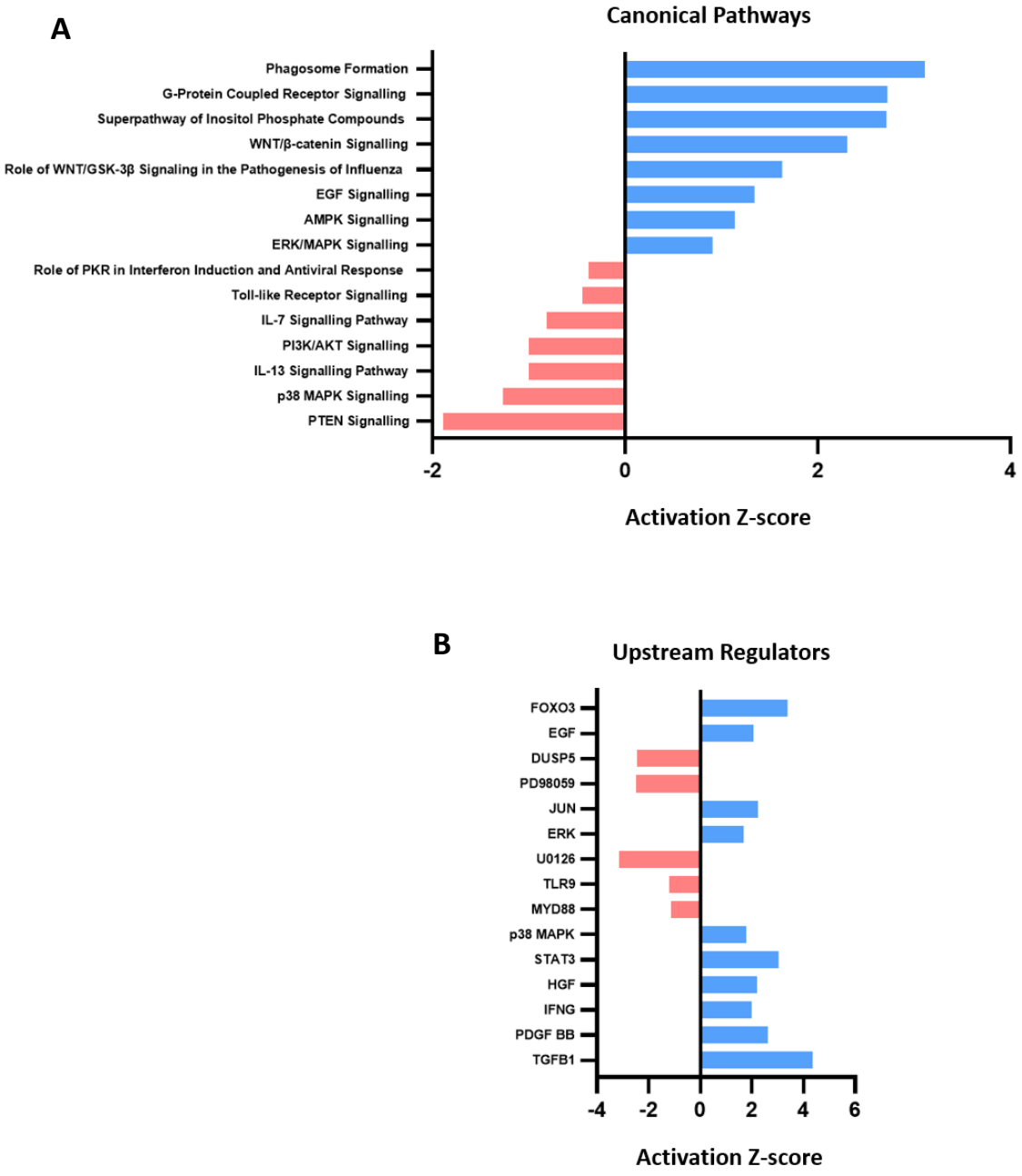

Figure 6.6: PI3K inhibition in RAW264.7 macrophages represses pro-inflammatory canonical biological pathways and upstream regulators. All statistically significant differentially expressed genes (≤ 0.05 p-value) obtained from RNA-Seq output of LY294002 (100 µM; PI3K inhibitor) treatment compared to DMSO (0.02% v/v) treatment with LPS inflammatory stimulation were inputted into IPA[691]. **A)** Indicates the top biological canonical pathways which are repressed (red bars) or upregulated (blue bars) with cordycepin treatment. **B)** Indicates the top upstream regulators which act in an opposite way (red bars) or act similarly (blue bars) to cordycepin treatment based on differential gene expression.

Previous results have already shown some similarity in the repression of inflammatory biological pathways with PI3K inhibition (figure 6.5A), and cordycepin treatment (figure 3.15A), as well as LY294002 having a proposed similar effect on expression to cordycepin downstream (figures 3.16B, 4.2B, 4.5B, 4.7B, & 4.8B). For more of a direct comparison between the treatment conditions, all statistically significant genes were compared based on gene nomenclature, showing an overlap of 2,110 genes between cordycepin treatment and LY294002 PI3K inhibition (figure 6.7A). These overlapped genes had a positive correlation based on Log_2 fold change ($R^2 = 0.482$, figure 6.7B), indicating that the two treatments have some relative similarity.

Many inflammatory biological pathways were repressed based on downregulated overlapped genes between cordycepin treatment and PI3K inhibition (figure 6.7C). These pathways include cellular response to TNF, LPS, and Interferon-γ, general inflammatory response and immune process, NF-κB activity, and IL-8 production (figure 6.7C). Signalling pathways such as JUN kinase and the ERK1/2 cascade are also enriched with overlapped downregulated genes, as well as transcription from RNAP II promoter (figure 6.7C).

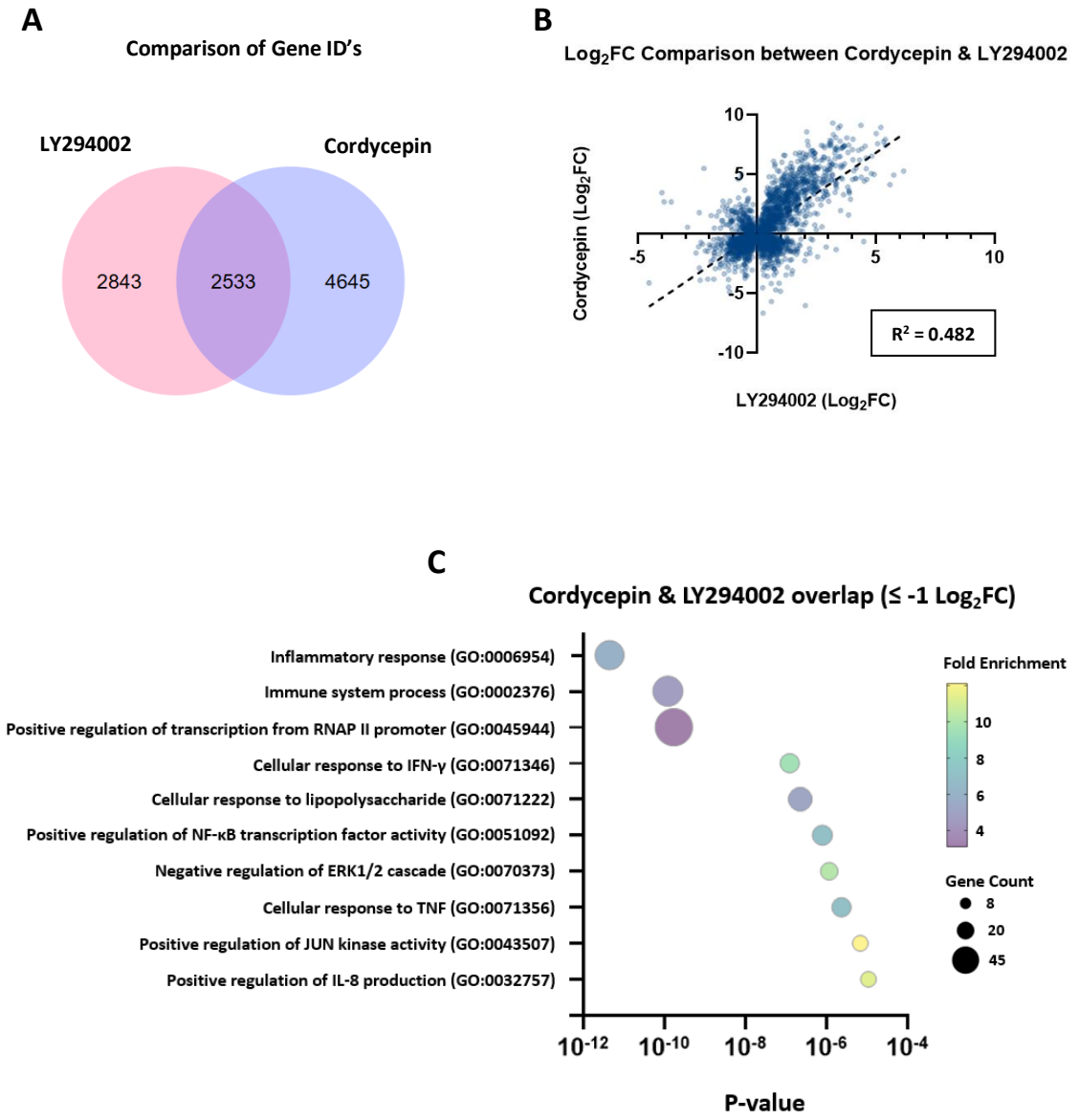

Figure 6.7: Overlap of differentially expressed genes between cordycepin treatment (RNA-Seq) and PI3K inhibition. Differentially expressed genes for cordycepin treatment (20 µM; RNA-Seq) was compared to LY294002 (100 µM; PI3K inhibitor) with 1-hour LPS inflammatory stimulation (1 µg/mL) in RAW264.7 macrophages. **A)** Venn diagram of all genes with statistical significance (≤0.05 p-value and FDR) for each treatment condition including overlapping genes. **B)** Scatter plot of Log_2FC of the overlapping genes (2,110) with R^2 value (0.482) indicating regression. **C)** Top 10 enriched GO biological pathway terms obtained through DAVID[690] for all repressed genes which overlapped between cordycepin and PI3K inhibition.

Comparison of all significantly differentially expressed genes (≤ -1 log_2FC and ≥ 1 log_2FC; ≤ 0.05 p-value) for cordycepin treatment (RNA-Seq) and LY294002 are linked to repression of PI3K/Akt, PTEN, RHOGDI, and interleukin-17 signalling pathways through Comparison analysis in IPA (figure 6.8A). Multiple inflammatory based upstream regulators were found to have negative activation z-scores and a predicted opposite effect on expression to cordycepin and PI3K inhibition through LY294002. These included MYD88, IRAK4, NOS2, RIPK2, TLR9, CCL20, TICAM1, and IFIH1, which is stimulated by LPS-MyD88 activation during M1 macrophage polarisation[825] (figure 6.8B). Besides the opposite effect of the RIPK2 kinase, known to modulate NOD1/2 and NF-κB signalling[724, 725], cordycepin and LY294002 also shows repression of NF-κB through having a similar effect to expression to the transcription regulators, KLF4 and SGK1, known inhibit NF-κB signalling[826, 827] (figure 6.8B).

Both cordycepin treatment and LY294002 PI3K inhibition were found to upregulate multiple signalling pathways, such as ERK/MAPK, Wnt/GSK3β, SNARE, protein kinase A, FAK, GPCR, Rho GTPase, and CREB signalling (figure 6.8A). This could be why the upstream regulators, CREB, JAK1/2, transcription regulator CEBBP, and G-protein coupled receptor PTGER4 have positive activation z-scores and similar effects on downstream expression as cordycepin treatment and LY294002 (figure 6.8B). PPAR signalling was consistently predicted to be upregulated with cordycepin treatment (figures 4.2A, 4.5A, & 4.8A), which is potentially why the ligand-dependent nuclear receptor, PPARγ (PPARG), has a positive activation z-score with overlapping genes (figure 6.8B). Similarly to previous results, phagosome formation, and superpathway of inositol phosphate compounds were upregulated with cordycepin and LY294002 (figures 3.16A & 6.6A).

Altogether, overlapping genes for both cordycepin treatment and PI3K inhibition through LY294002 can lead to repression of inflammatory biological pathways, and upregulation of ERK/MAPK, CREB, GPCR, and Wnt signalling pathways, which could be feedback loops of the inhibition of PI3K. Statistically significant genes show a positive correlation in Log_2 fold change (R^2 = 0.482, figure 6.7B), suggesting that cordycepin could affect inflammation in RAW264.7 macrophages partly through inhibiting PI3K, which will need further validation in future work.

A

Canonical Pathways

	Cordycepin + LPS	LY294002 + LPS
PI3K/AKT Signalling	-2.982	-1.000
RHOGDI Signalling	-2.400	-1.342
Crosstalk between Dendritic Cells and Natural Killer Cells	-1.604	-1.342
Pyroptosis Signalling Pathway	-1.279	-1.633
IL-7 Signalling Pathway	-0.816	-0.816
PTEN Signalling	-0.688	-1.890
Erythropoietin Signalling Pathway	-0.667	-0.632
ERK/MAPK Signalling	1.095	0.905
Signalling by Rho Family GTPases	1.616	2.828
Superpathway of Inositol Phosphate Compounds	1.667	2.714
Role of WNT/GSK-3β Signalling in the Pathogenesis of Influenza	1.941	1.633
Pathogen Induced Cytokine Storm Signalling Pathway	2.475	2.200
Protein Kinase A Signalling	2.626	1.155
SNARE Signalling Pathway	4.802	1.633
Breast Cancer Regulation by Stathmin1	5.277	2.967
G-Protein Coupled Receptor Signalling	6.384	2.722
FAK Signalling	6.565	2.994
Synaptogenesis Signalling Pathway	6.677	2.324
Phagosome Formation	7.309	3.111
CREB Signalling in Neurons	7.544	2.967

Activation Z-score

B

Upstream regulators

Upstream Regulators	Molecule Type	Cordycepin + LPS	LY294002 + LPS
METTL3	Enzyme	4.434	1.830
PTGER4	G-protein coupled receptor	4.139	1.612
SMARCA4	Transcription regulator	2.848	2.240
SGK1	Kinase	2.629	2.000
CREBBP	Transcription regulator	2.222	1.166
MEF2C	Transcription regulator	1.984	1.875
KLF4	Transcription regulator	1.946	1.809
PPP3R1	Phosphatase	1.937	2.000
JAK1/2	Group	1.886	1.134
PPARG	Ligand-dependent nuclear receptor	1.589	2.419
CREB	Group	1.000	2.043
IRAK4	Kinase	-1.358	-1.460
IFIH1	Enzyme	-1.615	-1.025
H-89	Kinase inhibitor (PKA)	-1.636	-1.464
MYD88	Adaptor	-2.248	-1.144
TLR9	Toll-like receptor	-2.592	-1.180
NOS2	Enzyme	-2.652	-1.772
CCL20	Cytokine	-2.736	-1.342
RIPK2	Kinase	-3.002	-1.589
TICAM1	Adaptor	-3.140	-1.295

Activation Z-score

Figure 6.8: Comparison of biological canonical pathways and upstream regulators consistently affected between cordycepin treatment and PI3K inhibition (RNA-Seq). Differentially expressed genes for cordycepin treatment (20 µM; RNA-Seq) was compared to LY294002 (100 µM; PI3K inhibitor) with 1-hour LPS inflammatory stimulation (1 µg/mL) in RAW 264.7 macrophages. All significantly differentially expressed genes (≤ -1 $\log_2$FC and ≥ 1 $\log_2$FC; ≤ 0.05 p-value) for both treatments were compared in IPA[691]. **A)** biological canonical pathways and **B)** upstream regulators.

6.5 Knockdown of WDR33 represses activation of PI3K/Akt/mTOR signalling kinases in RAW264.7 macrophages

As shown in a previous chapter, the effect of cordycepin and knockdown of poly(A) machinery, WDR33, were found to be similar in repression of inflammatory stimulation in RAW264.7 macrophages (figures 3.5, 3.11-3.13, 3.18, & 3.19). For both cordycepin and WDR33 knockdown, there was also repression of PI3K/Akt and MEK1/2 signalling (figures 3.13A & 3.19A), prompting for further validation. For the knockdown of WDR33 and scrambled control for comparison, RAW264.7 macrophages were treated with siRNA twice for 24-hours (48-hour siRNA knockdown in total), incubated in media containing less FBS (0.5%) for the final 24-hour knockdown, and either not treated or stimulated with LPS (1 μg/ml) for 1-hour prior to extraction of total protein following Methods sections 2.1.3 and 2.3.

Through comparison of no treatment and LPS stimulation in siRNA scrambled control (siCtrl), there is an increase in phosphorylation in AMPK (Thr172), 4E-BP1 (Thr37/46), and GSK3β (Ser9) (figure 6.9). When compared to siCtrl, knockdown of WDR33 increased the phosphorylation of AMPK (Thr172) and reduced the phosphorylation of GSK3β (Ser9) and 4E-BP1 (Thr37/46) with and without LPS stimulation (Figure 6.9). Confirmation of WDR33 knockdown was shown with depletion of WDR33 protein bands for WDR33 knockdown compared to siCtrl (figure 6.9). GAPDH loading control was used to show that protein was loaded equally for both siCtrl and siWDR33 protein samples, and any effects of protein abundance is through treatment conditions (figure 6.9).

These results show that in RAW264.7 macrophages, when you knockdown WDR33, there is a repression of mTOR signalling which induces reduction in the phosphorylation of 4E-BP1 (Thr37/46) and phosphorylation and activation of AMPK (Thr172) (figure 6.9). There is also a repression in the phosphorylation of GSK3β (Ser9), however total GSK3β was also affected, so this is not conclusive that WDR33 knockdown represses AKT (figure 6.9).

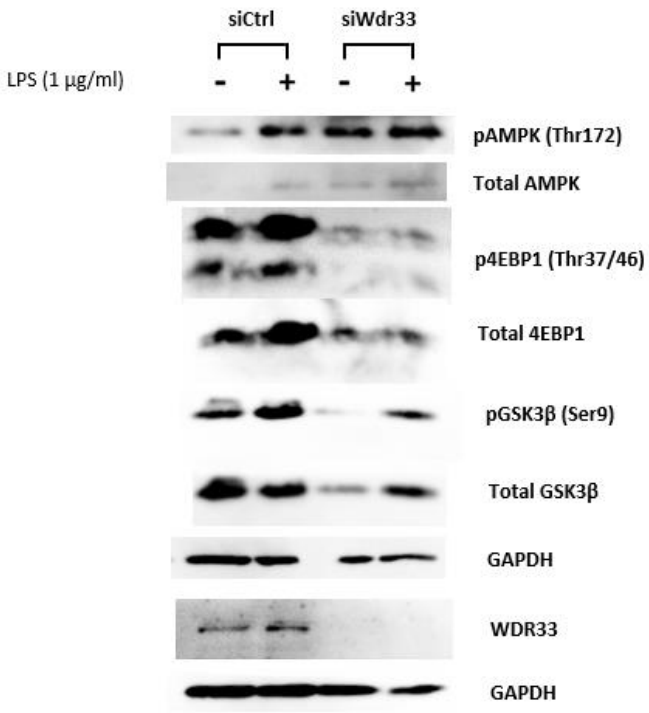

Figure 6.9: Knockdown of WDR33 in RAW264.7 macrophages represses PI3K/Akt/mTOR signalling through modulating kinase activation. RAW264.7 macrophages were subjected to siRNA knockdown of either WDR33 (siWDR33) or scramble control (siCtrl) for a total of 48 hours prior to 1-hour LPS (1 µg/mL) inflammatory stimulation. Total protein was extracted following Methods section 2.3.1. Western blotting and primary antibody incubation followed Methods section 2.3.3. Antibodies used is described in Table 2.4. (Diagram representative of one of three biological replicates).

6.6 Discussion

This chapter shows that cordycepin pre-treatment consistently represses many inflammatory mRNA markers that are induced by LPS in RAW264.7 macrophages (figures 6.2 & 6.3), as seen previously (figures 3.5 & 3.7). PI3K inhibition repressed some inflammatory genes, but not as effectively as cordycepin (figure 6.2), including the LY294002 inhibitor which was seen previously to have similar effects on downstream expression of inflammatory genes in RAW264.7 macrophages (figures 3.16 & 3.17C). Interestingly, there is some overlap between cordycepin and LY294002 treatments in RNA-Seq of statistically significant differential gene expression ($R^2 = 0.482$, figure 6.7B). As the p110δ isoform of PI3K is abundant in immune cells, there may be higher correlation to cordycepin treatment than LY294002, and future work could include comparing to the PI3Kδ inhibitor, Idelalisib[27, 45-47]. Similarly, cordycepin and modulators such as PI3K inhibitors, led to repression of mTORC1 signalling, as 4E-BP1 (Thr37/46) compared to LPS & DMSO treatment in RAW264.7 macrophages (figure 6.1), suggesting similar effect on translation.

Treatment with other kinase modulators; mTOR and AKT inhibitors, and an AMPK activation, prior to inflammatory stimulation failed to repress mRNA expression, except for Il1β (figure 6.3). This also shows that cordycepin does not appear to be acting through mTOR and AKT inhibition, or AMPK activation in repressing inflammatory mRNA marker expression in RAW264.7 macrophages. As PI3K/Akt activation is known to upregulate transcription of pro-inflammatory mRNAs with inflammatory stimulation[222, 223], it is a surprise that AKT inhibition did not lead to more substantial repression of inflammatory mRNA markers (figure 6.3) and PI3K inhibition repressed some inflammatory markers (figure 6.2). As LPS can also stimulate Tpl2, which phosphorylates and activates ERK1/2, MEK1 and JNK signalling pathways[248-250], upstream to transcription of proinflammatory cytokines IL-10, IL-6, and TNF-α[246, 247], the effect with the PI3K and AKT inhibitors could be through a feedback activation of MAPK signalling[281-284]. However, this is speculative, and future work should include the inhibition of MAPK pathways to show effects on inflammatory stimulation on mRNA expression.

Activated TLR's, such as TLR2, 4, 5, and 9 are known to activate PI3K/Akt via MyD88, leading to phosphorylation and inaction of GSK3β (Ser9). This process leads to activation and nuclear translocation of NF-κB, CREB, STAT, and AP-1 of pro-inflammatory mRNAs[828-830]. Overlapping statistically significant repressed genes between cordycepin treatment and the PI3K inhibitor, LY294002, is associated with

MyD88, IRAK4, NOS2, RIPK2, and TLR9, which could be why PI3K/Akt signalling is also repressed (figure 6.8). This repression of the RIPK2 kinase, which is known to modulate NF-κB signalling[724, 725], and the similar expression to transcription regulators which inhibit NF-κB signalling, KLF4 and SGK1[826, 827] (figure 6.8B), also relates to repression of nuclear translocation of NF-κB (p65) through cordycepin treatment (figure 3.4). Consistently, PPAR signalling has been found to be upregulated by cordycepin treatment (figures 3.10A, 4.2A, 4.5A, & 4.8A), which is known to repress cytokine production and NF-κB signalling[714-717]. This is potentially why the ligand-dependent nuclear receptor, PPARγ (PPARG), has a positive activation z-score with overlapping genes between cordycepin treatment and LY294002 (figure 6.8B). This altogether could suggest that cordycepin acts through PI3K inhibition in upregulating kinases, and signalling pathways such as PPAR signalling, which modulates NF-κB signalling.

Alternatively, knockdown of WDR33 was also found to repress phosphorylation of GSK3β (Ser9) and 4E-BP1 (Thr37/46), and activate AMPK through phosphorylation at Thr172, with and without LPS inflammatory stimulation in RAW264.7 macrophages (figure 6.9). This suggests that knockdown of WDR33 can repress AKT and mTORC1 signalling, which was shown previously in figures 3.13 and 3.19, as WDR33 knockdown had a similar effect on downstream expression as LY294002, and the MEK1/2 inhibitor, U0126. This effect on MEK/ERK signalling was also seen in figures 3.10B & 3.11. This is also partly substantiated as knockdown of CPSF4 can repress phosphorylation of PI3K (Tyr458) and Akt (S473)[635], which also links cleavage and polyadenylation machinery to signalling pathways. The repression of inflammatory pathways (figures 3.9A & 3.10A) and NF-κB signalling (figures 3.9, 3.13, & 3.19) through WDR33 knockdown could also be through modulating signalling machinery. Previously, knockdown of CPSF4 has been linked to reduced phosphorylation of IKKα/β and IκBα and nuclear translocation of NF-κB[630], which was further proven by Ashraf *et al*. 2019[384], demonstrating that cleavage and polyadenylation factors play a role in inflammation. As overlapping repressed genes for cordycepin treatment and WDR33 knockdown have a similar effect on downstream expression as PI3K, MEK, and p38 MAPK inhibitors (3.13, 3.18C, & 3.19), this altogether suggests that there is a link between polyadenylation and signalling pathways.

As cordycepin represses AKT-mediated phosphorylation of GSK3β (Ser9), it is probable that this leads to reduced activation of pro-inflammatory transcription factors downstream, and inflammatory mRNA

shown in figures 3.5, 3.7, 6.2, & 6.3). The PI3K inhibitors did not appear to have the same effect on the phosphorylation of GSK3β (Ser9) as cordycepin treatment, with little to no effect of Pictilisib compared to DMSO, and increased phosphorylation seen with LY294002 and Alpelisib (figure 6.1). This upregulation of GSK3β for LY294002 and Alpelisib is consistent with figures 6.1 and 6.8A, as both cordycepin and PI3K inhibition can lead to the upregulation of Wnt/GSK3β, however this is not consistent with the effect of cordycepin treatment (figure 6.1). This therefore suggests that the GSK3β (Ser9) site is phosphorylated by another kinase in RAW264.7 macrophages. It is already known than GPER activation can mediate activation of ERK1/2 signalling and second messengers such as cAMP, which can lead to activation of CREB[322]. Increased cAMP levels through cAMP-dependent protein kinase (PKA) can also lead to activation of AMPK through phosphorylation at Thr172 in the T-loop by LKB1[144]. This upregulation of cAMP through GPER can explain the increased phosphorylation and activation of AMPK by cordycepin treatment and PI3K inhibition by LY294002 and Alpelisib prior to inflammatory stimulation (figure 6.1). This is also suggested through the upregulation of GPCR signalling with LY294002 treatment prior to inflammatory stimulation (figure 6.6A). This crosstalk between GSK3β, CREB, and cAMP could also be why the AMPK activation causes an increase in GSK3β phosphorylation (figure 6.1).

The increased phosphorylation of AMPK could explain the reduced phosphorylation of 4E-BP1 (Thr37/46) downstream from mTORC1, as AMPK is known to repress mTORC1 through phosphorylating TSC2 at Ser1387, and Raptor at Ser722 and Ser792[153, 154]. Repression of 4E-BP1 (Thr37/46) through cordycepin has been shown to be abrogated with AMPK inhibition through compound C[369], which is consistent with this link. Activation of AMPK through cordycepin treatment was not seen in MCF-7 Breast Adenocarcinomas in the previous chapter (figure 5.1), suggesting cordycepin activates AMPK during inflammatory response, but not growth factor response. However this is not supported by previous results from Dr. Jialiang Lin[766]. Altogether, results from this chapter, in combination with results from chapter 5, suggests that cordycepin may not act directly through PI3K inhibition, however there is a link between polyadenylation and signalling pathways. As AMPK could still be a key mechanism of cordycepin, it will be reviewed in a CRISPR-Cas9 knockout cell line to see whether ablation of AMPK mitigates downstream effects of cordycepin in the next chapter.

7 AMPK CRISPR-Cas9 knockout does not restrict the effects of Cordycepin in EGF-stimulated HEK293 cells

7.1 Introduction

AMPK signalling is an intracellular ATP:AMP ratio sensing pathway known to repress mTOR through phosphorylating upstream regulator, TSC2, and mTORC1 subunit, Raptor[153, 154]. Cordycepin has been suggested to activate AMPK through interaction with the γ1 subunit of AMPK, or by allosteric activation as cordycepin monophosphate (CoMP)[13, 369, 831, 832]. Recently, the systematic review by Radhi *et al*. (2021)[3] has also highlighted that research unequivocally shows activation of AMPK by cordycepin through phosphorylation at Thr172 and Ser108 residues[369, 371, 373, 831, 833, 834]. Cordycepin has also been shown to enhance chemosensitivity through AMPK in Human Glioblastoma[372]. AMPK is known to regulate transcription of genes associated with lipid metabolism, such as PPARα, PPARγ and SREBP1c[835-837], which could be why PPAR and LXR/RXR signalling have positive activation z-score with cordycepin treatment in previous results (figures 3.3A, 3.10A, 3.16A, 4.2A, 4.5A, 4.7A, & 4.8A). It can therefore be suggested that the downstream effects of cordycepin are through activation of AMPK. However, as shown previously, cordycepin consistently had much more of a significant effect to expression of inflammatory and growth-dependent mRNAs than an AMPK activator in RAW264.7 macrophages and MCF-7 Breast Adenocarcinomas (figures 5.3 & 6.3), suggesting alternative effects by cordycepin.

It has been suggested by Hawley *et al.* (2020)[13] that cordycepin monophosphate (CoMP) acts as a less potent mimic of the adenosine mono-phosphate (AMP) substrate to AMPK, which was suggested as the causal effect of cordycepin on AMPK activation. They also found that CoMP could not activate AMPK with a mutant γ2 subunit in HepG2 cells, highlighting binding of CoMP to the γ subunit of AMPK, however AMPK knockout did not stop CoMP's effect on clonal survival in U2OS cells, suggesting that cordycepin is also acting through alternative mechanisms[13]. To review this further, both wild type and double AMPK γ-subunit CRISPR-Cas9 knockout (AMPK KO) HEK293 Human Embryonic Kidney cells, gifted from Professor Grahame Hardie's lab from the University of Dundee, were investigated to see if AMPK knockout depletes the effect of cordycepin.

7.2 EGF stimulates early growth response and EGF-stimulated biological pathways in both wild type and AMPK CRISPR-Cas9 knockout

HEK293 cells express endogenous EGF receptors and are well-characterised to respond to EGF stimulation[650, 651, 777-780]. For this reason, HEK293 cells were incubated in media containing less FBS (0.1%) for 24 hours, and then treated with cordycepin (25 µM) for 20 minutes before 30 minutes of EGF (15 nM) stimulation and compared to DMSO (0.025 v/v) treatment with EGF stimulation. HEK293 cells were also treated with DMSO (0.025% v/v) without EGF and compared to DMSO & EGF to check for EGF stimulation. These concentrations were chosen based on validations performed by Elizabeth Rider (figure A.6). RNA samples were sent to Azenta/GENEWIZ for Illumina NovaSeq RNA-Seq, with the FASTQ files sent back for RNA-Seq analysis of RPKM values after Upper Quartile normalisation (UQ)[688, 689, 712]. Principle component analysis (PCA) of the HEK293 biological replicates showed that biological replicate 1 for all treatment conditions was very different from the other biological replicates (figure A.5). For this reason, biological replicate 1 was taken out and only two biological replicates were taken forward for Upper Quartile normalisation (UQ)[688, 689, 712]. Total RNA was also converted to cDNA and qPCR was used to validate changes in EGF-induced mRNA markers with and without cordycepin treatment. EGF-related mRNA markers were chosen based on genes which were consistently found to be associated with EGF as an upstream regulator from IPA analysis output (figure 4.8).

To check the spread of differential gene expression with DMSO & EGF treatment compared to DMSO treatment on its own, volcano plots were plotted for both wild type (WT) and AMPK knockout (AMPK KO/AKO) HEK293 cells (figure 7.1). Most genes (25,885 for WT; 25,927 for AMPK KO) were not statistically significant (p-value = ≥ 0.05) and/or did not have a Log_2 fold change of over +1 or under -1 (figure 7.1). For WT HEK293 cells, there were less downregulated genes (54; ≤ -1 Log_2FC, p-value = ≤ 0.05) than upregulated genes (119; ≥ 1 Log_2FC, p-value = ≤ 0.05). The opposite was found for AMPK KO HEK293 cells, there were slightly more downregulated genes (68; ≤ -1 Log_2FC, p-value = ≤ 0.05) than upregulated genes (63; ≥ 1 Log_2FC, p-value = ≤ 0.05) (figure 7.1). Crucially, in both WT and AMPK KO HEK293 cells, EGF stimulation upregulated expression of transcription factors FOS and FOSB, as well as the early response genes, EGR1. However, EGR2 and EGR3 were only upregulated to ≥ 1 Log_2FC in WT cells (figure 7.1). This altogether shows that AMPK KO can potentially have an influence on the extent of upregulation of EGF-

stimulated genes. However, upregulation of FOS was confirmed through qPCR, and showed that c-FOS mRNA expression had a Log_2FC of ~10 (WT) and ~17 (AMPK KO) compared to DMSO treatment (figure 7.2), which highlights that AMPK KO is not restricting upregulation of FOS.

Other transcription factors, c-JUN, ATF3, and FOSL1, serine/threonine kinase, PLK2, and phosphatase, DUSP1, are also upregulated and above the DMSO expression line for both WT and AMPK KO (figure 7.2). SPRY2, known to modulate EGF stimulation[838], was also upregulated predominantly in AMPK KO HEK293 cells (figure 7.2). There were notable differences in the upregulation of mRNAs between WT and AMPK KO. For WT cells, there was a higher upregulation in ATF3 and TGIF1, compared to AMPK KO cells (figure 7.2). However, AMPK KO cells had a higher upregulation in c-FOS, c-JUN, PLK2, SPRY2, ERRFI1, and DUSP1, suggesting that initial EGF stimulation is higher for AMPK KO cells, potentially due to a lack of restriction from over-stimulation by AMPK (figure 7.2).

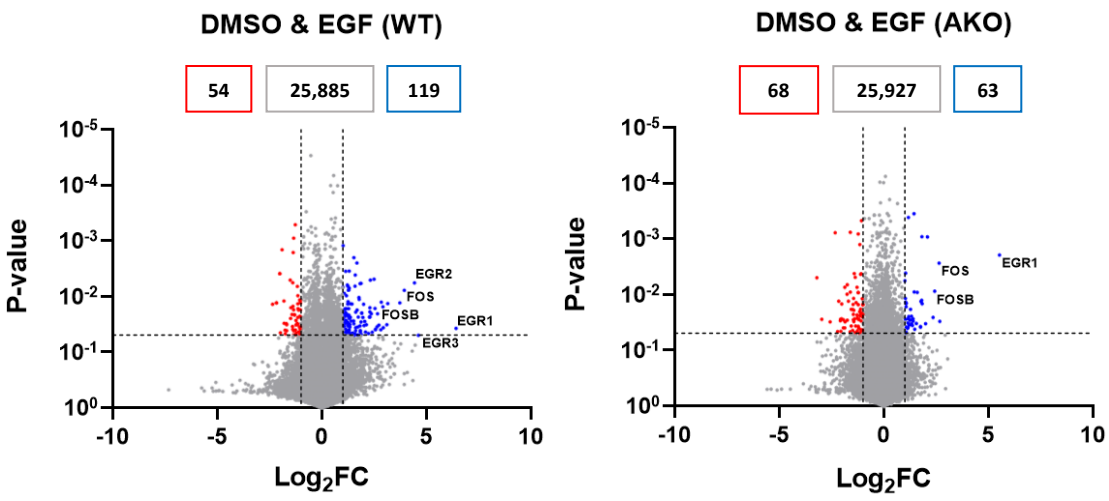

Figure 7.1: EGF treatment stimulates early growth response and EGF-stimulated mRNA transcripts in both wild type (WT) and AMPK knockdown HEK293 cells. HEK293 cells were gifted from Professor Grahame Hardie's lab at the University of Dundee. AMPK CRISPR-Cas9 knockout and wild type HEK293 cells were incubated in media containing less FBS (0.1%) for 24 hours prior to treatment with DMSO (0.025% v/v) for 20 minutes before stimulation with EGF (15 nM) for 30 minutes, or DMSO (0.025% v/v) on its own. Total RNA was extracted and sent off for RNA-Seq with output analysed through Log_2 fold change of treatment versus control of RPKM values after Upper Quartile normalisation (UQ)[688, 689, 712]. Each dot represents a differentially expressed gene with DMSO (0.025% v/v) and EGF stimulation. Red denotes downregulated genes with ≤ -1 Log_2FC & ≤ 0.05 p-value, blue denotes upregulated genes with ≥ 1 Log_2FC & ≤ 0.05 p-value, grey denotes genes which do not meet these requirements.

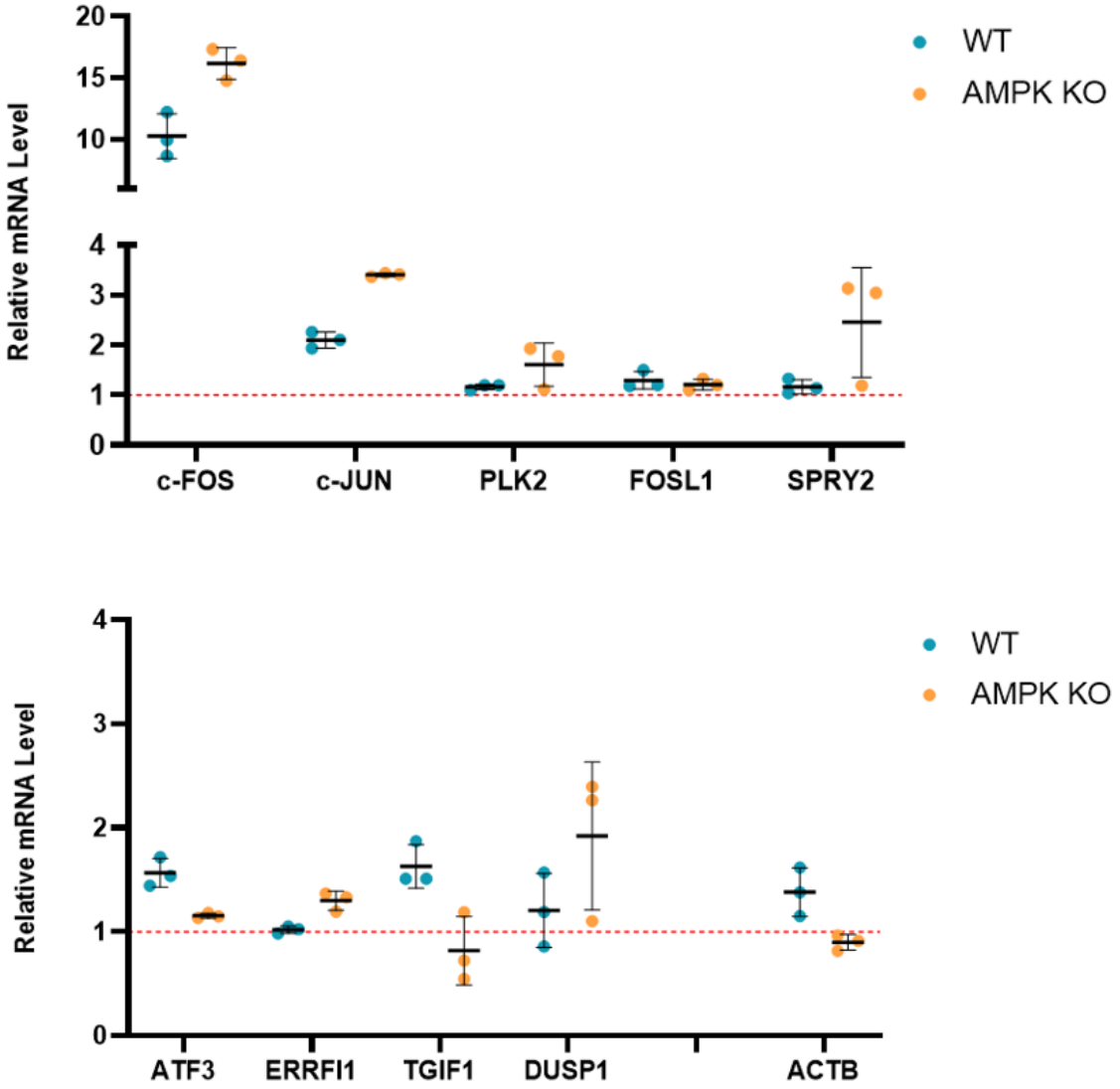

Figure 7.2: AMPK knockdown more consistently upregulates EGF-stimulated mRNA compared to wild type (WT). HEK293 cells were gifted from Professor Grahame Hardie's lab at the University of Dundee. AMPK CRISPR-Cas9 knockout and wild type HEK293 cells were incubated with media containing less FBS (0.1%) for 24 hours prior to treatment with DMSO (0.025% v/v) for 20 minutes before stimulation with EGF (15 nM) for 30 minutes, or DMSO (0.025% v/v) on its own. Total RNA was extracted prior to cDNA synthesis and qPCR. Output was analysed using the 2-ΔΔCt method[660] and normalised to GAPDH (housekeeping gene). Relative mRNA expression level of tested genes are presented relative to DMSO (0.025% v/v). (mean ± SD; n=3 independent experiments).

To confirm EGF stimulation further in both WT and AMPK KO HEK293 cells, all statistically significant upregulated genes (positive Log_2FC & p-value = ≤ 0.05) for WT (119) and AMPK KO (63) (figure 7.1) were inputted into DAVID Gene Ontology Analysis tool[690] to ensure there is enough input genes for more meaningful output. This was because of a lack of high differentially expressed genes in the datasets (figure 7.1).

Upregulated genes with EGF-stimulation in wild type HEK293 cells were enriched in RNA processing, response to hormone stimulus, cell differentiation and migration, and DNA biosynthetic process highlighting increased cellular and nucleic acid processing (figure 7.3A). However, the rate or frequency of transcription may be moderated as the upregulated genes with DMSO and EGF stimulation were enriched in the negative regulation of sequence-specific DNA binding biological pathway (figure 7.3A). Many genes enriched in RNA processing were small nucleolar RNAs (snoRNAs), important in many physiological and pathological cellular processes[839] (figure A.2.8A). The transcription factors FOS and FOSB, and the phosphatase DUSP1 were upregulated with DMSO and EGF stimulation in the enriched cellular response to hormone stimulus biological pathway (figures 7.3A & A.2.8A). This shows that in wild type HEK293 cells, EGF stimulation upregulates some key transcription factors and RNAs important for many cellular processes.

EGF stimulation in CRISPR-Cas9 AMPK knockout HEK293 cells upregulated genes enriched in cell cycle and migration, protein stabilisation and intracellular transport, response to DNA damage, and macromolecular complex assembly (figure 7.3B). Upregulated genes enriched in these biological pathways appear to be heterogeneous and span multiple protein types and groups (figure A.2.8B). Unlike in the wild type cells, EGF stimulation in AMPK knockout cells has an enrichment of upregulated genes in the regulation of transcription, such as the transcription factors FOS, JUNB, and FOXO4, early response genes, EGR1 and EGR3, as well as transcription mediators, MED23 and MED31 (figures 7.3B & A.2.8B). Altogether, EGF stimulation shows upregulation of biological pathways enriched with transcription factors, early response genes, and RNAs important for many cellular processes in both WT and AMPK KO. This, including the results of figure 7.1 and 7.2, demonstrates that EGF stimulation upregulates growth factor-related transcription factors and kinases in both WT and AMPK KO HEK293 cells, with some differences in biological pathways and genes specific to AMPK KO.

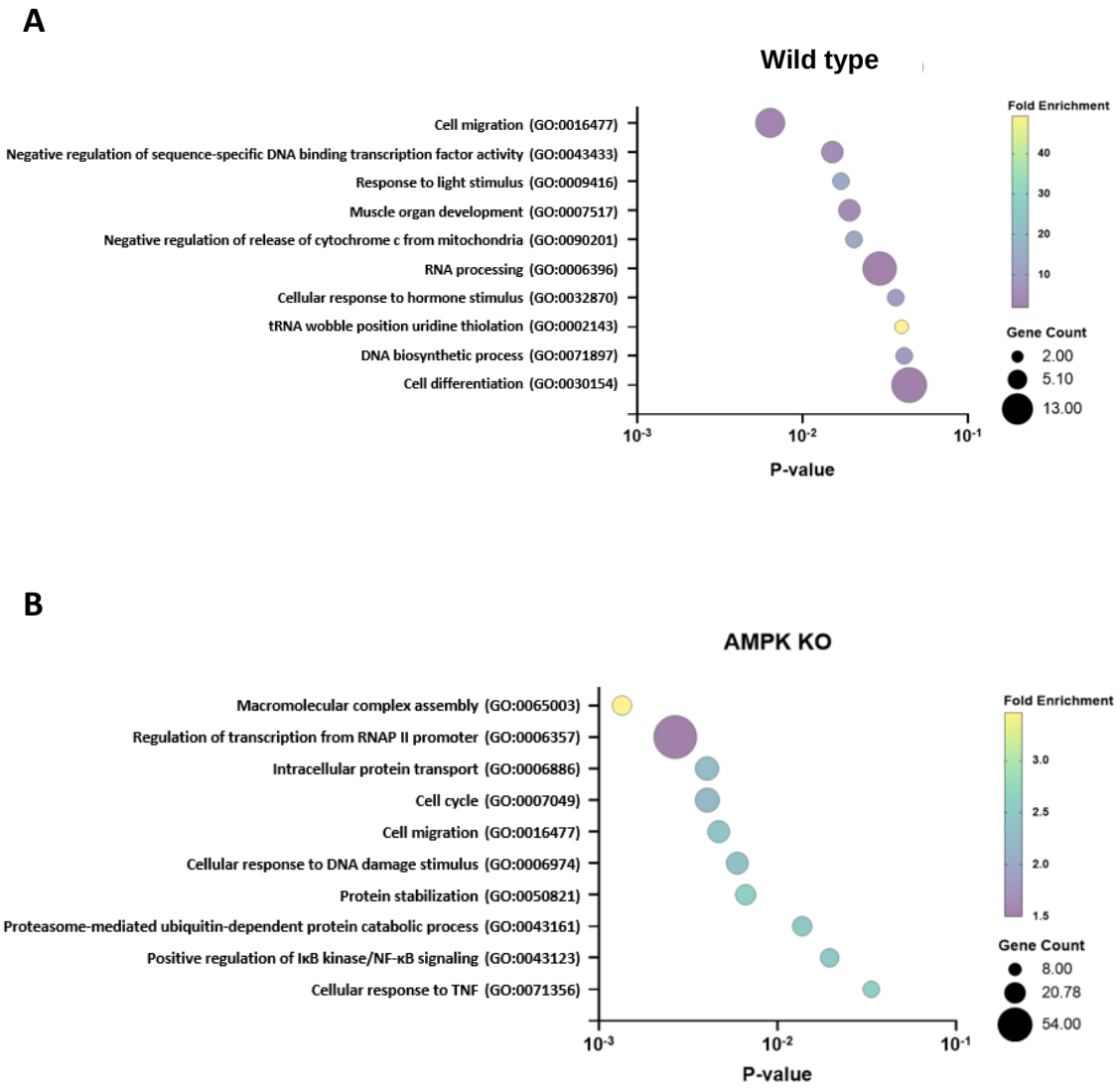

Figure 7.3: EGF-stimulated biological pathways are upregulated in both WT and AMPK KO HEK293 cells. HEK293 cells were gifted from Professor Grahame Hardie's lab at the University of Dundee. Wild type and CRISPR-Cas9 AMPK knockout HEK293 cells were incubated in media containing less FBS (0.1%) for 24 hours prior to treatment with DMSO (0.025% v/v) for 20 minutes before stimulation with EGF (15 nM) for 30 minutes. Total RNA was extracted and sent off for RNA-Seq, with output analysed through Log_2 fold change of treatment versus control of RPKM values after Upper Quartile normalisation (UQ)[688, 689, 712]. All statistically significant upregulated genes (positive Log_2FC & ≤ 0.05 p-value) compared to DMSO (0.025% v/v) on its own were included into DAVID Gene Ontology[690]. Bubble plots indicate enriched upregulated biological pathways in **A)** wild type HEK293 cells and **B)** CRIPSR-Cas9 AMPK knockout HEK293 cells.

7.3 Cordycepin represses EGF-stimulated transcription and early response mRNAs in both wild type and CRISPR-Cas9 AMPK knockout

As EGF stimulation can be seen in both wild type (WT) and AMPK KO HEK293 cells (figures 7.1-7.3), the effect of cordycepin (25 µM) treatment for 20 minutes prior to EGF (15 nM) stimulation for a further 30 minutes was investigated to check if AMPK KO depletes the effect of cordycepin. Differentially expressed genes for the comparison of cordycepin & EGF to DMSO & EGF treatment was obtained through Log_2 fold change of RPKM values after Upper Quartile normalisation (UQ)[688, 689, 712]. Differential expression was visualised through volcano plots, and most genes (25,078 for WT; 25,651 for AMPK KO) were not statistically significant (p-value = > 0.05) and/or did not have a Log_2 fold change of over +1 or under -1 (figure 7.4). For both WT and AMPK KO HEK293 cells, there were less downregulated genes (114 for WT, 62 for AMPK KO; ≤ -1 Log_2FC, p-value = ≤ 0.05) than upregulated genes (307 for WT, 345 for AMPK KO; ≥ 1 Log_2FC, p-value = ≤ 0.05) (figure 7.4). In WT HEK293 cells, cordycepin and EGF treatment led to downregulation of early growth response gene, EGR1, and the transcription factor, MYC (figure 7.4). Also repressed by cordycepin in WT HEK293 cells were mRNA encoding TTC26, HCG15, and the lncRNA MIR222HG (figure 7.4), which are either linked to the regulation of gene expression or poly(A) machinery[839-841]. Downregulated mRNAs found specifically in AMPK KO HEK293 cells with cordycepin treatment included CPAMD8, PSMD12P and mitochondrial encoded tRNAs, MT-TG and MT-TA (figure 7.4), of which are known to also attribute to cancer progression and translational efficiency[842-844].

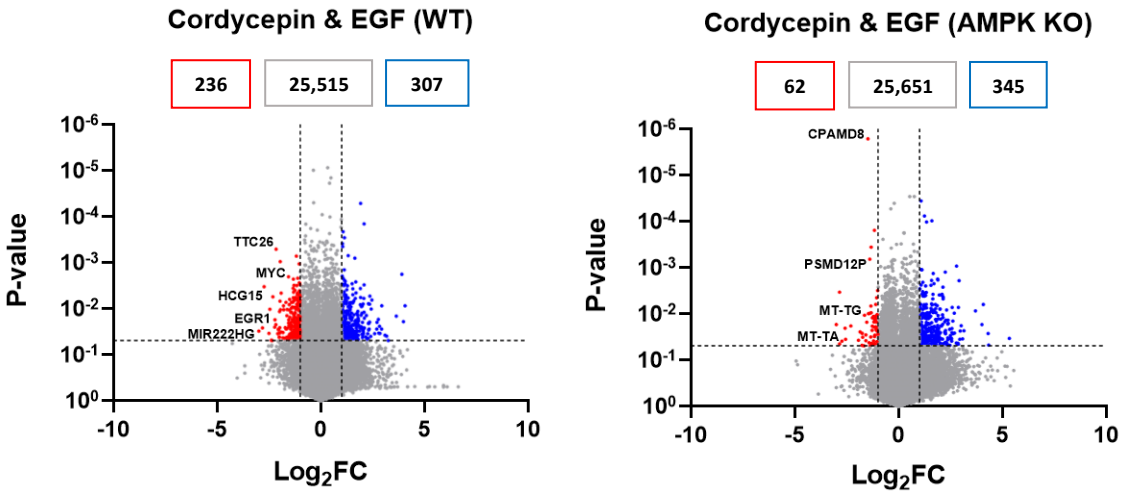

Figure 7.4: Cordycepin treatment represses early growth response and EGF-stimulated mRNA transcripts in both wild type and CRISPR-Cas9 AMPK knockout HEK293 cells. HEK293 cells were gifted from Professor Grahame Hardie's lab at the University of Dundee. AMPK CRISPR-Cas9 knockout and wild type HEK293 cells were incubated with media containing less FBS (0.1%) for 24 hours prior to treatment with cordycepin (25 µM) or DMSO (0.025% v/v) for 20 minutes before stimulation with EGF (15 nM) for 30 minutes. Total RNA was extracted and sent off for RNA-Seq, with output analysed through Log_2 fold change of treatment versus control of RPKM values after Upper Quartile normalisation (UQ)[688, 689, 712]. Each dot represents a differentially expressed gene with cordycepin (25 µM) and EGF stimulation. Red denotes genes with ≤ -1 Log_2FC & ≤ 0.05 p-value, blue denotes genes with ≥ 1 Log_2FC & ≤ 0.05 p-value, grey denotes genes with -1 to 1 Log_2FC & > 0.05 p-value.

To confirm repression of EGF-related mRNA marker expression, qPCR was used to show changes in mRNA abundance for cordycepin & EGF treatment compared to DMSO & EGF (figures 7.5 & 7.6). For WT HEK293 cells, the transcription factors, c-FOS, c-JUN, and ATF3, as well as SPRY2 and DUSP1 had statistically significant repression (p-value = ≤ 0.05-0.001) (figure 7.5). PLK2 and ERRFI1 had non-statistically significant repression, and the transcription factor, FOSL1, had a slight upregulation which was not statistically significant with cordycepin treatment in WT cells (figure 7.5). In comparison to WT, AMPK KO HEK293 cells also had statistically significant repression of transcription factors c-FOS (p-value = ≤ 0.0001), the phosphatase DUSP1, and SPRY2 (p-value = ≤ 0.05), but not the transcription factors, c-JUN and ATF3 (figure 7.6). Just like with the WT cells, cordycepin treatment did not have a big change in mRNA

expression for PLK2 and FOSL1, and a non-statistically significant repression of ERRFI1 in AMPK KO cells (figure 7.6). ACTB was used as a housekeeping gene and did not show statistically significant change for both WT and AMPK KO for cordycepin treatment (figure 7.5 & 7.6). Altogether, cordycepin still causes repression of EGF-related mRNA markers with AMPK Knockout, however transcription factors c-JUN and ATF3 were not repressed with statistical significance with AMPK Knockout. Further comparison of downregulated biological pathways for WT and AMPK KO HEK293 cells will be reviewed next to check if AMPK KO represses the effect of cordycepin on EGF-stimulated biological pathways.

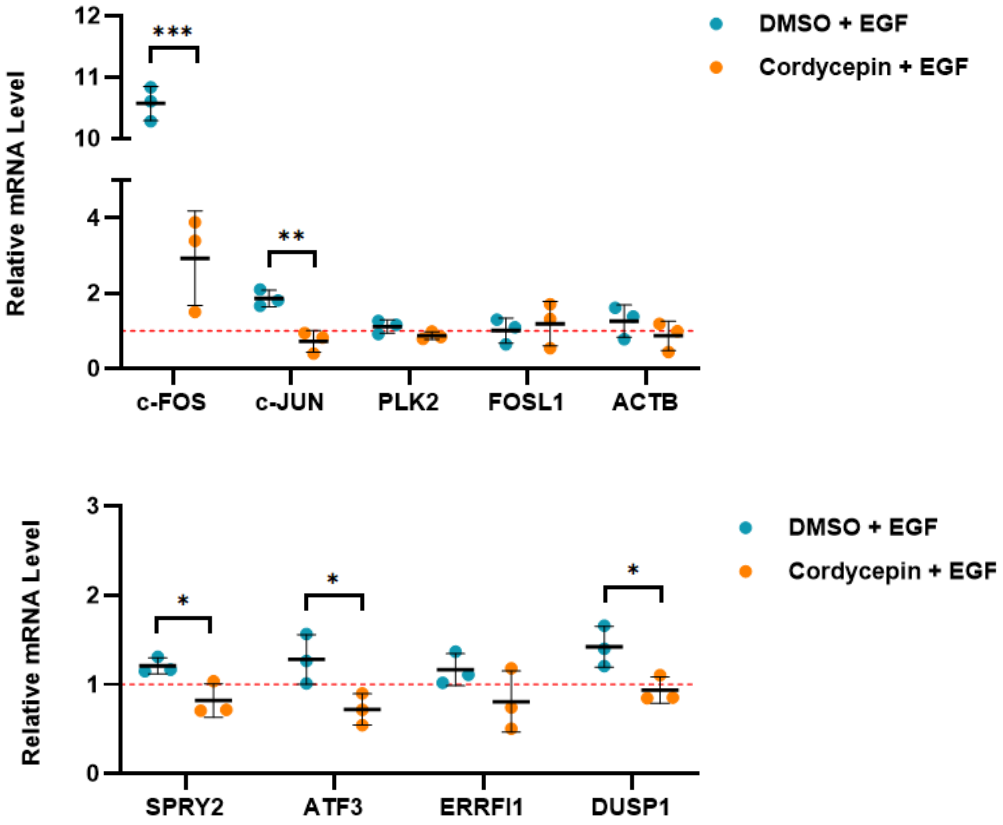

Figure 7.5: Cordycepin represses EGF-stimulated mRNA in wild type HEK293 Human Embryonic Kidney Cells. HEK293 cells were gifted from Professor Grahame Hardie's lab at the University of Dundee. Wild type HEK293 cells were incubated with media containing less FBS (0.1%) for 24 hours prior to treatment with either cordycepin (25 µM) or DMSO (0.025% v/v) for 20 minutes before stimulation with EGF (15 nM) for 30 minutes, or DMSO (0.025% v/v) on its own. Total RNA was extracted prior to cDNA synthesis and qPCR. Output was analysed using the 2-ΔΔCt method[660] and normalised to GAPDH (housekeeping gene). Relative mRNA expression level of tested genes are presented relative to DMSO (0.025% v/v). (mean ± SD; n=3 independent experiments; Students T-test was used to obtain statistical significance against DMSO (0.025% v/v) & EGF (15 nM) and representative of; *P<0.05, **P<0.01, ***P<0.001, ****P<0.0001).

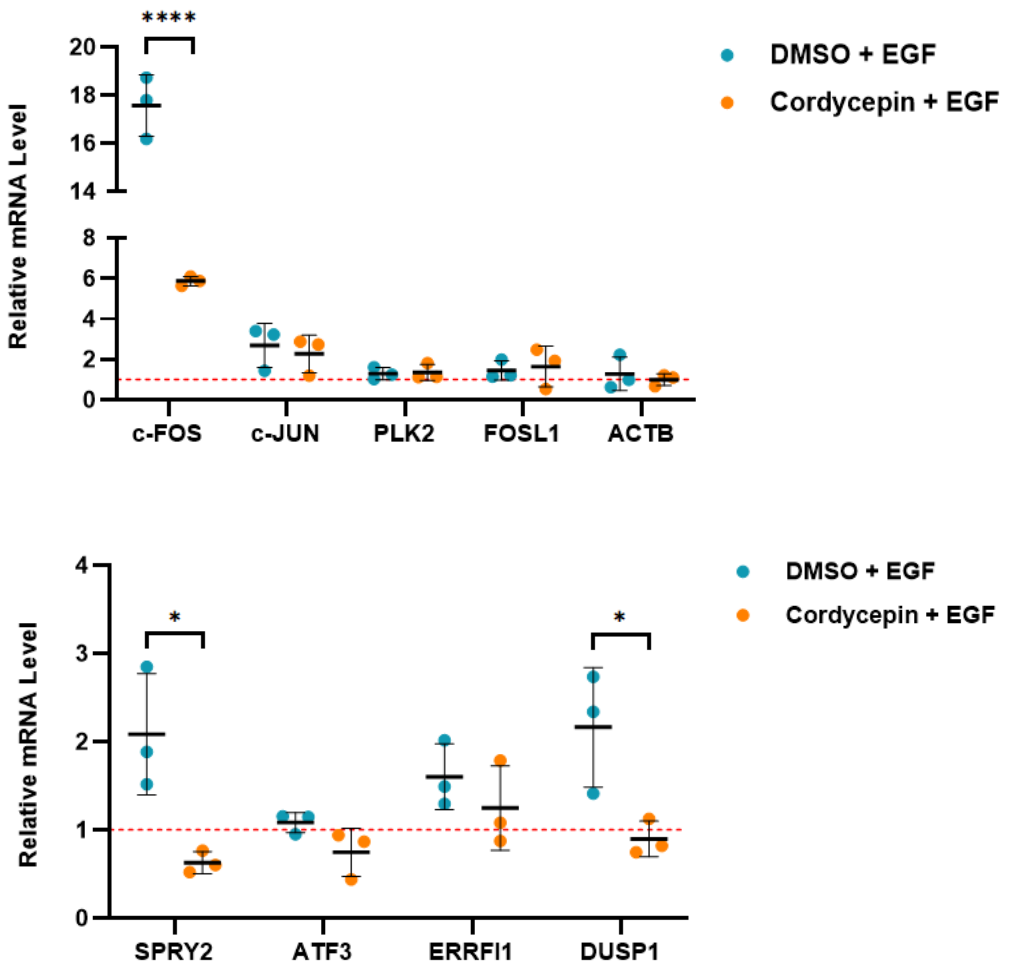

Figure 7.6: Cordycepin represses EGF-stimulated mRNA in CRISPR-Cas9 AMPK Knockout HEK293 Human Embryonic Kidney Cells. HEK293 cells were gifted from Professor Grahame Hardie's lab at the University of Dundee. AMPK CRISPR-Cas9 knockout HEK293 cells were incubated in media containing less FBS (0.1%) for 24 hours prior to treatment with either cordycepin (25 µM) or DMSO (0.025% v/v) for 20 minutes before stimulation with EGF (15 nM) for 30 minutes, or DMSO (0.025% v/v) on its own. Total RNA was extracted prior to cDNA synthesis and qPCR. Output was analysed using the 2-ΔΔCt method[660] and normalised to GAPDH (housekeeping gene). Relative mRNA expression level of tested genes are presented relative to DMSO (0.025% v/v). (mean ± SD; n=3 independent experiments; Students T-test was used to obtain statistical significance against DMSO (0.025% v/v) & EGF (15 nM) and representative of; *P<0.05, **P<0.01, ***P<0.001, ****P<0.0001).

To see whether AMPK Knockout (AMPK KO) restricts the effect of cordycepin on repressing EGF stimulation, all statistically significant downregulated genes (negative Log_2FC & p-value = ≤ 0.05) from the analyse of RNA-Seq datasets for wild type (WT) and AMPK KO HEK293 cells were entered into the DAVID Gene Ontology Analysis tool[690]. For WT HEK293 cells, cordycepin treatment repressed genes enriched in the response of EGF stimulus, transcription by RNAP II promoter, cell cycle and division, cytoskeleton organisation, and chromatic remodelling (figure 7.7A). Notable transcription regulators, MYC, ATF4, FOXO3, JUN, and early response genes EGR1 and EGR2, and the EGFR gene were all repressed with cordycepin treatment and enriched in the transcription biological pathway with WT HEK293 cells (figure A.2.9A). Signal transduction is also enriched with downregulated genes, including regulation of small GTPase mediated signal transduction, negative regulation of Wnt signalling and cyclin-dependent Ser/Thr kinase activity (figure 7.7A). Downregulated genes enriched for signal transduction pathways were heterogeneous, however mRNA's encoding Rho GTPase activating proteins were specifically enriched in the regulation of small GTPase mediated signal transduction (figure A.2.9A).

In AMPK KO HEK293 cells, cordycepin also repressed genes enriched in transcription (DNA-templated), cell cycle and division, and chromatin organisation and remodelling (figures 7.7B & A.2.9B). However, there is very little overlap between the genes repressed by cordycepin treatment which are enriched in these biological pathways between WT and AMPK KO HEK293 cells, with the notable absence of key transcription factors and early response genes in AMPK KO (figure A.2.9). Multiple repressed genes encoding RNA-binding proteins (RBPs) are enriched with cordycepin treatment in the protein ubiquitination pathway, including RBBP6, MED11, Ring Finger proteins RNF6, RNF25, and RNF38, and F-box proteins FBXO21, FBXW7, FBXL15, and FBXO30 (figure A.2.9B). Other pathways which are enriched with repressed genes with AMPK KO were the regulation of circadian rhythm, protein ubiquitination, DNA repair, and autophagosome assembly (figures 7.7B & A.2.9B). Cordycepin also repressed genes enriched in the Inositol phosphate biosynthetic process biological pathway, which encode multiple kinases, including IPPK, PPIP5K2, IPMK, and IP6K1 (figures 7.7B & A.2.9B).

Altogether, cordycepin treatment does appear to have different effects to biological pathways in WT and AMPK KO HEK293 cells, however regulation of transcription, cell cycle and division, and chromatin remodelling appear to consistently be repressed with cordycepin treatment (figure 7.7).

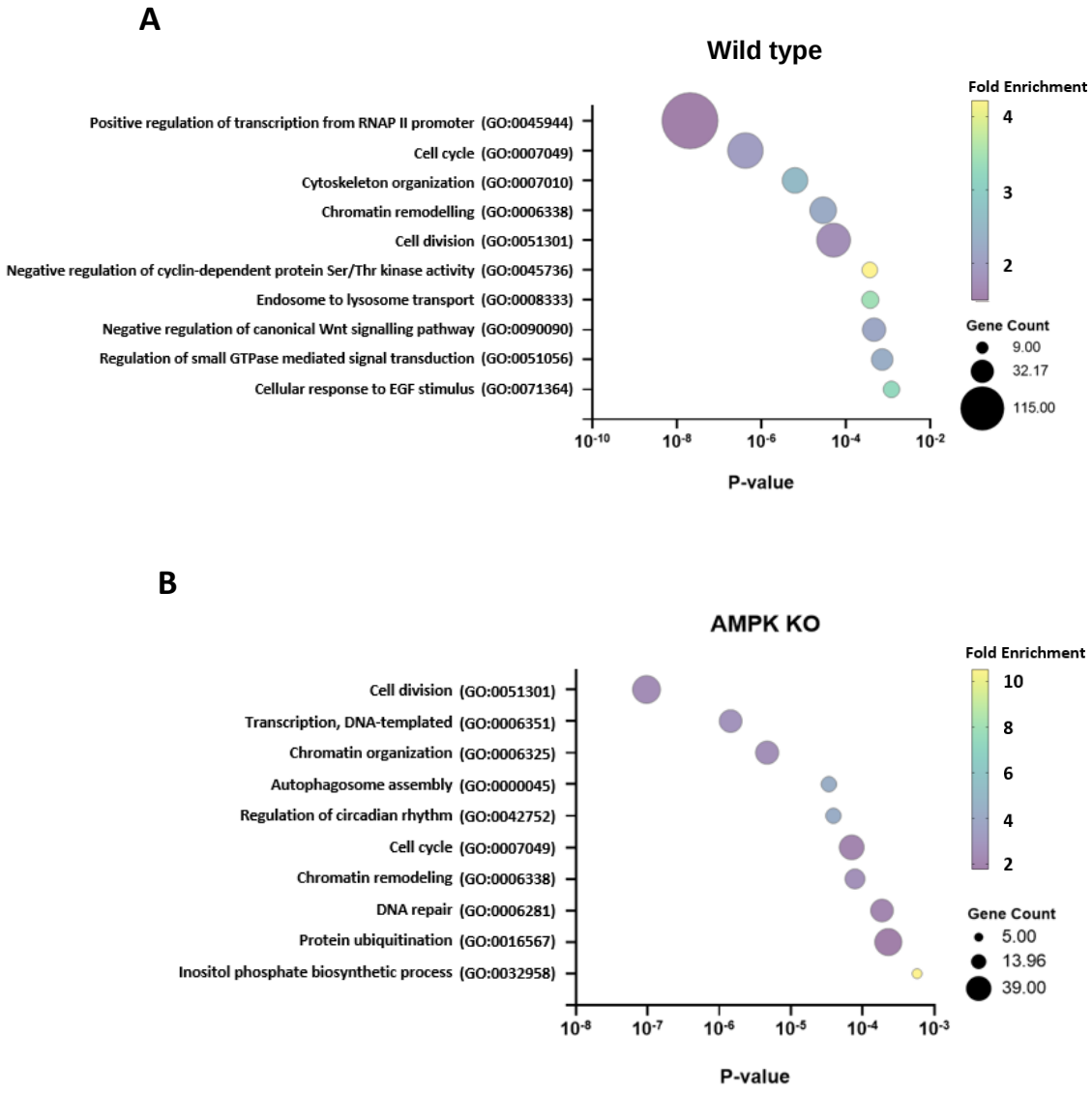

Figure 7.7: Cordycepin represses multiple EGF-stimulated signalling pathways & transcription in HEK293 cells. HEK293 cells were gifted from Professor Grahame Hardie's lab at the University of Dundee. Wild type and CRISPR-Cas9 AMPK knockout HEK293 cells were incubated in media containing less FBS (0.1%) for 24 hours prior to treatment with cordycepin (25 µM) or DMSO (0.025% v/v) for 20 minutes before stimulation with EGF (15 nM) for 30 minutes. Total RNA was extracted and sent off for RNA-Seq, with output analysed through Log_2 fold change of treatment versus control of RPKM values after Upper Quartile normalisation (UQ)[688, 689, 712]. All statistically repressed genes (≤ 0.05 p-value with a negative Log_2FC) were inputted into DAVID Gene Ontology[690]. Bubble plots indicate enriched biological pathways associated with significantly repressed genes (≤ 0.05 p-value cut-off only) for **(A)** wild type HEK293 cells, and **(B)** CRISPR-Cas9 AMPK knockout HEK293 cells.

7.4 Discussion

Results from this chapter has found that there are slight changes in the stimulation of EGF (figures 7.1-7.3), and effects of cordycepin treatment prior to EGF stimulation between wild type (WT) and AMPK knockout (KO) HEK293 cells (figures 7.4-7.7). However, the effect of cordycepin treatment is not completely abrogated by AMPK KO as there are consistent biological pathways affected by cordycepin in both HEK293 cell lines (figure 7.7). For both HEK293 cell lines, there was an upregulation of the immediate response genes (IEGs), EGR1, FOS, and FOSB with DMSO and EGF (figure 7.1). EGR1 is a known transcriptional regulator which upregulates mRNAs associated with cell growth, proliferation, and apoptosis, and is known to be induced by EGF binding to the EGF-responsive region of the EGR1 gene, and ERK1/2 signalling[845]. Both FOS and FOSB are known to form complexes the transcription factors, AP-1, JUN and ATF, which are important in the transcription of mRNAs linked to cellular proliferation and differentiation[846]. This shows that transcription is upregulated with EGF stimulation in both cell lines, which is consistent with upregulation of transcription factors in figure 7.2, and in the enriched growth-factor dependent biological pathways (figures 7.3 & A.2.8). However, AMPK KO was found to have higher regulation of c-FOS, c-JUN, PLK2, SPRY2, ERRFI1, and DUSP1, compared to WT HEK293 cells (figure 7.2). Based on all upregulated genes with DMSO & EGF treatment which were statistically significant (≤ 0.05 p-value), the regulation of transcription from RNAP II promoter and positive regulation of NF-κB signalling are enriched with transcription factors in AMPK KO HEK293 cells, which also shows that EGF stimulates transcription in AMPK KO HEK293 cells (figure 7.3 & A.2.8B). These pathways were not enriched in WT HEK293 cells, also suggesting differences in EGF stimulation in both cell lines (figure 7.3 & A.2.8A). This effect could potentially be due to the fact AMPK moderates growth and reprogramming of cellular metabolism via suppression of the mTORC1 pathway[153, 154, 847], and this is not occurring in the AMPK KO cell line, which leads to unrestricted induction of transcription factors.

Genes enriched with DMSO & EGF treatment in AMPK KO HEK293 cells in the regulation of transcription from RNAP II promoter included a few zinc-finger proteins, and growth factor dependent genes which regulate gene transcription, such as FOS, FOSL1, JUNB, FOXO4, FOXA3, EGR1, EGR3, and MED23 (figure A.2.8B). FOXO4 and FOXA3 are important transcription factors which can be regulated by the PI3K/Akt signalling pathway, and regulate transcription of mRNA associated with lipid metabolism, autophagy, cell

growth, cell differentiation, and apoptosis[848]. MED23 is a subunit of the large Mediator complex associated with RNAP II transcription initiation through the recruitment of transcription factors, important in mRNA splicing, chromatin conformation, RNAP II elongation, and ubiquitination-mediated cell fate[849]. This links to enrichment of repressed genes with cordycepin treatment prior to EGF stimulation in AMPK KO HEK293 cells in chromatin organisation and remodelling, and ubiquitination biological pathways (figure 7.3 & 7.7), as seen previously (figures 3.17C, 4.1B, 4.4B, A.2.5A, & A.2.6A). As c-MYC can be upregulated downstream from AKT activation through FoxO acetylation[820], and FOXN3 expression is linked to the regulation of MYC[850], it is likely this is synergistic downregulation of growth-related gene expression. Also, there could be a link between the downregulation of MYC, CREBBP, and ATF4, as the MYC/Max dimer is known to recruit the CREB p300/CBP-associated factor (PCAF), which further recruits ATF's[791, 792], and links to chromatin remodelling and transcription through RNAP II pathways via histone acetylation[791, 792]. Key inositol phosphate kinases were also found to be repressed and enriched in the Inositol phosphate biosynthetic process pathway with cordycepin treatment (figure 7.7B & A.2.9B). This could also explain a link to MYC repression, due to repression of PI3K/Akt signalling and FoxO acetylation[820].

RBPs enriched in the ubiquitination biological pathway with cordycepin treatment in AMPK KO included RBBP6, MED11, Ring Finger proteins RNF6, RNF25, and RNF38, and F-box proteins FBXO21, FBXW7, FBXL15, and FBXO30 (figure A.2.9B). RBBP6 is part of the CF complex which interacts with CPSF3 and WDR33 and influences cleavage in the presence of CSTF and CFIIm subcomplexes[394, 419], suggesting that cordycepin treatment can still affect cleavage and polyadenylation machinery with AMPK KO. RBBP6 can also facilitate ubiquitination and degradation of p53[570], which with the repression of PSMD12P (figure 7.4), a proteasome 26S subunit associated to K63-linked ubiquitination[851], links cordycepin treatment to affecting ubiquitination.

As cordycepin treatment with AMPK KO shows enrichment of repressed genes in a transcription biological pathway (figures 7.7B & A.2.9), which was upregulated in DMSO treatment (figure 7.3). In wild type HEK293 cells, cordycepin also downregulated transcription factors such as MYC, RUNX1, ATF4, FOXO3, CREBBP, FOS, JUN, EGR's 1-3, and EGFR, enriched in the positive regulation of transcription from RNAP II promoter biological pathway in wild type HEK293 cells (figures 7.7A & A.2.9A). Also, the mitochondrial

tRNAs, MT-TA and MT-TG are also repressed by cordycepin treatment in AMPK KO HEK293 cells (figure 7.4), and are associated with translational efficiency on oncogenes[844], which could also link the effect of cordycepin on translation. This shows that AMPK KO does not prevent typical effects of cordycepin on growth factor response.

Altogether, this chapter has shown that AMPK KO alters but does not abolish EGF induced gene expression, and that AMPK is not required for the repression of EGF stimulation by cordycepin. AMPK KO did not abolish the typical repression of chromatin remodelling, and ubiquitination biological processes by cordycepin treatment. Cordycepin is known to effect cleavage and polyadenylation, and poly(A) tails, which are processes associated regulated by RBPs. As RBPs were found to be enriched in repressed biological pathways with cordycepin treatment, it could be that cordycepin treatment is exerting downstream effects through RBPs. This will be investigated further in the next chapter.

8 Cordycepin and PI3K inhibition shift RNA-binding proteins towards the RNA-bound Interphase involved in RNA processing pathways

8.1 Introduction

RNA-binding proteins (RBPs) are a large class of proteins associated with post-transcriptional RNA metabolism through interaction with nucleotides of RNA via RNA-binding domains (RBDs)[852]. There are many forms of RBDs, and RBPs can contain multiple RBDs, which can interact in an RNA nucleobase-specific manner, and function through stabilising protein-RNA interfaces, and coordinating RBD-RNA interactions[852-856]. The most common RBDs are RNA recognition motifs (RRM's), such as DEAD-box helicase domains (DDX), LA motifs, and ribosomal S1-like domains[857]. Through these interactions, RBPs play crucial roles in of post-transcriptional RNA metabolism, including translation, splicing, modifications, intracellular trafficking, and decay. Examples include the eIF4F RBP complex which is important in translation initiation[597, 598], U1 and U2 small nuclear RNPs (snRNPs) which play a crucial role in splicing[858], and RNA methylation RBPs such as methyltransferases and hnRNPs, important in RNA turnover and DNA damage repair[859].

Cleavage and polyadenylation, deadenylation, and poly(A) tail metabolism also require RBP complexes. The nuclear cleavage and polyadenylation specificity factor (CPSF) pre-mRNA 3'processing multiprotein complex (detailed in figure 1.2), incorporates several core RNP subunits within the polyadenylation specificity factor (PSF) and cleavage factor (CF) complexes[393, 394]. This includes CPSF4 and WDR33 which recognises and interacts to the poly(A) site (PAS) on the 3'UTR of mRNA[393, 402, 403, 412], cleavage components, CPSF2, CPSF3, Symplekin[393], and interacting RBPs such as RBBP6[394, 419], and poly(A) polymerases (PAPs) such as PAPOLA, PAPOLB, and TUT1[446, 447]. Alternatively, cytoplasmic polyadenylation also relies on core RBPs such as cytoplasmic polyadenylation element (CPE) binding proteins (CPEBs)[501, 860, 861], and PABPC1 which plays a role in translation initiation through interacting with Eukaryotic translation initiation factors[587-589]. PABPC1 also interacts with the PAN2-PAN3 DEDD exonuclease complex in the removal of the poly(A) tail in deadenylation[590, 619, 620, 862, 863]. Altogether, RBPs play crucial roles in poly(A) metabolism, vital for mRNA transcription termination and translation, export from the nucleus, subcellular localisation, and promoting stability[398, 864-866].

RBPs are also known to play regulatory roles in PI3K/Akt/mTOR and AMPK signalling pathways. This includes the La-related protein 1 (LARP1) which binds to Raptor in the mTORC1 complex and facilitates translation downstream to mTOR[867], and the AXIN:APC-containing RNP complex which initiates LKB1 phosphorylation, upstream to AMPK activation[868]. Furthermore, knockdown of poly(A) machinery such as CPSF4, was found to repress PI3K (Tyr458) and AKT (S473) phosphorylation[635], suggesting a link of RBP's and 3'-UTR machinery to PI3K/Akt/mTOR signal transduction.

Results from the previous chapters (3 and 6) indicate that cordycepin affects gene expression through its effects on PI3K/Akt signalling (figures 3.13, 3.16, & 3.19), and that cordycepin may affect signal transduction through its effects on polyadenylation. As RBPs play key roles in RNA and poly(A) metabolism and have a link to PI3K/Akt/mTOR and AMPK signalling, this Chapter aims to see if cordycepin and PI3K inhibition can affect RBP-RNA interactions, and whether this is leading to downstream effects on signalling and inflammation in RAW264.7 macrophages.

8.2 OOPS Validations – RAW264.7 Macrophages

RNP complexes are dynamic and RBP composition changes naturally over time and in response to stimulus[852, 853, 869]. Due to the natural changes in RBP composition in RNP complexes, a validation time course for cordycepin treatment was necessary as we want to catch the early effects of cordycepin which is not due to natural changes. To do this, RAW264.7 macrophages were treated with LPS (1 µg/ml) and cordycepin (20 µM) together in 5-minute intervals from 5 minutes to 30 minutes, with protein extracted at each interval for comparison (figure 8.1). A total of 30 minutes was used as Dr. Jialiang Lin[766] had previously reported an effect on mTOR signalling by cordycepin within 30 minutes treatment. The downstream phosphorylation of 4E-BP1, and AMPK, associated with mTOR signalling[141, 153, 154], was found previously to be affected by cordycepin treatment (figure 6.1), and were chosen to compare the effect of cordycepin during the treatment time course (figure 8.1).

The phosphorylation of AMPK leads to the repression of mTOR signalling[141, 153, 154], and cordycepin was found to phosphorylate and activate AMPK (Thr172) after 20 minutes treatment (figure 8.1). There was also a reduction in band intensity for total AMPK protein at around 20 minutes treatment with cordycepin (figure 8.1). Unphosphorylated 4E-BP1 is known to repress translation through blocking translation initiation factors, eIF4E and eIF4G[124-126]. Cordycepin was found to influence total 4E-BP1 levels, and the phosphorylation of 4E-BP1 (Thr37/46) within 5 minutes, with marked reduction in band intensity within 20 minutes.

To test for inflammatory induction of mTOR signalling, RAW264.7 macrophages were treated for 30 minutes with LPS (1 µg/ml). As expected, 4E-BP1 (Thr37/46) was phosphorylated, whereas AMPK was not phosphorylated and active. This effect was the same for 30 minutes LPS & DMSO (0.02% v/v) treatment, suggesting that DMSO is no causing the effect we see with cordycepin, and there is still an inflammatory response (figure 8.1). However, these results were like RAW264.7 macrophages with no treatment, which suggests the RAW264.7 macrophages may have already been active (figure 8.1). As it was previously suggested that cordycepin acts through adenosine receptors[380, 382, 386], RAW264.7 were treated for 30 minutes with LPS & adenosine (20 µM), which showed no induction of AMPK phosphorylation, but an increase in 4E-BP1 phosphorylation, showing no correlation to cordycepin treatment (figure 8.1), as highlighted previously (figure 3.7). Altogether, 20 minutes appears to be a general indicative treatment time to see clear effects of cordycepin treatment in RAW264.7 macrophages.

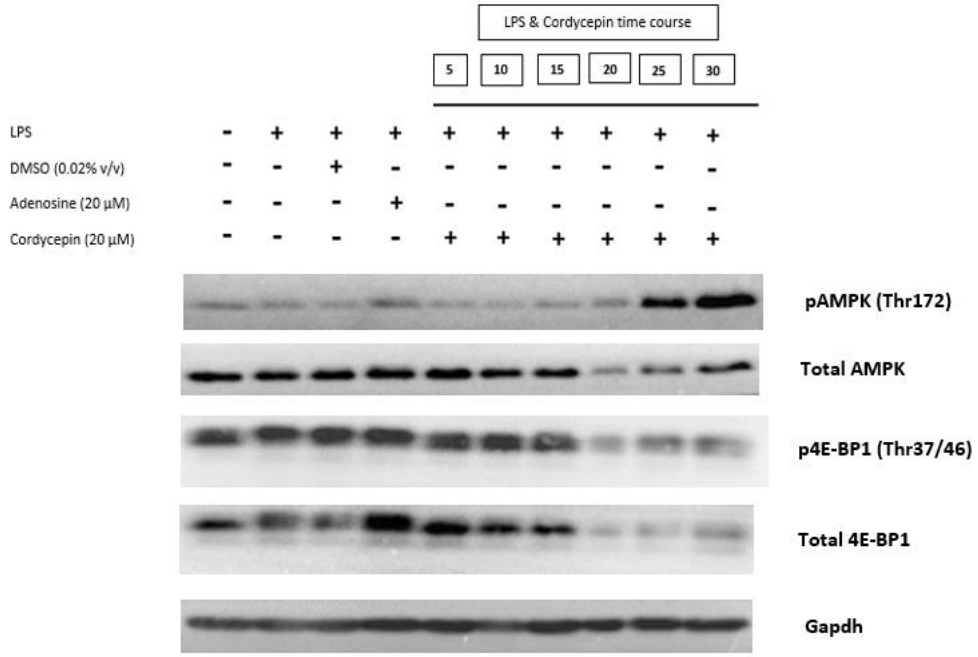

Figure 8.1: Cordycepin effects the phosphorylation of signalling machinery between 15-25 minutes. RAW264.7 macrophages were treated at 5-minute intervals separately between 5-30 minutes with LPS (1 µg/ml) & cordycepin (20 µM) to highlight how quickly we see the effects of cordycepin with inflammatory stimulation. For comparison, RAW264.7 macrophages were also treated for a maximum of 30 minutes with either LPS (1 µg/ml), LPS & DMSO (0.02% v/v), or LPS & adenosine (20 µM). Total protein was extracted using RIPA lysis buffer after treatment, and western blots were performed of target phosphorylation sites known to be affected by cordycepin treatment. (N = 1).

Prior to investigating whether cordycepin can shift RBPs from RNA-bound to unbound phases, validations for optimal conditions of crosslinking and RBP retention were necessary for the OOPS procedure. UV crosslinking is used in the original OOPS protocol[661], however this is irreversible. Formaldehyde crosslinking was used in this study as it also causes protein-protein crosslinks, which would allow us to see RBP associated proteins and perhaps discover direct links between signal transduction machinery and RBPs. Previous studies have used formaldehyde at 1% in PBS during a 10-minute incubation period for crosslinking[471, 662]. To see whether this is the optimal conditions to see RBPs in the interphase through western blotting, RAW264.7 macrophages were stimulated for 30 minutes with LPS (1 µg/ml), and

crosslinked for 2, 5, and 10 minutes with either 0.5% and 1% formaldehyde in PBS and compared to no crosslinking. As highlighted in figure 8.2A, the RBP, CELF1, was only seen in the unbound (organic) phase without crosslinking, and not in the interphase, with the highest protein intensity of CELF1 found with 2-minute incubation with 0.5% formaldehyde. Crosslinking was required for CELF1 to be found in the interphase (figure 8.2A).

The original OOPS procedure also aimed to concentrate RBPs in the interphase through multiple stringent acidified guanidinium thiocyanate-phenol-chloroform (AGPC) separations of the interphase[661]. To validate this, RAW264.7 macrophages were treated for 30 minutes with LPS (1 µg/ml) to induce inflammation, and the interphase and unbound phases were obtained for 1 to 4 AGPC cycles. Using CELF1 as an RBP example, it was clear that CELF1 protein intensity reduced in the interphase, and increased in the unbound phase, with every AGPC cycle with 0.5% formaldehyde crosslinking (figure 8.2B). This was also seen without crosslinking, however the band intensity of CELF1 was lower, which is consistent with the no formaldehyde control from figure 8.2A. Altogether, these results highlight that optimal retrieval in western blotting for CELF1 in RAW264.7 macrophages is through 2-minutes formaldehyde crosslinking at 0.5%, and that sequential AGPC cycles leads to the loss of CELF1 from the RNA-bound interphase to the unbound (organic) phase. As this is based on two biological replicates, further replicates will be needed in future work.

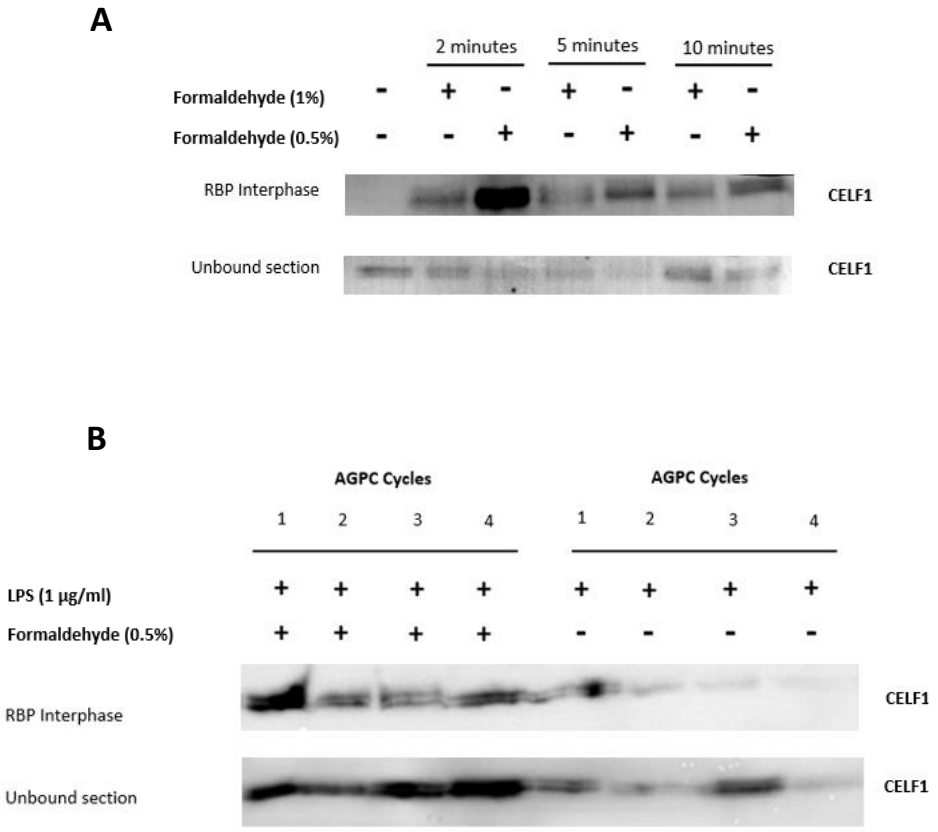

Figure 8.2: OOPS with 0.5% Formaldehyde is optimal, with multiple washes leading to loss of RBPs in the Interphase. RAW264.7 macrophages were treated for a maximum of 20 minutes with LPS (1 µg/ml) before: **(A)** testing for optimal formaldehyde crosslinking, or **(B)** testing for optimal AGPC separation cycles to concentrate RBPs in the Interphase. In **(A)**, formaldehyde crosslinking at either 1% or 0.5% for either 2, 5, or 10 minutes before glycine quenching were compared prior to OOPS to separate the Interphase (RBP Interphase), and Unbound (Organic) phases. In **(B)**, RAW264.7 macrophages were crosslinked at 0.5% or not at all as a control (0%) and subjected to between 1 to 4 AGPC separations for comparison. For both **(A)** and **(B)**, 3x SDS PAGE loading buffer was added to protein lysates before loading onto western blots. CELF1 was used as a known RBP to show changes in RBP abundance. (Image representative of two independent biological replicates).

8.3 Label-free Quantitative Proteomics shows RBP shifts to the interphase with PI3K inhibition

Since cordycepin has a clear effect on PI3K/Akt signalling in RAW264.7 macrophages, which correlates with the PI3K inhibition through LY294002 (figures 3.13, 3.16, & 3.19), and as RBPs can play roles in regulating PI3K/Akt/mTOR signalling[635, 867, 868, 870, 871], it is possible that cordycepin could affect signalling through RBPs. To test this, RAW264.7 macrophages were treated with DMSO (0.02%), LPS (1 μg/ml) & DMSO, LPS & cordycepin (20 μM), or LPS & LY294002 (100 mM) for 20-minutes before crosslinking with 0.5% formaldehyde based on validations (figures 8.1 & 8.2), prior to OOPS. To check that RBPs are shifting to the interphase with crosslinking, RAW264.7 macrophages were also treated with LPS & DMSO without formaldehyde crosslinking for comparison to with crosslinking. Protein pellets were sent to the Advanced Mass Spectrometry Facility of the University of Birmingham for trypsin digestion, liquid chromatography, and label-free quantitative mass spectrometry. Protein abundances for each treatment condition for both Interphase and Unbound (organic) phases for identified proteins, which included at least two unique peptides, were sent back for UQ normalisation[688, 689, 712].

Proteins were excluded if the average abundance values equalled '0'. Following the original OOPS procedure, glycoproteins were removed from analysis as glycans and RNAs are hydrophilic polymers and indistinguishable[661]. RBPs were identified through using EMBL's RBPbase (v0.2.1). To try to mediate variability, five biological replicates were used for analysis, which included two replicates with 1-hour liquid chromatography, and three replicates with 2-hour liquid chromatography peptide separations. Ideally more biological replicates will be needed in future for the same duration of liquid chromatography for robust interpretation of the data.

To see if RBPs shift to the Interphase with formaldehyde crosslinking, abundances with and without formaldehyde crosslinking with LPS & DMSO treatment were graphed, with the abundances ranked from highest to lowest for the without formaldehyde control. As shown in figure 8.3, RBPs had a general trend of higher abundance with formaldehyde crosslinking (red dots), as they were found predominantly above the ranked without formaldehyde protein abundance line in the Interphase (INT). In the Unbound (Organic phase; UNB), some RBPs with crosslinking also had higher protein abundance, and was above the ranked without formaldehyde crosslinking line, however it's clear there is more of a spread of

abundance below the ranked line than in the Interphase (figure 8.3). This suggests that formaldehyde crosslinking does concentrate and shift RBPs towards the Interphase, as protein abundance is higher for the RBPs. But some RBPs with formaldehyde crosslinking can be found in the Unbound (organic phase; UNB), which could be through technical variability of the biological replicate and imperfect crosslinking conditions, and worth considering in the interpretation of the data.

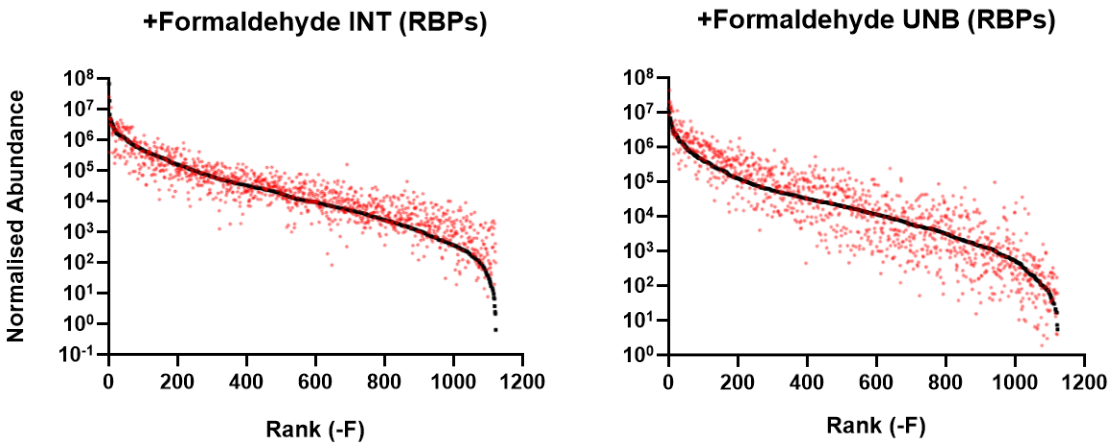

Figure 8.3: Formaldehyde crosslinking shifts some but not all RBPs towards the Interphase. RAW264.7 macrophages were treated for 20 minutes with LPS (1 µg/ml) to induce inflammation, and either crosslinked with formaldehyde at 0.5% or not at all as a control before OOPS with one AGPC phase separation cycle based on validations. Protein pellets were sent off for Label-free MS-based proteomics and protein abundance quantification at the University of Birmingham. Protein abundances were normalised using the Upper Quartile (UQ) method[688, 689, 712], and RBPs were identified using EMBL's RBPbase (v0.2.1). Normalised protein abundance for RBPs were averaged between biological replicates for treatment condition, abundances were ranked from highest to lowest for the no formaldehyde control, and plotted to show whether RBP abundances were above or below the ranked abundance line for no formaldehyde. (Figure includes the average of x5 biological replicates).

To see whether cordycepin treatment and PI3K inhibition influences RBP localisation between RNA-bound to unbound phases, the protein abundances of RBPs were compared between LPS (1 μg/ml) & DMSO (0.02% v/v), LPS & cordycepin (20 μM), and LPS & LY294002 (100 μM) with formaldehyde crosslinking (figure 8.4). Initially, to see if LPS inflammatory stimulation in RAW264.7 macrophages shifts RBPs, averaged LPS & DMSO protein abundances was compared to DMSO (0.02% v/v) treatment (figure 8.4A). In comparison, 20 minutes treatment, RBPs have less abundance in the Interphase (INT) with LPS inflammatory stimulation compared to the DMSO treatment only abundance line, suggesting that RBPs dissociate from being in an RNA-bound complex with inflammatory stimulation (figure 8.4A). Comparably, 20-minute LPS & cordycepin treatment shifted RBP abundance towards the Interphase compared with LPS & DMSO, as the protein abundances were above the LPS & DMSO abundance line (figure 8.4B). However, RBP protein abundance was also predominantly higher in the unbound phase (organic; UNB) with LPS & cordycepin treatment, with only slightly fewer RBPs below the LPS & DMSO abundance line (figure 8.4B). Comparably, PI3K inhibition through 20-minutes LPS & LY294002 treatment has a much more convincing shift of RBP protein abundance towards the Interphase compared to LPS & DMSO, with much higher RBP protein abundance with PI3K inhibition (figure 8.4B). It is also clear that RBP protein abundance with PI3K inhibition of RBPs are smaller than LPS & DMSO in the unbound phase, and below the ranked LPS & DMSO abundance line (figure 8.4B). Just interpreting the abundances in the Interphase suggests that LPS inflammatory stimulation shifts RBPs toward the unbound phase, with cordycepin treatment and PI3K inhibition shifting RBPs towards the Interphase. However, as opposed to PI3K inhibition, LPS & cordycepin treatment is less convincing in shifting RBPs out of the unbound phase through interpreting the unbound phase protein abundances of RBPs compared to LPS & DMSO (figure 8.4B). This effect could be through outlier protein abundance values skewing the interpretation, and further replicates and robust statistical analysis are therefore needed.

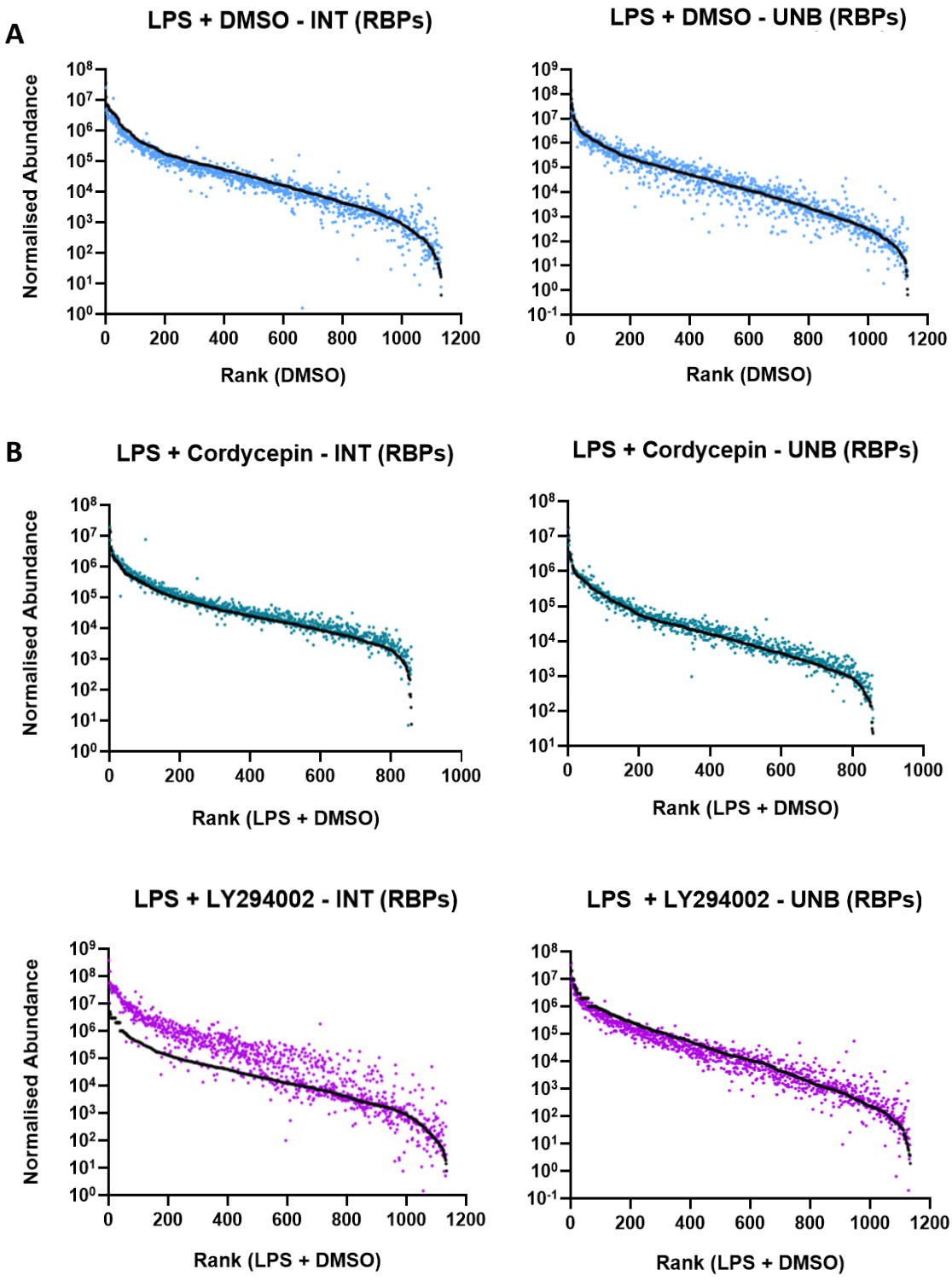

Figure 8.4: PI3K inhibition has a greater shift of RBPs towards the Interphase than cordycepin treatment. RAW264.7 macrophages were treated for 20 minutes with either LPS (1 µg/ml) & DMSO (0.02% v/v), LPS & cordycepin (20 µM), or LPS & LY294002 (PI3K inhibitor, 100 µM) at the same time prior to 0.5% formaldehyde crosslinking and OOPS with one AGPC phase separation. Protein pellets were sent off for Label-free MS-based proteomics and protein abundance quantification at the University of Birmingham. Protein abundances were normalised using the Upper Quartile (UQ) method[688, 689, 712], and RBPs were identified using EMBL's RBPbase (v0.2.1). Normalised protein abundance for RBPs

were averaged between biological replicates for treatment condition, abundances were ranked from highest to lowest for either **(A)** DMSO (0.02% v/v) without LPS inflammatory stimulation, or **(B)** LPS & DMSO. Abundances were plotted to show whether RBP abundances (dots) were above or below the ranked abundance lines. (Figure includes the average of x5 biological replicates).

As PI3K inhibition, and potentially cordycepin treatment, can shift RBPs from the unbound phase in LPS & DMSO treatment towards the Interphase (figure 8.4), it was important to identify the RBPs which shift towards being RNA-bound, and what their biological functions are. To do this, the ratio of the Interphase and unbound (INT/UNB) protein abundances for RBPs was calculated for each treatment condition. The INT/UNB ratio for LPS & cordycepin and LPS & LY294002 treatments were compared against LPS & DMSO, and RPBs with a ratio of ≥ 2 were included into DAVID Gene Ontology analysis[690] to obtain enriched biological pathways of these RBPs.

In comparison to LPS & DMSO treatment in RAW264.7 macrophages, cordycepin treatment shifted RBPs which had an INT/UNB ratio of ≥ 2 associated in many RNA processing pathways, such as mRNA, rRNA, and RNA processing, RNA splicing, mRNA transport, ribosome biogenesis and translation (figure 8.5A), consistent with effects on protein synthesis. These pathways were also enriched with RBPs with PI3K inhibition, however many more RBPs had an INT/UNB ratio of ≥ 2 in comparison to LPS & DMSO with LPS & LY294002 treatment (figure 8.5B). For both cordycepin treatment and PI3K inhibition, cleavage and polyadenylation, and poly(A) machinery, such as RBBP6, THOC2 and 3, and TUT1 (Star-PAP), were enriched in the mRNA processing biological pathway, and had higher abundance in the Interphase (figure 8.5). Specifically, for PI3K inhibition, WDR33, CPSF2, PABPC1, hnRNPLL, and ALYREF are also enriched in the Interphase for the mRNA processing and RNA splicing biological pathways based on an INT/UNB ratio of ≥ 2 in comparison to LPS & DMSO (figure 8.5B). This shows an effect of PI3K inhibition on polyadenylation. For both treatment conditions, the adenosine deaminase, ADAR, important in dynamic local rearrangements between RBPs and RNA[872, 873], was also enriched in mRNA and RNA processing. Likewise, multiple DEAD-Box RNA helicases (DDX) and RNA-Binding Motif (RBM) proteins are enriched

throughout the biological pathways for both treatments, which also suggests effects on RNA metabolism with cordycepin treatment and PI3K inhibition (figure 8.5).

PI3K inhibition was found to have enrichment of specific protein families in the Interphase for the biological pathways (figure 8.5B). This includes accumulation of exosome complex (EXOSC) and nucleolar (NOL) proteins in RNA and rRNA processing, small nuclear ribonucleoproteins (SNRPD) in splicing, ribosomal protein L (RPL) units in cytoplasmic translation, and Eukaryotic initiation factors (eIF) and elongation factors (EEF) proteins in translation (figure 8.5B). Altogether, key RBPs associated with RNA metabolism are enriched in the Interphase with both cordycepin treatment and PI3K inhibition.

A

Gene Ontology Term	P-value	Genes	Fold Enrichment
mRNA processing (GO:0006397)	1.07E-15	RBM26, SFSWAP, RNMT, PRKRIP1, DDX20, ADAR, HNRNPLL, PRPF8, CWC22, DHX15, RBBP6, APOBEC1, SF3A3, RBM38, AQR, ZRANB2, NCBP1, THOC3, THOC2, PUS7, CRNKL1, SRRM1, CD2BP2, TUT1, CLASRP, CDK13, SNRNP200	7.790234
RNA splicing (GO:0008380)	2.41E-12	SF3A3, RBM38, AQR, ZRANB2, NCBP1, PRMT1, SFSWAP, PRKRIP1, DDX20, THOC3, THOC2, PUS7, CRNKL1, PRPF8, SRRM1, CWC22, DHX15, CD2BP2, CLASRP, CDK13, SNRNP200	7.913448
Ribosome biogenesis (GO:0042254)	9.5E-09	DDX28, EMG1, XPO1, DDX27, NVL, PAK1IP1, DDX56, UTP23, DHX37, TSR1, PWP1, BYSL	11.2449
rRNA processing (GO:0006364)	2.26E-06	WDR36, EMG1, DDX27, NVL, DDX56, UTP23, PPAN, PWP1, UTP18, BYSL, MRPL44	7.466565
mRNA transport (GO:0051028)	4.43E-05	ENY2, XPO1, NCBP1, DDX25, NUP50, THOC3, THOC2, LRPPRC	8.471158
RNA processing (GO:0006396)	9.3E-05	ZRANB2, SFSWAP, ZFC3H1, DNTTIP2, ADAR, CRNKL1, MRPL44	9.502901
Protein import into nucleus (GO:0006606)	0.000698	NUP50, CSE1L, NUP153, ADAR, TNPO2, IPO7, IPO5	6.559525
tRNA aminoacylation for protein translation (GO:0006418)	0.003941	RARS1, NARS1, IARS2, IARS1	12.45759
Nuclear-transcribed mRNA catabolic process, nonsense-mediated decay (GO:0000184)	0.006245	UPF1, NCBP1, UPF3B, GSPT1	10.58895
Translation (GO:0006412)	0.00805	EIF2B5, RARS1, MRPL1, RPL21, NARS1, SRBD1, IARS2, IARS1, GSPT1	3.145232

B

Gene Ontology Term	P-value	Genes	Fold Enrichment
mRNA processing (GO:0006397)	3.79E-60	ZFP326, TCERG1, RAMAC, FMR1, CASC3, CCAR2, LGALS3, SNRPD2, SNRPD1, KHSRP, CWC22, MTREX, SNRPD3, SRRM2, THOC3, PUS7, CRNKL1, SRRM1, PRPF6, RBMXL1, PRPF3, XRN2, SRSF3, SNRPE, SNRNP200, SRSF6, SRSF7, SNRPA, SF1, SRSF9, KHDRBS1, RBM8A, YTHDC1, DDX1, PRKRIP1, SNU13, HNRNPLL, PRPF8, SUPT6H, PDCD11, PCBP1, HSPA8, ZRANB2, ALYREF, CPSF2, YJU2, CWC15, SMU1, HNRNPK, SNW1, SON, HNRNPF, CLASRP, SUGP1, RBM28, RBM25, RBM26, DDX46, CELF2, PPWD1, ADAR, YBX1, PRPF19, SART1, SYNCRIP, SART3, DHX15, RBM17, NCBP1, PRPF40A, PLRG1, WDR33, SFPQ, THRAP3, LUC7L3, TUT1, NCBP3, SNRPA1, PABPC1, SF3B4, RNMT, SFSWAP, SF3B6, SRRT, SCAF8, PUF60, U2AF2, TRA2B, RALY, RBBP6, SF3A3, RBM39, SF3A1, CDC5L, RRP1B, SCAF1, NUDT21, PHF5A, HNRNPA2B1, PRPF31, FAM50A	7.700746
RNA splicing (GO:0008380)	4.78E-54	ZFP326, TCERG1, RBM28, RBM25, DDX46, FMR1, PPWD1, CASC3, YBX1, PRPF19, CCAR2, SART1, SYNCRIP, LGALS3, SART3, SNRPD2, SNRPD1, KHSRP, CWC22, DHX15, MTREX, SNRPD3, SRRM2, RBM17, NCBP1, PRMT1, PRPF40A, THOC3, PLRG1, PUS7, CRNKL1, SRRM1, SFPQ, PRPF6, RBMXL1, THRAP3, PRPF3, SRSF3, LUC7L3, SNRPE, SNRPA1, PABPC1, SRSF6, SNRNP200, SRSF7, SNRPA, SF1, SRSF9, SF3B4, RBM8A, YTHDC1, SFSWAP, SF3B6, PRKRIP1, SNU13, PRPF8, SUPT6H, PUF60, U2AF2, TRA2B, RALY, SF3A3, RBM39, HSPA8, SF3A1, TAF15, ZRANB2, FUS, ALYREF, YJU2, CDC5L, RRP1B, CWC15, SCAF1, SMU1, HNRNPK, SON, SNW1, PHF5A, HNRNPF, HNRNPA2B1, PRPF31, CLASRP, FAM50A, SUGP1	8.464282
rRNA processing (GO:0006364)	1.25E-48	DDX49, NVL, EIF4A3, PPAN, NAT10, PWP2, PWP1, WDR43, RPL7, RPS15, FBL, MTREX, RRP12, UTP14A, RRP15, WDR36, IMP3, DDX10, DDX54, WDR75, UTP18, FTSJ3, MRPL44, NSA2, EBNA1BP2, NHP2, RPL27, UTP25, DDX27, RPL11, DDX21, NOL8, NOL9, RPF2, RPF1, NOL6, EXOSC6, EMG1, EXOSC4, EXOSC10, PDCD11, EXOSC9, BRIX1, EXOSC2, LYAR, DCAF13, MDN1, UTP6, NOP14, KRR1, WDR18, RPL35A, RRP1B, PA2G4, BYSL, BOP1, RPS25, TBL3, RPS28, RPS27, MPHOSPH10, NOL11, NOP53	11.30039
Translation (GO:0006412)	7.54E-43	RPL4, MRPS15, GFM1, MRPS16, RPL3, RPL32, RPL34, MRPL39, RPL8, RPL6, RPL7, RPS4X, MRPL41, RPS15, MRPL1, RPL18A, NARS1, RACK1, RPL35, RPL38, EIF2A, EIF5A, RPS9, RARS1, RPL21, RPS8, RPL23, RPS3A, MRPS7, TUFM, EEF1A1, EEF1G, SARS2, RPL27, TARS2, EEF1B, CARS1, RPL29, EIF4E2, RPL12, RPL11, SRBD1, MRPL16, RPS27L, MRPL15, GSPT1, RPS15A, RPL13, IARS2, RPS2, IARS1, RPS27A, YARS, EIF2B5, GM45713, RPL35A, RPL23A, EIF2S2, EEF2, EIF2S1, GARS1, RPS28, RPS27, EIF6, EIF3K, EIF3L, RPS29, EIF3I, RPL27A, RPS20, EIF3C, FARSA, EIF3D, RPS21, EIF3A, EIF4G1	7.110917
Cytoplasmic translation (GO:0002181)	1.4E-28	RPL4, RPL3, RPL32, RPL12, RPL34, RPL11, RPL8, RPL6, RPL7, RPS4X, RPS15, RPS15A, RPL18A, RPL13, RPLP2, RPL38, RPS2, RPS27A, RPS10, RPS9, RPL21, RPS8, RPL23, RPL35A, RPL23A, RPS3A, CKAP5, RPS25, RPS28,	11.37726

		RPS29, RPL27A, DRG1, DRG2, RPS20, RPL27, RPL29, RPS21	
Ribosome biogenesis (GO:0042254)	1.23E-23	DDX28, DDX27, NVL, PAK1IP1, SNU13, RPF2, PWP1, WDR43, IPO4, RPF1, EMG1, XPO1, BRIX1, RIOK1, UTP14A, DCAF13, NOP56, NOP14, NOP58, KRR1, IMP3, WDR75, GTPBP4, FTSJ3, BYSL, BOP1, EBNA1BP2, NSA2, RPS28, MYBBP1A, EIF6, NHP2, MPHOSPH10, TSR1, NOL11, NOP53	8.914594
Nucleosome assembly (GO:0006334)	1.9E-15	HP1BP3, SMARCA5, NAP1L1, SSRP1, H1-1, MACROH2A1, H1-0, H1-3, H1-2, H1-4, H3-5, SART3, RBBP4, H4C1, ANP32B, SUPT16	6.99548
RNA processing (GO:0006396)	1.91E-15	SF3A1, UTP6, ZRANB2, SFSWAP, DDX54, ADAR, NOL9, TRNT1, CRNKL1, U2SURP, MRPL44, EXOSC6, EXOSC10, SART3, PRPF6, EXOSC4, HNRNPK, PDCD11, HNRNPUL1, SNRPD1, EXOSC9, SNRPD3, EXOSC2, SUGP1	8.609821
mRNA transport (GO:0051028)	7.71E-14	RBM8A, DDX25, FMR1, EIF4A3, CASC3, SUPT6H, NUP160, XPO1, KHSRP, TPR, NUP88, EIF5A, RANBP2, NCBP1, ALYREF, THOC3, LRPPRC, NUP93, MYO1C, THRAP3, SARNP, HNRNPA2B1, SRSF3, NCBP3, SRSF7	6.99548
DNA-templated transcription, initiation (GO:0006352)	9.58E-10	SMARCA5, H4C1	9.554802

Figure 8.5: RBPs with higher abundance in the Interphase for both cordycepin treatment & PI3K inhibition are enriched in translation and RNA-based biological pathways. Normalised protein abundances of RBPs for the Interphase and Unbound (Organic) phases were compared, and a ratio of Interphase/Unbound (INT/UNB) abundance was calculated for 20 minutes LPS (1 µg/ml) & DMSO (0.02% v/v), or LPS & **(A)** cordycepin (20 µM), or **(B)** LY294002 (PI3K inhibitor, 100 µM) treatments of RAW264.7 macrophages. The INT/UNB ratio for **(A)** LPS & cordycepin or **(B)** LPS & LY294002 was compared to LPS & DMSO treatment, with RBPs with a 2-fold increase in INT/UNB ratio compared to LPS & DMSO control included into DAVID Gene Ontology analysis[690] to obtain enriched biological pathways.

8.4 Discussion

The aim of this chapter was to evaluate whether the effect we see with cordycepin treatment on PI3K/Akt signalling (figures 3.13, 3.16, 3.19, 4.2, 4.4-4.5, 4.7, 4.8, 5.1, 6.1, & 6.8) could be through affecting the association of RBPs to RNA-bound complexes. This was in part through known associations of RBPs with PI3K/Akt/mTOR and AMPK signalling pathways[635, 867, 868, 870, 871]. This chapter has shown that LPS induction of RAW264.7 macrophages shifts RBPs into an unbound phase from RNA, which is mitigated by PI3K inhibition, and to a less extent by cordycepin treatment, based solely on comparing protein abundances (figure 8.4).

Previous results in this Thesis have linked signalling and poly(A) machinery through the knockdown of WDR33 (figures 3.13A & 3.19A), and results from interpreting quantitative MS-based proteomics in this Chapter has shown that WDR33 is enriched in the Interphase and associated with mRNA processing with PI3K inhibition (figure 8.5B). The restriction of WDR33 from leaving an RNA-bound state in cleavage and polyadenylation and aiding in further cleavage and polyadenylation has been attributed to how cordycepin triphosphate (CoTP) inhibits this process[644, 645, 696, 697]. Furthermore, PI3K inhibition also shifted CPSF2, a core component of the cleavage (CF) complex required for pre-mRNA 3'end cleavage and interaction with the scaffolding component, Symplekin, important for cleavage and polyadenylation[393, 402, 403, 412, 420, 421], towards the Interphase (figure 8.5B). This could therefore suggest that PI3K regulates cleavage and polyadenylation.

CPSF2 was also found to co-fractionate with CPEB1[501], an important protein associated with cytoplasmic polyadenylation and mRNA translation[488-490], which coupled with the fact that PABPC1 was also enriched in the Interphase with PI3K inhibition, suggests that PI3K may play a role in polyadenylation (figure 8.5B). The heterogeneous nuclear ribonucleoprotein L-like (hnRNPLL) also shifted to the Interphase with PI3K inhibition (figure 8.5B) and is known to interact with PABPC1 and promote proximal alternative polyadenylation (APA) in B cell differentiation[482]. This could suggest that hnRNPLL shifted towards RNA in a complex with PABPC1 during PI3K inhibition. PABPC1 is known to contain N-terminal RNA recognition motifs and play a key role in translation initiation[587-589]. Multiple PABPC1s can bind across the poly(A) tail creating a 'head-to-tail' formation which supports interaction and stability of translational machinery[505, 589, 592-596]. In addition, PABPC1 can influence mRNA stability through recruiting the DEDD exonuclease

PAN2-PAN3 complex and poly(A) RNP complexes during deadenylation[590, 619, 620, 862, 863], and through helping form the 5'-m^{7}G-eIF4E-eIF4G-PABPC-poly(A)-3' closed loop structure which restricts access of exonucleases to mRNA[599, 617]. As many Eukaryotic initiation and elongation factors (eIF's and eEF's) enriched in translation shift to the Interphase with PI3K inhibition (figure 8.5B), and PABPC1 associates with translation factors, this could be as PI3K inhibition enhances translation repression by 4E-BP and lead to a reduction in translation. This is likely to shift the composition of PABPC complexes.

The Ubiquitin-ligase, RBBP6, known to interact with CPSF3 and WDR33 and aid in activating cleavage in the presence of CSTF and CFIIm subcomplexes[394, 419], was also enriched in mRNA processing and found to shift to the Interphase with cordycepin treatment and PI3K inhibition (figure 8.5). RBBP6 is also known to facilitate ubiquitination and degradation of p53[570], again associating cordycepin treatment to ubiquitination as seen previously (figures 3.17C, 4.1B, 4.4B, 7.7B, & A.2.6A). The THO subcomplexes, THOC2 and THOC3, form part of the TREX (TRanscription EXport) complex associated with mRNA transport[578-582], and were found to have a higher protein abundance in the Interphase with cordycepin treatment and PI3K inhibition (figure 8.5). The ALYREF (Aly/REF) adaptor in the TREX complex, which associates with the NXF1:NXT1 complex for export of mature mRNAs and poly(A)+ RNAs from the nuclear pores to the cytoplasm[577, 584, 585, 695], also has higher abundance in the Interphase with PI3K inhibition (figure 8.5B). This coupled which the enrichment of RBPs in mRNA transport (Figure 8.5), demonstrates that PI3K inhibition and cordycepin treatment could influence mRNA export through mediating RNA-association of RBPs.

Both LPS & cordycepin treatment and LPS & PI3K inhibition also had a higher abundance of the poly(A) polymerase, TUT1 (Star-PAP), in the Interphase compared to LPS & DMSO treatment (figure 8.5). TUT1 functions as a U6-TUTase, which catalyses the uridylylation of U6 snRNA, which is a component of the spliceosome[445]. This coupled with enrichment of RBPs in RNA splicing (figure 8.5), demonstrates that cordycepin and PI3K inhibition can affect RNA splicing. TUT1 can also promote recruitment of CPSF3 and CPSF1 to the CPA site, and forms a complex incorporating CSTF2, RNAP II and Symplekin to promote 3'end CPSF3 cleavage[446, 447], which also shows a link to cordycepin and PI3K inhibition to cleavage and polyadenylation. TUT1 can also inhibit PPARγ and SREBP-1c through upregulating miRNA-24 and miRNA-

29a[535], which links cordycepin treatment to PPAR signalling as shown previously (figures 3.3A, 3.16A, 4.2A, 4.5A, 4.7A, & 4.8A).

As stated previously, there are limitations in this Chapter which should not be ignored in the interpretation of the data, such as the need for robust statistical analyses of the data and to assess outliers in the replicates skewing the output. This Chapter included both 1-hour and 2-hour liquid chromatography biological replicates, equalling five replicates altogether, which could influence the results. There were also RBPs which had higher protein abundance in the unbound phase with formaldehyde crosslinking, which could suggest technical issues or variability in crosslinking between biological replicates (figure 8.3). Due to the higher protein abundance in RBPs with LPS & cordycepin in the unbound phase compared to LPS & DMSO treatment, it is inconclusive if cordycepin does shift RBPs towards the Interphase (figure 8.4B). Altogether, more biological replicates are required in future work for added confidence in the results, including for figures 8.1 & 8.2, however this preliminary data shows a potential link between PI3K signalling and poly(A) machinery, as well as cordycepin and PI3K inhibition in RNA metabolism, which needs further validation, probably through western blot.

9 Conclusions and Discussions

This study aimed to investigate the elusive mechanisms of action and regulatory targets of cordycepin, and build on previous systematic reviews which have shown clear effects of cordycepin on inflammation, cancer progression, and PI3K/Akt/mTOR signalling in literature[3, 4]. Results from this study has shown consistently that cordycepin treatment has a similar effect on differential expression to the PI3K inhibitor, LY294002 (figures 3.13B, 3.16B, 3.19B, 4.2B, 4.5B, 4.7B, & 4.8B). Interestingly, PI3K inhibition led to the accumulation of polyadenylation and cleavage machinery, such as WDR33, to an RNA-bound state, similarly to the effect of cordycepin triphosphate (CoTP)[5, 369, 646]. As siRNA knockdown of WDR33 in RAW264.7 macrophages led to repression of PI3K/Akt/mTOR signalling (figures 3.13B, 3.19B, 6.9), there is a clear association between cleavage and polyadenylation machinery, and PI3K/Akt/mTOR signalling (illustrated by figure 9.2).

Activation of AMPK through cordycepin is consistent in previous research findings[3, 369, 371, 373, 831, 833, 834], and has been suggested to be the main mechanistic target of cordycepin[13]. However, this study has shown that the effect of cordycepin on inflammatory and growth factor mRNA marker expression is not the same as the AMPK activator, A-769662, (figures 5.2, 5.3, 6.2, & 6.3), and cordycepin treatment still affected EGF stimulation in CRISPR-Cas9 AMPK knockout HEK293 cells (chapter 7). This shows that AMPK may be a target of cordycepin, but it is not the key target. Alternatively, this study has introduced new potential mechanisms of action of cordycepin, as the effect on PI3K/Akt/mTOR and NF-κB signalling could be through the upregulation of PPARγ or cAMP, which will be explained in more detail in this chapter and illustrated by figure 9.1.

9.1 Cordycepin modulates inflammatory and growth factor stimulation through inhibiting PI3K signalling

Throughout this study, cordycepin has consistently been shown to have a similar effect to the PI3K inhibitor, LY294002, during inflammatory response (figures 3.13B, 3.16B, & 3.19B), and growth factor stimulation (figures 4.2B, 4.5B, 4.7B, & 4.8B). This indicates that the two treatments have similarity in

downstream differential expression. Furthermore, cordycepin and LY294002 were both found to repress phosphorylation of downstream kinases, including the AKT target, GSK3β (Ser9), and mTORC1 targets, 4E-BP1 (Thr37/46) and S6K1 (Thr389) (figures 5.1 & 6.1). The effect of cordycepin on PI3K has been shown previously by Holbein *et al*. (2009)[362], who illustrated that a mutant yeast strain, vps15, of a regulatory subunit of PI3K was sensitive to cordycepin and had altered polyadenylation. Also, cordycepin has been predicted to be able to interact directly with the active pocket of PI3K, and thereby can inhibit PI3K activity[874]. Combinational treatment of cordycepin and the VEGFR2 inhibitor, apatinib, also represses phosphorylation of PI3K in non-small cell lung cancer cells[874]. This is consistent with the results from this study as VEGF stimulation was shown to have an opposite effect to expression compared to cordycepin treatment (figure 4.8B). GPERs are known to directly interact with EGFR, IGF-1Rs, HIF-1α, and Notch signalling components to trigger release of growth factors such as VEGF[320, 321]. This is upstream to activation of MAPK/ERK, PI3K/Akt signalling cascades and second messengers such as cAMP[322, 325-328]. Interestingly, the G protein-coupled estrogen receptor, GPER1, was also found to have an opposite effect to expression compared to cordycepin treatment (figures 4.2B, 4.5B, 4.7B, & 4.8B). This all suggests that cordycepin can repress receptor stimulation and growth factor receptor responses which mitigate activation of downstream signalling pathways such as PI3K/Akt/mTOR signalling. Interestingly, cordycepin upregulated CREB and cAMP signalling in RAW264.7 macrophages (figures 3.9B, 3.10, 3.15B, and 3.16), which could link to the upregulation of AMPK phosphorylation in figure 6.1 as increased cAMP levels upregulates PKA which induces LKB1-mediated phosphorylation of AMPK[144].

As opposed to the clear effects of cordycepin on PI3K/Akt signalling (figures 3.16, 4.2, 4.4, & 6.8), a previous study found that PI3K inhibition can abrogate the anti-apoptotic and anti-inflammatory effects of cordycepin in vascular endothelial cells[875]. However, this paper also suggested that downregulation of AKT led to nuclear activation of NF-κB. This does not relate to the fact that activated AKT leads to the phosphorylation of kinases upstream to the nuclear translocation of the NF-κB:p65:RelA heterodimer, which regulates transcription of pro-inflammatory cytokines in macrophages[219, 220, 222, 223] (figure 1.5). Also, upon LPS inflammatory stimulation, PI3K is recruited towards the LPS:TLR4:MD2 complex[185] and anchors to BCAP, where PI3K is activated and thereby stimulates activation and nuclear translocation of NF-κB[217, 218] (figure 1.5). In this study, inhibition of PI3K through LY294002 in RAW264.7 macrophages

was found to repress IκB kinase/NF-κB signalling (figure 6.5A), as well as MyD88, and TLR signalling (figure 6.6). Overlap of all statistically significant repressed genes (≤0.05 p-value and FDR) between cordycepin treatment and PI3K inhibition showed enrichment of genes linked to NF-κB transcription factor activation, and transcription from RNAP II promoter (figure 6.7C). Also, both cordycepin and PI3K inhibition through LY294002 had opposite effects to expression of activated upstream regulators of inflammation, including IRAK4, NOS2, TLR9, CCL20, TICAM1, and RIPK2, which is known to modulate NOD1/2 and NF-κB signalling[724, 725] (figure 6.8B). Cordycepin and LY294002 also have similar effects to expression to the transcription regulators, KLF4 and SGK1, which are both known to inhibit NF-κB signalling[826, 827] (figure 6.8B). These results show that cordycepin is likely acting through PI3K/Akt in inhibiting NF-κB and does not show the same result to the previous study that PI3K inhibition abrogates cordycepin[875].

These findings also add more clarity to the obscurity of the effects of cordycepin on NF-κB in current literature, which was highlighted in our systematic review of the biological effects of cordycepin by Radhi, *et al.* (2021)[3]. In this review, studies varied on whether cordycepin repressed nuclear translocation[364, 365, 698-700], activated NF-κB subunits through phosphorylation[371, 700-702], or had no effects on NF-κB at all[7, 703, 704]. In this study, cordycepin has been shown to repress NF-κB signalling through high-throughput analysis (figures 3.2, 3.3, 3.12, 3.13, 3.16, 3.17, 3.18 & 3.19), and restrict NF-κB (p65) nuclear translocation with inflammatory stimulation (figure 3.4), which supports previous research[364, 365, 698-700].

The effect on NF-κB by cordycepin treatment could be through PPAR signalling, which was consistently predicted to be upregulated with cordycepin treatment (figures 3.13A, 4.2A, 4.5A, & 4.8A). As the ligand-dependent nuclear receptor, PPARγ (PPARG) has a positive activation z-score with overlapping genes between cordycepin treatment and PI3K inhibition (figure 6.8B), it could be that cordycepin affects PPAR signalling through PI3K inhibition. Interestingly, inhibition of PI3K through LY294002 in RAW264.7 macrophages has a similar gene expression signature to activation of PTEN signalling (figures 6.6 & 6.8). As PPARγ is known to upregulate PTEN gene expression, which is linked to negatively regulating inflammatory response and enhancing tumour suppression[876], it is likely that PI3K inhibition upregulates PTEN signalling through activation of PPARγ. Also, PPARγ is a known inhibitor of the transcription factors NF-κB, AP-1, and STAT in macrophages and monocytes, which represses transcription of cytokine mRNAs[716, 717]. This could be a link to the repression of NF-κB by both cordycepin treatment and PI3K

inhibition (figure 6.7C). Besides PPARγ, the Class III PI3K regulatory subunit, Vps15 (p150), in hepatocytes has been shown to associate with PPARα, which is important in autophagy and mitochondrial lipid catabolism[877]. Vps15 is required for the stability and activity of the lipid kinase Vps34[67], upstream from the synthesis of Phosphatidylinositol 3-phosphate (PtdIns3P/PI3P/PIP)[68, 69], known to facilitate autophagic flux and vesicular trafficking of the lysosome[67, 877]. As Vps34 is stimulated at the phagophore membrane, which is required for autophagy initiation in conditions of nutrient withdrawal[70, 71], this could be another link to why phagosome formation, and superpathway of inositol phosphate compounds were upregulated with both cordycepin and LY294002 in RAW264.7 macrophages (figures 3.16A & 6.6A).

It has also been shown previously that enhanced PPARα DNA binding can inhibit NF-κB and ERK1/2 activity[878], and could be why cordycepin treatment leads to repression of NF-κB and ERK1/2 (figures 3.2, 3.3, 3.12, 3.13, 3.16, 3.17, 3.18, 3.19 4.5, & 4.8), potentially through the association of PI3K and PPARα[877]. Although ERK/MAPK signalling was upregulated in overlapped genes between cordycepin treatment and PI3K inhibition (figure 6.8A), which is potentially through a feedback effect with inhibition of PI3K/Akt signalling[281-284]. PPARs can heterodimerise with LXR/RXR, leading to repression of cytokine production and NF-κB signalling[714-717], which could be why both PPAR and LXR/RXR signalling are both upregulated with cordycepin treatment (figures 3.13A, 4.2A, 4.5A, & 4.8A). Interestingly, AMPK has been found to increase expression of PPARα, but repress expression of PPARγ[835, 836]. Furthermore, Takahashi, *et al.* (2012)[879] found that cordycepin treatment blocked both adipogenesis and lipid accumulation in 3T3-L1 pre-adipocytes via AMPK activation which repressed mTORC1-mediated activation of PPARγ. This is not supported by the upregulation of PPAR signalling through cordycepin treatment in this study (figures 3.13A, 4.2A, 4.5A, & 4.8A), neither is it consistent with the increased AMPK signalling and similarity of gene expression to activated PPARγ with LY294002 treatment (figures 6.6A & 6.8B). As cordycepin increased phosphorylation of AMPK at Thr172 in RAW264.7 macrophages (figure 6.1), which is consistent with literature[369, 371, 373, 831, 833, 834], and was also seen with treatment with LY294002 (figure 6.1), it is again suggestible that cordycepin acts through PI3K in upregulating PPARγ, and not through activating AMPK. Altogether, the downstream effects of cordycepin on NF-κB could be through PPAR signalling through inhibition of PI3K.

Growth factors and their respective receptor tyrosine kinases (RTKs) play important roles in the activation of downstream signalling pathways, such as PI3K/Akt, Ras/Raf/MEK/ERK, MAPK, and JAK/STAT signalling[278-280]. RTKs such as EGFRs[302-306], PDGFRα[334], VEGFRs[325, 326], and TGF-βRs[337, 340, 880] are known to stimulate PI3K/Akt signalling leading to downstream activation of transcription factors. In this study, cordycepin was found to repress growth factor signalling and had an opposite effect to gene expression compared to stimulation of growth factors, such as EGF and TGF-β, and associated RTKs (figures 4.2B, 4.5B, 4.7B, and 4.8). Also, on multiple occasions in chapter 4, cordycepin treatment was shown to repress PI3K/Akt/mTOR signalling during growth factor responses and has been found to have similar effects to expression downstream to growth factor stimulation to the PI3K inhibitor, LY294002 (figures 4.2, 4.4, 4.5, 4.7, & 4.8). Using qPCR, cordycepin was shown to repress mRNA expression of key transcription factors such as MYC, JUNB, ATF3, and early response genes such as c-FOS, c-JUN, EGR1 in the presence of growth factors such as EGF (figures 4.2, 4.9, 5.2, 5.3, 7.4, & 7.5), which was partly similar, but not identical to PI3K and mTOR inhibition (figure 5.2 & 5.3). As JUNB and FOS can be transcribed downstream from EGFR stimulation of ERK1/2 and JNK signalling by activated transcription factors, Sp1, E2F, Elk-1, and AP-1[301, 307-310], this suggests that cordycepin can repress transcription downstream from EGFR stimulation. Altogether, this shows that cordycepin represses the activation of growth factor stimulated RTKs upstream to signalling pathways (figure 9.1).

The MYC transcription factor can be upregulated through mTORC2-mediated FoxO acetylation[820], and through the downregulation of AMPK signalling by ablation of the α1 catalytic subunit[169]. Through qPCR, the treatment of the mTOR inhibitor, Torin1, and AMPK activator, A-769662, did not lead to repression of MYC mRNA expression, but there was clear repression of MYC through cordycepin (figure 5.3). This suggests that cordycepin is not acting via mTOR or AMPK activation in the repression of MYC mRNA expression. This was further suggested by no effect on the activation of AMPK through treatment with LY294002 treatment, which is known to be able to inhibit mTOR as well as PI3K[652] (figure 5.1). Also, CRISPR-Cas9 knockout of AMPK modified growth factor responses but did not abrogate repression the effect of cordycepin on the expression of growth factor induced gene expression in HEK293 cells (figures 7.6 & 7.7). MYC is also known to dimerise with the Max protein, which recruits a protein complex with the CREB p300/CBP-associated factor (PCAF)[789, 790]. This complex acetylates histone H3 and H4, opening

chromatin structure and allowing RNAP II machinery to access the E-box promoter and induce transcription[791, 792]. As cordycepin consistently represses MYC mRNA expression (figures 4.2, 5.2, & 5.3), this could link to the enrichment of repressed genes associated with chromatin remodelling and transcription through RNAP II biological pathways with CRISPR-Cas9 AMPK knockout (figures 7.7 & A.2.9A). Also, as cordycepin consistently repressed genes enriched in the regulation of transcription from RNAP II promoter with growth factor stimulation (figure 4.1B, 4.4B, 4.6B, A.2.5A, A.2.6A, & A.2.7A), this shows that AMPK knockout is not restricting the effect of cordycepin on transcription downstream to EGF stimulation. This also suggests that AMPK is not the key target of cordycepin and builds on this area of research.

Inositol phosphates (InsPs) are known to mediate many cellular processes, including proliferation, differentiation, apoptosis, migration, and mRNA export through modulating signalling cascades[35]. Multiple kinases are associated in the dynamic synthesis of InsPs, and this study has shown that cordycepin can downregulate expression of genes enriched in multiple inositol phosphate pathways (figure 4.8A) associated with growth factor stimulation. Cordycepin was also shown to inhibit expression of key inositol phosphate kinases (IPKs) in the Inositol phosphate biosynthetic process pathway in CRISPR-Cas9 AMPK knockout HEK293 cells (figures 7.7B & A.2.9B), showing again that AMPK ablation does not restrict the effect of cordycepin treatment in growth factor response. These included IPPK, IPMK, IP6K1, PPIP5K2, and ITPKC (figure A.2.9B). IPMK is known to convert IP_3 to IP_4, and then to IP_5, and acts similarly to PI3K in the phosphorylation of PIP_2 to PIP_3, important in the translocation and subsequent action of AKT at the plasma membrane[37, 72]. Downregulation of IPMK through cordycepin could be why PI3K/Akt signalling is consistently downregulated in this study (figures 3.16, 4.2, 4.4, & 6.8). Also, as IPPK phosphorylates IP_5 to IP_6, which is further phosphorylated by both PPIP5K2 and IP6K1 to IP_7 in the presence of growth factors or insulin, this suggests that cordycepin is repressing growth factor stimulation of the synthesis from IP_5 to IP_7[35]. It is known that IP_7 can fine-tune signalling downstream to PIP_2 to PIP_3 through interacting with the PH-domains of PIP-associating proteins at subcellular membranes[35, 38]. For this reason, as cordycepin represses expression of IPPK, PPIP5K2, and IP6K1 (figure A.2.9B), it is likely that cordycepin is affecting the metabolism of the inositol phosphates, which can then affect signalling downstream from PIP_2 and PIP_3. This is further proven through repression of ITPKC, which encodes an

isoform of the inositol-tetrakisphosphate 1-kinase (ITPK1) known to metabolise multiple inositol phosphates and produce substrates for multiple IPKs[35]. This effect was not seen in RAW264.7 macrophages with inflammatory stimulation as the superpathway of inositol phosphate compounds pathway is upregulated by both cordycepin treatment and PI3K inhibition (figures 3.16 & 6.6A). Altogether, cordycepin is repressing inositol phosphate metabolism in the presence of growth factors (figures 4.8A, 7.7B & A.2.9B) which could be causing the repression of downstream signalling pathways, such as PI3K/Akt signalling, even in the absence of AMPK.

The effects of cordycepin on the MAPK signalling pathways have been reviewed previously in Radhi *et al*. (2021)[3] and showed that the effect of cordycepin on the activity of p38 MAPK are ambiguous, whereas ERK signalling is consistently repressed. This study confirmed that cordycepin can repress MEK/ERK signalling (figures 3.10, 4.2, 4.5, & 4.8) and had similar effects to gene expression to the MEK1/2 inhibitor, U0126 (figures 3.13, 3.16, 3.19, 4.2, 4.5, 4.7, & 4.8). Also, this study confirmed ambiguity in the effects of cordycepin on p38 MAPK based on pathway analysis of differential gene expression, as for NIH3T3 fibroblasts, cordycepin both activate p38 MAPK signalling (figure 4.7A) and had an opposite effect to activation of p38 MAPK as an upstream regulator (figure 4.7B). Cordycepin treatment also led to repression of p38 MAPK signalling in MCF-7 cells (figure 4.2B) but had a similar effect to downstream expression to the p38 MAPK inhibitor, SB203580, in NIH3T3 fibroblasts, MCF-7 cells, and MDA-MB-231 cells (figure 4.8B). Interestingly, overlapping of statistically significant differentially expressed genes between cordycepin and PI3K inhibition led to activation of ERK/MAPK and p38 MAPK signalling in this study (≤ 0.05 p-value; figure 6.6A). This effect could be through crosstalk between the MAPK/MEK/ERK signalling pathway and PI3K/Akt signalling[281-284], as MEK/ERK is upregulated to counteract the downregulation of the PI3K/Akt pathways. As GSK3β is known to phosphorylate numerous proteins and transcription factors associated with the Wnt/β-catenin signalling pathway[95], and AKT is known to phosphorylate and inactivate GSK3β at Ser9[89], it is not surprising that PI3K led to upregulation of WNT/β-catenin and WNT/GSK3β pathways (figure 6.6A). This altogether provides more evidence that cordycepin treatment and PI3K inhibition can have similar effects on expression and signalling pathways. As cellular stress may trigger these signalling pathways, future work could include investigating pathways not affected by cordycepin to show that these effects are not through induction of stress.

Altogether, this study has shown that cordycepin consistently represses PI3K activity, which could be through the effect of cordycepin on cleavage and polyadenylation, which will be described in the next section. Cordycepin analogues such as Nucarna's ProTide (NUC-7738) are now entering the clinic[15], and preliminary data has also shown that NUC-7738 can restrict transcription of c-MYC and CD44 in AML cells through reduced PI3K-P110α, and repressed phosphorylation and activation of AKT (Ser473), and GSK3β (Ser9)[881]. This coupled with the data from this study highlights the importance and relevance of studying the effect of cordycepin on PI3K/Akt/mTOR signalling and shows exciting potential benefits of cordycepin treatment to reduce disease propagation linked to PI3K/Akt/mTOR signalling.

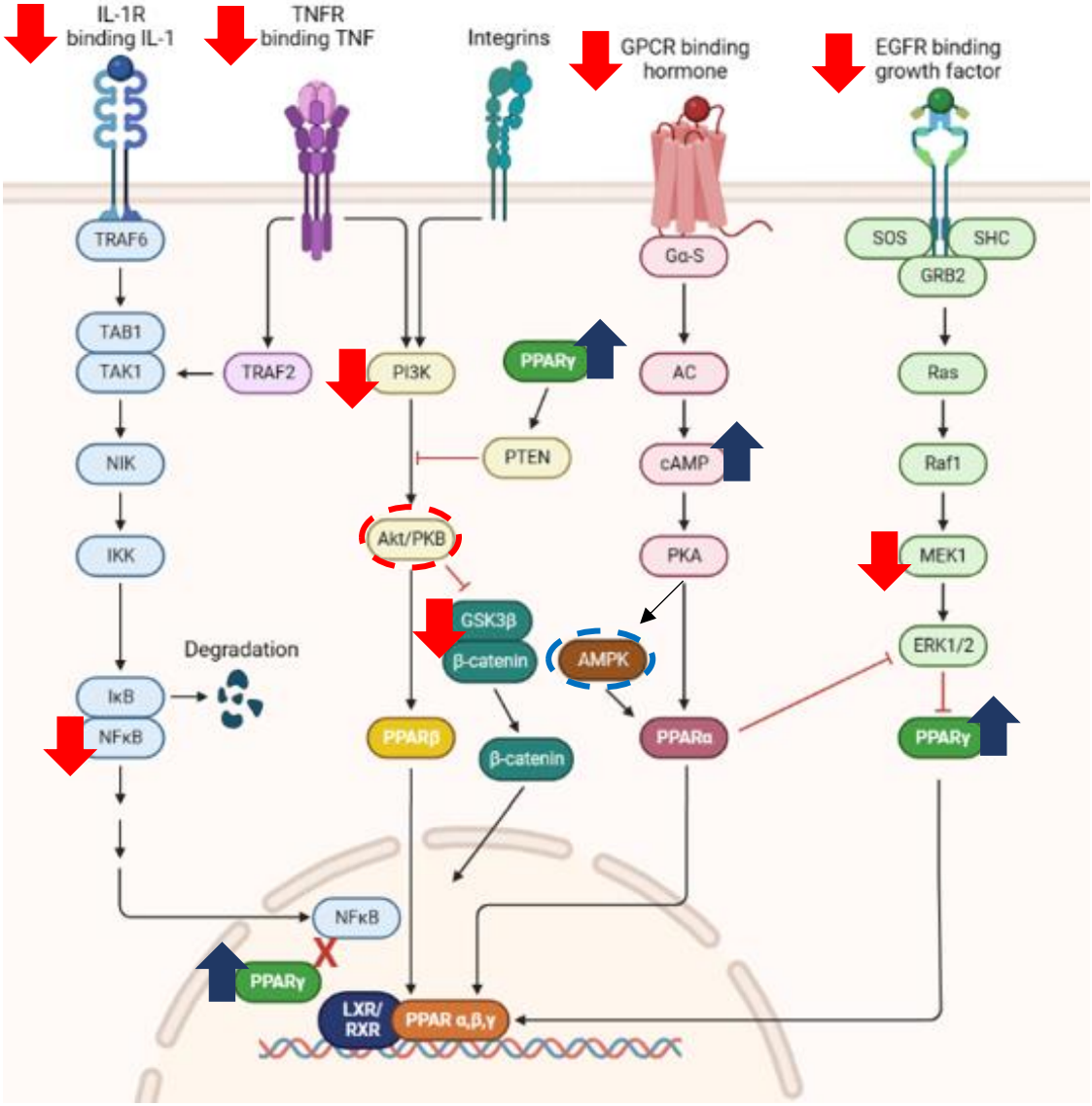

Figure 9.1: Targets of cordycepin in signalling cascades identified in this study. Diagram illustrating targets of cordycepin based on results from this study (in arrows; red means downregulated, blue means upregulated) relating to signalling cascades downstream of activated membrane receptors. Circles are previously known targets of cordycepin, AKT/PKB and AMPK, based on literature reviews[3, 4].

9.2 Cordycepin could be affecting PI3K/Akt/mTOR signalling through restricting cleavage and polyadenylation

Cleavage and polyadenylation is a crucial mechanism in the maturation of mRNA transcripts which composes of a cleavage and polyadenylation specificity factor (CPSF) pre-mRNA 3'processing multiprotein complex (detailed in figure 1.2)[393, 394]. The formation of the poly(A) tail and associated 3'end processing machinery can contribute to transcription termination, translational control, and the stability of mRNA, thereby regulating gene expression[391, 392]. In this study, label-free quantitative proteomics of RNA-bound Interphases and Unbound phases obtained through Orthogonal Organic Phase Separation (OOPS)[661], was used to gain protein abundances of RNA binding proteins (RBPs). Chapter 8 set out to use the RBP protein abundances to see whether cordycepin is repressing PI3K/Akt signalling, shown throughout the study (figures 3.13, 3.16, 3.19, 4.2, 4.4-4.5, 4.7, 4.8, 5.1, 6.1, & 6.8) through affecting the association of RBPs to RNA-bound complexes, as RBPs can modulate PI3K/Akt/mTOR and AMPK signalling[635, 867, 868, 870, 871]. Through comparing UQ normalised protein abundances, it was clear that PI3K inhibition had a more significant effect on shifting RBPs towards the RNA-bound Interphase than cordycepin treatment when compared to DMSO treatment (figure 8.4). This could however be due to unknown outlier abundances skewing interpretation of the data. However, both treatments shifted RBPs towards the RNA-bound Interphase which are associated with mRNA processing, RNA splicing, mRNA transport, and translation, and included the factors, RBBP6, THOC2 and 3, and TUT1 (Star-PAP), which are associated with polyadenylation and poly(A) tail metabolism (figure 8.5).

TUT1 is known to inhibit PPARγ and SREBP-1c through upregulating miRNA-24 and miRNA-29a[535], which shows again that both cordycepin treatment and PI3K inhibition can influence PPAR signalling as seen previously in figures 3.3A, 3.16A, 4.2A, 4.5A, 4.7A, 4.8A, & 6.8. Interestingly, TUT1 is also known to be regulated by the phosphatidylinositol phosphate kinase, PIPKIα, and PIP_2[882], suggesting that cordycepin can sequester TUT1 to the nucleus through PI3K inhibition, linked to the repression of inositol phosphate metabolic pathways shown previously (figures 4.8A, 7.7B, & A.2.9B). TUT1 can promote recruitment of CPSF3 and CPSF1 to the CPA site to induce 3'end CPSF3 cleavage[446, 447], and the ubiquitin-ligase RBBP6, which interacts with CPSF3 and WDR33 can also play a crucial role in activating cleavage in the presence of CSTF and CFIIm subcomplexes[394, 419]. This shows that cordycepin and PI3K inhibition can shift RBPs

towards an RNA-bound phase which can affect 3'end cleavage. RBBP6 also facilitates ubiquitination and degradation of p53[570], and results from this study has consistently shown that cordycepin can repress ubiquitination (figures 3.17C, 4.1B, 4.4B, 7.3, 7.7B, A.2.5A, A.2.6A, & A.2.9B), even in CRISPR-Cas9 AMPK knockout HEK293 cells. As both cordycepin and PI3K inhibition sequesters RBBP6 to RNA-bound Interphase, this might suggest that cordycepin can repress ubiquitination through PI3K inhibition.

The association between PI3K and polyadenylation machinery is not a new concept, with previous research highlighting interaction between PI3K and CPSF4[632, 633], with reduced expression of CPSF4 linked to repressed phosphorylation and activation of PI3K p85 (Tyr458)/p55 (Tyr199), AKT (Ser473), ERK1/2 (Thr202/Tyr204), and JNK (Thr183/Tyr185) in H1299 non-small cell lung carcinomas[635, 637]. In this study, siRNA knockdown of the cleavage and polyadenylation factor, WDR33, in RAW264.7 macrophages led to reduced phosphorylation of AKT target, GSK3β (Ser9), and mTORC1 target, 4E-BP1 (Thr37/46) (figure 6.9). Also, depletion of WDR33 increased the phosphorylation of AMPK (Thr172) (figure 6.9), known to repress mTORC1 signalling[153, 154]. Coupled with this is the similarity of gene expression pattern between the overlapped genes of cordycepin treatment and WDR33 knockdown to the PI3K inhibitor, LY294002, in RAW264.7 macrophages, and the repression of PI3K/Akt signalling pathway (figures 3.13B & 3.19B). This altogether clearly shows that knockdown of WDR33 leads to repression of PI3K/Akt/mTOR signalling, illustrated by figure 9.2. Also, as with cordycepin treatment (figures 3.2, 3.3, 3.12, 3.13, 3.16, 3.17, 3.18 & 3.19), and PI3K inhibition (figures 6.5-6.8), knockdown of WDR33 also repressed inflammatory stimulation and NF-κB transcription (figures 3.10 & 3.12, 3.13, 3.18, 3.19), which was linked to overlapping genes with cordycepin treatment. This is consistent with a previous publication in our lab which showed that depleting polyadenylation machinery can restrict NF-κB nuclear translocation, and repress inflammatory gene expression[384], and also highlights that ablation of polyadenylation machinery is repressing PI3K/Akt/NF-κB signalling.

Interestingly, analysis of label-free quantitative proteomics of PI3K inhibition through LY294002 in RAW264.7 macrophages also showed a higher accumulation of WDR33 towards the RNA-bound Interphase section compared to the unbound phase (figure 8.5B), obtained through OOPS[661]. This was shown within 20 minutes treatment of PI3K inhibition and LPS stimulation compared to DMSO and LPS stimulation (chapter 8), so this effect on WDR33 was relatively quick and potentially quite a direct effect.

This sequestering of WDR33 to RNA through PI3K inhibition could be linked to the restricted dissociation of WDR33 seen with CoTP[5, 369, 646], illustrated by figure 9.2. Altogether, there is apparent feedback between PI3K and WDR33. As knockdown of WDR33 was over two courses for a total of 48 hours, it is worth performing shorter knockdown experiments or longer treatment of PI3K inhibition and cordycepin for better comparison in RAW264.7 macrophages. Indeed, a limitation of this study is that the longer incubation with siRNA of WDR33 could be why there is a relatively low positive correlation between RNA-Seq output of WDR33 knockdown and cordycepin treatment (R^2 = 0.207; figure 3.18B).

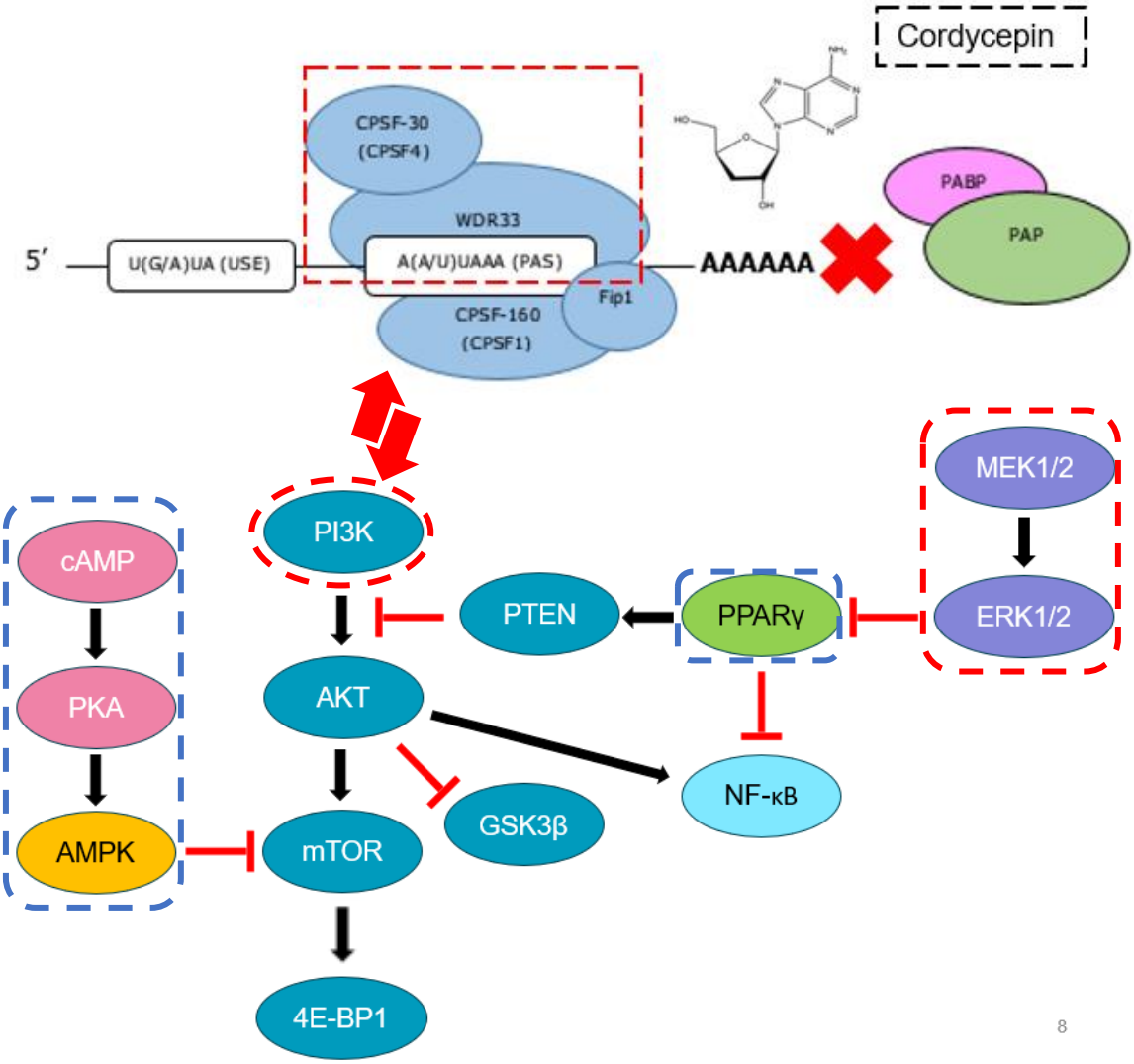

Figure 9.2: There is crosstalk between the inhibition of polyadenylation and signalling machinery. Diagram illustrating results from this study highlighting that inhibiting polyadenylation machinery, WDR33, represses PI3K/Akt signalling via upregulating PPARγ, cAMP, and AMPK signalling. The effect of cordycepin on signalling could be through trapping WDR33 on the poly(A) tail, similarly to PI3K inhibition.

Besides WDR33, other factors also accumulated towards the RNA-bound Interphase, including CPSF2, PABPC1, hnRNPLL, and ALYREF specifically with PI3K inhibition (figure 8.5B). CPSF2 forms as part of the CPSF complex and is a core component of the cleavage factor (CF) subcomplex[393], and plays key roles in tethering cleavage machinery, such as CPSF3, with polyadenylation specificity factors (PSFs), such as CPSF4 and Symplekin[393, 402, 403, 412, 420, 421]. This again shows that LY294002 treatment can affect CPSF3 cleavage as suggested previously. CPSF2 can also associate with CPEB1[501], an important protein associated with cytoplasmic polyadenylation and mRNA translation, and PABPC1[488-490]. Multiple PABPC1's can bind to RNA recognition motifs on mRNA and link together in a 'head-to-tail' formation, which supports interaction and stability of translational machinery[505, 589, 592-596]. Altogether with the repression of the phosphorylation of 4E-BP1 (Thr37/46) downstream from mTORC1 (figure 5.1 and 6.1), this study has shown that cordycepin and PI3K inhibition can restrict mRNA translation, with PI3K inhibition affecting key polyadenylation machinery.

As both cordycepin treatment and PI3K inhibition had higher abundance of THOC2 and THOC3 proteins in the RNA-bound Interphase, and PI3K inhibition shifted ALYREF (Aly/REF) towards the RNA-bound Interphase (figure 8.5), it can be suggested that cordycepin affects mRNA transport through PI3K inhibition. This is due to THOC2, THOC3 and ALYREFs involvement in the TREX (TRanscription EXport) complex, which associates with NXF1:NXT1 to export mature mRNAs[578-582, 584, 585]. As the TREX complex is released through NXF1:NXT1 mRNA:protein rearrangements at the nuclear pore, this fixing of THOC2, THOC3, and ALYREF to RNA-bound complexes could be mitigating mRNA export for translation in the cytoplasm[578-582, 584-586]. This also links to previous results through enrichment of RBPs in translation and cytoplasmic translation biological pathways that cordycepin and LY294002 treatment can affect translation (figure 8.5). Future work to confirm these shifts of polyadenylation machinery with PI3K inhibition could be through performing western blots of protein from Interphase and Unbound phases after OOPS. Also, association studies could include immunoprecipitation (IP) experiments of PI3K after OOPS on the phases and visualisation of polyadenylation machinery targets through western blot, or through quantifying mRNA abundance of these target polyadenylation machinery after RNA-IP.

As highlighted in the discussion section of chapter 8, there are clear limitations in the interpretation of the label-free quantitative proteomics data in this study as both 1-hour and 2-hour liquid chromatography

biological replicates were used for analysis in chapter 8. Also, the shifting of RBPs towards the RNA-bound Interphase with addition of formaldehyde crosslinking was not conclusive in figure 8.3. For this reason, more biological replicates will be needed to improve output, or potentially using labelling methods can be used to increase precision of peptide calling, which will be discussed further in the next section.

9.3 Concluding remarks & future work

Throughout this study, cordycepin was found to repress growth factor stimulation and had an opposite effect to the activation of receptor tyrosine kinases (RTKs) (figures 4.2B, 4.5B, 4.7B, and 4.8), which are upstream to the activation of PI3K/Akt, Ras/Raf/MEK/ERK, MAPK, and JAK/STAT signalling[278-280]. To substantiate this predicted effect of cordycepin treatment on RTK activity, which could be why downstream signalling pathways are repressed, a potential next step could be through using commercial ELISA kits with RTK-specific polymer substrate-coated multi-well plates (such as the Sigma Protein Tyrosine Kinase Assay Kit; PTK101). This will allow for the quantification and specific detection of phosphorylated tyrosine residues of the receptors and indicate whether cordycepin treatment inhibits activity of the RTKs.

This study has also shown that cordycepin treatment had an opposite gene expression profile to VEGF stimulation (figure 4.8B), potentially through reduced GPER1 activity (figures 4.2B, 4.5B, 4.7B, & 4.8B) leading to repression of MAPK/ERK, PI3K/Akt signalling and cAMP production[322, 325-328]. However, cordycepin treatment also upregulated CREB and cAMP signalling in RAW264.7 macrophages (figures 3.9B, 3.10, 3.15B, and 3.16), which could be why AMPK is phosphorylated by cordycepin in RAW264.7 macrophages (figure 6.1) as increased cAMP levels upregulates PKA which induces LKB1-mediated phosphorylation of AMPK[144], highlighted by figures 9.1 & 9.2. To conclusively check to see if increased cAMP through cordycepin is triggering AMPK in RAW264.7 macrophages, future work should include quantifying cAMP through LC-MS/MS, such as the method detailed by Tsjokajev *et al.* (2020)[883]. Also. western blotting for phosphorylated PKA with and without cordycepin treatment can also be used as an

indicator for increased cAMP. Likewise, this will also show whether cordycepin is modulating signalling pathways via regulating cAMP levels.

The systematic review of Radhi, *et al.* (2021)[3] showed that the effect of cordycepin on NF-κB signalling is ambiguous in literature, with papers suggesting repressed nuclear translocation of NF-κB[364, 365, 698-700], activated NF-κB subunits through phosphorylation[371, 700-702], or had no effect at all[7, 703, 704]. This study also suggested that cordycepin can repress NF-κB signalling through differential gene expression (figures 3.2, 3.3, 3.12, 3.13, 3.16, 3.17, 3.18 & 3.19), and shifted NF-κB (p65) towards the cytoplasm and out of the nucleus in RAW264.7 macrophages (figure 3.4), which supports previous research[364, 365, 698-700]. Going forward, further work to show that cordycepin represses NF-κB signalling could include confirmation that PI3K inhibition also represses NF-κB nuclear localisation in RAW264.7 macrophages, as this is suggested by results in chapter 6. Another possibility in future work could be to use immunofluorescence with antibodies of alternative upstream mediators of NF-κB such as phosphorylated IκB kinase or RIPK2 with cordycepin treatment which will also build on these results and give more evidence that cordycepin represses NF-κB signalling. Alternatively, commercial DNA-binding ELISA assays for multiple NF-κB subunits (p50, p52, p65, c-Rel, and RelB) could be used to show that cordycepin represses NF-κB activity quantitatively through colourimetry.

This study has shown that multiple inositol phosphate kinases (IPKs), IPPK, IPMK, IP6K1, PPIP5K2, and ITPKC, have downregulated expression with cordycepin treatment (figure A.2.9B), and multiple Inositol phosphate metabolism pathways are predicted to the repressed with cordycepin with growth factor stimulation (figures 4.8A & 7.7B). These IPKs play crucial roles in the metabolism of Inositol phosphates (InsPs), which play crucial roles in regulating signalling cascades downstream from PIP_3 and PIP_2[35, 37, 38, 72]. For this reason, more work is needed to investigate whether the effect of cordycepin on PI3K/Akt signalling is through affecting IPK activity and InsP metabolism. Future work to prove that cordycepin is affecting PIP_2 or PIP_3 could be through transfecting RAW264.7 macrophages with fluorescently tagged sensor vectors, such as the AKT-PH-Venus or AKT-PH-mCherry vector. Through confocal microscopy, this will illuminate AKT, which will be cytosolic in the absence of PIP_3 and translocates to the plasma membrane upon PIP_3 generation, which has been shown previously to indicate AKT activity and PIP production[884]. Through treatment with cordycepin, it would be apparent whether cordycepin affects PIP

metabolism and AKT activity. Quantifying inositol phosphates is trickier and requires more advanced high-pressure liquid chromatography (HPLC) with electrospray ionisation mass spectrometry (ESI-MS) techniques[885]. However, using these techniques, it might be possible to quantitatively show that cordycepin is changing InsP metabolism linking to downstream effects on signal transduction.

Throughout this study, cordycepin treatment was found to upregulate LXR/RXR and PPAR signalling (figures 3.13A, 4.2A, 4.5A, & 4.8A), which could be why we see repression of cytokine production, ERK1/2 and NF-κB signalling (figures 3.2, 3.3, 3.12, 3.13, 3.16, 3.17, 3.18, 3.19 4.5, & 4.8), as PPAR heterodimerisation of LXR/RXR can cause this repression[714-717, 878]. Also, there is an association between PI3K and PPARα[877], and AMPK can increase the expression of PPARα, but repress expression of PPARγ[835, 836]. This means there is an association between pathways affected by cordycepin to PPAR signalling. Very few papers have linked cordycepin treatment with PPAR signalling, with one suggesting that cordycepin activates AMPK, which represses mTORC1-mediated PPARγ activation[879]. Results from this study do not support this as PPAR signalling is upregulated, and therefore more work is needed to see if the effects we see through cordycepin is through PPAR signalling. To provide further clarification, co-inhibition of PPAR activity, such as by treating cells with GW6471 for PPARα[886], or GW9662 for PPARγ[887], could show whether this abrogates the anti-inflammatory effects of cordycepin treatment and PI3K inhibition (seen in chapter 6), thereby confirming whether these downstream effects are through PPARs.

This study showed that both cordycepin treatment and PI3K inhibition can shift cleavage and polyadenylation machinery towards the RNA-bound Interphase (figures 8.4 & 8.5). Specifically with PI3K inhibition, there was a shift of PABPC1, linked to cytoplasmic polyadenylation and translation[505, 589, 592-596], and WDR33, important for recognising the poly(A) site (PAS)[402, 403], towards the RNA-bound Interphase. This study also showed that WDR33 knockdown can lead to repression of PI3K/Akt/mTOR signalling (figure 6.9) and had a similar effect to differential gene expression to LY294002 (figures 3.13 & 3.19). For this reason, it would be interesting for future work to include immunoprecipitation (IP) experiments of PI3K after OOPS on the phases and visualisation of polyadenylation machinery targets through western blot, or through quantifying mRNA abundance of these target polyadenylation machinery after RNA-IP. Alternatively, more sensitive quantitative proteomic analysis and precise peptide calling methods such as SILAC or TMT labelling[888], can be used in future experiments to help alleviate

technical variability of label-free proteomics[889]. Also, other methods to study protein-RNA complexes are available, such as thermal proteome profiling (TPP), which uses multiplexed quantitative mass spectrometry-based proteomics which can monitor the melting profile of expressed proteins in a sample[890]. There are also other RBP extraction methods, such as the Phenol Toluol extraction (PTex) protocol which uses phenol:toluol extraction to purify RNA-protein complexes based on their physiochemical differences due to toluol being less water-soluble than phenol[891]. Therefore, future work could include labelling, or alternative methods to obtain RBPs, which can be used to compare to the data from this study for reproducible outcomes. Also, there is a lack of statistical analyses of the current proteomics data, so future work must include performing statistical tests to establish if high-variability and extreme outliers are leading to differences between cordycepin and LY294002 treatments.

It should be noted that a lot of the interpretation of the differential expression of cordycepin and LY294002 treatment in this study was through IPA. As this platform uses the differential expression data to predict affected biological pathways and similarity to upstream regulators on expression, further experimental evidence will be needed to show that this data is reliable and accurate. Due to restrictions through a global pandemic during this study, causing a big disruption and halt to experimental work, it was impossible to gain this experimental evidence within the set PhD deadline. However, this study forms the basis of potentially new target pathways and regulators of cordycepin treatment, and consistent link between polyadenylation and PI3K inhibition, prompting for further investigations in the future and expanding our understanding of the effects of cordycepin.

10 References

1. CUNNINGHAM, K. G., MANSON, W., SPRING, F. S. & HUTCHINSON, S. A. (1950). Cordycepin, a metabolic product isolated from cultures of cordyceps militaris (linn.) link. *Nature,* **166,** 949.
2. Das, S. K., Masuda, M., Sakurai, A. & Sakakibara, M. (2010). Medicinal uses of the mushroom cordyceps militaris: Current state and prospects. *Fitoterapia,* **81,** 961-8.
3. Radhi, M., Ashraf, S., Lawrence, S., Tranholm, A. A., Wellham, P. A. D., Hafeez, A., Khamis, A. S., Thomas, R., McWilliams, D. & de Moor, C. H. (2021). A systematic review of the biological effects of cordycepin. *Molecules,* **26**.
4. Khan, M. A. & Tania, M. (2022). Cordycepin and kinase inhibition in cancer. *Drug Discov Today,* **28,** 103481.
5. KLENOW, H. (1963). Formation of the mono-, di- and triphosphate of cordycepin in ehrlich ascites-tumor cells in vitro. *Biochim Biophys Acta,* **76,** 347-53.
6. Jeong, J. W., Jin, C. Y., Kim, G. Y., Lee, J. D., Park, C., Kim, G. D., Kim, W. J., Jung, W. K., Seo, S. K., Choi, I. W.*, et al.* (2010). Anti-inflammatory effects of cordycepin via suppression of inflammatory mediators in bv2 microglial cells. *Int Immunopharmacol,* **10,** 1580-6.
7. Kondrashov, A., Meijer, H. A., Barthet-Barateig, A., Parker, H. N., Khurshid, A., Tessier, S., Sicard, M., Knox, A. J., Pang, L. & De Moor, C. H. (2012). Inhibition of polyadenylation reduces inflammatory gene induction. *RNA,* **18,** 2236-50.
8. Hwang, J. H., Park, S. J., Ko, W. G., Kang, S. M., Lee, D. B., Bang, J., Park, B. J., Wee, C. B., Kim, D. J., Jang, I. S.*, et al.* (2017). Cordycepin induces human lung cancer cell apoptosis by inhibiting nitric oxide mediated erk/slug signaling pathway. *Am J Cancer Res,* **7,** 417-432.
9. Hwang, I. H., Oh, S. Y., Jang, H. J., Jo, E., Joo, J. C., Lee, K. B., Yoo, H. S., Lee, M. Y., Park, S. J. & Jang, I. S. (2017). Cordycepin promotes apoptosis in renal carcinoma cells by activating the mkk7-jnk signaling pathway through inhibition of c-flipl expression. *PLoS One,* **12,** e0186489.
10. Zhou, X., Luo, L., Dressel, W., Shadier, G., Krumbiegel, D., Schmidtke, P., Zepp, F. & Meyer, C. U. (2008). Cordycepin is an immunoregulatory active ingredient of cordyceps sinensis. *Am J Chin Med,* **36,** 967-80.
11. Huang, F., Li, W., Xu, H., Qin, H. & He, Z. G. (2019). Cordycepin kills mycobacterium tuberculosis through hijacking the bacterial adenosine kinase. *PLoS One,* **14,** e0218449.
12. Jiang, Q., Lou, Z., Wang, H. & Chen, C. (2019). Antimicrobial effect and proposed action mechanism of cordycepin against escherichia coli and bacillus subtilis. *J Microbiol,* **57,** 288-297.
13. Hawley, S. A., Ross, F. A., Russell, F. M., Atrih, A., Lamont, D. J. & Hardie, D. G. (2020). Mechanism of activation of ampk by cordycepin. *Cell Chem Biol,* **27,** 214-222.e4.
14. Li, G., Nakagome, I., Hirono, S., Itoh, T. & Fujiwara, R. (2015). Inhibition of adenosine deaminase (ada)-mediated metabolism of cordycepin by natural substances. *Pharmacol Res Perspect,* **3,** e00121.
15. Schwenzer, H., De Zan, E., Elshani, M., van Stiphout, R., Kudsy, M., Morris, J., Ferrari, V., Um, I. H., Chettle, J., Kazmi, F.*, et al.* (2021). The novel nucleoside analogue protide nuc-7738 overcomes cancer resistance mechanisms. *Clin Cancer Res,* **27,** 6500-6513.
16. Majumder, A. L., Johnson, M. D. & Henry, S. A. (1997). 1l-myo-inositol-1-phosphate synthase. *Biochim Biophys Acta,* **1348,** 245-56.
17. Falkenburger, B. H., Jensen, J. B., Dickson, E. J., Suh, B. C. & Hille, B. (2010). Phosphoinositides: Lipid regulators of membrane proteins. *J Physiol,* **588,** 3179-85.

18. Raghu, P., Joseph, A., Krishnan, H., Singh, P. & Saha, S. (2019). Phosphoinositides: Regulators of nervous system function in health and disease. *Front Mol Neurosci,* **12,** 208.
19. Burke, J. E. (2018). Structural basis for regulation of phosphoinositide kinases and their involvement in human disease. *Mol Cell,* **71,** 653-673.
20. Balla, T. (2013). Phosphoinositides: Tiny lipids with giant impact on cell regulation. *Physiol Rev,* **93,** 1019-137.
21. Berridge, M. J. (2009). Inositol trisphosphate and calcium signalling mechanisms. *Biochim Biophys Acta,* **1793,** 933-40.
22. Saiardi, A., Bhandari, R., Resnick, A. C., Snowman, A. M. & Snyder, S. H. (2004). Phosphorylation of proteins by inositol pyrophosphates. *Science,* **306,** 2101-5.
23. Shen, X., Xiao, H., Ranallo, R., Wu, W. H. & Wu, C. (2003). Modulation of atp-dependent chromatin-remodeling complexes by inositol polyphosphates. *Science,* **299,** 112-4.
24. Odom, A. R., Stahlberg, A., Wente, S. R. & York, J. D. (2000). A role for nuclear inositol 1,4,5-trisphosphate kinase in transcriptional control. *Science,* **287,** 2026-9.
25. York, J. D., Odom, A. R., Murphy, R., Ives, E. B. & Wente, S. R. (1999). A phospholipase c-dependent inositol polyphosphate kinase pathway required for efficient messenger rna export. *Science,* **285,** 96-100.
26. Malek, M., Kielkowska, A., Chessa, T., Anderson, K. E., Barneda, D., Pir, P., Nakanishi, H., Eguchi, S., Koizumi, A., Sasaki, J.*, et al.* (2017). Pten regulates pi(3,4)p. *Mol Cell,* **68,** 566-580.e10.
27. Vanhaesebroeck, B., Guillermet-Guibert, J., Graupera, M. & Bilanges, B. (2010). The emerging mechanisms of isoform-specific pi3k signalling. *Nat Rev Mol Cell Biol,* **11,** 329-41.
28. Gaidarov, I., Smith, M. E., Domin, J. & Keen, J. H. (2001). The class ii phosphoinositide 3-kinase c2alpha is activated by clathrin and regulates clathrin-mediated membrane trafficking. *Mol Cell,* **7,** 443-9.
29. Noda, T., Matsunaga, K., Taguchi-Atarashi, N. & Yoshimori, T. (2010). Regulation of membrane biogenesis in autophagy via pi3p dynamics. *Semin Cell Dev Biol,* **21,** 671-6.
30. Balla, A. & Balla, T. (2006). Phosphatidylinositol 4-kinases: Old enzymes with emerging functions. *Trends Cell Biol,* **16,** 351-61.
31. D'Angelo, G., Vicinanza, M., Di Campli, A. & De Matteis, M. A. (2008). The multiple roles of ptdins(4)p -- not just the precursor of ptdins(4,5)p2. *J Cell Sci,* **121,** 1955-63.
32. Shisheva, A., Sbrissa, D. & Ikonomov, O. (2015). Plentiful ptdins5p from scanty ptdins(3,5)p2 or from ample ptdins? Pikfyve-dependent models: Evidence and speculation (response to: Doi 10.1002/bies.201300012). *Bioessays,* **37,** 267-77.
33. Grainger, D. L., Tavelis, C., Ryan, A. J. & Hinchliffe, K. A. (2011). Involvement of phosphatidylinositol 5-phosphate in insulin-stimulated glucose uptake in the l6 myotube model of skeletal muscle. *Pflugers Arch,* **462,** 723-32.
34. Vanhaesebroeck, B., Leevers, S. J., Ahmadi, K., Timms, J., Katso, R., Driscoll, P. C., Woscholski, R., Parker, P. J. & Waterfield, M. D. (2001). Synthesis and function of 3-phosphorylated inositol lipids. *Annu Rev Biochem,* **70,** 535-602.
35. Tu-Sekine, B. & Kim, S. F. (2022). The inositol phosphate system-a coordinator of metabolic adaptability. *Int J Mol Sci,* **23**.
36. Irvine, R. F. (2003). 20 years of ins(1,4,5)p3, and 40 years before. *Nat Rev Mol Cell Biol,* **4,** 586-90.
37. Maag, D., Maxwell, M. J., Hardesty, D. A., Boucher, K. L., Choudhari, N., Hanno, A. G., Ma, J. F., Snowman, A. S., Pietropaoli, J. W., Xu, R.*, et al.*

(2011). Inositol polyphosphate multikinase is a physiologic pi3-kinase that activates akt/pkb. *Proc Natl Acad Sci U S A,* **108,** 1391-6.
38. Lee, S., Kim, M. G., Ahn, H. & Kim, S. (2020). Inositol pyrophosphates: Signaling molecules with pleiotropic actions in mammals. *Molecules,* **25**.
39. Fruman, D. A., Chiu, H., Hopkins, B. D., Bagrodia, S., Cantley, L. C. & Abraham, R. T. (2017). The pi3k pathway in human disease. *Cell,* **170,** 605-635.
40. Escobedo, J. A., Navankasattusas, S., Kavanaugh, W. M., Milfay, D., Fried, V. A. & Williams, L. T. (1991). Cdna cloning of a novel 85 kd protein that has sh2 domains and regulates binding of pi3-kinase to the pdgf beta-receptor. *Cell,* **65,** 75-82.
41. Hiles, I. D., Otsu, M., Volinia, S., Fry, M. J., Gout, I., Dhand, R., Panayotou, G., Ruiz-Larrea, F., Thompson, A. & Totty, N. F. (1992). Phosphatidylinositol 3-kinase: Structure and expression of the 110 kd catalytic subunit. *Cell,* **70,** 419-29.
42. Miller, M. S., Schmidt-Kittler, O., Bolduc, D. M., Brower, E. T., Chaves-Moreira, D., Allaire, M., Kinzler, K. W., Jennings, I. G., Thompson, P. E., Cole, P. A., *et al.* (2014). Structural basis of nsh2 regulation and lipid binding in pi3kα. *Oncotarget,* **5,** 5198-208.
43. Hu, P., Mondino, A., Skolnik, E. Y. & Schlessinger, J. (1993). Cloning of a novel, ubiquitously expressed human phosphatidylinositol 3-kinase and identification of its binding site on p85. *Mol Cell Biol,* **13,** 7677-88.
44. Stoyanov, B., Volinia, S., Hanck, T., Rubio, I., Loubtchenkov, M., Malek, D., Stoyanova, S., Vanhaesebroeck, B., Dhand, R. & Nürnberg, B. (1995). Cloning and characterization of a g protein-activated human phosphoinositide-3 kinase. *Science,* **269,** 690-3.
45. Vanhaesebroeck, B., Welham, M. J., Kotani, K., Stein, R., Warne, P. H., Zvelebil, M. J., Higashi, K., Volinia, S., Downward, J. & Waterfield, M. D. (1997). P110delta, a novel phosphoinositide 3-kinase in leukocytes. *Proc Natl Acad Sci U S A,* **94,** 4330-5.
46. Chantry, D., Vojtek, A., Kashishian, A., Holtzman, D. A., Wood, C., Gray, P. W., Cooper, J. A. & Hoekstra, M. F. (1997). P110delta, a novel phosphatidylinositol 3-kinase catalytic subunit that associates with p85 and is expressed predominantly in leukocytes. *J Biol Chem,* **272,** 19236-41.
47. Whitman, M., Downes, C. P., Keeler, M., Keller, T. & Cantley, L. (1988). Type i phosphatidylinositol kinase makes a novel inositol phospholipid, phosphatidylinositol-3-phosphate. *Nature,* **332,** 644-6.
48. Otsu, M., Hiles, I., Gout, I., Fry, M. J., Ruiz-Larrea, F., Panayotou, G., Thompson, A., Dhand, R., Hsuan, J. & Totty, N. (1991). Characterization of two 85 kd proteins that associate with receptor tyrosine kinases, middle-t/pp60c-src complexes, and pi3-kinase. *Cell,* **65,** 91-104.
49. Skolnik, E. Y., Margolis, B., Mohammadi, M., Lowenstein, E., Fischer, R., Drepps, A., Ullrich, A. & Schlessinger, J. (1991). Cloning of pi3 kinase-associated p85 utilizing a novel method for expression/cloning of target proteins for receptor tyrosine kinases. *Cell,* **65,** 83-90.
50. Fruman, D. A., Cantley, L. C. & Carpenter, C. L. (1996). Structural organization and alternative splicing of the murine phosphoinositide 3-kinase p85 alpha gene. *Genomics,* **37,** 113-21.
51. Antonetti, D. A., Algenstaedt, P. & Kahn, C. R. (1996). Insulin receptor substrate 1 binds two novel splice variants of the regulatory subunit of phosphatidylinositol 3-kinase in muscle and brain. *Mol Cell Biol,* **16,** 2195-203.
52. Inukai, K., Anai, M., Van Breda, E., Hosaka, T., Katagiri, H., Funaki, M., Fukushima, Y., Ogihara, T., Yazaki, Y., Kikuchi, *et al.* (1996). A novel 55-kda regulatory subunit for phosphatidylinositol 3-kinase structurally similar

to p55pik is generated by alternative splicing of the p85alpha gene. *J Biol Chem,* **271,** 5317-20.
53. Thorpe, L. M., Yuzugullu, H. & Zhao, J. J. (2015). Pi3k in cancer: Divergent roles of isoforms, modes of activation and therapeutic targeting. *Nat Rev Cancer,* **15,** 7-24.
54. Yu, J., Wjasow, C. & Backer, J. M. (1998). Regulation of the p85/p110alpha phosphatidylinositol 3'-kinase. Distinct roles for the n-terminal and c-terminal sh2 domains. *J Biol Chem,* **273,** 30199-203.
55. Dhand, R., Hara, K., Hiles, I., Bax, B., Gout, I., Panayotou, G., Fry, M. J., Yonezawa, K., Kasuga, M. & Waterfield, M. D. (1994). Pi 3-kinase: Structural and functional analysis of intersubunit interactions. *EMBO J,* **13,** 511-21.
56. Burke, J. E. & Williams, R. L. (2015). Synergy in activating class i pi3ks. *Trends Biochem Sci,* **40,** 88-100.
57. Kurig, B., Shymanets, A., Bohnacker, T., Prajwal, Brock, C., Ahmadian, M. R., Schaefer, M., Gohla, A., Harteneck, C., Wymann, M. P.*, et al.* (2009). Ras is an indispensable coregulator of the class ib phosphoinositide 3-kinase p87/p110gamma. *Proc Natl Acad Sci U S A,* **106,** 20312-7.
58. Schmid, M. C., Avraamides, C. J., Dippold, H. C., Franco, I., Foubert, P., Ellies, L. G., Acevedo, L. M., Manglicmot, J. R., Song, X., Wrasidlo, W.*, et al.* (2011). Receptor tyrosine kinases and tlr/il1rs unexpectedly activate myeloid cell pi3kγ, a single convergent point promoting tumor inflammation and progression. *Cancer Cell,* **19,** 715-27.
59. Virbasius, J. V., Guilherme, A. & Czech, M. P. (1996). Mouse p170 is a novel phosphatidylinositol 3-kinase containing a c2 domain. *J Biol Chem,* **271,** 13304-7.
60. Braccini, L., Ciraolo, E., Campa, C. C., Perino, A., Longo, D. L., Tibolla, G., Pregnolato, M., Cao, Y., Tassone, B., Damilano, F.*, et al.* (2015). Pi3k-c2γ is a rab5 effector selectively controlling endosomal akt2 activation downstream of insulin signalling. *Nat Commun,* **6,** 7400.
61. Ono, F., Nakagawa, T., Saito, S., Owada, Y., Sakagami, H., Goto, K., Suzuki, M., Matsuno, S. & Kondo, H. (1998). A novel class ii phosphoinositide 3-kinase predominantly expressed in the liver and its enhanced expression during liver regeneration. *J Biol Chem,* **273,** 7731-6.
62. Marat, A. L. & Haucke, V. (2016). Phosphatidylinositol 3-phosphates-at the interface between cell signalling and membrane traffic. *EMBO J,* **35,** 561-79.
63. Franco, I., Gulluni, F., Campa, C. C., Costa, C., Margaria, J. P., Ciraolo, E., Martini, M., Monteyne, D., De Luca, E., Germena, G.*, et al.* (2014). Pi3k class ii α controls spatially restricted endosomal ptdins3p and rab11 activation to promote primary cilium function. *Dev Cell,* **28,** 647-58.
64. Pirola, L., Zvelebil, M. J., Bulgarelli-Leva, G., Van Obberghen, E., Waterfield, M. D. & Wymann, M. P. (2001). Activation loop sequences confer substrate specificity to phosphoinositide 3-kinase alpha (pi3kalpha). Functions of lipid kinase-deficient pi3kalpha in signaling. *J Biol Chem,* **276,** 21544-54.
65. Lo, W. T., Zhang, Y., Vadas, O., Roske, Y., Gulluni, F., De Santis, M. C., Zagar, A. V., Stephanowitz, H., Hirsch, E., Liu, F.*, et al.* (2022). Structural basis of phosphatidylinositol 3-kinase c2α function. *Nat Struct Mol Biol,* **29,** 218-228.
66. Bilanges, B., Posor, Y. & Vanhaesebroeck, B. (2019). Pi3k isoforms in cell signalling and vesicle trafficking. *Nat Rev Mol Cell Biol,* **20,** 515-534.
67. Backer, J. M. (2016). The intricate regulation and complex functions of the class iii phosphoinositide 3-kinase vps34. *Biochem J,* **473,** 2251-71.
68. Devereaux, K., Dall'Armi, C., Alcazar-Roman, A., Ogasawara, Y., Zhou, X., Wang, F., Yamamoto, A., De Camilli, P. & Di Paolo, G. (2013). Regulation of mammalian autophagy by class ii and iii pi 3-kinases through pi3p synthesis. *PLoS One,* **8,** e76405.

69. Kutateladze, T. G. (2010). Translation of the phosphoinositide code by pi effectors. *Nat Chem Biol,* **6,** 507-13.
70. Matsunaga, K., Saitoh, T., Tabata, K., Omori, H., Satoh, T., Kurotori, N., Maejima, I., Shirahama-Noda, K., Ichimura, T., Isobe, T.*, et al.* (2009). Two beclin 1-binding proteins, atg14l and rubicon, reciprocally regulate autophagy at different stages. *Nat Cell Biol,* **11,** 385-96.
71. Zhong, Y., Wang, Q. J., Li, X., Yan, Y., Backer, J. M., Chait, B. T., Heintz, N. & Yue, Z. (2009). Distinct regulation of autophagic activity by atg14l and rubicon associated with beclin 1-phosphatidylinositol-3-kinase complex. *Nat Cell Biol,* **11,** 468-76.
72. Toker, A. & Marmiroli, S. (2014). Signaling specificity in the akt pathway in biology and disease. *Adv Biol Regul,* **55,** 28-38.
73. Cho, H., Thorvaldsen, J. L., Chu, Q., Feng, F. & Birnbaum, M. J. (2001). Akt1/pkbalpha is required for normal growth but dispensable for maintenance of glucose homeostasis in mice. *J Biol Chem,* **276,** 38349-52.
74. Garofalo, R. S., Orena, S. J., Rafidi, K., Torchia, A. J., Stock, J. L., Hildebrandt, A. L., Coskran, T., Black, S. C., Brees, D. J., Wicks, J. R.*, et al.* (2003). Severe diabetes, age-dependent loss of adipose tissue, and mild growth deficiency in mice lacking akt2/pkb beta. *J Clin Invest,* **112,** 197-208.
75. Dummler, B., Tschopp, O., Hynx, D., Yang, Z. Z., Dirnhofer, S. & Hemmings, B. A. (2006). Life with a single isoform of akt: Mice lacking akt2 and akt3 are viable but display impaired glucose homeostasis and growth deficiencies. *Mol Cell Biol,* **26,** 8042-51.
76. Tschopp, O., Yang, Z. Z., Brodbeck, D., Dummler, B. A., Hemmings-Mieszczak, M., Watanabe, T., Michaelis, T., Frahm, J. & Hemmings, B. A. (2005). Essential role of protein kinase b gamma (pkb gamma/akt3) in postnatal brain development but not in glucose homeostasis. *Development,* **132,** 2943-54.
77. Calleja, V., Laguerre, M. & Larijani, B. (2012). Role of the c-terminal regulatory domain in the allosteric inhibition of pkb/akt. *Adv Biol Regul,* **52,** 46-57.
78. Calleja, V., Laguerre, M., Parker, P. J. & Larijani, B. (2009). Role of a novel ph-kinase domain interface in pkb/akt regulation: Structural mechanism for allosteric inhibition. *PLoS Biol,* **7,** e17.
79. Mahadevan, D., Powis, G., Mash, E. A., George, B., Gokhale, V. M., Zhang, S., Shakalya, K., Du-Cuny, L., Berggren, M., Ali, M. A.*, et al.* (2008). Discovery of a novel class of akt pleckstrin homology domain inhibitors. *Mol Cancer Ther,* **7,** 2621-32.
80. Franke, T. F., Kaplan, D. R., Cantley, L. C. & Toker, A. (1997). Direct regulation of the akt proto-oncogene product by phosphatidylinositol-3,4-bisphosphate. *Science,* **275,** 665-8.
81. Frech, M., Andjelkovic, M., Ingley, E., Reddy, K. K., Falck, J. R. & Hemmings, B. A. (1997). High affinity binding of inositol phosphates and phosphoinositides to the pleckstrin homology domain of rac/protein kinase b and their influence on kinase activity. *J Biol Chem,* **272,** 8474-81.
82. Klippel, A., Kavanaugh, W. M., Pot, D. & Williams, L. T. (1997). A specific product of phosphatidylinositol 3-kinase directly activates the protein kinase akt through its pleckstrin homology domain. *Mol Cell Biol,* **17,** 338-44.
83. Alessi, D. R., Andjelkovic, M., Caudwell, B., Cron, P., Morrice, N., Cohen, P. & Hemmings, B. A. (1996). Mechanism of activation of protein kinase b by insulin and igf-1. *EMBO J,* **15,** 6541-51.
84. Sarbassov, D. D., Guertin, D. A., Ali, S. M. & Sabatini, D. M. (2005). Phosphorylation and regulation of akt/pkb by the rictor-mtor complex. *Science,* **307,** 1098-101.
85. Yang, J., Cron, P., Good, V. M., Thompson, V., Hemmings, B. A. & Barford, D. (2002). Crystal structure of an activated akt/protein kinase b ternary complex with gsk3-peptide and amp-pnp. *Nat Struct Biol,* **9,** 940-4.

86. Andjelković, M., Jakubowicz, T., Cron, P., Ming, X. F., Han, J. W. & Hemmings, B. A. (1996). Activation and phosphorylation of a pleckstrin homology domain containing protein kinase (rac-pk/pkb) promoted by serum and protein phosphatase inhibitors. *Proc Natl Acad Sci U S A,* **93,** 5699-704.
87. Gao, T., Furnari, F. & Newton, A. C. (2005). Phlpp: A phosphatase that directly dephosphorylates akt, promotes apoptosis, and suppresses tumor growth. *Mol Cell,* **18,** 13-24.
88. Manning, B. D. & Toker, A. (2017). Akt/pkb signaling: Navigating the network. *Cell,* **169,** 381-405.
89. Cross, D. A., Alessi, D. R., Cohen, P., Andjelkovich, M. & Hemmings, B. A. (1995). Inhibition of glycogen synthase kinase-3 by insulin mediated by protein kinase b. *Nature,* **378,** 785-9.
90. Inoki, K., Li, Y., Zhu, T., Wu, J. & Guan, K. L. (2002). Tsc2 is phosphorylated and inhibited by akt and suppresses mtor signalling. *Nat Cell Biol,* **4,** 648-57.
91. Sancak, Y., Thoreen, C. C., Peterson, T. R., Lindquist, R. A., Kang, S. A., Spooner, E., Carr, S. A. & Sabatini, D. M. (2007). Pras40 is an insulin-regulated inhibitor of the mtorc1 protein kinase. *Mol Cell,* **25,** 903-15.
92. Risso, G., Blaustein, M., Pozzi, B., Mammi, P. & Srebrow, A. (2015). Akt/pkb: One kinase, many modifications. *Biochem J,* **468,** 203-14.
93. Wang, Y., Zhou, Y. & Graves, D. T. (2014). Foxo transcription factors: Their clinical significance and regulation. *Biomed Res Int,* **2014,** 925350.
94. Pandey, M. K. & DeGrado, T. R. (2016). Glycogen synthase kinase-3 (gsk-3)-targeted therapy and imaging. *Theranostics,* **6,** 571-93.
95. Dokken, B. B., Sloniger, J. A. & Henriksen, E. J. (2005). Acute selective glycogen synthase kinase-3 inhibition enhances insulin signaling in prediabetic insulin-resistant rat skeletal muscle. *Am J Physiol Endocrinol Metab,* **288,** E1188-94.
96. Yang, H., Rudge, D. G., Koos, J. D., Vaidialingam, B., Yang, H. J. & Pavletich, N. P. (2013). Mtor kinase structure, mechanism and regulation. *Nature,* **497,** 217-23.
97. Saxton, R. A. & Sabatini, D. M. (2017). Mtor signaling in growth, metabolism, and disease. *Cell,* **169,** 361-371.
98. Nojima, H., Tokunaga, C., Eguchi, S., Oshiro, N., Hidayat, S., Yoshino, K., Hara, K., Tanaka, N., Avruch, J. & Yonezawa, K. (2003). The mammalian target of rapamycin (mtor) partner, raptor, binds the mtor substrates p70 s6 kinase and 4e-bp1 through their tor signaling (tos) motif. *J Biol Chem,* **278,** 15461-4.
99. Yang, H., Jiang, X., Li, B., Yang, H. J., Miller, M., Yang, A., Dhar, A. & Pavletich, N. P. (2017). Mechanisms of mtorc1 activation by rheb and inhibition by pras40. *Nature,* **552,** 368-373.
100. Wälchli, M., Berneiser, K., Mangia, F., Imseng, S., Craigie, L. M., Stuttfeld, E., Hall, M. N. & Maier, T. (2021). Regulation of human mtor complexes by deptor. *Elife,* **10**.
101. Chen, J., Ou, Y., Luo, R., Wang, J., Wang, D., Guan, J., Li, Y., Xia, P., Chen, P. R. & Liu, Y. (2021). Sar1b senses leucine levels to regulate mtorc1 signalling. *Nature,* **596,** 281-284.
102. Wolfson, R. L., Chantranupong, L., Saxton, R. A., Shen, K., Scaria, S. M., Cantor, J. R. & Sabatini, D. M. (2016). Sestrin2 is a leucine sensor for the mtorc1 pathway. *Science,* **351,** 43-8.
103. Saxton, R. A., Knockenhauer, K. E., Wolfson, R. L., Chantranupong, L., Pacold, M. E., Wang, T., Schwartz, T. U. & Sabatini, D. M. (2016). Structural basis for leucine sensing by the sestrin2-mtorc1 pathway. *Science,* **351,** 53-8.
104. Chantranupong, L., Scaria, S. M., Saxton, R. A., Gygi, M. P., Shen, K., Wyant, G. A., Wang, T., Harper, J. W., Gygi, S. P. & Sabatini, D. M. (2016). The

castor proteins are arginine sensors for the mtorc1 pathway. *Cell,* **165,** 153-164.
105. Bar-Peled, L., Chantranupong, L., Cherniack, A. D., Chen, W. W., Ottina, K. A., Grabiner, B. C., Spear, E. D., Carter, S. L., Meyerson, M. & Sabatini, D. M. (2013). A tumor suppressor complex with gap activity for the rag gtpases that signal amino acid sufficiency to mtorc1. *Science,* **340,** 1100-6.
106. Cai, W., Wei, Y., Jarnik, M., Reich, J. & Lilly, M. A. (2016). The gator2 component wdr24 regulates torc1 activity and lysosome function. *PLoS Genet,* **12,** e1006036.
107. Jiang, C., Dai, X., He, S., Zhou, H., Fang, L., Guo, J., Liu, S., Zhang, T., Pan, W., Yu, H*., et al.* (2023). Ring domains are essential for gator2-dependent mtorc1 activation. *Mol Cell,* **83,** 74-89.e9.
108. Sekiguchi, T., Hirose, E., Nakashima, N., Ii, M. & Nishimoto, T. (2001). Novel g proteins, rag c and rag d, interact with gtp-binding proteins, rag a and rag b. *J Biol Chem,* **276,** 7246-57.
109. Fawal, M. A., Brandt, M. & Djouder, N. (2015). Mcrs1 binds and couples rheb to amino acid-dependent mtorc1 activation. *Dev Cell,* **33,** 67-81.
110. Rabanal-Ruiz, Y. & Korolchuk, V. I. (2018). Mtorc1 and nutrient homeostasis: The central role of the lysosome. *Int J Mol Sci,* **19**.
111. Sancak, Y., Bar-Peled, L., Zoncu, R., Markhard, A. L., Nada, S. & Sabatini, D. M. (2010). Ragulator-rag complex targets mtorc1 to the lysosomal surface and is necessary for its activation by amino acids. *Cell,* **141,** 290-303.
112. Yonehara, R., Nada, S., Nakai, T., Nakai, M., Kitamura, A., Ogawa, A., Nakatsumi, H., Nakayama, K. I., Li, S., Standley, D. M*., et al.* (2017). Structural basis for the assembly of the ragulator-rag gtpase complex. *Nat Commun,* **8,** 1625.
113. Rebsamen, M., Pochini, L., Stasyk, T., de Araújo, M. E., Galluccio, M., Kandasamy, R. K., Snijder, B., Fauster, A., Rudashevskaya, E. L., Bruckner, M*., et al.* (2015). Slc38a9 is a component of the lysosomal amino acid sensing machinery that controls mtorc1. *Nature,* **519,** 477-81.
114. Wang, S., Tsun, Z. Y., Wolfson, R. L., Shen, K., Wyant, G. A., Plovanich, M. E., Yuan, E. D., Jones, T. D., Chantranupong, L., Comb, W*., et al.* (2015). Metabolism. Lysosomal amino acid transporter slc38a9 signals arginine sufficiency to mtorc1. *Science,* **347,** 188-94.
115. Zoncu, R., Bar-Peled, L., Efeyan, A., Wang, S., Sancak, Y. & Sabatini, D. M. (2011). Mtorc1 senses lysosomal amino acids through an inside-out mechanism that requires the vacuolar h(+)-atpase. *Science,* **334,** 678-83.
116. Wolfson, R. L., Chantranupong, L., Wyant, G. A., Gu, X., Orozco, J. M., Shen, K., Condon, K. J., Petri, S., Kedir, J., Scaria, S. M*., et al.* (2017). Kicstor recruits gator1 to the lysosome and is necessary for nutrients to regulate mtorc1. *Nature,* **543,** 438-442.
117. Peng, M., Yin, N. & Li, M. O. (2017). Szt2 dictates gator control of mtorc1 signalling. *Nature,* **543,** 433-437.
118. Demetriades, C., Doumpas, N. & Teleman, A. A. (2014). Regulation of torc1 in response to amino acid starvation via lysosomal recruitment of tsc2. *Cell,* **156,** 786-99.
119. Chong-Kopera, H., Inoki, K., Li, Y., Zhu, T., Garcia-Gonzalo, F. R., Rosa, J. L. & Guan, K. L. (2006). Tsc1 stabilizes tsc2 by inhibiting the interaction between tsc2 and the herc1 ubiquitin ligase. *J Biol Chem,* **281,** 8313-6.
120. Inoki, K., Li, Y., Xu, T. & Guan, K. L. (2003). Rheb gtpase is a direct target of tsc2 gap activity and regulates mtor signaling. *Genes Dev,* **17,** 1829-34.
121. Zhang, Y., Gao, X., Saucedo, L. J., Ru, B., Edgar, B. A. & Pan, D. (2003). Rheb is a direct target of the tuberous sclerosis tumour suppressor proteins. *Nat Cell Biol,* **5,** 578-81.
122. Wullschleger, S., Loewith, R. & Hall, M. N. (2006). Tor signaling in growth and metabolism. *Cell,* **124,** 471-84.

123. Ben-Sahra, I. & Manning, B. D. (2017). Mtorc1 signaling and the metabolic control of cell growth. *Curr Opin Cell Biol,* **45,** 72-82.
124. Sekiyama, N., Arthanari, H., Papadopoulos, E., Rodriguez-Mias, R. A., Wagner, G. & Léger-Abraham, M. (2015). Molecular mechanism of the dual activity of 4egi-1: Dissociating eif4g from eif4e but stabilizing the binding of unphosphorylated 4e-bp1. *Proc Natl Acad Sci U S A,* **112,** E4036-45.
125. Peter, D., Igreja, C., Weber, R., Wohlbold, L., Weiler, C., Ebertsch, L., Weichenrieder, O. & Izaurralde, E. (2015). Molecular architecture of 4e-bp translational inhibitors bound to eif4e. *Mol Cell,* **57,** 1074-1087.
126. Bah, A., Vernon, R. M., Siddiqui, Z., Krzeminski, M., Muhandiram, R., Zhao, C., Sonenberg, N., Kay, L. E. & Forman-Kay, J. D. (2015). Folding of an intrinsically disordered protein by phosphorylation as a regulatory switch. *Nature,* **519,** 106-9.
127. Dawson, J. E., Bah, A., Zhang, Z., Vernon, R. M., Lin, H., Chong, P. A., Vanama, M., Sonenberg, N., Gradinaru, C. C. & Forman-Kay, J. D. (2020). Non-cooperative 4e-bp2 folding with exchange between eif4e-binding and binding-incompatible states tunes cap-dependent translation inhibition. *Nat Commun,* **11,** 3146.
128. Holz, M. K., Ballif, B. A., Gygi, S. P. & Blenis, J. (2005). Mtor and s6k1 mediate assembly of the translation preinitiation complex through dynamic protein interchange and ordered phosphorylation events. *Cell,* **123,** 569-80.
129. Guertin, D. A., Stevens, D. M., Thoreen, C. C., Burds, A. A., Kalaany, N. Y., Moffat, J., Brown, M., Fitzgerald, K. J. & Sabatini, D. M. (2006). Ablation in mice of the mtorc components raptor, rictor, or mlst8 reveals that mtorc2 is required for signaling to akt-foxo and pkcalpha, but not s6k1. *Dev Cell,* **11,** 859-71.
130. Fu, W. & Hall, M. N. (2020). Regulation of mtorc2 signaling. *Genes (Basel),* **11**.
131. Stuttfeld, E., Aylett, C. H., Imseng, S., Boehringer, D., Scaiola, A., Sauer, E., Hall, M. N., Maier, T. & Ban, N. (2018). Architecture of the human mtorc2 core complex. *Elife,* **7**.
132. Scaiola, A., Mangia, F., Imseng, S., Boehringer, D., Berneiser, K., Shimobayashi, M., Stuttfeld, E., Hall, M. N., Ban, N. & Maier, T. (2020). The 3.2-å resolution structure of human mtorc2. *Sci Adv,* **6**.
133. Hwang, Y., Kim, L. C., Song, W., Edwards, D. N., Cook, R. S. & Chen, J. (2019). Disruption of the scaffolding function of mlst8 selectively inhibits mtorc2 assembly and function and suppresses mtorc2-dependent tumor growth. *Cancer Res,* **79,** 3178-3184.
134. Kazyken, D., Lentz, S. I. & Fingar, D. C. (2021). Alkaline intracellular ph (phi) activates ampk-mtorc2 signaling to promote cell survival during growth factor limitation. *J Biol Chem,* **297,** 101100.
135. Huang, J., Dibble, C. C., Matsuzaki, M. & Manning, B. D. (2008). The tsc1-tsc2 complex is required for proper activation of mtor complex 2. *Mol Cell Biol,* **28,** 4104-15.
136. Jacinto, E., Facchinetti, V., Liu, D., Soto, N., Wei, S., Jung, S. Y., Huang, Q., Qin, J. & Su, B. (2006). Sin1/mip1 maintains rictor-mtor complex integrity and regulates akt phosphorylation and substrate specificity. *Cell,* **127,** 125-37.
137. Hagiwara, A., Cornu, M., Cybulski, N., Polak, P., Betz, C., Trapani, F., Terracciano, L., Heim, M. H., Rüegg, M. A. & Hall, M. N. (2012). Hepatic mtorc2 activates glycolysis and lipogenesis through akt, glucokinase, and srebp1c. *Cell Metab,* **15,** 725-38.
138. Tang, Y., Wallace, M., Sanchez-Gurmaches, J., Hsiao, W. Y., Li, H., Lee, P. L., Vernia, S., Metallo, C. M. & Guertin, D. A. (2016). Adipose tissue mtorc2 regulates chrebp-driven de novo lipogenesis and hepatic glucose metabolism. *Nat Commun,* **7,** 11365.

139. Tao, R., Xiong, X., Liangpunsakul, S. & Dong, X. C. (2015). Sestrin 3 protein enhances hepatic insulin sensitivity by direct activation of the mtorc2-akt signaling. *Diabetes,* **64,** 1211-23.
140. Oh, W. J., Wu, C. C., Kim, S. J., Facchinetti, V., Julien, L. A., Finlan, M., Roux, P. P., Su, B. & Jacinto, E. (2010). Mtorc2 can associate with ribosomes to promote cotranslational phosphorylation and stability of nascent akt polypeptide. *EMBO J,* **29,** 3939-51.
141. Hardie, D. G. (2014). Amp-activated protein kinase: Maintaining energy homeostasis at the cellular and whole-body levels. *Annu Rev Nutr,* **34,** 31-55.
142. Lin, S. C. & Hardie, D. G. (2018). Ampk: Sensing glucose as well as cellular energy status. *Cell Metab,* **27,** 299-313.
143. Sanders, M. J., Grondin, P. O., Hegarty, B. D., Snowden, M. A. & Carling, D. (2007). Investigating the mechanism for amp activation of the amp-activated protein kinase cascade. *Biochem J,* **403,** 139-48.
144. Collins, S. P., Reoma, J. L., Gamm, D. M. & Uhler, M. D. (2000). Lkb1, a novel serine/threonine protein kinase and potential tumour suppressor, is phosphorylated by camp-dependent protein kinase (pka) and prenylated in vivo. *Biochem J,* **345 Pt 3,** 673-80.
145. Woods, A., Johnstone, S. R., Dickerson, K., Leiper, F. C., Fryer, L. G., Neumann, D., Schlattner, U., Wallimann, T., Carlson, M. & Carling, D. (2003). Lkb1 is the upstream kinase in the amp-activated protein kinase cascade. *Curr Biol,* **13,** 2004-8.
146. Hawley, S. A., Pan, D. A., Mustard, K. J., Ross, L., Bain, J., Edelman, A. M., Frenguelli, B. G. & Hardie, D. G. (2005). Calmodulin-dependent protein kinase kinase-beta is an alternative upstream kinase for amp-activated protein kinase. *Cell Metab,* **2,** 9-19.
147. Yeh, L. A., Lee, K. H. & Kim, K. H. (1980). Regulation of rat liver acetyl-coa carboxylase. Regulation of phosphorylation and inactivation of acetyl-coa carboxylase by the adenylate energy charge. *J Biol Chem,* **255,** 2308-14.
148. Hawley, S. A., Davison, M., Woods, A., Davies, S. P., Beri, R. K., Carling, D. & Hardie, D. G. (1996). Characterization of the amp-activated protein kinase kinase from rat liver and identification of threonine 172 as the major site at which it phosphorylates amp-activated protein kinase. *J Biol Chem,* **271,** 27879-87.
149. Oakhill, J. S., Chen, Z. P., Scott, J. W., Steel, R., Castelli, L. A., Ling, N., Macaulay, S. L. & Kemp, B. E. (2010). B-subunit myristoylation is the gatekeeper for initiating metabolic stress sensing by amp-activated protein kinase (ampk). *Proc Natl Acad Sci U S A,* **107,** 19237-41.
150. Davies, S. P., Helps, N. R., Cohen, P. T. & Hardie, D. G. (1995). 5'-amp inhibits dephosphorylation, as well as promoting phosphorylation, of the amp-activated protein kinase. Studies using bacterially expressed human protein phosphatase-2c alpha and native bovine protein phosphatase-2ac. *FEBS Lett,* **377,** 421-5.
151. Xiao, B., Sanders, M. J., Underwood, E., Heath, R., Mayer, F. V., Carmena, D., Jing, C., Walker, P. A., Eccleston, J. F., Haire, L. F.*, et al.* (2011). Structure of mammalian ampk and its regulation by adp. *Nature,* **472,** 230-3.
152. Ross, F. A., Jensen, T. E. & Hardie, D. G. (2016). Differential regulation by amp and adp of ampk complexes containing different γ subunit isoforms. *Biochem J,* **473,** 189-99.
153. Gwinn, D. M., Shackelford, D. B., Egan, D. F., Mihaylova, M. M., Mery, A., Vasquez, D. S., Turk, B. E. & Shaw, R. J. (2008). Ampk phosphorylation of raptor mediates a metabolic checkpoint. *Mol Cell,* **30,** 214-26.
154. Inoki, K., Zhu, T. & Guan, K. L. (2003). Tsc2 mediates cellular energy response to control cell growth and survival. *Cell,* **115,** 577-90.

155. Engelman, J. A. (2009). Targeting pi3k signalling in cancer: Opportunities, challenges and limitations. *Nat Rev Cancer,* **9,** 550-62.
156. Gerstung, M., Jolly, C., Leshchiner, I., Dentro, S. C., Gonzalez, S., Rosebrock, D., Mitchell, T. J., Rubanova, Y., Anur, P., Yu, K.*, et al.* (2020). The evolutionary history of 2,658 cancers. *Nature,* **578,** 122-128.
157. Tsolakos, N., Durrant, T. N., Chessa, T., Suire, S. M., Oxley, D., Kulkarni, S., Downward, J., Perisic, O., Williams, R. L., Stephens, L.*, et al.* (2018). Quantitation of class ia pi3ks in mice reveals p110-free-p85s and isoform-selective subunit associations and recruitment to receptors. *Proc Natl Acad Sci U S A,* **115,** 12176-12181.
158. Gulluni, F., Martini, M., De Santis, M. C., Campa, C. C., Ghigo, A., Margaria, J. P., Ciraolo, E., Franco, I., Ala, U., Annaratone, L.*, et al.* (2017). Mitotic spindle assembly and genomic stability in breast cancer require pi3k-c2α scaffolding function. *Cancer Cell,* **32,** 444-459.e7.
159. Li, J., Yen, C., Liaw, D., Podsypanina, K., Bose, S., Wang, S. I., Puc, J., Miliaresis, C., Rodgers, L., McCombie, R.*, et al.* (1997). Pten, a putative protein tyrosine phosphatase gene mutated in human brain, breast, and prostate cancer. *Science,* **275,** 1943-7.
160. Chen, L. & Guo, D. (2017). The functions of tumor suppressor pten in innate and adaptive immunity. *Cell Mol Immunol,* **14,** 581-589.
161. Cantley, L. C. & Neel, B. G. (1999). New insights into tumor suppression: Pten suppresses tumor formation by restraining the phosphoinositide 3-kinase/akt pathway. *Proc Natl Acad Sci U S A,* **96,** 4240-5.
162. Khan, S., Kumagai, T., Vora, J., Bose, N., Sehgal, I., Koeffler, P. H. & Bose, S. (2004). Pten promoter is methylated in a proportion of invasive breast cancers. *Int J Cancer,* **112,** 407-10.
163. Garcia-Junco-Clemente, P. & Golshani, P. (2014). Pten: A master regulator of neuronal structure, function, and plasticity. *Commun Integr Biol,* **7,** e28358.
164. Matsuda, S., Ikeda, Y., Murakami, M., Nakagawa, Y., Tsuji, A. & Kitagishi, Y. (2019). Roles of pi3k/akt/gsk3 pathway involved in psychiatric illnesses. *Diseases,* **7**.
165. Kitagishi, Y., Nakanishi, A., Ogura, Y. & Matsuda, S. (2014). Dietary regulation of pi3k/akt/gsk-3β pathway in alzheimer's disease. *Alzheimers Res Ther,* **6,** 35.
166. Franke, T. F., Yang, S. I., Chan, T. O., Datta, K., Kazlauskas, A., Morrison, D. K., Kaplan, D. R. & Tsichlis, P. N. (1995). The protein kinase encoded by the akt proto-oncogene is a target of the pdgf-activated phosphatidylinositol 3-kinase. *Cell,* **81,** 727-36.
167. Carpten, J. D., Faber, A. L., Horn, C., Donoho, G. P., Briggs, S. L., Robbins, C. M., Hostetter, G., Boguslawski, S., Moses, T. Y., Savage, S.*, et al.* (2007). A transforming mutation in the pleckstrin homology domain of akt1 in cancer. *Nature,* **448,** 439-44.
168. Milburn, C. C., Deak, M., Kelly, S. M., Price, N. C., Alessi, D. R. & Van Aalten, D. M. (2003). Binding of phosphatidylinositol 3,4,5-trisphosphate to the pleckstrin homology domain of protein kinase b induces a conformational change. *Biochem J,* **375,** 531-8.
169. Faubert, B., Boily, G., Izreig, S., Griss, T., Samborska, B., Dong, Z., Dupuy, F., Chambers, C., Fuerth, B. J., Viollet, B.*, et al.* (2013). Ampk is a negative regulator of the warburg effect and suppresses tumor growth in vivo. *Cell Metab,* **17,** 113-24.
170. Kishton, R. J., Barnes, C. E., Nichols, A. G., Cohen, S., Gerriets, V. A., Siska, P. J., Macintyre, A. N., Goraksha-Hicks, P., de Cubas, A. A., Liu, T.*, et al.* (2016). Ampk is essential to balance glycolysis and mitochondrial metabolism to control t-all cell stress and survival. *Cell Metab,* **23,** 649-62.

171. Steinberg, G. R. & Carling, D. (2019). Amp-activated protein kinase: The current landscape for drug development. *Nat Rev Drug Discov,* **18,** 527-551.
172. Steinberg, G. R. & Schertzer, J. D. (2014). Ampk promotes macrophage fatty acid oxidative metabolism to mitigate inflammation: Implications for diabetes and cardiovascular disease. *Immunol Cell Biol,* **92,** 340-5.
173. Price, N. L., Gomes, A. P., Ling, A. J., Duarte, F. V., Martin-Montalvo, A., North, B. J., Agarwal, B., Ye, L., Ramadori, G., Teodoro, J. S.*, et al.* (2012). Sirt1 is required for ampk activation and the beneficial effects of resveratrol on mitochondrial function. *Cell Metab,* **15,** 675-90.
174. Janeway, C. A. (1989). Approaching the asymptote? Evolution and revolution in immunology. *Cold Spring Harb Symp Quant Biol,* **54 Pt 1,** 1-13.
175. Medzhitov, R. (2001). Toll-like receptors and innate immunity. *Nat Rev Immunol,* **1,** 135-45.
176. Akira, S., Takeda, K. & Kaisho, T. (2001). Toll-like receptors: Critical proteins linking innate and acquired immunity. *Nat Immunol,* **2,** 675-80.
177. Janeway, C. A. & Medzhitov, R. (2002). Innate immune recognition. *Annu Rev Immunol,* **20,** 197-216.
178. Netea, M. G., Balkwill, F., Chonchol, M., Cominelli, F., Donath, M. Y., Giamarellos-Bourboulis, E. J., Golenbock, D., Gresnigt, M. S., Heneka, M. T., Hoffman, H. M.*, et al.* (2017). A guiding map for inflammation. *Nat Immunol,* **18,** 826-831.
179. Yoneyama, M. & Fujita, T. (2009). Rna recognition and signal transduction by rig-i-like receptors. *Immunol Rev,* **227,** 54-65.
180. Fitzgerald, M. E., Rawling, D. C., Vela, A. & Pyle, A. M. (2014). An evolving arsenal: Viral rna detection by rig-i-like receptors. *Curr Opin Microbiol,* **20,** 76-81.
181. Fan, X. & Jin, T. (2019). Structures of rig-i-like receptors and insights into viral rna sensing. *Adv Exp Med Biol,* **1172,** 157-188.
182. Franchi, L., Eigenbrod, T., Muñoz-Planillo, R. & Nuñez, G. (2009). The inflammasome: A caspase-1-activation platform that regulates immune responses and disease pathogenesis. *Nat Immunol,* **10,** 241-7.
183. Platnich, J. M. & Muruve, D. A. (2019). Nod-like receptors and inflammasomes: A review of their canonical and non-canonical signaling pathways. *Arch Biochem Biophys,* **670,** 4-14.
184. Jin, M. S. & Lee, J. O. (2008). Structures of the toll-like receptor family and its ligand complexes. *Immunity,* **29,** 182-91.
185. Kim, H. M., Park, B. S., Kim, J. I., Kim, S. E., Lee, J., Oh, S. C., Enkhbayar, P., Matsushima, N., Lee, H., Yoo, O. J.*, et al.* (2007). Crystal structure of the tlr4-md-2 complex with bound endotoxin antagonist eritoran. *Cell,* **130,** 906-17.
186. Park, B. S., Song, D. H., Kim, H. M., Choi, B. S., Lee, H. & Lee, J. O. (2009). The structural basis of lipopolysaccharide recognition by the tlr4-md-2 complex. *Nature,* **458,** 1191-5.
187. Poltorak, A., He, X., Smirnova, I., Liu, M. Y., Van Huffel, C., Du, X., Birdwell, D., Alejos, E., Silva, M., Galanos, C.*, et al.* (1998). Defective lps signaling in c3h/hej and c57bl/10sccr mice: Mutations in tlr4 gene. *Science,* **282,** 2085-8.
188. Beutler, B. & Rietschel, E. T. (2003). Innate immune sensing and its roots: The story of endotoxin. *Nat Rev Immunol,* **3,** 169-76.
189. Wright, S. D., Tobias, P. S., Ulevitch, R. J. & Ramos, R. A. (1989). Lipopolysaccharide (lps) binding protein opsonizes lps-bearing particles for recognition by a novel receptor on macrophages. *J Exp Med,* **170,** 1231-41.
190. Wright, S. D., Ramos, R. A., Tobias, P. S., Ulevitch, R. J. & Mathison, J. C. (1990). Cd14, a receptor for complexes of lipopolysaccharide (lps) and lps binding protein. *Science,* **249,** 1431-3.

191. Shimazu, R., Akashi, S., Ogata, H., Nagai, Y., Fukudome, K., Miyake, K. & Kimoto, M. (1999). Md-2, a molecule that confers lipopolysaccharide responsiveness on toll-like receptor 4. *J Exp Med,* **189,** 1777-82.
192. Gioannini, T. L., Teghanemt, A., Zhang, D., Coussens, N. P., Dockstader, W., Ramaswamy, S. & Weiss, J. P. (2004). Isolation of an endotoxin-md-2 complex that produces toll-like receptor 4-dependent cell activation at picomolar concentrations. *Proc Natl Acad Sci U S A,* **101,** 4186-91.
193. O'Neill, L. A. & Bowie, A. G. (2007). The family of five: Tir-domain-containing adaptors in toll-like receptor signalling. *Nat Rev Immunol,* **7,** 353-64.
194. Lin, S. C., Lo, Y. C. & Wu, H. (2010). Helical assembly in the myd88-irak4-irak2 complex in tlr/il-1r signalling. *Nature,* **465,** 885-90.
195. Keating, S. E., Maloney, G. M., Moran, E. M. & Bowie, A. G. (2007). Irak-2 participates in multiple toll-like receptor signaling pathways to nfkappab via activation of traf6 ubiquitination. *J Biol Chem,* **282,** 33435-33443.
196. Kollewe, C., Mackensen, A. C., Neumann, D., Knop, J., Cao, P., Li, S., Wesche, H. & Martin, M. U. (2004). Sequential autophosphorylation steps in the interleukin-1 receptor-associated kinase-1 regulate its availability as an adapter in interleukin-1 signaling. *J Biol Chem,* **279,** 5227-36.
197. Jiang, Z., Ninomiya-Tsuji, J., Qian, Y., Matsumoto, K. & Li, X. (2002). Interleukin-1 (il-1) receptor-associated kinase-dependent il-1-induced signaling complexes phosphorylate tak1 and tab2 at the plasma membrane and activate tak1 in the cytosol. *Mol Cell Biol,* **22,** 7158-67.
198. Ordureau, A., Smith, H., Windheim, M., Peggie, M., Carrick, E., Morrice, N. & Cohen, P. (2008). The irak-catalysed activation of the e3 ligase function of pellino isoforms induces the lys63-linked polyubiquitination of irak1. *Biochem J,* **409,** 43-52.
199. Cao, Z., Xiong, J., Takeuchi, M., Kurama, T. & Goeddel, D. V. (1996). Traf6 is a signal transducer for interleukin-1. *Nature,* **383,** 443-6.
200. Deng, L., Wang, C., Spencer, E., Yang, L., Braun, A., You, J., Slaughter, C., Pickart, C. & Chen, Z. J. (2000). Activation of the ikappab kinase complex by traf6 requires a dimeric ubiquitin-conjugating enzyme complex and a unique polyubiquitin chain. *Cell,* **103,** 351-61.
201. Kanayama, A., Seth, R. B., Sun, L., Ea, C. K., Hong, M., Shaito, A., Chiu, Y. H., Deng, L. & Chen, Z. J. (2004). Tab2 and tab3 activate the nf-kappab pathway through binding to polyubiquitin chains. *Mol Cell,* **15,** 535-48.
202. Windheim, M., Stafford, M., Peggie, M. & Cohen, P. (2008). Interleukin-1 (il-1) induces the lys63-linked polyubiquitination of il-1 receptor-associated kinase 1 to facilitate nemo binding and the activation of ikappabalpha kinase. *Mol Cell Biol,* **28,** 1783-91.
203. Sato, S., Sanjo, H., Takeda, K., Ninomiya-Tsuji, J., Yamamoto, M., Kawai, T., Matsumoto, K., Takeuchi, O. & Akira, S. (2005). Essential function for the kinase tak1 in innate and adaptive immune responses. *Nat Immunol,* **6,** 1087-95.
204. Schröfelbauer, B., Polley, S., Behar, M., Ghosh, G. & Hoffmann, A. (2012). Nemo ensures signaling specificity of the pleiotropic ikkβ by directing its kinase activity toward iκbα. *Mol Cell,* **47,** 111-21.
205. Roff, M., Thompson, J., Rodriguez, M. S., Jacque, J. M., Baleux, F., Arenzana-Seisdedos, F. & Hay, R. T. (1996). Role of ikappabalpha ubiquitination in signal-induced activation of nfkappab in vivo. *J Biol Chem,* **271,** 7844-50.
206. Ghosh, S., May, M. J. & Kopp, E. B. (1998). Nf-kappa b and rel proteins: Evolutionarily conserved mediators of immune responses. *Annu Rev Immunol,* **16,** 225-60.
207. Savinova, O. V., Hoffmann, A. & Ghosh, G. (2009). The nfkb1 and nfkb2 proteins p105 and p100 function as the core of high-molecular-weight heterogeneous complexes. *Mol Cell,* **34,** 591-602.

208. Oeckinghaus, A. & Ghosh, S. (2009). The nf-kappab family of transcription factors and its regulation. *Cold Spring Harb Perspect Biol,* **1,** a000034.
209. Ghosh, G., Wang, V. Y., Huang, D. B. & Fusco, A. (2012). Nf-κb regulation: Lessons from structures. *Immunol Rev,* **246,** 36-58.
210. Oganesyan, G., Saha, S. K., Guo, B., He, J. Q., Shahangian, A., Zarnegar, B., Perry, A. & Cheng, G. (2006). Critical role of traf3 in the toll-like receptor-dependent and -independent antiviral response. *Nature,* **439,** 208-11.
211. Guo, B. & Cheng, G. (2007). Modulation of the interferon antiviral response by the tbk1/ikki adaptor protein tank. *J Biol Chem,* **282,** 11817-26.
212. Hiscott, J., Pitha, P., Genin, P., Nguyen, H., Heylbroeck, C., Mamane, Y., Algarte, M. & Lin, R. (1999). Triggering the interferon response: The role of irf-3 transcription factor. *J Interferon Cytokine Res,* **19,** 1-13.
213. Fitzgerald, K. A., McWhirter, S. M., Faia, K. L., Rowe, D. C., Latz, E., Golenbock, D. T., Coyle, A. J., Liao, S. M. & Maniatis, T. (2003). Ikkepsilon and tbk1 are essential components of the irf3 signaling pathway. *Nat Immunol,* **4,** 491-6.
214. Hemmi, H., Takeuchi, O., Sato, S., Yamamoto, M., Kaisho, T., Sanjo, H., Kawai, T., Hoshino, K., Takeda, K. & Akira, S. (2004). The roles of two ikappab kinase-related kinases in lipopolysaccharide and double stranded rna signaling and viral infection. *J Exp Med,* **199,** 1641-50.
215. Matsumoto, M. & Seya, T. (2008). Tlr3: Interferon induction by double-stranded rna including poly(i:C). *Adv Drug Deliv Rev,* **60,** 805-12.
216. Farina, G. A., York, M. R., Di Marzio, M., Collins, C. A., Meller, S., Homey, B., Rifkin, I. R., Marshak-Rothstein, A., Radstake, T. R. & Lafyatis, R. (2010). Poly(i:C) drives type i ifn- and tgfβ-mediated inflammation and dermal fibrosis simulating altered gene expression in systemic sclerosis. *J Invest Dermatol,* **130,** 2583-93.
217. Troutman, T. D., Hu, W., Fulenchek, S., Yamazaki, T., Kurosaki, T., Bazan, J. F. & Pasare, C. (2012). Role for b-cell adapter for pi3k (bcap) as a signaling adapter linking toll-like receptors (tlrs) to serine/threonine kinases pi3k/akt. *Proc Natl Acad Sci U S A,* **109,** 273-8.
218. Miao, Y., Jiang, M., Qi, L., Yang, Xiao, W. & Fang, F. (2020). Bcap regulates dendritic cell maturation through the dual-regulation of nf-κb and pi3k/akt signaling during infection. *Front Immunol,* **11,** 250.
219. Bai, D., Ueno, L. & Vogt, P. K. (2009). Akt-mediated regulation of nfkappab and the essentialness of nfkappab for the oncogenicity of pi3k and akt. *Int J Cancer,* **125,** 2863-70.
220. Hayden, M. S. & Ghosh, S. (2008). Shared principles in nf-kappab signaling. *Cell,* **132,** 344-62.
221. Hayden, M. S. & Ghosh, S. (2004). Signaling to nf-kappab. *Genes Dev,* **18,** 2195-224.
222. Siggers, T., Chang, A. B., Teixeira, A., Wong, D., Williams, K. J., Ahmed, B., Ragoussis, J., Udalova, I. A., Smale, S. T. & Bulyk, M. L. (2011). Principles of dimer-specific gene regulation revealed by a comprehensive characterization of nf-κb family DNA binding. *Nat Immunol,* **13,** 95-102.
223. Sun, S. C., Chang, J. H. & Jin, J. (2013). Regulation of nuclear factor-κb in autoimmunity. *Trends Immunol,* **34,** 282-9.
224. Chen, I. T., Hsu, P. H., Hsu, W. C., Chen, N. J. & Tseng, P. H. (2015). Polyubiquitination of transforming growth factor β-activated kinase 1 (tak1) at lysine 562 residue regulates tlr4-mediated jnk and p38 mapk activation. *Sci Rep,* **5,** 12300.
225. Zarnegar, B., Yamazaki, S., He, J. Q. & Cheng, G. (2008). Control of canonical nf-kappab activation through the nik-ikk complex pathway. *Proc Natl Acad Sci U S A,* **105,** 3503-8.

226. Shi, J. H. & Sun, S. C. (2018). Tumor necrosis factor receptor-associated factor regulation of nuclear factor κb and mitogen-activated protein kinase pathways. *Front Immunol,* **9,** 1849.
227. Liu, T., Zhang, L., Joo, D. & Sun, S. C. (2017). Nf-κb signaling in inflammation. *Signal Transduct Target Ther,* **2,** 17023-.
228. Barnabei, L., Laplantine, E., Mbongo, W., Rieux-Laucat, F. & Weil, R. (2021). Nf-κb: At the borders of autoimmunity and inflammation. *Front Immunol,* **12,** 716469.
229. Kyriakis, J. M. & Avruch, J. (2012). Mammalian mapk signal transduction pathways activated by stress and inflammation: A 10-year update. *Physiol Rev,* **92,** 689-737.
230. Huang, P., Han, J. & Hui, L. (2010). Mapk signaling in inflammation-associated cancer development. *Protein Cell,* **1,** 218-26.
231. Johnson, G. L. & Lapadat, R. (2002). Mitogen-activated protein kinase pathways mediated by erk, jnk, and p38 protein kinases. *Science,* **298,** 1911-2.
232. Li, S., Wang, L. & Dorf, M. E. (2009). Pkc phosphorylation of traf2 mediates ikkalpha/beta recruitment and k63-linked polyubiquitination. *Mol Cell,* **33,** 30-42.
233. Carpenter, S. & O'Neill, L. A. (2009). Recent insights into the structure of toll-like receptors and post-translational modifications of their associated signalling proteins. *Biochem J,* **422,** 1-10.
234. Kenny, E. F. & O'Neill, L. A. (2008). Signalling adaptors used by toll-like receptors: An update. *Cytokine,* **43,** 342-9.
235. Wang, C., Deng, L., Hong, M., Akkaraju, G. R., Inoue, J. & Chen, Z. J. (2001). Tak1 is a ubiquitin-dependent kinase of mkk and ikk. *Nature,* **412,** 346-51.
236. Xia, Z. P., Sun, L., Chen, X., Pineda, G., Jiang, X., Adhikari, A., Zeng, W. & Chen, Z. J. (2009). Direct activation of protein kinases by unanchored polyubiquitin chains. *Nature,* **461,** 114-9.
237. Yu, Y., Ge, N., Xie, M., Sun, W., Burlingame, S., Pass, A. K., Nuchtern, J. G., Zhang, D., Fu, S., Schneider, M. D.*, et al.* (2008). Phosphorylation of thr-178 and thr-184 in the tak1 t-loop is required for interleukin (il)-1-mediated optimal nfkappab and ap-1 activation as well as il-6 gene expression. *J Biol Chem,* **283,** 24497-505.
238. Charlaftis, N., Suddason, T., Wu, X., Anwar, S., Karin, M. & Gallagher, E. (2014). The mekk1 phd ubiquitinates tab1 to activate mapks in response to cytokines. *EMBO J,* **33,** 2581-96.
239. Vallabhapurapu, S., Matsuzawa, A., Zhang, W., Tseng, P. H., Keats, J. J., Wang, H., Vignali, D. A., Bergsagel, P. L. & Karin, M. (2008). Nonredundant and complementary functions of traf2 and traf3 in a ubiquitination cascade that activates nik-dependent alternative nf-kappab signaling. *Nat Immunol,* **9,** 1364-70.
240. Jin, J., Xiao, Y., Hu, H., Zou, Q., Li, Y., Gao, Y., Ge, W., Cheng, X. & Sun, S. C. (2015). Proinflammatory tlr signalling is regulated by a traf2-dependent proteolysis mechanism in macrophages. *Nat Commun,* **6,** 5930.
241. Zarnegar, B. J., Wang, Y., Mahoney, D. J., Dempsey, P. W., Cheung, H. H., He, J., Shiba, T., Yang, X., Yeh, W. C., Mak, T. W.*, et al.* (2008). Noncanonical nf-kappab activation requires coordinated assembly of a regulatory complex of the adaptors ciap1, ciap2, traf2 and traf3 and the kinase nik. *Nat Immunol,* **9,** 1371-8.
242. Cuadrado, A. & Nebreda, A. R. (2010). Mechanisms and functions of p38 mapk signalling. *Biochem J,* **429,** 403-17.
243. Raman, M., Chen, W. & Cobb, M. H. (2007). Differential regulation and properties of mapks. *Oncogene,* **26,** 3100-12.
244. Rossa, C., Ehmann, K., Liu, M., Patil, C. & Kirkwood, K. L. (2006). Mkk3/6-p38 mapk signaling is required for il-1beta and tnf-alpha-induced rankl

expression in bone marrow stromal cells. *J Interferon Cytokine Res,* **26,** 719-29.
245. Jeffrey, K. L., Camps, M., Rommel, C. & Mackay, C. R. (2007). Targeting dual-specificity phosphatases: Manipulating map kinase signalling and immune responses. *Nat Rev Drug Discov,* **6,** 391-403.
246. Scherle, P. A., Jones, E. A., Favata, M. F., Daulerio, A. J., Covington, M. B., Nurnberg, S. A., Magolda, R. L. & Trzaskos, J. M. (1998). Inhibition of map kinase kinase prevents cytokine and prostaglandin e2 production in lipopolysaccharide-stimulated monocytes. *J Immunol,* **161,** 5681-6.
247. Guha, M., O'Connell, M. A., Pawlinski, R., Hollis, A., McGovern, P., Yan, S. F., Stern, D. & Mackman, N. (2001). Lipopolysaccharide activation of the mek-erk1/2 pathway in human monocytic cells mediates tissue factor and tumor necrosis factor alpha expression by inducing elk-1 phosphorylation and egr-1 expression. *Blood,* **98,** 1429-39.
248. Sweet, M. J. & Hume, D. A. (1996). Endotoxin signal transduction in macrophages. *J Leukoc Biol,* **60,** 8-26.
249. Salmeron, A., Ahmad, T. B., Carlile, G. W., Pappin, D., Narsimhan, R. P. & Ley, S. C. (1996). Activation of mek-1 and sek-1 by tpl-2 proto-oncoprotein, a novel map kinase kinase kinase. *EMBO J,* **15,** 817-26.
250. Belich, M. P., Salmerón, A., Johnston, L. H. & Ley, S. C. (1999). Tpl-2 kinase regulates the proteolysis of the nf-kappab-inhibitory protein nf-kappab1 p105. *Nature,* **397,** 363-8.
251. Furman, D., Campisi, J., Verdin, E., Carrera-Bastos, P., Targ, S., Franceschi, C., Ferrucci, L., Gilroy, D. W., Fasano, A., Miller, G. W.*, et al.* (2019). Chronic inflammation in the etiology of disease across the life span. *Nat Med,* **25,** 1822-1832.
252. Gabay, C. & Kushner, I. (1999). Acute-phase proteins and other systemic responses to inflammation. *N Engl J Med,* **340,** 448-54.
253. Tisoncik, J. R., Korth, M. J., Simmons, C. P., Farrar, J., Martin, T. R. & Katze, M. G. (2012). Into the eye of the cytokine storm. *Microbiol Mol Biol Rev,* **76,** 16-32.
254. Mantovani, A. (2005). Cancer: Inflammation by remote control. *Nature,* **435,** 752-3.
255. Pirmohamed, M., James, S., Meakin, S., Green, C., Scott, A. K., Walley, T. J., Farrar, K., Park, B. K. & Breckenridge, A. M. (2004). Adverse drug reactions as cause of admission to hospital: Prospective analysis of 18 820 patients. *BMJ,* **329,** 15-9.
256. Davis, A. & Robson, J. (2016). The dangers of nsaids: Look both ways. *Br J Gen Pract,* **66,** 172-3.
257. Barrett, K., Saxena, S. & Pollok, R. (2018). Using corticosteroids appropriately in inflammatory bowel disease: A guide for primary care. *Br J Gen Pract,* **68,** 497-498.
258. Bruscoli, S., Febo, M., Riccardi, C. & Migliorati, G. (2021). Glucocorticoid therapy in inflammatory bowel disease: Mechanisms and clinical practice. *Front Immunol,* **12,** 691480.
259. Riccardi, C., Bruscoli, S. & Migliorati, G. (2002). Molecular mechanisms of immunomodulatory activity of glucocorticoids. *Pharmacol Res,* **45,** 361-8.
260. Cancer research uk (2023). breast cancer statistics | cancer research uk. *Accessed[February][2023].*
261. DeSantis, C. E., Ma, J., Gaudet, M. M., Newman, L. A., Miller, K. D., Goding Sauer, A., Jemal, A. & Siegel, R. L. (2019). Breast cancer statistics, 2019. *CA Cancer J Clin,* **69,** 438-451.
262. Li, Y., Yang, D., Yin, X., Zhang, X., Huang, J., Wu, Y., Wang, M., Yi, Z., Li, H. & Ren, G. (2020). Clinicopathological characteristics and breast cancer-specific survival of patients with single hormone receptor-positive breast cancer. *JAMA Netw Open,* **3,** e1918160.

263. Oh, D. Y. & Bang, Y. J. (2020). Her2-targeted therapies - a role beyond breast cancer. *Nat Rev Clin Oncol,* **17,** 33-48.
264. Shan, N. L., Shin, Y., Yang, G., Furmanski, P. & Suh, N. (2021). Breast cancer stem cells: A review of their characteristics and the agents that affect them. *Mol Carcinog,* **60,** 73-100.
265. Perou, C. M., Sørlie, T., Eisen, M. B., van de Rijn, M., Jeffrey, S. S., Rees, C. A., Pollack, J. R., Ross, D. T., Johnsen, H., Akslen, L. A.*, et al.* (2000). Molecular portraits of human breast tumours. *Nature,* **406,** 747-52.
266. Sørlie, T., Perou, C. M., Tibshirani, R., Aas, T., Geisler, S., Johnsen, H., Hastie, T., Eisen, M. B., van de Rijn, M., Jeffrey, S. S.*, et al.* (2001). Gene expression patterns of breast carcinomas distinguish tumor subclasses with clinical implications. *Proc Natl Acad Sci U S A,* **98,** 10869-74.
267. Sorlie, T., Tibshirani, R., Parker, J., Hastie, T., Marron, J. S., Nobel, A., Deng, S., Johnsen, H., Pesich, R., Geisler, S.*, et al.* (2003). Repeated observation of breast tumor subtypes in independent gene expression data sets. *Proc Natl Acad Sci U S A,* **100,** 8418-23.
268. Zhang, X. (2023). Molecular classification of breast cancer: Relevance and challenges. *Arch Pathol Lab Med,* **147,** 46-51.
269. Howlader, N., Altekruse, S. F., Li, C. I., Chen, V. W., Clarke, C. A., Ries, L. A. & Cronin, K. A. (2014). Us incidence of breast cancer subtypes defined by joint hormone receptor and her2 status. *J Natl Cancer Inst,* **106**.
270. Pérez-Fidalgo, J. A., Criscitiello, C., Carrasco, E., Regan, M. M., Di Leo, A., Ribi, K., Adam, V. & Bedard, P. L. (2022). A phase iii trial of alpelisib + trastuzumab ± fulvestrant versus trastuzumab + chemotherapy in her2+. *Future Oncol,* **18,** 2339-2349.
271. Hartman, Z. C., Yang, X. Y., Glass, O., Lei, G., Osada, T., Dave, S. S., Morse, M. A., Clay, T. M. & Lyerly, H. K. (2011). Her2 overexpression elicits a proinflammatory il-6 autocrine signaling loop that is critical for tumorigenesis. *Cancer Res,* **71,** 4380-91.
272. Dent, R., Trudeau, M., Pritchard, K. I., Hanna, W. M., Kahn, H. K., Sawka, C. A., Lickley, L. A., Rawlinson, E., Sun, P. & Narod, S. A. (2007). Triple-negative breast cancer: Clinical features and patterns of recurrence. *Clin Cancer Res,* **13,** 4429-34.
273. Lin, N. U., Claus, E., Sohl, J., Razzak, A. R., Arnaout, A. & Winer, E. P. (2008). Sites of distant recurrence and clinical outcomes in patients with metastatic triple-negative breast cancer: High incidence of central nervous system metastases. *Cancer,* **113,** 2638-45.
274. (EBCTCG), E. B. C. T. C. G. (2005). Effects of chemotherapy and hormonal therapy for early breast cancer on recurrence and 15-year survival: An overview of the randomised trials. *Lancet,* **365,** 1687-717.
275. Quail, D. F. & Joyce, J. A. (2013). Microenvironmental regulation of tumor progression and metastasis. *Nat Med,* **19,** 1423-37.
276. Polyak, K. & Weinberg, R. A. (2009). Transitions between epithelial and mesenchymal states: Acquisition of malignant and stem cell traits. *Nat Rev Cancer,* **9,** 265-73.
277. Vella, V., De Francesco, E. M., Lappano, R., Muoio, M. G., Manzella, L., Maggiolini, M. & Belfiore, A. (2020). Microenvironmental determinants of breast cancer metastasis: Focus on the crucial interplay between estrogen and insulin/insulin-like growth factor signaling. *Front Cell Dev Biol,* **8,** 608412.
278. Hubbard, S. R. & Miller, W. T. (2007). Receptor tyrosine kinases: Mechanisms of activation and signaling. *Curr Opin Cell Biol,* **19,** 117-23.
279. Montor, W. R., Salas, A. R. O. S. & Melo, F. H. M. (2018). Receptor tyrosine kinases and downstream pathways as druggable targets for cancer treatment: The current arsenal of inhibitors. *Mol Cancer,* **17,** 55.

280. Yarden, Y. & Sliwkowski, M. X. (2001). Untangling the erbb signalling network. *Nat Rev Mol Cell Biol,* **2,** 127-37.
281. Witsch, E., Sela, M. & Yarden, Y. (2010). Roles for growth factors in cancer progression. *Physiology (Bethesda),* **25,** 85-101.
282. Elliott, R. L. & Blobe, G. C. (2005). Role of transforming growth factor beta in human cancer. *J Clin Oncol,* **23,** 2078-93.
283. Demoulin, J. B. & Essaghir, A. (2014). Pdgf receptor signaling networks in normal and cancer cells. *Cytokine Growth Factor Rev,* **25,** 273-83.
284. Dieci, M. V., Arnedos, M., Andre, F. & Soria, J. C. (2013). Fibroblast growth factor receptor inhibitors as a cancer treatment: From a biologic rationale to medical perspectives. *Cancer Discov,* **3,** 264-79.
285. Katzenellenbogen, J. A., Mayne, C. G., Katzenellenbogen, B. S., Greene, G. L. & Chandarlapaty, S. (2018). Structural underpinnings of oestrogen receptor mutations in endocrine therapy resistance. *Nat Rev Cancer,* **18,** 377-388.
286. Neve, R. M., Chin, K., Fridlyand, J., Yeh, J., Baehner, F. L., Fevr, T., Clark, L., Bayani, N., Coppe, J. P., Tong, F.*, et al.* (2006). A collection of breast cancer cell lines for the study of functionally distinct cancer subtypes. *Cancer Cell,* **10,** 515-27.
287. Carey, L. A., Dees, E. C., Sawyer, L., Gatti, L., Moore, D. T., Collichio, F., Ollila, D. W., Sartor, C. I., Graham, M. L. & Perou, C. M. (2007). The triple negative paradox: Primary tumor chemosensitivity of breast cancer subtypes. *Clin Cancer Res,* **13,** 2329-34.
288. Mitchell, R. A., Luwor, R. B. & Burgess, A. W. (2018). Epidermal growth factor receptor: Structure-function informing the design of anticancer therapeutics. *Exp Cell Res,* **371,** 1-19.
289. Huang, Y., Ognjenovic, J., Karandur, D., Miller, K., Merk, A., Subramaniam, S. & Kuriyan, J. (2021). A molecular mechanism for the generation of ligand-dependent differential outputs by the epidermal growth factor receptor. *Elife,* **10**.
290. Hubbard, S. R. & Till, J. H. (2000). Protein tyrosine kinase structure and function. *Annu Rev Biochem,* **69,** 373-98.
291. Carpenter, G. (1987). Receptors for epidermal growth factor and other polypeptide mitogens. *Annu Rev Biochem,* **56,** 881-914.
292. Roskoski, R. (2014). Erbb/her protein-tyrosine kinases: Structures and small molecule inhibitors. *Pharmacol Res,* **87,** 42-59.
293. Kim, H. H., Vijapurkar, U., Hellyer, N. J., Bravo, D. & Koland, J. G. (1998). Signal transduction by epidermal growth factor and heregulin via the kinase-deficient erbb3 protein. *Biochem J,* **334 (Pt 1),** 189-95.
294. Carrera, A. C., Alexandrov, K. & Roberts, T. M. (1993). The conserved lysine of the catalytic domain of protein kinases is actively involved in the phosphotransfer reaction and not required for anchoring atp. *Proc Natl Acad Sci U S A,* **90,** 442-6.
295. Wilson, K. J., Gilmore, J. L., Foley, J., Lemmon, M. A. & Riese, D. J. (2009). Functional selectivity of egf family peptide growth factors: Implications for cancer. *Pharmacol Ther,* **122,** 1-8.
296. Burgess, A. W., Cho, H. S., Eigenbrot, C., Ferguson, K. M., Garrett, T. P., Leahy, D. J., Lemmon, M. A., Sliwkowski, M. X., Ward, C. W. & Yokoyama, S. (2003). An open-and-shut case? Recent insights into the activation of egf/erbb receptors. *Mol Cell,* **12,** 541-52.
297. Moasser, M. M. (2007). The oncogene her2: Its signaling and transforming functions and its role in human cancer pathogenesis. *Oncogene,* **26,** 6469-87.
298. Zaczek, A., Brandt, B. & Bielawski, K. P. (2005). The diverse signaling network of egfr, her2, her3 and her4 tyrosine kinase receptors and the consequences for therapeutic approaches. *Histol Histopathol,* **20,** 1005-15.

299. Batzer, A. G., Rotin, D., Ureña, J. M., Skolnik, E. Y. & Schlessinger, J. (1994). Hierarchy of binding sites for grb2 and shc on the epidermal growth factor receptor. *Mol Cell Biol,* **14,** 5192-201.
300. Lowenstein, E. J., Daly, R. J., Batzer, A. G., Li, W., Margolis, B., Lammers, R., Ullrich, A., Skolnik, E. Y., Bar-Sagi, D. & Schlessinger, J. (1992). The sh2 and sh3 domain-containing protein grb2 links receptor tyrosine kinases to ras signaling. *Cell,* **70,** 431-42.
301. Katz, M., Amit, I. & Yarden, Y. (2007). Regulation of mapks by growth factors and receptor tyrosine kinases. *Biochim Biophys Acta,* **1773,** 1161-76.
302. Way, T. D. & Lin, J. K. (2005). Role of her2/her3 co-receptor in breast carcinogenesis. *Future Oncol,* **1,** 841-9.
303. Schulze, W. X., Deng, L. & Mann, M. (2005). Phosphotyrosine interactome of the erbb-receptor kinase family. *Mol Syst Biol,* **1,** 2005.0008.
304. Lamothe, B., Yamada, M., Schaeper, U., Birchmeier, W., Lax, I. & Schlessinger, J. (2004). The docking protein gab1 is an essential component of an indirect mechanism for fibroblast growth factor stimulation of the phosphatidylinositol 3-kinase/akt antiapoptotic pathway. *Mol Cell Biol,* **24,** 5657-66.
305. Mattoon, D. R., Lamothe, B., Lax, I. & Schlessinger, J. (2004). The docking protein gab1 is the primary mediator of egf-stimulated activation of the pi-3k/akt cell survival pathway. *BMC Biol,* **2,** 24.
306. Wheeler, M. & Domin, J. (2001). Recruitment of the class ii phosphoinositide 3-kinase c2beta to the epidermal growth factor receptor: Role of grb2. *Mol Cell Biol,* **21,** 6660-7.
307. Han, J. S. & Crowe, D. L. (2010). Jun amino-terminal kinase 1 activation promotes cell survival in erbb2-positive breast cancer. *Anticancer Res,* **30,** 3407-12.
308. Davis, R. J. (2000). Signal transduction by the jnk group of map kinases. *Cell,* **103,** 239-52.
309. Iliopoulos, D., Hirsch, H. A. & Struhl, K. (2009). An epigenetic switch involving nf-kappab, lin28, let-7 microrna, and il6 links inflammation to cell transformation. *Cell,* **139,** 693-706.
310. Ancrile, B., Lim, K. H. & Counter, C. M. (2007). Oncogenic ras-induced secretion of il6 is required for tumorigenesis. *Genes Dev,* **21,** 1714-9.
311. Nahta, R., Yuan, L. X., Zhang, B., Kobayashi, R. & Esteva, F. J. (2005). Insulin-like growth factor-i receptor/human epidermal growth factor receptor 2 heterodimerization contributes to trastuzumab resistance of breast cancer cells. *Cancer Res,* **65,** 11118-28.
312. Valentinis, B. & Baserga, R. (2001). Igf-i receptor signalling in transformation and differentiation. *Mol Pathol,* **54,** 133-7.
313. Daubriac, J., Han, S., Grahovac, J., Smith, E., Hosein, A., Buchanan, M., Basik, M. & Boucher, Y. (2018). The crosstalk between breast carcinoma-associated fibroblasts and cancer cells promotes rhoa-dependent invasion. *Oncotarget,* **9,** 10375-10387.
314. Zhang, X. H., Jin, X., Malladi, S., Zou, Y., Wen, Y. H., Brogi, E., Smid, M., Foekens, J. A. & Massagué, J. (2013). Selection of bone metastasis seeds by mesenchymal signals in the primary tumor stroma. *Cell,* **154,** 1060-1073.
315. Hiraga, T., Myoui, A., Hashimoto, N., Sasaki, A., Hata, K., Morita, Y., Yoshikawa, H., Rosen, C. J., Mundy, G. R. & Yoneda, T. (2012). Bone-derived igf mediates crosstalk between bone and breast cancer cells in bony metastases. *Cancer Res,* **72,** 4238-49.
316. De Francesco, E. M., Sims, A. H., Maggiolini, M., Sotgia, F., Lisanti, M. P. & Clarke, R. B. (2017). Gper mediates the angiocrine actions induced by igf1 through the hif-1α/vegf pathway in the breast tumor microenvironment. *Breast Cancer Res,* **19,** 129.

317. Molina, L., Figueroa, C. D., Bhoola, K. D. & Ehrenfeld, P. (2017). Gper-1/gpr30 a novel estrogen receptor sited in the cell membrane: Therapeutic coupling to breast cancer. *Expert Opin Ther Targets,* **21,** 755-766.
318. Lappano, R., Pisano, A. & Maggiolini, M. (2014). Gper function in breast cancer: An overview. *Front Endocrinol (Lausanne),* **5,** 66.
319. Hsu, L. H., Chu, N. M., Lin, Y. F. & Kao, S. H. (2019). G-protein coupled estrogen receptor in breast cancer. *Int J Mol Sci,* **20**.
320. De Francesco, E. M., Maggiolini, M. & Musti, A. M. (2018). Crosstalk between notch, hif-1α and gper in breast cancer emt. *Int J Mol Sci,* **19**.
321. De Marco, P., Lappano, R., De Francesco, E. M., Cirillo, F., Pupo, M., Avino, S., Vivacqua, A., Abonante, S., Picard, D. & Maggiolini, M. (2016). Gper signalling in both cancer-associated fibroblasts and breast cancer cells mediates a feedforward il1β/il1r1 response. *Sci Rep,* **6,** 24354.
322. Barton, M., Filardo, E. J., Lolait, S. J., Thomas, P., Maggiolini, M. & Prossnitz, E. R. (2018). Twenty years of the g protein-coupled estrogen receptor gper: Historical and personal perspectives. *J Steroid Biochem Mol Biol,* **176,** 4-15.
323. Schweighofer, B., Schultes, J., Pomyje, J. & Hofer, E. (2007). Signals and genes induced by angiogenic growth factors in comparison to inflammatory cytokines in endothelial cells. *Clin Hemorheol Microcirc,* **37,** 57-62.
324. Simons, M., Gordon, E. & Claesson-Welsh, L. (2016). Mechanisms and regulation of endothelial vegf receptor signalling. *Nat Rev Mol Cell Biol,* **17,** 611-25.
325. Schoeffner, D. J., Matheny, S. L., Akahane, T., Factor, V., Berry, A., Merlino, G. & Thorgeirsson, U. P. (2005). Vegf contributes to mammary tumor growth in transgenic mice through paracrine and autocrine mechanisms. *Lab Invest,* **85,** 608-23.
326. Wu, Y., Hooper, A. T., Zhong, Z., Witte, L., Bohlen, P., Rafii, S. & Hicklin, D. J. (2006). The vascular endothelial growth factor receptor (vegfr-1) supports growth and survival of human breast carcinoma. *Int J Cancer,* **119,** 1519-29.
327. Nakopoulou, L., Stefanaki, K., Panayotopoulou, E., Giannopoulou, I., Athanassiadou, P., Gakiopoulou-Givalou, H. & Louvrou, A. (2002). Expression of the vascular endothelial growth factor receptor-2/flk-1 in breast carcinomas: Correlation with proliferation. *Hum Pathol,* **33,** 863-70.
328. Weigand, M., Hantel, P., Kreienberg, R. & Waltenberger, J. (2005). Autocrine vascular endothelial growth factor signalling in breast cancer. Evidence from cell lines and primary breast cancer cultures in vitro. *Angiogenesis,* **8,** 197-204.
329. Santolla, M. F. & Maggiolini, M. (2020). The fgf/fgfr system in breast cancer: Oncogenic features and therapeutic perspectives. *Cancers (Basel),* **12**.
330. Krook, M. A., Reeser, J. W., Ernst, G., Barker, H., Wilberding, M., Li, G., Chen, H. Z. & Roychowdhury, S. (2021). Fibroblast growth factor receptors in cancer: Genetic alterations, diagnostics, therapeutic targets and mechanisms of resistance. *Br J Cancer,* **124,** 880-892.
331. Kelleher, F. C., O'Sullivan, H., Smyth, E., McDermott, R. & Viterbo, A. (2013). Fibroblast growth factor receptors, developmental corruption and malignant disease. *Carcinogenesis,* **34,** 2198-205.
332. Chen, L., Zhang, Y., Yin, L., Cai, B., Huang, P., Li, X. & Liang, G. (2021). Fibroblast growth factor receptor fusions in cancer: Opportunities and challenges. *J Exp Clin Cancer Res,* **40,** 345.
333. Kazlauskas, A. (2017). Pdgfs and their receptors. *Gene,* **614,** 1-7.
334. Carvalho, I., Milanezi, F., Martins, A., Reis, R. M. & Schmitt, F. (2005). Overexpression of platelet-derived growth factor receptor alpha in breast cancer is associated with tumour progression. *Breast Cancer Res,* **7,** R788-95.

335. Vander Ark, A., Cao, J. & Li, X. (2018). Tgf-β receptors: In and beyond tgf-β signaling. *Cell Signal,* **52,** 112-120.
336. Nickel, J., Ten Dijke, P. & Mueller, T. D. (2018). Tgf-β family co-receptor function and signaling. *Acta Biochim Biophys Sin (Shanghai),* **50,** 12-36.
337. Lee, M. K., Pardoux, C., Hall, M. C., Lee, P. S., Warburton, D., Qing, J., Smith, S. M. & Derynck, R. (2007). Tgf-beta activates erk map kinase signalling through direct phosphorylation of shca. *EMBO J,* **26,** 3957-67.
338. Frey, R. S. & Mulder, K. M. (1997). Involvement of extracellular signal-regulated kinase 2 and stress-activated protein kinase/jun n-terminal kinase activation by transforming growth factor beta in the negative growth control of breast cancer cells. *Cancer Res,* **57,** 628-33.
339. Yu, L., Hébert, M. C. & Zhang, Y. E. (2002). Tgf-beta receptor-activated p38 map kinase mediates smad-independent tgf-beta responses. *EMBO J,* **21,** 3749-59.
340. Yi, J. Y., Shin, I. & Arteaga, C. L. (2005). Type i transforming growth factor beta receptor binds to and activates phosphatidylinositol 3-kinase. *J Biol Chem,* **280,** 10870-6.
341. Burguin, A., Diorio, C. & Durocher, F. (2021). Breast cancer treatments: Updates and new challenges. *J Pers Med,* **11**.
342. McGale, P., Taylor, C., Correa, C., Cutter, D., Duane, F., Ewertz, M., Gray, R., Mannu, G., Peto, R., Whelan, T.*, et al.* (2014). Effect of radiotherapy after mastectomy and axillary surgery on 10-year recurrence and 20-year breast cancer mortality: Meta-analysis of individual patient data for 8135 women in 22 randomised trials. *Lancet,* **383,** 2127-35.
343. Cheng, Y. J., Nie, X. Y., Ji, C. C., Lin, X. X., Liu, L. J., Chen, X. M., Yao, H. & Wu, S. H. (2017). Long-term cardiovascular risk after radiotherapy in women with breast cancer. *J Am Heart Assoc,* **6**.
344. Tao, J. J., Visvanathan, K. & Wolff, A. C. (2015). Long term side effects of adjuvant chemotherapy in patients with early breast cancer. *Breast,* **24 Suppl 2,** S149-53.
345. Ross, J. S., Slodkowska, E. A., Symmans, W. F., Pusztai, L., Ravdin, P. M. & Hortobagyi, G. N. (2009). The her-2 receptor and breast cancer: Ten years of targeted anti-her-2 therapy and personalized medicine. *Oncologist,* **14,** 320-68.
346. Sperinde, J., Jin, X., Banerjee, J., Penuel, E., Saha, A., Diedrich, G., Huang, W., Leitzel, K., Weidler, J., Ali, S. M.*, et al.* (2010). Quantitation of p95her2 in paraffin sections by using a p95-specific antibody and correlation with outcome in a cohort of trastuzumab-treated breast cancer patients. *Clin Cancer Res,* **16,** 4226-35.
347. Cardoso, F., Paluch-Shimon, S., Senkus, E., Curigliano, G., Aapro, M. S., André, F., Barrios, C. H., Bergh, J., Bhattacharyya, G. S., Biganzoli, L.*, et al.* (2020). 5th eso-esmo international consensus guidelines for advanced breast cancer (abc 5). *Ann Oncol,* **31,** 1623-1649.
348. Faratian, D., Goltsov, A., Lebedeva, G., Sorokin, A., Moodie, S., Mullen, P., Kay, C., Um, I. H., Langdon, S., Goryanin, I.*, et al.* (2009). Systems biology reveals new strategies for personalizing cancer medicine and confirms the role of pten in resistance to trastuzumab. *Cancer Res,* **69,** 6713-20.
349. Chumsri, S., Sperinde, J., Liu, H., Gligorov, J., Spano, J. P., Antoine, M., Moreno Aspitia, A., Tan, W., Winslow, J., Petropoulos, C. J.*, et al.* (2018). High p95her2/her2 ratio associated with poor outcome in trastuzumab-treated her2-positive metastatic breast cancer ncctg n0337 and ncctg 98-32-52 (alliance). *Clin Cancer Res,* **24,** 3053-3058.
350. Jain, S., Shah, A. N., Santa-Maria, C. A., Siziopikou, K., Rademaker, A., Helenowski, I., Cristofanilli, M. & Gradishar, W. J. (2018). Phase i study of alpelisib (byl-719) and trastuzumab emtansine (t-dm1) in her2-positive

metastatic breast cancer (mbc) after trastuzumab and taxane therapy. *Breast Cancer Res Treat,* **171,** 371-381.
351. Xing, Y., Lin, N. U., Maurer, M. A., Chen, H., Mahvash, A., Sahin, A., Akcakanat, A., Li, Y., Abramson, V., Litton, J.*, et al.* (2019). Phase ii trial of akt inhibitor mk-2206 in patients with advanced breast cancer who have tumors with pik3ca or akt mutations, and/or pten loss/pten mutation. *Breast Cancer Res,* **21,** 78.
352. Chien, A. J., Tripathy, D., Albain, K. S., Symmans, W. F., Rugo, H. S., Melisko, M. E., Wallace, A. M., Schwab, R., Helsten, T., Forero-Torres, A.*, et al.* (2020). Mk-2206 and standard neoadjuvant chemotherapy improves response in patients with human epidermal growth factor receptor 2-positive and/or hormone receptor-negative breast cancers in the i-spy 2 trial. *J Clin Oncol,* **38,** 1059-1069.
353. Ma, C. X., Sanchez, C., Gao, F., Crowder, R., Naughton, M., Pluard, T., Creekmore, A., Guo, Z., Hoog, J., Lockhart, A. C.*, et al.* (2016). A phase i study of the akt inhibitor mk-2206 in combination with hormonal therapy in postmenopausal women with estrogen receptor-positive metastatic breast cancer. *Clin Cancer Res,* **22,** 2650-8.
354. Wahba, H. A. & El-Hadaad, H. A. (2015). Current approaches in treatment of triple-negative breast cancer. *Cancer Biol Med,* **12,** 106-16.
355. Lehmann, B. D. & Pietenpol, J. A. (2014). Identification and use of biomarkers in treatment strategies for triple-negative breast cancer subtypes. *J Pathol,* **232,** 142-50.
356. Gonzalez-Angulo, A. M., Timms, K. M., Liu, S., Chen, H., Litton, J. K., Potter, J., Lanchbury, J. S., Stemke-Hale, K., Hennessy, B. T., Arun, B. K.*, et al.* (2011). Incidence and outcome of brca mutations in unselected patients with triple receptor-negative breast cancer. *Clin Cancer Res,* **17,** 1082-9.
357. Gelmon, K. A., Tischkowitz, M., Mackay, H., Swenerton, K., Robidoux, A., Tonkin, K., Hirte, H., Huntsman, D., Clemons, M., Gilks, B.*, et al.* (2011). Olaparib in patients with recurrent high-grade serous or poorly differentiated ovarian carcinoma or triple-negative breast cancer: A phase 2, multicentre, open-label, non-randomised study. *Lancet Oncol,* **12,** 852-61.
358. Matulonis, U. A., Wulf, G. M., Barry, W. T., Birrer, M., Westin, S. N., Farooq, S., Bell-McGuinn, K. M., Obermayer, E., Whalen, C., Spagnoletti, T.*, et al.* (2017). Phase i dose escalation study of the pi3kinase pathway inhibitor bkm120 and the oral poly (adp ribose) polymerase (parp) inhibitor olaparib for the treatment of high-grade serous ovarian and breast cancer. *Ann Oncol,* **28,** 512-518.
359. Reddy, T. P., Rosato, R. R., Li, X., Moulder, S., Piwnica-Worms, H. & Chang, J. C. (2020). A comprehensive overview of metaplastic breast cancer: Clinical features and molecular aberrations. *Breast Cancer Res,* **22,** 121.
360. Basho, R. K., Gilcrease, M., Murthy, R. K., Helgason, T., Karp, D. D., Meric-Bernstam, F., Hess, K. R., Herbrich, S. M., Valero, V., Albarracin, C.*, et al.* (2017). Targeting the pi3k/akt/mtor pathway for the treatment of mesenchymal triple-negative breast cancer: Evidence from a phase 1 trial of mtor inhibition in combination with liposomal doxorubicin and bevacizumab. *JAMA Oncol,* **3,** 509-515.
361. Yang, M. H., Chen, I. C. & Lu, Y. S. (2019). Pi3k inhibitor provides durable response in metastatic metaplastic carcinoma of the breast: A hidden gem in the belle-4 study. *J Formos Med Assoc,* **118,** 1333-1338.
362. Holbein, S., Wengi, A., Decourty, L., Freimoser, F. M., Jacquier, A. & Dichtl, B. (2009). Cordycepin interferes with 3' end formation in yeast independently of its potential to terminate rna chain elongation. *RNA,* **15,** 837-49.
363. Yoon, J. Y., Kim, J. H., Baek, K. S., Kim, G. S., Lee, S. E., Lee, D. Y., Choi, J. H., Kim, S. Y., Park, H. B., Sung, G. H.*, et al.* (2015). A direct protein kinase

b-targeted anti-inflammatory activity of cordycepin from artificially cultured fruit body of cordyceps militaris. *Pharmacogn Mag,* **11,** 477-85.
364. Kim, H. G., Shrestha, B., Lim, S. Y., Yoon, D. H., Chang, W. C., Shin, D. J., Han, S. K., Park, S. M., Park, J. H., Park, H. I.*, et al.* (2006). Cordycepin inhibits lipopolysaccharide-induced inflammation by the suppression of nf-kappab through akt and p38 inhibition in raw 264.7 macrophage cells. *Eur J Pharmacol,* **545,** 192-9.
365. Cui, Z. Y., Park, S. J., Jo, E., Hwang, I. H., Lee, K. B., Kim, S. W., Kim, D. J., Joo, J. C., Hong, S. H., Lee, M. G.*, et al.* (2018). Cordycepin induces apoptosis of human ovarian cancer cells by inhibiting ccl5-mediated akt/nf-κb signaling pathway. *Cell Death Discov,* **4,** 62.
366. Jeong, J. W., Jin, C. Y., Park, C., Han, M. H., Kim, G. Y., Moon, S. K., Kim, C. G., Jeong, Y. K., Kim, W. J., Lee, J. D.*, et al.* (2012). Inhibition of migration and invasion of lncap human prostate carcinoma cells by cordycepin through inactivation of akt. *Int J Oncol,* **40,** 1697-704.
367. Pan, B. S., Wang, Y. K., Lai, M. S., Mu, Y. F. & Huang, B. M. (2015). Cordycepin induced ma-10 mouse leydig tumor cell apoptosis by regulating p38 mapks and pi3k/akt signaling pathways. *Sci Rep,* **5,** 13372.
368. Li, T., Wen, L. & Cheng, B. (2019). Cordycepin alleviates hepatic lipid accumulation by inducing protective autophagy via pka/mtor pathway. *Biochem Biophys Res Commun,* **516,** 632-638.
369. Wong, Y. Y., Moon, A., Duffin, R., Barthet-Barateig, A., Meijer, H. A., Clemens, M. J. & de Moor, C. H. (2010). Cordycepin inhibits protein synthesis and cell adhesion through effects on signal transduction. *J Biol Chem,* **285,** 2610-21.
370. Bain, J., Plater, L., Elliott, M., Shpiro, N., Hastie, C. J., McLauchlan, H., Klevernic, I., Arthur, J. S., Alessi, D. R. & Cohen, P. (2007). The selectivity of protein kinase inhibitors: A further update. *Biochem J,* **408,** 297-315.
371. Zhang, J. L., Xu, Y. & Shen, J. (2014). Cordycepin inhibits lipopolysaccharide (lps)-induced tumor necrosis factor (tnf)-α production via activating amp-activated protein kinase (ampk) signaling. *Int J Mol Sci,* **15,** 12119-34.
372. Bi, Y., Li, H., Yi, D., Sun, Y., Bai, Y., Zhong, S., Song, Y., Zhao, G. & Chen, Y. (2018). Cordycepin augments the chemosensitivity of human glioma cells to temozolomide by activating ampk and inhibiting the akt signaling pathway. *Mol Pharm,* **15,** 4912-4925.
373. Wu, W. D., Hu, Z. M., Shang, M. J., Zhao, D. J., Zhang, C. W., Hong, D. F. & Huang, D. S. (2014). Cordycepin down-regulates multiple drug resistant (mdr)/hif-1α through regulating ampk/mtorc1 signaling in gbc-sd gallbladder cancer cells. *Int J Mol Sci,* **15,** 12778-90.
374. Yan, L. J., Yang, H. T., Duan, H. Y., Wu, J. T., Qian, P., Fan, X. W. & Wang, S. (2017). Cordycepin inhibits vascular adhesion molecule expression in tnf-α-stimulated vascular muscle cells. *Exp Ther Med,* **14,** 2335-2340.
375. Lee, S. J., Kim, S. K., Choi, W. S., Kim, W. J. & Moon, S. K. (2009). Cordycepin causes p21waf1-mediated g2/m cell-cycle arrest by regulating c-jun n-terminal kinase activation in human bladder cancer cells. *Arch Biochem Biophys,* **490,** 103-9.
376. Kitamura, M., Kato, H., Saito, Y., Nakajima, S., Takahashi, S., Johno, H., Gu, L. & Katoh, R. (2011). Aberrant, differential and bidirectional regulation of the unfolded protein response towards cell survival by 3'-deoxyadenosine. *Cell Death Differ,* **18,** 1876-88.
377. Liao, Y., Ling, J., Zhang, G., Liu, F., Tao, S., Han, Z., Chen, S., Chen, Z. & Le, H. (2015). Cordycepin induces cell cycle arrest and apoptosis by inducing DNA damage and up-regulation of p53 in leukemia cells. *Cell Cycle,* **14,** 761-71.
378. Hsu, P. Y., Lin, Y. H., Yeh, E. L., Lo, H. C., Hsu, T. H. & Su, C. C. (2017). Cordycepin and a preparation from. *Oncotarget,* **8,** 93712-93728.

379. Wang, Z., Wu, X., Liang, Y. N., Wang, L., Song, Z. X., Liu, J. L. & Tang, Z. S. (2016). Cordycepin induces apoptosis and inhibits proliferation of human lung cancer cell line h1975 via inhibiting the phosphorylation of egfr. *Molecules,* **21**.
380. Nakamura, K., Yoshikawa, N., Yamaguchi, Y., Kagota, S., Shinozuka, K. & Kunitomo, M. (2006). Antitumor effect of cordycepin (3'-deoxyadenosine) on mouse melanoma and lung carcinoma cells involves adenosine a3 receptor stimulation. *Anticancer Res,* **26,** 43-7.
381. Wang, J., Gong, Y., Tan, H., Li, W., Yan, B., Cheng, C., Wan, J., Sun, W., Yuan, C. & Yao, L. H. (2022). Cordycepin suppresses glutamatergic and gabaergic synaptic transmission through activation of a. *Biomed Pharmacother,* **145,** 112446.
382. Kadomatsu, M., Nakajima, S., Kato, H., Gu, L., Chi, Y., Yao, J. & Kitamura, M. (2012). Cordycepin as a sensitizer to tumour necrosis factor (tnf)-α-induced apoptosis through eukaryotic translation initiation factor 2α (eif2α)- and mammalian target of rapamycin complex 1 (mtorc1)-mediated inhibition of nuclear factor (nf)-κb. *Clin Exp Immunol,* **168,** 325-32.
383. Imamura, K., Asai, M., Sugamoto, K., Matsumoto, T., Yamasaki, Y., Kamei, I., Hattori, T., Kishimoto, M., Niisaka, S., Kubo, M.*, et al.* (2015). Suppressing effect of cordycepin on the lipopolysaccharide-induced nitric oxide production in raw 264.7 cells. *Biosci Biotechnol Biochem,* **79,** 1021-5.
384. Ashraf, S., Radhi, M., Gowler, P., Burston, J. J., Gandhi, R. D., Thorn, G. J., Piccinini, A. M., Walsh, D. A., Chapman, V. & de Moor, C. H. (2019). The polyadenylation inhibitor cordycepin reduces pain, inflammation and joint pathology in rodent models of osteoarthritis. *Sci Rep,* **9,** 4696.
385. Tania, M., Shawon, J., Saif, K., Kiefer, R., Khorram, M. S., Halim, M. A. & Khan, M. A. (2019). Cordycepin downregulates cdk-2 to interfere with cell cycle and increases apoptosis by generating ros in cervical cancer cells: In vitro and in silico study. *Curr Cancer Drug Targets,* **19,** 152-159.
386. Chen, Y., Chen, Y. C., Lin, Y. T., Huang, S. H. & Wang, S. M. (2010). Cordycepin induces apoptosis of cgth w-2 thyroid carcinoma cells through the calcium-calpain-caspase 7-parp pathway. *J Agric Food Chem,* **58,** 11645-52.
387. Kim, H., Naura, A. S., Errami, Y., Ju, J. & Boulares, A. H. (2011). Cordycepin blocks lung injury-associated inflammation and promotes brca1-deficient breast cancer cell killing by effectively inhibiting parp. *Mol Med,* **17,** 893-900.
388. Li, X. Y., Tao, H., Jin, C., DU, Z. Y., Liao, W. F., Tang, Q. J. & Ding, K. (2020). Cordycepin inhibits pancreatic cancer cell growth in vitro and in vivo via targeting fgfr2 and blocking erk signaling. *Chin J Nat Med,* **18,** 345-355.
389. Chen, S., Ni, M., Hu, T., Gu, Y., Feng, C., Pan, C., Zhang, S., Wen, S., Zhao, N., Wang, W.*, et al.* (2021). Tank-binding kinase 1 inhibitor gsk8612 enhances daunorubicin sensitivity in acute myeloid leukemia cells via the akt-cdk2 pathway. *Am J Transl Res,* **13,** 13640-13653.
390. Cohen-Armon, M., Yeheskel, A. & Pascal, J. M. (2019). Signal-induced parp1-erk synergism mediates ieg expression. *Signal Transduct Target Ther,* **4,** 8.
391. Wang, Z. Y., Leushkin, E., Liechti, A., Ovchinnikova, S., Mößinger, K., Brüning, T., Rummel, C., Grützner, F., Cardoso-Moreira, M., Janich, P.*, et al.* (2020). Transcriptome and translatome co-evolution in mammals. *Nature,* **588,** 642-647.
392. Xiang, K. & Bartel, D. P. (2021). The molecular basis of coupling between poly(a)-tail length and translational efficiency. *Elife,* **10**.
393. Zhang, Y., Sun, Y., Shi, Y., Walz, T. & Tong, L. (2020). Structural insights into the human pre-mrna 3'-end processing machinery. *Mol Cell,* **77,** 800-809.e6.

394. Boreikaite, V., Elliott, T. S., Chin, J. W. & Passmore, L. A. (2022). Rbbp6 activates the pre-mrna 3' end processing machinery in humans. *Genes Dev,* **36,** 210-224.
395. Mandel, C. R., Bai, Y. & Tong, L. (2008). Protein factors in pre-mrna 3'-end processing. *Cell Mol Life Sci,* **65,** 1099-122.
396. Millevoi, S. & Vagner, S. (2010). Molecular mechanisms of eukaryotic pre-mrna 3' end processing regulation. *Nucleic Acids Res,* **38,** 2757-74.
397. Chan, S., Choi, E. A. & Shi, Y. (2011). Pre-mrna 3'-end processing complex assembly and function. *Wiley Interdiscip Rev RNA,* **2,** 321-35.
398. Neve, J., Patel, R., Wang, Z., Louey, A. & Furger, A. M. (2017). Cleavage and polyadenylation: Ending the message expands gene regulation. *RNA Biol,* **14,** 865-890.
399. Shi, Y., Di Giammartino, D. C., Taylor, D., Sarkeshik, A., Rice, W. J., Yates, J. R., Frank, J. & Manley, J. L. (2009). Molecular architecture of the human pre-mrna 3' processing complex. *Mol Cell,* **33,** 365-76.
400. Proudfoot, N. J. & Brownlee, G. G. (1976). 3' non-coding region sequences in eukaryotic messenger rna. *Nature,* **263,** 211-4.
401. Proudfoot, N. J. (2011). Ending the message: Poly(a) signals then and now. *Genes Dev,* **25,** 1770-82.
402. Sun, Y., Zhang, Y., Hamilton, K., Manley, J. L., Shi, Y., Walz, T. & Tong, L. (2018). Molecular basis for the recognition of the human aauaaa polyadenylation signal. *Proc Natl Acad Sci U S A,* **115,** E1419-E1428.
403. Clerici, M., Faini, M., Muckenfuss, L. M., Aebersold, R. & Jinek, M. (2018). Structural basis of aauaaa polyadenylation signal recognition by the human cpsf complex. *Nat Struct Mol Biol,* **25,** 135-138.
404. Tian, B., Hu, J., Zhang, H. & Lutz, C. S. (2005). A large-scale analysis of mrna polyadenylation of human and mouse genes. *Nucleic Acids Res,* **33,** 201-12.
405. Wilusz, J., Pettine, S. M. & Shenk, T. (1989). Functional analysis of point mutations in the aauaaa motif of the sv40 late polyadenylation signal. *Nucleic Acids Res,* **17,** 3899-908.
406. Beaudoing, E., Freier, S., Wyatt, J. R., Claverie, J. M. & Gautheret, D. (2000). Patterns of variant polyadenylation signal usage in human genes. *Genome Res,* **10,** 1001-10.
407. Mitschka, S. & Mayr, C. (2022). Context-specific regulation and function of mrna alternative polyadenylation. *Nat Rev Mol Cell Biol,* **23,** 779-796.
408. Wang, R., Zheng, D., Yehia, G. & Tian, B. (2018). A compendium of conserved cleavage and polyadenylation events in mammalian genes. *Genome Res,* **28,** 1427-1441.
409. Kaufmann, I., Martin, G., Friedlein, A., Langen, H. & Keller, W. (2004). Human fip1 is a subunit of cpsf that binds to u-rich rna elements and stimulates poly(a) polymerase. *EMBO J,* **23,** 616-26.
410. Chan, S. L., Huppertz, I., Yao, C., Weng, L., Moresco, J. J., Yates, J. R., Ule, J., Manley, J. L. & Shi, Y. (2014). Cpsf30 and wdr33 directly bind to aauaaa in mammalian mrna 3' processing. *Genes Dev,* **28,** 2370-80.
411. Schönemann, L., Kühn, U., Martin, G., Schäfer, P., Gruber, A. R., Keller, W., Zavolan, M. & Wahle, E. (2014). Reconstitution of cpsf active in polyadenylation: Recognition of the polyadenylation signal by wdr33. *Genes Dev,* **28,** 2381-93.
412. Clerici, M., Faini, M., Aebersold, R. & Jinek, M. (2017). Structural insights into the assembly and polya signal recognition mechanism of the human cpsf complex. *Elife,* **6**.
413. Dantonel, J. C., Murthy, K. G., Manley, J. L. & Tora, L. (1997). Transcription factor tfiid recruits factor cpsf for formation of 3' end of mrna. *Nature,* **389,** 399-402.

414. Fitzgerald, M. & Shenk, T. (1981). The sequence 5'-aauaaa-3'forms parts of the recognition site for polyadenylation of late sv40 mrnas. *Cell,* **24,** 251-60.
415. Gruber, A. J., Schmidt, R., Gruber, A. R., Martin, G., Ghosh, S., Belmadani, M., Keller, W. & Zavolan, M. (2016). A comprehensive analysis of 3' end sequencing data sets reveals novel polyadenylation signals and the repressive role of heterogeneous ribonucleoprotein c on cleavage and polyadenylation. *Genome Res,* **26,** 1145-59.
416. Murthy, K. G. & Manley, J. L. (1995). The 160-kd subunit of human cleavage-polyadenylation specificity factor coordinates pre-mrna 3'-end formation. *Genes Dev,* **9,** 2672-83.
417. Mandel, C. R., Kaneko, S., Zhang, H., Gebauer, D., Vethantham, V., Manley, J. L. & Tong, L. (2006). Polyadenylation factor cpsf-73 is the pre-mrna 3'-end-processing endonuclease. *Nature,* **444,** 953-6.
418. Hamilton, K. & Tong, L. (2020). Molecular mechanism for the interaction between human cpsf30 and hfip1. *Genes Dev,* **34,** 1753-1761.
419. Schmidt, M., Kluge, F., Sandmeir, F., Kühn, U., Schäfer, P., Tüting, C., Ihling, C., Conti, E. & Wahle, E. (2022). Reconstitution of 3' end processing of mammalian pre-mrna reveals a central role of rbbp6. *Genes Dev,* **36,** 195-209.
420. Takagaki, Y. & Manley, J. L. (2000). Complex protein interactions within the human polyadenylation machinery identify a novel component. *Mol Cell Biol,* **20,** 1515-25.
421. Sullivan, K. D., Steiniger, M. & Marzluff, W. F. (2009). A core complex of cpsf73, cpsf100, and symplekin may form two different cleavage factors for processing of poly(a) and histone mrnas. *Mol Cell,* **34,** 322-32.
422. MacDonald, C. C., Wilusz, J. & Shenk, T. (1994). The 64-kilodalton subunit of the cstf polyadenylation factor binds to pre-mrnas downstream of the cleavage site and influences cleavage site location. *Mol Cell Biol,* **14,** 6647-54.
423. Takagaki, Y. & Manley, J. L. (1997). Rna recognition by the human polyadenylation factor cstf. *Mol Cell Biol,* **17,** 3907-14.
424. Grozdanov, P. N., Masoumzadeh, E., Latham, M. P. & MacDonald, C. C. (2018). The structural basis of cstf-77 modulation of cleavage and polyadenylation through stimulation of cstf-64 activity. *Nucleic Acids Res,* **46,** 12022-12039.
425. Fong, N. & Bentley, D. L. (2001). Capping, splicing, and 3' processing are independently stimulated by rna polymerase ii: Different functions for different segments of the ctd. *Genes Dev,* **15,** 1783-95.
426. Fong, N., Bird, G., Vigneron, M. & Bentley, D. L. (2003). A 10 residue motif at the c-terminus of the rna pol ii ctd is required for transcription, splicing and 3' end processing. *EMBO J,* **22,** 4274-82.
427. Yang, W., Hsu, P. L., Yang, F., Song, J. E. & Varani, G. (2018). Reconstitution of the cstf complex unveils a regulatory role for cstf-50 in recognition of 3'-end processing signals. *Nucleic Acids Res,* **46,** 493-503.
428. McCracken, S., Fong, N., Yankulov, K., Ballantyne, S., Pan, G., Greenblatt, J., Patterson, S. D., Wickens, M. & Bentley, D. L. (1997). The c-terminal domain of rna polymerase ii couples mrna processing to transcription. *Nature,* **385,** 357-61.
429. Muckenfuss, L. M., Migenda Herranz, A. C., Boneberg, F. M., Clerici, M. & Jinek, M. (2022). Fip1 is a multivalent interaction scaffold for processing factors in human mrna 3' end biogenesis. *Elife,* **11**.
430. Schäfer, P., Tüting, C., Schönemann, L., Kühn, U., Treiber, T., Treiber, N., Ihling, C., Graber, A., Keller, W., Meister, G.*, et al.* (2018). Reconstitution of mammalian cleavage factor ii involved in 3' processing of mrna precursors. *RNA,* **24,** 1721-1737.

431. Birse, C. E., Minvielle-Sebastia, L., Lee, B. A., Keller, W. & Proudfoot, N. J. (1998). Coupling termination of transcription to messenger rna maturation in yeast. *Science,* **280,** 298-301.
432. de Vries, H., Rüegsegger, U., Hübner, W., Friedlein, A., Langen, H. & Keller, W. (2000). Human pre-mrna cleavage factor ii(m) contains homologs of yeast proteins and bridges two other cleavage factors. *EMBO J,* **19,** 5895-904.
433. West, S. & Proudfoot, N. J. (2008). Human pcf11 enhances degradation of rna polymerase ii-associated nascent rna and transcriptional termination. *Nucleic Acids Res,* **36,** 905-14.
434. Kamieniarz-Gdula, K., Gdula, M. R., Panser, K., Nojima, T., Monks, J., Wiśniewski, J. R., Riepsaame, J., Brockdorff, N., Pauli, A. & Proudfoot, N. J. (2019). Selective roles of vertebrate pcf11 in premature and full-length transcript termination. *Mol Cell,* **74,** 158-172.e9.
435. Kyriakopoulou, C. B., Nordvarg, H. & Virtanen, A. (2001). A novel nuclear human poly(a) polymerase (pap), pap gamma. *J Biol Chem,* **276,** 33504-11.
436. Kerwitz, Y., Kühn, U., Lilie, H., Knoth, A., Scheuermann, T., Friedrich, H., Schwarz, E. & Wahle, E. (2003). Stimulation of poly(a) polymerase through a direct interaction with the nuclear poly(a) binding protein allosterically regulated by rna. *EMBO J,* **22,** 3705-14.
437. Dettwiler, S., Aringhieri, C., Cardinale, S., Keller, W. & Barabino, S. M. (2004). Distinct sequence motifs within the 68-kda subunit of cleavage factor im mediate rna binding, protein-protein interactions, and subcellular localization. *J Biol Chem,* **279,** 35788-97.
438. Kühn, U., Gündel, M., Knoth, A., Kerwitz, Y., Rüdel, S. & Wahle, E. (2009). Poly(a) tail length is controlled by the nuclear poly(a)-binding protein regulating the interaction between poly(a) polymerase and the cleavage and polyadenylation specificity factor. *J Biol Chem,* **284,** 22803-14.
439. Wahle, E. (1991). Purification and characterization of a mammalian polyadenylate polymerase involved in the 3' end processing of messenger rna precursors. *J Biol Chem,* **266,** 3131-9.
440. Wahle, E. (1991). A novel poly(a)-binding protein acts as a specificity factor in the second phase of messenger rna polyadenylation. *Cell,* **66,** 759-68.
441. Bienroth, S., Keller, W. & Wahle, E. (1993). Assembly of a processive messenger rna polyadenylation complex. *EMBO J,* **12,** 585-94.
442. Martin, G. & Keller, W. (2007). Rna-specific ribonucleotidyl transferases. *RNA,* **13,** 1834-49.
443. Rissland, O. S., Mikulasova, A. & Norbury, C. J. (2007). Efficient rna polyuridylation by noncanonical poly(a) polymerases. *Mol Cell Biol,* **27,** 3612-24.
444. Balbo, P. B. & Bohm, A. (2007). Mechanism of poly(a) polymerase: Structure of the enzyme-mgatp-rna ternary complex and kinetic analysis. *Structure,* **15,** 1117-31.
445. Trippe, R., Guschina, E., Hossbach, M., Urlaub, H., Lührmann, R. & Benecke, B. J. (2006). Identification, cloning, and functional analysis of the human u6 snrna-specific terminal uridylyl transferase. *RNA,* **12,** 1494-504.
446. Laishram, R. S. & Anderson, R. A. (2010). The poly a polymerase star-pap controls 3'-end cleavage by promoting cpsf interaction and specificity toward the pre-mrna. *EMBO J,* **29,** 4132-45.
447. Kandala, D. T., Mohan, N., A, V., A P, S., G, R. & Laishram, R. S. (2016). Cstf-64 and 3'-utr cis-element determine star-pap specificity for target mrna selection by excluding papα. *Nucleic Acids Res,* **44,** 811-23.
448. Buratowski, S. (2005). Connections between mrna 3' end processing and transcription termination. *Curr Opin Cell Biol,* **17,** 257-61.

449. Eaton, J. D. & West, S. (2020). Termination of transcription by rna polymerase ii: Boom! *Trends Genet,* **36,** 664-675.
450. Eaton, J. D., Davidson, L., Bauer, D. L. V., Natsume, T., Kanemaki, M. T. & West, S. (2018). Xrn2 accelerates termination by rna polymerase ii, which is underpinned by cpsf73 activity. *Genes Dev,* **32,** 127-139.
451. Cortazar, M. A., Sheridan, R. M., Erickson, B., Fong, N., Glover-Cutter, K., Brannan, K. & Bentley, D. L. (2019). Control of rna pol ii speed by pnuts-pp1 and spt5 dephosphorylation facilitates termination by a "sitting duck torpedo" mechanism. *Mol Cell,* **76,** 896-908.e4.
452. Gregersen, L. H., Mitter, R., Ugalde, A. P., Nojima, T., Proudfoot, N. J., Agami, R., Stewart, A. & Svejstrup, J. Q. (2019). Scaf4 and scaf8, mrna anti-terminator proteins. *Cell,* **177,** 1797-1813.e18.
453. Dubbury, S. J., Boutz, P. L. & Sharp, P. A. (2018). Cdk12 regulates DNA repair genes by suppressing intronic polyadenylation. *Nature,* **564,** 141-145.
454. Jenal, M., Elkon, R., Loayza-Puch, F., van Haaften, G., Kühn, U., Menzies, F. M., Oude Vrielink, J. A., Bos, A. J., Drost, J., Rooijers, K.*, et al.* (2012). The poly(a)-binding protein nuclear 1 suppresses alternative cleavage and polyadenylation sites. *Cell,* **149,** 538-53.
455. Kaida, D., Berg, M. G., Younis, I., Kasim, M., Singh, L. N., Wan, L. & Dreyfuss, G. (2010). U1 snrnp protects pre-mrnas from premature cleavage and polyadenylation. *Nature,* **468,** 664-8.
456. Zhang, H., Rigo, F. & Martinson, H. G. (2015). Poly(a) signal-dependent transcription termination occurs through a conformational change mechanism that does not require cleavage at the poly(a) site. *Mol Cell,* **59,** 437-48.
457. Osheim, Y. N., Sikes, M. L. & Beyer, A. L. (2002). Em visualization of pol ii genes in drosophila: Most genes terminate without prior 3' end cleavage of nascent transcripts. *Chromosoma,* **111,** 1-12.
458. Eaton, J. D., Francis, L., Davidson, L. & West, S. (2020). A unified allosteric/torpedo mechanism for transcriptional termination on human protein-coding genes. *Genes Dev,* **34,** 132-145.
459. Fong, N., Brannan, K., Erickson, B., Kim, H., Cortazar, M. A., Sheridan, R. M., Nguyen, T., Karp, S. & Bentley, D. L. (2015). Effects of transcription elongation rate and xrn2 exonuclease activity on rna polymerase ii termination suggest widespread kinetic competition. *Mol Cell,* **60,** 256-67.
460. Gruber, A. J. & Zavolan, M. (2019). Alternative cleavage and polyadenylation in health and disease. *Nat Rev Genet*.
461. Fu, Y., Sun, Y., Li, Y., Li, J., Rao, X., Chen, C. & Xu, A. (2011). Differential genome-wide profiling of tandem 3' utrs among human breast cancer and normal cells by high-throughput sequencing. *Genome Res,* **21,** 741-7.
462. Hoque, M., Ji, Z., Zheng, D., Luo, W., Li, W., You, B., Park, J. Y., Yehia, G. & Tian, B. (2013). Analysis of alternative cleavage and polyadenylation by 3' region extraction and deep sequencing. *Nat Methods,* **10,** 133-9.
463. Tian, B. & Manley, J. L. (2017). Alternative polyadenylation of mrna precursors. *Nat Rev Mol Cell Biol,* **18,** 18-30.
464. Hoffman, Y., Bublik, D. R., Ugalde, A. P., Elkon, R., Biniashvili, T., Agami, R., Oren, M. & Pilpel, Y. (2016). 3'utr shortening potentiates microrna-based repression of pro-differentiation genes in proliferating human cells. *PLoS Genet,* **12,** e1005879.
465. Mayya, V. K. & Duchaine, T. F. (2019). Ciphers and executioners: How 3'-untranslated regions determine the fate of messenger rnas. *Front Genet,* **10,** 6.
466. Kim, H. H. & Gorospe, M. (2008). Gu-rich rna: Expanding cugbp1 function, broadening mrna turnover. *Mol Cell,* **29,** 151-2.

467. Mayr, C. (2017). Regulation by 3'-untranslated regions. *Annu Rev Genet,* **51,** 171-194.
468. Alt, F. W., Bothwell, A. L., Knapp, M., Siden, E., Mather, E., Koshland, M. & Baltimore, D. (1980). Synthesis of secreted and membrane-bound immunoglobulin mu heavy chains is directed by mrnas that differ at their 3' ends. *Cell,* **20,** 293-301.
469. Mayr, C. & Bartel, D. P. (2009). Widespread shortening of 3'utrs by alternative cleavage and polyadenylation activates oncogenes in cancer cells. *Cell,* **138,** 673-84.
470. Sandberg, R., Neilson, J. R., Sarma, A., Sharp, P. A. & Burge, C. B. (2008). Proliferating cells express mrnas with shortened 3' untranslated regions and fewer microrna target sites. *Science,* **320,** 1643-7.
471. Berkovits, B. D. & Mayr, C. (2015). Alternative 3' utrs act as scaffolds to regulate membrane protein localization. *Nature,* **522,** 363-7.
472. Djebali, S., Davis, C. A., Merkel, A., Dobin, A., Lassmann, T., Mortazavi, A., Tanzer, A., Lagarde, J., Lin, W., Schlesinger, F.*, et al.* (2012). Landscape of transcription in human cells. *Nature,* **489,** 101-8.
473. Zhang, Z. & Carmichael, G. G. (2001). The fate of dsrna in the nucleus: A p54(nrb)-containing complex mediates the nuclear retention of promiscuously a-to-i edited rnas. *Cell,* **106,** 465-75.
474. Chen, L. L. & Carmichael, G. G. (2008). Gene regulation by sines and inosines: Biological consequences of a-to-i editing of alu element inverted repeats. *Cell Cycle,* **7,** 3294-301.
475. Chen, L. L., DeCerbo, J. N. & Carmichael, G. G. (2008). Alu element-mediated gene silencing. *EMBO J,* **27,** 1694-705.
476. Rüegsegger, U., Beyer, K. & Keller, W. (1996). Purification and characterization of human cleavage factor im involved in the 3' end processing of messenger rna precursors. *J Biol Chem,* **271,** 6107-13.
477. Martin, G., Gruber, A. R., Keller, W. & Zavolan, M. (2012). Genome-wide analysis of pre-mrna 3' end processing reveals a decisive role of human cleavage factor i in the regulation of 3' utr length. *Cell Rep,* **1,** 753-63.
478. Gruber, A. R., Martin, G., Keller, W. & Zavolan, M. (2012). Cleavage factor im is a key regulator of 3' utr length. *RNA Biol,* **9,** 1405-12.
479. Sartini, B. L., Wang, H., Wang, W., Millette, C. F. & Kilpatrick, D. L. (2008). Pre-messenger rna cleavage factor i (cfim): Potential role in alternative polyadenylation during spermatogenesis. *Biol Reprod,* **78,** 472-82.
480. Lackford, B., Yao, C., Charles, G. M., Weng, L., Zheng, X., Choi, E. A., Xie, X., Wan, J., Xing, Y., Freudenberg, J. M.*, et al.* (2014). Fip1 regulates mrna alternative polyadenylation to promote stem cell self-renewal. *EMBO J,* **33,** 878-89.
481. Li, W., You, B., Hoque, M., Zheng, D., Luo, W., Ji, Z., Park, J. Y., Gunderson, S. I., Kalsotra, A., Manley, J. L.*, et al.* (2015). Systematic profiling of poly(a)+ transcripts modulated by core 3' end processing and splicing factors reveals regulatory rules of alternative cleavage and polyadenylation. *PLoS Genet,* **11,** e1005166.
482. Peng, Y., Yuan, J., Zhang, Z. & Chang, X. (2017). Cytoplasmic poly(a)-binding protein 1 (pabpc1) interacts with the rna-binding protein hnrnpll and thereby regulates immunoglobulin secretion in plasma cells. *J Biol Chem,* **292,** 12285-12295.
483. Paris, J. & Richter, J. D. (1990). Maturation-specific polyadenylation and translational control: Diversity of cytoplasmic polyadenylation elements, influence of poly(a) tail size, and formation of stable polyadenylation complexes. *Mol Cell Biol,* **10,** 5634-45.
484. Cooperstock, R. L. & Lipshitz, H. D. (1997). Control of mrna stability and translation during drosophila development. *Semin Cell Dev Biol,* **8,** 541-9.

485. Kashiwabara, S., Noguchi, J., Zhuang, T., Ohmura, K., Honda, A., Sugiura, S., Miyamoto, K., Takahashi, S., Inoue, K., Ogura, A.*, et al.* (2002). Regulation of spermatogenesis by testis-specific, cytoplasmic poly(a) polymerase tpap. *Science,* **298,** 1999-2002.
486. Cui, J., Sartain, C. V., Pleiss, J. A. & Wolfner, M. F. (2013). Cytoplasmic polyadenylation is a major mrna regulator during oogenesis and egg activation in drosophila. *Dev Biol,* **383,** 121-31.
487. Vassalli, J. D., Huarte, J., Belin, D., Gubler, P., Vassalli, A., O'Connell, M. L., Parton, L. A., Rickles, R. J. & Strickland, S. (1989). Regulated polyadenylation controls mrna translation during meiotic maturation of mouse oocytes. *Genes Dev,* **3,** 2163-71.
488. Burgess, H. M. & Gray, N. K. (2010). Mrna-specific regulation of translation by poly(a)-binding proteins. *Biochem Soc Trans,* **38,** 1517-22.
489. Novoa, I., Gallego, J., Ferreira, P. G. & Mendez, R. (2010). Mitotic cell-cycle progression is regulated by cpeb1 and cpeb4-dependent translational control. *Nat Cell Biol,* **12,** 447-56.
490. Hosoda, N., Lejeune, F. & Maquat, L. E. (2006). Evidence that poly(a) binding protein c1 binds nuclear pre-mrna poly(a) tails. *Mol Cell Biol,* **26,** 3085-97.
491. Gorgoni, B. & Gray, N. K. (2004). The roles of cytoplasmic poly(a)-binding proteins in regulating gene expression: A developmental perspective. *Brief Funct Genomic Proteomic,* **3,** 125-41.
492. Féral, C., Guellaën, G. & Pawlak, A. (2001). Human testis expresses a specific poly(a)-binding protein. *Nucleic Acids Res,* **29,** 1872-83.
493. Kleene, K. C., Mulligan, E., Steiger, D., Donohue, K. & Mastrangelo, M. A. (1998). The mouse gene encoding the testis-specific isoform of poly(a) binding protein (pabp2) is an expressed retroposon: Intimations that gene expression in spermatogenic cells facilitates the creation of new genes. *J Mol Evol,* **47,** 275-81.
494. Guzeloglu-Kayisli, O., Pauli, S., Demir, H., Lalioti, M. D., Sakkas, D. & Seli, E. (2008). Identification and characterization of human embryonic poly(a) binding protein (epab). *Mol Hum Reprod,* **14,** 581-8.
495. Blanco, P., Sargent, C. A., Boucher, C. A., Howell, G., Ross, M. & Affara, N. A. (2001). A novel poly(a)-binding protein gene (pabpc5) maps to an x-specific subinterval in the xq21.3/yp11.2 homology block of the human sex chromosomes. *Genomics,* **74,** 1-11.
496. Kini, H. K., Kong, J. & Liebhaber, S. A. (2014). Cytoplasmic poly(a) binding protein c4 serves a critical role in erythroid differentiation. *Mol Cell Biol,* **34,** 1300-9.
497. Hake, L. E. & Richter, J. D. (1994). Cpeb is a specificity factor that mediates cytoplasmic polyadenylation during xenopus oocyte maturation. *Cell,* **79,** 617-27.
498. Afroz, T., Skrisovska, L., Belloc, E., Guillén-Boixet, J., Méndez, R. & Allain, F. H. (2014). A fly trap mechanism provides sequence-specific rna recognition by cpeb proteins. *Genes Dev,* **28,** 1498-514.
499. Stebbins-Boaz, B., Cao, Q., de Moor, C. H., Mendez, R. & Richter, J. D. (1999). Maskin is a cpeb-associated factor that transiently interacts with elf-4e. *Mol Cell,* **4,** 1017-27.
500. Mendez, R. & Richter, J. D. (2001). Translational control by cpeb: A means to the end. *Nat Rev Mol Cell Biol,* **2,** 521-9.
501. Duran-Arqué, B., Cañete, M., Castellazzi, C. L., Bartomeu, A., Ferrer-Caelles, A., Reina, O., Caballé, A., Gay, M., Arauz-Garofalo, G., Belloc, E.*, et al.* (2022). Comparative analyses of vertebrate cpeb proteins define two subfamilies with coordinated yet distinct functions in post-transcriptional gene regulation. *Genome Biol,* **23,** 192.
502. Gallie, D. R. (1991). The cap and poly(a) tail function synergistically to regulate mrna translational efficiency. *Genes Dev,* **5,** 2108-16.

503. Tarun, S. Z. & Sachs, A. B. (1996). Association of the yeast poly(a) tail binding protein with translation initiation factor eif-4g. *EMBO J,* **15,** 7168-77.
504. Imataka, H., Gradi, A. & Sonenberg, N. (1998). A newly identified n-terminal amino acid sequence of human eif4g binds poly(a)-binding protein and functions in poly(a)-dependent translation. *EMBO J,* **17,** 7480-9.
505. Tarun, S. Z., Wells, S. E., Deardorff, J. A. & Sachs, A. B. (1997). Translation initiation factor eif4g mediates in vitro poly(a) tail-dependent translation. *Proc Natl Acad Sci U S A,* **94,** 9046-51.
506. Andrésson, T. & Ruderman, J. V. (1998). The kinase eg2 is a component of the xenopus oocyte progesterone-activated signaling pathway. *EMBO J,* **17,** 5627-37.
507. Frank-Vaillant, M., Haccard, O., Thibier, C., Ozon, R., Arlot-Bonnemains, Y., Prigent, C. & Jessus, C. (2000). Progesterone regulates the accumulation and the activation of eg2 kinase in xenopus oocytes. *J Cell Sci,* **113 (Pt 7),** 1127-38.
508. Mendez, R., Hake, L. E., Andresson, T., Littlepage, L. E., Ruderman, J. V. & Richter, J. D. (2000). Phosphorylation of cpe binding factor by eg2 regulates translation of c-mos mrna. *Nature,* **404,** 302-7.
509. Benoit, P., Papin, C., Kwak, J. E., Wickens, M. & Simonelig, M. (2008). Pap- and gld-2-type poly(a) polymerases are required sequentially in cytoplasmic polyadenylation and oogenesis in drosophila. *Development,* **135,** 1969-79.
510. Lim, J., Kim, D., Lee, Y. S., Ha, M., Lee, M., Yeo, J., Chang, H., Song, J., Ahn, K. & Kim, V. N. (2018). Mixed tailing by tent4a and tent4b shields mrna from rapid deadenylation. *Science,* **361,** 701-704.
511. Kuchta, K., Muszewska, A., Knizewski, L., Steczkiewicz, K., Wyrwicz, L. S., Pawlowski, K., Rychlewski, L. & Ginalski, K. (2016). Fam46 proteins are novel eukaryotic non-canonical poly(a) polymerases. *Nucleic Acids Res,* **44,** 3534-48.
512. Anderson, S., Bankier, A. T., Barrell, B. G., de Bruijn, M. H., Coulson, A. R., Drouin, J., Eperon, I. C., Nierlich, D. P., Roe, B. A., Sanger, F.*, et al.* (1981). Sequence and organization of the human mitochondrial genome. *Nature,* **290,** 457-65.
513. Yokokawa, T., Kido, K., Suga, T., Isaka, T., Hayashi, T. & Fujita, S. (2018). Exercise-induced mitochondrial biogenesis coincides with the expression of mitochondrial translation factors in murine skeletal muscle. *Physiol Rep,* **6,** e13893.
514. Sousa, J. S., D'Imprima, E. & Vonck, J. (2018). Mitochondrial respiratory chain complexes. *Subcell Biochem,* **87,** 167-227.
515. Ojala, D., Montoya, J. & Attardi, G. (1981). Trna punctuation model of rna processing in human mitochondria. *Nature,* **290,** 470-4.
516. Saoji, M., Sen, A. & Cox, R. T. (2021). Loss of individual mitochondrial ribonuclease p complex proteins differentially affects mitochondrial trna processing in vivo. *Int J Mol Sci,* **22**.
517. Sanchez, M. I., Mercer, T. R., Davies, S. M., Shearwood, A. M., Nygård, K. K., Richman, T. R., Mattick, J. S., Rackham, O. & Filipovska, A. (2011). Rna processing in human mitochondria. *Cell Cycle,* **10,** 2904-16.
518. Rossmanith, W., Tullo, A., Potuschak, T., Karwan, R. & Sbisà, E. (1995). Human mitochondrial trna processing. *J Biol Chem,* **270,** 12885-91.
519. Chang, J. H. & Tong, L. (2012). Mitochondrial poly(a) polymerase and polyadenylation. *Biochim Biophys Acta,* **1819,** 992-7.
520. Tomecki, R., Dmochowska, A., Gewartowski, K., Dziembowski, A. & Stepien, P. P. (2004). Identification of a novel human nuclear-encoded mitochondrial poly(a) polymerase. *Nucleic Acids Res,* **32,** 6001-14.
521. Nagaike, T., Suzuki, T., Katoh, T. & Ueda, T. (2005). Human mitochondrial mrnas are stabilized with polyadenylation regulated by mitochondria-specific

poly(a) polymerase and polynucleotide phosphorylase. *J Biol Chem,* **280,** 19721-7.
522. Antonicka, H. & Shoubridge, E. A. (2015). Mitochondrial rna granules are centers for posttranscriptional rna processing and ribosome biogenesis. *Cell Rep,* **10,** 920-932.
523. Bai, Y., Srivastava, S. K., Chang, J. H., Manley, J. L. & Tong, L. (2011). Structural basis for dimerization and activity of human papd1, a noncanonical poly(a) polymerase. *Mol Cell,* **41,** 311-20.
524. Zorkau, M., Albus, C. A., Berlinguer-Palmini, R., Chrzanowska-Lightowlers, Z. M. A. & Lightowlers, R. N. (2021). High-resolution imaging reveals compartmentalization of mitochondrial protein synthesis in cultured human cells. *Proc Natl Acad Sci U S A,* **118**.
525. Xavier, V. J. & Martinou, J. C. (2021). Rna granules in the mitochondria and their organization under mitochondrial stresses. *Int J Mol Sci,* **22**.
526. Borowski, L. S., Dziembowski, A., Hejnowicz, M. S., Stepien, P. P. & Szczesny, R. J. (2013). Human mitochondrial rna decay mediated by pnpase-hsuv3 complex takes place in distinct foci. *Nucleic Acids Res,* **41,** 1223-40.
527. Pietras, Z., Wojcik, M. A., Borowski, L. S., Szewczyk, M., Kulinski, T. M., Cysewski, D., Stepien, P. P., Dziembowski, A. & Szczesny, R. J. (2018). Dedicated surveillance mechanism controls g-quadruplex forming non-coding rnas in human mitochondria. *Nat Commun,* **9,** 2558.
528. Bedrat, A., Lacroix, L. & Mergny, J. L. (2016). Re-evaluation of g-quadruplex propensity with g4hunter. *Nucleic Acids Res,* **44,** 1746-59.
529. Toompuu, M., Tuomela, T., Laine, P., Paulin, L., Dufour, E. & Jacobs, H. T. (2018). Polyadenylation and degradation of structurally abnormal mitochondrial trnas in human cells. *Nucleic Acids Res,* **46,** 5209-5226.
530. Xiang, Y., Ye, Y., Lou, Y., Yang, Y., Cai, C., Zhang, Z., Mills, T., Chen, N. Y., Kim, Y., Muge Ozguc, F.*, et al.* (2018). Comprehensive characterization of alternative polyadenylation in human cancer. *J Natl Cancer Inst,* **110,** 379-389.
531. Komini, C., Theohari, I., Lambrianidou, A., Nakopoulou, L. & Trangas, T. (2021). Papola contributes to cyclin d1 mrna alternative polyadenylation and promotes breast cancer cell proliferation. *J Cell Sci,* **134**.
532. Bresson, S. M. & Conrad, N. K. (2013). The human nuclear poly(a)-binding protein promotes rna hyperadenylation and decay. *PLoS Genet,* **9,** e1003893.
533. Bresson, S. M., Hunter, O. V., Hunter, A. C. & Conrad, N. K. (2015). Canonical poly(a) polymerase activity promotes the decay of a wide variety of mammalian nuclear rnas. *PLoS Genet,* **11,** e1005610.
534. Kim, J., Tsuruta, F., Okajima, T., Yano, S., Sato, B. & Chiba, T. (2017). Klhl7 promotes tut1 ubiquitination associated with nucleolar integrity: Implications for retinitis pigmentosa. *Biochem Biophys Res Commun,* **494,** 220-226.
535. Zhu, D. Q., Lou, Y. F., He, Z. G. & Ji, M. (2014). Nucleotidyl transferase tut1 inhibits lipogenesis in osteosarcoma cells through regulation of microrna-24 and microrna-29a. *Tumour Biol,* **35,** 11829-35.
536. Wang, L., Eckmann, C. R., Kadyk, L. C., Wickens, M. & Kimble, J. (2002). A regulatory cytoplasmic poly(a) polymerase in caenorhabditis elegans. *Nature,* **419,** 312-6.
537. Kwak, J. E., Wang, L., Ballantyne, S., Kimble, J. & Wickens, M. (2004). Mammalian gld-2 homologs are poly(a) polymerases. *Proc Natl Acad Sci U S A,* **101,** 4407-12.
538. Barnard, D. C., Ryan, K., Manley, J. L. & Richter, J. D. (2004). Symplekin and xgld-2 are required for cpeb-mediated cytoplasmic polyadenylation. *Cell,* **119,** 641-51.

539. Warkocki, Z., Liudkovska, V., Gewartowska, O., Mroczek, S. & Dziembowski, A. (2018). Terminal nucleotidyl transferases (tents) in mammalian rna metabolism. *Philos Trans R Soc Lond B Biol Sci,* **373**.
540. Mansur, F., Alarcon, J. M., Stackpole, E. E., Wang, R. & Richter, J. D. (2021). Noncanonical cytoplasmic poly(a) polymerases regulate rna levels, alternative rna processing, and synaptic plasticity but not hippocampal-dependent behaviours. *RNA Biol,* **18,** 962-971.
541. Shin, J., Paek, K. Y., Ivshina, M., Stackpole, E. E. & Richter, J. D. (2017). Essential role for non-canonical poly(a) polymerase gld4 in cytoplasmic polyadenylation and carbohydrate metabolism. *Nucleic Acids Res,* **45,** 6793-6804.
542. Barragán, I., Borrego, S., Abd El-Aziz, M. M., El-Ashry, M. F., Abu-Safieh, L., Bhattacharya, S. S. & Antiñolo, G. (2008). Genetic analysis of fam46a in spanish families with autosomal recessive retinitis pigmentosa: Characterisation of novel vntrs. *Ann Hum Genet,* **72,** 26-34.
543. Diener, S., Bayer, S., Sabrautzki, S., Wieland, T., Mentrup, B., Przemeck, G. K., Rathkolb, B., Graf, E., Hans, W., Fuchs, H.*, et al.* (2016). Exome sequencing identifies a nonsense mutation in fam46a associated with bone abnormalities in a new mouse model for skeletal dysplasia. *Mamm Genome,* **27,** 111-21.
544. Doyard, M., Bacrot, S., Huber, C., Di Rocco, M., Goldenberg, A., Aglan, M. S., Brunelle, P., Temtamy, S., Michot, C., Otaify, G. A.*, et al.* (2018). Mutations are responsible for autosomal recessive osteogenesis imperfecta. *J Med Genet,* **55,** 278-284.
545. Etokebe, G. E., Jotanovic, Z., Mihelic, R., Mulac-Jericevic, B., Nikolic, T., Balen, S., Sestan, B. & Dembic, Z. (2015). Susceptibility to large-joint osteoarthritis (hip and knee) is associated with bag6 rs3117582 snp and the vntr polymorphism in the second exon of the fam46a gene on chromosome 6. *J Orthop Res,* **33,** 56-62.
546. Etokebe, G. E., Zienolddiny, S., Kupanovac, Z., Enersen, M., Balen, S., Flego, V., Bulat-Kardum, L., Radojčić-Badovinac, A., Skaug, V., Bakke, P.*, et al.* (2015). Association of the fam46a gene vntrs and bag6 rs3117582 snp with non small cell lung cancer (nsclc) in croatian and norwegian populations. *PLoS One,* **10,** e0122651.
547. Mroczek, S., Chlebowska, J., Kuliński, T. M., Gewartowska, O., Gruchota, J., Cysewski, D., Liudkovska, V., Borsuk, E., Nowis, D. & Dziembowski, A. (2017). The non-canonical poly(a) polymerase fam46c acts as an onco-suppressor in multiple myeloma. *Nat Commun,* **8,** 619.
548. Liudkovska, V., Krawczyk, P. S., Brouze, A., Gumińska, N., Wegierski, T., Cysewski, D., Mackiewicz, Z., Ewbank, J. J., Drabikowski, K., Mroczek, S.*, et al.* (2022). Tent5 cytoplasmic noncanonical poly(a) polymerases regulate the innate immune response in animals. *Sci Adv,* **8,** eadd9468.
549. Hu, J. L., Liang, H., Zhang, H., Yang, M. Z., Sun, W., Zhang, P., Luo, L., Feng, J. X., Bai, H., Liu, F.*, et al.* (2020). Fam46b is a prokaryotic-like cytoplasmic poly(a) polymerase essential in human embryonic stem cells. *Nucleic Acids Res,* **48,** 2733-2748.
550. Chapman, M. A., Lawrence, M. S., Keats, J. J., Cibulskis, K., Sougnez, C., Schinzel, A. C., Harview, C. L., Brunet, J. P., Ahmann, G. J., Adli, M.*, et al.* (2011). Initial genome sequencing and analysis of multiple myeloma. *Nature,* **471,** 467-72.
551. Lohr, J. G., Stojanov, P., Carter, S. L., Cruz-Gordillo, P., Lawrence, M. S., Auclair, D., Sougnez, C., Knoechel, B., Gould, J., Saksena, G.*, et al.* (2014). Widespread genetic heterogeneity in multiple myeloma: Implications for targeted therapy. *Cancer Cell,* **25,** 91-101.
552. Walker, B. A., Boyle, E. M., Wardell, C. P., Murison, A., Begum, D. B., Dahir, N. M., Proszek, P. Z., Johnson, D. C., Kaiser, M. F., Melchor, L.*, et al.*

(2015). Mutational spectrum, copy number changes, and outcome: Results of a sequencing study of patients with newly diagnosed myeloma. *J Clin Oncol,* **33,** 3911-20.
553. Boyd, K. D., Ross, F. M., Walker, B. A., Wardell, C. P., Tapper, W. J., Chiecchio, L., Dagrada, G., Konn, Z. J., Gregory, W. M., Jackson, G. H.*, et al.* (2011). Mapping of chromosome 1p deletions in myeloma identifies fam46c at 1p12 and cdkn2c at 1p32.3 as being genes in regions associated with adverse survival. *Clin Cancer Res,* **17,** 7776-84.
554. Wan, X. Y., Zhai, X. F., Jiang, Y. P., Han, T., Zhang, Q. Y. & Xin, H. L. (2017). Antimetastatic effects of norcantharidin on hepatocellular carcinoma cells by up-regulating fam46c expression. *Am J Transl Res,* **9,** 155-166.
555. Zhang, Q. Y., Yue, X. Q., Jiang, Y. P., Han, T. & Xin, H. L. (2017). Author correction: Fam46c is critical for the anti-proliferation and pro-apoptotic effects of norcantharidin in hepatocellular carcinoma cells. *Sci Rep,* **7,** 17576.
556. Tanaka, H., Kanda, M., Shimizu, D., Tanaka, C., Kobayashi, D., Hayashi, M., Iwata, N., Yamada, S., Fujii, T., Nakayama, G.*, et al.* (2017). Fam46c serves as a predictor of hepatic recurrence in patients with resectable gastric cancer. *Ann Surg Oncol,* **24,** 3438-3445.
557. Van Eyck, L., Bruni, F., Ronan, A., Briggs, T. A., Roscioli, T., Rice, G. I., Vassallo, G., Rodero, M. P., He, L., Taylor, R. W.*, et al.* (2020). Biallelic mutations in mtpap associated with a lethal encephalopathy. *Neuropediatrics,* **51,** 178-184.
558. Kleiman, F. E. & Manley, J. L. (1999). Functional interaction of brca1-associated bard1 with polyadenylation factor cstf-50. *Science,* **285,** 1576-9.
559. Kleiman, F. E., Wu-Baer, F., Fonseca, D., Kaneko, S., Baer, R. & Manley, J. L. (2005). Brca1/bard1 inhibition of mrna 3' processing involves targeted degradation of rna polymerase ii. *Genes Dev,* **19,** 1227-37.
560. Shinohara, A., Ogawa, H. & Ogawa, T. (1992). Rad51 protein involved in repair and recombination in s. Cerevisiae is a reca-like protein. *Cell,* **69,** 457-70.
561. Maldonado, E., Shiekhattar, R., Sheldon, M., Cho, H., Drapkin, R., Rickert, P., Lees, E., Anderson, C. W., Linn, S. & Reinberg, D. (1996). A human rna polymerase ii complex associated with srb and DNA-repair proteins. *Nature,* **381,** 86-9.
562. Scully, R., Chen, J., Plug, A., Xiao, Y., Weaver, D., Feunteun, J., Ashley, T. & Livingston, D. M. (1997). Association of brca1 with rad51 in mitotic and meiotic cells. *Cell,* **88,** 265-75.
563. Scully, R., Anderson, S. F., Chao, D. M., Wei, W., Ye, L., Young, R. A., Livingston, D. M. & Parvin, J. D. (1997). Brca1 is a component of the rna polymerase ii holoenzyme. *Proc Natl Acad Sci U S A,* **94,** 5605-10.
564. Cevher, M. A., Zhang, X., Fernandez, S., Kim, S., Baquero, J., Nilsson, P., Lee, S., Virtanen, A. & Kleiman, F. E. (2010). Nuclear deadenylation/polyadenylation factors regulate 3' processing in response to DNA damage. *EMBO J,* **29,** 1674-87.
565. López de Silanes, I., Quesada, M. P. & Esteller, M. (2007). Aberrant regulation of messenger rna 3'-untranslated region in human cancer. *Cell Oncol,* **29,** 1-17.
566. Zhang, Y., Liu, L., Qiu, Q., Zhou, Q., Ding, J., Lu, Y. & Liu, P. (2021). Alternative polyadenylation: Methods, mechanism, function, and role in cancer. *J Exp Clin Cancer Res,* **40,** 51.
567. Wang, L., Lang, G. T., Xue, M. Z., Yang, L., Chen, L., Yao, L., Li, X. G., Wang, P., Hu, X. & Shao, Z. M. (2020). Dissecting the heterogeneity of the alternative polyadenylation profiles in triple-negative breast cancers. *Theranostics,* **10,** 10531-10547.

568. Mbita, Z., Meyer, M., Skepu, A., Hosie, M., Rees, J. & Dlamini, Z. (2012). De-regulation of the rbbp6 isoform 3/dwnn in human cancers. *Mol Cell Biochem,* **362,** 249-62.
569. Di Giammartino, D. C., Li, W., Ogami, K., Yashinskie, J. J., Hoque, M., Tian, B. & Manley, J. L. (2014). Rbbp6 isoforms regulate the human polyadenylation machinery and modulate expression of mrnas with au-rich 3' utrs. *Genes Dev,* **28,** 2248-60.
570. Li, L., Deng, B., Xing, G., Teng, Y., Tian, C., Cheng, X., Yin, X., Yang, J., Gao, X., Zhu, Y.*, et al.* (2007). Pact is a negative regulator of p53 and essential for cell growth and embryonic development. *Proc Natl Acad Sci U S A,* **104,** 7951-6.
571. Kim, J., Nakamura, J., Hamada, C., Taketomi, T., Yano, S., Okajima, T., Kashiwabara, S. I., Baba, T., Sato, B., Chiba, T.*, et al.* (2020). Usp15 deubiquitinates tut1 associated with rna metabolism and maintains cerebellar homeostasis. *Mol Cell Biol,* **40**.
572. Stewart, M. (2019). Polyadenylation and nuclear export of mrnas. *J Biol Chem,* **294,** 2977-2987.
573. Xie, Y. & Ren, Y. (2019). Mechanisms of nuclear mrna export: A structural perspective. *Traffic,* **20,** 829-840.
574. Galloway, A. & Cowling, V. H. (2019). Mrna cap regulation in mammalian cell function and fate. *Biochim Biophys Acta Gene Regul Mech,* **1862,** 270-279.
575. Viphakone, N., Sudbery, I., Griffith, L., Heath, C. G., Sims, D. & Wilson, S. A. (2019). Co-transcriptional loading of rna export factors shapes the human transcriptome. *Mol Cell,* **75,** 310-323.e8.
576. Williams, T., Ngo, L. H. & Wickramasinghe, V. O. (2018). Nuclear export of rna: Different sizes, shapes and functions. *Semin Cell Dev Biol,* **75,** 70-77.
577. Grüter, P., Tabernero, C., von Kobbe, C., Schmitt, C., Saavedra, C., Bachi, A., Wilm, M., Felber, B. K. & Izaurralde, E. (1998). Tap, the human homolog of mex67p, mediates cte-dependent rna export from the nucleus. *Mol Cell,* **1,** 649-59.
578. Chang, C. T., Hautbergue, G. M., Walsh, M. J., Viphakone, N., van Dijk, T. B., Philipsen, S. & Wilson, S. A. (2013). Chtop is a component of the dynamic trex mrna export complex. *EMBO J,* **32,** 473-86.
579. Katahira, J., Inoue, H., Hurt, E. & Yoneda, Y. (2009). Adaptor aly and co-adaptor thoc5 function in the tap-p15-mediated nuclear export of hsp70 mrna. *EMBO J,* **28,** 556-67.
580. Zolotukhin, A. S., Uranishi, H., Lindtner, S., Bear, J., Pavlakis, G. N. & Felber, B. K. (2009). Nuclear export factor rbm15 facilitates the access of dbp5 to mrna. *Nucleic Acids Res,* **37,** 7151-62.
581. Folco, E. G., Lee, C. S., Dufu, K., Yamazaki, T. & Reed, R. (2012). The proteins pdip3 and zc11a associate with the human trex complex in an atp-dependent manner and function in mrna export. *PLoS One,* **7,** e43804.
582. Dufu, K., Livingstone, M. J., Seebacher, J., Gygi, S. P., Wilson, S. A. & Reed, R. (2010). Atp is required for interactions between uap56 and two conserved mrna export proteins, aly and cip29, to assemble the trex complex. *Genes Dev,* **24,** 2043-53.
583. Hautbergue, G. M., Hung, M. L., Walsh, M. J., Snijders, A. P., Chang, C. T., Jones, R., Ponting, C. P., Dickman, M. J. & Wilson, S. A. (2009). Uif, a new mrna export adaptor that works together with ref/aly, requires fact for recruitment to mrna. *Curr Biol,* **19,** 1918-24.
584. Golovanov, A. P., Hautbergue, G. M., Tintaru, A. M., Lian, L. Y. & Wilson, S. A. (2006). The solution structure of ref2-i reveals interdomain interactions and regions involved in binding mrna export factors and rna. *RNA,* **12,** 1933-48.
585. Hautbergue, G. M., Hung, M. L., Golovanov, A. P., Lian, L. Y. & Wilson, S. A. (2008). Mutually exclusive interactions drive handover of mrna from export adaptors to tap. *Proc Natl Acad Sci U S A,* **105,** 5154-9.

586. Domínguez-Sánchez, M. S., Barroso, S., Gómez-González, B., Luna, R. & Aguilera, A. (2011). Genome instability and transcription elongation impairment in human cells depleted of tho/trex. *PLoS Genet,* **7,** e1002386.
587. Burd, C. G., Matunis, E. L. & Dreyfuss, G. (1991). The multiple rna-binding domains of the mrna poly(a)-binding protein have different rna-binding activities. *Mol Cell Biol,* **11,** 3419-24.
588. Kühn, U. & Pieler, T. (1996). Xenopus poly(a) binding protein: Functional domains in rna binding and protein-protein interaction. *J Mol Biol,* **256,** 20-30.
589. Deo, R. C., Bonanno, J. B., Sonenberg, N. & Burley, S. K. (1999). Recognition of polyadenylate rna by the poly(a)-binding protein. *Cell,* **98,** 835-45.
590. Xie, J., Kozlov, G. & Gehring, K. (2014). The "tale" of poly(a) binding protein: The mlle domain and pam2-containing proteins. *Biochim Biophys Acta,* **1839,** 1062-8.
591. Baer, B. W. & Kornberg, R. D. (1983). The protein responsible for the repeating structure of cytoplasmic poly(a)-ribonucleoprotein. *J Cell Biol,* **96,** 717-21.
592. Gu, S., Jeon, H. M., Nam, S. W., Hong, K. Y., Rahman, M. S., Lee, J. B., Kim, Y. & Jang, S. K. (2022). The flip-flop configuration of the pabp-dimer leads to switching of the translation function. *Nucleic Acids Res,* **50,** 306-321.
593. Uchida, N., Hoshino, S., Imataka, H., Sonenberg, N. & Katada, T. (2002). A novel role of the mammalian gspt/erf3 associating with poly(a)-binding protein in cap/poly(a)-dependent translation. *J Biol Chem,* **277,** 50286-92.
594. Hoshino, S., Imai, M., Kobayashi, T., Uchida, N. & Katada, T. (1999). The eukaryotic polypeptide chain releasing factor (erf3/gspt) carrying the translation termination signal to the 3'-poly(a) tail of mrna. Direct association of erf3/gspt with polyadenylate-binding protein. *J Biol Chem,* **274,** 16677-80.
595. Wigington, C. P., Williams, K. R., Meers, M. P., Bassell, G. J. & Corbett, A. H. (2014). Poly(a) rna-binding proteins and polyadenosine rna: New members and novel functions. *Wiley Interdiscip Rev RNA,* **5,** 601-22.
596. Smith, B. L., Gallie, D. R., Le, H. & Hansma, P. K. (1997). Visualization of poly(a)-binding protein complex formation with poly(a) rna using atomic force microscopy. *J Struct Biol,* **119,** 109-17.
597. Shirokikh, N. E. & Preiss, T. (2018). Translation initiation by cap-dependent ribosome recruitment: Recent insights and open questions. *Wiley Interdiscip Rev RNA,* **9,** e1473.
598. Leppek, K., Das, R. & Barna, M. (2018). Functional 5' utr mrna structures in eukaryotic translation regulation and how to find them. *Nat Rev Mol Cell Biol,* **19,** 158-174.
599. Safaee, N., Kozlov, G., Noronha, A. M., Xie, J., Wilds, C. J. & Gehring, K. (2012). Interdomain allostery promotes assembly of the poly(a) mrna complex with pabp and eif4g. *Mol Cell,* **48,** 375-86.
600. Kapp, L. D. & Lorsch, J. R. (2004). The molecular mechanics of eukaryotic translation. *Annu Rev Biochem,* **73,** 657-704.
601. Preiss, T. & Hentze, M. W. (1998). Dual function of the messenger rna cap structure in poly(a)-tail-promoted translation in yeast. *Nature,* **392,** 516-20.
602. Rau, M., Ohlmann, T., Morley, S. J. & Pain, V. M. (1996). A reevaluation of the cap-binding protein, eif4e, as a rate-limiting factor for initiation of translation in reticulocyte lysate. *J Biol Chem,* **271,** 8983-90.
603. Yanagiya, A., Suyama, E., Adachi, H., Svitkin, Y. V., Aza-Blanc, P., Imataka, H., Mikami, S., Martineau, Y., Ronai, Z. A. & Sonenberg, N. (2012). Translational homeostasis via the mrna cap-binding protein, eif4e. *Mol Cell,* **46,** 847-58.

604. Iizuka, N., Najita, L., Franzusoff, A. & Sarnow, P. (1994). Cap-dependent and cap-independent translation by internal initiation of mrnas in cell extracts prepared from saccharomyces cerevisiae. *Mol Cell Biol,* **14,** 7322-30.
605. Preiss, T., Muckenthaler, M. & Hentze, M. W. (1998). Poly(a)-tail-promoted translation in yeast: Implications for translational control. *RNA,* **4,** 1321-31.
606. Eisen, T. J., Li, J. J. & Bartel, D. P. (2022). The interplay between translational efficiency, poly(a) tails, micrornas, and neuronal activation. *RNA,* **28,** 808-831.
607. Sheiness, D., Puckett, L. & Darnell, J. E. (1975). Possible relationship of poly(a) shortening to mrna turnover. *Proc Natl Acad Sci U S A,* **72,** 1077-81.
608. Sawicki, S. G., Jelinek, W. & Darnell, J. E. (1977). 3'-terminal addition to hela cell nuclear and cytoplasmic poly (a). *J Mol Biol,* **113,** 219-35.
609. Legnini, I., Alles, J., Karaiskos, N., Ayoub, S. & Rajewsky, N. (2019). Flam-seq: Full-length mrna sequencing reveals principles of poly(a) tail length control. *Nat Methods,* **16,** 879-886.
610. Workman, R. E., Tang, A. D., Tang, P. S., Jain, M., Tyson, J. R., Razaghi, R., Zuzarte, P. C., Gilpatrick, T., Payne, A., Quick, J.*, et al.* (2019). Nanopore native rna sequencing of a human poly(a) transcriptome. *Nat Methods,* **16,** 1297-1305.
611. Subtelny, A. O., Eichhorn, S. W., Chen, G. R., Sive, H. & Bartel, D. P. (2014). Poly(a)-tail profiling reveals an embryonic switch in translational control. *Nature,* **508,** 66-71.
612. Lima, S. A., Chipman, L. B., Nicholson, A. L., Chen, Y. H., Yee, B. A., Yeo, G. W., Coller, J. & Pasquinelli, A. E. (2017). Short poly(a) tails are a conserved feature of highly expressed genes. *Nat Struct Mol Biol,* **24,** 1057-1063.
613. Mattijssen, S., Iben, J. R., Li, T., Coon, S. L. & Maraia, R. J. (2020). Single molecule poly(a) tail-seq shows larp4 opposes deadenylation throughout mrna lifespan with most impact on short tails. *Elife,* **9**.
614. Chang, H., Lim, J., Ha, M. & Kim, V. N. (2014). Tail-seq: Genome-wide determination of poly(a) tail length and 3' end modifications. *Mol Cell,* **53,** 1044-52.
615. Lim, J., Lee, M., Son, A., Chang, H. & Kim, V. N. (2016). Mtail-seq reveals dynamic poly(a) tail regulation in oocyte-to-embryo development. *Genes Dev,* **30,** 1671-82.
616. Brewer, G. & Ross, J. (1988). Poly(a) shortening and degradation of the 3' a+u-rich sequences of human c-myc mrna in a cell-free system. *Mol Cell Biol,* **8,** 1697-708.
617. Archer, S. K., Shirokikh, N. E., Hallwirth, C. V., Beilharz, T. H. & Preiss, T. (2015). Probing the closed-loop model of mrna translation in living cells. *RNA Biol,* **12,** 248-54.
618. Bernstein, P., Peltz, S. W. & Ross, J. (1989). The poly(a)-poly(a)-binding protein complex is a major determinant of mrna stability in vitro. *Mol Cell Biol,* **9,** 659-70.
619. Siddiqui, N., Mangus, D. A., Chang, T. C., Palermino, J. M., Shyu, A. B. & Gehring, K. (2007). Poly(a) nuclease interacts with the c-terminal domain of polyadenylate-binding protein domain from poly(a)-binding protein. *J Biol Chem,* **282,** 25067-75.
620. Schäfer, I. B., Yamashita, M., Schuller, J. M., Schüssler, S., Reichelt, P., Strauss, M. & Conti, E. (2019). Molecular basis for poly(a) rnp architecture and recognition by the pan2-pan3 deadenylase. *Cell,* **177,** 1619-1631.e21.
621. Tucker, M., Valencia-Sanchez, M. A., Staples, R. R., Chen, J., Denis, C. L. & Parker, R. (2001). The transcription factor associated ccr4 and caf1 proteins are components of the major cytoplasmic mrna deadenylase in saccharomyces cerevisiae. *Cell,* **104,** 377-86.

622. Chen, J., Chiang, Y. C. & Denis, C. L. (2002). Ccr4, a 3'-5' poly(a) rna and ssdna exonuclease, is the catalytic component of the cytoplasmic deadenylase. *EMBO J,* **21,** 1414-26.
623. Alhusaini, N. & Coller, J. (2016). The deadenylase components not2p, not3p, and not5p promote mrna decapping. *RNA,* **22,** 709-21.
624. Raisch, T., Chang, C. T., Levdansky, Y., Muthukumar, S., Raunser, S. & Valkov, E. (2019). Reconstitution of recombinant human ccr4-not reveals molecular insights into regulated deadenylation. *Nat Commun,* **10,** 3173.
625. Jiang, H., Wolgast, M., Beebe, L. M. & Reese, J. C. (2019). Ccr4-not maintains genomic integrity by controlling the ubiquitylation and degradation of arrested rnapii. *Genes Dev,* **33,** 705-717.
626. Panasenko, O. O. (2014). The role of the e3 ligase not4 in cotranslational quality control. *Front Genet,* **5,** 141.
627. Webster, M. W., Chen, Y. H., Stowell, J. A. W., Alhusaini, N., Sweet, T., Graveley, B. R., Coller, J. & Passmore, L. A. (2018). Mrna deadenylation is coupled to translation rates by the differential activities of ccr4-not nucleases. *Mol Cell,* **70,** 1089-1100.e8.
628. Liu, J., Lu, X., Zhang, S., Yuan, L. & Sun, Y. (2022). Molecular insights into mrna polyadenylation and deadenylation. *Int J Mol Sci,* **23**.
629. Yamashita, A., Chang, T. C., Yamashita, Y., Zhu, W., Zhong, Z., Chen, C. Y. & Shyu, A. B. (2005). Concerted action of poly(a) nucleases and decapping enzyme in mammalian mrna turnover. *Nat Struct Mol Biol,* **12,** 1054-63.
630. Yi, C., Wang, Y., Zhang, C., Xuan, Y., Zhao, S., Liu, T., Li, W., Liao, Y., Feng, X., Hao, J.*, et al.* (2016). Cleavage and polyadenylation specific factor 4 targets nf-κb/cyclooxygenase-2 signaling to promote lung cancer growth and progression. *Cancer Lett,* **381,** 1-13.
631. Yang, Q., Fan, W., Zheng, Z., Lin, S., Liu, C., Wang, R., Li, W., Zuo, Y., Sun, Y., Hu, S.*, et al.* (2019). Cleavage and polyadenylation specific factor 4 promotes colon cancer progression by transcriptionally activating htert. *Biochim Biophys Acta Mol Cell Res,* **1866,** 1533-1543.
632. Twu, K. Y., Noah, D. L., Rao, P., Kuo, R. L. & Krug, R. M. (2006). The cpsf30 binding site on the ns1a protein of influenza a virus is a potential antiviral target. *J Virol,* **80,** 3957-65.
633. Rosário-Ferreira, N., Preto, A. J., Melo, R., Moreira, I. S. & Brito, R. M. M. (2020). The central role of non-structural protein 1 (ns1) in influenza biology and infection. *Int J Mol Sci,* **21**.
634. Zhang, M., Lin, H., Ge, X. & Xu, Y. (2021). Overproduced cpsf4 promotes cell proliferation and invasion via pi3k-akt signaling pathway in oral squamous cell carcinoma. *J Oral Maxillofac Surg,* **79,** 1177.e1-1177.e14.
635. Chen, W., Guo, W., Li, M., Shi, D., Tian, Y., Li, Z., Wang, J., Fu, L., Xiao, X., Liu, Q. Q.*, et al.* (2013). Upregulation of cleavage and polyadenylation specific factor 4 in lung adenocarcinoma and its critical role for cancer cell survival and proliferation. *PLoS One,* **8,** e82728.
636. Li, Z., Xu, X., Li, Y., Zou, K., Zhang, Z., Liao, Y., Zhao, X., Jiang, W., Yu, W., Guo, W.*, et al.* (2018). Synergistic antitumor effect of bkm120 with prima-1met via inhibiting pi3k/akt/mtor and cpsf4/htert signaling and reactivating mutant p53. *Cell Physiol Biochem,* **45,** 1772-1786.
637. Wu, J., Miao, J., Ding, Y., Zhang, Y., Huang, X., Zhou, X. & Tang, R. (2019). Mir-4458 inhibits breast cancer cell growth, migration, and invasiveness by targeting cpsf4. *Biochem Cell Biol,* **97,** 722-730.
638. Li, N., Jiang, S., Fu, R., Lv, J., Yao, J., Mai, J., Hua, X., Chen, H., Liu, J. & Lu, M. (2021). Cleavage and polyadenylation-specific factor 3 induces cell cycle arrest via pi3k/akt/gsk-3β signaling pathways and predicts a negative prognosis in hepatocellular carcinoma. *Biomark Med,* **15,** 347-358.

639. Zu, Y., Wang, D., Ping, W. & Sun, W. (2022). The roles of cpsf6 in proliferation, apoptosis and tumorigenicity of lung adenocarcinoma. *Aging (Albany NY),* **14,** 9300-9316.
640. An, W. & Yu, F. (2022). Silencing of. *Open Med (Wars),* **17,** 1655-1663.
641. Ogorodnikov, A., Levin, M., Tattikota, S., Tokalov, S., Hoque, M., Scherzinger, D., Marini, F., Poetsch, A., Binder, H., Macher-Göppinger, S.*, et al.* (2018). Transcriptome 3'end organization by pcf11 links alternative polyadenylation to formation and neuronal differentiation of neuroblastoma. *Nat Commun,* **9,** 5331.
642. Xiong, M., Chen, L., Zhou, L., Ding, Y., Kazobinka, G., Chen, Z. & Hou, T. (2019). Nudt21 inhibits bladder cancer progression through anxa2 and limk2 by alternative polyadenylation. *Theranostics,* **9,** 7156-7167.
643. Tseng, H. W., Mota-Sydor, A., Leventis, R., Jovanovic, P., Topisirovic, I. & Duchaine, T. F. (2022). Distinct, opposing functions for cfim59 and cfim68 in mrna alternative polyadenylation of pten and in the pi3k/akt signalling cascade. *Nucleic Acids Res,* **50,** 9397-9412.
644. Penman, S., Rosbash, M. & Penman, M. (1970). Messenger and heterogeneous nuclear rna in hela cells: Differential inhibition by cordycepin. *Proc Natl Acad Sci U S A,* **67,** 1878-85.
645. Rose, K. M., Bell, L. E. & Jacob, S. T. (1977). Specific inhibition of chromatin-associated poly(a) synthesis in vitro by cordycepin 5'-triphosphate. *Nature,* **267,** 178-80.
646. Müller, W. E., Seibert, G., Beyer, R., Breter, H. J., Maidhof, A. & Zahn, R. K. (1977). Effect of cordycepin on nucleic acid metabolism in l5178y cells and on nucleic acid-synthesizing enzyme systems. *Cancer Res,* **37,** 3824-33.
647. Turner, R. E., Harrison, P. F., Swaminathan, A., Kraupner-Taylor, C. A., Goldie, B. J., See, M., Peterson, A. L., Schittenhelm, R. B., Powell, D. R., Creek, D. J.*, et al.* (2021). Genetic and pharmacological evidence for kinetic competition between alternative poly(a) sites in yeast. *Elife,* **10**.
648. Li, M., Zhang, C. S., Feng, J. W., Wei, X., Zhang, C., Xie, C., Wu, Y., Hawley, S. A., Atrih, A., Lamont, D. J.*, et al.* (2021). Aldolase is a sensor for both low and high glucose, linking to ampk and mtorc1. *Cell Res,* **31,** 478-481.
649. Cheratta, A. R., Thayyullathil, F., Hawley, S. A., Ross, F. A., Atrih, A., Lamont, D. J., Pallichankandy, S., Subburayan, K., Alakkal, A., Rezgui, R.*, et al.* (2022). Caspase cleavage and nuclear retention of the energy sensor ampk-α1 during apoptosis. *Cell Rep,* **39,** 110761.
650. Schmidt, M. H. H., Furnari, F. B., Cavenee, W. K. & Bögler, O. (2003). Epidermal growth factor receptor signaling intensity determines intracellular protein interactions, ubiquitination, and internalization. *Proc Natl Acad Sci U S A,* **100,** 6505-10.
651. Yavas, S., Macháň, R. & Wohland, T. (2016). The epidermal growth factor receptor forms location-dependent complexes in resting cells. *Biophys J,* **111,** 2241-2254.
652. Gharbi, S. I., Zvelebil, M. J., Shuttleworth, S. J., Hancox, T., Saghir, N., Timms, J. F. & Waterfield, M. D. (2007). Exploring the specificity of the pi3k family inhibitor ly294002. *Biochem J,* **404,** 15-21.
653. Folkes, A. J., Ahmadi, K., Alderton, W. K., Alix, S., Baker, S. J., Box, G., Chuckowree, I. S., Clarke, P. A., Depledge, P., Eccles, S. A.*, et al.* (2008). The identification of 2-(1h-indazol-4-yl)-6-(4-methanesulfonyl-piperazin-1-ylmethyl)-4-morpholin-4-yl-thieno[3,2-d]pyrimidine (gdc-0941) as a potent, selective, orally bioavailable inhibitor of class i pi3 kinase for the treatment of cancer. *J Med Chem,* **51,** 5522-32.
654. Stirrups, R. (2019). Alpelisib plus fulvestrant for pik3ca-mutated breast cancer. *Lancet Oncol,* **20,** e347.
655. Markham, A. (2019). Alpelisib: First global approval. *Drugs,* **79,** 1249-1253.

656. Liu, Q., Chang, J. W., Wang, J., Kang, S. A., Thoreen, C. C., Markhard, A., Hur, W., Zhang, J., Sim, T., Sabatini, D. M.*, et al.* (2010). Discovery of 1-(4-(4-propionylpiperazin-1-yl)-3-(trifluoromethyl)phenyl)-9-(quinolin-3-yl)benzo[h][1,6]naphthyridin-2(1h)-one as a highly potent, selective mammalian target of rapamycin (mtor) inhibitor for the treatment of cancer. *J Med Chem,* **53,** 7146-55.
657. Kim, A. S., Miller, E. J., Wright, T. M., Li, J., Qi, D., Atsina, K., Zaha, V., Sakamoto, K. & Young, L. H. (2011). A small molecule ampk activator protects the heart against ischemia-reperfusion injury. *J Mol Cell Cardiol,* **51,** 24-32.
658. Göransson, O., McBride, A., Hawley, S. A., Ross, F. A., Shpiro, N., Foretz, M., Viollet, B., Hardie, D. G. & Sakamoto, K. (2007). Mechanism of action of a-769662, a valuable tool for activation of amp-activated protein kinase. *J Biol Chem,* **282,** 32549-60.
659. Alessi, D. R., Cuenda, A., Cohen, P., Dudley, D. T. & Saltiel, A. R. (1995). Pd 098059 is a specific inhibitor of the activation of mitogen-activated protein kinase kinase in vitro and in vivo. *J Biol Chem,* **270,** 27489-94.
660. Schmittgen, T. D., Lee, E. J. & Jiang, J. (2008). High-throughput real-time pcr. *Methods Mol Biol,* **429,** 89-98.
661. Queiroz, R. M. L., Smith, T., Villanueva, E., Marti-Solano, M., Monti, M., Pizzinga, M., Mirea, D. M., Ramakrishna, M., Harvey, R. F., Dezi, V.*, et al.* (2019). Comprehensive identification of rna-protein interactions in any organism using orthogonal organic phase separation (oops). *Nat Biotechnol,* **37,** 169-178.
662. Niranjanakumari, S., Lasda, E., Brazas, R. & Garcia-Blanco, M. A. (2002). Reversible cross-linking combined with immunoprecipitation to study rna-protein interactions in vivo. *Methods,* **26,** 182-90.
663. Matsunaga, F., Forterre, P., Ishino, Y. & Myllykallio, H. (2001). In vivo interactions of archaeal cdc6/orc1 and minichromosome maintenance proteins with the replication origin. *Proc Natl Acad Sci U S A,* **98,** 11152-7.
664. Khurshid, A. (2015). *The effect of the polyadenylation inhibitor cordycepin on mcf-7 cells. phd thesis, university of nottingham.*
665. Ritchie, M. E., Phipson, B., Wu, D., Hu, Y., Law, C. W., Shi, W. & Smyth, G. K. (2015). Limma powers differential expression analyses for rna-sequencing and microarray studies. *Nucleic Acids Res,* **43,** e47.
666. Peart, M. J., Smyth, G. K., van Laar, R. K., Bowtell, D. D., Richon, V. M., Marks, P. A., Holloway, A. J. & Johnstone, R. W. (2005). Identification and functional significance of genes regulated by structurally different histone deacetylase inhibitors. *Proc Natl Acad Sci U S A,* **102,** 3697-702.
667. Caiazzo, M., Dell'Anno, M. T., Dvoretskova, E., Lazarevic, D., Taverna, S., Leo, D., Sotnikova, T. D., Menegon, A., Roncaglia, P., Colciago, G.*, et al.* (2011). Direct generation of functional dopaminergic neurons from mouse and human fibroblasts. *Nature,* **476,** 224-7.
668. Hubert, F. X., Kinkel, S. A., Crewther, P. E., Cannon, P. Z., Webster, K. E., Link, M., Uibo, R., O'Bryan, M. K., Meager, A., Forehan, S. P.*, et al.* (2009). Aire-deficient c57bl/6 mice mimicking the common human 13-base pair deletion mutation present with only a mild autoimmune phenotype. *J Immunol,* **182,** 3902-18.
669. Mannsperger, H. A., Gade, S., Henjes, F., Beissbarth, T. & Korf, U. (2010). Rppanalyzer: Analysis of reverse-phase protein array data. *Bioinformatics,* **26,** 2202-3.
670. Sheridan, J. M., Ritchie, M. E., Best, S. A., Jiang, K., Beck, T. J., Vaillant, F., Liu, K., Dickins, R. A., Smyth, G. K., Lindeman, G. J.*, et al.* (2015). A pooled shrna screen for regulators of primary mammary stem and progenitor cells identifies roles for asap1 and prox1. *BMC Cancer,* **15,** 221.

671. R Core Team (2021). R: A language and environment for statistical computing. R foundation for statistical computing, vienna, austria. Url https://www.R-project.Org/.
672. Silver, J. D., Ritchie, M. E. & Smyth, G. K. (2009). Microarray background correction: Maximum likelihood estimation for the normal-exponential convolution. *Biostatistics,* **10,** 352-63.
673. Bolstad, B. M., Irizarry, R. A., Astrand, M. & Speed, T. P. (2003). A comparison of normalization methods for high density oligonucleotide array data based on variance and bias. *Bioinformatics,* **19,** 185-93.
674. Smyth, G. K. (2004). Linear models and empirical bayes methods for assessing differential expression in microarray experiments. *Stat Appl Genet Mol Biol,* **3,** Article3.
675. Benjamini, Y., & Hochberg, Y. (1995). Controlling the false discovery rate: A practical and powerful approach to multiple testing. J*. R. Stat. Soc. Ser. B (methodol.),5***7,**289-300.
676. Kukurba, K. R. & Montgomery, S. B. (2015). Rna sequencing and analysis. *Cold Spring Harb Protoc,* **2015,** 951-69.
677. Tellier, M. & Murphy, S. (2020). Incomplete removal of ribosomal rna can affect chromatin rna-seq data analysis. *Transcription,* **11,** 230-235.
678. Andrews, S. (2010). Fastqc: A quality control tool for high throughput sequence data [online]. Available online at: Http://www.Bioinformatics.Babraham.Ac.Uk/projects/fastqc/.
679. Li, P., Piao, Y., Shon, H. S. & Ryu, K. H. (2015). Comparing the normalization methods for the differential analysis of illumina high-throughput rna-seq data. *BMC Bioinformatics,* **16,** 347.
680. Corchete, L. A., Rojas, E. A., Alonso-López, D., De Las Rivas, J., Gutiérrez, N. C. & Burguillo, F. J. (2020). Systematic comparison and assessment of rna-seq procedures for gene expression quantitative analysis. *Sci Rep,* **10,** 19737.
681. Liao, Y., Smyth, G. K. & Shi, W. (2013). The subread aligner: Fast, accurate and scalable read mapping by seed-and-vote. *Nucleic Acids Res,* **41,** e108.
682. Liao, Y., Smyth, G. K. & Shi, W. (2019). The r package rsubread is easier, faster, cheaper and better for alignment and quantification of rna sequencing reads. *Nucleic Acids Res,* **47,** e47.
683. Liao, Y., Smyth, G. K. & Shi, W. (2014). Featurecounts: An efficient general purpose program for assigning sequence reads to genomic features. *Bioinformatics,* **30,** 923-30.
684. Robinson, M. D., McCarthy, D. J. & Smyth, G. K. (2010). Edger: A bioconductor package for differential expression analysis of digital gene expression data. *Bioinformatics,* **26,** 139-40.
685. Mortazavi, A., Williams, B. A., McCue, K., Schaeffer, L. & Wold, B. (2008). Mapping and quantifying mammalian transcriptomes by rna-seq. *Nat Methods,* **5,** 621-8.
686. Conesa, A., Madrigal, P., Tarazona, S., Gomez-Cabrero, D., Cervera, A., McPherson, A., Szcześniak, M. W., Gaffney, D. J., Elo, L. L., Zhang, X.*, et al.* (2016). A survey of best practices for rna-seq data analysis. *Genome Biol,* **17,** 13.
687. Bullard, J. H., Purdom, E., Hansen, K. D. & Dudoit, S. (2010). Evaluation of statistical methods for normalization and differential expression in mrna-seq experiments. *BMC Bioinformatics,* **11,** 94.
688. Abbas-Aghababazadeh, F., Li, Q. & Fridley, B. L. (2018). Comparison of normalization approaches for gene expression studies completed with high-throughput sequencing. *PLoS One,* **13,** e0206312.
689. Dillies, M. A., Rau, A., Aubert, J., Hennequet-Antier, C., Jeanmougin, M., Servant, N., Keime, C., Marot, G., Castel, D., Estelle, J.*, et al.* (2013). A

comprehensive evaluation of normalization methods for illumina high-throughput rna sequencing data analysis. *Brief Bioinform,* **14,** 671-83.
690. Huang, d. W., Sherman, B. T. & Lempicki, R. A. (2009). Systematic and integrative analysis of large gene lists using david bioinformatics resources. *Nat Protoc,* **4,** 44-57.
691. Krämer, A., Green, J., Pollard, J. & Tugendreich, S. (2014). Causal analysis approaches in ingenuity pathway analysis. *Bioinformatics,* **30,** 523-30.
692. Iglesias, N., Tutucci, E., Gwizdek, C., Vinciguerra, P., Von Dach, E., Corbett, A. H., Dargemont, C. & Stutz, F. (2010). Ubiquitin-mediated mrnp dynamics and surveillance prior to budding yeast mrna export. *Genes Dev,* **24,** 1927-38.
693. Johnson, S. A., Cubberley, G. & Bentley, D. L. (2009). Cotranscriptional recruitment of the mrna export factor yra1 by direct interaction with the 3' end processing factor pcf11. *Mol Cell,* **33,** 215-26.
694. Morris, K. J. & Corbett, A. H. (2018). The polyadenosine rna-binding protein zc3h14 interacts with the tho complex and coordinately regulates the processing of neuronal transcripts. *Nucleic Acids Res,* **46,** 6561-6575.
695. Silla, T., Karadoulama, E., Mąkosa, D., Lubas, M. & Jensen, T. H. (2018). The rna exosome adaptor zfc3h1 functionally competes with nuclear export activity to retain target transcripts. *Cell Rep,* **23,** 2199-2210.
696. Zarkower, D. & Wickens, M. (1987). Formation of mrna 3' termini: Stability and dissociation of a complex involving the aauaaa sequence. *EMBO J,* **6,** 177-86.
697. Ryner, L. C. & Manley, J. L. (1987). Requirements for accurate and efficient mrna 3' end cleavage and polyadenylation of a simian virus 40 early pre-rna in vitro. *Mol Cell Biol,* **7,** 495-503.
698. Cheng, C. & Zhu, X. (2019). Cordycepin mitigates mptp-induced parkinson's disease through inhibiting tlr/nf-κb signaling pathway. *Life Sci,* **223,** 120-127.
699. Choi, Y. H., Kim, G. Y. & Lee, H. H. (2014). Anti-inflammatory effects of cordycepin in lipopolysaccharide-stimulated raw 264.7 macrophages through toll-like receptor 4-mediated suppression of mitogen-activated protein kinases and nf-κb signaling pathways. *Drug Des Devel Ther,* **8,** 1941-53.
700. Sun, T., Dong, W., Jiang, G., Yang, J., Liu, J., Zhao, L. & Ma, P. (2019). Improves chronic kidney disease by affecting tlr4/nf-. *Oxid Med Cell Longev,* **2019,** 7850863.
701. Guo, Z., Chen, W., Dai, G. & Huang, Y. (2020). Cordycepin suppresses the migration and invasion of human liver cancer cells by downregulating the expression of cxcr4. *Int J Mol Med,* **45,** 141-150.
702. Kim, J., Lee, H., Kang, K. S., Chun, K. H. & Hwang, G. S. (2015). Cordyceps militaris mushroom and cordycepin inhibit rankl-induced osteoclast differentiation. *J Med Food,* **18,** 446-52.
703. Noh, E. M., Youn, H. J., Jung, S. H., Han, J. H., Jeong, Y. J., Chung, E. Y., Jung, J. Y., Kim, B. S., Lee, S. H., Lee, Y. R.*, et al.* (2010). Cordycepin inhibits tpa-induced matrix metalloproteinase-9 expression by suppressing the mapk/ap-1 pathway in mcf-7 human breast cancer cells. *Int J Mol Med,* **25,** 255-60.
704. Baik, J. S., Kim, K. S., Moon, H. I., An, H. K., Park, S. J., Kim, C. H. & Lee, Y. C. (2014). Cordycepin-mediated transcriptional regulation of human gd3 synthase (hst8sia i) in human neuroblastoma sk-n-be(2)-c cells. *Acta Biochim Biophys Sin (Shanghai),* **46,** 65-71.
705. Patin, E. C., Orr, S. J. & Schaible, U. E. (2017). Macrophage inducible c-type lectin as a multifunctional player in immunity. *Front Immunol,* **8,** 861.
706. Wu, R., Chen, F., Wang, N., Tang, D. & Kang, R. (2020). Acod1 in immunometabolism and disease. *Cell Mol Immunol,* **17,** 822-833.

707. Seibert, K. & Masferrer, J. L. (1994). Role of inducible cyclooxygenase (cox-2) in inflammation. *Receptor,* **4,** 17-23.
708. Al-Mutairi, M. S., Cadalbert, L. C., McGachy, H. A., Shweash, M., Schroeder, J., Kurnik, M., Sloss, C. M., Bryant, C. E., Alexander, J. & Plevin, R. (2010). Map kinase phosphatase-2 plays a critical role in response to infection by leishmania mexicana. *PLoS Pathog,* **6,** e1001192.
709. Guo, Y., Tian, L., Liu, X., He, Y., Chang, S. & Shen, Y. (2019). Errfi1 inhibits proliferation and inflammation of nucleus pulposus and is negatively regulated by mir-2355-5p in intervertebral disc degeneration. *Spine (Phila Pa 1976),* **44,** E873-E881.
710. Wataya, Y. & Hiraoka, O. (1984). 3'-deoxyinosine as an anti-leishmanial agent: The metabolism and cytotoxic effects of 3'-deoxyinosine in leishmania tropica promastigotes. *Biochem Biophys Res Commun,* **123,** 677-83.
711. Lee, J. B., Radhi, M., Cipolla, E., Gandhi, R. D., Sarmad, S., Zgair, A., Kim, T. H., Feng, W., Qin, C., Adrower, C.*, et al.* (2019). A novel nucleoside rescue metabolic pathway may be responsible for therapeutic effect of orally administered cordycepin. *Sci Rep,* **9,** 15760.
712. Glusman, G., Caballero, J., Robinson, M., Kutlu, B. & Hood, L. (2013). Optimal scaling of digital transcriptomes. *PLoS One,* **8,** e77885.
713. Canovas, B. & Nebreda, A. R. (2021). Diversity and versatility of p38 kinase signalling in health and disease. *Nat Rev Mol Cell Biol,* **22,** 346-366.
714. Kliewer, S. A., Umesono, K., Noonan, D. J., Heyman, R. A. & Evans, R. M. (1992). Convergence of 9-cis retinoic acid and peroxisome proliferator signalling pathways through heterodimer formation of their receptors. *Nature,* **358,** 771-4.
715. Evans, R. M. & Mangelsdorf, D. J. (2014). Nuclear receptors, rxr, and the big bang. *Cell,* **157,** 255-66.
716. Ricote, M., Li, A. C., Willson, T. M., Kelly, C. J. & Glass, C. K. (1998). The peroxisome proliferator-activated receptor-gamma is a negative regulator of macrophage activation. *Nature,* **391,** 79-82.
717. Jiang, C., Ting, A. T. & Seed, B. (1998). Ppar-gamma agonists inhibit production of monocyte inflammatory cytokines. *Nature,* **391,** 82-6.
718. Xu, X., Zhang, Y., Williams, J., Antoniou, E., McCombie, W. R., Wu, S., Zhu, W., Davidson, N. O., Denoya, P. & Li, E. (2013). Parallel comparison of illumina rna-seq and affymetrix microarray platforms on transcriptomic profiles generated from 5-aza-deoxy-cytidine treated ht-29 colon cancer cells and simulated datasets. *BMC Bioinformatics,* **14 Suppl 9,** S1.
719. Wang, C., Gong, B., Bushel, P. R., Thierry-Mieg, J., Thierry-Mieg, D., Xu, J., Fang, H., Hong, H., Shen, J., Su, Z.*, et al.* (2014). The concordance between rna-seq and microarray data depends on chemical treatment and transcript abundance. *Nat Biotechnol,* **32,** 926-32.
720. Zhao, S., Fung-Leung, W. P., Bittner, A., Ngo, K. & Liu, X. (2014). Comparison of rna-seq and microarray in transcriptome profiling of activated t cells. *PLoS One,* **9,** e78644.
721. Kim, G. D., Das, R., Goduni, L., McClellan, S., Hazlett, L. D. & Mahabeleshwar, G. H. (2016). Kruppel-like factor 6 promotes macrophage-mediated inflammation by suppressing b cell leukemia/lymphoma 6 expression. *J Biol Chem,* **291,** 21271-21282.
722. Darnell, J. E., Kerr, I. M. & Stark, G. R. (1994). Jak-stat pathways and transcriptional activation in response to ifns and other extracellular signaling proteins. *Science,* **264,** 1415-21.
723. Ivashkiv, L. B. & Donlin, L. T. (2014). Regulation of type i interferon responses. *Nat Rev Immunol,* **14,** 36-49.
724. He, S. & Wang, X. (2018). Rip kinases as modulators of inflammation and immunity. *Nat Immunol,* **19,** 912-922.

725. McCarthy, J. V., Ni, J. & Dixit, V. M. (1998). Rip2 is a novel nf-kappab-activating and cell death-inducing kinase. *J Biol Chem,* **273,** 16968-75.
726. Cho, Y., Noshiro, M., Choi, M., Morita, K., Kawamoto, T., Fujimoto, K., Kato, Y. & Makishima, M. (2009). The basic helix-loop-helix proteins differentiated embryo chondrocyte (dec) 1 and dec2 function as corepressors of retinoid x receptors. *Mol Pharmacol,* **76,** 1360-9.
727. Koschinski, A. & Zaccolo, M. (2017). Activation of pka in cell requires higher concentration of camp than in vitro: Implications for compartmentalization of camp signalling. *Sci Rep,* **7,** 14090.
728. Hamm, H. E. (1998). The many faces of g protein signaling. *J Biol Chem,* **273,** 669-72.
729. Smrcka, A. V. (2008). G protein βγ subunits: Central mediators of g protein-coupled receptor signaling. *Cell Mol Life Sci,* **65,** 2191-214.
730. Tesmer, J. J., Sunahara, R. K., Gilman, A. G. & Sprang, S. R. (1997). Crystal structure of the catalytic domains of adenylyl cyclase in a complex with gsalpha.Gtpgammas. *Science,* **278,** 1907-16.
731. Sunahara, R. K., Tesmer, J. J., Gilman, A. G. & Sprang, S. R. (1997). Crystal structure of the adenylyl cyclase activator gsalpha. *Science,* **278,** 1943-7.
732. Dhyani, V., Gare, S., Gupta, R. K., Swain, S., Venkatesh, K. V. & Giri, L. (2020). Gpcr mediated control of calcium dynamics: A systems perspective. *Cell Signal,* **74,** 109717.
733. Nathan, C. (2003). Immunology: Oxygen and the inflammatory cell. *Nature,* **422,** 675-6.
734. Scortegagna, M., Cataisson, C., Martin, R. J., Hicklin, D. J., Schreiber, R. D., Yuspa, S. H. & Arbeit, J. M. (2008). Hif-1alpha regulates epithelial inflammation by cell autonomous nfkappab activation and paracrine stromal remodeling. *Blood,* **111,** 3343-54.
735. Candelario-Jalil, E., de Oliveira, A. C., Gräf, S., Bhatia, H. S., Hüll, M., Muñoz, E. & Fiebich, B. L. (2007). Resveratrol potently reduces prostaglandin e2 production and free radical formation in lipopolysaccharide-activated primary rat microglia. *J Neuroinflammation,* **4,** 25.
736. Annabi, B., Lord-Dufour, S., Vézina, A. & Béliveau, R. (2012). Resveratrol targeting of carcinogen-induced brain endothelial cell inflammation biomarkers mmp-9 and cox-2 is sirt1-independent. *Drug Target Insights,* **6,** 1-11.
737. Smits, E. L., Cools, N., Lion, E., Van Camp, K., Ponsaerts, P., Berneman, Z. N. & Van Tendeloo, V. F. (2010). The toll-like receptor 7/8 agonist resiquimod greatly increases the immunostimulatory capacity of human acute myeloid leukemia cells. *Cancer Immunol Immunother,* **59,** 35-46.
738. Chaudhary, R., Slebos, R. J. C., Song, F., McCleary-Sharpe, K. P., Masannat, J., Tan, A. C., Wang, X., Amaladas, N., Wu, W., Hall, G. E.*, et al.* (2021). Effects of checkpoint kinase 1 inhibition by prexasertib on the tumor immune microenvironment of head and neck squamous cell carcinoma. *Mol Carcinog,* **60,** 138-150.
739. Do, K. T., Manuszak, C., Thrash, E., Giobbie-Hurder, A., Hu, J., Kelland, S., Powers, A., de Jonge, A., Shapiro, G. I. & Severgnini, M. (2021). Immune modulating activity of the chk1 inhibitor prexasertib and anti-pd-l1 antibody ly3300054 in patients with high-grade serous ovarian cancer and other solid tumors. *Cancer Immunol Immunother,* **70,** 2991-3000.
740. Illi, B., Puri, P., Morgante, L., Capogrossi, M. C. & Gaetano, C. (2000). Nuclear factor-kappab and camp response element binding protein mediate opposite transcriptional effects on the flk-1/kdr gene promoter. *Circ Res,* **86,** E110-7.
741. Francis, S. H. & Corbin, J. D. (1994). Structure and function of cyclic nucleotide-dependent protein kinases. *Annu Rev Physiol,* **56,** 237-72.
742. Hilger, D., Masureel, M. & Kobilka, B. K. (2018). Structure and dynamics of gpcr signaling complexes. *Nat Struct Mol Biol,* **25,** 4-12.

743. Jewell, J. L., Fu, V., Hong, A. W., Yu, F. X., Meng, D., Melick, C. H., Wang, H., Lam, W. M., Yuan, H. X., Taylor, S. S.*, et al.* (2019). Gpcr signaling inhibits mtorc1 via pka phosphorylation of raptor. *Elife,* **8**.
744. Melick, C. H., Meng, D. & Jewell, J. L. (2020). A-kinase anchoring protein 8l interacts with mtorc1 and promotes cell growth. *J Biol Chem,* **295,** 8096-8105.
745. Ghisletti, S., Huang, W., Ogawa, S., Pascual, G., Lin, M. E., Willson, T. M., Rosenfeld, M. G. & Glass, C. K. (2007). Parallel sumoylation-dependent pathways mediate gene- and signal-specific transrepression by lxrs and ppargamma. *Mol Cell,* **25,** 57-70.
746. Ghisletti, S., Huang, W., Jepsen, K., Benner, C., Hardiman, G., Rosenfeld, M. G. & Glass, C. K. (2009). Cooperative ncor/smrt interactions establish a corepressor-based strategy for integration of inflammatory and anti-inflammatory signaling pathways. *Genes Dev,* **23,** 681-93.
747. Ito, A., Hong, C., Rong, X., Zhu, X., Tarling, E. J., Hedde, P. N., Gratton, E., Parks, J. & Tontonoz, P. (2015). Lxrs link metabolism to inflammation through abca1-dependent regulation of membrane composition and tlr signaling. *Elife,* **4,** e08009.
748. Fadok, V. A., Bratton, D. L., Konowal, A., Freed, P. W., Westcott, J. Y. & Henson, P. M. (1998). Macrophages that have ingested apoptotic cells in vitro inhibit proinflammatory cytokine production through autocrine/paracrine mechanisms involving tgf-beta, pge2, and paf. *J Clin Invest,* **101,** 890-8.
749. A-Gonzalez, N., Bensinger, S. J., Hong, C., Beceiro, S., Bradley, M. N., Zelcer, N., Deniz, J., Ramirez, C., Díaz, M., Gallardo, G.*, et al.* (2009). Apoptotic cells promote their own clearance and immune tolerance through activation of the nuclear receptor lxr. *Immunity,* **31,** 245-58.
750. Thomas, D. G., Doran, A. C., Fotakis, P., Westerterp, M., Antonson, P., Jiang, H., Jiang, X. C., Gustafsson, J., Tabas, I. & Tall, A. R. (2018). Lxr suppresses inflammatory gene expression and neutrophil migration through cis-repression and cholesterol efflux. *Cell Rep,* **25,** 3774-3785.e4.
751. Chawla, A., Boisvert, W. A., Lee, C. H., Laffitte, B. A., Barak, Y., Joseph, S. B., Liao, D., Nagy, L., Edwards, P. A., Curtiss, L. K.*, et al.* (2001). A ppar gamma-lxr-abca1 pathway in macrophages is involved in cholesterol efflux and atherogenesis. *Mol Cell,* **7,** 161-71.
752. Dunnwald, L. K., Rossing, M. A. & Li, C. I. (2007). Hormone receptor status, tumor characteristics, and prognosis: A prospective cohort of breast cancer patients. *Breast Cancer Res,* **9,** R6.
753. Yao, H., He, G., Yan, S., Chen, C., Song, L., Rosol, T. J. & Deng, X. (2017). Triple-negative breast cancer: Is there a treatment on the horizon? *Oncotarget,* **8,** 1913-1924.
754. Akman, B. H., Can, T. & Erson-Bensan, A. E. (2012). Estrogen-induced upregulation and 3'-utr shortening of cdc6. *Nucleic Acids Res,* **40,** 10679-88.
755. Masamha, C. P., Xia, Z., Yang, J., Albrecht, T. R., Li, M., Shyu, A. B., Li, W. & Wagner, E. J. (2014). Cfim25 links alternative polyadenylation to glioblastoma tumour suppression. *Nature,* **510,** 412-6.
756. Chu, Y., Elrod, N., Wang, C., Li, L., Chen, T., Routh, A., Xia, Z., Li, W., Wagner, E. J. & Ji, P. (2019). Nudt21 regulates the alternative polyadenylation of pak1 and is predictive in the prognosis of glioblastoma patients. *Oncogene,* **38,** 4154-4168.
757. Liu, H., Heller-Trulli, D. & Moore, C. L. (2022). Targeting the mrna endonuclease cpsf73 inhibits breast cancer cell migration, invasion, and self-renewal. *iScience,* **25,** 104804.
758. Chen, W., Qin, L., Wang, S., Li, M., Shi, D., Tian, Y., Wang, J., Fu, L., Li, Z., Guo, W.*, et al.* (2014). Cpsf4 activates telomerase reverse transcriptase and

predicts poor prognosis in human lung adenocarcinomas. *Mol Oncol,* **8,** 704-16.
759. Lee, K., Zheng, Q., Lu, Q., Xu, F., Qin, G., Zhai, Q., Hong, R., Chen, M., Deng, W. & Wang, S. (2021). Cpsf4 promotes triple negative breast cancer metastasis by upregulating mdm4. *Signal Transduct Target Ther,* **6,** 184.
760. Wang, Y., Lv, Y., Liu, T. S., Yan, W. D., Chen, L. Y., Li, Z. H., Piao, Y. S., An, R. B., Lin, Z. H. & Ren, X. S. (2019). Cordycepin suppresses cell proliferation and migration by targeting clec2 in human gastric cancer cells via akt signaling pathway. *Life Sci,* **223,** 110-119.
761. Yu, Q. & Stamenkovic, I. (2000). Cell surface-localized matrix metalloproteinase-9 proteolytically activates tgf-beta and promotes tumor invasion and angiogenesis. *Genes Dev,* **14,** 163-76.
762. Jeong, J. W., Jin, C. Y., Park, C., Han, M. H., Kim, G. Y., Moon, S. K., Kim, C. G., Jeong, Y. K., Kim, W. J., Lee, J. D.*, et al.* (2012). Inhibition of migration and invasion of lncap human prostate carcinoma cells by cordycepin through inactivation of akt. *Int J Oncol,* **40,** 1697-704.
763. Lee, D. Y., Lee, S. Y., Yun, S. H., Jeong, J. W., Kim, J. H., Kim, H. W., Choi, J. S., Kim, G. D., Joo, S. T., Choi, I.*, et al.* (2022). Review of the current research on fetal bovine serum and the development of cultured meat. *Food Sci Anim Resour,* **42,** 775-799.
764. Chen, Y., Lun, A. T. & Smyth, G. K. (2016). From reads to genes to pathways: Differential expression analysis of rna-seq experiments using rsubread and the edger quasi-likelihood pipeline. *F1000Res,* **5,** 1438.
765. Rzymowska, J., Wilkołaski, A., Szatkowska, L. & Grzybowska, L. (2022). The expression of signaling genes in breast cancer cells. *Biology (Basel),* **11**.
766. Lin, J. (2017). *Cordycepin affects growth factor-dependent gene expression. Phd thesis, university of nottingham.*
767. Singhania, R., Thorn,G.J., Williams,K., Gandhi,R.D., Daher,C., Barthet-Barateig,A., Parker,H.N., Utami,W., Al-Siraj,M., Barrett,D.A., *et al*. (2019). Nuclear poly(a) tail size is regulated by cnot1 during the serum response. *bioRxiv***,** 10.1101/773432.
768. Greenberg, M. E. & Ziff, E. B. (1984). Stimulation of 3t3 cells induces transcription of the c-fos proto-oncogene. *Nature,* **311,** 433-8.
769. Greenberg, M. E., Hermanowski, A. L. & Ziff, E. B. (1986). Effect of protein synthesis inhibitors on growth factor activation of c-fos, c-myc, and actin gene transcription. *Mol Cell Biol,* **6,** 1050-7.
770. Kallergi, G., Agelaki, S., Kalykaki, A., Stournaras, C., Mavroudis, D. & Georgoulias, V. (2008). Phosphorylated egfr and pi3k/akt signaling kinases are expressed in circulating tumor cells of breast cancer patients. *Breast Cancer Res,* **10,** R80.
771. Rozakis-Adcock, M., Fernley, R., Wade, J., Pawson, T. & Bowtell, D. (1993). The sh2 and sh3 domains of mammalian grb2 couple the egf receptor to the ras activator msos1. *Nature,* **363,** 83-5.
772. Roberts, P. J. & Der, C. J. (2007). Targeting the raf-mek-erk mitogen-activated protein kinase cascade for the treatment of cancer. *Oncogene,* **26,** 3291-310.
773. Humtsoe, J. O. & Kramer, R. H. (2010). Differential epidermal growth factor receptor signaling regulates anchorage-independent growth by modulation of the pi3k/akt pathway. *Oncogene,* **29,** 1214-26.
774. Corcoran, R. B., Ebi, H., Turke, A. B., Coffee, E. M., Nishino, M., Cogdill, A. P., Brown, R. D., Della Pelle, P., Dias-Santagata, D., Hung, K. E.*, et al.* (2012). Egfr-mediated re-activation of mapk signaling contributes to insensitivity of braf mutant colorectal cancers to raf inhibition with vemurafenib. *Cancer Discov,* **2,** 227-35.
775. Ponsioen, B., Post, J. B., Buissant des Amorie, J. R., Laskaris, D., van Ineveld, R. L., Kersten, S., Bertotti, A., Sassi, F., Sipieter, F., Cappe, B.*, et al.*

(2021). Quantifying single-cell erk dynamics in colorectal cancer organoids reveals egfr as an amplifier of oncogenic mapk pathway signalling. *Nat Cell Biol,* **23,** 377-390.
776. Weston, C. R., Wong, A., Hall, J. P., Goad, M. E., Flavell, R. A. & Davis, R. J. (2004). The c-jun nh2-terminal kinase is essential for epidermal growth factor expression during epidermal morphogenesis. *Proc Natl Acad Sci U S A,* **101,** 14114-9.
777. Kramer, H. K., Onoprishvili, I., Andria, M. L., Hanna, K., Sheinkman, K., Haddad, L. B. & Simon, E. J. (2002). Delta opioid activation of the mitogen-activated protein kinase cascade does not require transphosphorylation of receptor tyrosine kinases. *BMC Pharmacol,* **2,** 5.
778. Kiyatkin, A., Aksamitiene, E., Markevich, N. I., Borisov, N. M., Hoek, J. B. & Kholodenko, B. N. (2006). Scaffolding protein grb2-associated binder 1 sustains epidermal growth factor-induced mitogenic and survival signaling by multiple positive feedback loops. *J Biol Chem,* **281,** 19925-38.
779. Yarwood, S. J. & Woodgett, J. R. (2001). Extracellular matrix composition determines the transcriptional response to epidermal growth factor receptor activation. *Proc Natl Acad Sci U S A,* **98,** 4472-7.
780. Tan, X., Thapa, N., Sun, Y. & Anderson, R. A. (2015). A kinase-independent role for egf receptor in autophagy initiation. *Cell,* **160,** 145-60.
781. Healy, S., Khan, P. & Davie, J. R. (2013). Immediate early response genes and cell transformation. *Pharmacol Ther,* **137,** 64-77.
782. Lu, C., Shen, Q., DuPré, E., Kim, H., Hilsenbeck, S. & Brown, P. H. (2005). Cfos is critical for mcf-7 breast cancer cell growth. *Oncogene,* **24,** 6516-24.
783. Liu, Z. G., Jiang, G., Tang, J., Wang, H., Feng, G., Chen, F., Tu, Z., Liu, G., Zhao, Y., Peng, M. J.*, et al.* (2016). C-fos over-expression promotes radioresistance and predicts poor prognosis in malignant glioma. *Oncotarget,* **7,** 65946-65956.
784. Vleugel, M. M., Greijer, A. E., Bos, R., van der Wall, E. & van Diest, P. J. (2006). C-jun activation is associated with proliferation and angiogenesis in invasive breast cancer. *Hum Pathol,* **37,** 668-74.
785. Wang, Q., Liu, H., Zhou, F., Liu, Y., Zhang, Y., Ding, H., Yuan, M., Li, F. & Chen, Y. (2017). Involvement of c-fos in cell proliferation, migration, and invasion in osteosarcoma cells accompanied by altered expression of wnt2 and fzd9. *PLoS One,* **12,** e0180558.
786. Huang, C., Ma, R., Xu, Y., Li, N., Li, Z., Yue, J., Li, H., Guo, Y. & Qi, D. (2015). Wnt2 promotes non-small cell lung cancer progression by activating wnt/β-catenin pathway. *Am J Cancer Res,* **5,** 1032-46.
787. Karasawa, T., Yokokura, H., Kitajewski, J. & Lombroso, P. J. (2002). Frizzled-9 is activated by wnt-2 and functions in wnt/beta -catenin signaling. *J Biol Chem,* **277,** 37479-86.
788. Zhang, M. Z., Ferrigno, O., Wang, Z., Ohnishi, M., Prunier, C., Levy, L., Razzaque, M., Horne, W. C., Romero, D., Tzivion, G.*, et al.* (2015). Tgif governs a feed-forward network that empowers wnt signaling to drive mammary tumorigenesis. *Cancer Cell,* **27,** 547-60.
789. Blackwood, E. M. & Eisenman, R. N. (1991). Max: A helix-loop-helix zipper protein that forms a sequence-specific DNA-binding complex with myc. *Science,* **251,** 1211-7.
790. Struntz, N. B., Chen, A., Deutzmann, A., Wilson, R. M., Stefan, E., Evans, H. L., Ramirez, M. A., Liang, T., Caballero, F., Wildschut, M. H. E.*, et al.* (2019). Stabilization of the max homodimer with a small molecule attenuates myc-driven transcription. *Cell Chem Biol,* **26,** 711-723.e14.
791. Chen, H., Liu, H. & Qing, G. (2018). Targeting oncogenic myc as a strategy for cancer treatment. *Signal Transduct Target Ther,* **3,** 5.

792. Ahmadi, S. E., Rahimi, S., Zarandi, B., Chegeni, R. & Safa, M. (2021). Myc: A multipurpose oncogene with prognostic and therapeutic implications in blood malignancies. *J Hematol Oncol,* **14,** 121.
793. Thomas, L. R., Wang, Q., Grieb, B. C., Phan, J., Foshage, A. M., Sun, Q., Olejniczak, E. T., Clark, T., Dey, S., Lorey, S.*, et al.* (2015). Interaction with wdr5 promotes target gene recognition and tumorigenesis by myc. *Mol Cell,* **58,** 440-52.
794. Gerlach, J. M., Furrer, M., Gallant, M., Birkel, D., Baluapuri, A., Wolf, E. & Gallant, P. (2017). Paf1 complex component leo1 helps recruit. *Proc Natl Acad Sci U S A,* **114,** E9224-E9232.
795. Pommier, R. M., Gout, J., Vincent, D. F., Cano, C. E., Kaniewski, B., Martel, S., Rodriguez, J., Fourel, G., Valcourt, U., Marie, J. C.*, et al.* (2012). The human nupr1/p8 gene is transcriptionally activated by transforming growth factor β via the smad signalling pathway. *Biochem J,* **445,** 285-93.
796. Briscoe, J. & Thérond, P. P. (2013). The mechanisms of hedgehog signalling and its roles in development and disease. *Nat Rev Mol Cell Biol,* **14,** 416-29.
797. Sari, I. N., Phi, L. T. H., Jun, N., Wijaya, Y. T., Lee, S. & Kwon, H. Y. (2018). Hedgehog signaling in cancer: A prospective therapeutic target for eradicating cancer stem cells. *Cells,* **7**.
798. Fiaschi, M., Rozell, B., Bergström, A. & Toftgård, R. (2009). Development of mammary tumors by conditional expression of gli1. *Cancer Res,* **69,** 4810-7.
799. He, M., Fu, Y., Yan, Y., Xiao, Q., Wu, H., Yao, W., Zhao, H., Zhao, L., Jiang, Q., Yu, Z.*, et al.* (2015). The hedgehog signalling pathway mediates drug response of mcf-7 mammosphere cells in breast cancer patients. *Clin Sci (Lond),* **129,** 809-22.
800. Yin, X., Wolford, C. C., Chang, Y. S., McConoughey, S. J., Ramsey, S. A., Aderem, A. & Hai, T. (2010). Atf3, an adaptive-response gene, enhances tgf{beta} signaling and cancer-initiating cell features in breast cancer cells. *J Cell Sci,* **123,** 3558-65.
801. Liu, C., Qi, M., Li, L., Yuan, Y., Wu, X. & Fu, J. (2020). Natural cordycepin induces apoptosis and suppresses metastasis in breast cancer cells by inhibiting the hedgehog pathway. *Food Funct,* **11,** 2107-2116.
802. van Roy, F. & Berx, G. (2008). The cell-cell adhesion molecule e-cadherin. *Cell Mol Life Sci,* **65,** 3756-88.
803. Song, Y., Ye, M., Zhou, J., Wang, Z. & Zhu, X. (2019). Targeting e-cadherin expression with small molecules for digestive cancer treatment. *Am J Transl Res,* **11,** 3932-3944.
804. Kalluri, R. (2016). The biology and function of fibroblasts in cancer. *Nat Rev Cancer,* **16,** 582-98.
805. Chen, X. & Song, E. (2019). Turning foes to friends: Targeting cancer-associated fibroblasts. *Nat Rev Drug Discov,* **18,** 99-115.
806. Guo, S. & Deng, C. X. (2018). Effect of stromal cells in tumor microenvironment on metastasis initiation. *Int J Biol Sci,* **14,** 2083-2093.
807. Takiyama, Y., Miyokawa, N., Sugawara, A., Kato, S., Ito, K., Sato, K., Oikawa, K., Kobayashi, H., Kimura, S. & Tateno, M. (2004). Decreased expression of retinoid x receptor isoforms in human thyroid carcinomas. *J Clin Endocrinol Metab,* **89,** 5851-61.
808. Ando, N., Shimizu, M., Okuno, M., Matsushima-Nishiwaki, R., Tsurumi, H., Tanaka, T. & Moriwaki, H. (2007). Expression of retinoid x receptor alpha is decreased in 3'-methyl-4-dimethylaminoazobenzene-induced hepatocellular carcinoma in rats. *Oncol Rep,* **18,** 879-84.
809. Lotan, Y., Xu, X. C., Shalev, M., Lotan, R., Williams, R., Wheeler, T. M., Thompson, T. C. & Kadmon, D. (2000). Differential expression of nuclear retinoid receptors in normal and malignant prostates. *J Clin Oncol,* **18,** 116-21.

810. Zhong, C., Yang, S., Huang, J., Cohen, M. B. & Roy-Burman, P. (2003). Aberration in the expression of the retinoid receptor, rxralpha, in prostate cancer. *Cancer Biol Ther,* **2,** 179-84.
811. Pozzi, A., Ibanez, M. R., Gatica, A. E., Yang, S., Wei, S., Mei, S., Falck, J. R. & Capdevila, J. H. (2007). Peroxisomal proliferator-activated receptor-alpha-dependent inhibition of endothelial cell proliferation and tumorigenesis. *J Biol Chem,* **282,** 17685-95.
812. Garrido-Urbani, S., Jemelin, S., Deffert, C., Carnesecchi, S., Basset, O., Szyndralewiez, C., Heitz, F., Page, P., Montet, X., Michalik, L.*, et al.* (2011). Targeting vascular nadph oxidase 1 blocks tumor angiogenesis through a pparα mediated mechanism. *PLoS One,* **6,** e14665.
813. Lappano, R. & Maggiolini, M. (2018). Gper is involved in the functional liaison between breast tumor cells and cancer-associated fibroblasts (cafs). *J Steroid Biochem Mol Biol,* **176,** 49-56.
814. Pisano, A., Santolla, M. F., De Francesco, E. M., De Marco, P., Rigiracciolo, D. C., Perri, M. G., Vivacqua, A., Abonante, S., Cappello, A. R., Dolce, V.*, et al.* (2017). Gper, igf-ir, and egfr transduction signaling are involved in stimulatory effects of zinc in breast cancer cells and cancer-associated fibroblasts. *Mol Carcinog,* **56,** 580-593.
815. Peng, Y., Wang, Y., Zhou, C., Mei, W. & Zeng, C. (2022). Pi3k/akt/mtor pathway and its role in cancer therapeutics: Are we making headway? *Front Oncol,* **12,** 819128.
816. He, Y., Sun, M. M., Zhang, G. G., Yang, J., Chen, K. S., Xu, W. W. & Li, B. (2021). Targeting pi3k/akt signal transduction for cancer therapy. *Signal Transduct Target Ther,* **6,** 425.
817. Wee, P. & Wang, Z. (2017). Epidermal growth factor receptor cell proliferation signaling pathways. *Cancers (Basel),* **9**.
818. Li, L., Wang, N., Xiong, Y., Guo, G., Zhu, M. & Gu, Y. (2022). Transcription factor fosl1 enhances drug resistance of breast cancer through dusp7-mediated dephosphorylation of pea15. *Mol Cancer Res,* **20,** 515-526.
819. Zhang, Y. E. (2017). Non-smad signaling pathways of the tgf-β family. *Cold Spring Harb Perspect Biol,* **9**.
820. Masui, K., Tanaka, K., Akhavan, D., Babic, I., Gini, B., Matsutani, T., Iwanami, A., Liu, F., Villa, G. R., Gu, Y.*, et al.* (2013). Mtor complex 2 controls glycolytic metabolism in glioblastoma through foxo acetylation and upregulation of c-myc. *Cell Metab,* **18,** 726-39.
821. Burnett, P. E., Barrow, R. K., Cohen, N. A., Snyder, S. H. & Sabatini, D. M. (1998). Raft1 phosphorylation of the translational regulators p70 s6 kinase and 4e-bp1. *Proc Natl Acad Sci U S A,* **95,** 1432-7.
822. Hawley, S. A., Boudeau, J., Reid, J. L., Mustard, K. J., Udd, L., Mäkelä, T. P., Alessi, D. R. & Hardie, D. G. (2003). Complexes between the lkb1 tumor suppressor, strad alpha/beta and mo25 alpha/beta are upstream kinases in the amp-activated protein kinase cascade. *J Biol,* **2,** 28.
823. Habibian, J. S., Jefic, M., Bagchi, R. A., Lane, R. H., McKnight, R. A., McKinsey, T. A., Morrison, R. F. & Ferguson, B. S. (2017). Dusp5 functions as a feedback regulator of tnfα-induced erk1/2 dephosphorylation and inflammatory gene expression in adipocytes. *Sci Rep,* **7,** 12879.
824. Brandstetter, B., Dalwigk, K., Platzer, A., Niederreiter, B., Kartnig, F., Fischer, A., Vladimer, G. I., Byrne, R. A., Sevelda, F., Holinka, J.*, et al.* (2019). Foxo3 is involved in the tumor necrosis factor-driven inflammatory response in fibroblast-like synoviocytes. *Lab Invest,* **99,** 648-658.
825. Zhang, S., Chu, C., Wu, Z., Liu, F., Xie, J., Yang, Y. & Qiu, H. (2020). Contributes to m1 macrophage polarization in ards. *Front Immunol,* **11,** 580838.

826. Hamik, A., Lin, Z., Kumar, A., Balcells, M., Sinha, S., Katz, J., Feinberg, M. W., Gerzsten, R. E., Edelman, E. R. & Jain, M. K. (2007). Kruppel-like factor 4 regulates endothelial inflammation. *J Biol Chem,* **282,** 13769-79.
827. Han, X., Ren, J., Lohner, H., Yakoumatos, L., Liang, R. & Wang, H. (2022). Sgk1 negatively regulates inflammatory immune responses and protects against alveolar bone loss through modulation of traf3 activity. *J Biol Chem,* **298,** 102036.
828. Ko, R. & Lee, S. Y. (2016). Glycogen synthase kinase 3β in toll-like receptor signaling. *BMB Rep,* **49,** 305-10.
829. Martin, M., Rehani, K., Jope, R. S. & Michalek, S. M. (2005). Toll-like receptor-mediated cytokine production is differentially regulated by glycogen synthase kinase 3. *Nat Immunol,* **6,** 777-84.
830. Yang, D., Li, S., Duan, X., Ren, J., Liang, S., Yakoumatos, L., Kang, Y., Uriarte, S. M., Shang, J., Li, W.*, et al.* (2020). Tlr4 induced wnt3a-dvl3 restrains the intensity of inflammation and protects against endotoxin-driven organ failure through gsk3β/β-catenin signaling. *Mol Immunol,* **118,** 153-164.
831. Wu, C., Guo, Y., Su, Y., Zhang, X., Luan, H., Zhu, H., He, H., Wang, X., Sun, G., Sun, X.*, et al.* (2014). Cordycepin activates amp-activated protein kinase (ampk) via interaction with the γ1 subunit. *J Cell Mol Med,* **18,** 293-304.
832. Wang, Z., Wang, X., Qu, K., Zhu, P., Guo, N., Zhang, R., Abliz, Z., Yu, H. & Zhu, H. (2010). Binding of cordycepin monophosphate to amp-activated protein kinase and its effect on amp-activated protein kinase activation. *Chem Biol Drug Des,* **76,** 340-4.
833. Wang, Z., Chen, Z., Jiang, Z., Luo, P., Liu, L., Huang, Y., Wang, H., Wang, Y., Long, L., Tan, X.*, et al.* (2019). Cordycepin prevents radiation ulcer by inhibiting cell senescence via nrf2 and ampk in rodents. *Nat Commun,* **10,** 2538.
834. Guo, P., Kai, Q., Gao, J., Lian, Z. Q., Wu, C. M., Wu, C. A. & Zhu, H. B. (2010). Cordycepin prevents hyperlipidemia in hamsters fed a high-fat diet via activation of amp-activated protein kinase. *J Pharmacol Sci,* **113,** 395-403.
835. Lee, S. K., Lee, J. O., Kim, J. H., Kim, N., You, G. Y., Moon, J. W., Sha, J., Kim, S. J., Lee, Y. W., Kang, H. J.*, et al.* (2012). Coenzyme q10 increases the fatty acid oxidation through ampk-mediated pparα induction in 3t3-l1 preadipocytes. *Cell Signal,* **24,** 2329-36.
836. Vingtdeux, V., Chandakkar, P., Zhao, H., Davies, P. & Marambaud, P. (2011). Small-molecule activators of amp-activated protein kinase (ampk), rsva314 and rsva405, inhibit adipogenesis. *Mol Med,* **17,** 1022-30.
837. Yap, F., Craddock, L. & Yang, J. (2011). Mechanism of ampk suppression of lxr-dependent srebp-1c transcription. *Int J Biol Sci,* **7,** 645-50.
838. Rubin, C., Litvak, V., Medvedovsky, H., Zwang, Y., Lev, S. & Yarden, Y. (2003). Sprouty fine-tunes egf signaling through interlinked positive and negative feedback loops. *Curr Biol,* **13,** 297-307.
839. Liang, J., Wen, J., Huang, Z., Chen, X. P., Zhang, B. X. & Chu, L. (2019). Small nucleolar rnas: Insight into their function in cancer. *Front Oncol,* **9,** 587.
840. Jing, F., Ruan, X., Liu, X., Yang, C., Wang, D., Zheng, J., Xue, Y., Shen, S., Shao, L., Yang, Y.*, et al.* (2020). The pabpc5/hcg15/znf331 feedback loop regulates vasculogenic mimicry of glioma via stau1-mediated mrna decay. *Mol Ther Oncolytics,* **17,** 216-231.
841. Sun, Q., Hao, Q., Lin, Y. C., Song, Y. J., Bangru, S., Arif, W., Tripathi, V., Zhang, Y., Cho, J. H., Freier, S. M.*, et al.* (2020). Antagonism between splicing and microprocessor complex dictates the serum-induced processing of lnc-. *RNA,* **26,** 1603-1620.

842. Du, X., Shen, X., Dai, L., Bi, F., Zhang, H. & Lu, C. (2020). Psmd12 promotes breast cancer growth via inhibiting the expression of pro-apoptotic genes. *Biochem Biophys Res Commun,* **526,** 368-374.
843. Wang, Z., Li, Z., Xu, H., Liao, Y., Sun, C., Chen, Y., Sheng, M. & Lan, Q. (2021). Psmd12 promotes glioma progression by upregulating the expression of nrf2. *Ann Transl Med,* **9,** 700.
844. Pavon-Eternod, M., Gomes, S., Geslain, R., Dai, Q., Rosner, M. R. & Pan, T. (2009). Trna over-expression in breast cancer and functional consequences. *Nucleic Acids Res,* **37,** 7268-80.
845. Gregg, J. & Fraizer, G. (2011). Transcriptional regulation of egr1 by egf and the erk signaling pathway in prostate cancer cells. *Genes Cancer,* **2,** 900-9.
846. Gazon, H., Barbeau, B., Mesnard, J. M. & Peloponese, J. M. (2017). Hijacking of the ap-1 signaling pathway during development of atl. *Front Microbiol,* **8,** 2686.
847. Gowans, G. J., Hawley, S. A., Ross, F. A. & Hardie, D. G. (2013). Amp is a true physiological regulator of amp-activated protein kinase by both allosteric activation and enhancing net phosphorylation. *Cell Metab,* **18,** 556-66.
848. Schmitt-Ney, M. (2020). The foxo's advantages of being a family: Considerations on function and evolution. *Cells,* **9**.
849. Yang, Y., Li, C., Chen, Z., Zhang, Y., Tian, Q., Sun, M., Zhang, S., Yu, M. & Wang, G. (2023). An intellectual disability-related med23 mutation dysregulates gene expression by altering chromatin conformation and enhancer activities. *Nucleic Acids Res,* **51,** 2137-2150.
850. Lee, S. H., Singh, I., Tisdale, S., Abdel-Wahab, O., Leslie, C. S. & Mayr, C. (2018). Widespread intronic polyadenylation inactivates tumour suppressor genes in leukaemia. *Nature,* **561,** 127-131.
851. Hui, X., Cao, L., Xu, T., Zhao, L., Huang, K., Zou, Z., Ren, P., Mao, H., Yang, Y., Gao, S.*, et al.* (2022). Psmd12-mediated m1 ubiquitination of influenza a virus at k102 regulates viral replication. *J Virol,* **96,** e0078622.
852. Hentze, M. W., Castello, A., Schwarzl, T. & Preiss, T. (2018). A brave new world of rna-binding proteins. *Nat Rev Mol Cell Biol,* **19,** 327-341.
853. Corley, M., Burns, M. C. & Yeo, G. W. (2020). How rna-binding proteins interact with rna: Molecules and mechanisms. *Mol Cell,* **78,** 9-29.
854. Liao, S., Sun, H. & Xu, C. (2018). Yth domain: A family of n. *Genomics Proteomics Bioinformatics,* **16,** 99-107.
855. Oubridge, C., Ito, N., Evans, P. R., Teo, C. H. & Nagai, K. (1994). Crystal structure at 1.92 a resolution of the rna-binding domain of the u1a spliceosomal protein complexed with an rna hairpin. *Nature,* **372,** 432-8.
856. Wilson, K. A., Holland, D. J. & Wetmore, S. D. (2016). Topology of rna-protein nucleobase-amino acid π-π interactions and comparison to analogous DNA-protein π-π contacts. *RNA,* **22,** 696-708.
857. Nowacka, M., Boccaletto, P., Jankowska, E., Jarzynka, T., Bujnicki, J. M. & Dunin-Horkawicz, S. (2019). Rrmdb-an evolutionary-oriented database of rna recognition motif sequences. *Database (Oxford),* **2019**.
858. Fu, X. D. & Ares, M. (2014). Context-dependent control of alternative splicing by rna-binding proteins. *Nat Rev Genet,* **15,** 689-701.
859. Zhao, Y., Shi, Y., Shen, H. & Xie, W. (2020). M. *J Hematol Oncol,* **13,** 35.
860. Wang, X. P. & Cooper, N. G. (2010). Comparative in silico analyses of cpeb1-4 with functional predictions. *Bioinform Biol Insights,* **4,** 61-83.
861. Guillén-Boixet, J., Buzon, V., Salvatella, X. & Méndez, R. (2016). Cpeb4 is regulated during cell cycle by erk2/cdk1-mediated phosphorylation and its assembly into liquid-like droplets. *Elife,* **5**.
862. Tang, T. T. L., Stowell, J. A. W., Hill, C. H. & Passmore, L. A. (2019). The intrinsic structure of poly(a) rna determines the specificity of pan2 and caf1 deadenylases. *Nat Struct Mol Biol,* **26,** 433-442.

863. Wolf, J., Valkov, E., Allen, M. D., Meineke, B., Gordiyenko, Y., McLaughlin, S. H., Olsen, T. M., Robinson, C. V., Bycroft, M., Stewart, M.*, et al.* (2014). Structural basis for pan3 binding to pan2 and its function in mrna recruitment and deadenylation. *EMBO J,* **33,** 1514-26.
864. Lewis, J. D., Gunderson, S. I. & Mattaj, I. W. (1995). The influence of 5' and 3' end structures on pre-mrna metabolism. *J Cell Sci Suppl,* **19,** 13-9.
865. Jacobson, A. & Peltz, S. W. (1996). Interrelationships of the pathways of mrna decay and translation in eukaryotic cells. *Annu Rev Biochem,* **65,** 693-739.
866. Huang, Y. & Carmichael, G. G. (1996). Role of polyadenylation in nucleocytoplasmic transport of mrna. *Mol Cell Biol,* **16,** 1534-42.
867. Hong, S., Freeberg, M. A., Han, T., Kamath, A., Yao, Y., Fukuda, T., Suzuki, T., Kim, J. K. & Inoki, K. (2017). Larp1 functions as a molecular switch for mtorc1-mediated translation of an essential class of mrnas. *Elife,* **6**.
868. Pronobis, M. I., Rusan, N. M. & Peifer, M. (2015). A novel gsk3-regulated apc:Axin interaction regulates wnt signaling by driving a catalytic cycle of efficient βcatenin destruction. *Elife,* **4,** e08022.
869. Dreyfuss, G., Kim, V. N. & Kataoka, N. (2002). Messenger-rna-binding proteins and the messages they carry. *Nat Rev Mol Cell Biol,* **3,** 195-205.
870. Tcherkezian, J., Cargnello, M., Romeo, Y., Huttlin, E. L., Lavoie, G., Gygi, S. P. & Roux, P. P. (2014). Proteomic analysis of cap-dependent translation identifies larp1 as a key regulator of 5'top mrna translation. *Genes Dev,* **28,** 357-71.
871. Fonseca, B. D., Zakaria, C., Jia, J. J., Graber, T. E., Svitkin, Y., Tahmasebi, S., Healy, D., Hoang, H. D., Jensen, J. M., Diao, I. T.*, et al.* (2015). La-related protein 1 (larp1) represses terminal oligopyrimidine (top) mrna translation downstream of mtor complex 1 (mtorc1). *J Biol Chem,* **290,** 15996-6020.
872. Matthews, M. M., Thomas, J. M., Zheng, Y., Tran, K., Phelps, K. J., Scott, A. I., Havel, J., Fisher, A. J. & Beal, P. A. (2016). Structures of human adar2 bound to dsrna reveal base-flipping mechanism and basis for site selectivity. *Nat Struct Mol Biol,* **23,** 426-33.
873. Leulliot, N. & Varani, G. (2001). Current topics in rna-protein recognition: Control of specificity and biological function through induced fit and conformational capture. *Biochemistry,* **40,** 7947-56.
874. Liao, X., Tao, L., Guo, W., Wu, Z. X., Du, H., Wang, J., Zhang, J., Chen, H., Chen, Z. S., Lin, L.*, et al.* (2020). Combination of cordycepin and apatinib synergistically inhibits nsclc cells by down-regulating vegf/pi3k/akt signaling pathway. *Front Oncol,* **10,** 1732.
875. Ku, C. W., Ho, T. J., Huang, C. Y., Chu, P. M., Ou, H. C. & Hsieh, P. L. (2021). Cordycepin attenuates palmitic acid-induced inflammation and apoptosis of vascular endothelial cells through mediating pi3k/akt/enos signaling pathway. *Am J Chin Med,* **49,** 1703-1722.
876. Patel, L., Pass, I., Coxon, P., Downes, C. P., Smith, S. A. & Macphee, C. H. (2001). Tumor suppressor and anti-inflammatory actions of ppargamma agonists are mediated via upregulation of pten. *Curr Biol,* **11,** 764-8.
877. Iershov, A., Nemazanyy, I., Alkhoury, C., Girard, M., Barth, E., Cagnard, N., Montagner, A., Chretien, D., Rugarli, E. I., Guillou, H.*, et al.* (2019). The class 3 pi3k coordinates autophagy and mitochondrial lipid catabolism by controlling nuclear receptor pparα. *Nat Commun,* **10,** 1566.
878. Chandran, K., Goswami, S. & Sharma-Walia, N. (2016). Implications of a peroxisome proliferator-activated receptor alpha (pparα) ligand clofibrate in breast cancer. *Oncotarget,* **7,** 15577-99.
879. Takahashi, S., Tamai, M., Nakajima, S., Kato, H., Johno, H., Nakamura, T. & Kitamura, M. (2012). Blockade of adipocyte differentiation by cordycepin. *Br J Pharmacol,* **167,** 561-75.

880. Yang, W. L., Wang, J., Chan, C. H., Lee, S. W., Campos, A. D., Lamothe, B., Hur, L., Grabiner, B. C., Lin, X., Darnay, B. G.*, et al.* (2009). The e3 ligase traf6 regulates akt ubiquitination and activation. *Science,* **325,** 1134-8.
881. Shahid, A. M., Um, I. H., Elshani, M., Zhang, Y. & Harrison, D. J. (2022). Nuc-7738 regulates β-catenin signalling resulting in reduced proliferation and self-renewal of aml cells. *PLoS One,* **17,** e0278209.
882. Mellman, D. L., Gonzales, M. L., Song, C., Barlow, C. A., Wang, P., Kendziorski, C. & Anderson, R. A. (2008). A ptdins4,5p2-regulated nuclear poly(a) polymerase controls expression of select mrnas. *Nature,* **451,** 1013-7.
883. Tsjokajev, A., Røberg-Larsen, H., Wilson, S. R., Dyve Lingelem, A. B., Skotland, T., Sandvig, K. & Lundanes, E. (2020). Mass spectrometry-based measurements of cyclic adenosine monophosphate in cells, simplified using reversed phase liquid chromatography with a polar characterized stationary phase. *J Chromatogr B Analyt Technol Biomed Life Sci,* **1160,** 122384.
884. Wijayaratna, D., Ratnayake, K., Ubeysinghe, S., Kankanamge, D., Tennakoon, M. & Karunarathne, A. (2023). The spatial distribution of gpcr and gβγ activity across a cell dictates pip3 dynamics. *Sci Rep,* **13,** 2771.
885. Duong, Q. H. & Pegg, R. B. (2020). Quantitation of inositol phosphates by hplc-esi-ms. *Methods Mol Biol,* **2091,** 31-37.
886. Castelli, V., Catanesi, M., Alfonsetti, M., Laezza, C., Lombardi, F., Cinque, B., Cifone, M. G., Ippoliti, R., Benedetti, E., Cimini, A.*, et al.* (2021). Pparɑ-selective antagonist gw6471 inhibits cell growth in breast cancer stem cells inducing energy imbalance and metabolic stress. *Biomedicines,* **9**.
887. Seargent, J. M., Yates, E. A. & Gill, J. H. (2004). Gw9662, a potent antagonist of ppargamma, inhibits growth of breast tumour cells and promotes the anticancer effects of the ppargamma agonist rosiglitazone, independently of ppargamma activation. *Br J Pharmacol,* **143,** 933-7.
888. Rozanova, S., Barkovits, K., Nikolov, M., Schmidt, C., Urlaub, H. & Marcus, K. (2021). Quantitative mass spectrometry-based proteomics: An overview. *Methods Mol Biol,* **2228,** 85-116.
889. Schubert, O. T., Röst, H. L., Collins, B. C., Rosenberger, G. & Aebersold, R. (2017). Quantitative proteomics: Challenges and opportunities in basic and applied research. *Nat Protoc,* **12,** 1289-1294.
890. Mateus, A., Kurzawa, N., Becher, I., Sridharan, S., Helm, D., Stein, F., Typas, A. & Savitski, M. M. (2020). Thermal proteome profiling for interrogating protein interactions. *Mol Syst Biol,* **16,** e9232.
891. Urdaneta, E. C., Vieira-Vieira, C. H., Hick, T., Wessels, H. H., Figini, D., Moschall, R., Medenbach, J., Ohler, U., Granneman, S., Selbach, M.*, et al.* (2019). Purification of cross-linked rna-protein complexes by phenol-toluol extraction. *Nat Commun,* **10,** 990.

11 Appendix

11.1 Cell Viability Assays of bioactive compounds: PI3K inhibitors

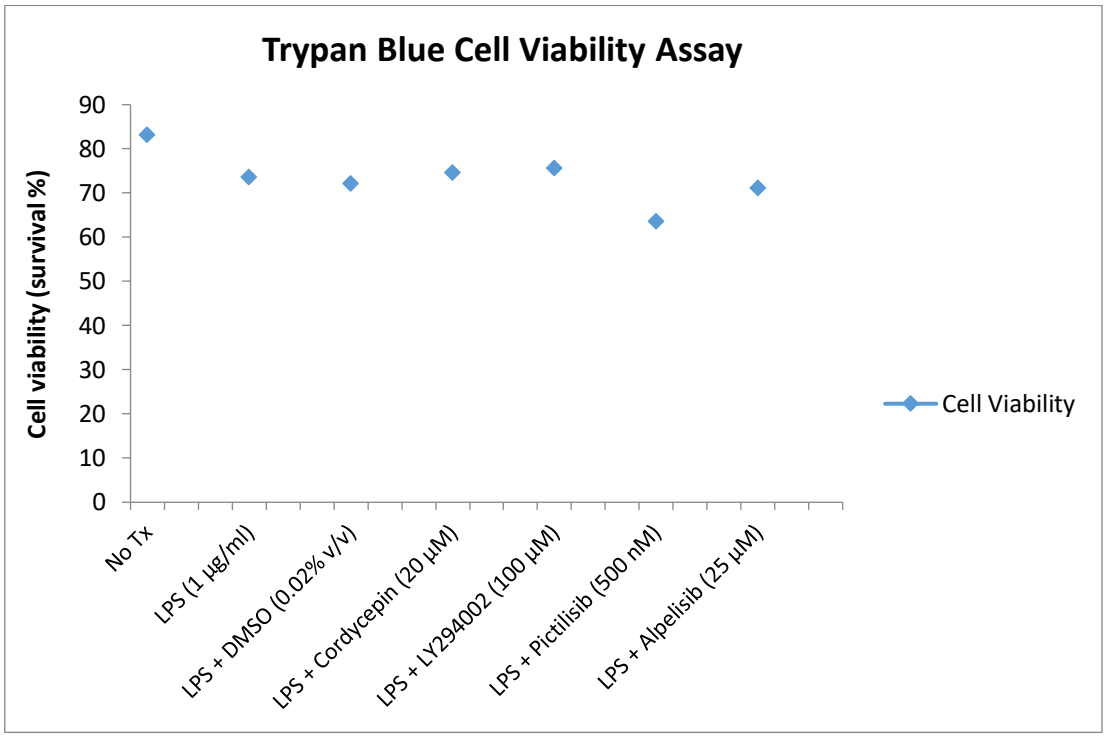

Figure A.1: Cell viability results for DMSO, cordycepin, and PI3K inhibitors in RAW264.7 macrophages. RAW264.7 macrophages were incubated in media containing less FBS (0.5%) for 24-hours prior to treatment with either DMSO, cordycepin, or the PI3K inhibitors, LY294002, Pictilisib, or Alpelisib for concentrations detailed above for 1-hour prior to a further 1-hour LPS (1 µg/ml) inflammatory stimulation. After treatment, culture media is taken off and kept, cells were washed with PBS, and cells were pelleted with original media taken off. Media was taken off, and the cell pellet was washed with PBS before resuspension with fresh culture media. A 1:1 solution of suspended cells and trypan blue (0.4%) was made and visualised under the microscope to assess cell viability (death). Healthy and dead cells were counted through haemocytometry and a percentage of alive/healthy cells were calculated from mean values using the formula = 1-(mean dead cells/mean total (alive) cells)x100.

11.2 Additional Output from DAVID Gene Ontology Analyses

11.2.1 RAW264.7 Microarray (DMSO + LPS treatment)

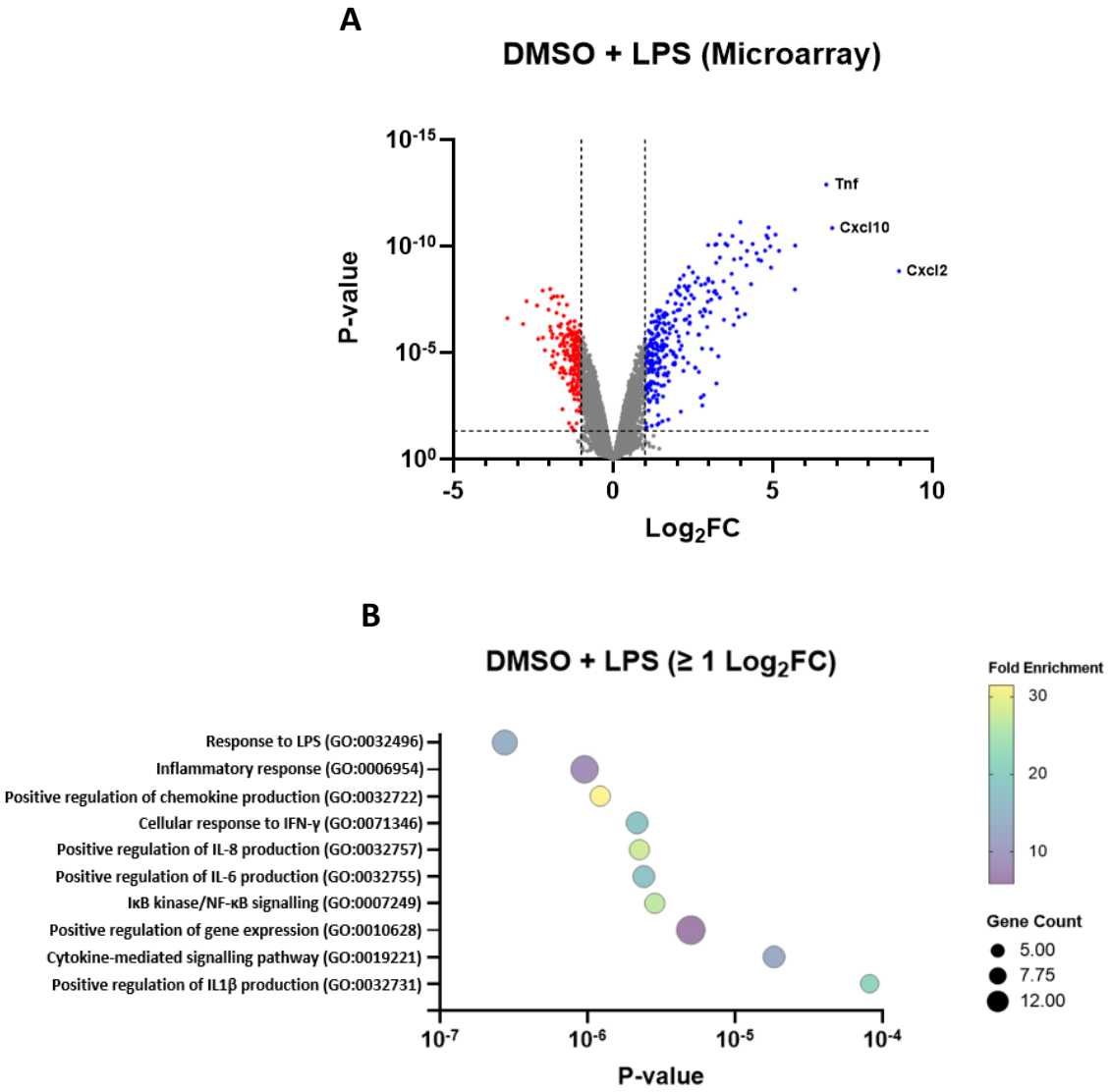

Figure A.2.1: Biological pathways upregulated with LPS & DMSO. Differentially expressed genes for 1-hour DMSO (0.02% v/v; RNA-Seq) treatment prior to a further 1-hour LPS inflammatory stimulation (1 µg/mL) in RAW264.7 macrophages was compared to DMSO (0.02% v/v) treatment only. The LIMMA[665] method was used to obtain differentially expressed genes. (**A**) A volcano plot of differentially expressed genes shows downregulated genes in red (≤ -1 Log_2FC & ≤ 0.05 p-value), upregulated genes in blue (≥ 1 Log_2FC & ≤ 0.05 p-value), and genes which do not meet the requirements for up or downregulated genes in grey (-1 to 1 Log_2FC & > 0.05 p-value). (**B**) All upregulated differentially expressed genes (≥ 1 Log_2FC & ≤ 0.05 p-value) were included into DAVID[690] gene ontology. The top 10 GO biological pathways was plotted for LPS & DMSO treatment.

11.2.2 RAW264.7 RNA-Seq (DMSO + LPS treatment)

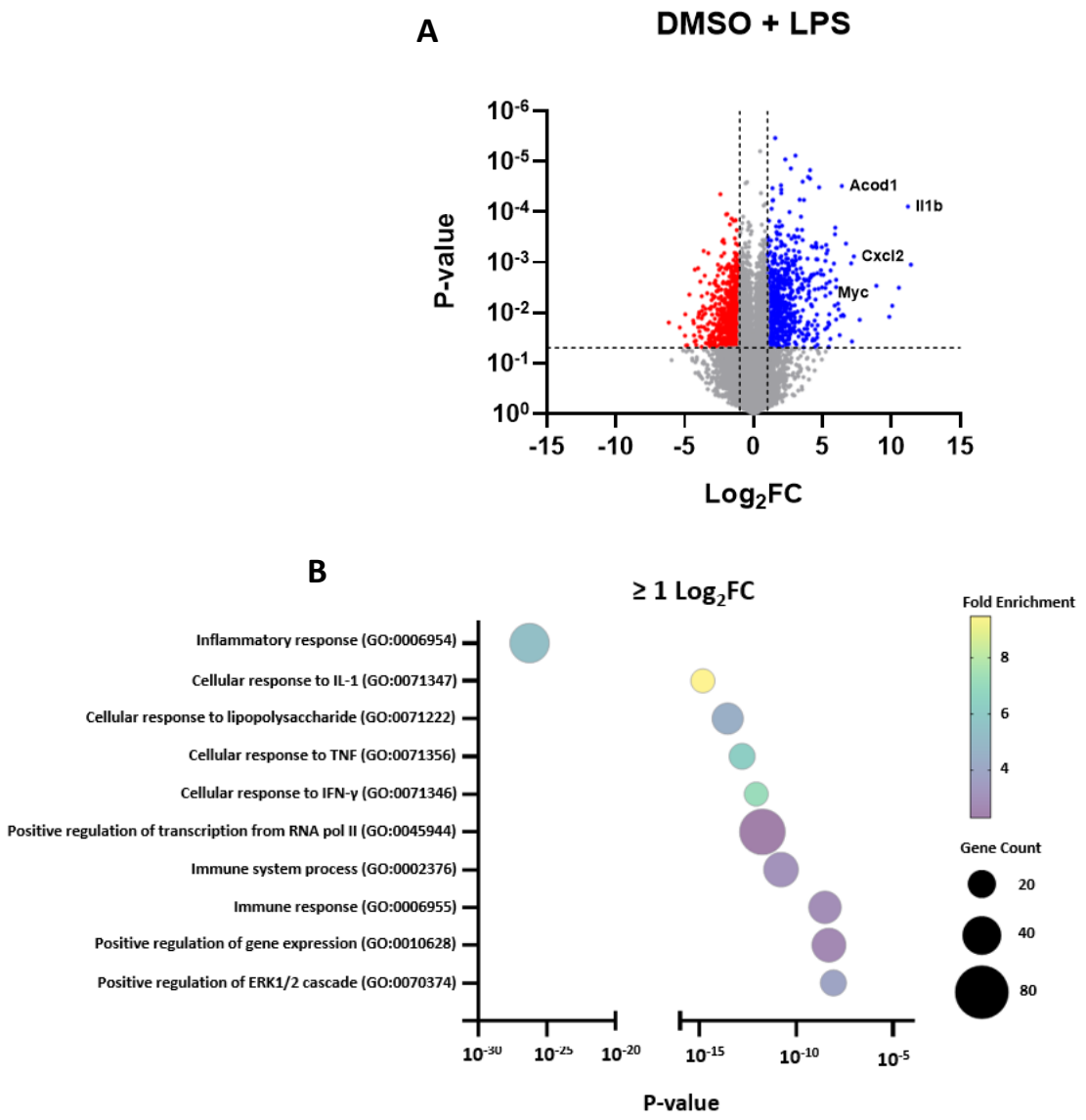

Figure A.2.2: Biological pathways upregulated with LPS & DMSO (RNA-Seq). Differentially expressed genes were obtained from RPKM values from RNA-Seq analysed through computing the Log_2 fold change after Upper Quartile normalisation (UQ)[688, 689, 712] of 1-hour DMSO (0.02% v/v; RNA-Seq) treatment prior to a further 1-hour LPS inflammatory stimulation (1 µg/mL) in RAW264.7 macrophages compared to DMSO (0.02% v/v) treatment only. (**A**) A volcano plot of differentially expressed genes shows downregulated genes in red (≤ -1 Log_2FC & ≤ 0.05 p-value), upregulated genes in blue (≥ 1 Log_2FC & ≤ 0.05 p-value), and genes which do not meet the requirements for up or downregulated genes in grey (-1 to 1 Log_2FC & > 0.05 p-value). (**B**) All upregulated differentially expressed genes (≥ 1 Log_2FC & ≤ 0.05 p-value) were included into DAVID[690] gene ontology. The top 10 GO biological pathways was plotted for LPS & DMSO treatment.

11.2.3 RAW264.7 RNA-Seq (siCtrl + LPS)

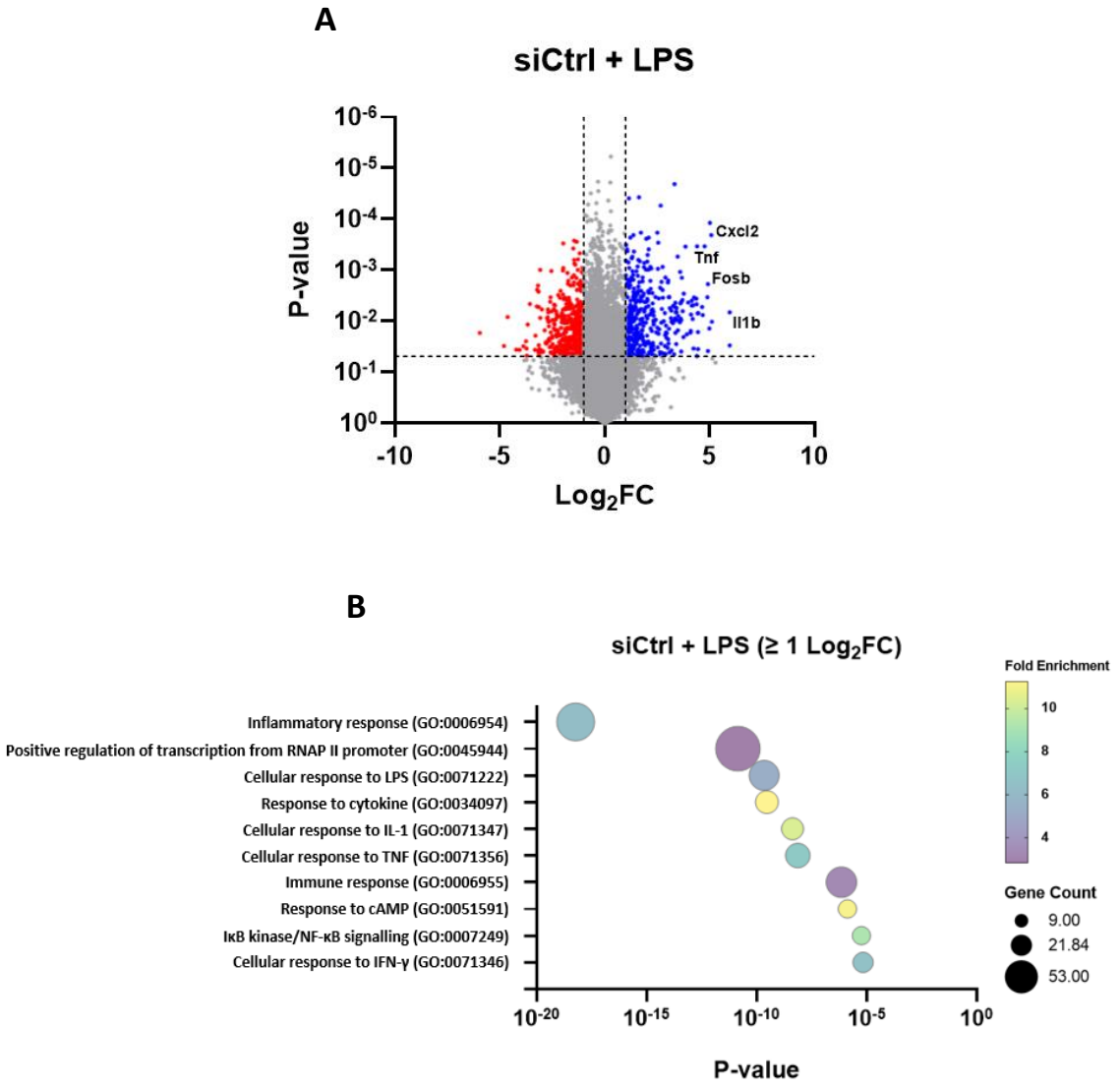

Figure A.2.3: Biological pathways upregulated with siCtrl & LPS (RNA-Seq). Differentially expressed genes for RAW264.7 macrophages subjected to siRNA knockdown of scramble control (siCtrl) for a total of 48 hours prior to 1-hour LPS (1 µg/mL) inflammatory stimulation, compared to siRNA knockdown of scramble control (siCtrl) without LPS stimulation. RPKM values were used to compute Log_2 fold change after Upper Quartile normalisation (UQ)[688, 689, 712] for differential expression. (**A**) A volcano plot of differentially expressed genes shows downregulated genes in red (≤ -1 Log_2FC & ≤ 0.05 p-value), upregulated genes in blue (≥ 1 Log_2FC & ≤ 0.05 p-value), and genes which do not meet the requirements for up or downregulated genes in grey (-1 to 1 Log_2FC & > 0.05 p-value). (**B**) All upregulated differentially expressed genes (≥ 1 Log_2FC & ≤ 0.05 p-value) were included into DAVID[690] gene ontology. The top 10 GO biological pathways was plotted for LPS & DMSO treatment.

11.2.4 RAW264.7 RNA-Seq (Wdr33 Knockdown)

Gene Ontology ID	Biological Process	Genes
GO:0006954	Inflammatory response	KDM6B, TNFRSF9, C5AR1, TNFAIP3, ACOD1, CXCL3, MEFV, PTGS2, TNF, SELE, CXCL2, IL1A, IL23A, IL1B, CCL4, ZC3H12A, NFKBIZ, REL, OLR1, TLR8, NLRP3, NFKBID, PF4
GO:0032496	Response to lipopolysaccharide	CEBPB, JUN, TNFRSF9, IL10RA, C5AR1, ACOD1, CXCL3, SOD2, PTGS2, TNF, CXCL2, NFKBIA, NOCT, IL1B, TRIB1, PTGES, PF4
GO:0006955	Immune response	CSF3, TNFRSF9, OSM, LIF, CXCL3, TNF, CXCL2, IL1A, IL23A, IL1B, CCL4, CLEC4E, OASL1, PF4
GO:0071347	Cellular response to interleukin-1	CEBPB, SAA3, ZC3H12A, SERPINE1, CCL4, ACOD1, CXCL2, KLF2
GO:0006915	Apoptotic process	PPP1R15A, CSRNP1, PLK3, GADD45B, TNFRSF9, C5AR1, TNFAIP3, TRAF1, CFLAR, TNF, MALT1, GADD45G, RHOB, NR4A1, ZC3H12A, PIM1, CHAC1, PHLDA1, MAP2K6
GO:0045944	Positive regulation of transcription from RNA polymerase II promoter	CSRNP1, CEBPB, CSF3, TNF, SERTAD1, ZC3H12A, NLRP3, KDM6B, EGR1, EGR2, JUN, JAG1, IFRD1, ARID5A, OSM, LIF, KLF2, VEGFA, FOSL1, NFKBIA, NR4A1, IL1A, IL23A, IL1B, REL, PF4
GO:0043123	Positive regulation of I-kappaB kinase/NF-kappaB signaling	IL1A, SLC20A1, IL1B, REL, TRIM13, CFLAR, TNF, IKBKE, MALT1, TGM2
GO:1900745	Positive regulation of p38MAPK cascade	GADD45B, GADD45A, ZC3H12A, VEGFA, GADD45G
GO:0006469	Negative regulation of protein kinase activity	SOCS3, FABP4, GADD45B, CISH, FLRT3, GADD45A, TRIB1, GADD45G
GO:0034097	Response to cytokine	FOSL1, JUN, CTRB1, REL, PTGS2, SKIL, PTGES

Figure A.2.4: Output of the enriched biological pathways and genes associated with Wdr33 knockdown with LPS inflammatory stimulation of RAW264.7 macrophages (RNA-Seq). RAW264.7 macrophages were subjected to siRNA knockdown of Wdr33 for a total of 48 hours with 1-hour LPS (1 µg/mL) inflammatory stimulation and compared to siRNA knockdown of scramble control (siCtrl) and 1-hour LPS (1 µg/mL) inflammatory stimulation. RPKM values were used to compute Log_2 fold change after Upper Quartile normalisation (UQ)[688, 689, 712] for differential expression. This table highlights the biological pathways enriched only for statistically significant downregulated genes (≤ -1 Log_2FC & ≤ 0.05 p-value). DAVID Gene Ontology[690] was used to obtain the biological pathways enriched with the input genes.

11.2.5 MCF-7 Microarray (Cordycepin treatment)

A

Gene Ontology ID	Biological process	Genes
GO:0006357	Regulation of transcription from RNA pol II promoter	FOXA1, ZNF331, CSRNP1, ZNF296, ZNF571, ZNF691, CCNT1, ZNF48, FOXQ1, SOX17, MYC, ZNF845, ZNF646, EPC2, ZNF689, ZNF567, JUNB, TGIF1, ZNF562, KLF10, KLF11, BRD2, ZNF165, TSC22D1, ZNF283, MED9, ARID5B, FOXL2, ZNF14, RUNX1, HIC2, ZSCAN20, RFX7, ZNF317, ZNF436, ZNF555, ATF3, DLX1, CEBPB, DLX2, FOXC1, ZNF394, GATA6, ZBTB45, ZNF2, ZNF8, ZBTB5, RLF, ZBTB3, ZNF629, ZNF628, NRIP1, ZNF668, ZSCAN12, PLAGL2, E2F3, E2F6, ZNF784, ZNF420, ZNF584, EGR1, JUN, ZNF263, KTI12, ARID3B, FOXN2, ZNF79, SMAD6, KLF3, KLF2, SMAD7, FOSL1, KLF6, KLF5, NR4A3, MAFF, SNAI1, ZNF416, ZNF614, ZNF613, FOSB, ZNF776, ZNF697, ZNF134, ZNF574
GO:0001570	Vasculogenesis	SOX17, CITED2, TIPARP, FBXW7, ADM, JUNB, EPHA2, ZFP36L1
GO:0043066	Negative regulation of apoptotic process	PLK3, CITED2, DUSP1, SIAH2, PLK2, GATA6, SMAD6, DKK1, SH3RF1, NFKBIA, SOCS3, NUAK2, MYC, TRAF6, ID1, PIM1, SPRY2, PIM3, ZNF830, STK40, IER3
GO:0016567	Protein ubiquitination	MYLIP, CISH, KLHL25, FEM1B, FBXW7, SIAH2, KLHL21, FBXO30, SH3RF1, HERPUD1, CNOT4, SOCS3, SPSB1, RNF113A, TRIM35, TRIM13, FBXO5, TRIM32, TRIM11, RNF111
GO:0071364	Cellular response to EGF stimulus	ERRFI1, ZFP36, FOXC1, MYC, ID1, ZFP36L1
GO:0042149	Cellular response to glucose starvation	NUAK1, NUAK2, SESN2, ZC3H12A, SIK1, HNRNPA1
GO:0045746	Negative regulation of Notch signaling pathway	NFKBIA, DLX1, DLX2, FBXW7, CHAC1
GO:0007049	Cell cycle	CCNT1, DUSP1, SIAH2, KLHL21, HJURP, ING1, CDC25A, RGS2, PIM1, GAS1, PIM3, SIK1, PELO
GO:0001525	Angiogenesis	EFNA1, FOXC1, JUN, KLF5, SOX17, FZD5, ZC3H12A, ID1, AMOTL2, RHOB
GO:0048008	PDGF receptor signaling pathway	CSRNP1, NR4A3, TIPARP, ARID5B

B

Gene Ontology ID	Biological process	Genes
GO:0009725	Response to hormone	SORD, HCLS1, RBM14, FHL2
GO:0030041	Actin filament polymerization	HCLS1, ARPC4-TTLL3, XLOC_011837
GO:0002188	Translation reinitiation	MCTS1, DENR
GO:0032790	Ribosome disassembly	MCTS1, DENR

Figure A.2.5: Output of the enriched genes associated with the key biological pathways for cordycepin treatment of MCF-7 Breast Adenocarcinomas (Microarray). MCF-7 cells were treated for 2 hours with cordycepin (50 µM) prior to LPS (1 µg/mL) inflammatory stimulation for a further 1-hour and compared to 1-hour DMSO (0.02% v/v) treatment prior to LPS (1 µg/mL) inflammatory stimulation. The LIMMA$^{(665)}$ method was used to obtain differentially expressed genes. (**A**) indicates the biological pathways enriched with statistically significant downregulated genes (≤ -1 Log_2FC

& ≤ 0.05 p-value). (**B**) represents the biological pathways enriched with statistically significant upregulated genes (≥ 1 Log_2FC & ≤ 0.05 p-value). DAVID Gene Ontology[690] was used to obtain the biological pathways enriched with the input genes.

11.2.6 MDA-MB-231 RNA-Seq (Cordycepin treatment)

Gene Ontology ID	Biological process	Genes
GO:0006357	Regulation of transcription from RNA pol II promoter	ZNF296, ZNF175, ZNF174, ZNF292, BACH1, SOX21, BACH2, ZXDA, MYC, ZXDB, ZSCAN32, ADNP2, JUNB, ZNF17, ZNF18, ZNF165, MEF2C, ZNF19, ZNF284, ZNF282, ZNF160, SOX13, ZNF10, MED9, ZNF12, ZNF14, ZNF16, ZSCAN20, RFX7, DDIT3, ZSCAN22, ZSCAN21, HOXB3, ZSCAN26, ZSCAN25, ZNF398, ZSCAN29, ZNF28, ZNF155, ZNF275, ZNF274, ZNF394, ZNF273, HOXD1, ZNF391, PRDM15, GATA6, MYNN, GATA3, GATA2, PRDM16, HOXC4, ZSCAN12, ZNF148, RREB1, ZBTB7A, ZSCAN16, ZNF267, ZNF264, ZNF142, JUN, ZNF263, ZNF383, ZNF140, ZNF382, ZNF260, IRF2BP1, IRF2BP2, NR2F2, ZNF35, FOSL2, FOSL1, MLLT10, ZNF30, REL, HOXD3, ZNF136, ZNF256, ZNF134, ZNF254, ZNF133, ZNF253, GMEB1, GMEB2, ZNF250, TCF20, HOXC13, CTCF, ZNF45, GLI1, MED18, ZNF48, MED17, GLI2, MECOM, ZNF280C, ZNF367, ZNF124, ZNF486, ZNF485, ZNF121, ZNF484, BRD2, BRD1, FOS, ZNF57, MED26, MTF1, PAX9, ZNF114, ZNF112, ZNF595, ZNF232, ZNF594, ZNF230, ZNF350, ZNF518B, PLAGL2, ZNF227, ZNF468, ZNF226, ZNF225, ZNF223, ZNF343, ZNF222, ZNF100, ZNF221, ZNF583, ZNF581, ZNF460, ZNF77, ZNF79, ZNF71, ZNF579, ZNF699, ZNF578, ZNF214, ZNF697, ZNF696, ZNF212, ZNF574, ZNF695, ZNF572, ZNF571, ZNF570, ZNF691, CCNT2, CCNT1, ZBTB24, ZBTB21, AHR, FOXQ1, ZFP30, ZNF569, ZNF205, ZNF689, ZNF567, ZNF446, PITX2, ZNF324, ZNF566, ZNF445, ZFP37, ZNF202, ZNF322, ZNF443, ZNF442, ZNF563, ZNF684, ZNF441, PIAS4, ZNF562, ZNF440, ZBTB39, ZNF561, ZNF681, ZNF680, ZBTB34, HIC1, PIAS1, HIC2, ZNF319, ERF, ZNF317, ZNF438, ZNF557, ZNF799, ZNF678, ZNF436, ADNP, TOX, ZNF555, ZNF311, ZNF432, ZNF551, ZNF430, ZNF671, ZNF550, ZNF792, ZNF791, ZNF670, DLX2, ZNF790, DLX3, NRF1, FOXO3, RLF, FOXO1, GLIS2, ZKSCAN7, ATXN7, ZNF549, ZKSCAN8, ZNF548, ZKSCAN3, ZNF669, ZNF426, ZKSCAN2, ZNF668, ZKSCAN5, ZNF546, ZNF425, ZNF304, ZKSCAN4, NKX6-1, ZNF543, ZNF784, ZNF420, ZNF782, BRPF1, ZBTB14, ZNF658B, BICRAL, ZBTB10, ZBTB11, FOXN2, MAFA, ZFP69, ZNF419, ZNF418, SP4, MAFF, ZNF417, ZNF416, SP6, ZNF658, TADA1, ZNF778, SP5, ZNF777, ZNF776, LHX4, ZNF775, ZNF654, ZNF653, ZNF530, ZNF772, NFE2L2, ZFP82, HHEX, ZNF408, ZNF649, ZNF527, ZNF526, ZNF888, ZNF646, ZNF525, ZNF644, ZNF765, ZNF764, NKX3-2, ZNF639, ZNF879, ZNF878, CEBPB, CEBPD, ZBTB49, ZBTB48, ZBTB43, ZBTB45, AMBRA1, STOX2, ZNF629, ZNF749, ZNF628, ZNF627, ZNF626, ZNF746, ZNF625, ZNF624, E2F2, ZNF502, ZNF623, E2F3, ZNF501, ZNF500, E2F6, E2F7, E2F8, IRX1, IRX5, IRX3, FOXJ3, KLF4, KLF3, KLF2, TBX2, KLF7, KLF6, ZNF619, KLF5, ZNF616, ZNF737, ZNF615, ZNF614, ZNF613, ZNF850, JMJD1C, IKZF2, IKZF3, ZNF608, ZNF607, ZNF727, ZNF724, ZNF845, DPF2, EPC1, ZNF844, EPC2, SOX9, CCNL1, ZFP1, ZFP3, RUNX2, OVOL2, RUNX1, ZNF836, ZNF710, ZNF324B, ZBTB5, ZBTB3, ZNF829, ZNF708, HIVEP1, ZNF823, ZNF701, PATZ1, XBP1, KTI12, ZBTB9, ZBTB6, ZNF816, ZNF813, RBAK, CSRNP1, CSRNP2, ZNF808, ZNF805, FOXD3, FOXD2, ZHX2, TSC22D1, TSC22D2, TFEB, ZFX, TOX3, ZNF780A, FOXC1, ZNF2, ZNF3, ZNF8, ZNF7, NFIL3, HDX, ZNF585A, GRHL2, NR6A1, TFAP4, FOXA3, NEUROG2, FOXA2, ZNF354B, ZSCAN9, JADE1, ARID4A, ARID4B, PRDM2, PRDM1, JADE2, ETS1, HOXA13, ETS2, SNIP1, ARID2, OSR2, MSX2, OSR1, ARID5B, ZNF92, ZNF93, RAI1, OTX1, TFAP2C, POU2F1, PHF12, NFXL1, ESR1, ZFHX4, SMAD7, BHLHE40, JMY, MXD1, MIDEAS, SIX1, CHD2, CHD1,

		IRF2BPL, LYL1, ZIC2, SIX4, BCL7A, TRPS1, TGIF1, KLF10, KLF11, TGIF2, ETV3, ARID1A, ELF1, ELF2, ELF3, IRF1, IRF9, KDM7A, ZNF197, BICRA, HLX, NRIP1, ZNF286B, HES1, ZNF189, ZNF286A, SPEN, TCF7L2, ZNF184, ZNF182, ZNF181, ARID3B, ZIC5, TBX15, TEF
GO:0006325	Chromatin organization	KMT2E, KDM5B, CHD9, ZNF518B, CHD7, KDM8, JMJD1C, ARID4B, CHD2, ING1, MBTD1, ING2, ALKBH4, TLK2, DPF2, KAT7, EPC2, ZNF304, ZBTB7A, CBX8, BRD2, BRD1, BRPF1, CBX4, C17ORF49, KMT5C, SETD1B, CBX2, SETD1A, TET2, TET1, HASPIN, SIRT1, RSBN1, JMJD6, RNF168, RIOX1, KANSL1, KANSL2, MTF2, TET3, PHF13, BCOR, TOX, BCORL1, KDM7A, FOXA3, FOXA2
GO:0016567	Protein ubiquitination	CCNF, CBLC, CBLB, FBXO24, JADE2, SH3RF1, IRF2BPL, MED17, TRIM4, ENC1, TRIM68, TRIM26, FBXO5, RNF152, RNF111, ARRDC4, VPS18, TRIM61, MYLIP, RNF43, CISH, FBXW7, MSL2, SIRT1, KCTD6, RNF168, RNF169, NFX1, GAN, SDE2, TRIM13, TRIM59, CBLL1, TRIM11, BIRC3, RNF34, KLHL15, RNF38, DTX2, SOCS3, VCPIP1, RNF113A, ZNRF3, SOCS1, KCTD21, TRIM47, FEM1C, SOCS6, SOCS5, BARD1, BRAP, KLHL25, FEM1B, RNF25, SMURF1, SIAH2, SIAH1, KLHL21, FBXL14, FBXO30, FBXL12, CNOT4, SPSB2, SPSB1, GID4, RNF227, TRIM35, ASB7, TRIM32, LNX2, NFE2L2
GO:0043065	Positive regulation of apoptotic process	USP27X, DCUN1D3, DDX20, ADM, BCL10, FOXO3, FOXO1, IFIT2, C3ORF38, BCL2L11, BMF, FADD, MAP3K9, ZNF622, CCN1, PHLDA1, SOX4, MCL1, BARD1, KLF11, JUN, GADD45B, GADD45A, DUSP1, SIAH1, OSGIN1, SIRT1, DUSP6, RHOB, BMP4, LATS1, FOSL1, BMP2, REST, RYBP, LATS2, TFAP4, MIR221, STK17B, JMY, TRIM35, TXNIP, ID3, SPRY1, RNF122
GO:0000188	Inactivation of MAPK activity	DUSP4, RGS4, DUSP5, DUSP2, DUSP10, RGS3, DUSP1, DUSP6, DUSP7
GO:1902459	Positive regulation of stem cell population maintenance	BICRAL, ARID4A, TET1, ARID4B, ARID1A, ING1, BICRA, ING2, REST, BCL7A, SIN3A, DPF2, ZNF322
GO:0006338	Chromatin remodelling	KDM5B, INO80D, CHD9, CHD7, GATA3, CHD2, CHD1, BICRA, BCL7A, ZNF827, MYC, MIER1, DPF2, SOX9, JARID2, ARID2, ZBTB7A, KDM6A, KDM6B, BRD2, KDM4D, BICRAL, ARID1A, ESR1, GATAD2B, ERCC6, RAD54L2
GO:0043551	Regulation of PI3K activity	SOCS3, SOCS1, CISH, WDR81, PIK3R2, PIK3R1, SOCS6, SOCS5
GO:0043409	Negative regulation of MAPK cascade	DUSP4, EFNA1, DUSP5, DUSP2, DUSP10, DUSP1, PRDM15, PIK3R2, NF2, DUSP6, DUSP7
GO:0071364	Cellular response to EGF stimulus	ERRFI1, ZFP36, FOXC1, GAREM1, MYC, ID1, SNAI2, FOS, SOX9, ZFP36L2, ZFP36L1

Figure A.2.6: Output of the enriched biological pathways and genes associated with cordycepin treatment of MDA-MB-231 Breast Adenocarcinomas (RNA-Seq). MDA-MB-231 cells were treated for 2 hours with cordycepin (50 μM) and compared to 2-hours DMSO treatment. RPKM values were used to compute Log_2 fold change after Upper Quartile normalisation (UQ)[688, 689, 712] for differential expression. This table highlights the biological pathways enriched only for statistically significant downregulated genes (≤ -1 Log_2FC & ≤ 0.05 p-value). DAVID Gene Ontology[690] was used to obtain the biological pathways enriched with the input genes.

11.2.7 NIH3T3 Microarray (Cordycepin treatment)

Gene Ontology ID	Biological process	Genes
GO:0006357	Regulation of transcription from RNA pol II promoter	ZFP169, ZFP846, PRDM2, IKZF2, ZFP119A, ZFP36, ZFP281, ZXDB, MYC, ZXDC, EPC1, ZFP282, ZFP960, JUNB, ZFP442, ZFP458, ZFP334, IFRD1, ARID5A, RFX3, CASK, RUNX2, HIC1, RUNX1, FOXP1, NPAS4, HIC2, ISL2, MYCN, ZSCAN22, ERF, ZFP7, ATF3, ZFP623, DLX2, ZFP229, ZFP108, ZFP867, ZFP866, ZBTB1, ZFP628, ZBTB5, HIF1A, ZBTB3, ZFP58, E430018J23RIK, ZKSCAN6, ZFP740, NKX2-5, ZBTB7B, EGR1, ZFP599, JUN, EGR3, SMAD3, ZFP873, EGR4, 2810021J22RIK, 2610008E11RIK, INHBA, SMAD5, FOSL2, SMAD7, ZBTB9, FOSL1, NR4A1, NR4A3, BCL6, MAFF, SNAI1, 5430403G16RIK, PHF14, ZFP111, ZFP128, CSRNP1, ZFP644, CITED2, ZFP526, ZFP955A, BMYC, ZFP955B, ZFP809, ANKRD1, TGIF1, KLF10, TEAD4, ZFP655, ZHX3, ZFP418, FOS, MED26, KLF16, LCOR, LCORL, ZFP941, FOXC2, CEBPB, AU041133, ZBTB49, SRF, ZBTB43, ZFP12, FOXS1, HES1, ZFP382, MEF2D, ZFP266, E2F8, ZFP953, ZFP799, ZFP433, ZFP319, ZFP438, KLF3, TBX18, KLF2, HINFP, KLF7, KLF6, KLF9, FOSB, ZFP553, ZFP27, ZFP398, ZFP397
GO:0030154	Cell differentiation	CITED2, D16ERTD472E, FGF7, ZFP281, ALKBH1, ZC3H12A, TLK2, UTP14B, SRRM4, ZHX3, TNFRSF12A, IFRD1, RFX3, DUSP6, RUNX2, EREG, RHOB, NPAS4, ERF, KCTD11, MEG3, FOXC2, CEBPB, DLX2, SEMA3A, ZBTB1, PRKX, HIF1A, FOXS1, NKX2-5, ZBTB7B, MEF2D, PDLIM7, MCL1, FGF21, SMAD3, FZD5, GADD45B, CAV2, CAVIN4, OSGIN1, MICAL2, NR1D1, SMAD5, TBX18, GADD45G, SMAD7, ID2, ID1, ID4, ID3
GO:0000188	Inactivation of MAPK activity	DUSP4, DUSP5, DUSP2, DUSP10, DUSP1, DUSP8, DUSP6
GO:0007623	Circadian rhythm	KLF10, PER1, JUN, NFIL3, NOCT, ID2, KLF9, ID1, ID4, ID3, NR1D1, NGF
GO:0044344	Cellular response to FGF stimulus	KDM5B, NR4A1, ZFP36, EGR3, MYC, ZFP36L2, CD44
GO:0009611	Response to wounding	ZFP36, PVT1, MYC, MIR17HG, TNC, TNFAIP3, ID3, ADM, PIK3CB, ZFP36L2, SNHG17
GO:0001525	Angiogenesis	JUN, TNFRSF12A, FZD5, SERPINE1, PTEN, FZD8, PRKX, PTGS2, SMAD5, HIF1A, RHOB, EREG, PLAU, ZC3H12A, MYH9, ITGA5, ANGPTL4, HBEGF
GO:0006915	Apoptotic process	CSRNP1, PLEKHF1, SGMS1, PDCD7, SEMA3A, PRUNE2, PTEN, TNFAIP3, NUAK2, EVA1A, ZC3H12A, CHAC1, PHLDA1, RELT, MEF2D, MCL1, PLK3, EPHA7, TNFRSF12A, GADD45B, TRAF2, RNF41, GADD45G, RHOB, HIPK2, NR4A1, TCIM, SGK1
GO:0071356	Cellular response to TNF	ZFP36, EDN1, SGMS1, CCL7, MIR143, ZC3H12A, ANKRD1, NR1D1, THBS1, ZFP36L2, KLF2, FOXP1
GO:0007179	TGF-β receptor signalling pathway	JUN, SMAD3, CITED2, MIR143, GCNT2, FOS, SMAD5, HIPK2, SMAD7

Figure A.2.7: Output of the enriched genes associated with the key biological pathways for cordycepin treatment of NIH3T3 fibroblasts (Microarray). NIH3T3 fibroblasts were treated after 24-hour serum-starvation for 90-minute cordycepin (20 µM) prior to 30-minute 10% NBCS serum stimulation compared to serum stimulation alone. The LIMMA[665] method was used to obtain differentially expressed genes. This table highlights the biological pathways enriched only for statistically significant downregulated genes (≤ -1 Log_2FC & ≤ 0.05 p-value). DAVID Gene Ontology[690] was used to obtain the biological pathways enriched with the input genes.

11.2.8 HEK293 RNA-Seq (DMSO + EGF)

A

Gene Ontology ID	Biological pathway	Genes
GO:0016477	Cell migration	CDC42, RHBDF1, SPEF1, PXN, PTK6, SCRIB, USH2A, PTPRF, PAK5
GO:0043433	Negative regulation of sequence-specific DNA binding transcription factor activity	TNFSF4, MIR199A1, BHLHE40, ID3, TRIB1
GO:0009416	Response to light stimulus	DUSP1, FOS, DNM2
GO:0007517	Muscle organ development	UNC45A, SPEG, ID3, ITGA7, POU6F1
GO:0090201	Negative regulation of release of cytochrome c from mitochondria	PRELID1, GPX1, TRIAP1
GO:0006396	RNA processing	SNORA68B, NOVA1, SNORD12C, SNORD62A, SNHG10, SNORA47, SNORD91A, SNORD3A, SNHG7, GRSF1, SNORA65, SCARNA18B
GO:0032870	Cellular response to hormone stimulus	DUSP1, FOSB, FOS
GO:0002143	tRNA wobble position uridine thiolation	TRMU, CTU1
GO:0071897	DNA biosynthetic process	POLE4, TERT, POLL
GO:0030154	Cell differentiation	UNC45A, DLX1, RARG, PKDCC, THRA, TNFAIP2, OSGIN1, PTK6, NR1D1, KAZALD1, ID3, TESMIN, CDHR5

B

Gene Ontology ID	Biological pathway	Genes
GO:0065003	Macromolecular complex assembly	GCH1, PARD3, MDM2, CHCHD10, LIN7A, CD247, LAMC1, DNM1L, WASF3, TEAD2, CD2AP
GO:0006357	Regulation of transcription from RNAP II promoter	ECM1, PSIP1, HMGB1, DPF3, ZNF205, KMT5A, LRRFIP1, CCNL1, JUNB, TEAD2, PRKCB, SP110, IFRD1, ZBTB33, BAZ1A, FOS, BAZ1B, ZNF14, MED23, KAT2B, ZFP41, HOXB2, PFN1, ZNF396, CBFB, DLX6, TAF9, FOXO4, HTATSF1, HOXB13, ZNF876P, CUX1, PLAGL1, MED31, PLAGL2, ALX4, ZNF227, ZBED6, E2F7, EGR1, EGR3, PHF10, BRPF3, IRF2BP2, FOSL1, NR4A1, MLLT10, MT-RNR1, MDM2, ZNF416, TAF4, MXD1, ZBTB8B, FOXA3
GO:0006886	Intracellular protein transport	RABGAP1L, USP6, STXBP1, TIMM23, VPS26A, AP2B1, SYTL4, RAB22A, RHOB, TBC1D1, STX1B, RAB14, APPBP2, XPOT, VTI1A, TMED7
GO:0007049	Cell cycle	TSPYL2, CASP8AP2, SUV39H2, DCLRE1A, ANAPC13, RIF1, PRPF40A, SMC4, WAPL, CD2AP, NEDD1, KAT2B, PARD3, TP53BP2, FAM32A, ANAPC1, NUP37
GO:0016477	Cell migration	ITGB3, LAMB4, WWC2, PRSS37, PRPF40A, GFRA1, LAMC1, PHB2, VAV1, RHOB, CD2AP, RHOU, EPHA3, NOX1

GO:0006974	Cellular response to DNA damage stimulus	PPP1R15A, BTG2, SLF1, WDR48, RIF1, MCM9, TAF9, SIRT4, MCM10, BAZ1B, DDB1, SFPQ, RAD50, ZC3H12A
GO:0050821	Protein stabilization	USP13, PDCL3, BAG4, MORC3, CDC37, GNAQ, STXBP1, TAF9, SUGT1, PFN1, PLPP3, PHB2
GO:0043161	Proteasome-mediated ubiquitin-dependent protein catabolic process	DDB1, PSMD12, WDR26, RMND5A, APPBP2, PSMD3, MDM2, KIF14, KCTD2, PSMF1, CD2AP
GO:0043123	Positive regulation of IκB kinase/NF-κB signalling	TRIM8, ECM1, VAPA, CHUK, PRKCB, MIER1, LPAR1, DDX21, ROR1, ZDHHC17
GO:0071356	Cellular response to TNF	BAG4, ASAH1, CHUK, ZC3H12A, FOS, CLDN1, TNFRSF21, MAP3K5

Figure A.2.8: Output of the enriched biological pathways and genes associated with DMSO treatment with EGF stimulation in HEK293 cells (RNA-Seq). HEK293 cells were gifted from Professor Grahame Hardie's lab at the University of Dundee. CRISPR-Cas9 AMPK knockout and wild type HEK293 cells were incubated in media containing less FBS (0.1%) for 24 hours prior to treatment with DMSO (0.025% v/v) for 20 minutes before stimulation with EGF (15 nM) for 30 minutes. Total RNA was extracted and sent off for RNA-Seq, with output analysed through Log_2 fold change of treatment versus control of RPKM values after Upper Quartile normalisation (UQ)[688, 689, 712]. All statistically significant genes (≤ 0.05 p-value) with a positive Log_2FC compared to DMSO (0.025% v/v) on its own were included into DAVID Gene Ontology[690]. Biological pathways enriched with upregulated genes with EGF stimulation are shown for **A)** wild type, and **B)** CRISPR-Cas9 AMPK knockout HEK293 cells.

11.2.9 HEK293 RNA-Seq (Cordycepin + EGF)

A

Gene Ontology ID	Biological pathway	Genes
GO:0045944	Positive regulation of transcription from RNAP II promoter	CRTC3, KDM1A, NUCKS1, HOXA13, FGF2, ELK3, ZNF609, SALL2, ZNF606, MYC, MYB, DPF3, AKT1, MEN1, GTF2I, EBF2, ISL1, GTF2F2, POU3F3, RUNX1, RFX6, KAT6B, MAML3, TP53, ATF4, NOTCH3, ZNF395, KMT2A, FOXO3, ZNF24, MED12L, ZNF827, RIPK1, ZNF148, RREB1, S100A10, EGR1, SMAD1, DR1, CREBBP, JUN, EGR2, POU2F1, BCL11B, PHF10, PBX3, HMGA2, NR2F2, TRERF1, SMARCA2, AHI1, MKRN2, HNRNPD, TCF4, CSRNP1, RARG, CSRNP2, THRB, ONECUT3, PKD2, LITAF, ZNF48, MED12, HHEX, SUMO2, NCK2, ZNF521, TEAD1, TEAD4, PARP1, FOS, KLF14, PAX2, RGMA, HAX1, TFDP2, ZNF780B, YAP1, ZNF473, SATB2, TAF9, HOXD13, EGFR, MLLT6, STOX2, PLAGL2, E2F3, MTA2, E2F7, STOX1, E2F8, BRD4, TCF7L2, PRRX1, EYA1, ATAD2, FOXJ3, STAT3, NR1H3, HIPK2, GRIN1, ASXL1, SKI, REST, MEIS1, NFIA, NFIB, TTC5, ASXL2, FOSB, CTNNB1, SSBP2, PFKM, SSBP3, ZNF212
GO:0007049	Cell cycle	CDKN1C, ANKLE2, CDCA2, MCM7, PRCC, NEDD9, AMBRA1, LIN9, KIF11, GSPT2, CDC73, SMC2, TTC28, PPP1CC, KIF13A, MAP3K20, NUP43, RIOK2, STOX1, MAPK4, LRRCC1, RBM38, TSPYL2, CDKN2C, URGCP, BOD1, CSNK1A1, STRADB, PRKCE, MICAL3, HMGA2, CABLES1, PIMREG, TERF2, KLHL42, TFDP2, SGSM3, CINP, MCM3, MCM5, ZMYND11, MNAT1, KIF20B, AJUBA, TP53, ARL8B
GO:0007010	Cytoskeleton organization	SEMA6A, MAST3, MAST2, MICAL3, NEDD9, FITM2, SIPA1L3, SYNE3, FGD4, ARHGAP10, ARHGAP21, ARC, DPYSL2, EPB41L3, MAP3K20, RANBP10, PACSIN2, PACSIN3, CSPG5, PLCE1, AJUBA, PAK5, PACSIN1, CAP2
GO:0006338	Chromatin remodelling	RERE, INO80C, SATB2, BAZ2A, CHD2, MTA1, BCL7A, ZNF827, MYC, MYB, EP400, DPF3, RBBP7, MTA2, ARID2, KDM6A, BRD4, SMARCE1, DR1, KDM4D, PHF10, RING1, CHD1L, ARID1A, SMARCA2, ARID1B
GO:0051301	Cell division	ANKLE2, CDCA2, MIS12, NEDD9, KIF11, CDC73, SMC2, TTC28, PPP1CC, CCND3, CCNB1, PTTG1, TPR, KIF13A, ZNF207, NUP43, NEK3, MAP4, FAM83D, STOX1, LRRCC1, NEK4, LIG1, BOD1, CSNK1A1, PRKCE, MICAL3, HMGA2, CABLES1, VRK1, PIMREG, KLHL42, EML3, LATS1, CENPF, CCNY, CENPJ, CINP, TACC3, MCM5, KIF20B, ARL8B
GO:0045736	Negative regulation of cyclin-dependent protein Ser/Thr kinase activity	CDKN1C, LATS1, HHEX, CDKN2C, CASP3, PLK1, NR2F2, CDK5RAP2, MEN1
GO:0008333	Endosome to lysosome transport	RNF157, SNAPIN, HMGXB4, DTX3L, HOOK1, TGFBRAP1, KIF13A, TRAK1, ATG14, RHOB, MTM1
GO:0090090	Negative regulation of canonical Wnt signalling pathway	TLE4, INVS, EGR1, TCF7L2, TLE2, FZD4, CSNK1A1, AMFR, CAV1, SHISA3, FOXO3, TMEM170B, ISL1, BICC1, UBAC2, LATS1, FERMT1, G3BP1, CTNNB1, ANKRD6

GO:0051056	Regulation of small GTPase mediated signal transduction	PLEKHG1, TRIO, ARHGEF12, ARHGEF28, SIPA1L2, SIPA1L3, ARHGAP44, FGD4, ARHGAP10, AKAP13, ARHGAP21, ARHGAP20, RACGAP1, DLC1, PLEKHG4B, ARHGEF1, NGEF
GO:0071364	Cellular response to EGF stimulus	DUSP3, GAREM1, MCM7, MYC, ERBB2, AKT1, FOS, CFLAR, PAX2, EGFR

B

Gene Ontology ID	Biological pathway	Genes
GO:0051301	Cell division	AHCTF1, TSG101, CCNT1, CCDC124, NCAPG2, KIF14, NCAPG, CDCA8, SMC5, SKA3, SKA1, SKA2, PARD6B, DSN1, MAEA, CDC23, CHMP1B, RBBP8, KMT5A, FAM83D, MISP, PELO, CDT1, TIPIN, CENPW, UBE2C, NSMCE2, ACTR8, KNL1, HAUS2, PPP1CA, WEE1, CDC34, PPP1R1C, CDK2, ANAPC4, MAPRE3, NCAPD3, CDK13
GO:0006351	Transcription, DNA-templated	CCNT1, LIN9, TAF1B, POLR2B, TDG, ZXDC, LPXN, GPBP1L1, POLR2H, MAPK3, BRD4, AKIRIN2, SMAD1, AKIRIN1, KDM2A, EAF1, GTF2H1, TBX3, SAP30, XAB2, RYBP, POLR3A, AEBP2, FUBP3, CDK2, CNOT8
GO:0006325	Chromatin organization	PHF20, SUPT4H1, EHMT1, ARID4B, CHD3, DCAF1, MBTD1, TDG, SPIN1, BANF1, KMT5A, ATXN7L3, BRD4, RNF20, BRD2, DAXX, KDM2A, EED, EYA3, DAPK3, ATRX, RSBN1, MORF4L1, AEBP2, WAC, BAP1, EZH2
GO:0000045	Autophagosome assembly	STX12, GABARAPL1, MAP1LC3B, UBXN2B, BAG3, RB1CC1, UBQLN1, ATP2A2, WIPI2, ATG12, ATG5, ATG2B
GO:0042752	Regulation of circadian rhythm	KLF10, GSK3B, MAPK8, KDM2A, FBXW7, NOCT, UBE3A, CSNK1D, CSNK1E, PPARA, EZH2, PPP1CA
GO:0007049	Cell cycle	KLLN, AHCTF1, TSG101, RABGAP1, CCNT1, UHRF2, CCDC124, HJURP, LIN9, PDCD2L, MAEA, CDC45, RB1CC1, PIM1, SPIN1, WDR6, EP300, PELO, APPL2, MAPK3, CDKN2D, CDT1, TIPIN, NSMCE2, ACTR8, PPP1CA, THAP5, PPP1R1C, PSME3, ANAPC4, TAF1
GO:0006338	Chromatin remodelling	BRD2, SMARCC1, DAXX, INO80D, ATRX, BAZ1A, CHD3, ACTR8, CECR2, ZNHIT1, RYBP, TADA2A, CFDP1, MYBBP1A, POLE3, PWWP2A, SMARCAD1, RAD54L, NFRKB, BRD4
GO:0006281	DNA repair	PAXIP1, INO80D, FMR1, XPC, SAMHD1, BACH1, ALKBH1, RBBP8, RAD54L, TOPBP1, POLE, NFRKB, UPF1, SLX1B, FBXW7, EYA3, INTS3, ATRX, RECQL, GTF2H1, ACTR8, CSNK1E, POLA1, RRM2B, CDK2, NABP2
GO:0016567	Protein ubiquitination	CUL5, UHRF2, RNF38, UBR4, RNF6, ARRB2, FBXO21, DCAF1, MED11, COP1, MAEA, CDC23, UBR7, MED10, VPS11, RBBP6, ARIH1, DCAF11, SOCS4, ATG5, KLHDC10, ARRDC4, VPS18, RNF25, UBE2C, FBXW7, MSL2, FBXL15, FBXO30, KCTD9, AIMP2, CDC34, GAN, RFWD3, MDM2, CUL4B, ASB1
GO:0032958	Inositol phosphate biosynthetic process	IPPK, ITPKC, PPIP5K2, IPMK, IP6K1

Figure A.2.9: Output of the enriched biological pathways and genes associated with cordycepin treatment with EGF stimulation in HEK293 cells (RNA-Seq). HEK293 cells were gifted from Professor Grahame Hardie's lab at the University of Dundee. CRISPR-Cas9 AMPK knockout and wild type HEK293 cells were incubated in media containing

less FBS (0.1%) for 24 hours prior to treatment with cordycepin (25 µM) for 20 minutes before stimulation with EGF (15 nM) for 30 minutes. Total RNA was extracted and sent off for RNA-Seq, with output analysed through Log_2 fold change of treatment versus control of RPKM values after Upper Quartile normalisation (UQ)[688, 689, 712]. All statistically significant genes (≤ 0.05 p-value) with a negative Log_2FC compared to DMSO (0.025% v/v) and EGF (15 nM) treatment were included into DAVID Gene Ontology[690]. Biological pathways enriched with downregulated genes with cordycepin treatment are shown for **A)** wild type, and **B)** CRISPR-Cas9 AMPK knockout HEK293 cells.

11.3 RNA-Seq: Rsubread & EdgeR differential expression output

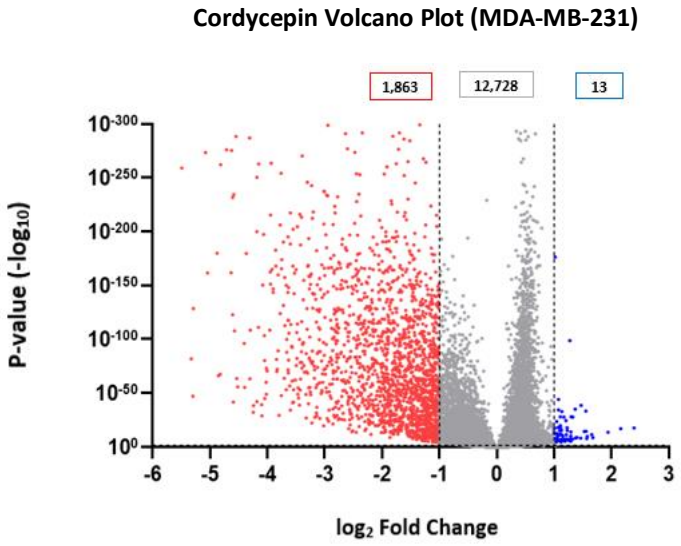

Figure A.3: Differential expression analysis of cordycepin treatment in MDA-MB-231 analysed through Rsubread. Volcano plot showing the spread of expression with cordycepin treatment in MDA-MB-231 Breast Adenocarcinomas. Differentially expressed genes obtained from RNA-Seq output was analysed using the Rsubread method[764] of 2-hour cordycepin (50 µM) treatment compared to DMSO (0.05% v/v). Red denotes genes with ≤ -1 Log_2FC & ≤ 0.05 p-value, blue denotes genes with ≥ 1 Log_2FC & ≤ 0.05 p-value, grey denotes genes with -1 to 1 Log_2FC & > 0.05 p-value.

11.4 Primary antibody validation of phospho-AKT antibodies

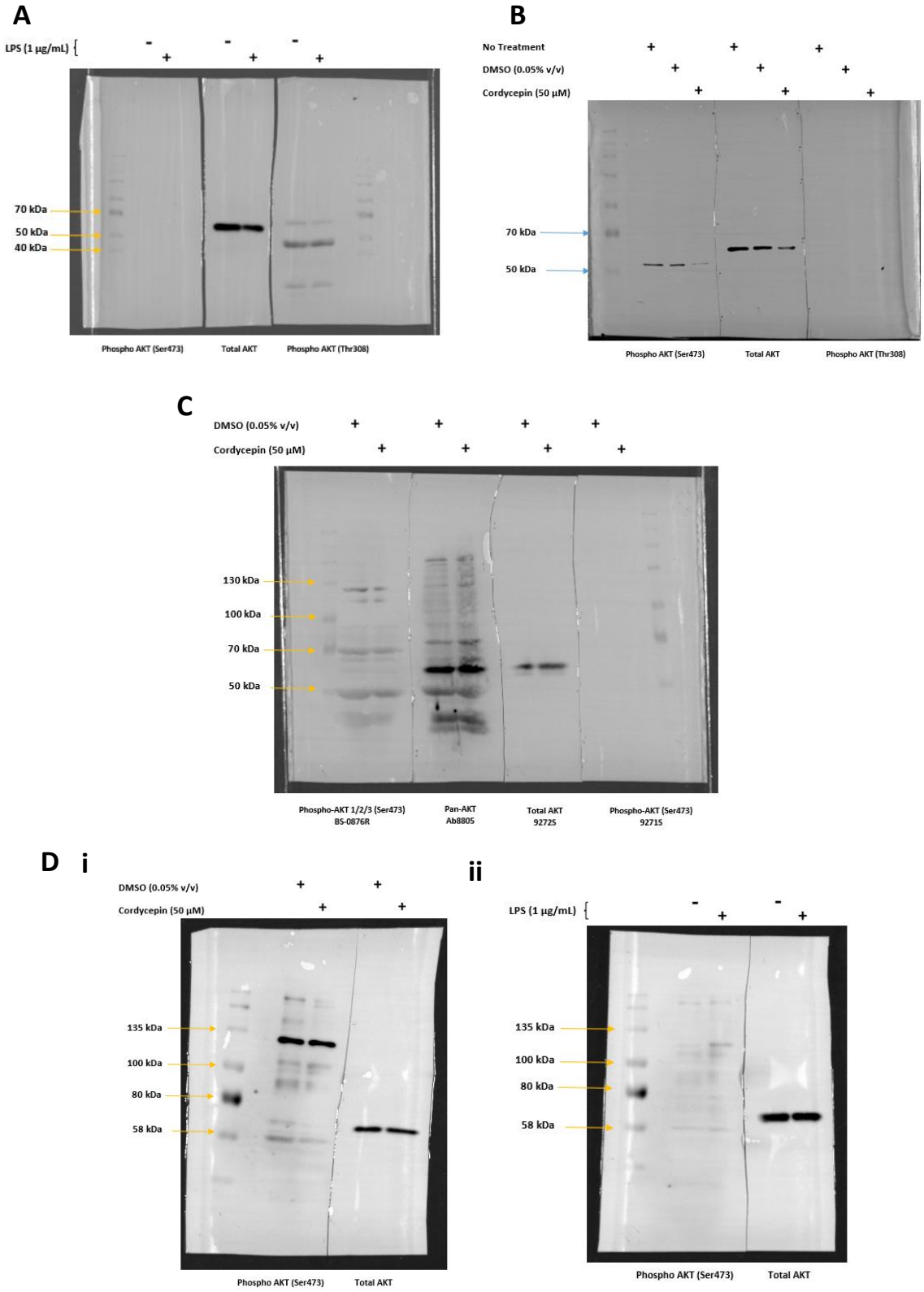

Figure A.4: Primary antibodies against phospho-AKT were unspecific for Mouse and Human proteins. Protein was extracted from either MCF-7 Human cells (**B**, **C**, **Di**) or RAW264.7 Mouse cells (**A** & **Dii**) and western blots of antibodies

following Method sections 2.3.1 & 2.3.3. Antibodies: Phospho-AKT (Ser473): 4058S (**A**), AF3263 (**B**), 587F11 (**D**). Phospho-AKT (Thr308): 4056S (**A**), AF3262 (**B**). **C)** detailed in image. Total AKT: 9272S (**A-D**).

11.5 HEK293 RNA-Seq MDS Plot – distribution of expression for each biological replicate

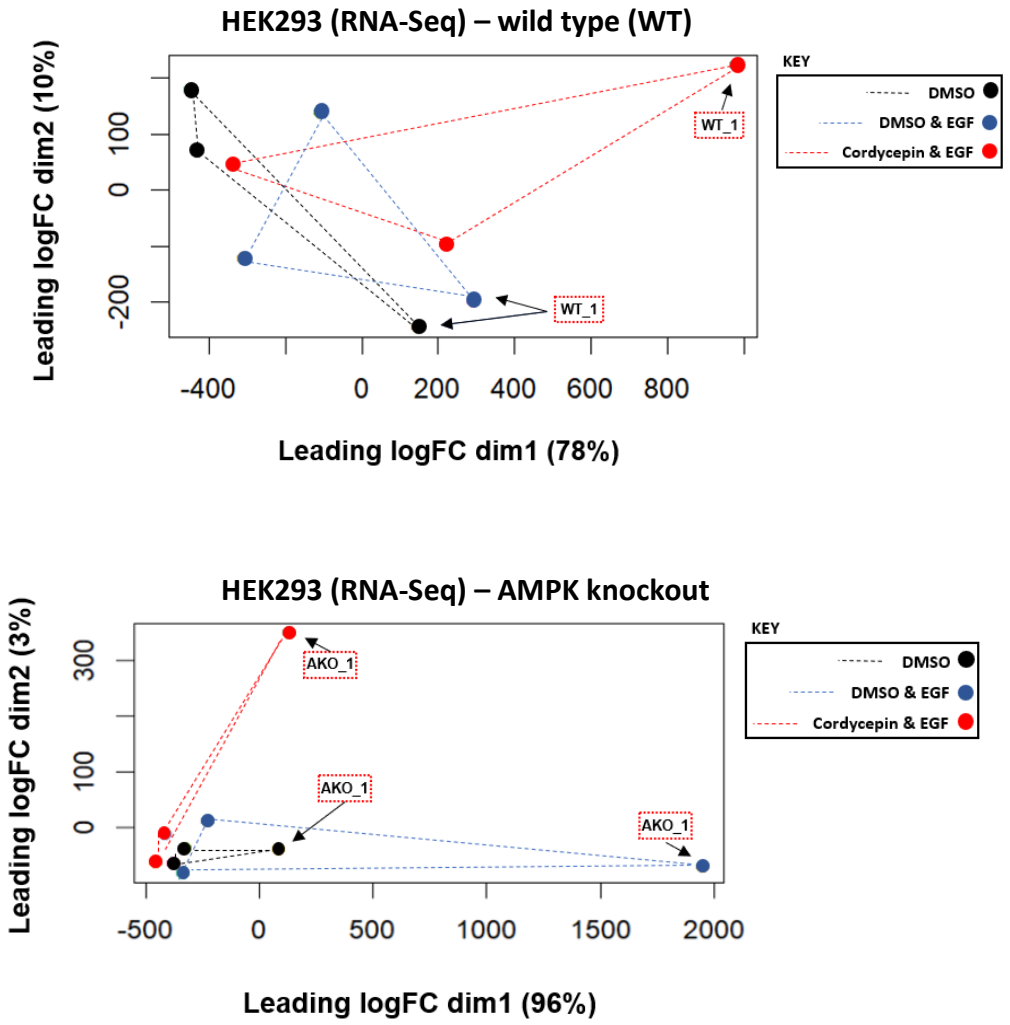

Figure A.5: Multidimensional scaling (MDS) plot of HEK293 RNA-Seq biological replicates. RPKM values of HEK293 RNA-Seq samples were used for MDS using the 'plotMDS' function within the LIMMA tool[665]. The distances between the plots correlates to the dissimilarity between the expression (Log_2FC) of the top 500 genes. The X- and Y-axis represent the Euclidean distances (difference between two plots). The dimensions (dim1 and dim2) explain the percentage of total variance between the expression of the samples. The dotted lines show the spread of expression between biological replicates of treatment conditions to show outliers in the replicates.

11.6 Validations of DMSO & EGF treatment concentrations in HEK293 cells by Elizabeth Rider

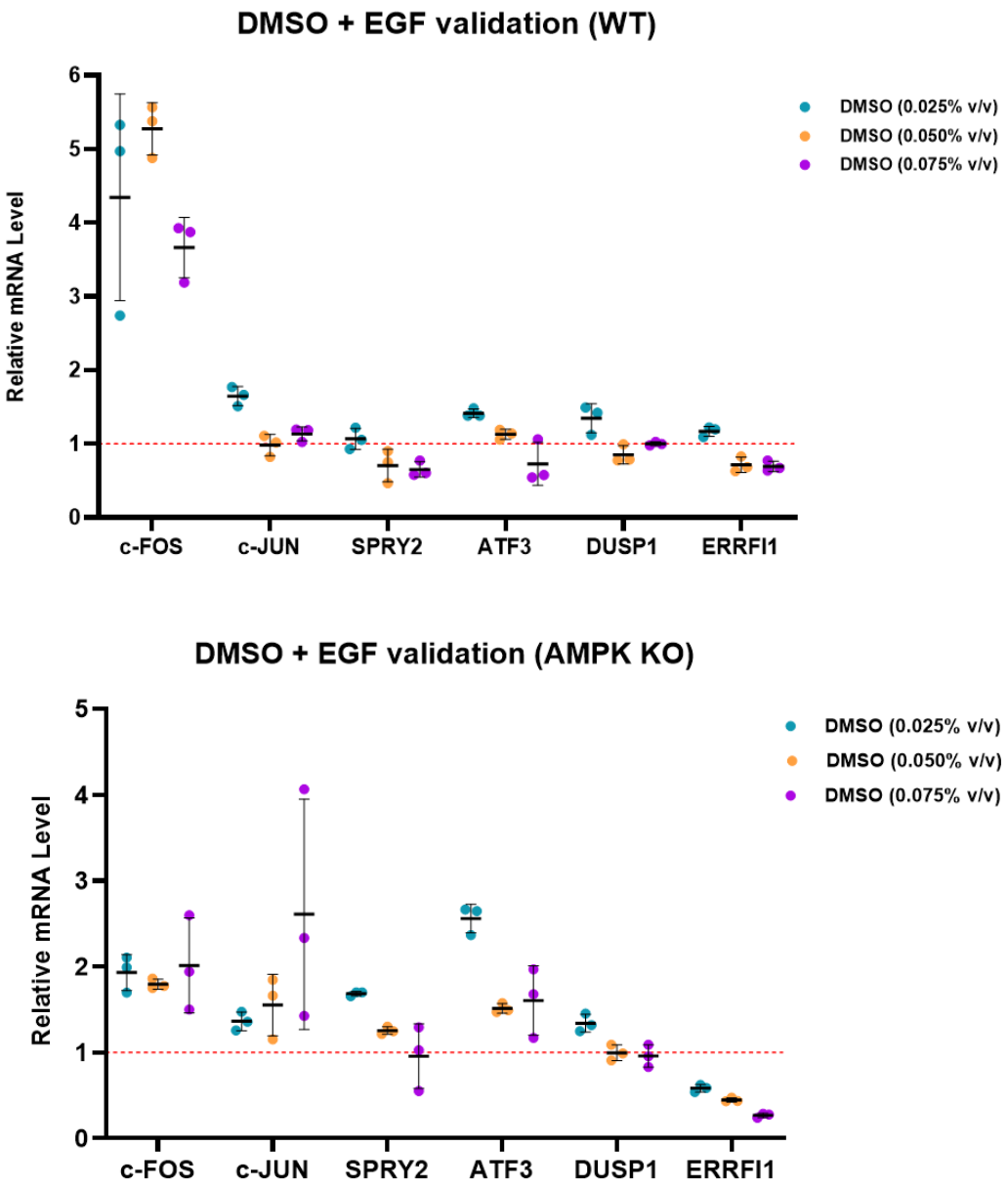

Figure A.6: Validation of DMSO & EGF stimulation of WT and AMPK KO HEK293 cells. HEK293 cells were gifted from Professor Grahame Hardie's lab at the University of Dundee. AMPK CRISPR-Cas9 knockout and wild type HEK293 cells were incubated in media containing less FBS (0.1%) for 24 hours prior to treatment with DMSO (0.025-0.075% v/v) for 20 minutes before stimulation with EGF (15 nM) for 30 minutes, or DMSO (0.025-0.075% v/v) on its own. Total RNA was extracted prior to cDNA synthesis and qPCR. Output was analysed using the 2-ΔΔCt method[660] and normalised to GAPDH (housekeeping gene). Relative mRNA expression level of tested genes are presented relative to DMSO (0.025-0.075% v/v). (mean ± SD; n=1 independent experiments). Experiment was performed by Elizabeth Rider under my training and guidance.

11.7 Additional biological replicates of western blots for cordycepin treatment and PI3K inhibitors for MCF-7 cells

A

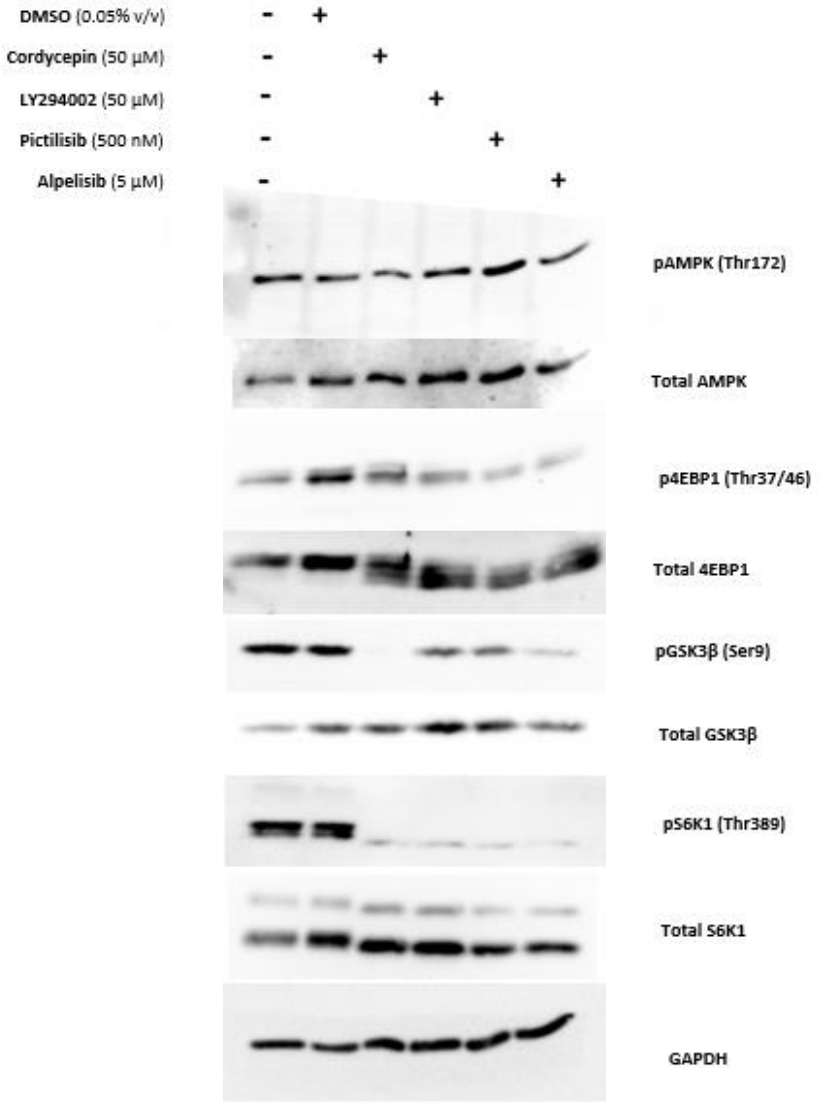

B

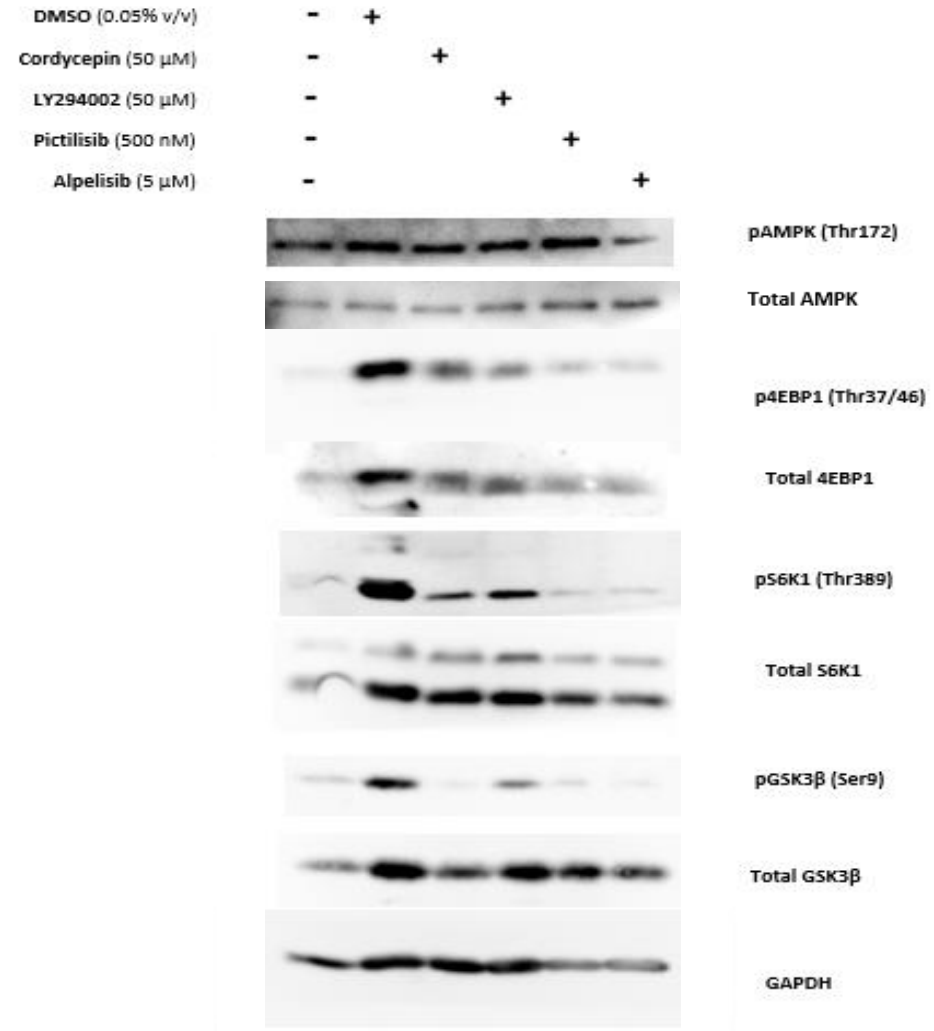

Figure A.7: Additional biological replicates of cordycepin treatment and PI3K inhibitors showing repression of AKT and mTOR signalling in MCF-7 cells. MCF-7 cells were treated for 2-hours with either cordycepin (50 µM), DMSO (0.05% v/v) or PI3K inhibitors; LY294002 (50 µM), Pictilisib (500 nM), or Alpelisib (5 µM). Total protein was extracted following Methods section 2.3.1. Western blotting and primary antibody incubation followed Methods section 2.3.3. Antibodies used is described in Table 2.4. **A)** Biological replicate 2, **B)** biological replicate 3.

11.8 PIPS Reflective Statement

Note to examiners: PhD candidates on the BBSRC-funded Doctoral Training Partnership programme are required to undergo a compulsory 3-month placement on a project which is not related to the PhD project.

PIPS Reflective Statement:

I reached out to Pip Peakman (Director of Research and Innovation (R&I), University of Nottingham) to join her team for my internship to gain an insight into how research and business interplay within the Institutional setting on a broad scale, and to attribute my skills gained from my PhD studies in project development and management.

As an intern for R&I, my original focus was on the R&I Roadmap project; with the aim of developing an expert framework to support the transition towards operational excellence for delivery of research excellence and knowledge exchange across the University (both Central and Faculty level). This roadmap would then integrate with Research Planning Working Groups (RPWG's) and Research Performance management to set priorities and 'quick wins' to optimise operational delivery and excellence of research and knowledge exchange (RKE).

The internship further separated into working for specific factions of R&I, including working specifically with Research Performance management with Dr. Sophie Berckhan (Research and Knowledge Exchange Business analysis & Reporting Manager (R&I)). I also worked with Dr. Maria Augusta Arruda (Head of Researcher Development) and Dr. Maria Letizia Cassioli (previous PhD Researcher) as a Research Development Officer on the Universities COVID-19 Research Portfolio.

11.9 Covid-19 Statement

Between March 2020 to September 2020, the Gene Regulation and RNA Biology (GRRB) lab was closed due to the COVID-19 pandemic and University of Nottingham guidance. From September 2020 to around May 2021, the GRRB lab was under a strict booking system and much reduced lab opening times than before the COVID-19 pandemic. Due to these issues, the lack of access to a lab, and subsequent problems with procuring lab consumables due to the consequence of lock-down in the UK and Europe, my PhD was severely impacted. As a result of the interruption of my PhD, I applied and was accepted by the School of Pharmacy for a 6-month extension to my deadline of my PhD thesis. I am very grateful for this extension as it enabled me to achieve as much practical results as I could with the restricted time and gave me the time to write the PhD thesis whilst working full-time at Prostate Cancer UK.